FINAL REPORT

MARCH 1997

DEVELOP ADVANCED NONLINEAR SIGNAL ANALYSIS TOPOGRAPHICAL MAPPING SYSTEM

NASA CONTRACT NO. NAS8-39393

Prepared for

NATIONAL AERONAUTICS AND SPACE ADMINISTRATION
GEORGE C. MARSHALL SPACE FLIGHT CENTER
MARSHALL SPACE FLIGHT CENTER, AL 35812

by

AI SIGNAL RESEARCH, INC.
3322 South Memorial Parkway, Suite 67
Huntsville, AL 35801
(205) 880-1968

AI SIGNAL RESEARCH
Program Manager: J. Jong

NASA
Contract Monitor: J. McBride
Contracting Officer: S. Presnell

TABLE OF CONTENTS

FOREWORD

This report was prepared by AI Signal Research, Inc. (ASRI) for the George C. Marshall Space Flight Center (MSFC), National Aeronautics and Space Administration (NASA). The work was performed under contract NAS8-39393, entitled "Develop Advanced Nonlinear Signal Analysis Topographical Mapping System (ATMS)". It covers work completed during January 12, 1993 through April 11, 1997.

The effort was managed out by Dr. Jen-Yi Jong serving as Program Manager. Dr. Jong was the Principle Investigator and key contributor responsible for the software design, development, and evaluation of ATMS. Mr. Ken Wang and Mr. Kim Ong, computer programmers, were responsible for implementing the ATMS software on both ASRI's SUN/330 and MSFC/ED33 OISPS computer systems using C, Fortran and Clips programming languages.

Mr. James McBride and Mr. Tony Fiorucci, MSFC/ED23, provided valuable management and technical support through the coordination of computer resources and definition of task requirements and priority. In addition, Mr. Michael Wright, MSFC/ED23 provided valuable assistance in integrating the ATMS into MSFC's OISPS Computer System. Prior to his retirement, Mr. Jess Jones, ED/32, provided key program direction for this contractual effort.

1.0 PROGRAM SUMMARY

During the past two decades, The National Aeronautics and Space Administration (NASA) has conducted extensive flight certification and developmental testing for the Space Shuttle Main Engine (SSME)/Advanced Turbopump Development (ATD). The testing involved the collection and analysis of a large number of health monitoring measurements. It was found that numerous major component failures have occurred as a result of severe temperature, pressure, and dynamic environments sustained during operation causing extensive engine hardware damage and scheduling impacts. This contractual effort focused on enhancing engine safety and reliability through the use of detailed analysis and evaluation of the measured signals to assess the engine's dynamic characteristics and operational condition. Results have shown that efficient and reliable signal detection techniques will reduce the risk of catastrophic system failures and expedite the evaluation of both flight and ground test data thereby reducing launch turn-around time.

During the development of the SSME, a hierarchy of advanced signal analysis techniques for mechanical signature analysis has been developed by NASA and AI Signal Research Inc. (ASRI) to improve the safety and reliability for Space Shuttle operations. These techniques can process and identify intelligent information hidden in a measured signal, which are often unidentifiable using conventional signal analysis methods. By providing additional insight into measured signals, the techniques can better identify well-hidden system defects as well as false-alarm signatures. Efforts to date have shown that using advanced signal analysis techniques reduces false alarm/misinterpretation rates and greatly improves system reliability. These techniques have been extensively tested using SSME static test and flight data. Results appear to be extremely promising for failure analysis and detection in other complex machinery. These advanced signature analysis techniques have proven valuable in supporting critical day to day MSFC SSME Project flight and test program operations.

The detection and understanding of anomalous signatures and their physical implications is the most important function of advanced signal analysis techniques. Currently, due to the highly interactive processing requirements and the volume of dynamic data involved, detailed diagnostic analysis is being performed manually which requires immense man-hours with extensive human interface. To overcome this manual process, NASA implemented this program to develop an Advanced nonlinear signal Analysis Topographical Mapping System (ATMS) to provide automatic/unsupervised engine diagnostic capabilities. The ATMS will utilize a rule-based Clips expert system to supervise a hierarchy of diagnostic signature analysis techniques in the Advanced Signal Analysis Library (ASAL). ASAL will perform automatic signal processing, archiving, and anomaly detection/identification tasks in order to provide an intelligent and fully automated engine diagnostic capability. The ATMS has been successfully developed under this contract through the following four major tasks:

- Development of a hierarchy of advanced nonlinear signal analysis techniques for reliable engine health monitoring and failure prediction and prevention and integrating the signal diagnostic techniques into an Advanced Signal Analysis Library (ASAL) within the ATMS system.

- Development of the ATMS Automated Signal Processing Subsystem (ASPS) and Anomaly Detection and Identification Subsystem (ADIS) utilizing an expert system to supervise the diagnostic signal analysis programs in the ASAL. The ASPS and ADIS subsystems perform automatic/unsupervised engine health monitoring and diagnostic evaluation.

- Creation of a compressed TOPO Data Base (CTDB) utilizing ASPS/ADI subsystems to convert high frequency dynamic signals from engine test history into a bank of succinct image-like patterns, while preserving valuable dynamic statistics, failure history, fault symptoms and anomalous signatures in the CTDB.

- Development of a signature Retrieval Subsystem (SRS) by integrating the ASAL with the CTDB data base to provide fast signature retrieval, trending and fault pattern comparison/identification capabilities which would allow the entire engine test history to be readily accessible.

The significance of the ATMS developed under this program is attributed to the fully automated coherence analysis capability for anomaly detection and identification, which can greatly enhance the power and reliability of engine diagnostic evaluation. The ATMS will provide rapid turn-around time for engine performance evaluation and a detailed engineering assessment of engine dynamic data in order to insure it's operational integrity. The system will allow NASA engineers to quickly evaluate engine operational conditions of both flight and ground test data, thereby reducing launch turn-around time and enhancing flight safety and reliability. In addition, ATMS will provide timely assessment of engine performance, identify probable causes of malfunction & anomaly, and indicate feasible engineering solutions to enhance engine performance. Failure history, fault symptoms, and anomalous signatures created in the CTDB Data base will provide a foundation for future propulsion development programs.

In summary, the program objectives to design, develop, test and conduct performance evaluation for an automated engine diagnostic system have been successfully achieved. Software implementation of the entire ATMS system on MSFC's OISPS computer has been completed. The results have demonstrated that ***ATMS can significantly save time and man-hours in performing engine test/flight data analysis and performance evaluation of large volumes of dynamic test data.***

2.0 TECHNICAL DISCUSSION

2.1 Introduction

This section presents an overview of the Space Shuttle Vehicle (SSV) system and Space Shuttle Main Engine (SSME) in particular. The SSME test program and history are briefly described, and underlined is the need for advanced signal detection techniques for diagnostic assessment of SSME dynamic measurements. The SSV is composed of the Orbiter, an External Tank (ET), which contains fuel for the Orbiter's three SSMEs, and two Solid Rocket Boosters (SRB). The orbiter and SRBs are reusable; the ET is expended on each launch. The Orbiter vehicle main propulsion system consists of three SSMEs. The SSMEs are reusable, high-performance, liquid-propellant rocket engines with variable thrust. All three engines are ignited on the ground at launch and operate for approximately 500 seconds total of firing duration. Each engine operates at a mixture ratio (liquid oxygen/liquid hydrogen) of 6:1 and a chamber pressure of approximately 3000 psia to produce a sea-level thrust of 375,000 pounds and a vacuum thrust of 470,400 pounds. The SSMEs are extremely sophisticated machines, designed to provide maximum performance within stringent constraints on size, weight and efficiency. As a result, the SSMEs are required to operate under extreme temperatures with high fluid pressures and rotational pump speeds. Furthermore, developmental work is currently proceeding to improve SSME performance. Since a key to SSV cost effectiveness and flight safety is hardware reusability, system reliability is of paramount importance. Consequently, the SSME and its components are subjected to extensive hot firing testing. Acceleration, temperature, dynamic pressure and strain data are acquired during these tests along with SSV during flights.

Development and qualification testing of the engine and its components is conducted at several NASA and contractor locations. Full-scale engine test firings for development and flight acceptance purposes are performed on three single-engine test stands at the Stennis Space Center, Bay St. Louis, Mississippi. In addition, propulsion system testing is performed at the NASA Engine Technology Test Bed (TTB) , Marshall Space Flight Center, Alabama. Testing is performed on a continuous basis. The length of a given test is dependent on specific test objectives and may range anywhere from an ignition test of only 1.5 seconds to a component certification test of over 1000 seconds. Tests are generally designed to satisfy multiple objectives which fall into two broad categories: (1) Acceptance/certification firing of flight hardware; and (2) Developmental testing directed toward design verification, and performance/reliability improvement. SSME operation is controlled by a computer called the Command and Data Simulator (CADS) which communicates with the engine, displays vital measurements for on-line observation/control, and initiates pre- and post-test procedures.

Approximately 250 measurements are recorded during a given test. They include wide band vibration, dynamic pressure and strain readings at critical engine locations. Some of

the dynamic measurements are utilized as on-line emergency cut-off indicators. All data are recorded as analog signals on magnetic tape or stored digitally for subsequent analysis and evaluation. Limited SSME vibration measurements are recorded on magnetic tape during SSV flight for evaluation after orbiter landing. The extensive dynamic database available from this test program is highly valuable in the calibration and verification of analysis/statistical models comprising a wide range of operational engine conditions.

During the development of the propulsion system for the Space Shuttle, state-of-the-art technology in rocket engines has seen significant advances. In several instances, these advances have resulted in high fluid velocities and dynamic pressures in engine pumps, turbines, and valves. These critical operational parameters have in turn given rise to several fluid pressure fluctuations and destructive vibrations within the SSME. The character of these vibration signatures varies from random in nature to that of a complex periodic function, and even a pure tone in some cases. To analyze and thereby quantify these complex signatures, non-standard analysis techniques together with an experienced analyst are required.

Under the severe temperatures, pressures, and dynamic environments sustained during operation, engine systems and components have been subject to malfunction and failure. Over the past two decades of SSME development, a number of major component failures have occurred, causing extensive damage to engine hardware and test facilities along with considerable expense in cost and scheduling. In addition to numerous off normal operations of less severe nature including turbine blade cracks and bearing element failures. Through extensive data evaluation and analytical effort, turbomachinery and related component vibrations have been implicated as the sources of many high cycle fatigue problems which induced some of these catastrophic failures. This failure history underlines the need for a reliable incipient failure detection and diagnostic evaluation methodology. Signal processing has become one of the most important components in any machine monitoring and diagnostic system. Improving such system reliability has required a more complete understanding of the vibration signals associated with various failure mechanisms.

Conventional frequency spectrum signature analysis has been a useful technique for defect signature identification. However, under a complex multi-source operational environment, vibration signals are often subjected to noise corruption and signal interference, which can cause false detection/identification and greatly reduce the diagnostic reliability. In addition, nonlinear mechanisms of a rotor system will cause different frequency components to interact with one another, which would further complicate the vibration spectrum with various harmonic/modulation/sideband patterns. This nonlinear interaction thus provides some unique defect signature for failure identification.

The ATMS utilizes both the conventional linear and a hierarchy of novel nonlinear coherence analysis techniques to detect and identify these signatures. The unique linear/nonlinear phase/correlation information of machinery vibration signals plays a significant role for fault diagnostics and better identifies well-hidden defect symptoms, which are often unidentifiable using conventional spectral analysis. These techniques have been tested using SSME engine data for post-test/flight analysis, and proven to be highly promising for failure detection in complex machinery. ***The significance of the ATMS developed under this program is attributed to the fully automated coherence analysis capability for anomaly detection and identification, which can greatly enhance the power and reliability of engine diagnostic evaluation.***

2.2 Overall System Structure of ATMS

ATMS utilizes an expert system to supervise a sequence of mechanical signature analysis techniques in the Advanced Signal Analysis Library (ASAL) to perform automatic signal processing, anomaly detection and identification tasks in order to provide automated SSME post-test engine diagnostic capability. Figure 2.2.1 shows the overall ATMS system flow diagram. Typical input to the system for SSME ground tests contains 60 to 80 channels of dynamic data at a sample frequency of 10,240 Hz for a test duration of approximately 550 seconds. SSME flight data inputs range from 24 to 36 dynamic channels sampled at 10,240 Hz for approximately 520 seconds. The interfaces between the CLIPS expert system and the ASAL programs were developed first. A set of ASAL execution rules of how to perform the analysis of each ASAL program with correct parameter settings were established in the Automated Signal Processing Subsystem (ASPS) Knowledge Base (ASPS-KB). Based on this knowledge base, the ASPS then utilizes the CLIPS expert system to supervise the ASAL in performing a sequence of standard analysis tasks for engine post-flight/test evaluation. The ASPS will automatically convert high frequency dynamic signals from the engine operational run into a bank of succinct image-like patterns in a compressed TOPO format and other various special formats to be stored in the Compressed TOPO Data Base (CTDB). The results of the ASPS operations thus provides the basic fact database and key statistic information for more detailed analysis in the subsequent Anomaly Detection and Identification Subsystem (ADIS). In addition, the Signature Retrieval Subsystem (SRS) can be enacted to provide fast signature retrieval, trending, and fault pattern comparison/identification capabilities which allows the entire engine test history to be readily accessible. The ADIS is the most intelligent element of the ATMS. Its major function is to first detect the existence of any anomaly in the CTDB database created by ASPS. Anomaly identification will then be performed in order to determine the physical underlying cause of the anomaly. The signature analysis techniques in ASAL can often provide valuable insight about the source of an anomaly and identify its underlying causes. This anomaly detection and identification task requires interactive processing of various signal analysis techniques in ASAL. An ADIS Knowledge Base (ADIS-KB) was designed and established by extracting the knowledge and thought logic of experienced human experts in performing such anomaly detection/identification, and reducing them into a set of rules for expert system execution. The ADIS then utilizes the CLIPS expert system to automate an intelligent ADIS analysis task by performing an extensive and highly interactive analysis for anomaly detection and identification. Figure 2.2.2 shows the overall ATMS system flow diagram along with the ASAL analysis program associated with each ATMS subsystem.

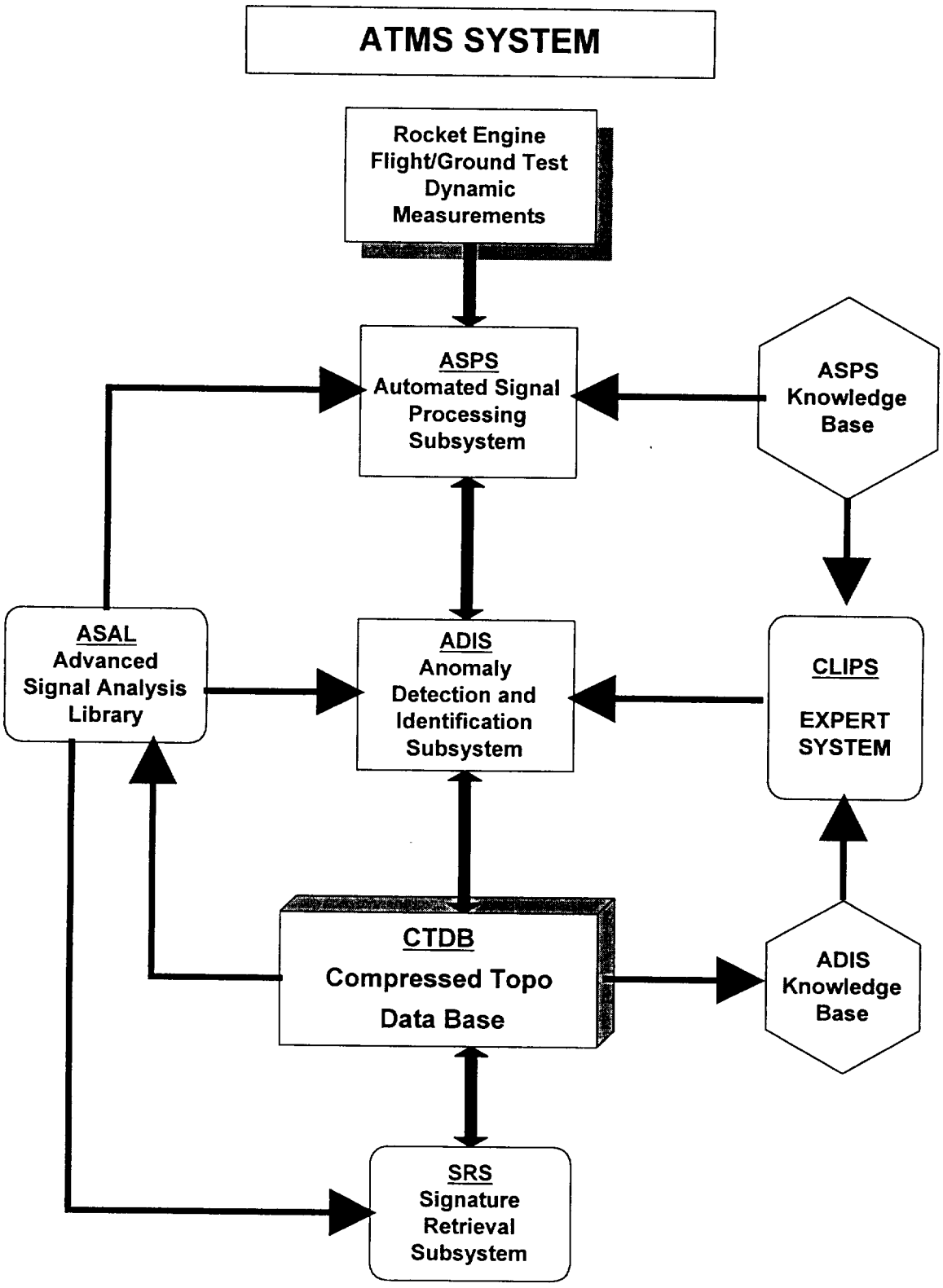

Figure 2.2.1 ATMS System Flow Diagram

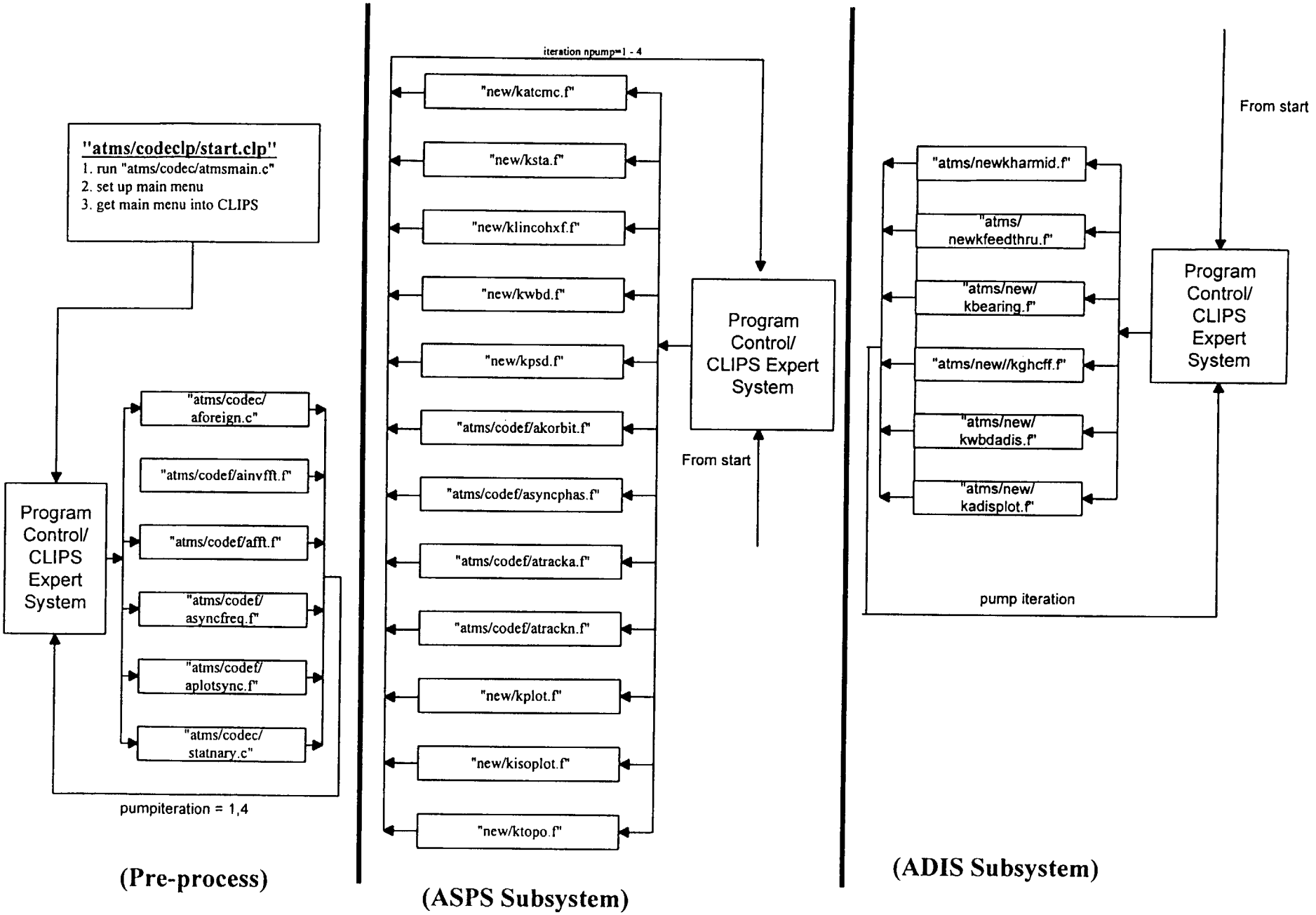

Figure 2.2.2 ATMS Overall System Flow Diagram

2.3 ATMS Advanced Signal Analysis Library (ATMS-ASAL)

During the development of the Space Shuttle Main Engine (SSME), NASA and ASRI have developed a hierarchy of advanced signal analysis techniques for mechanical signature analysis for the improvement of safety and reliability of Space Shuttle operations. These techniques can process and identify intelligent information hidden in a measurement signal, which is often unidentifiable using conventional signal analysis methods. By providing additional insight into the system response, the techniques can better identify well-hidden defect symptoms as well as false-alarm signatures. As a result, use of these signal analysis techniques reduces false-alarm/mis-interpretation rates and greatly improves system reliability. These techniques have been tested using SSME hot-firing test and flight data, and they appear to be highly promising for failure analysis and detection in other complex machinery.

Under this program, these hierarchy of mechanical signature analysis techniques have been integrated into the ATMS Advanced Signal Analysis Library (ATMS-ASAL) as shown in Table-2.3.1. Each of these ASAL techniques can identify a specific type of signal coherence and characteristic along with the particular physical mechanism associated with it. In many situation, interactive operation of various analysis techniques will also be required. The interface of each ASAL program has been converted from the original manual user-interface mode into a Clips-interface mode so that they can be executed directly from the CLIPS expert system for automated processing. This conversion involved reprogramming of a number of utility subroutines in the OISPS system controlling the communication between the main analysis programs and all the other I/O routines and database.

In the following sections, several application examples utilizing the ASAL signature analysis techniques will be used to demonstrate the principle and effectiveness of ASAL in fault diagnosis. As will be shown later in section 2.8 for Case Study, most of the anomalies discussed in these example can be automatically detected and identified by ADIS.

2.3.1 Bandwidth Coherence (BWC) Analysis - Discrete Line Noise Identification

Some of the most commonly observed false-alarm components found very frequently in dynamic data measurements are; the discrete line noise component emanating from the power supply of the data acquisition system (i.e. 60 Hz line noise and its harmonics), the tape multiplex/demultiplex devices; and other elements within the measurement/sensor system. In an effort to classify discrete line noise, the Bandwidth Coherence (BWC) Analysis technique was developed by ASRI. The BWC method is an effective tool in measuring the relative bandwidth, i.e. the discreteness, of a spectral component. This method is based on identifying a coherent phase relationship at the frequency of a discrete component within contiguous ensemble blocks of data. The strength of such a coherent phase relationship is proportional to the degree of discreteness of the spectral component. Therefore, for a pure-tone discrete component (such as line noise or its harmonics), a strong coherent phase relationship would exist and its Bandwidth Coherence should be unity. On the other hand, for a narrow band random component, the coherent phase would be diminished (in proportion to its bandwidth) relative to a pure tone, and its

THIS PAGE

INTENTIONALLY

LEFT BLANK

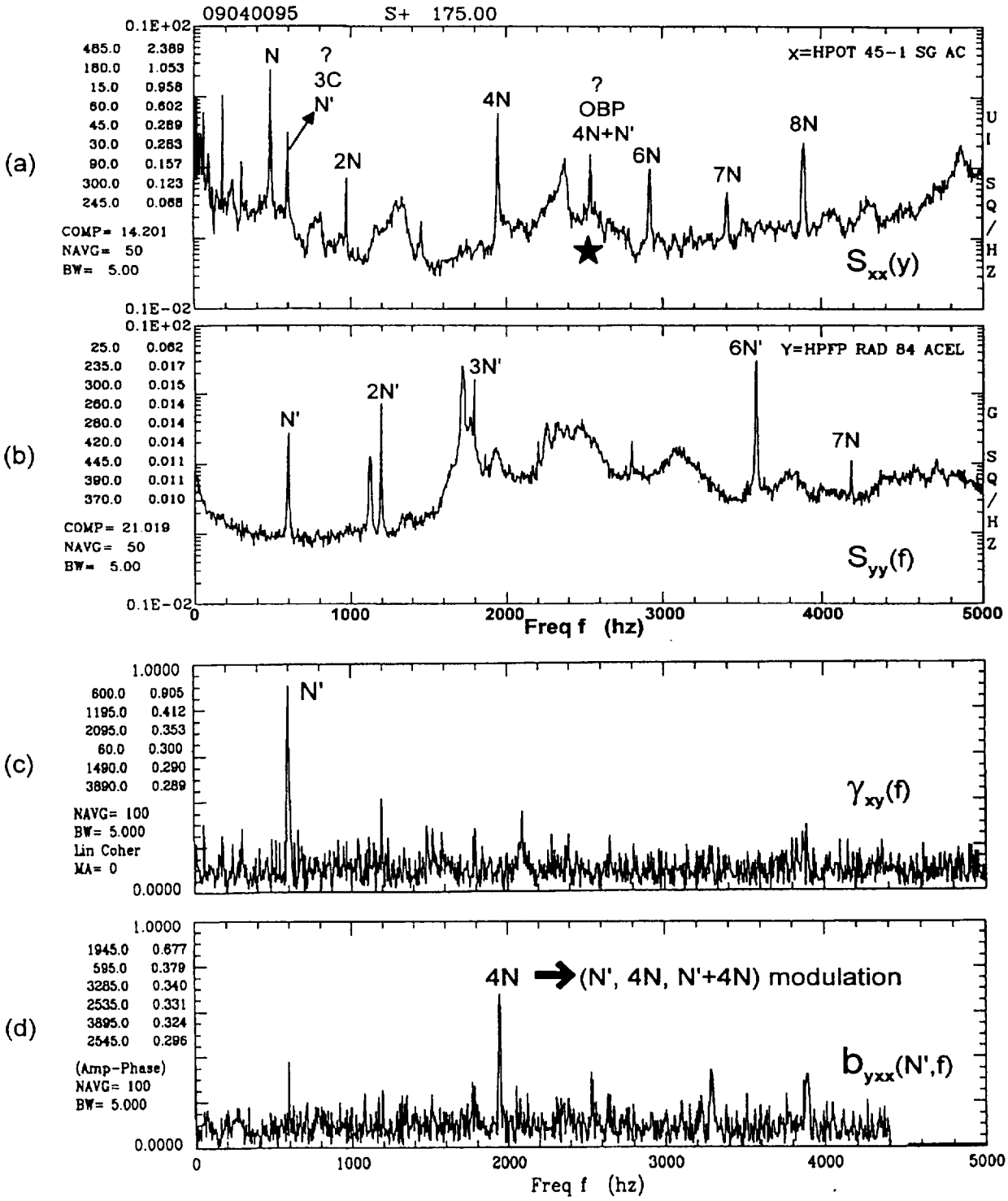

Figure 2.3.2 (a): PSD of SSME HPOTP Strain Gauge Measurement.
(b): PSD of SSME HPFTP Accelerometer Measurement.
(c): Linear Cross Coherence γxy(f) Between HPOTP & HPFTP
(d): Cross Bi-Coherence Byxx(N', f) Between HPOTP & HPFTP

A typical example of the application of linear coherence is shown in Figure 2.3.2. Figure 2.3.2-(a) shows a PSD taken from a SSME HPOTP external strain gauge measurement . The peaks marked "N", "2N", "3N",... are the Sync component and its harmonics. The peak marked "LN" is the third harmonic of 60 Hz line noise. However, two anomalies are observed in the PSD. The first one marked "3C (or N')" is near the third harmonic of the turbine-end bearing cage frequency, while the other anomaly marked "OBP (or 4N+N')" is near the turbine-end Outer Ball Pass (OBP) frequency. Since both anomalies are near critical bearing characteristic frequencies, it is imperative to identify the sources of these anomalies. Figure 2.3.2-(b) shows the PSD of an accelerometer of the nearby High Pressure Fuel TurboPump (HPFTP). The peaks marked N', 2N', 3N' are the Sync and harmonics of HPFTP. Since the frequency of N' is at the same frequency of the 3C anomaly of the HPOTP, linear cross-coherence is first performed in order to identify if the 3C anomaly as simply a feed through from the sync of HPFTP. Figure 2.3.2-(c) shows the linear cross-coherence between the two measurements in Figure 2.3.2(a) and 2.3.2(b). The linear coherence indeed identifies a strong correlation at 600 Hz (N' component). This indicates that this N' component in the HPOTP signal is simply a Sync feed-through from the HPFTP. However, the identification of the remaining anomaly marked "OBP" in the HPOTP measurement requires the use of nonlinear coherence analysis and will be discussed next.

2.3.3 Cross Bi-Coherence Analysis - Amplitude Modulation Identification

The dynamic response of a rotating machine can exhibit frequency sum or difference phenomena. This type of nonlinear phenomena is primarily due to amplitude modulation between various rotational components and/or fluid/structure interactions. The characteristics of such nonlinear interactions are usually reflected in a response waveform, which can be identified by using the bi-spectral technique. As the linear coherence is a second moment statistic of a random signal, the bi-coherence represents the third joint moment among three different waves at frequency w_1, w_2 and the sum frequency w_1+w_2. Even though a PSD can identify the power distribution at these three particular frequencies, the existence of modulation can only be proven by identifying their nonlinear coherent phase relationship. Bicoherence provides such an effective method to identify such nonlinear phase coupling.

As discussed before, the anomaly present at OBP frequency in the HPOTP measurement is coincident with the outer ball pass (OBP) frequency of the HPOTP pump-end bearings. If it was concluded to be a bearing defect signature based on this assessment, a costly turbomachine would have been rejected for flight and been subjected to an in-depth hardware tear-down inspection. However, bispectral analysis showed this anomaly to be a false-alarm defect signature. By closely examining the frequency relationships of all these components, the OBP frequency was observed to be 4N plus the Sync feed-through (N') from the nearby HPFTP. Therefore, a new question was raised, that is, whether this OBP anomaly was truly an OBP defect signature or was it just the modulation between 4N of the HPOTP, and the Sync of the HPFTP. The latter phenomenon has been frequently observed in multiple machinery environments where two rotational processes interact with each other. To answer this question, the nonlinear correlation between the frequency components emanating from the two separate pumps had to be determined through bispectral analysis. Figure 2.3.2(d) depicts the cross bi-coherence function between the HPFTP and HPOTP measurements, A significant bicoherence peak is detected at the 4N frequency which corresponds to the bi-coherence function bxxx(N', 4N). This indicates that the N' and 4N components, along with their sum frequency, the OBP anomaly, are highly correlated with each other quadratically. Therefore, this OBP anomaly is actually due to the modulation between 4N of the HPOTP and the Sync the

HPFTP (N'). This nonlinear phenomenon is identifiable only through bi-spectral analysis. In this case, the OBP anomaly turned out to be a false alarm rather than a true OBP defect signature as it appeared to be. Moreover, this finding exonerated a healthy multi-million dollar turbopump for flight purposes.

2.3.4 Auto Bi-Coherence Analysis - Bearing Fault Patterns Identification

Faults in bearings will tend to generate characteristic frequencies and signature patterns evident in the dynamic monitoring signal. As a fault in an inner race moves into and out of the load zone within each revolution, its can cause amplitude modulation with a modulating frequency of Sync (once per rev), and a carrier frequency of Inner Race Defect (IRD) frequency. Similarly, as a defect on a rolling element moves into and out of the load zone, as well as the line of contact, it will also cause amplitude modulation with a modulating frequency of Cage (ball/roller train frequency), and a carrier frequency of ball/roller spin frequency. These nonlinear interactions among various frequency components provide important signatures for bearing fault diagnostics. Such bearing faults with their associated nonlinear modulations will typically generate modulation/sideband patterns as shown in Figuress 2.3.3, which are composed of a fundamental and its harmonics of some bearing characteristic frequency, plus a family of sidebands around each. The fundamental frequency could be Inner Race Frequency (IRF) or Ball/Roller Spin Frequency, and the modulating frequency (the spacing between sidebands) could be Sync frequency or the Cage frequency, depending on the fault mechanism. However, this analytically predicted bearing fault patterns are often confused with rotordynamic, fluid dynamic, structural, environmental responses, other elements in the machinery system, and background noise. These additional sources collectively mask bearing distress signals emanating from the defective bearing. Under these conditions, bearing diagnostics based on PSD analysis would not be effective, and the bicoherence must be utilized to discriminate the presence of nonlinearly coupled fault pattern.

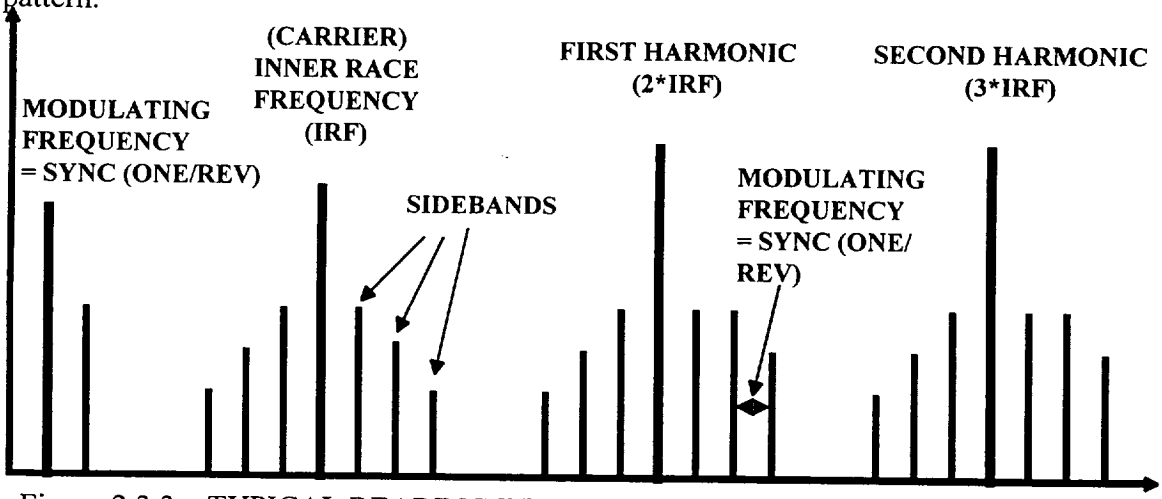

Figure 2.3.3. TYPICAL BEARING INNER RACE FAULT PATTERN TEMPLATE

An application example from a helicopter drive-train system are utilized to demonstrate the performance of the auto bi-spectral techniques for bearing diagnostics. The test data were captured from externally mounted accelerometers at the output end of a 42 degree gearbox, which is a component in the H-46 drive train and couples to the tail rotor gearbox. Both input pinion and output gears have 27 teeth. The shaft rotational frequency (RPM or Sync) is running at approximately 71.667 Hz during the tests. The

content of these tests included nominal and induced fault conditions within the transmission systems. Figure 2.3.4 shows the raw PSDs of 4 sets of tests of the accelerometer measurements. These spectra's are cluttered with a gamut of discrete signals. Some of these components could represent critical bearing defect signatures, while others may be nominal system responses. The complexity of the spectral content makes it very difficult to extract the analytically predicted bearing fault patterns (modulation/sideband patterns) depicted in Figure 2.3.3. In addition, a sequence of spectral peaks matching the sideband pattern does not ensure that such a pattern is indicative of a fault-generated modulation sideband.

Bicoherence analysis provides an effective way to identify such bearing fault patterns since the cluster of sidebands around various carrier frequencies (e.g. IRD+k*N, and 2IRD+k*N,..) are nonlinearly correlated with each other. Therefore, a bearing fault pattern due to an inner race defect can be identified using bicoherence with the first frequency argument w1 fixed at the IRD frequency, while the second frequency argument, w2, sweeps through the entire analysis frequency range. Figure 2.3.5 depicts a bicoherence with w1 fixed at 510 Hz, the IRD frequency of the ball bearings, for the 4 sets of gearbox test data. A clear pattern identical to the inner race fault pattern template is immediately identified for test 3. In the bicoherence function for test 3, two clusters of sidebands are shown. The carrier frequency of the first cluster is the IRD frequency, and the carrier of the second cluster is the second harmonic of IRD (i.e. 2*IRD). The spacing frequency between the sidebands within each cluster is equal to the Sync frequency, 71.67 Hz. The identification of this fault template clearly indicates that an inner race defect is present in the ball bearing of test 3. Notice that the bicoherence for test 2 also picks up strong coherence at N and it harmonics but without the presence of rich sideband clusters. This modulation phenomenon between the IRD and the Sync/harmonics also indicates a ball-bearing related fault. Later discussion with test representative confirmed that the bispectral analysis correctly identified seeded bearing faults in tests 2, and 3.

Bicoherence analysis provides an effective way to identify such bearing fault patterns since the cluster of sidebands around various carrier frequencies (e.g. IRD+k*N, and 2IRD+k*N,..) are nonlinearly correlated with each other. Therefore, a bearing fault pattern due to an inner race defect can be identified using bicoherence with the first frequency argument w1 fixed at the IRD frequency, while the second frequency argument, w2, sweeps through the entire analysis frequency range. Figure 2.3.5 depicts a bicoherence with w1 fixed at 510 Hz, the IRD frequency of the ball bearings, for the 4 sets of gearbox test data. A clear pattern identical to the inner race fault pattern template is immediately identified for test 3. In the bicoherence function for test 3, two clusters of sidebands are shown. The carrier frequency of the first cluster is the IRD frequency, and the carrier of the second cluster is the second harmonic of IRD (i.e. 2*IRD). The spacing frequency between the sidebands within each cluster is equal to the Sync frequency, 71.67 Hz. The identification of this fault template clearly indicates that an inner race defect is present in the ball bearing of test 3. Notice that the bicoherence for test 2 also picks up strong coherence at N and it harmonics but without the presence of rich sideband clusters. This modulation phenomenon between the IRD and the Sync/harmonics also indicates a ball-bearing related fault. Later discussion with test representative confirmed that the bispectral analysis correctly identified seeded bearing faults in tests 2, and 3.

2.3.5 Generalized Hyper-Coherence (GHC) - Bearing Fault identification

Frequency Modulation (FM) is an important type of fault signature common in a gearbox/bearing system. For example, spacing errors due to an excessively deflecting gear tooth, or shaft torsional oscillation, will cause frequency modulation. Valuable information is contained in the instantaneous frequency (IF) or the instantaneous phase of the carrier frequency component. This instantaneous frequency/phase information can be recovered using several digital frequency demodulation methods, such as the complex demodulation (heterodyne) technique and Phase Lock Loop (PLL) method. The instantaneous frequency can provide valuable information in identifying well-hidden defect signatures associated with gearbox/bearing defects. During steady state operation of a rotor system, the dynamic load variation on a rotating shaft tends to momentarily speed up or slow down the shaft rotational speed. This fundamental shaft rotational component drives other rotational mechanisms and generates various spectral components associated with, tooth meshing, bearing cage, or inner/outer ball pass frequencies along with related harmonics and modulations. When RPM reduces or increases even slightly, the frequencies of all the corresponding rotational components will also respond in kind. These characteristic components along with their modulation or sideband signatures are all correlated with each other in some particular fashion, and non-linear spectral and coherence analysis such as bi-spectral estimation provides an effective way to identify such correlation. Information regarding such correlation is also contained in instantaneous frequency variation and may be invaluable in identifying complex modulation phenomena associated with bearing distress.

An example of such a complex modulation phenomenon that was observed in the Space Shuttle Main Engine (SSME) test data and has been associated with turbopump bearing defects will be discussed here. Figure 2.3.6-a shows the PSD of a SSME High Pressure Oxygen Turbopump (HPOTP) internal Strain Gauge measurement data recorded during an engine hot firing. The peaks marked "N", "2N", "4N", etc., are the synchronous frequency component and its harmonics. The other peaks marked "C" and "2C" are the cage train frequency component and its second harmonic, and are normally seen in such internal measurements. However, a strong anomalous component, marked "A", is observed around a frequency of 8.5N. The frequency of this anomaly does not correspond to any bearing characteristic frequencies. In order to assess if this anomaly is an indication of a bearing related defect, the correlation between "A", the ball cage train frequency, and synchronous must be determined.

By examining the frequencies of these components, the component at 8.5N is observed to be equal to 14N-12C, or 12(N-C)+2N. This implies that the 8.5N component might be caused by the modulation between the inner ball pass component (for a 12-ball bearing set), which is at a frequency of 12(N-C), and the second harmonic of Sync. If the existence of such modulation could be proven, then the anomalous 8.5N component would represent a bearing related defect signature. However, the potential modulating harmonics at 14N, 12C and the inner race frequency, 12(N-C), do not exist in the PSD. Therefore, nonlinear spectral analysis techniques are not applicable in identifying whether such a modulation creates the anomaly 8.5N.

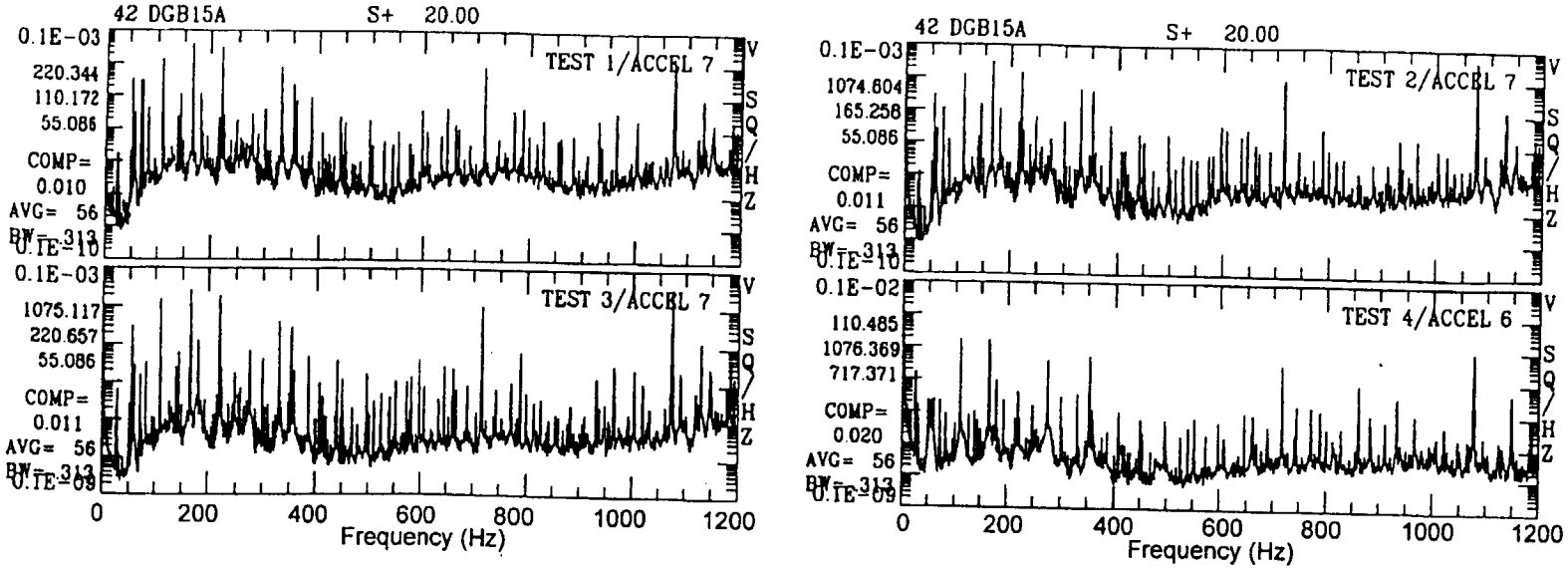

Figure 2.3.4 PSDs of 4 Sets of 42 Degree Gearbox Tests Data (0 to 1,200 Hz).

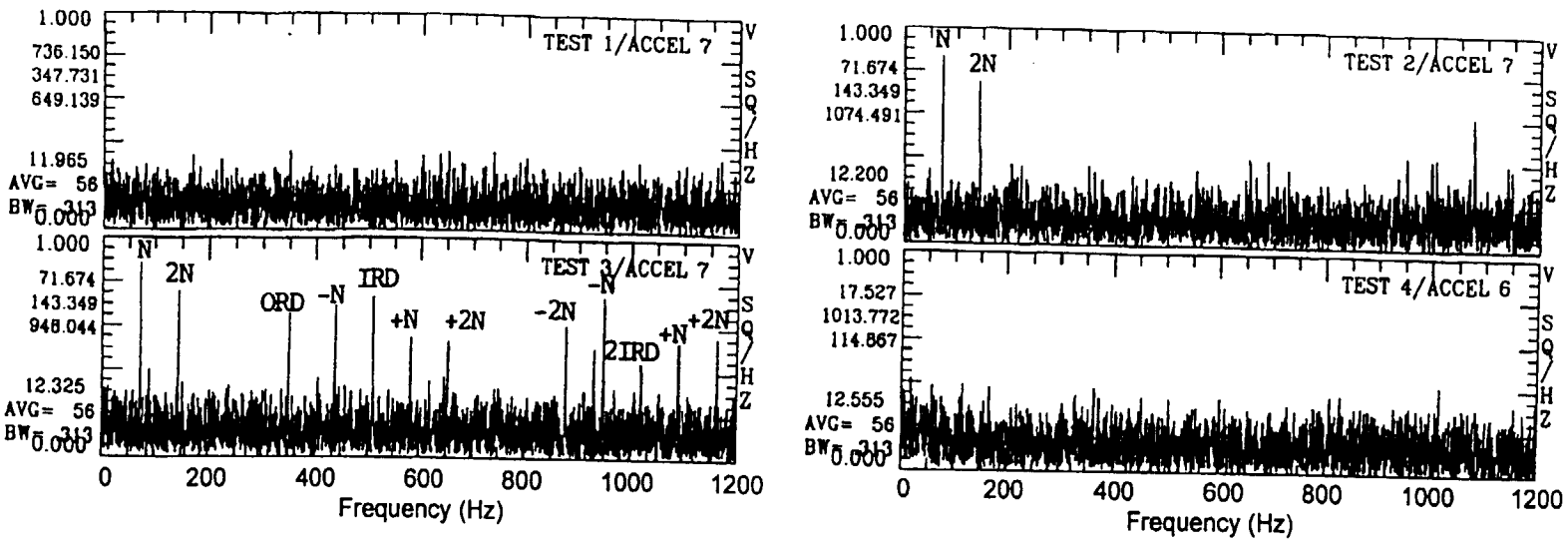

Figure 2.3.5 Auto Bi-Coherence Bxxx(510 Hz, f) of 42 Degree Gearbox Tests Data.

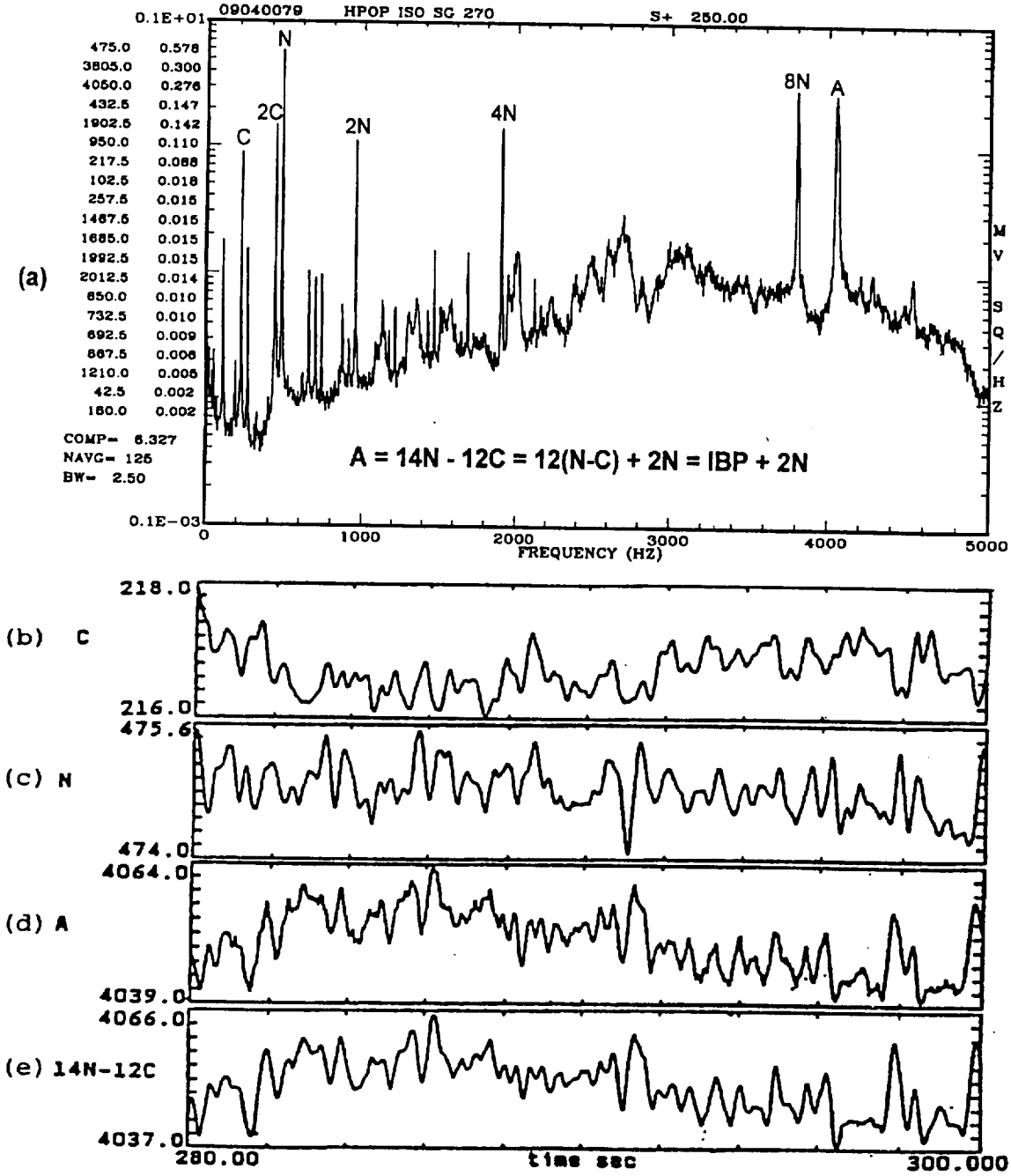

Figure 2.3.6 (a) PSD of HPOTP Strain Gauge Measurement.
(b) Instantaneous Frequency (IF) of Cage (C).
(c) Instantaneous Frequency (IF) of Sync (N).
(d) Instantaneous Frequency (IF) of Anomaly (A).
(e) 14 times of IF Signal of N (Figure 6-c) minus. 12 times of IF Signal of C (Figure 6-b).

Instantaneous frequency manipulation provides an alternative way to identify such correlation between fundamental rotor and bearing components by matching the appropriate integer multiple of each fundamental IF signal corresponding to each of the modulating components. In this example, the IF signals are first estimated at the cage frequency "C", the SYNC frequency "N" and the anomalous frequency "A", as shown in Figuress 2.3.6-b, 2.3.6-c and 2.3.6-d respectively. Figure 2.3.6-e shows the summation of negative twelve times the IF signal of "C" and 14 times the IF signal of "N". If modulation does exist, this composite IF signal in Figure 2.3.6-e should be equal to the IF signal of the anomaly "A" at frequency IRD+2N. Comparison of the reconstructed composite waveform (Figure 2.3.6-e) with the IF signal of "A" (Figure 2.3.6-d) reveals a strong correlation between the two Figuress. Therefore, anomaly "A" is a true bearing defect signature. It is both a Sync and cage related component being generated from the modulation of the inner ball pass frequency at 12(N-C) with 2 times Sync. A later hardware teardown inspection indeed indicates uneven wear on the inner race of the bearing. In this case, the turbopump was a developmental unit, which was used for continued testing following identification of the anomaly. However, if the unit had been in the flight inventory, the turbopump would have been rejected for flight.

2.3.6 Phase Synchronized Enhancement Method for Diagnostic Signal Enhancement

As discussed in the last section, shaft rotational speed in a rotor system tends to momentarily speed up or slow down due to dynamic load variation. This micro-frequency variation phenomenon can be observed from the instantaneous frequency at synchronous (Sync) frequency using a Frequency Demodulation technique. With this instantaneous frequency, useful information for bearing/gearbox diagnosis can then be obtained using a new method called the Phase Synchronized Enhancement Method (PSEM). The basic principle of the PSEM is to force the quasi-periodic Sync component whose frequency is slightly fluctuating around some center frequency into a pure-tone discrete component whose frequency is constant. PSEM, with its unique capability of transforming a quasi-periodic Sync into a pure-tone discrete component, generates a highly desirable effect on an entire diagnostic signal with all Sync-related components becoming discrete. With this enhanced frequency resolution, the PSEM signal can recover detailed spectral information useful in diagnostic evaluation. This method is especially useful for machinery diagnostics, in which case a quasi-periodic driving process (Sync) generates many other rotational components. These related components such as Sync harmonics, bearing element spin and passing frequencies, modulation and sideband components can provide useful information about a machine's operational condition.

Test data from an application example is used to demonstrate the signal enhancement capability of PSEM. The PSD shown in Figure 2.3.7(a) is taken from a spindle motor during a vibration test. The FFT block size is 16K, which gives a very high bandwidth resolution of 1.6 Hz bandwidth. During steady state operation, the fundamental Sync frequency is very constant. Therefore, a PSD of spindle motor vibration data shows a very discrete peak at synchronous frequency(Sync = of 74 Hz, not shown in Figure 2.3.7(a)). A joint time-frequency plot (waterfall plot) of the test data also shows a very steady state peak at sync whose frequency never moves outside an analysis frequency bandwidth. However, instantaneous frequency analysis indicates that the instantaneous frequency of Sync is moving periodically with small frequency variation, which is even less than the bandwidth of the PSDs. At higher frequency region as in Figure 2.3.7(a), due to such micro-frequency variation of Sync, the spectral bandwidth broadening effect start to smear its spectral peaks and makes it difficult to identify them.

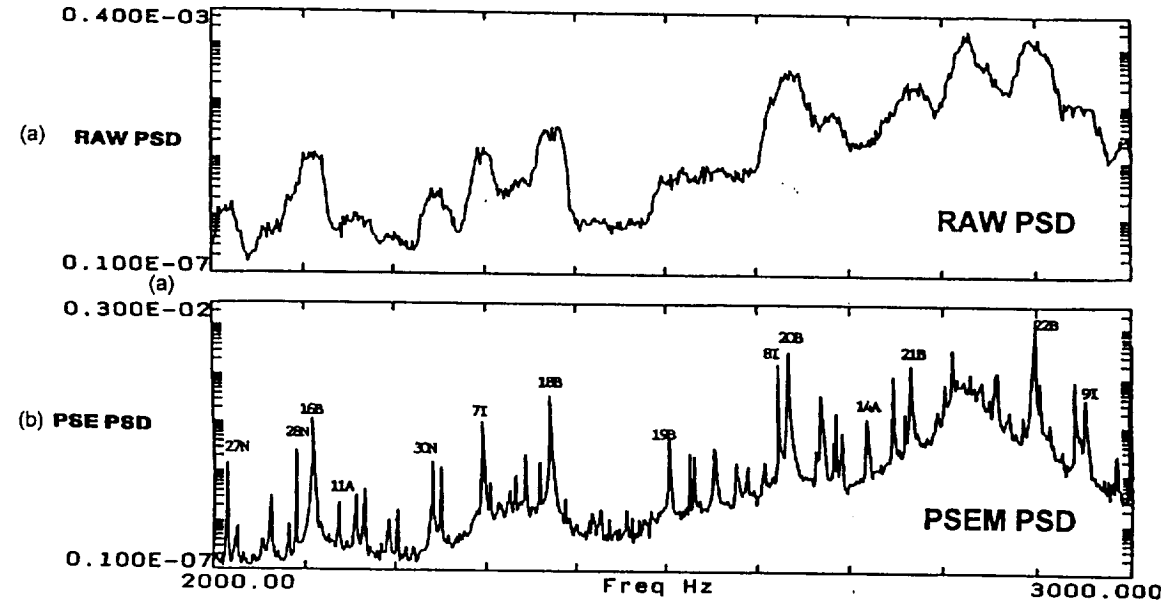

Figure 2.3.7 (a) Raw PSDs of Spindle Motor Test Data.
(b) PSEM PSDs of Spindle Motor Test Data

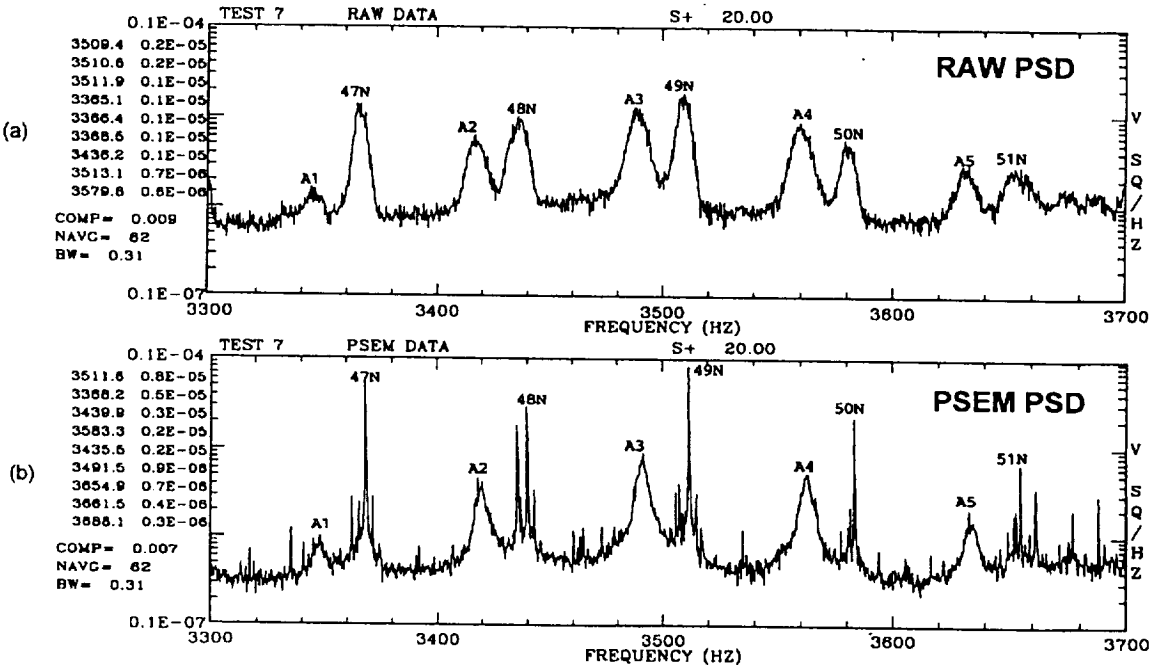

Figure 2.3.8 (a) Raw PSD for Test 7/Accel 6 of 42 Degree Gearbox Data.
(b) PSEM PSD for Test 7/Accel 6 of 42 Degree Gearbox Data.
(Anomalies at A1, A2, A3, A4, & A5)

Based on this IF information, the PSEM algorithm forces the frequency of Sync from this periodic variation into a constant frequency. As a result, a highly desirable effect is generated on the entire signal. Figure 2.3.7-b shows its corresponding PSEM PSD in the same frequency range as Figure 2.3.7(a). Since all the Sync-related components become discrete, the signal's frequency resolution becomes much sharper. The enhanced PSEM PSD indeed recovers all the sync-related components such as such as the Ball Spin (B) components and its harmonics (16B, 18B, 20B, 22B, etc.), Inner Ball Pass (I) component and its harmonics (7I, 8I, 9I), as well as the Outer Ball Pass (A) component and its harmonics (11A, 14A). These critical sync-related components useful for diagnostic evaluation are completely smeared in the original PSD.

2.3.7 PSEM for Non-Sync-Related Component Identification

As discussed before, the major function of the PSEM is to transform all the sync-related components into discrete. On the other hand, for a non-sync-related component such as structural mode or an independent feedthrough from other rotor systems, its PSEM spectral peak will retain its original broadness in spite of this discretization process. This leads to another highly desirable property of PSEM for anomaly identification, in which case one wish to identify whether a spectral component is a sync-related and a non-sync-related component within a particular rotor system.

As example from the gearbox data can best demonstrate this. Figure 2.3.8(a) shows the raw PSD of the 42 degree Gearbox for test 7 in the frequency range of 3300 Hz to 3700 Hz. The peaks marked 47N, 48N, 49N, 50N, & 51N are the harmonic of Sync. However, a sequence of anomalies marked "A1", "A2", "A3", "A4", & "A5" are also observed. From this raw PSD, it would be difficult to identify whether these anomalies are Sync-related or not since they all have similar spectral peak bandwidth as these sync harmonics. However, this would become clear after the PSEM algorithm transforms all the sync-related components into discrete. Figure 2.3.8(b) shows the corresponding PSEM PSDs. First of all, all the Sync harmonics such as 47N, 48N, 49N, 50N, & 51N have indeed become discrete as expected. However, all these anomalies still retain its original broadness in spite of the PSEM discretization process. This indicates that these anomalies are non-sync-related components. Also notice that, the spacing frequencies between these anomalies happen to be the sync frequency. This indicates that these anomalies are due to the modulation between the shaft rotational motion with a non-sync-related component such as a structure mode (eg. bending or torsional mode of the shaft). In this particular case, even though the source of these anomalies was not identified since the major structural properties of the gearbox system were not available. However, this example has demonstrated that the PSEM can be an effective tool in discriminating between a sync-related and a non-sync-related components, which can provide critical insight for diagnostics or failure identification.

2.3.8 PSEM for False Bearing Signature Identification

Another example that was recently encountered on the SSME ATD High Pressure Fuel TurboPump is used to demonstrate how PSEM can identify false bearing signature. During a sequence of developmental testing of ATD HPFTP, strong 6N sideband anomaly was consistently observed. The presence of this anomaly severely impacted the schedule of this shuttle main engine development. Figure 2.3.9(A) shows a typical zoomed PSD of this anomaly. The peak marked "6N", is the 6 harmonic of Sync frequency. The two strong peaks marked $6N\pm\alpha$ around 6N are the 6N sideband

anomalies whose frequencies are equal-spaced from 6N. Since the left sideband, 6N-α is right around the predicted Outer Roller Pass (ORP) frequency, and the right sideband 6N+α is on the Inner Roller Pass (IRP) minus 2N (IRP-2N) frequency, this 6N sideband anomaly has been labeled as a possible bearing-related Defect signature. Based on this assumption, several tests have been designed and conducted in order to investigate this anomaly.

However, the PSEM method provided valuable insight concerning this anomaly. The Figure 2.3.9-b shows its corresponding enhanced PSEM PSD. First of all, the 6N component indeed becomes discrete as expected. However, there is another discrete peak that became enhanced and begins to show. Notice that, in the lower frequency region of the PSEM PSD (not shown in the frequency range of Figure 2.3.9), it also recovers the fundamental bearing cage frequency component and its harmonics. Since this is a 14 roller bearing system, therefore, the true ORP frequency can be pinpointed to be at 14th harmonic of Cage. It was apparent, the 14 harmonic of cage is exactly located at the newly recovered discrete peak. This indicates that, this newly-recovered discrete peak became the true ORP frequency component. Therefore, the original strong 6N left sideband anomaly is not the ORP component as was thought before. The true ORP component is the smaller discrete peak at a different frequency very close to the 6N left sideband anomaly. Based on this finding, anomaly investigation of the ATD HPFP has changed direction to identify other vibration sources, which is discussed next.

2.3.9 Wideband Demodulation Method - Cavitation Induced Vibration Identification

Cavitation is the process of boiling liquid when local hydrodynamic pressures in the areas of accelerated flow drop below the vapor pressure of the fluid. When cavitation occurs on turbopumps, it can (i) Severely degrade the overall system efficiency (ii) Cause excessive structural vibration (iii) Create erosion damage to the turbopump blades. Therefore, there is a critical need of an effective method for cavitation detection and monitoring in order to study and minimize cavitation-induced problems. The Principle for Cavitation Monitoring is based on a unique phenomenon associated with cavitation physics: That is when cavitation occurs in a rotor system, the Doppler effect of a stationary dynamic measurement will make the periodic shaft rotational motion to amplitude modulate with the wide-band random noise due to the collapse of cavitation bubbles. This phenomenon of wide-band modulation thus provides a unique signature for cavitation detection. That is: a hidden periodicity in the Wide-Band Noise Floor serves as an Indicator about the existence and Type of Cavitation conditions. However, due to the lack of phase information among different spectral components, the conventional spectral analysis method is unable to identify such a unique WBM signature. By searching for such a unique cavitation-generated hidden periodicity, the Wide-Band Demodulation method can detect and identify cavitation conditions in turbomachinery directly from dynamic measurement signals (eg. accel., pressure, etc.): It can (1) Detect the cavitation inception point when it occurs. (2) Determine severity or magnitude, and (3) Identify type of cavitation (Full-blade, alternate-blade, etc.)

Application of this WBD technique to the ATD High Pressure Fuel Pump problem as discussed in the last section, new evidence has been obtained which indicated that this 6N sideband anomaly is due to a cavitation-induced vibration at the first stage impeller of this fuel pump. Figures 2.3.10(a) and 2.3.10(b) show the raw PSDs of 2 different pressure measurements of the ATD HPFTP during test TTB-38. 6N sideband anomalies are present in the first measurements (HPFP INLET PRESSURE NO1). However, these anomalies are not observable at all in the raw PSDs of the second measurement (HPFP 1ST STAGE IMPELLER INLET PRESSURE.). In order to determine whether these

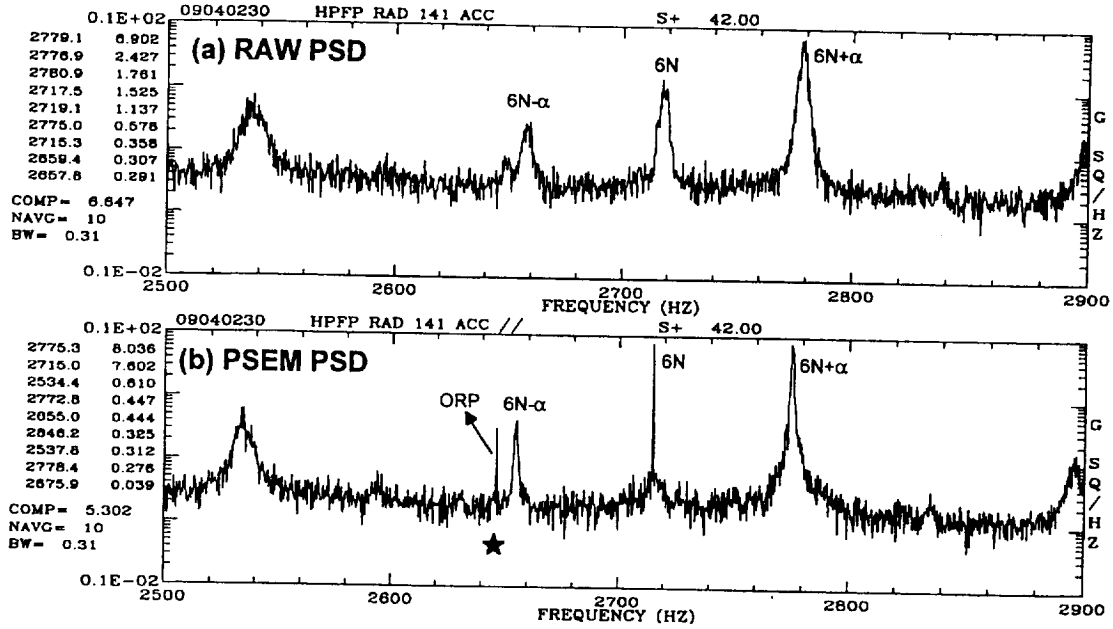

Figure 2.3.9 (a) Raw PSD of ATD HPFTP Accelerometer Test Data.
(b) PSEM PSD of ATD HPFTP Accelerometer Test Data.

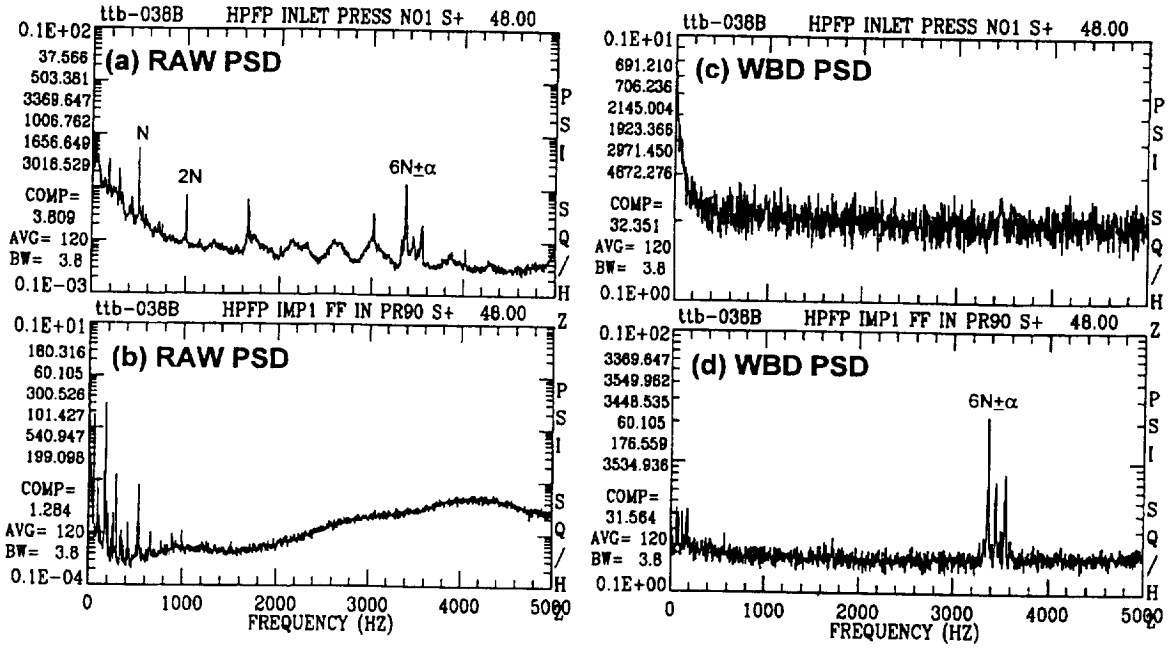

Figure 2.3.10 (a) Raw PSD of ATD HPFTP Inlet Pressure No 1.
(b) Raw PSD of ATD HPFTP 1st Stage Impeller Pressure.
(c) WBD PSD of ATD HPFTP Inlet Pressure No 1.
(d) WBD PSD of ATD HPFTP 1st Stage Impeller Pressure.

2.4 ATMS Automated Signal Processing Subsystem (ATMS-ASPS)

The ATMS-ASPS program utilizes an expert system to supervise a sequence of dynamic signal analysis programs in the Advanced Signal Analysis Library (ASAL) to perform automatic processing of a sequence of programs that are currently used for SSME post-test/flight evaluation. Such automation is achieved through the integration of the ASAL with the Automated Signal Processing Subsystem (ASPS) Knowledge Base (ASPS-KB). The ASPS-KB represents a set of rules of how to perform the analysis of each ASAL program with correct parameter settings. Based on this knowledge base, the ASPS then utilizes the CLIPS expert system to supervise the ASAL in performing a sequence of standard analysis tasks for engine post-flight/test evaluation. The ASPS will automatically convert high frequency dynamic signals from the engine operational run into a bank of succinct image-like patterns in a compressed TOPO time/frequency/amplitude/phase format and other various special formats to be stored in the Compressed TOPO Data Base (CTDB). The results of the ASPS operations thus provides the basic fact database and key statistic information for more detailed analysis in the subsequent Anomaly Detection and Identification Subsystem (ADIS).

As discussed in the last section, the interface of each ASAL programs has been converted from the original manual user-interfaced mode into Clips-interfaced mode so that the ASAL can be executed from the CLIPS expert system for unsupervised processing. In addition, an ASPS interface module was developed which will allow the ATMS system to access to the basic engine test information such as power level profile, test duration, and pump unit numbers for the entire SSME test history. This test history information will provide the baseline for ASPS processing (such as tracking, characteristic frequency identification, etc.), and will be reduced and stored in the Compressed SSME TOPO database.

Based on the power level profile information, the ASPS will first establish tracking frequency boundaries for Sync/harmonics frequency tracking. The power level profile first establishes the sync frequency boundaries of different pumps based on the regression equation between power level and sync frequency obtained from the current SSME data base. With this tracking baseline being established, the sync frequency is then identified to be the reference frequency within the boundary, which has the maximum Sync, plus harmonics energy. These basic operation are performed in the pre-process element of ATMS whose flowchart is shown in Figure 2.4.1.

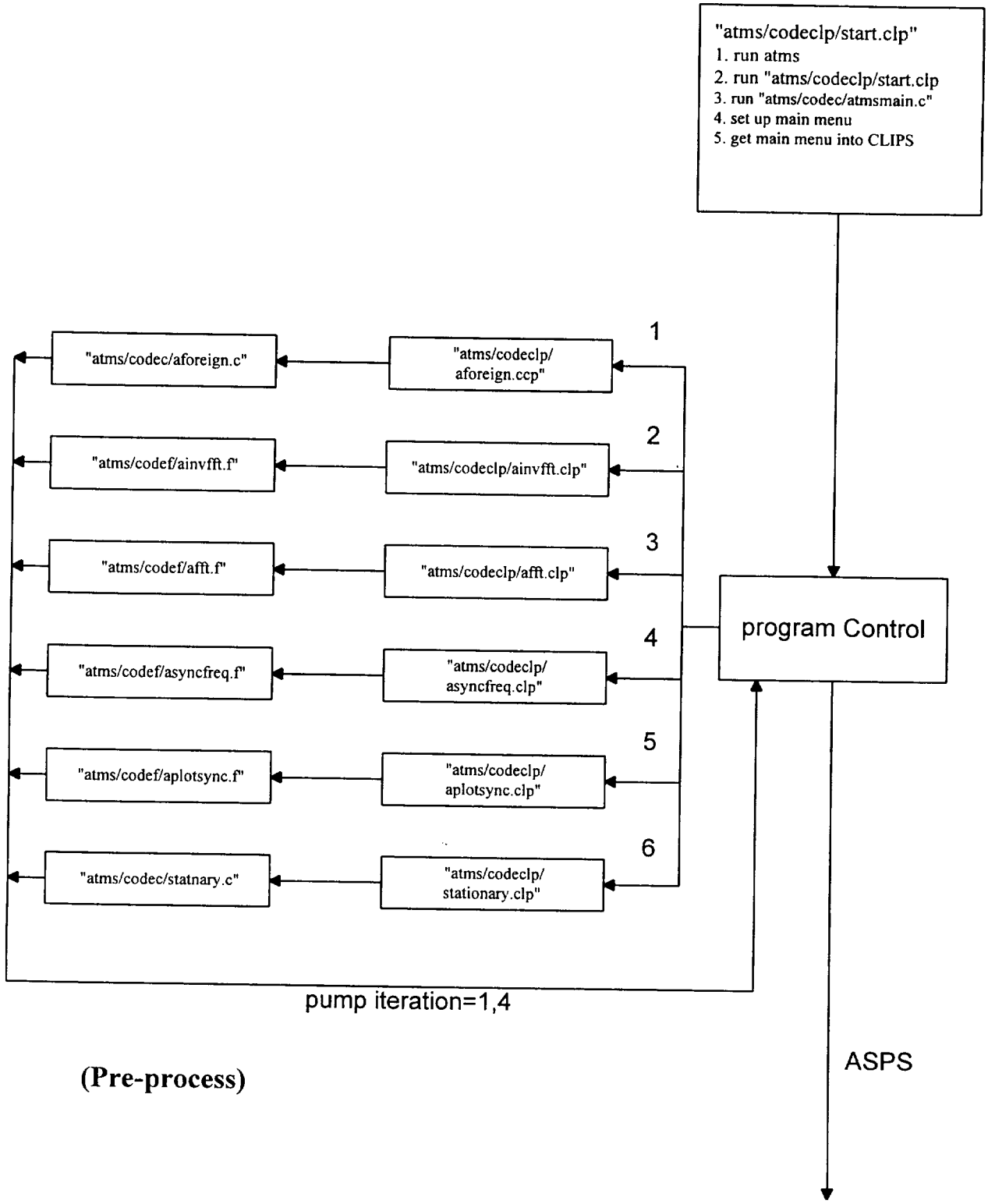

Figure 2.4.1 ATMS Pre_Pre-Processing Programs

Once the sync frequency is identified over the entire duration of an engine test, the sync frequency information will be stored in the ATMS database for subsequent analysis programs in ASPS and ADIS. Subsequently, the "syncfreq" program will perform amplitude tracking on sync and harmonics. In addition, the RMS tracking on the wide-band noise between harmonics will also be conducted. This tracking information will be summarized and stored in the ATMS database for different pump units within a test. Therefore, the measurement of the time domain basic dynamic information is summarized in this one Figure to allow quick detection of anomalous activities.

In addition to sync/harmonic tracking, ASPS will also perform bearing component tracking based on the Sync frequency database generated from the ATMS program "asyncfreq". The "atrackn" program can track an anomaly over a number of frequency band associated with each bearing. The default setting is at (1) Cage frequency C, 2C 3C & 4C (2) Rolling Element (RE) Spin (RS) & RS$\pm$C (3) Inner RE Pass IRP & IRP+N (4) Outer RE Passing ORP & ORP+N. In addition, a sync/harmonics rejection option is available so that it can track an anomaly whose frequency crossover sync/harmonics which will cause tracking frequency to be erroneously trapped by the sync/harmonic components.

Once the basic engine test information is acquire, the ASPS then performs the following analysis tasks:

1. Download the raw FFT data of all measurements of all four pumps (HPFP, HPOP, LPFP, LPOP) from OISPS optical disk (Jukebox) to user-specified OISPS processing database (e.g. 11a, 11b, etc.).
2. Inverse FFT from frequency to Time Domain
3. Identify the Power level profile, and establish the stationary/nonstationary time profile based on user specified method for stationary period determination.
4. Establish the frequency tracking window and tracking harmonics at each power level of each pump.
5. Establish and plot the Sync frequency tracking of each pump.
6. Perform amplitude tracking of sync and harmonics
7. Perform RMS tracking for all frequency bands between harmonics.
8. Perform composite phase tracking between sync and its first 3 harmonics.
9. Perform anomalous frequency/amplitude tracking.

10. Perform orbit analysis using rotary spectral analysis for pairs of measurements 90 degree apart.

11. Perform Synchronized Time Averaging (STA) to generate enhanced periodic signal associated with sync/harmonics.

12. Convert FFT into TOPO format which contains amplitude/bandwidth/phase in both time and frequency domains.

13. Generate all the TOPO plot for each measurement.

14. Generate the standard isoplot (3D waterfall)

15. Plot time history of major statistics including mean, RMS, skewness, kurtosis and max/min reduction throughout the test period.

16. Plot all PSD within each stationary period.

17. Perform Wide Band Demodulation and plot all WBDPSD within each stationary period.

18. Perform linear cross-coherence analysis between measurements within each pump.

19. Perform linear cross-coherence analysis between measurements across pumps.

20. Perform bi-coherence analysis using sync frequency as reference frequency.

21. Store the compressed TOPO format and other special formats in the CTDB.

22. etc.

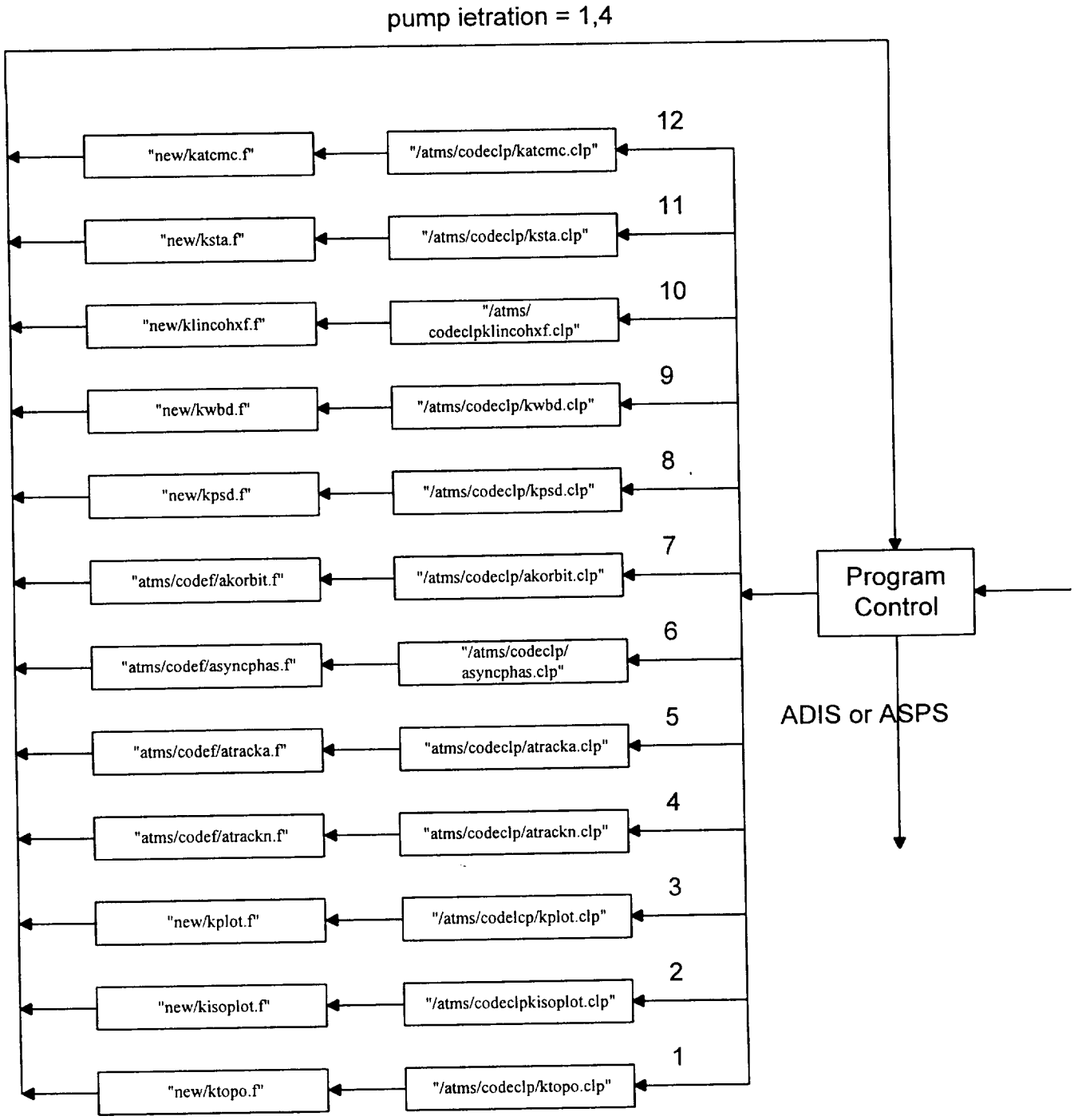

(ASPS Subsystem)

Figure 2.4.2 ATMS ASPS Subsystem Flow Diagram

Figure 2.4.2 depicts the flowchart of ASPS, which shows the unsupervised processing sequence of various ASAL programs controlled by its corresponding Clips file. A test run of the ASPS program using a sample set of SSME test data, 09010853, is utilized to demonstrate the basic dynamic information generated from ASPS. In this test run, multiple channels of standard SSME high frequency measurement data (10,240 Hz Sampling Frequency) for each pumps (HPFP, HPOP, LPFP, LPOP) are analyzed. The analysis programs shown within the ASPS flow diagram in Figure 2.4.2 are automatically executed with appropriate execution parameters determined by its program control CLIPS file.

The ASPS programs will generate a large volume of output data plots in various formats for each pump, each measurement, each stationary time period within each constant power level, and each pair of measurement for cross-pump or cross channel analysis. Such enormous complete processing/analysis task for SSME post-test evaluation would have taken long period of time to perform, and would require engineers' or data analysts' continuous attendance for detailed program interfaces. However, after certain basic information (such as power level profile, parameters, database specification, etc.) being setup, with a simple execution command, the ASPS will automatically perform this complete analysis without any human interface. Due to the large number of output plots of the entire engine test measurements, only the data plots of the HPFP at selected (4) measurements are shown in here for demonstration purpose.

- The Sync frequency for each pump will first be estimated, tracked from PSD, identified and plotted over the entire test period. In addition, the stationary time period within each constant power level will also be identified and plotted based on used selected method for stationary time partition. Figure A-1 shows such Sync frequency tracking of the 4 different pumps for test 09010853 along with the stationary time period identified within each constant power level.

- FFT data are converted into Topo format and plotted for each measurement over the entire test period. The Topo information including frequency, amplitude, phase and signal-to-noise ratio (SNR) are then compressed and stored into the Topo database. Figure A-2 to A-5 show the Topo plots of 4 channels of measurement (all channel are processed and plotted in this test run) of the HPFP pumps over the entire test period.

- Several dynamic characteristic including Composite RMS, White (noise floor) spectrum RMS, Rice frequency (expected frequency), and Noise floor RMS over various frequency bands are calculated and plotted for each measurement over the entire test period. These information are also compressed and stored into the Topo database. Figure A-6 to A-9 show such plots of 4 HPFP measurements over the entire test period.

- 3D PSD waterfall or isoplot are plotted for each measurement over the entire test period as shown in Figure A-10 to A-13 for the 4 HPFP measurement.

- Time domain statistical moment of each measurement signal will be generated over the entire test period. These include mean value, RMS, Max/Min Reduction, Skewness, and Kurtosis. Figure A-14 to A18 show the time histories of these statistical moments of the 4 different HPFP measurements.

- Sync/harmonics RMS tracking for each measurement upto to a desired harmonic (8th harmonic for this test) are performed and plotted. The RMS in between harmonics (e.g. between 1N and 2N, 2N to 3N, etc.) for anomaly detection are also generated. Figure A-19 to A-22 show the Sync/harmonics along with the in-between harmonics RMS tracking of the 4 different HPFP measurements over the entire test period.

- In addition to sync/harmonic tracking, ASPS will also perform bearing component tracking over a number of frequency band associated with each bearing. The default setting is at (1) Cage frequency C, 2C 3C & 4C (2) Rolling Element (RE) Spin (RS) & RS$\pm$C (3) Inner RE Pass IRP & IRP+N (4) Outer RE Passing ORP & ORP+N. In addition, a sync/harmonics rejection option is available so that it can track an anomaly whose frequency crossover sync/harmonics which will cause tracking frequency to be erroneously trapped by the sync/harmonic components. Figure A-23 to A-30 show the bearing component frequency/amplitude tracking for these 4 HPFP measurements.

- In addition to sync/harmonic and bearing components tracking, ASPS also provide an option to perform anomalous frequency tracking over used specified frequency band which are selected in the ATMS Main Menu. Figure A-31 to A-34 show anomalous frequency/amplitude tracking over (0.4 - 0.6N), (1.4 - 1.6N), (2.4-2.6N) etc., for these 4 HPFP measurements since 50% sync-sync and its harmonics at 1.5N 2.5N ... are presented in this test.

- Hyper-Coherence composite phase tracking between Sync and its first 3 harmonics (2N, 3N and 4N) are also performed over the entire test period. Figure A-35 to A-37 show such Sync/Harmonics phase tracking for three pairs of HPFP measurements.

- Rotary spectral analysis for any pairs of measurement which are 90 degree apart will be performed. The rotary spectral analysis can show the overall orbit and rotational direction over the entire test period. Figure A-38 to A-39 show the result of rotary spectral analysis for Accel pair HPFP135/HPFP 225 measurements.

- With the stationary time period identified, the PSDs for all measurements will be averaged over the stationary period and plotted. User has the option to set the length of stationary time period in the ATMS Main menu. FigureA-40 to A53 show the long averaged PSDs of the 4 different HPFP measurements over various stationary periods.

- Wide Band Demodulation (WBD) analysis for detecting wideband modulation phenomenon commonly associated with pump cavitation and electric noise modulation will be performed for all measurements over the stationary periods. Figure A-54 to A-67 show the WBD PSDs of the 4 different pumps over various stationary periods. Notice that, the hidden periodicities shown in the HPFP SPD NDF, which is the HPFP speed measurement, are actually due to the lack of noise-floor in this speed measurement. Therefore, the recovery of hidden periodicity in this measurement is due to erroneous phase information rippled from major spectral peak due to the well-recognized Gibbs phenomenon instead of the wideband modulation mechanism due to phenomenon such as pump cavitation.

- Linear cross coherence between different measurements within the same pump is generated over the stationary periods. Figure A-68 shows the linear coherence functions between HPFT RAD 135 and HPFP RAD 225 measurement over stationary period of S+6 to S+38 second.

- Linear cross coherence between measurements across different pumps is generated over the stationary periods for signal feedthru identification. Figure A-69 to A81 show the linear coherence functions between HPFP and HPOP over various stationary period. Figure A-82 to A-87 are between HPFP and LPOP

- Synchronous Time Averaging (STA) for Sync/harmonics periodic waveform enhancement are performed for all measurements of HPFP, LPFP, and LPOP. STA is not performed for HPOP since STA requirement a speed measurement which is not available for HPOP. Figure A-91 to A-104 show the STA waveform for these 4 HPFP measurements over different stationary periods.

- Bi-coherence with Sync as the reference frequency for all measurements over the stationary period is generated. Such bi-coherence function with Sync as the reference frequency can provide a quick and overall information about the existence of modulation/sideband pattern commonly generated by bearing fault mechanisms, sub-sync whirl and some unknown fluid/structure interaction phenomenon. Figure A-105

to A-117 show the bi-coherence Bxxx (Sync, f) of the 4 different HPFP measurements over different stationary period.

- ASPS provides user with the option to perform bi-coherence with other reference frequency other than Sync. The reference frequency for such optional bi-coherence can be selected in the ATMS Main Menu.

- After the ATMS finish the ASPS processing and store the processed into the ATDB database. ADIS subsystem is subsequently activated which will go through a sequence of analysis for anomaly detection and identification. Detailed discussion for such ADIS analysis and programming will be covered in next section. Figure A-118 to A-120 show the output ADIS PSD plots for the three HPFP measurements over the stationary period from S+241 to S+291 seconds.

2.5 ATMS Anomaly Detection and Identification Subsystem (ATMS-ADIS)

The ADIS is the most intelligent element of the ATMS. Its major function is to first detect the existence of any anomaly in the CTDB database created by ASPS. Anomaly identification will then be performed in order to determine the physical underlying cause of the anomaly. The signature analysis techniques in ASAL can often provide valuable insight about the source of an anomaly and identify its underlying causes. Table-2.5.1 lists the typical anomaly detection and identification capabilities offered by ASAL for engine diagnostic evaluation. This anomaly detection and identification task requires interactive processing of various signal analysis techniques in ASAL, and is a very time consuming procedure for even an experienced analyst to perform manually. Automation of the Anomaly Identification process is achieved in ATMS by integrated the ASAL with the Clips expert system. An ADIS Knowledge Base (ADIS-KB) was designed and established by extracting the knowledge and thought logic of experienced human experts in performing such anomaly detection/identification, and reducing them into a set of rules for expert system execution. The ADIS then utilizes the CLIPS expert system to automate an intelligent ADIS analysis task by performing an extensive and highly interactive analysis for anomaly detection and identification.

TABLE-2.5.1 ATMS-ADIS ANOMALY DETECTION/IDENTIFICATION CAPABILITIES

- Detect nonlinear modulation/sideband phenomenon associated with bearing fault mechanisms.
- Detect wideband modulation phenomenon associated with cavitation induced vibration.
- Identify feed-through or resonance from neighboring equipment
- Identify RPM/Harmonics interference/overlap within a multi-rotor system
- Discriminate Rotor-related vibration from independent non-rotor-driven source/noise.
- Identify Sync. (RPM) modulated spectral component associated various nonlinear vibration mechanisms (including mechanical-driven) such as deadband interaction, and fluid-driven such as cavitation-induced asynchronous vibration, etc.
- Identify Pure-tone Electric Line Noise.
- Identify Structural/acoustical resonant mode.
- Detect Frequency Modulation (FM) Phenomenon associated with various FM vibration mechanisms such as shaft torsional vibration or gearbox transmission error.
- Identify signal source through time-delay estimation
- Improve the signal-to-noise ratio in the vibration measurement data corrupted by noise
- Enhance spectral resolution for all RPM-related vibration components.

A typical example of the ADIS logic flow will now be given. If a strong anomaly is detected at some frequency in the accelerometer data from the SSME high-pressure fuel turbopump (HPFTP), the ADIS will perform a sequence of appropriate signal analyses in order to identify the potential sources of this anomaly as:

- apparent or true sync/harmonics within current pump
- a sync/harmonic frequency feed-through from other engine turbopumps.
- a high vibration level at the HPFTP synchronous and/or harmonic frequency due to rubbing, imbalance, misalignment, or instability.
- 50% sub-sync due to deadband interaction (high GHC with Sync)
- 50% sub-sync due to whirl (low GHC with Sync)
- bearing signature (inner race defect, outer race defect, rolling element defect) characteristic frequencies of various ball/roller bearings [pump-end ball (PEBB), turbine-end ball (TEBB), turbine-end roller (TERB)].
- a modulation/sideband spectral component of a bearing fault pattern.
- aliasing.
- electrical line noise.
- cavitation-induced vibration.
- a structural mode.
- etc. If the anomaly cannot be absolutely identified, ADIS will then try to identify certain dynamic characteristics associated with the anomaly such as:

- whether it is synchronous frequency related or sync.-independent.
- if the anomaly modulation with synchronous.
- a sync/harmonic frequency feed-through from other engine turbopumps.
- If it frequency synchronized with sync (GHC correlation)
- a sync/harmonic frequency feed-through from other engine turbopumps.
- if it is composite modulated with Sync and bearing Cage (CGHC correlation)
- the discreteness of the anomaly.
- the instantaneous frequency/amplitude characteristics (periodic or random) of the anomaly.

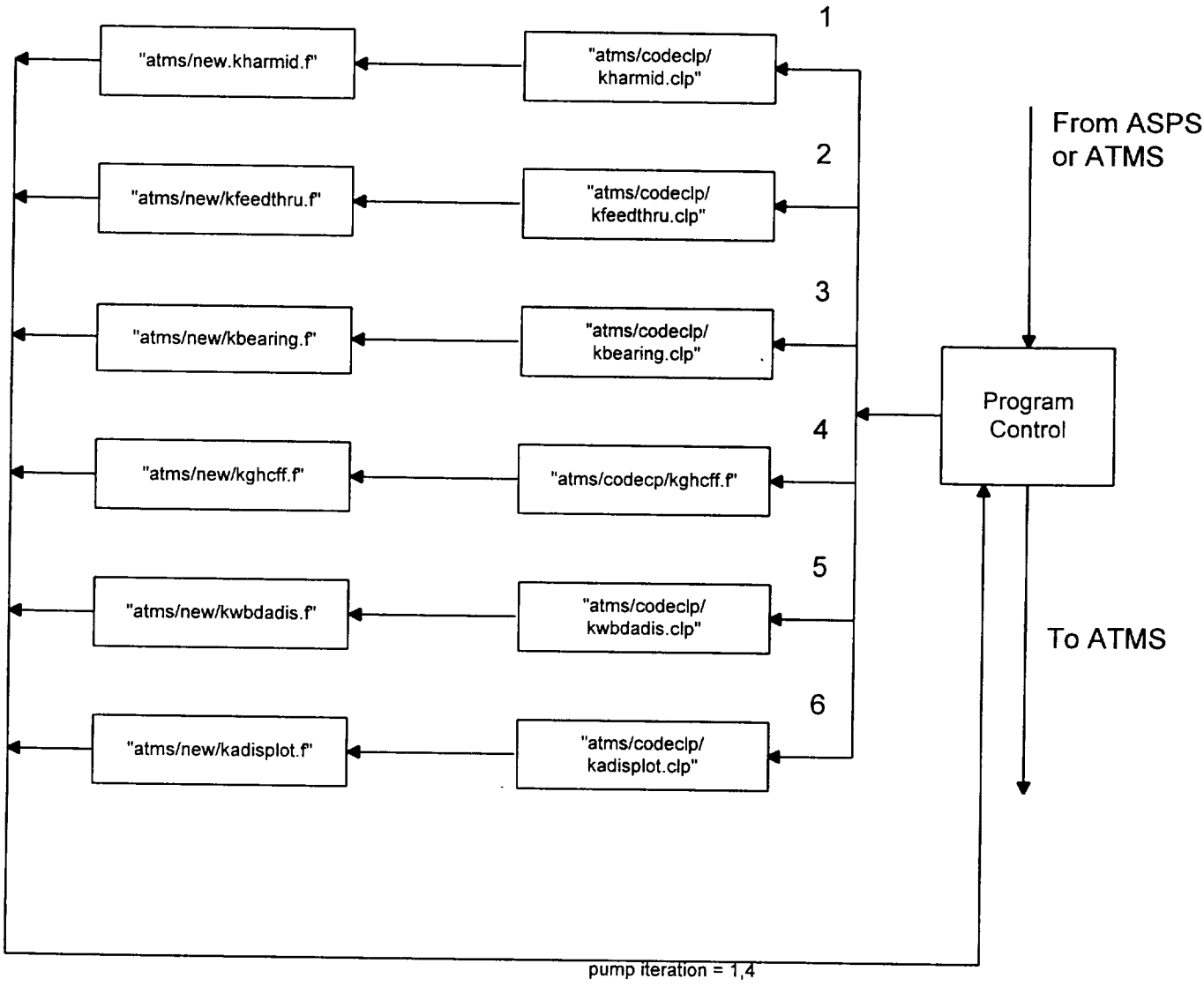

(ADIS SUBSYSTEM)

Figure 2.5.1 ATMS ADIS Subsystem Flow Diagram

These dynamic characteristics would provide valuable clues in determining the potential source of the anomaly (fluid dynamic, structural dynamic or rotordynamic). The above process requires intensive interactive processing of various signal analysis and is very time consuming. Automation of such anomaly identification task is the major function of the ATMS-ADIS program. ADIS flow diagram in Figure 2.5.1 shows the analysis programs executed within ADIS. Many detailed rules for various coherence analysis are implemented directly in the programs which are then automatically executed with appropriate execution parameters determined by its program control CLIPS file. The function of each ADIS program is described below:

(1) **Sync/harmonic Identification within current pump.**

The Sync/harmonics are the most fundamental vibration components to be identified within a vibration measurement. Within the SSME test history, spectral components from other vibration sources (e.g. feedthrough from other pumps, anomalous pseudo 3N, etc.) have been observed at harmonic frequency (coincidentally) and appear to be sync harmonic. Since many machinery failure modes (e.g. misalignment, rubbing, loose coupling, etc.) will generate strong sync harmonics, they are generally considered to be defect signature.

The purpose of the ADIS Sync/Harmonic identification is to identify whether an apparent spectral peak at harmonic frequency is truly a harmonic of the RPM of the current pump. To achieve this, a hierarchy of nonlinear coherence analysis techniques, hyper-coherence, bi-coherence and tri-coherence in ASAL are required which have been integrated in the ADIS. To run these coherence analysis programs correctly, several program parameters (such as reference channel, reference frequency, coherence threshold, etc.) must be determined by an experienced analyst. Interactive operation of these program will also be required. Furthermore, on order to obtain an optimal coherence for such sync/harmonic identification, extensive analysis is needed to search over different coherence function with different reference frequency settings. To automate this task, a number of rules governing such coherence analysis are implemented in the "kharmid" program, which are briefly summarized below:

Establish the linear coherence matrix at all harmonic between channels within the current pump as below:

Linear coherence | iharm =1

	ch1	ch2	ch3	ch4	ch5	Avg	Max	SNR	BW
ch1	0.0	.96	.98	.78	.84	.84	.86	22.2	2
ch2		0.0	.32	.29	.49	.49	.45	16.1	3
ch3			0.0	.86	.48	.48	.98	5.5	8
ch4				0.0	.68	.68	.78	7.9	.68
ch5					0.0	0.0	.84	5.8	0.0

Based on this linear coherence matrix, establish the channel with maximum linear coherence for each harmonic in array: ich-max-coh(iharm)= the channel number with max lin-coh for iharm.

based on the following rules:

for each harmonics K: K=1,max-harm/2 (max-harm/2 be round-off-to-next-highest integer)
if SNR(K)>0, then run hyper-coherence Hxy(w1=KC, w2=JC±1bin)
for all J where: snr(JC)>0, J/K=integer, J>K
If Hxy(KC, JC)=aa > max-coh(J), then max-coh(J) =aa, trace(J, "HC",KC,JC,0,0, x,y,0,0)

establish the hyper-coherence matrix for each harmonics (upto nharm/2:

Hyper-coherence									
ref	N1	N2	N3	N4	N5	N6	N7	N8	N9
N1		.96	.34	.78	0.2	.96	.34	.78	.84
N2				.29		0.22		.29	
N3						0.68	0.0	.	.48
N4								0.0	

Record trace-freq(ihram,1 to 9) = (maxcoh,w1,w2,w3,w4, ch1,ch2,ch3,ch4)
= hc(ref, hram, 0, 0) = abc(0, w2, w3, w2+w3) = atc(w1,w2,w3,w1+w2+w3)

based on the following rules:

if SNR(K) > 0, then run bi-coherence Txyzw(w1=0, w2=KC, w3=JC±1bin; w4=w1+w2+w3)
for all J where: snr(JC) GE 0, and (K+J)C<Fmax,
and chan-x= " "
chan-y= chan associated with KC
chan-z= chan associated with JC
chan-w= chan associated with (K+J)C
Let aa=Txyzw[0, KC, JC; (K+J)C], bb={"BC",0,KC,JC,(K+J)C,x,y,z,w}
if aa > max-coh(K), then max-coh(K) =aa, trace(K) =bb
if aa > max-coh(J), then max-coh(J) =aa, trace(J) =bb
if aa > max-coh(J+K),then max-coh(J+K) =aa, trace(J+K)=bb

establish the bi-coherence matrix for each harmonics upto nharm-1 (Symmetric matrix) as below:

bi-coherence									
ch#	2	3	3	1	6	3	2	3	2
w1	N1	N2	N3	N4	N5	N6	N7	N8	N9
N1	.34	.96	.34	.78	.34	.96	.34	.78	
N2	.23	0.0	.23	.29	.23	0.0	.23		
N3	.35	0.8	.35	.12	.35	0.68			
N4	.24	0.0	.24	.29	.24				
N5	.68	0.6 8	0.8 6	.49					
N6	.45	0.0	.45						
N7	.42	0.6 8							
N8	.47								

=> update trace-freq(ihram,1 to 9) = (maxcoh,w1,w2,w3,w4, ch1,ch2,ch3,ch4)
= hc(ref, hram , 0, 0) = abc(0, w2, w3, w2+w3) = atc(w1,w2,w3,w1+w2+w3)

based on the following rules, identify the remaining un-identified apparent harmonics:

For each unidentified apparent harmonics K: K=1,max-harm/2
Find all pairs of consecutive components: (L)*C and (K+L)*C
define snr2= min{ snr(L), snr(K+L) }
fine L which corresponding to the pair with the strongest snr2
Run aatcmc Txyzw(w1=-LC, w2=(K+L)C, w3=JC±1bin, w4=w1+w2+w3)
for all J where: snr(JC) GE 0 and (K+J)C<Fmax, and (J.NE.K)
and chan-x= chan associated with LC
chan-y= chan associated with (K+L)C
chan-z= chan associated with JC
chan-w= chan associated with (K+J)C
Let aa=Txyzw(-LC, (K+L)C, JC)=aa, and bb= {"TC", -LC, (K+L)C, JC,(K+J)C, x,y,z,w)
if aa > max-coh(L), then max-coh(L) =aa, trace(L)=bb
if aa > max-coh(K+L), then max-coh(K+L) =aa, trace(K+L)=bb
if aa > max-coh(J), then max-coh(J) =aa, trace(J) =bb
if aa > max-coh(J+K), then max-coh(J+K) =aa, trace(J+K) =bb

- For all J, if max-coh(J) > min-coh, then JC is true Harmonics
- For all other apparent harmonic not in the max-snr, use alincoh:
  all J, if Lxy(JC) > min-coh, then true harmonic
  where x = channel with highest SNR
  y = all other channel

(2) Sync/harmonic Feeedthru Identification from other pumps.

The function of the ADIS Sync/harmonic feedthru identification subsystem is to identify whether any spectral peak in the measurement PSD is a linear feedthru from other pumps. Such sync/harmonics feedthru is so commonly observed on the SSME measurement data. Previously, the human process to identify it was quite tedious. The data analyst has to keep tracking all the frequencies of Sync and its harmonics of four different pumps (HPFP, HPOP, LPFP, LPOP) at various power level, and compares and matches all these sync/harmonics frequencies to each spectral peaks within each measurement PSD. Once an apparent feedthru is found when the frequency of any particular PSD peak matching any one of these sync/harmonic frequencies, then the data analyst needs to run a linear cross-coherence program within the ASAL in order to verify it is indeed a linear feedthru. The purpose of the ADIS Sync/harmonic feedthru identification subsystem is to automate all the above tedious process by supervising and executing the linear coherence analysis program with rules of CLIPS expert system. All the tedious process of frequency matching, coherence program execution and coherence verification will all be performed in the background. The user will only see the result of this identification process from a final tag or attribute such as "$4N_2$" that is assigned to a PSD peak. Such a tag of "$4N_2$" would indicate it is as a feedthru of the 4th harmonic of Sync of HPOP (note: the notation for different pump's Sync within ATMS is: N1 =Sync of HPFP, N2=HPOP, N3=LPFP, N4=LPOP). An coherence value such as "83%LC" associated with the tag will also be recorded, which indicates its linear coherence obtained from "klincoh" program is 83%.

The basic rules of ATMS/ADIS Sync/harmonic feedthru identification subsystem is briefly summarized below:

1. At each power level, generate the sync/harmonic frequencies templates of each pump
2. For each measurement channel, generate all *major* PSD peaks to be identified from "kjpsd".
3. With each pump, identify all true sync/harmonic components using ADIS Sync/harmonic identification subsystem
4. For each PSD peak, match its frequency against the sync/harmonic frequencies templates of each pump. For each peaks with positive matching, an "apparent frequency" of i-th Sync harmonic feedthru from j-th pump (i*Nj) will be tagged to this peak.
5. For each peak with a tag of apparent frequency of iNj, search the measurement channel within the j-th pump which has the highest signal-to-noise ratio (SNR) at the i-th harmonic of Sync.
6. fire (execute) program "klincoh" between the current channel and the channel of j-th pump identified in step 5.
7. If the resulting coherence exceeding a pre specified threshold level, then tag (i*Nj) to this PSD peak as a true i-th Sync harmonic feedthru from j-th pump. Otherwise, repeat step 5 to 7 for the next PSD peak.

(3) Bearing Modulation/Sideband Signature Identification.

As a fault in an inner race moves into and out of the load zone within each revolution, its can cause amplitude modulation with a modulating frequency of Sync (once per rev), and a carrier frequency of Inner Race Defect (IRD) frequency. Similarly, as a defect on a rolling element moves into and out of the load zone, as well as the line of contact, it will also cause amplitude modulation with a modulating frequency of Cage (ball/roller train frequency), and a carrier frequency of ball/roller spin frequency. These nonlinear interactions among various frequency components provide important signatures for bearing fault diagnostics. Such bearing faults with their associated nonlinear modulations will typically generate modulation/sideband patterns as shown in Figures 2.3.3, which are composed of a fundamental and its harmonics of some bearing characteristic frequency, plus a family of sidebands around each. For example, the fundamental frequency components could be IRD or Ball/Roller Spin Frequency, and the modulating frequency (the spacing between sidebands) could be Sync frequency, the Cage frequency, or a structure's natural frequency, depending on the fault mechanism.

When a complete modulation/sideband pattern is presented in a PSD, computation of their coherence value among modulation/sideband component is quite straightforward. However, in many cases, the spectral components observed in the PSD may only contain partial pattern of the entire modulation/sideband pattern. In this case, coherence identification among modulation/sideband components would require many different

coherence functions interactively. The frequency arguments of the coherence function will be determined based on the available component within the partial modulation/sideband pattern. In this case, the representative coherence will be obtained by searching for the best correlation that might exist within the observed partial pattern. These dynamic characteristics would provide valuable clues in determining the potential source of the anomaly.

The function of the ADIS Bearing Signature Identification is to identify whether any spectral peak in the measurement PSD is a bearing-related signature. To achieve this, a set of bearing signature "templates" associated with various bearing fault mechanisms are created and stored within the ADIS. The spectral peaks to be identified will first be matched against all such bearing templates in order to determine whether the frequency of any particular spectral peak is associated with an "apparent" bearing signature. If it is, this peak will then be tagged in the "apparent frequency" slot with its associated bearing component, such as 2*IRP-N, 4*Cage, etc. Since multiple identification or matching could occur for the same spectral peak, a scoring logic is developed in order to rank the goodness-of-fit among multiple patterns. In addition, since there exists some degree of uncertainty of the bearing parameters such as the contact angle, ball diameter, and pitch diameter, bearing templates matching is performed over a pre-specified region in order to accommodate such parameter variation. The scoring logic will then determine the best fit among various templates and bearing parameters. Once a spectral component are identified to be an apparent bearing signature, ADIS bearing signature identification subsystem will then proceed to perform correlation analysis to further identify if the apparent bearing signature is truly a bearing signature or not. The following scoring logic is used: This correlation analysis utilizes several nonlinear signal analysis techniques supervised by a number of rule which are briefly summarized below:

Define

Modulation/Sideband (M/S) Pattern: $I_c * f_c \pm I_s * f_s$

(C,B,I,O)=(Sync,Cage, Ball/Roller Spin, IRP, ORP)

Where:
Ic & Is are harmonic # for carrier and sideband
fc and fs are carrier & sideband frequency.
fc and fs can be one of (N,C,S,I,O)

- perform apparent frequency matching against all possible modulation/sideband Pattern for each bearing, and obtain matching frequencies: $I_c * f_c \pm I_s * f_s$

- Perform harmonic Identification for carrier component at fc using the rules for Sync/harmonic identification as described in last section.

- Perform harmonic Identification for sideband component at fs using the rules for Sync/harmonic.
- Perform Modulation/Sideband Identification for : $I_c * f_c \pm I_s * f_s$ based on the following rules:

  - Search the channel with the best SNR for each modulation/sideband component.
  - For each harmonic of Sideband frequency fs with SNR exceeding a threshold, perform bi-coherence analysis using fs as the reference frequency, ie. Txyzw(w1=0, w2=fs, w3=w; w1+w2+w3). Record the coherence value at each modulation/sideband frequency.
  - For each pair of modulation/sideband components at f_{MS1} and f_{MS2}, with SNR exceeding a threshold, perform tri-coherence analysis using their difference frequency as reference frequency, ie. Txyzw(w1=-f_{MS1}, w2=f_{MS2}, w3=w; w1+w2+w3). Record the coherence value at each modulation/sideband frequency.
  - Search for the maximum coherence value and record the reference and channel information in the trace file.

(4) Sync-Related Signature Identification using GHC.

As discussed in section 2.3.5, valuable diagnostic information is contained in the instantaneous frequency (IF) in vibration measurement signal. Since the fundamental shaft rotational component (i.e. Sync) drives other rotational mechanisms and generates various spectral components associated with, tooth meshing, bearing cage, or inner/outer ball pass frequencies along with related harmonics and modulations. When RPM reduces or increases even slightly, the frequencies of all the corresponding rotational components will also respond in kind. These Sync-related property can be identified by the GHC technique. Therefore, for the major spectral components exceeding certain SNR threshold, the ADIS will automatically activate the GHC function, setup all appropriate parameters and generate their corresponding GHC coherence as a indication of the degree of frequency synchronization with Sync. In section 2.8 for Case Study, a number of SSME examples involving 50% sub-sync will be used to demonstrate the importance of GHC for anomaly identification.

(5) Discrete Line Noise Identification using BWC.

As discussed in section 2.3.1, the Bandwidth Coherence (BWC) Analysis technique is an effective tool in measuring the relative bandwidth, i.e. the discreteness, of a spectral component. This method is based on identifying a coherent phase relationship at the frequency of a discrete component within contiguous ensemble blocks of data. The strength of such a coherent phase relationship is proportional to the degree of discreteness of the spectral component. Therefore, for a pure-tone discrete component (such as line noise or its harmonics), a strong coherent phase relationship would exist and its Bandwidth Coherence should be unity. On the other hand, for a narrow band random component, the coherent phase would be diminished (in proportion to its bandwidth) relative to a pure tone, and its resulting bandwidth Coherence would be some value less than unity. In this manner, Bandwidth Coherence Analysis provides an effective way to identify whether an anomaly is benign discrete line noise or an important mechanical signature fault. Therefore, for each spectral components to be identified, the ADIS will automatically calculate the BWC as a indication of the degree of discreteness.

(6) Wideband Modulation Signature Identification using WBD.

As discussed in section 2.3.9, Cavitation is one of the known phenomenon that can cause wideband noise to amplitude modulate with discrete components and generates a unique wideband modulation phenomenon in the vibration signal. The Wide-Band Demodulation (WBD) method can be used to recover the hidden periodicity associated with the wideband modulation phenomenon and detect and identify cavitation conditions directly from dynamic measurement signals. Therefore, for those major spectral components exceeding certain SNR threshold, the ADIS will automatically activate the WBD function, setup all appropriate parameters and calculate their corresponding WBD PSD. The SNR (in dB) above noise floor in the resulting WBD PSD will the be listed in the tag of ADIS plot as a indication of hidden periodicity due to wideband modulation phenomenon.

(7) Composite Modulation Signature Identification using CGHC.

In a rotor system, the dynamic load variation on a rotating shaft tends to momentarily speed up or slow down the shaft rotational speed. When RPM reduces or increases even only slightly, the frequencies of all these Sync-related components will also respond in kind. As a result, critical correlation information is also contained in their instantaneous frequency, which can be used to detect some well-hidden correlation that can not be identified by other coherence analysis techniques. A unique phenomenon was observed in an SSME test data involving a more complicated modulation phenomenon called "composite-modulation". As discussed before, if two spectral components at frequencies w1 and w2 are modulated to each other and generate a new component at their sum frequency w1+w2, then the bi-spectrum can be used to identify the existence of such modulation. However, this modulation could also exist between the harmonics of w1 & w2 at N1w1 & N2w2 and then generate a new component at frequency N1w1 + N2w2 which is the sum of these 2 modulating harmonics. The spectra of the measurement signal might only shows the fundamental frequency components at w1 and w2 without the presence of these modulating harmonics. Therefore, the bi-coherence analysis would not be able to identify such modulation phenomenon. In this case, the IF signal can provide valuable information in identifying this well hidden correlation. Instantaneous frequency information provides an alternative way to identify such correlation between fundamental rotor and bearing components by matching the appropriate integer multiple of each fundamental IF signal corresponding to each of the modulating components. Such composite GHC (CGHC) analysis is also automatically performed by ADIS for major spectral peak with SNR exceeding some threshold level. It should be noted that, such CGHC analysis will only be performed when a bearing cage frequency component or its harmonics is present in the measurement signal with a representative coherence value greater than some user defined threshold value.

(8) ADIS Output display format

If frequency of a spectral peak is found to match any characteristic frequency, a tag will be assigned to this spectral peak for this particular match. The symbol for the ADIS tag

are listed in table 2.5.2. For example, 4N2 represents the 4th harmonic of Sync of pump #2 (ie. HPOP). I2-3N1 represent the Inner Ball Rolling Element Pass (I) of bearing # 2 (Turbine End Ball Bearing) minus 3rd harmonic of Sync of HPFP

Since multiple frequency matches of a spectral peak is possible, it is important to assign a representative coherence to a particular match. The purpose of this representative coherence is to provide a degree of statistical confidence level indicating the likelihood of any apparent match. The coherence would allow the ADIS to choose the most likely match as the final identification result. This representative coherence is the result of a sequence of ASAL analysis automatically performed by ADIS. The various type of representative coherence as shown in table 2.5.3 attached to the tag is used to indicate the degree and type of coherence performed. For example, a spectral peak at 540 Hz might have two matches, the tag of the first match is N1 with 12%3 and the tag of the second match is 9L with 96%5. The first match indicates that its frequency matches the Sync of HPFP with a representative bicoherence (%3) of 12%; while the second match indicates that its frequency matches the 9th harmonic of 60 Hz line noise with a representative Bandwidth coherence (%5) of 96%. From these information, the ADIS will choose the match with the highest representative coherence (ie. 9L) as the best match and list it in the final ADIS output plot.

Ifq	ifq represents:	idx	Symbol
1	N(Sync)	1/HPF 2/HPO 3/LPF 4/LPO	?N?
2	C (Cage)	1/bearing 1 2/bearing 2 ,etc	?C?
3	B (Ball Spin)	1/bearing 1 2/bearing 2 ,etc	?B?
4	I (IRP)	1/bearing 1 2/bearing 2 ,etc	?I?
5	O (ORP)	1/bearing 1 2/bearing 2 ,etc	?O?
6	SS (Sub-Sync)	1(50%);2(33%),3(25%)	?SS?
7	L (60 Hz L.N)		?L
8	A (Anomaly)		?A?

Table 2.5.2 symbol for the ADIS tag

%1	Hyper-Coherence
%2	Special Hyper-Coherence
%3	Bi-coherence
%4	Tri-Coherence
%5	Bandwidth Coherence
%6	Linear Coherence
%7	Generalized Hyper Coherence (GHC)
%8	Composite GHC (CGHC)
%9	Wideband Demodulation

Table 2.5.3 Type of representative coherence

Figure 2.5.2 shows a typical result of ADIS from measurement HPOP RAD 90 of SSME test 9010854. Various tag information are listed on the left portion of the PSD plot. Each major spectral peak is assigned a peak number, frequency, tag (i.e. symbol for frequency match), representative coherence, Bandwidth Coherence (WBC), GHC correlation with Sync (GHCN), and Wideband Demodulation SNR in dB. The tag such as L1, N1, N1-C1, etc., indicates the best match for this spectral peak with the highest representative coherence among multiple matches. In this Figure, peaks 2, 5, 7, 11 are identified to be 60 Hz line noise and its harmonics which are all supported by high representative coherence, the bandwidth coherence (%5). Peaks 8, 12, 16, 17, 19, 23 and 27 are identified to be the Sync and harmonics of the current pump, HPOP, which are all supported by high representative coherence. The representative coherence for N2, 2N2, 4N2 are 97%, 93% and 77% of hyper-coherence (%1). The representative coherence for 5N2, 6N2, 8N2 and 12N2 are 62%, 73%, 73% and 73% of bi-coherence-coherence (%3). Peaks 10, N1, is identified to be the Sync feedthru from other pump, HPFP, which is supported by 80% representative linear coherence (%1). Peaks 9, 5N4, has a frequency matching the 4th harmonic of Sync feedthru from LPOP. However, this match is not supported by its representative linear coherence (only 10%1). In addition to these nominal peaks (Sync/harmonic, feedthru, line noise) identified above, a number of matches at bearing modulation/sideband frequencies (such as 2N2+2C1, 2B2$\pm$C2, 4B2-2C2,etc.) are listed. Due to the weak SNR of these components, their representative coherence are all relatively weak. However, multiple components associated with a common modulation/sideband pattern are shown here which gives an alternative indication of being bearing signature. This example will be discussed in more details in the case study section.

2.6 ATMS Compressed Topo Data base (ATMS-CTDB)

Within the SSME program, the creation of a concise data base containing detailed dynamic spectral information is a formidable task due to the immensity of the SSME dynamic data pool acquired over the past decade. With well over 1000 SSME tests (averaging approximately 600 seconds apiece), storage for this test data requires an exceptional amount of storage capacity. This data pool is currently stored in a large collection of optical disk in FFT format, which requires extensive man-hours for data recall from the history of the SSME program. Effective archival of dynamic information for probability and statistical analysis is virtually impossible.

Using a TOPO mapping format, an intricate dynamic signal can be compressed and transformed into a simple image-like pattern. In this TOPO pattern, the amplitude and phase for each peak of the original PSD will be stored in order to preserve any linear or nonlinear correlations in the signal to allow their future recovery. In addition, since only the peak information is stored and the noise floor information is discarded, storage requirement will be dramatically reduced. A compression ratio of 50:1 can be achieved for a typical vibration signal from a turbomachine running at 36000 RPM. Clearly, TOPO provide an excellent reduction medium for the creation of a concise SSME data

base. Therefore, a Compressed TOPO Data Base (CTDB) representing the whole SSME test history can be created and stored in a few 10 GB optical discs while preserving all major dynamic information of the original signal.

As discussed in the previous section, the ATMS-ASPS program utilizes an expert system to supervise a sequence of dynamic signal analysis programs in the ASAL to perform automatic processing of large amount of dynamic data for SSME post-test/flight evaluation. ASPS automatically generate a series of output plots in various formats along with the compressed TOPO time/frequency/amplitude/phase information stored in the Compressed TOPO Data Base (CTDB). All the data in the CTDB can be retrieved by the ATMS Signature Retrieval Subsystem (ATMS-SRS) for future database recall and statistical/trend analysis. The CTDB database contains various key dynamics signatures representing major statistics, fault signatures, and anomalies. Complete generation of the CTDB will allow a wealth of engine test and failure history information to be readily accessible for diagnostic evaluation.

Three types of dynamic signatures as listed below will be created by the ATMS-ASPS and stored in the CTDB.

(1) Topo Format:

- The TOPO format contains the time-frequency, amplitude, phase and Signal-to-noise ratio information of each spectral components in the dynamic measurements. In the CTDB, the original large volume FFT data format will be converted into a bank of image-like pattern in compressed TOPO format which preserve the frequency, amplitude, phase as well as signal to noise (SNR) of each significant spectral peak. Two main programs, "atopo" and "aptopo" within the ASPS are used to transform the original FFT format into Topo format in order to achieve first level of compression for frequency, amplitude, phase and SNR information.. The information is then further compressed into a minimum number of bit representation to achieve the secondary compression. The compressed information is then stored in the CTDB.

(2) Time Format:

In addition to the Topo format, various time domain information representing major statistics, key dynamics signatures usefully for statistical and trend analysis are also compressed and stored in the CTDB. These include:

- Sync frequency of each pumps (HPFTP, HPOTP, LPFTP, LPOTP, etc.)
- Rice Frequency (expected frequency in a PSD)
- Composite Ave/RMS/Skewness/Kurtosis/Min/Max statistics.
- Sync/Harmonics RMS tracking (N, 2N, 3N,..8N) of each pumps

- RMS of signal in-between Sync
- Composite White Spectrum (Overall Noise Floor) RMS
- White Spectrum Bands (in 1000 Hz Interval) RMS

(3) Frequency Format:

A number of frequency domain spectral information representing either linear coherence across pump and measurement or non-linear coherence with are also compressed and stored in the CTDB. These include:

- Mean and Standard deviation of PSD
- Wide-band Demodulation PSD for cavitation analysis
- Bi-coherence Bxxx(N, f) for modulation analysis
- Linear coherence for feed-through analysis

The database format along with its appropriate data bit compression for various TOPO output parameters was designed to preserved the maximum accuracy and minimum storage for each CTDB signature. Table 2.6.1 shows the file system used in the CTDB along with the data bit compression for various CTDB signatures. Corresponding decompression routine to recover each type of information stored in CTDB in the ATMS-SRS would allow user to recall any dynamic signature in CTDB across the entire SSME test history. In general, a regular number (integer/real number) required 32 bits storage space in UNIX system This secondary compression will provide an additional 50% - 68.75% storage reduction. These compressed information is also stored in the CTDB.

	Description	Data File Extension	Header File Extension	Numbe of Bits	Source Program	Writing Routines	Reading Routines	Routine Location
TOPO FORMAT	Frequency	*.lopk	*.topo	11	ktopo.f	writetopo()		topodb.f
	Amplitude	*.sspk	*.topo	11	ktopo.f	writetopo()		topodb.f
	Phase	*.phas	*.topo	9	ktopo.f	writetopo()		topodb.f
	SNR(in dB)	*.snr	*.topo	7	ktopo.f	writetopo()		topodb.f
TIME FORMAT	Rice Frequency	*.rice	*.topo	10	ktopo.f	writetopo()		topodb.f
	Composite White Spectrum (Noise Floor) RMS	*.whit	*.topo	10	ktopo.f	writetopo()		topodb.f
	Sync Frequency	*.sync	*.syhd	32	asyncfreq.f	writesync()		syncdb.f
	Composite Average Reduction	*.aver	*.avhd	10	kplot.f	writered()		reddb.f
	Composite RMS Reduction	*.rmsr	*.rmhd	10	kplot.f	writered()		reddb.f
	Composite Skewness Reduction	*.skew	*.skhd	10	kplot.f	writered()		reddb.f
	Composite Kurtosis Reduction	*.kurt	*.kuhd	10	kplot.f	writered()		reddb.f
	Composite Minimum Reduction	*.mini	*.mihd	10	kplot.f	writered()		reddb.f
	Composite Maximum Reduction	*.maxi	*.mahd	10	kplot.f	writered()		reddb.f
	N/2N/3N/.../8N RMS	*.ampn	*.anhd	10	atrackn.f	writeampn()		ampndb.f
	0N-N/N-2N/2N-3N/.../7N-8N Between Sync RM	*.ampr	*.anhd	10	atrackn.f	writeampn()		ampndb.f
FREQ. FORMAT (station.)	PSD mean (average)	*.psda	*.pdhd	10	kpsd.f	writepsd()		psddb.f
	PSD dev.	*.psdd	*.pdhd	10	kpsd.f	writepsd()		psddb.f
	wbd PSD	*.wbd	*.wbhd	10	kwbd.f	writewbd()		wbddb.f
	Bi-Coherence Bxxx(N,f)	*.bcoh	*.bchd	7	katcmc.f	writebcoh()		bcohdb.f
	Linear Coherence	*.lcoh	*.lchd	7	klincohxf.f	writelcoh()		lcohdb.f

Note:

1. The second set of raw data is created when anomaly analysis is required.
2. The database created by second set of raw data include:
   ktopo.f, kplot.f, kpsd.f, atrackn.f, and atracka.f
3. The filename convension for the 2nd group of database is consist of
   *w.????
4. atracka.f will create following database:

*w.aahd ==> header file						
*w.ampf ==> data file	*w.ampf	*w.aahd	10	atracka.f	writeampa()	ampadb.f
*w.ampa ==> data file	*w.ampa	*w.aahd	10	atracka.f	writeampa()	ampadb.f

Table 2.6.1 File system used in the CTDB along with the data bit compression for various CTDB signatures.

2.7 ATMS Signature Retrieval Subsystem (ATMS-SRS)

The major function of the ATMS Signature Retrieval Subsystem (SRS) is to provide fast signature retrieval, statistical analysis, trending and fault pattern comparison/identification capabilities from the CTDB database. The SRS would allow a user to recall any dynamic information created by the ASPS from any SSME test stored in CTDB. Therefore, with the creation of CTDB and SRS, the entire engine test history would be readily accessible. In addition, SRS also provides graphic capabilities for displaying any retrieved information on a computer screen or printer. With such effective database recall capability, signature retrieval capability across a series of engine tests for trending or statistical analysis become feasible. Detailed description of the SRS program along with its menu system are documented and discussed below:

The initial task in SRS is to decompress the CTDB database and recover the original signature created by ASPS. Various time/spectral information representation as shown in table 2.6.1 in the compressed bit will first be decompress and retrieved from the CTDB and transformed back into standard REAL/INTEGER for further analysis or replot. As discussed the last section, the standard CTDB database consists of three major types of data formats: (1) Joint time-frequency Topo format; (2) Time domain information (Sync/harmonics tracking, RMS, Max/Min, Skewness, Kurtosis, etc.); and (3) Frequency domain information (Raw PSD, WBD PSD, linear and nonlinear Coherence, etc.). All these three formats of dynamic information can be retrieved from the CTDB database with the SRS program. The sequence of items in the SRS menu system as shown in Figure 2.7.1 will be discussed below:

1. TESTID

With new "testid" from user, the recall system will:

(1). Make file names for binary data files and ASCII data files.
The standard database of ATMS is in compressed form and storing in "testid" sub-directory. To retrieve the data and save as decompressed format is one of the options in this recall system. The decompressed data is stored in user's home directory under ".atmsmenu".

(2). Read SSME information data file.
The SSME data file is part of ATMS standard database which consists of power level profile, vent profile, number of channels, engine and pump serial number, testing time/date, sampling frequency, start time, stop time, measurement id, and units.

(3). Read ATMS main menu data file.
The ATMS main menu data file is part of ATMS standard database. These data consisting of pump type selection status, disk file id, pump selection attributes, atracka anomaly tracking range, sync frequency tracking window width, and time cut in stationary period is used to control entire ATMS operation in CLIPS environment. The combination of SSME data file and ATMS main menu file enables this recall system working properly.

(4). Read stationary data file.
The stationary data file is part of ATMS standard database. This data file consists of start time, stop time, power level, and sync frequency for each stationary period. User is allowed to select stationary periods only if this data file is available.

(5). Read header information for each data format.
The header information for each data format are used to be the default values in menu item # 4 (define output parameters). Basically, each set of data has its own header information. For instance, topo data created by program "ktopo.f" has header file "*.topo"; composite average reduction data created by program "kplot.f" has header file "*.avhd", and so on. However, the entire database is created under same condition and same parameter such as same start time, same stop time and same raw data. Thus, we can take any header information within database as the default values for plotting and assume all of them are to be identical to each other. In this case, we use header file "*.topo" as topo data format default values; "*.avhd" as time data format default values; and "*.pdhd" as frequency data format default values.

(6). Group channels into different pump types.
Once the recall system gets the channel selection attributes and all the channels' measurement ID. The channels are catalogued into different pump types according to attributes.

2. PUMP AND CHANNEL SELECTION

This selection displays all the available pumps and channels which allow user to select. The selection can be made by entering the number in front of channel measurement ID. The selected channels are marked with asterisk (*). To de-select just re-enter the same number again. The channel selecting results will be returned to main program as the searching key in the database recall.

3. DATA TYPE SELECTION

The available data types in this database include topo, time, and frequency data format. A sub menu will be displayed as follows if the user selects this menu item.

ATMS Database Recall Data Type Selection
1. Topo Format Data
2. Time Format Data
3. Frequency Format Data

(1). Topo format data

Four types of data are included in this data format. They are

ktopo.f	1. Frequency 2. Amplitude 3. Phase 4. SNR (in dB)

Each set of topo data may consist of two subset data: raw data topo and WBD data topo. Therefore, if user selects any topo format data, this recall system will prompt user to select raw data topo or WBD data topo.

(2). Time format data

Time format data consists of twelve types of data plus sync frequency tracking.

ktopo.f	1. Rice Frequency 2. Composite white spectrum
kplot.f	3. Composite average reduction 4. Composite RMS reduction 5. Composite Skewness reduction 6. Composite Kurtosis reduction 7. Composite Minimum reduction 8. Composite Maximum reduction 9. (Composite MaxMin reduction)
Atrackn.f	10. 1N/2N ... /8N RMS 11. 0-1N/1-2N/../7-8N between Sync RMS
Atracka.f	12. Atracka frequency tracking 13 Atracka amplitude tracking

Composite MaxMin reduction is not part of the ATMS standard database. However it is available if both composite minimum and maximum reduction can be retrieved. If user selects any data from "ktopo.f", "atrackn.f", or "atracka.f", he/she needs to specify raw data type or WBD data type. If user selects any data from "atrackn.f", he/she needs to select which sync is desired. If user selects any data from "atracka.f", he/she needs to indicate what is the tracking range.

(3). Frequency format data

kpsd.f	1. PSD mean 2. PSD deviation
kwbd.f	3. WBD PSD
katcmc.f	4. bi-coherence
klincohxf.f	5. linear coherence

The start time and stop time for each data record in the database depend on the stationary periods. Thus, it is required to get the stationary information first being able to process frequency format data. User will be prompted to select stationary period if any of the data set are selected from above table. If the data set is linear coherence, in addition to the selection of stationary period, user needs to select channel pairs. Thus all the available cross-files channel pairs will be listed on the screen for selection.

4. OUTPUT DEVICE SELECTION

Binary output file and ASCII output file are two extra options besides standard output devices. Multiple selection are possible in this system. That means user may send retrieved data to two or more printers at the same time.

5. DEFINE OUTPUT PARAMETER

Basically, output parameters are used to define three things in this system, the starting point, the stopping point, and number of plots per page.

(1). To process topo data, we need:
- [1] define start time
- [2] define stop time
- [3] define minimum frequency for plotting
- [4] define maximum frequency for plotting
- [5] define the broadness of topo line

(2). To process time data, we need:
- [1] define start time
- [2] define stop time
- [3] # of plots per page

(3). To process frequency data, we need:
- [1] define minimum frequency for plotting
- [2] define maximum frequency for plotting
- [3] # of plots per page

6. PLOT SYNC AND POWER LEVEL

This set of data is independent to others. Once user specifies the output devices, the process can be performed based on the previously chosen parameters.

2.8 Case Study from SSME Test History

A number of examples from actual SSME test history are discussed in this section. These case study examples demonstrate various anomaly detection and identification capabilities offered by ATMS-ADIS.

2.8.1 Sync/Harmonics and Feedthru Identification

In machinery diagnostics, the harmonic component content much subtle information about the operational condition. Many failure modes will cause waveform distortion and generate strong harmonics. For example, the radial rubbing of a rotating shaft will cause waveform clipping. This waveform clipping will then generate strong odd harmonic and can be easily identified from its PSD. However again, due to the complex operational environment of SSME, many other independent sources will coincidentally generate spectral component right at the harmonic frequency and appear to be a harmonic. In this case, nonlinear coherence analysis can be required to identify whether an apparent harmonic at harmonic frequency is truly a harmonics or not.

Figure 2.8.1.1 shows the ADIS summary PSD plot of an SSME example. The PSD is taken from an accelerometer measurement FASCOS HPFP 219 of SSME tests 9040277. Other than 60Hz line noise and its harmonics, other major peaks in the PSD are the Sync frequency component N1 of HPFP and its harmonics 2N1, 3N1 and 6N1 at peak number 8, 11, 12 and 16. Now notice that, the amplitude of 3N is pretty high which is generally considered to be fault signature. However, the representative coherence indicates that its correlation with other sync harmonics are pretty low (21% hyper-coherence). This indicates that most of the power at 3N is due to some other independent source and is not related to the machinery rotational process. Therefore, the apparent high level 3N PSD is just a false alarm defect signature instead of being a true 3rd harmonic. It turns out to be the so-called pseudo 3N component commonly observed in the HPFP measurements..

In addition to the representative coherence, the GHC correlation with Sync (GHCN, %7) also show strong GHCN for N1(84%7), 2N1(81%7) and 6N1(99%7) but a weak GHCN for N3 (3%7). Figure 2.8.1.2 shows the instantaneous frequency (IF) signal for components at center N1, 6N1 and 3N1. Strong correlation between the IF signal at N1 and 6N1 is evident; while no correlation can be observed between N1 and 3N1. This GHCN provides additional evidence for such sync/harmonic identification.

Sync/Harmonics Feedthru Identification

Spectral components due to Sync/harmonics feedthru from other pumps is a commonly observed phenomenon in SSME measurement data. Even though its identification is quite straightforward, however to completely identify all possible feedthru from all 4 pumps manually is still quite a tedious process since the data analyst has to keep tracking

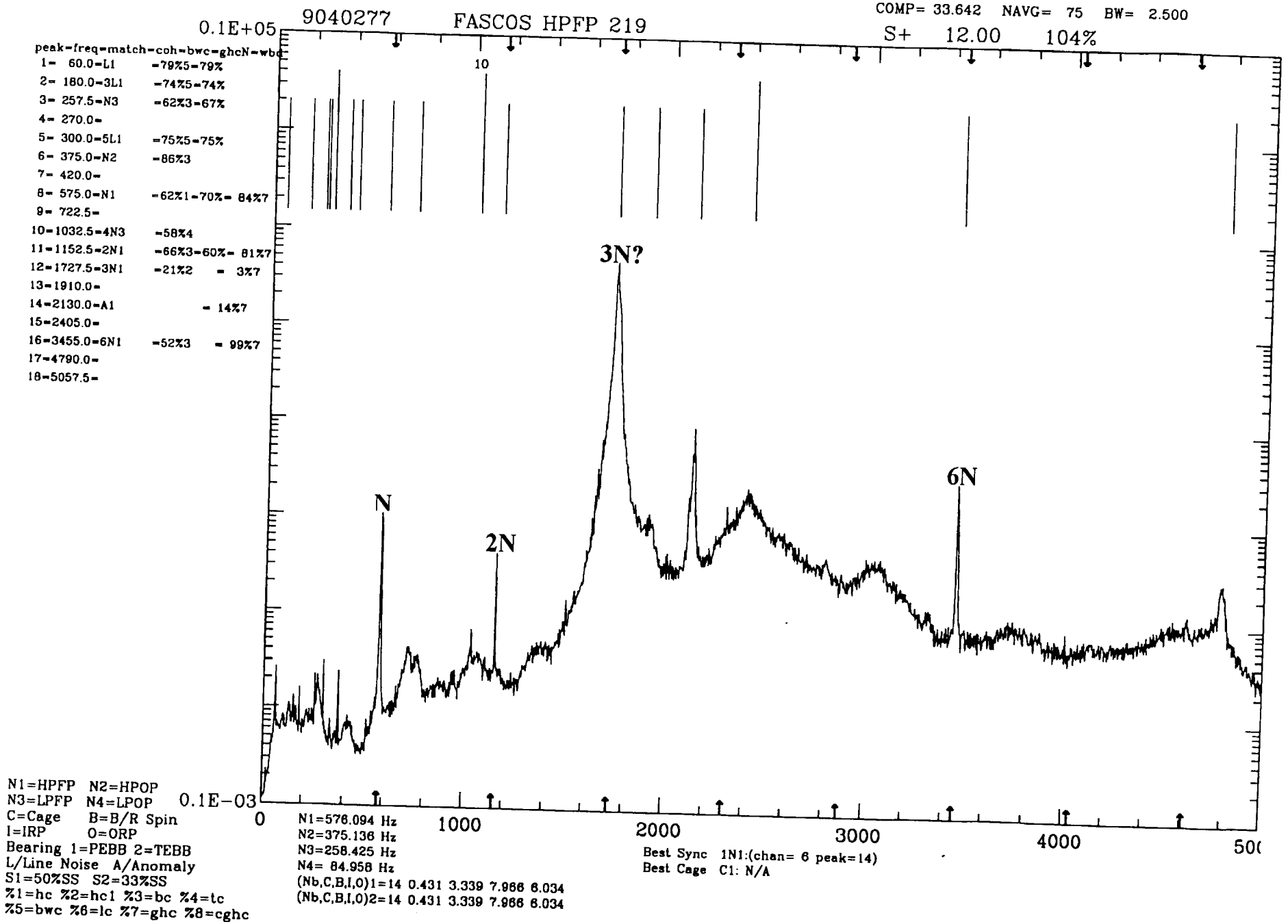

Figure 2.8.1.1 ADIS PSD: Strong 3N component due to non-sync related source

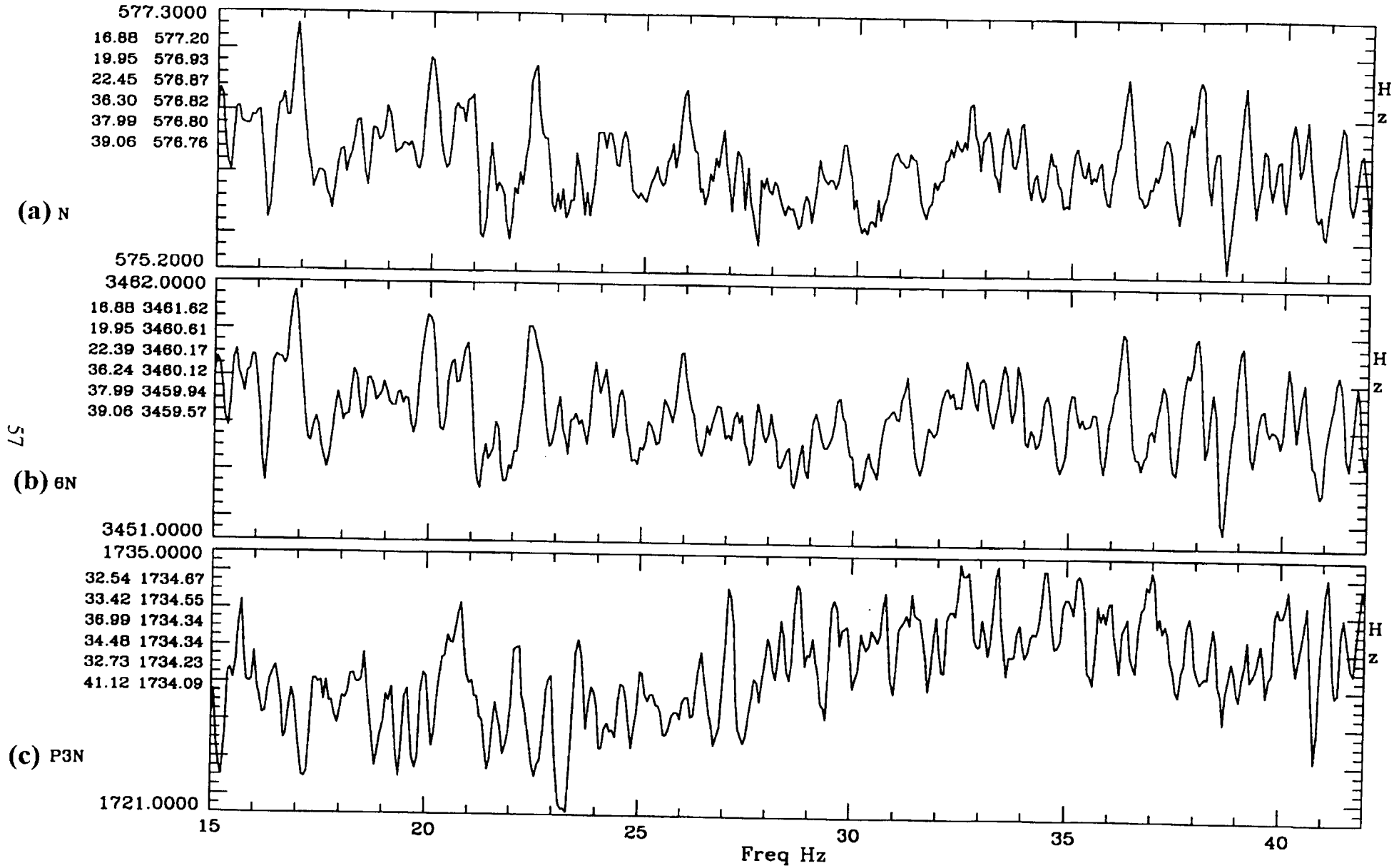

Figure 2.8.1.2 GHC Instantaneous Frequency signal: Weak Correlation between N1 and 3N1

all the frequencies of Sync and its harmonics of four different pumps (HPFP, HPOP, LPFP, LPOP) at various power level, in order to perform a linear cross coherence analysis. The ADIS Sync/harmonic feedthru identification can automatically identify whether any spectral peak in the measurement PSD is a linear feedthru from other pumps.

The PSD in Figure 2.8.1.1 shows a typical example for ADIS sync/harmonics feedthru identification. In this PSD, other than the line noise components and the Sync/harmonics of HPFP, a number of sync feedthru from the other pump are identified. For example, peak number 6 is the sync (N2) feedthru from HPOP with 86% bi-coherence. Peak number 10 is the sync harmonic (4N3) feedthru from LPFP with 58% tri-coherence. The weak coherence is due to the weak SNR the PSD peak. This process of coherence analysis for feedthru identification is entirely automated and transparent to user. In actual ATMS/ADIS processing, a large number of such identification will be performed in the background, while only the results (the attribute tags and representative coherence values) are shown in the final ADIS summary plot.

2.8.2 Discrete Line-Noise Identification

One other commonly observed false-alarm component in a dynamic measurement is the discrete line noise component. It is typically generated from the power supply of the data acquisition system (e.g. the 60 Hz line noise and its harmonics), the tape multiplex/demultiplex devices, and other elements within the measurement/sensor system. As discussed in previous section, the Bandwidth Coherence (BWC) method provides an effective tool within the ATMS system for discrete line noise identification. This method is based on the identification of the existence and coherent phase relationship at the frequency of a spectral component within contiguous ensemble data blocks. The strength of such coherent phase relationship is proportional to the degree of discreteness of the spectral component. Therefore, for a pure-tone discrete component (as a line noise or its harmonics), strong coherent phase relationship would exist and its Bandwidth Coherent should be unity (one). On the other hand, for a narrow band random component, its coherent phase would diminished (in proportional or its bandwidth), and its resulting bandwidth Coherence would be diminished. Therefore, the Bandwidth Coherence Analysis provides an effective way to identify whether an anomaly is a false-alarm discrete line noise instead of a rotor related important signature.

Figure 2.8.2.1 shows example for such ADIS discrete line noise identification. The PSD is taken from a turbine-end accelerometer measurement from HPOP during SSME test 9010823. The 60 Hz line noise and its harmonics along with the Sync/Harmonics and feedthru components have all been correctly identified by ADIS with supporting coherence value. The 18th peak marked I3 indicates it is an apparent Inner Ball Pass (IBP) component of the Turbine-End Ball Bearing (TEBB). This IBP component is considered to be a benign signature since it has been consistently observed at this measurement location and its amplitude is within the its normal level. However, the 19th

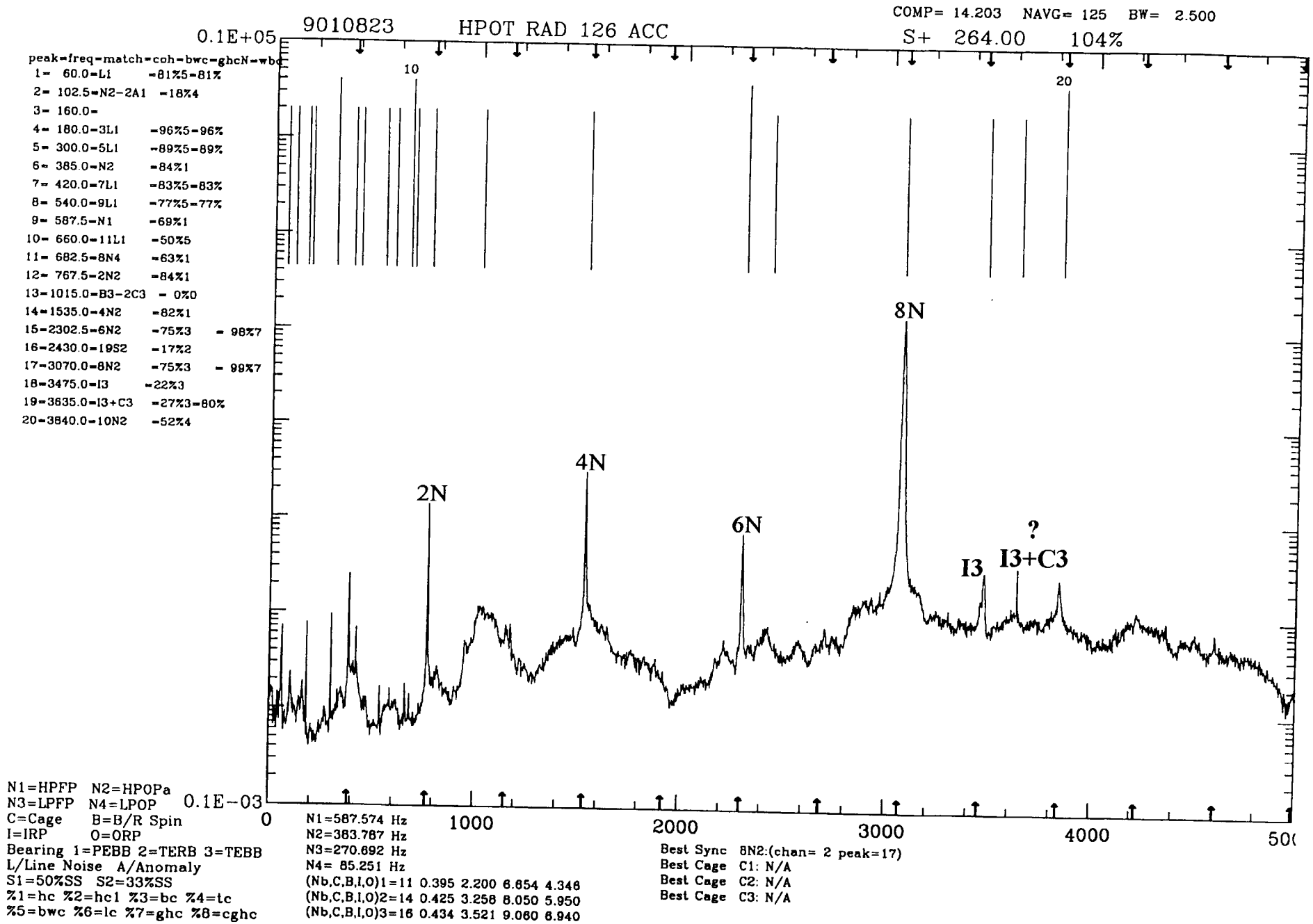

Figure 2.8.2.1 ADIS PSD: Anomaly I3+C3 at 3635 Hz.

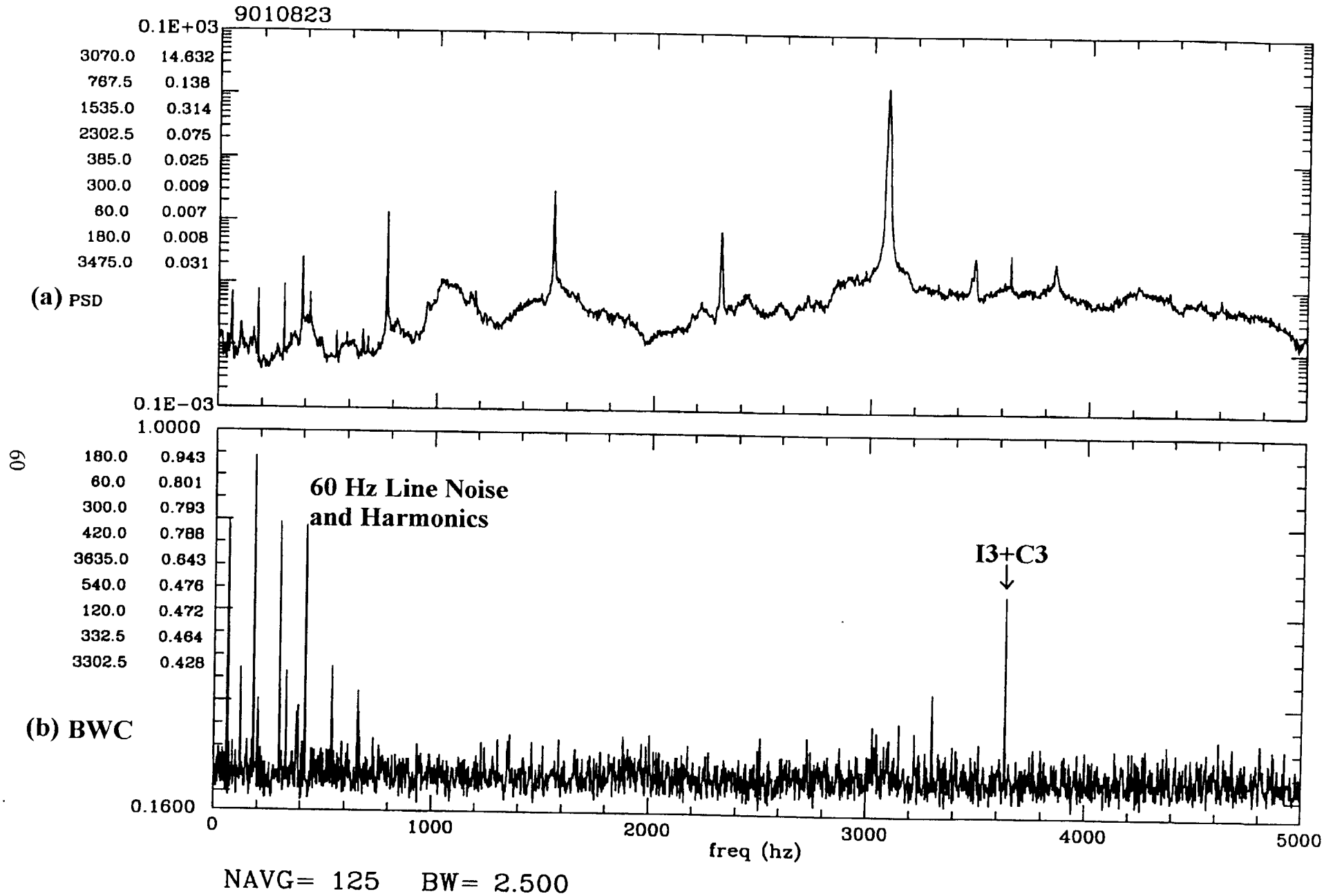

Figure 2.8.2.2 (a) PSD (b) Band-Width Coherence Function: Strong BWC at 3635 Hz

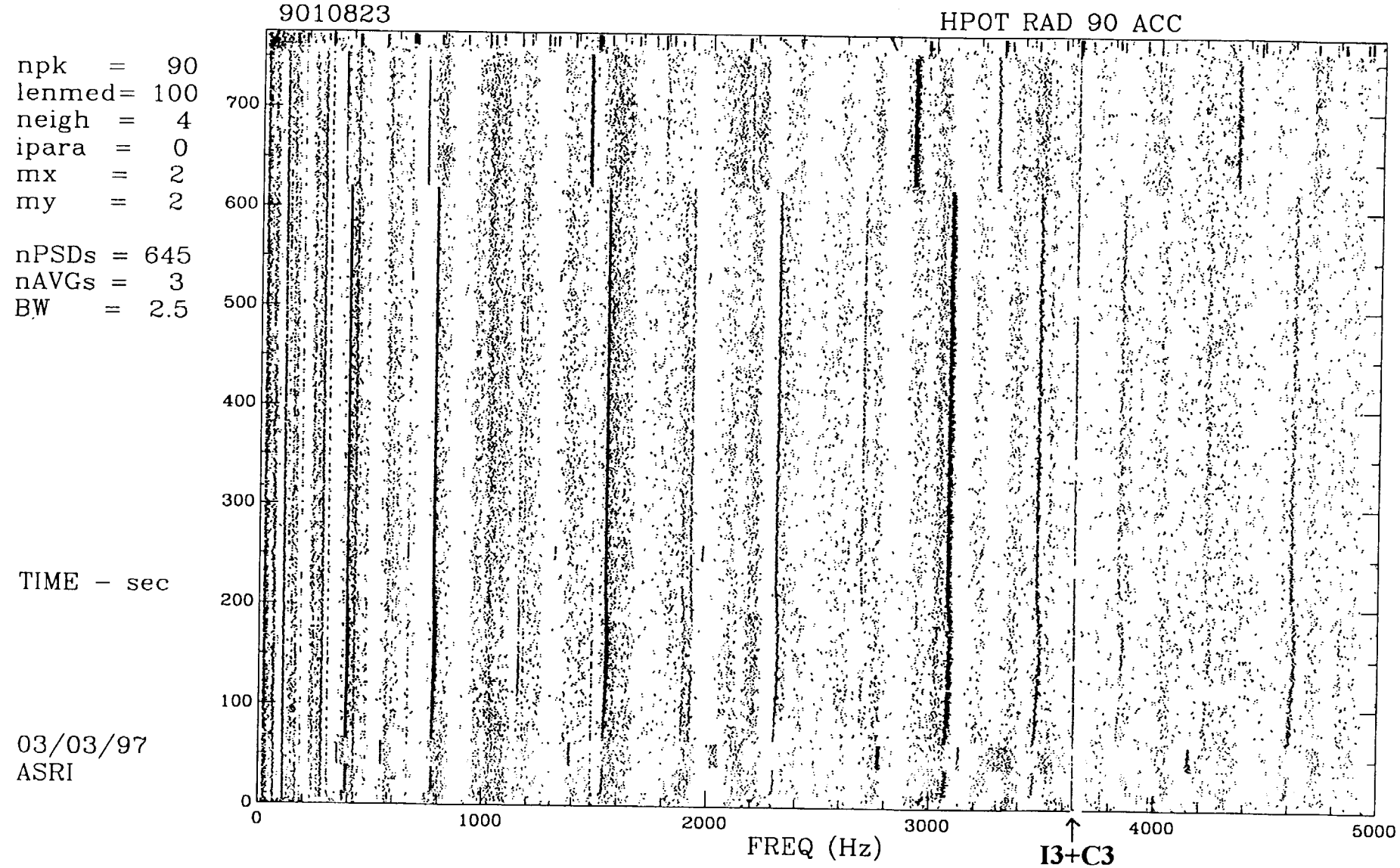

Figure 2.8.2.3 Topp spectrogram: Frequency of I3+C3 anomaly remains constant.

peak at 3635 Hz with tag I3+C3 indicates that it is the IBP (I3) of TEBB plus the Cage component (C3). Since amplitude modulation among different bearing characteristic frequency components could be an indicative of bearing-related defect, therefore, this I3+C3 anomaly could represent a defect signature. Since its representative coherence shows a weak bi-coherence, it indicates the lack of correlation among its corresponding modulation/sideband pattern. Also notice that, the ADIS also shows a strong 80% bandwidth coherence associated with it. This indicates that the I3+C3 anomaly is quite discrete, and is likely to be just a line noise, rather than a sync-related bearing signature. The BWC function in Figure 2.8.2.2(b) indeed shows strong bandwidth coherence at I3+C3 along with several other 60 Hz line noise and its harmonics, while very weak coherence at sync harmonic and IBP frequencies. This identification is also supported by the topo spectrogram in Figure 2.8.2.3 which shows the frequency of the I3+C3 anomaly remains constant during power level change. This example demonstrates how the ADIS utilize the BCA method for discrete line noise identification.

2.8.3 Bearing Signature Identification

As discussed in section 2.5 (Bearing Signature Identification), the ADIS will establish various bearing characteristic frequencies. This includes Cage, Ball/Roller Spin (BS), Inner Ball/Roller Pass (IBP), and Outer Ball/Roller Pass (OBP), (represented by C, B, I, O), within all allowable variation of bearing parameters (e.g. contact angle and bearing dimension variation). A set of bearing modulation/sideband pattern will then be generated for each set of analytically calculated (C,B,I,O). A coherence-based scoring which measure the goodness-of-fit is used to determine which set of (C, B, I, O) provides the best matching. Within the template, candidate carriers include (N, C, B, I, O) and the sidebands also include (N, C, B, I, O), where N is Sync frequency.

Since the number of possible permutations among various modulation/sideband patterns of different bearings is quite large, the possibility of a coincidental matching to some bearing frequency could be high. In this case, the coherence provide an effective indicator about the likelihood of an apparent matching. It should be pointed out that, the representative coherence only shows the existence of nonlinear correlation among different components within a modulation/sideband pattern, which is still not an absolute proof for it to be a bearing signature. However, since bearing faults do generate such nonlinear characteristic, the representative coherence can provide additional evidence than apparent frequency matching.

Figure 2.8.3.1 shows an example of such bearing signature identification. The PSD is taken from HPFP RAD 135 ACC of SSME test 9040287. Other than the normal 60 Hz line noise/harmonics, Sync/harmonics of current pump HPFP and feedthru from other pumps, a number of peaks show apparent frequency matching as bearing frequencies. For example, the peak number 4 and 10 have apparent frequencies at N1-2C2 (Sync - 2nd harmonic of Cage of Pump End Roller Bearing PERB) and 2C2. However, their

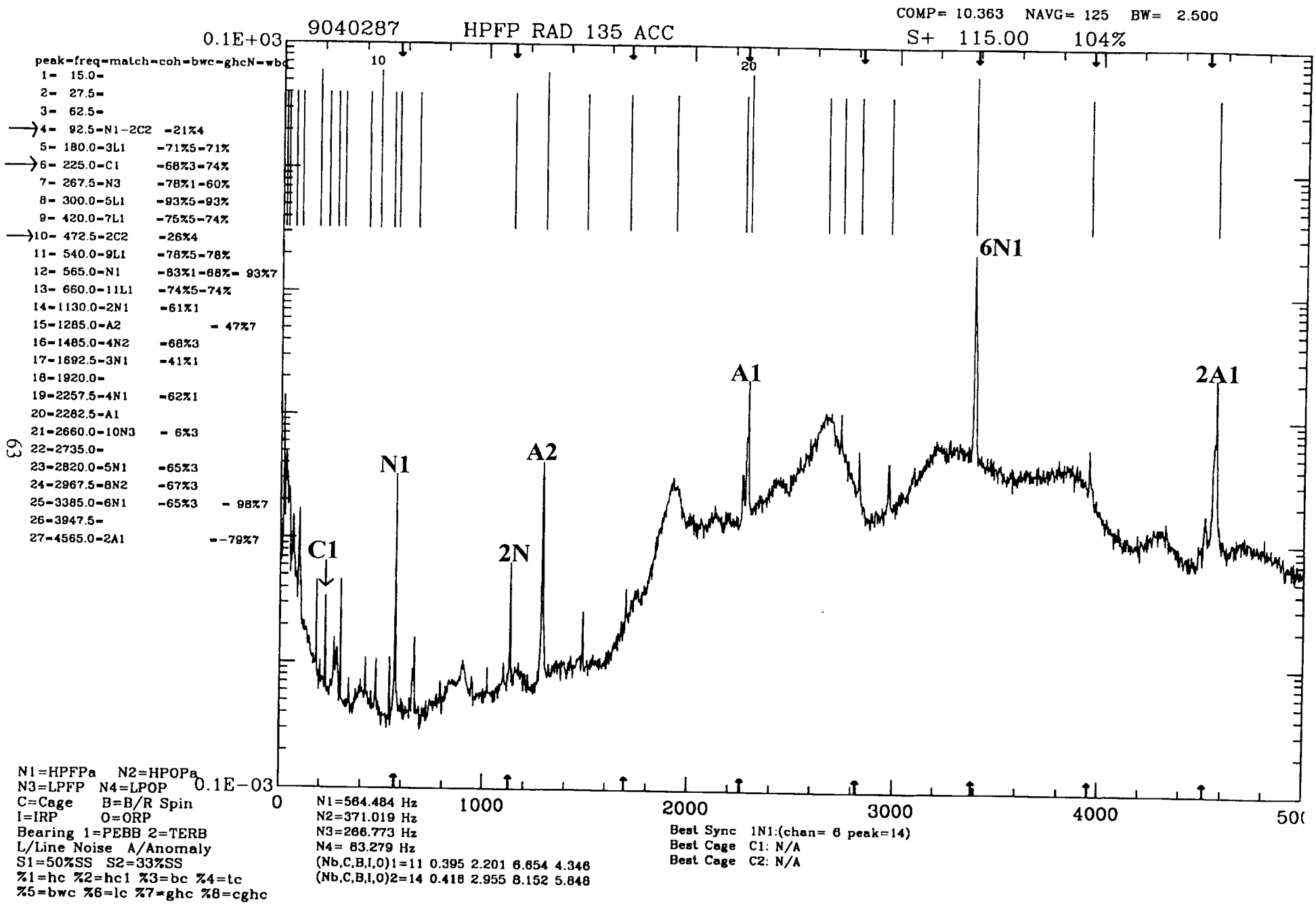

Figure 2.8.3.1 ADIS PSD: Anomalies at bearing frequencies: N1-2C2, 2C2 and C1.

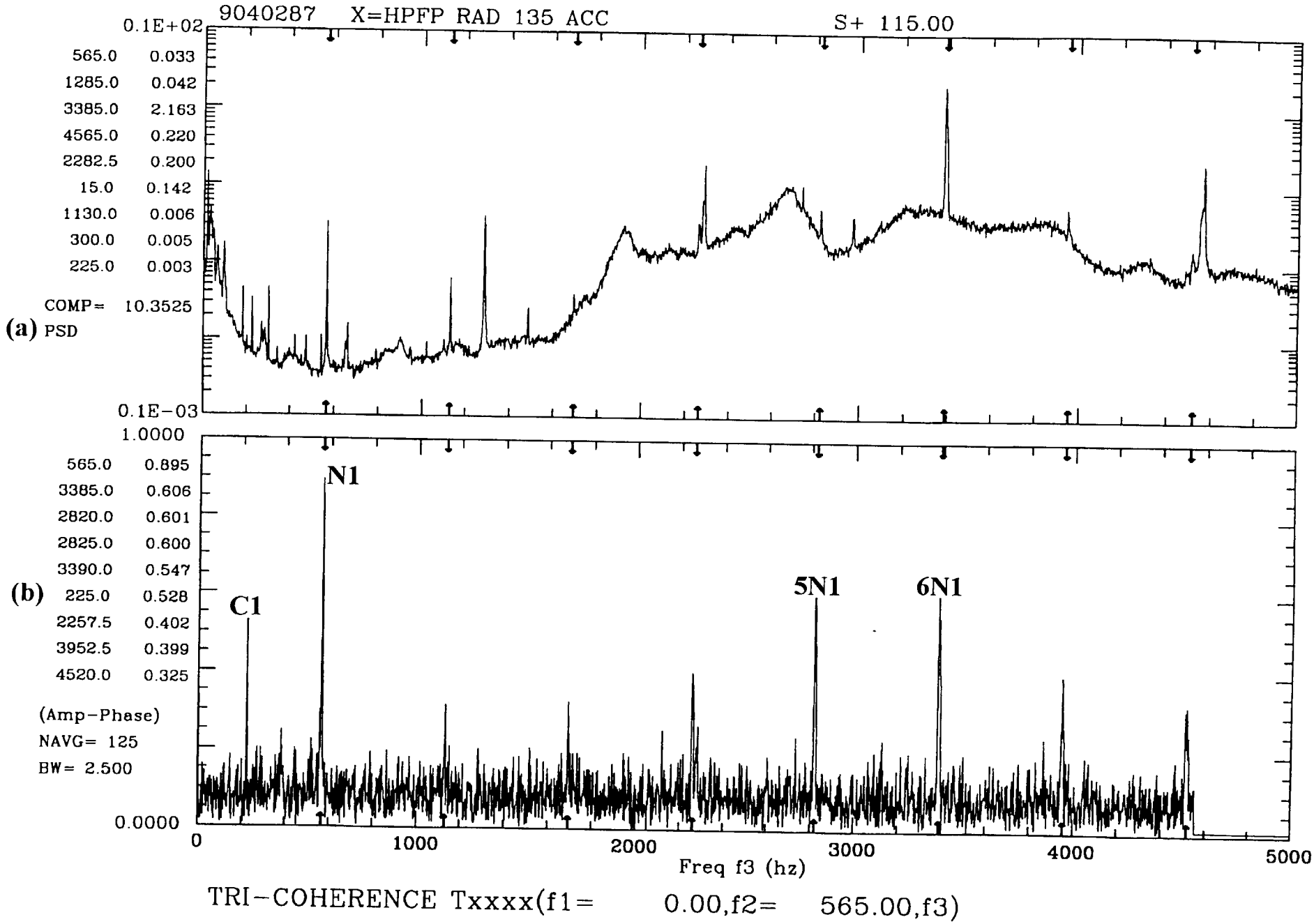

Figure 2.8.3.2 (a) PSD (b) Bi-coherence function: Strong correlation between C1 and N1

representative coherence are relatively low, which indicate the lack of nonlinear correlation among its corresponding modulation/sideband pattern. However, the representative coherence for peak number 6 (C1 = Cage of Pump End Ball Bearing PEBB) shows a 68% of bi-coherence. If the analyst need to find out more detailed supporting information about this cage frequency identification, a trace file generated by ADIS would contains all the relevant information about how this identification is performed. Figure 2.8.3.2(b) shows the detailed bi-coherence function using the sync as the reference frequency, which indeed shows bi-coherence peak at the cage frequency (225 Hz). Most of the spectral components in this PSD have been correctly identified by ADIS. However, there are two unidentified anomalies with tags A1 and A2. A1 has a 2nd harmonic 2A1 at peak # 27. The ADIS try to further identify these anomalies by providing certain dynamic characteristics associated with the anomaly such as the negative 79% GHC coherence with Sync for 2A1.

2.8.4 Bearing Modulation/Sideband Signature Identification (test 9010854)

As discussed in last section, the ADIS detect bearing signature by matching against various bearing modulation/sideband patterns within all allowable variation of bearing parameters. Any apparent matching is then further verified by a representative coherence since coincidental matching to some bearing frequencies is quite possible. However, due to either weak SNR or lack of required frequency combination for coherence analysis, sometimes the ADIS can only find a weak coherence. However, if there is a large number of apparent matches associated with a particular modulation/sideband pattern, the ADIS will list them in the final summary plot to alert the user about possible bearing signature.

Figure 2.8.4.1 shows a typical example of this case. The PSD is taken from measurement HPOP RAD 90 of SSME test 9010854. Again, other than the normal 60 Hz line noise/harmonics, and Sync/harmonics/feedthru of current pump HPOP and other pumps, a number of peaks with apparent frequency matching to a particular modulation/sideband pattern 2B2±?C2 are listed (such as 2B2-C2, 2B2+C2, 2B2+2C2). However, due to the lack of required frequency bridging for tri-coherence analysis, their representative coherence are all relatively weak. However, the fact that multiple components associated with a common modulation/sideband should provide a god indication of being bearing signature.

These bearing signatures have also been further identified the enhancement PSEM signal analysis as shown in Figure 2.8.4.2. Figure 2.8.4.2(b) shows its higher-resolution PSD from 2000 Hz to 3700 Hz with 65K FFT size which gives a very fine spectral bandwidth of 0.16 Hz. Figure 2.8.4.2.(b) shows its corresponding enhanced PSEM PSD in the same frequency range from 2000 Hz to 3700 Hz. First notice that, all the Sync harmonics at 6N , 7N and 8N have indeed become discrete as we expected. In addition, all these components at 2B2±?C2 have also become discrete. This indicates that these anomalies should be Sync-related components. Also notice that, there are several new discrete spectral components also got enhanced and start to show up here which are not

observable in the original raw PSD. Therefore, the a more complete pattern of 2B2±?C2 are recovered in the PSEM PSD which are all sync-related as the roller bearing signature usually exhibit. This indicates that the anomalies observed in this PSD should be TERB bearing signatures.

2.8.5 54% Sub-sync Signature Identification due to Whirl

Fluid flow in bearing when set in motion by rotating shaft can generate dynamic forces which may result in a well-recognized instability known as whirl. This is a lateral, self-excited sub-synchronous vibration whose frequency is typically around (usually less than) 50% of sync. Even though the relationship between whirl frequency and Sync is constant. However, their frequency ratio is not maintained absolutely constant especially in the micro-frequency variation of their instantaneous frequency signal. Therefore, such lack of frequency synchronization with Sync is an important characteristic of whirl, which can be identified by the GHC technique. In addition, the sub-sync whirl was commonly observed to be amplitude modulated with the sync/harmonics and generated a modulation/sideband pattern at ?N±?SS (SS represent Sub-Sync). Therefore, such modulation phenomenon with Sync is another important characteristic of whirl, which can be identified by the bi-coherence or tri-coherence analysis technique. Since these two dynamic characteristics are usually provided by ADIS, sub-sync whirl can usually be recognized from the ADIS summary plot.

Figure 2.8.5.1 shows a typical example of sub-sync whirl. The PSD is taken from measurement HPFP RAD 84 ACC of SSME test 9040180. Other than the normal sync and harmonics (N1, N2, N3, etc.), a strong anomaly (A1) and its harmonics (2A1, 4A1, 5A1 and 6A1) are also observed in the PSD. The frequency of A1 is around 54% of Sync. In addition, 2 modulation/sideband components at peak # 9 and 10 with tag symbol: 2N1-A1 and N1+A1) This indicate that there exist a modulation phenomenon between the 54% Sub-Sync and Sync which are proved by the representative bi-coherence (%3) of 75% and 74% respectively. Furthermore, the ADIS shows that the GHC coherence with Sync (%7) of this 54% sub-sync component is only 14%. This indicates that the micro-frequency variation of the 54% Sub-Sync is not synchronization with Sync. Figure 2.8.5.2 shows the instantaneous frequency signal of 54%N, N and 2N respectively. As expected, the correlation between N and 2N is evident, however, only very weak correlation exists between N and 54%N.

Again, it should be pointed out that, these two dynamic characteristic associated with sub-sync whirl do not absolutely guarantee it to be a true whirl component. However, since sub-sync whirl do exhibit such dynamic characteristic, (modulation with Sync and no GHC correlation with Sync), the information identified by ADIS can provide additional clue and/or evidence about the source of an anomaly.

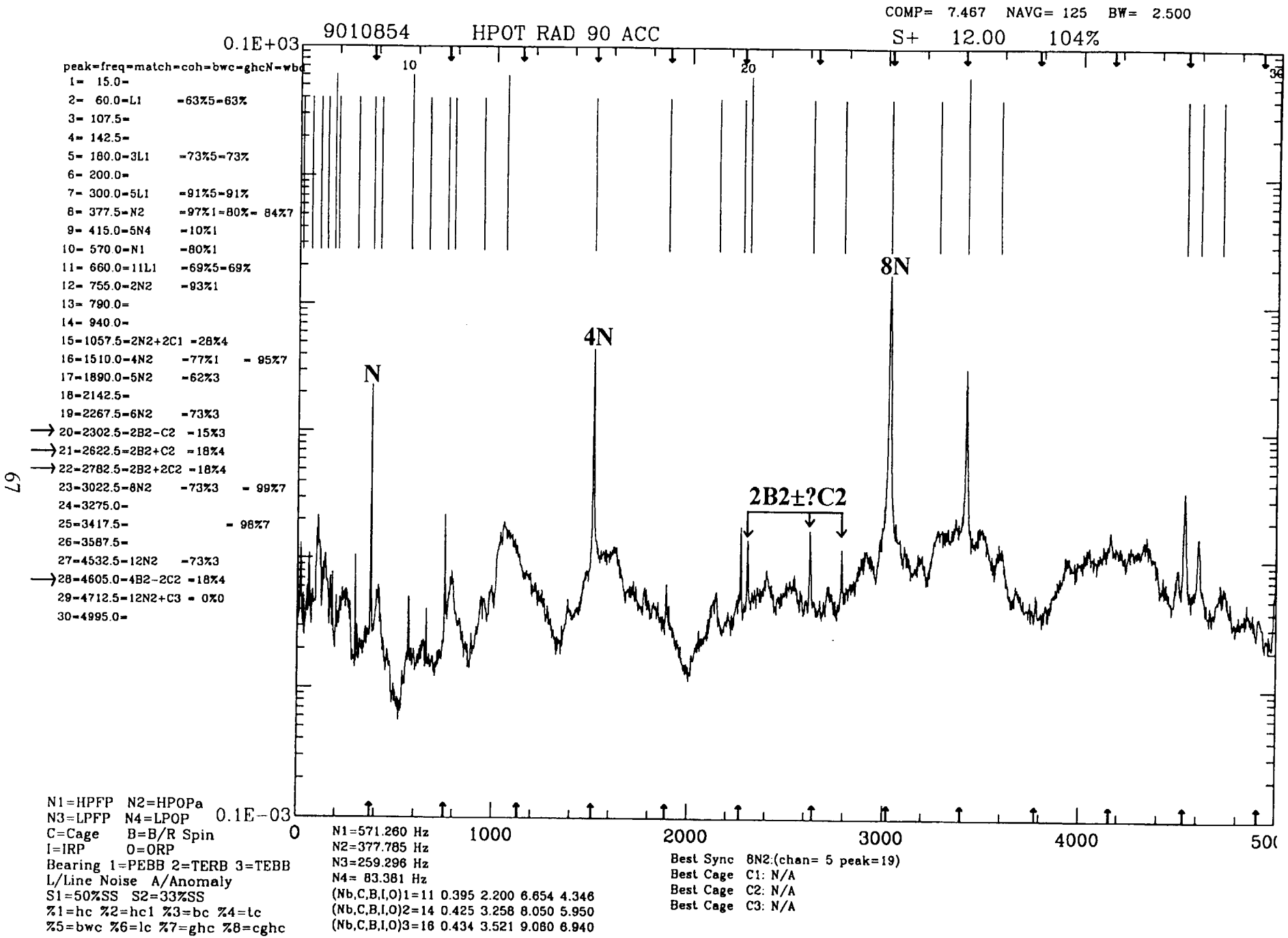

Figure 2.8.4.1 ADIS PSD: Anomalies at Bearing Modulation/Sideband Pattern 2B2+?C2

ATD HPOTP Roller Bearing	Number of Roller	Cage	Roller Spin (RS)	Outer Roller Pass(ORP)	Inner Roller Pass(IRP)
Turbine End Roller	14	0.425N	3.258N	5.95N	8.05N
ORP=2252.8 Hz = 5.95N => C=ORP/14=160.915 => IRP+N=(14N-ORP)+N=3423.75					

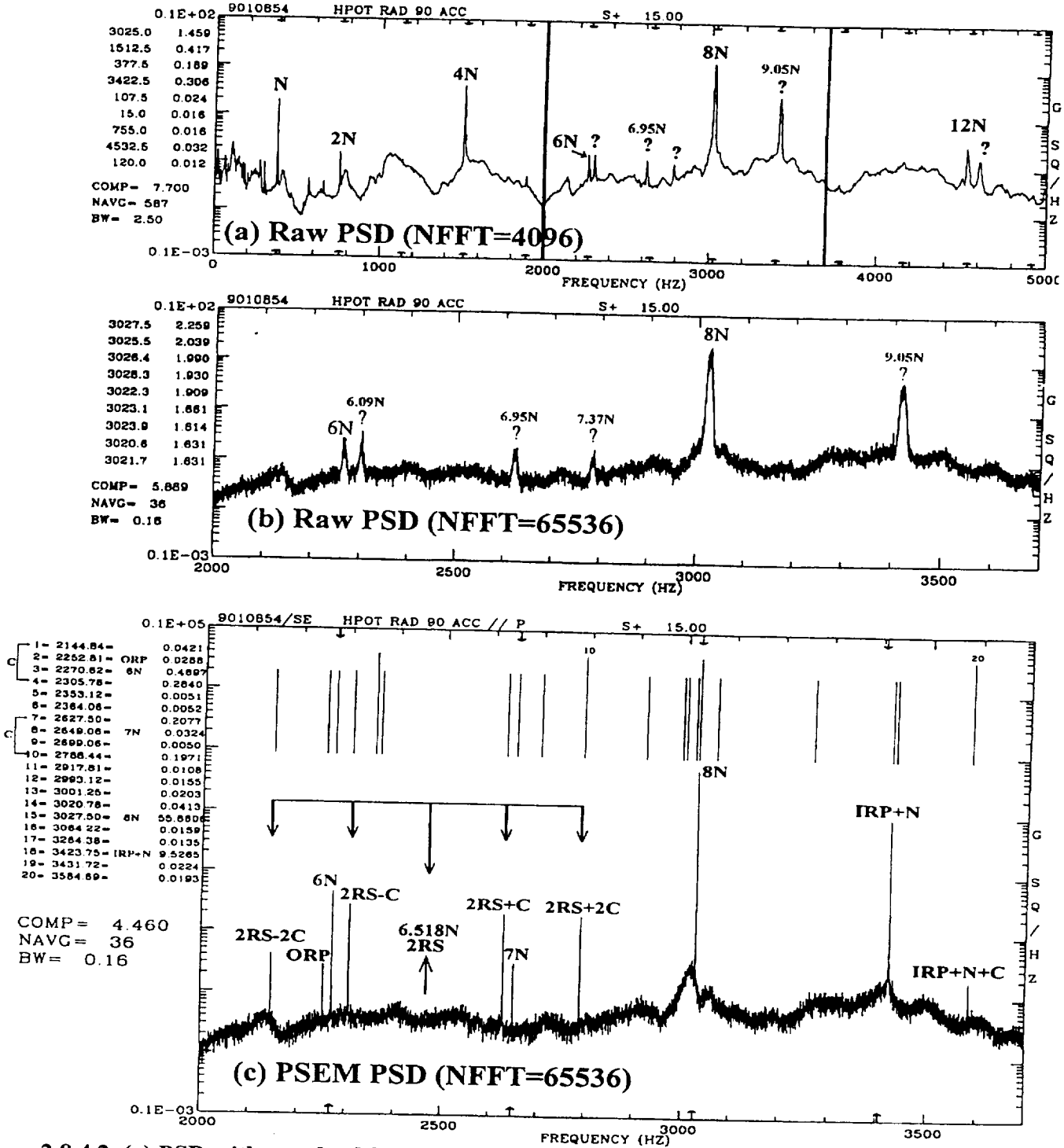

Figure 2.8.4.2 (a) PSD with standard 2.5 Hz spectral bandwidth
(b) PSD with finer spectral bandwidth of 0.16 Hz.
(c) PSEM PSD: Bearing Modulation/Sideband Pattern 2B2+?C2 become discrete enhanced.

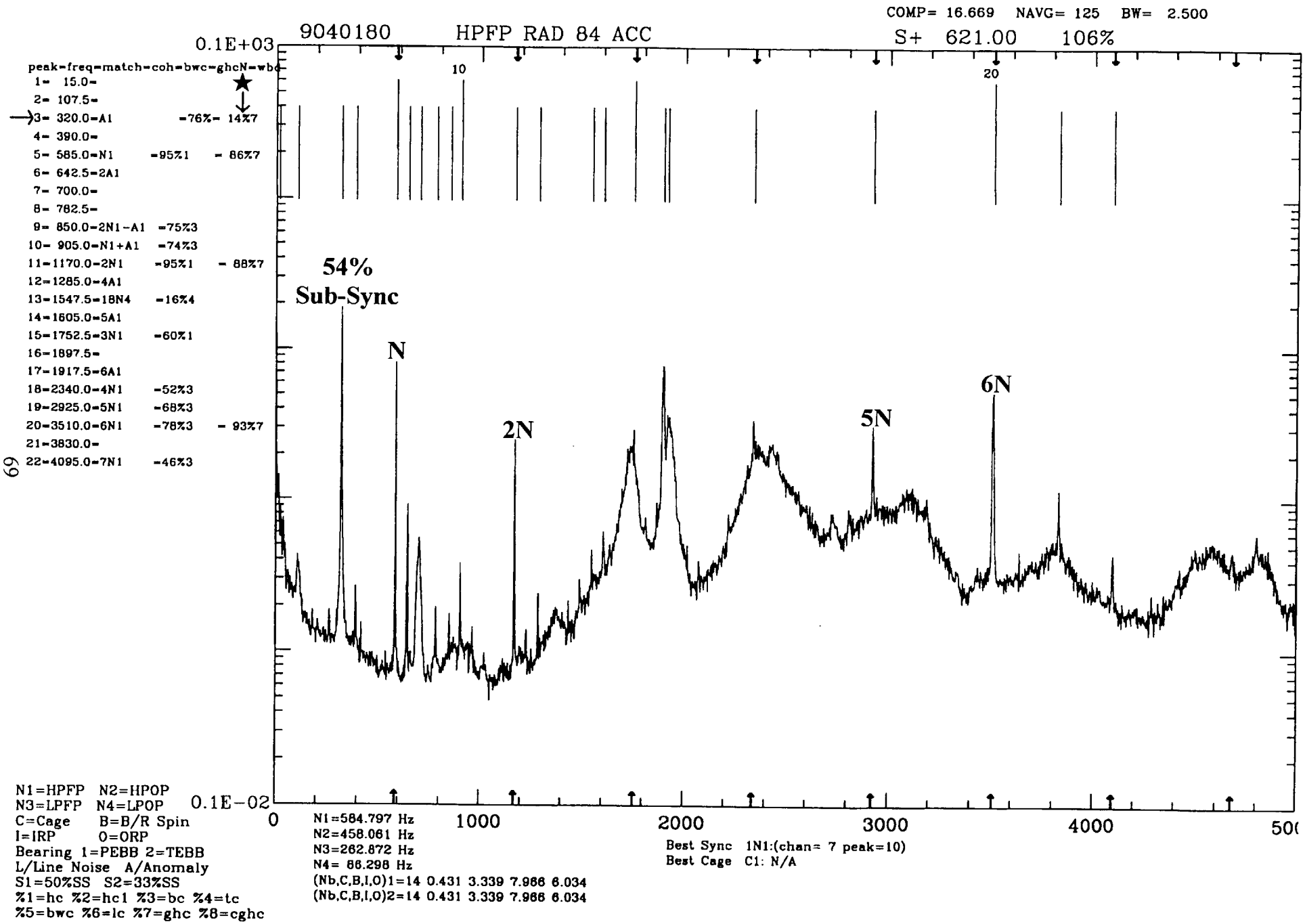

Figure 2.8.5.1 ADIS PSD: 54% Sub-Sync Anomaly (A1) at 320 Hz

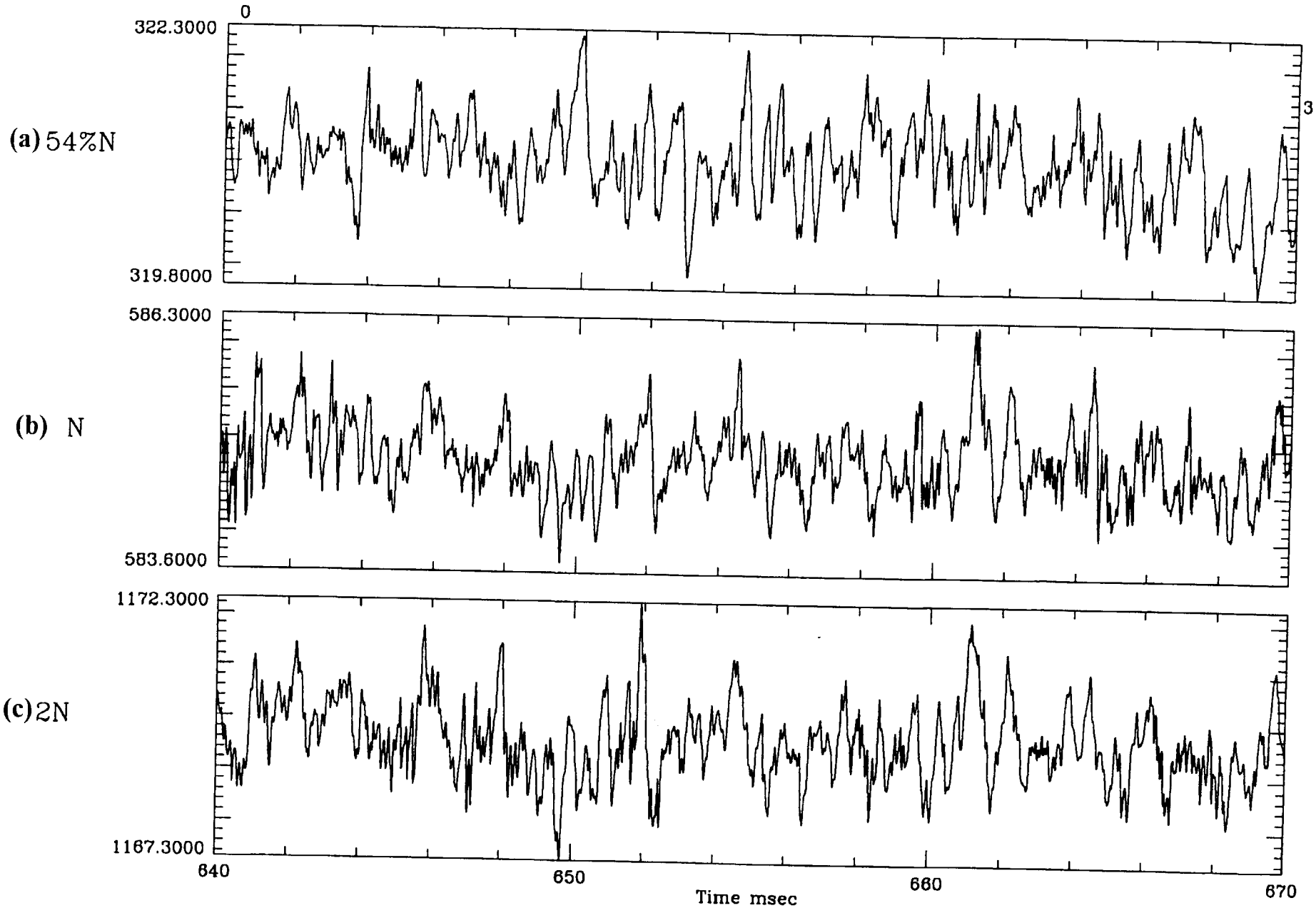

Figure 2.8.5.2 GHC instantaneous frequency signal of (a) 54%N (b) N (c) 2N showing weak GHC correlation between N and 54%N.

2.8.6 50% Sub-sync Signature Identification due to Deadband Interaction

Nonlinearity generated by rotor radial rub or deadband interaction due to insufficient clearance can generate sub-synchronous vibration. The frequency of this type of sub-harmonic vibration are would exact 1/2 , 1/3 or 1/4 of the Sync frequency. In other word, its frequency ratio with respect to Sync is maintained absolutely constant. Such constant frequency ratio applies to their micro-frequency variation of their instantaneous frequency signal. Therefore, the unique frequency synchronization with Sync is an important characteristic of this type of Sub-Sync vibration, which can be identified by the GHC technique.

An example from ATD HPFTP unit 6-4 pump is used here to demonstrate this. A failure occurred during a January 25 1995 firing test of unit 6-4 pump (test number: 9010853) at NASA Stennis Space Center. An unusual color flame was observed during the test, indicating metallic particles, and the engine was shut down 500 seconds into a 700-second test. In the subsequent teardown inspection, the first stage turbine blades and the second stage vanes and blades were found to be nearly destroyed.

Figure 2.8.6.1 shows the ADIS summary PSD taken from measurement HPFP RAD 225 of this test. An important anomaly at 50% sub-sync is observed at peak # 6 marked S1 (S1 represents 50% Sub-Sync; S2 represents 33% Sub-sync) which indicates possible rotor instability. The frequency of S1 is right at 50% of Sync (290Hz and 580 Hz). This Sub-Sync anomaly is observed at both pump and turbine end measurements. A critical question is that: is this 50%N anomaly actually correlated and frequency synchronize with the Sync due to nonlinear deadband interaction, or is it due to the sub-sync whirl whose instantaneous frequency does not correlate with Sync as discussed in last section.

The strong GHC coherence with Sync (%7) of 94% identified by the ADIS for this 50% sub-sync component provides an important clue about this anomaly. This high GHC with Sync indicates that the micro-frequency variation of the 50% Sub-Sync is highly synchronization with Sync. Figure 2.8.6.2 shows the GHC Instantaneous Frequencies (IF) of four different spectral components at 50%N, 1N, 1.5N, and 2N. The remarkable similarity among these IF signal indicates that the micro-frequency variation of the 50% sub-sync is highly lock-in or synchronized to the instantaneous frequency variation of sync. These dynamic characteristic associated with the 50% sub-sync indicates that the anomaly is more likely to be corresponding to a 50% sub-sync due to nonlinear deadband interaction, instead of the sub-sync whirl.

2.8.7 50% Sub-sync Signature Identification due to Whirl

As discussed in the last two sections, sub-sync vibration are important anomalous phenomenon for machinery diagnostics. Even though both phenomenons will generate similar spectral component in the PSD, there exists an important discriminator to distinguish between these two. The 50% sub-sync vibration due to deadband interaction is frequency synchronized with Sync (i.e. Strong GHC with Sync); while 50% sub-sync whirl is not frequency synchronized with Sync. When frequency of whirl becomes very close or even right at 50%N, it would be very difficult to distinguish them from their

spectrum. However, the dynamic characteristic identified by ADIS would provide valuable clue.

Figure 2.8.7.1 shows such an example. The PSD is taken from measurement HPFP RAD 225 of SSME test 9010892. Again, . An important anomaly at 50% sub-sync is observed at peak # 6 marked S1, which indicates possible rotor instability. . The frequency of S1 is right at 50% of Sync (285Hz and 570 Hz). Based on this spectrum, it would have been judged to be a exact 50% sub-sync due to deadband interaction. However, the ADIS summary PSD shows that the GHC coherence with Sync (%7) of this 5o% sub-sync component is only 13%. This indicates that the micro-frequency variation of the 50% Sub-Sync is not synchronization with Sync. Therefore, it should be a sub-sync whirl rather than an exact 50% sub-harmonic. Figure 2.8.7.2 shows the instantaneous frequency signal of 50%N, N, 1.5N and 2N respectively. The correlation between N and 2N is evident, but only very weak correlation exists between N and 50%N.

2.8.8 Composite GHC for Bearing Signature Identification

Within the bearing modulation/sideband pattern, there exists some correlation among these components, which can usually be identified by the nonlinear coherence analysis techniques. However, when only partial pattern is observed in the measurement data, it may not provide the required frequency combination or bridging for bi-coherence or tri-coherence to find such correlation within this partial pattern. In this case, the instantaneous frequency used by GHC analysis would provide critical information in identifying well-hidden bearing signatures. An example of such a well-hidden partial bearing pattern is shown in Figure 2.8.8.1 which was encountered in SSME test history.

The PSD is taken from an SSME HPOP internal Strain Gauge measurement recorded during an engine hot firing 9040079. The nominal peaks such as the 60 Hz line noise/harmonics, Sync/harmonics of HPOP have all been clearly identified by ADIS. In addition, a number of bearing-related components are also identified. These include C1 (Cage of PEBB) N2$\pm$C1, 2N2$\pm$C1, 3N2-C1, which are all supported by strong representative coherence. These cage train frequency components are normally seen in such internal measurements. However, a strong anomalous component, at 4050 Hz (peak # 34) is observed. The frequency of this anomaly does not match any bearing characteristic frequencies or modulation/sideband components. In order to assess if this anomaly is bearing related, the ADIS will further search for the correlation between the anomaly and the Sync/cage frequency.

The ADIS perform such Composite GHC analysis by first search for the existence of Cage component with strong supporting representative coherence. Then based on the best Sync and Cage components (with highest SNR and coherence) which can be found among various channels and harmonics (which are also listed in the ADIS summary plot). The ADIS will correlate the IF signal of the anomaly against various combination of IF signal of sync and cage. If a strong correlation is found, the ADIS will list it in the summary plot under the Composite GHC (CGHC).

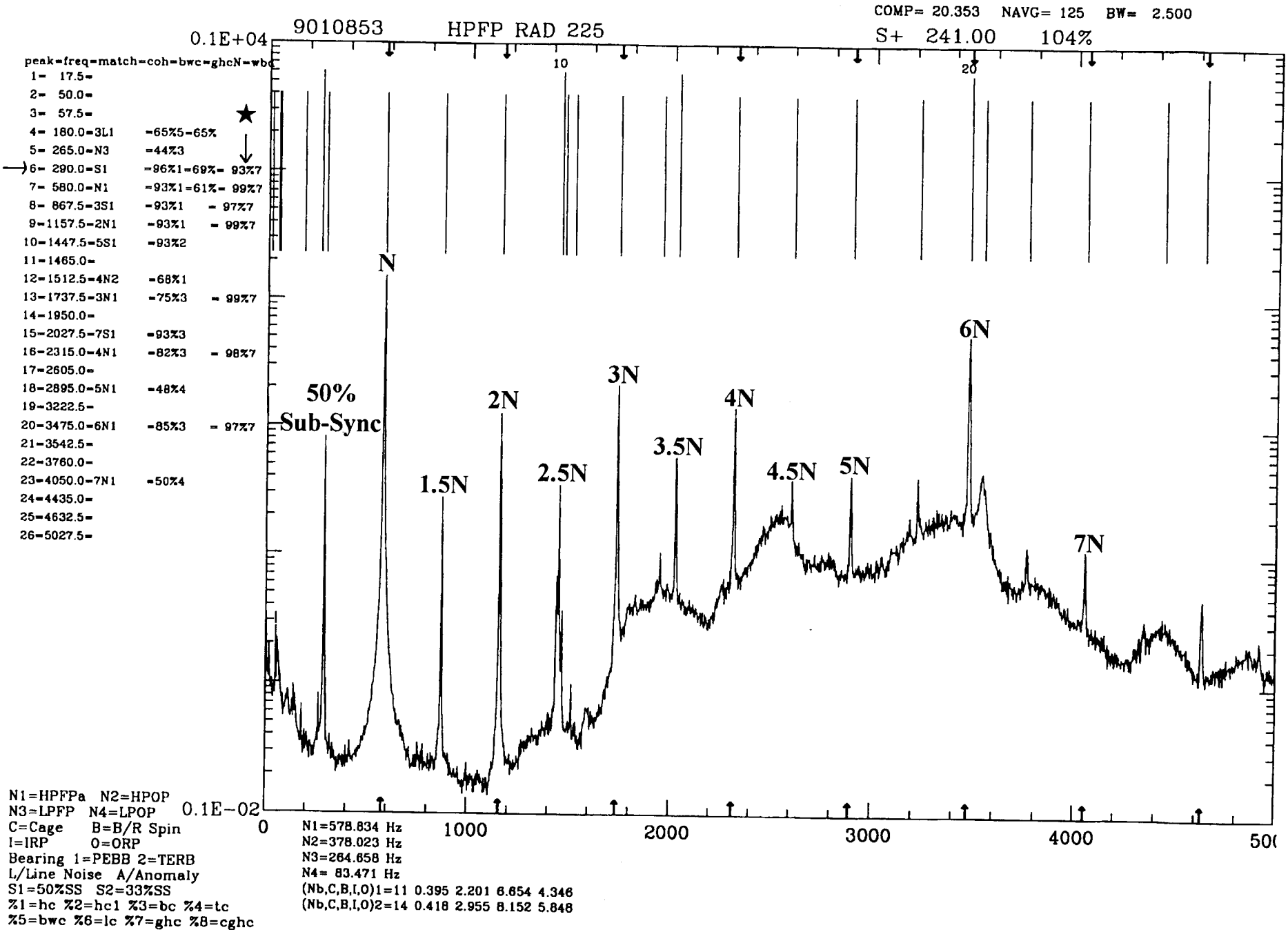

Figure 2.8.6.1 ADIS PSD: Exact 50% Sub-Sync Anomaly (S1) at 290 Hz

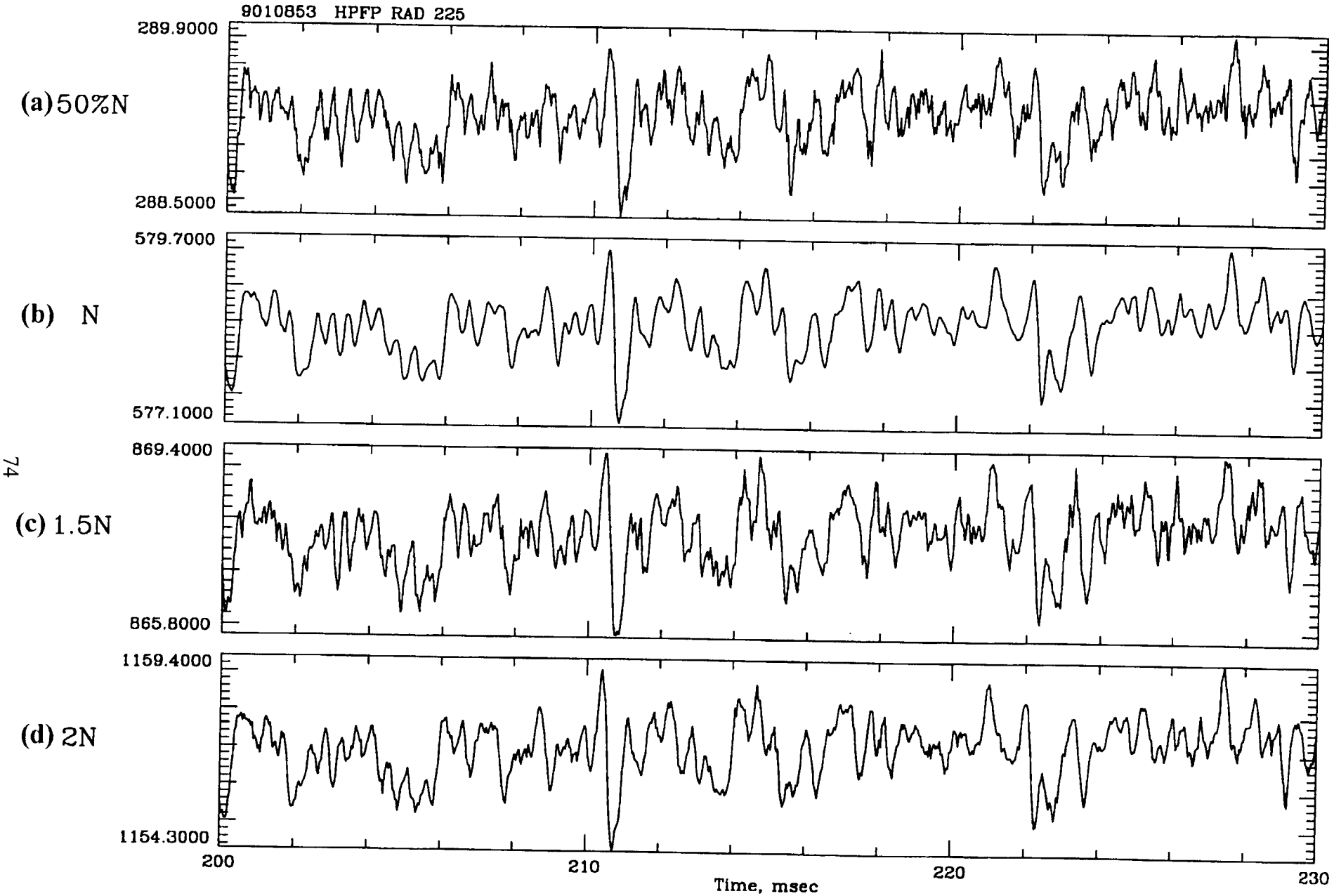

GHC Instantaneous Frequency

Figure 2.8.6.2 GHC instantaneous frequency of (a) 50%N (b) N (c) 1.5N (d) 2N showing strong GHC correlation between N and 50%N.

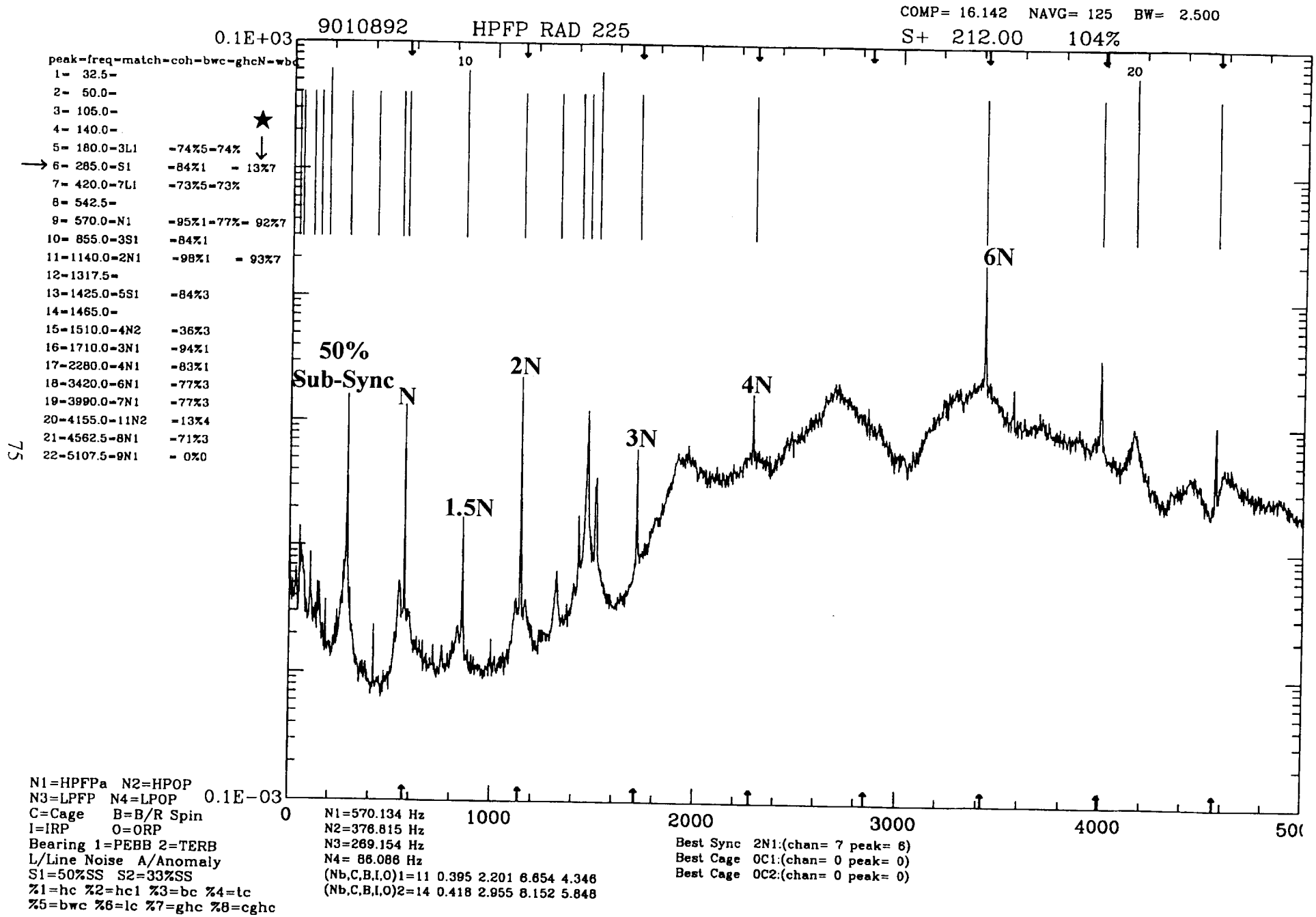

Figure 2.8.7.1 ADIS PSD: Exact 50% Sub-Sync Anomaly (S1) at 285 Hz

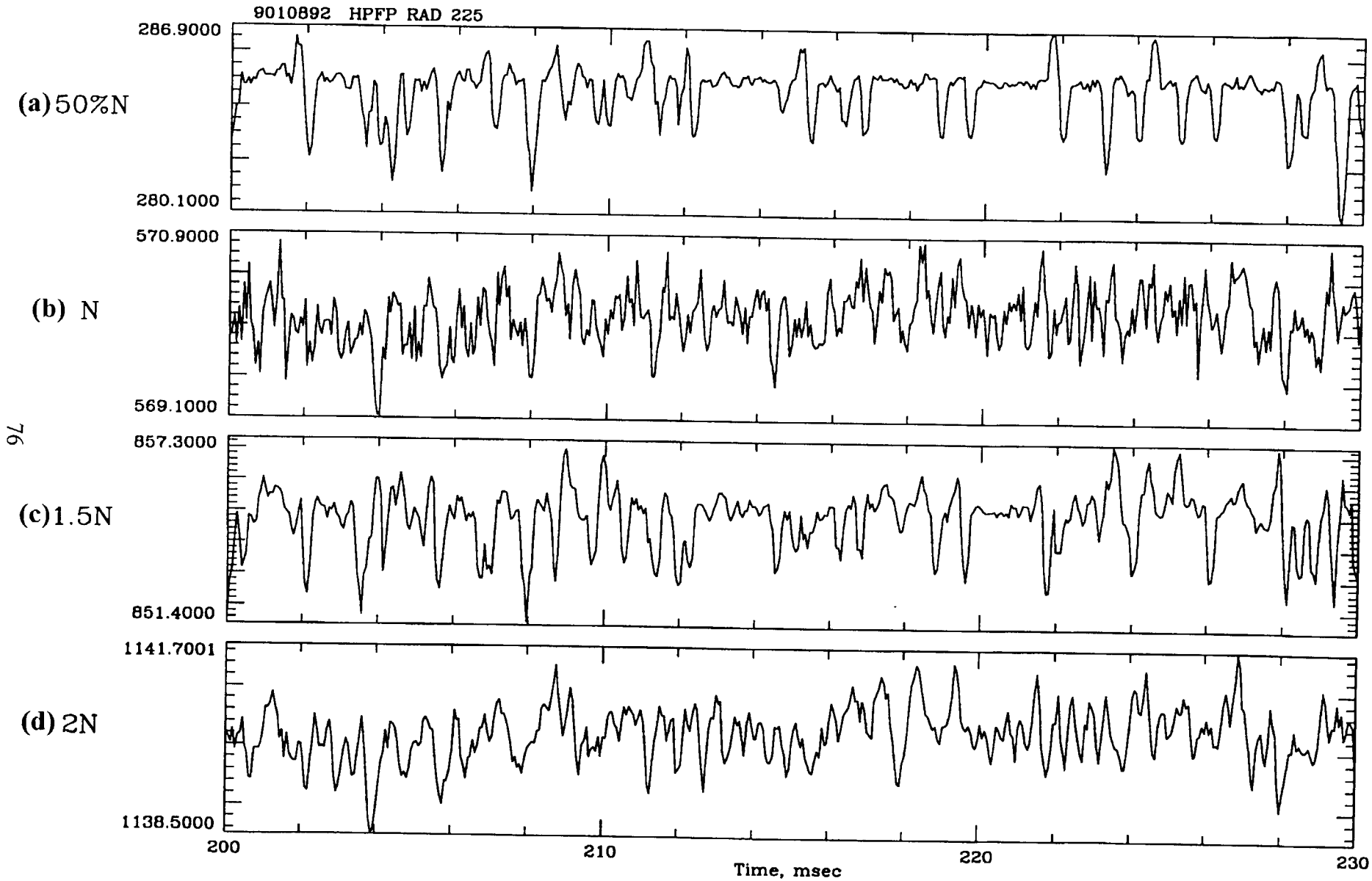

Figure 2.8.7.2 GHC instantaneous frequency of (a) 50%N (b) N (c) 1.5N (d) 2N showing weak GHC correlation between N and 50%N.

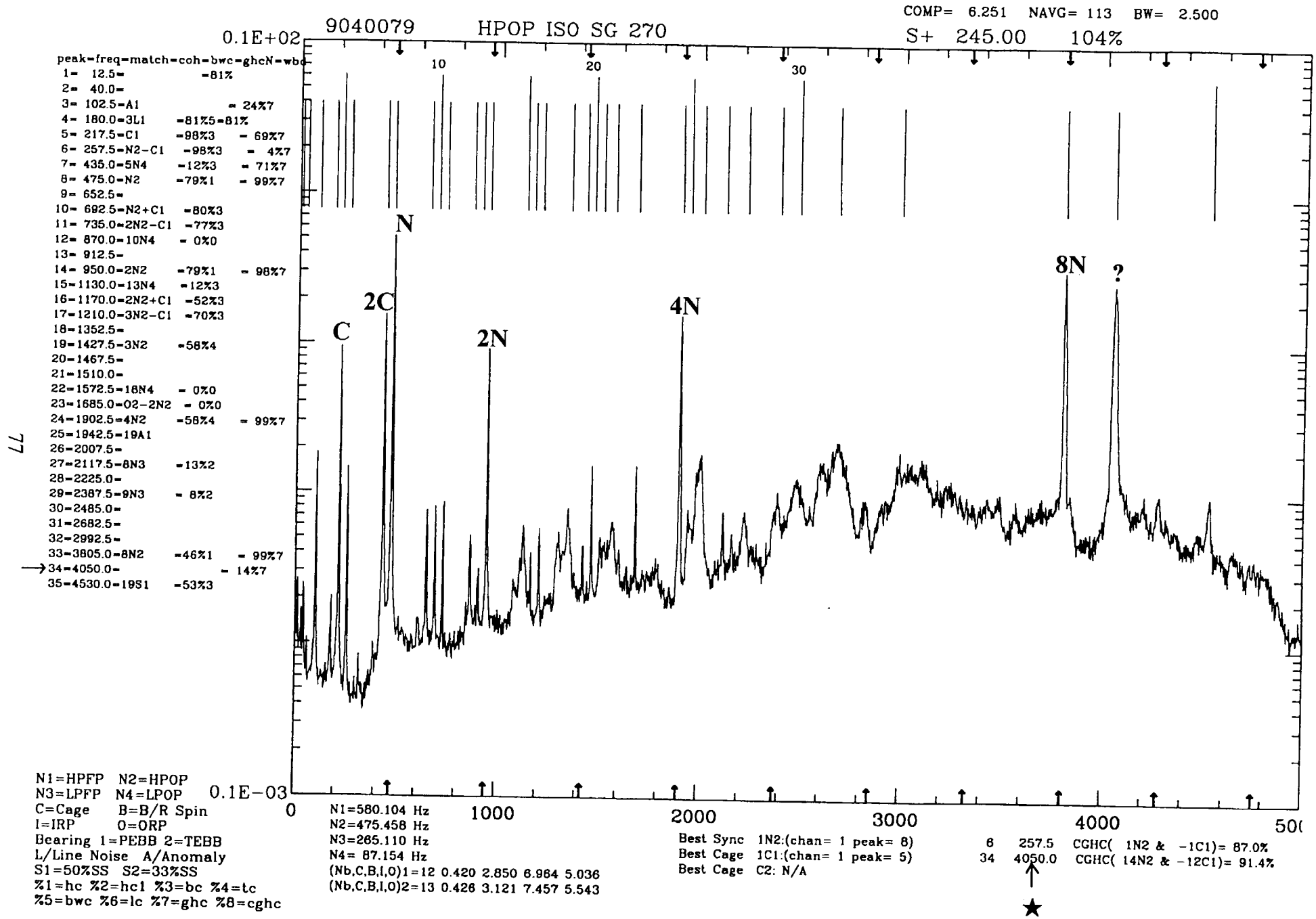

Figure 2.8.8.1 ADIS PSD: Strong Anomaly at 4050 Hz

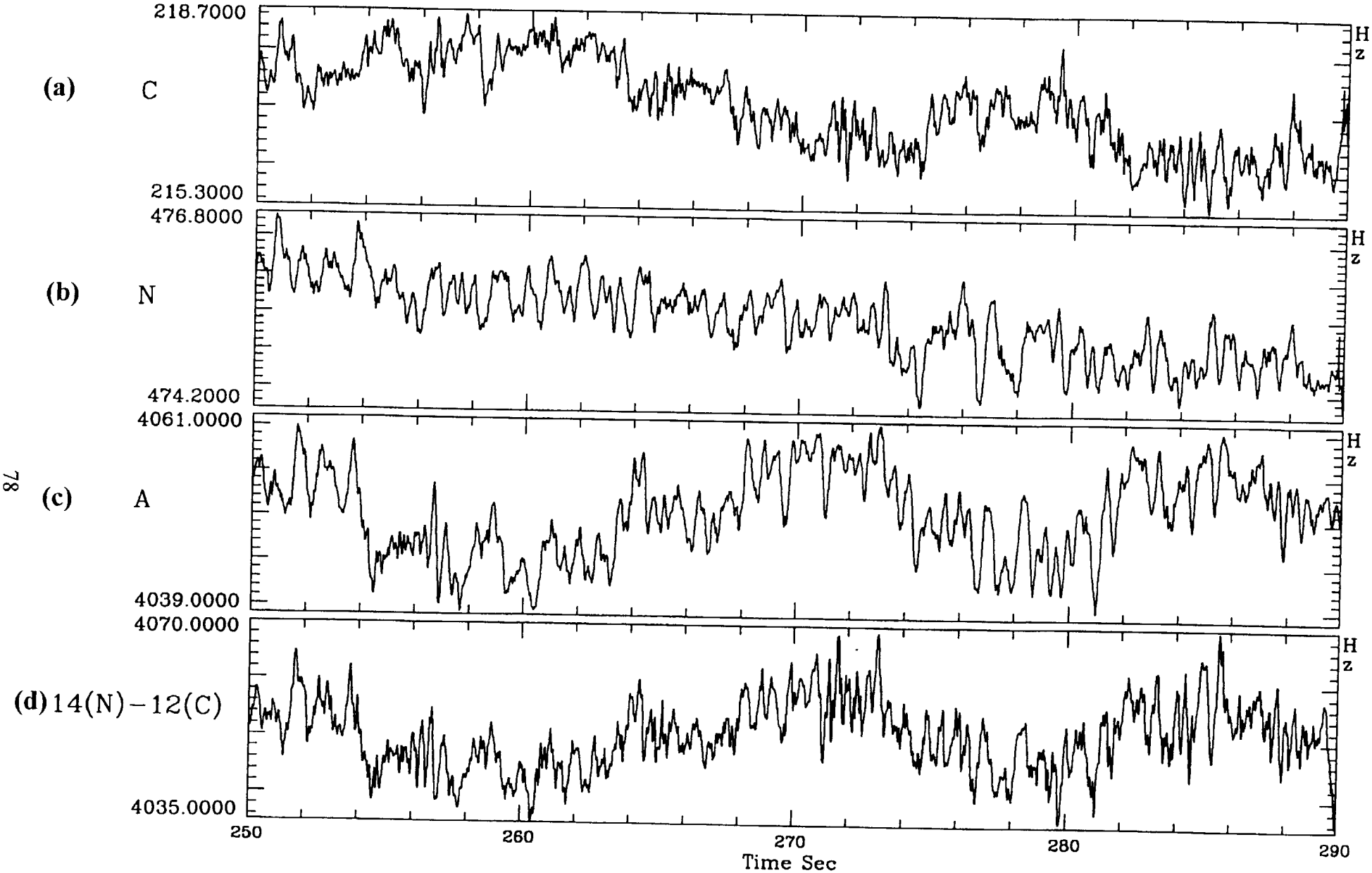

GHC IF SIGNAL 9040079 HPOP ISO SG 270

Figure 2.8.8.2 GHC instantaneous frequency (IF) of (a) C (b) N (c) A (d) 14N-12C showing Strong Composite GHC correlation between A and the reconstructed Composite IF Waveform.

Two such CGHC correlated are found in Figure 2.8.8.1, which are listed near the lower right corner. The first one is at 257.5 Hz (peak # 6), whose CGHC with N2-C1 is 87%. This indicates that it is a modulation component of N2-C1, which is already been identified by its representative bi-coherence of 98%. The second one is the strong anomaly at 4050 Hz (peak # 34), whose CGHC with 14N2-12C1 is 91%.

Since 14N2-12C1 equals 12(N2-C1)+2N2, which also equals I1+2N2 (note: 12(N2-C1) = Inner Ball Pass for this PEBB of 12-ball bearing set). This CGHC correlation indicates that the anomaly is actually a member of the modulation/sideband pattern between the inner ball pass component and Sync: I1$\pm$?N2. Since all the rest component (such as I1, I1$\pm$N, I1-2N, etc.) within this pattern are not shown in the PSD, it is difficult to identify such isolated signature using the bi- and tri-coherence analysis. However, the Composite GHC analysis performed by ADIS can provide addition insight in identifying such well-hidden bearing signature.

Figure 2.8.8.2 show the detailed information the Composite GHC analysis involves. Figure 2.8.8.2(a), (b) and (c) depict the IF signals of cage frequency "C1", the SYNC frequency "N2" and the anomalous frequency "A". Figure 2.8.8.2(d) shows the summation of 14 times the IF signal of "N2" minus twelve times the IF signal of "C1". Comparison of the reconstructed composite IF waveform (Figure 2.8.8.2(d)) with the IF signal of "A" (Figure 2.8.8.2(c)) reveals a strong correlation between the two Figuress. Therefore, anomaly "A" is a true bearing signature being generated from the modulation of the inner ball pass frequency at I1=12(N2-C1) with 2 times Sync (2N2). Again, all these detailed analysis and information are automatically performed by ADIS in the background with only the final CGHC information listed in the summary plot.

2.8.9 Cavitation Signature Identification using Wideband Modulation (WBD)

The so-called "330 Hz Anomaly" (LPFP) has been frequently observed on the SSME LPFP accelerometer data over the SSME test history. The frequency of the 330 HZ anomaly has a wandering characteristic and occasionally moves down into the LPFP Synchronous frequency range (260-270 Hz), causing a few pump to have abnormally high vibration. Dynamic analysis performed by correlating and comparing and trending the anomaly and pump performance data indicates that the 330 Hz anomaly should be a hydrodynamic-related phenomenon rather than structural or rotor dynamics. However, the source of this hydro-related anomaly was not clearly identified.

The Wideband Demodulation technique discussed in section 2.3 can be used to detect the existence of so-called "wideband modulation" phenomenon usually generated in the dynamic signal associated with pump cavitation. Figure 2.8.9.1 shows the raw PSD Topo of the external accelerometer measurement, LPFP RAD 330 ACC of SSME test 9040261. The dominant spectral components in this PSD include the Sync (N) and Sync harmonics (2N, 3N & 4N) along with the 60 Hz line noise and its harmonics. In addition, the 330

Hz anomaly (marked "T") and its modulation with sync (e.g. 4N ± T, 2N+T, etc.) are also present.

Figure 2.8.9.2 shows the ADIS summary PSD plot of this measurement. Again, most of the line noise, sync/harmonics and feedthru components are clearly identified. The "330 Hz" anomaly tagged as A1 at 352.5 Hz (peak # 10) are shown without any supporting coherence. However, the ADIS attaches an important parameter to this anomaly. This parameter represents the SNR (in dB) of this component in its corresponding WBD PSD. Two components at 352.5 Hz (A2) and 1015 Hz (4N3) are found to possesses strong WBD signature. Figure 2.8.9.3 and Figure 2.8.9.4 show the information processed in the background by ADIS, which represent the ordinary raw PSD along with WBD PSD; and the Topo plot of WBD PSD.

This results indicate that hidden periodicities at 352 Hz, 4N and 4N+352 Hz due to wide band modulation phenomenon indeed exists at this measurement data. In addition, the periodic modulating components which modulate the wideband noise due to cavitation bubble collapsing are composed of the 4N component along with the 352 Hz and 4N+352 Hz anomalies. This indicates that full-blade cavitation condition could be present during the period of the steady state operation. Furthermore, the 352 Hz anomaly should also be associated with the cavitation phenomenon as the nonsynchronous-related modulating component with the wide band bubble noise. Such nonsynchronous-related modulating component associated with cavitation phenomenon was also observed in other pump test data such as the ATD HPFP 6N sideband anomaly, and ATD HPOP Inducer test from MSFC Water Flow Test. However, the mechanism of such non-synchronous cavitation signature is still not clearly understood.

It should be pointed out that, the existence of wideband modulation phenomenon do not necessarily guarantee it is a cavitation signature since other mechanism could also generate similar WBM phenomenon. However, pump cavitation is known to exhibit such unique dynamic characteristic of hidden periodicity, the WBD information identified by ADIS can provide additional clue and/or evidence about the source of an anomaly.

2.8.10 Line Noise Modulation Signature Identification using WBD

As just mentioned, other mechanisms could also generate wideband modulation phenomenon in the dynamic measurement signal. Therefore, the interpretation of such WBD dynamic characteristic identified by ADIS may not be quite straightforward. Figure 2.8.10.1 shows another example involving wideband modulation phenomenon in vibration signal. The PSD Topo is taken from SSME Main Engine #2 HPFP Accel measurement during actual shuttle flight STS060. The peak marked N is the Sync of HPFP, and the two peaks marked α and 2α are anomaly α and its 2nd harmonic. Notice that, the frequency of the anomaly α at 35 Hz is maintained quite constant throughout the entire flight period regardless of power level changes. This usually indicates it is a line noise component or other non-sync related component totally independent of the rotor system. However, the two sideband around Sync marked N-α and N+α indicates that this

anomaly α also modulate with the Sync N. Similar phenomenon is observed in another measurement as shown in the PSD Topo plot in Figure 2.8.10.2. In this measurement, a line noise component β with constant frequency at 120 Hz also modulate with Sync and generate $N\pm\beta$ sideband components. Since any sideband phenomenon around Sync is always considered to be alarming signature, the source of this anomaly must be further identified. Such modulation between α/β and sync is further verified by the strong bi-coherence between them as shown in Figures 2.8.10.3(b) and 2.8.10.4(b). These two observations seem to contradict with each other, since it does not make sense to have an electrical generated line noise to selectively modulate certain frequency component (Sync) within a mechanical generated signal.

Figure 2.8.10.5 and Figure 2.8.10.6 show the ADIS summary PSD plots of these measurements. Again, many nominal sync/harmonics, feedthru and even some bearing modulation components are identified. However, the strong of WBD SNR at both α and β frequencies (12 dB and 9 dB respectively) show that both α and β do possess strong WBD phenomenon. This indicates that, electrically generated line noise components, α and β, are actually modulating the entire vibration signal rather than just selectively modulating the Sync frequency component within the mechanical generated signal as it appears to be. Even though the exact reason that cause electrical line noise to modulated the entire vibration signal is not understood, this wideband modulation mechanism as indicated by the WBD parameters of α and β provides a more reasonable explanation about the source of the $N+\alpha$ and $N+\beta$ sideband anomalies. Figure 2.8.10.7 and Figure 2.8.10.8 show the Topo plot of WBD PSD; processed by ADIS in the background.

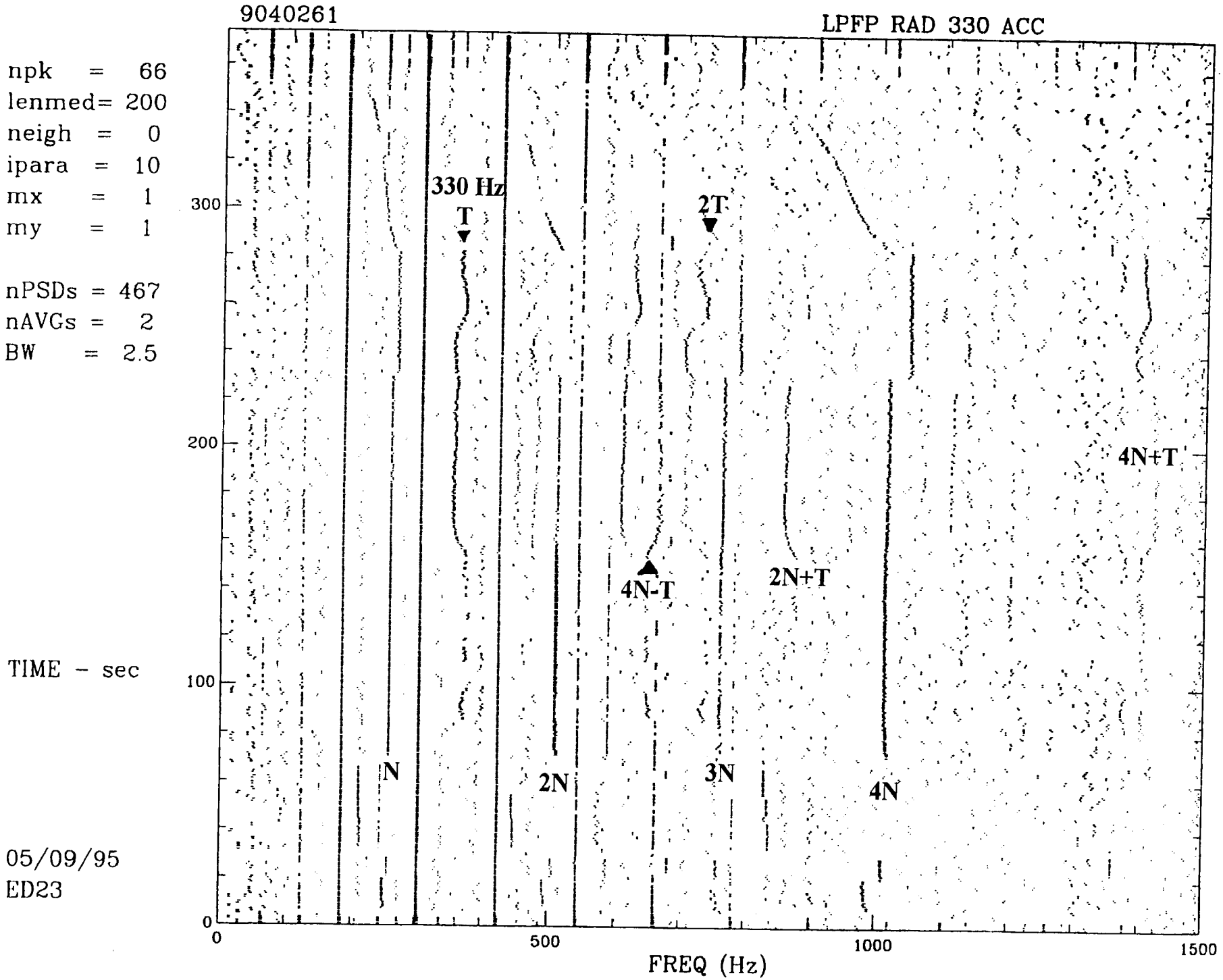

Figure 2.8.9.1 Raw PSD Topo: The 330 Hz anomaly (T) and its modulation with sync (4N ± T, 2N+T)

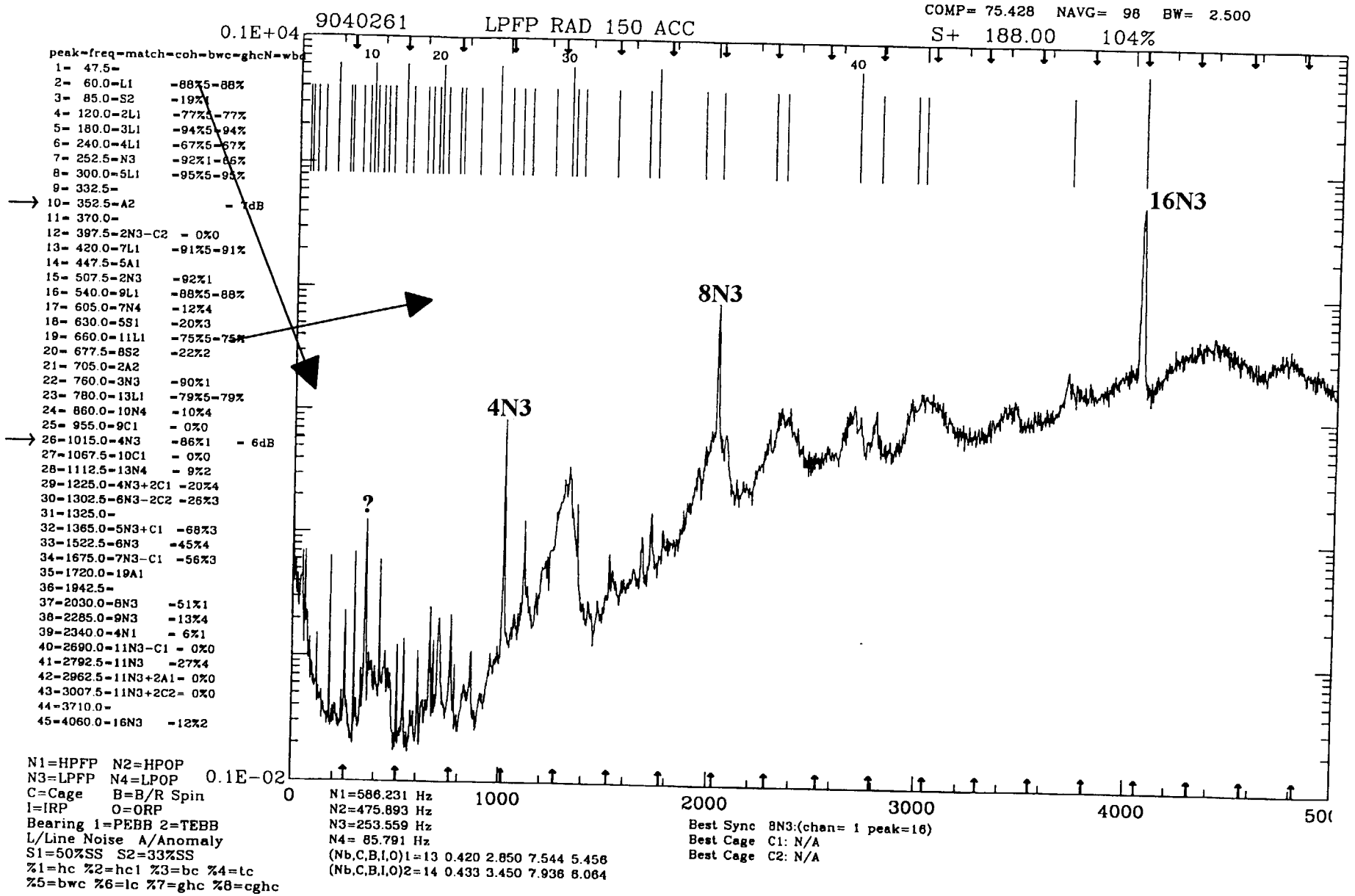

Figure 2.8.9.2 ADIS PSD: Strong WBD SNR at A2 and 4N3 indicating Wideband Modulation Phenomenon due to potential Cavitation-Induced Vibration

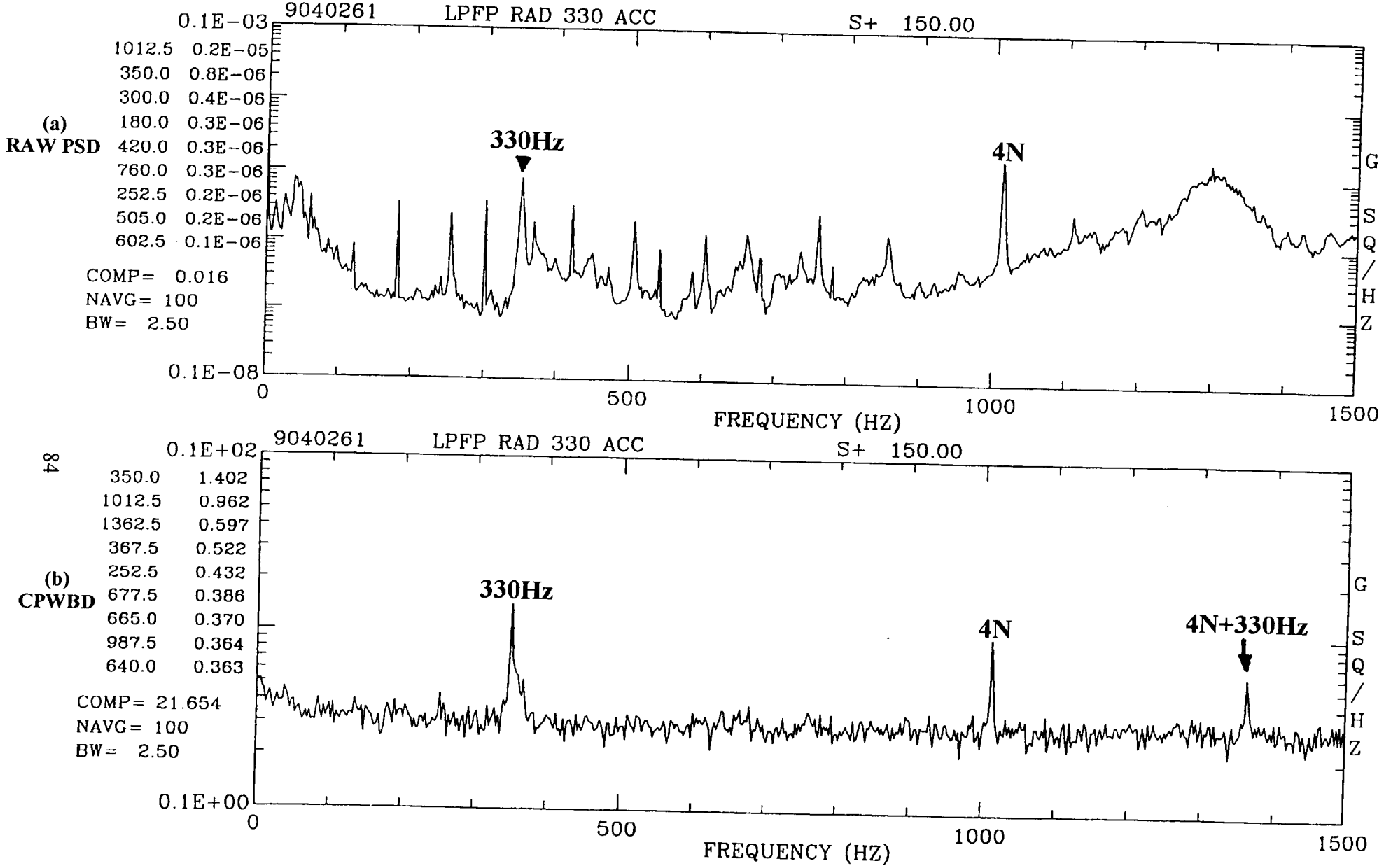

Figure 2.8.9.3 WBD PSD: Strong WBD SNR at A2, 4N3 and 4N3+A2

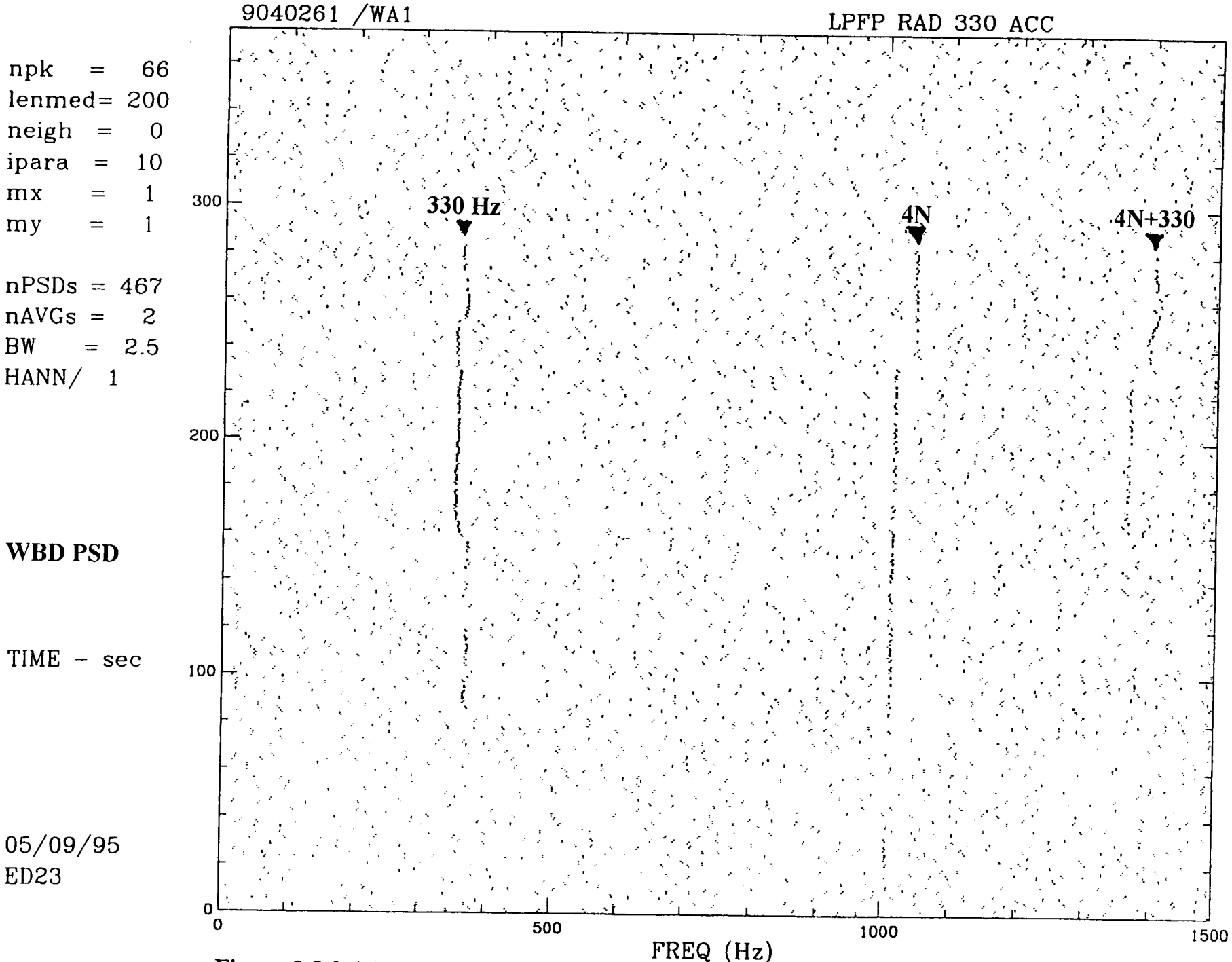

Figure 2.8.9.4 WBD PSD Topo: WBD Signature at A2, 4N3 and 4N3+A2

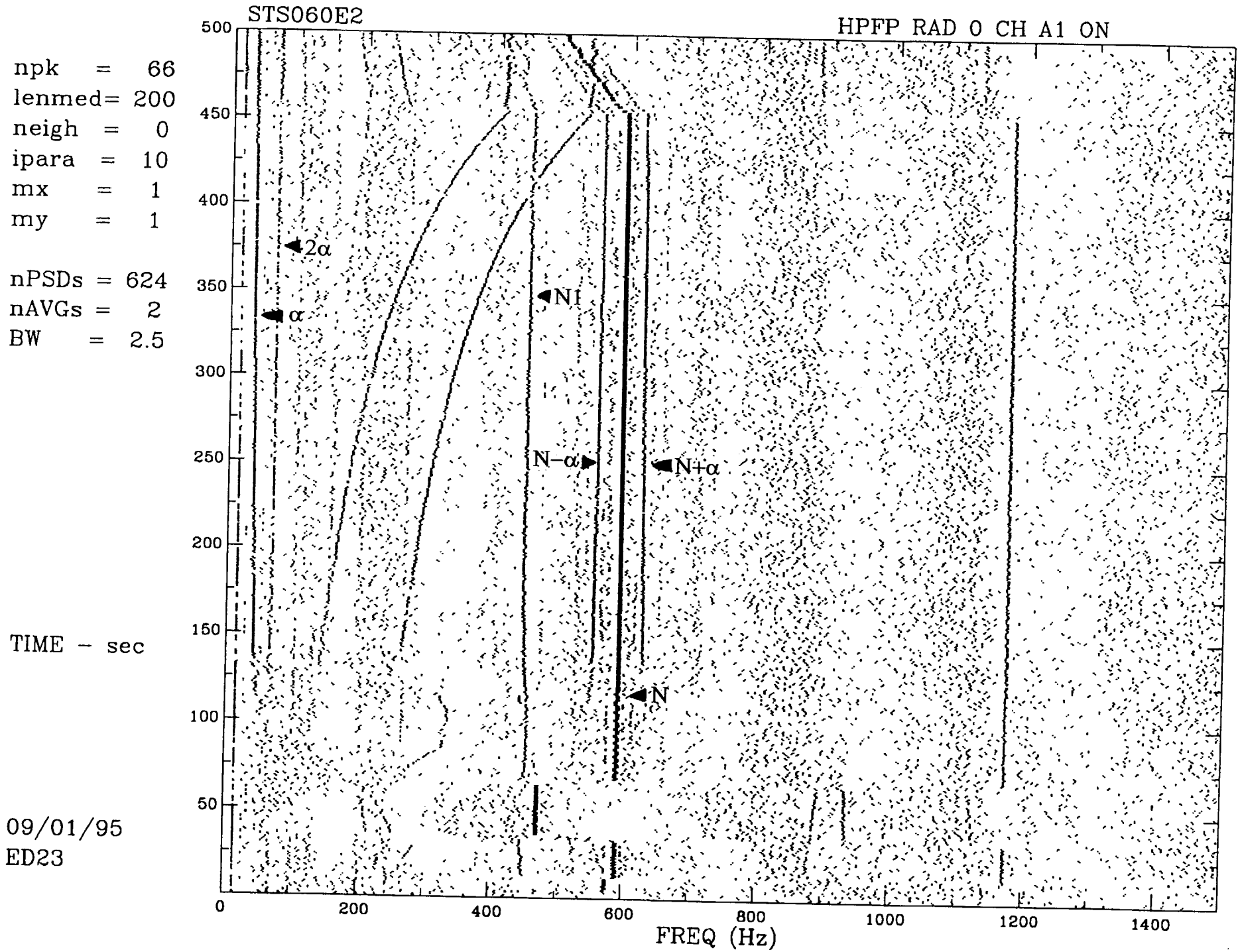

Figure 2.8.10.1 Raw PSD Topo: Electrical Noise α at 35 Hz and Modulation sideband at N-α and N+α

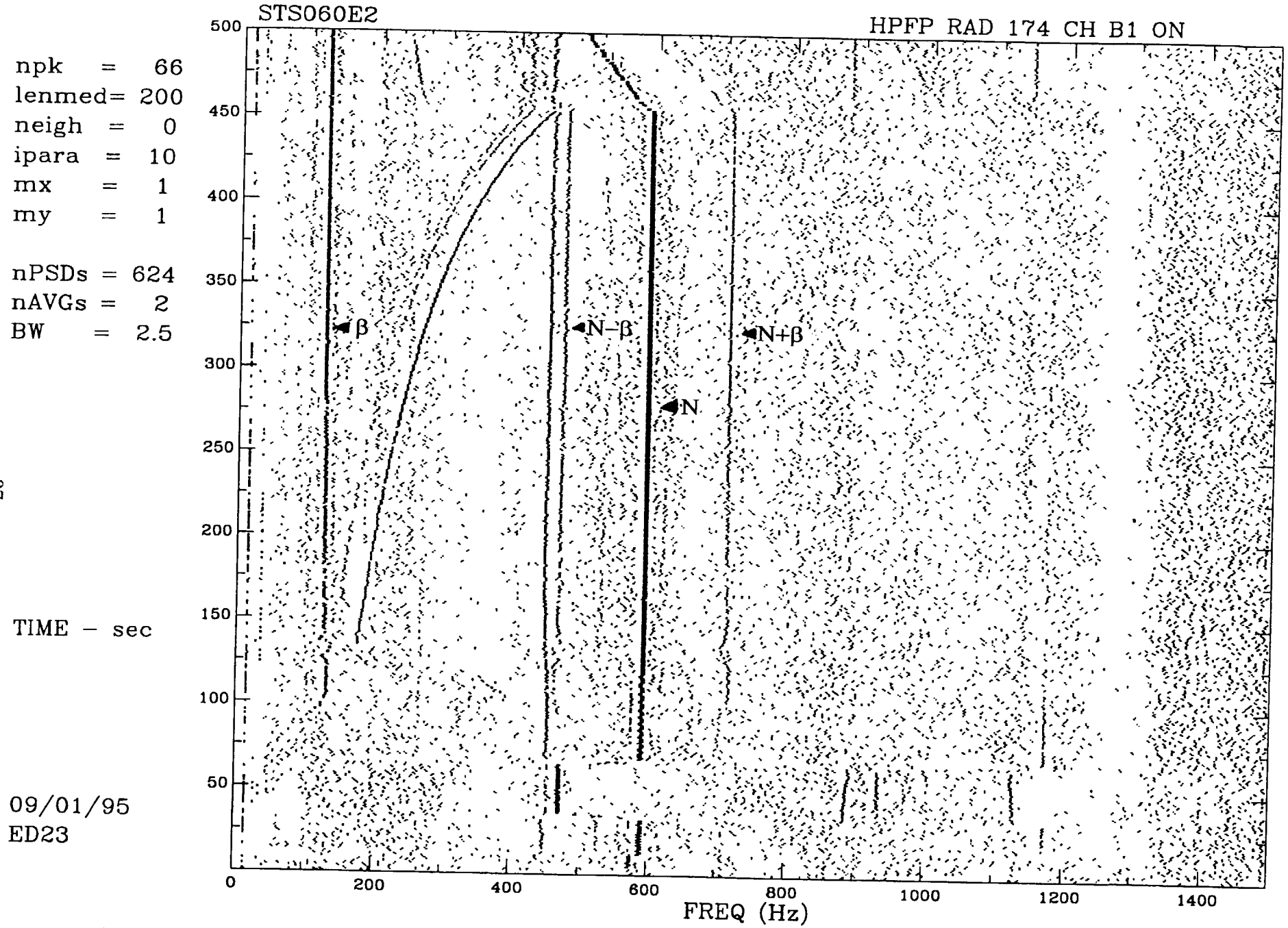

Figure 2.8.10.2 Raw PSD Topo: Electrical Noise β at 120 Hz and Modulation sideband at N-β and N+β

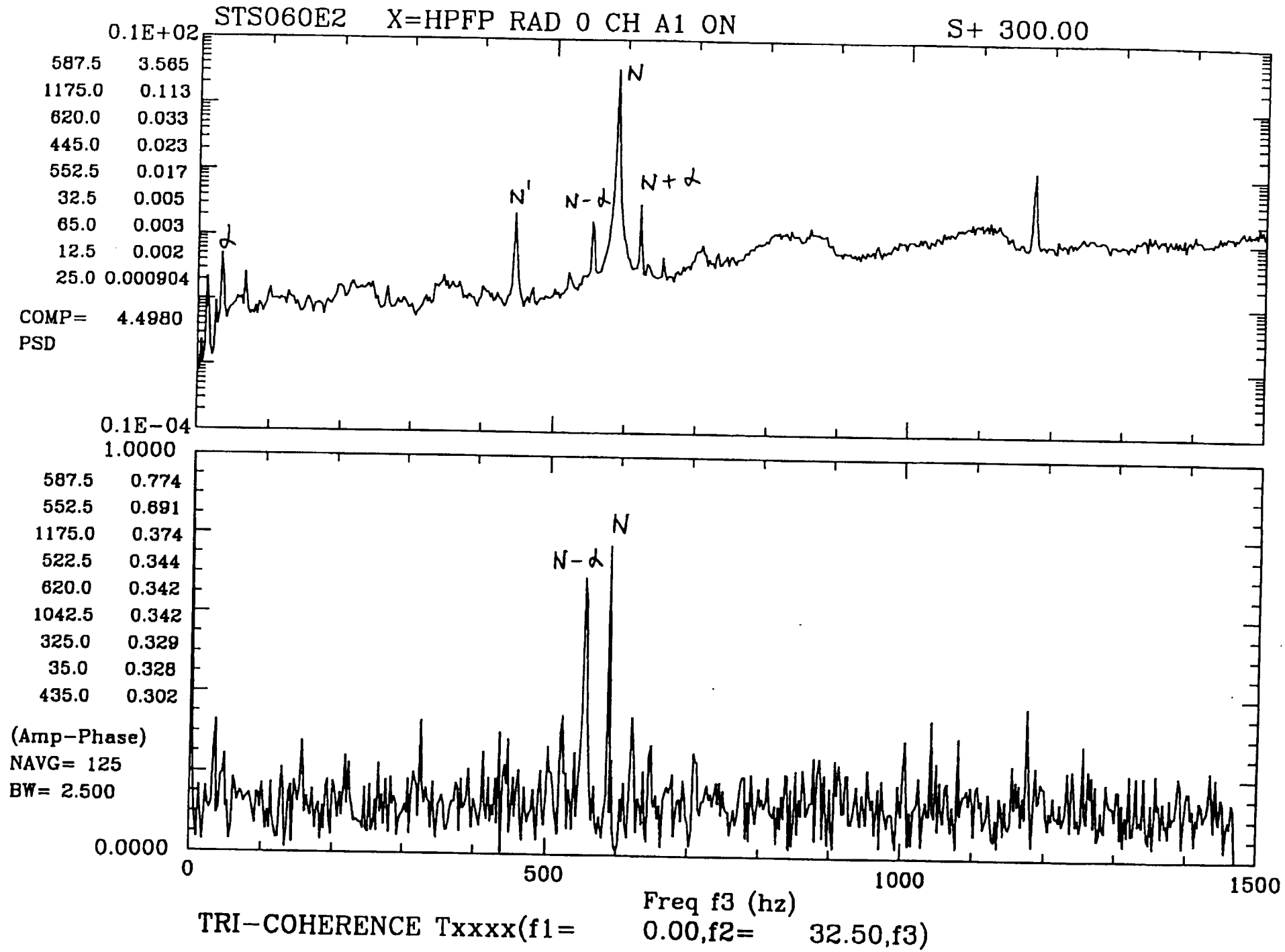

Figures 2.8.10.3(a) PSD (b) Bi-Coherence: Showing strong correlation between anomaly α and Sync (N)

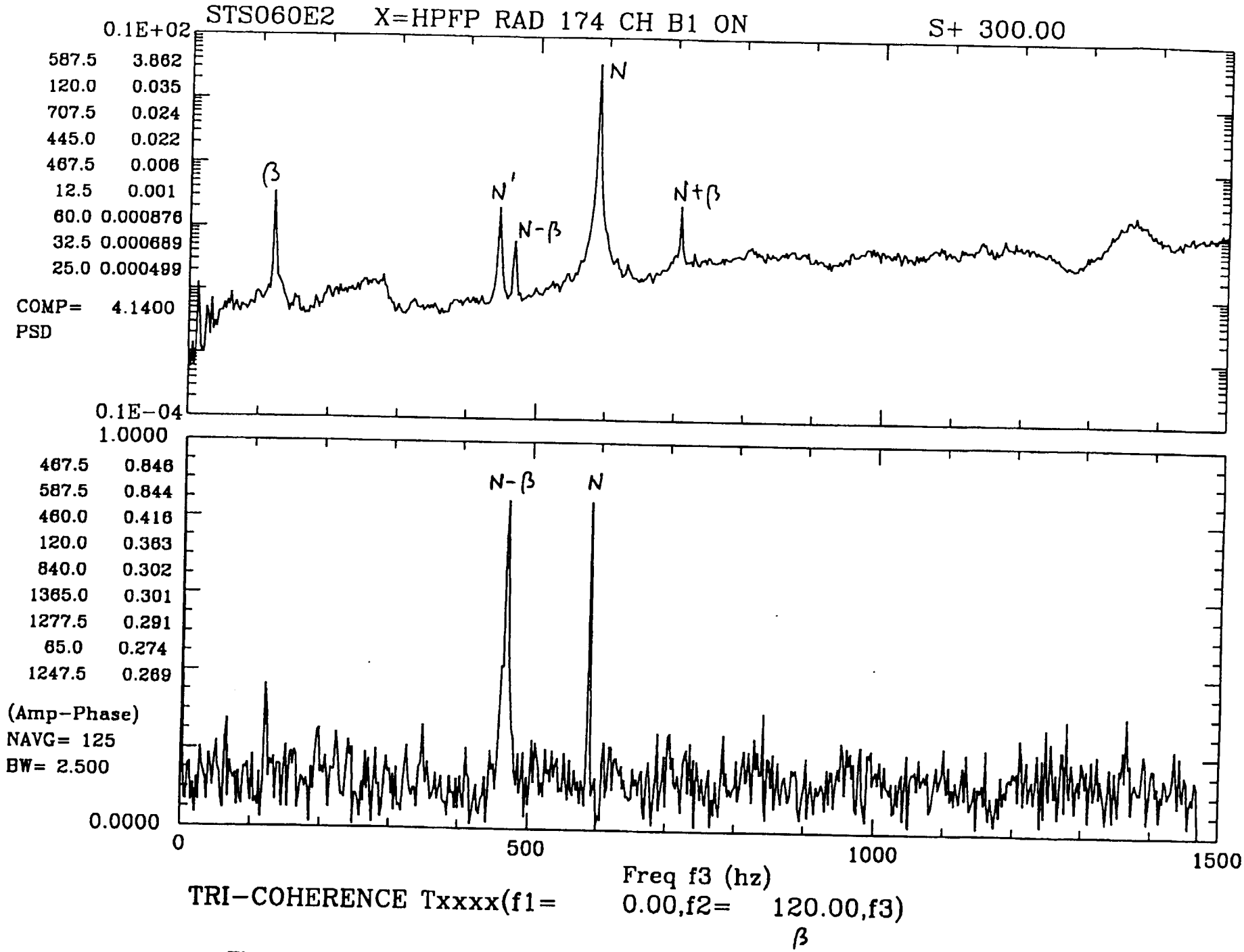

Figures 2.8.10.4(a) PSD (b) Bi-Coherence: Showing strong correlation between anomaly β and Sync (N)

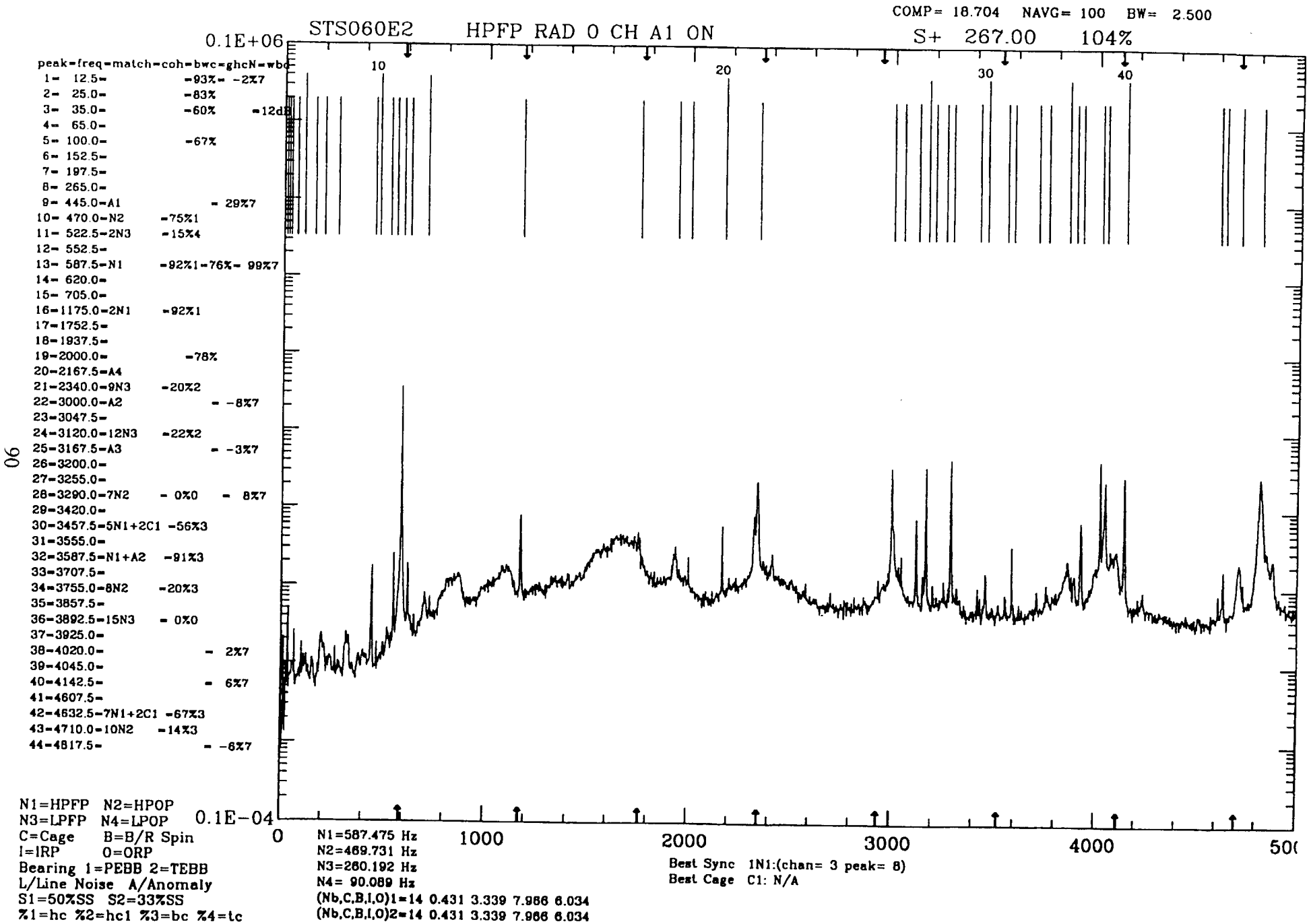

Figure 2.8.10.5 ADIS PSD: Strong WBD SNR at α indicating Wideband Modulation Phenomenon between α and the entire vibration signal

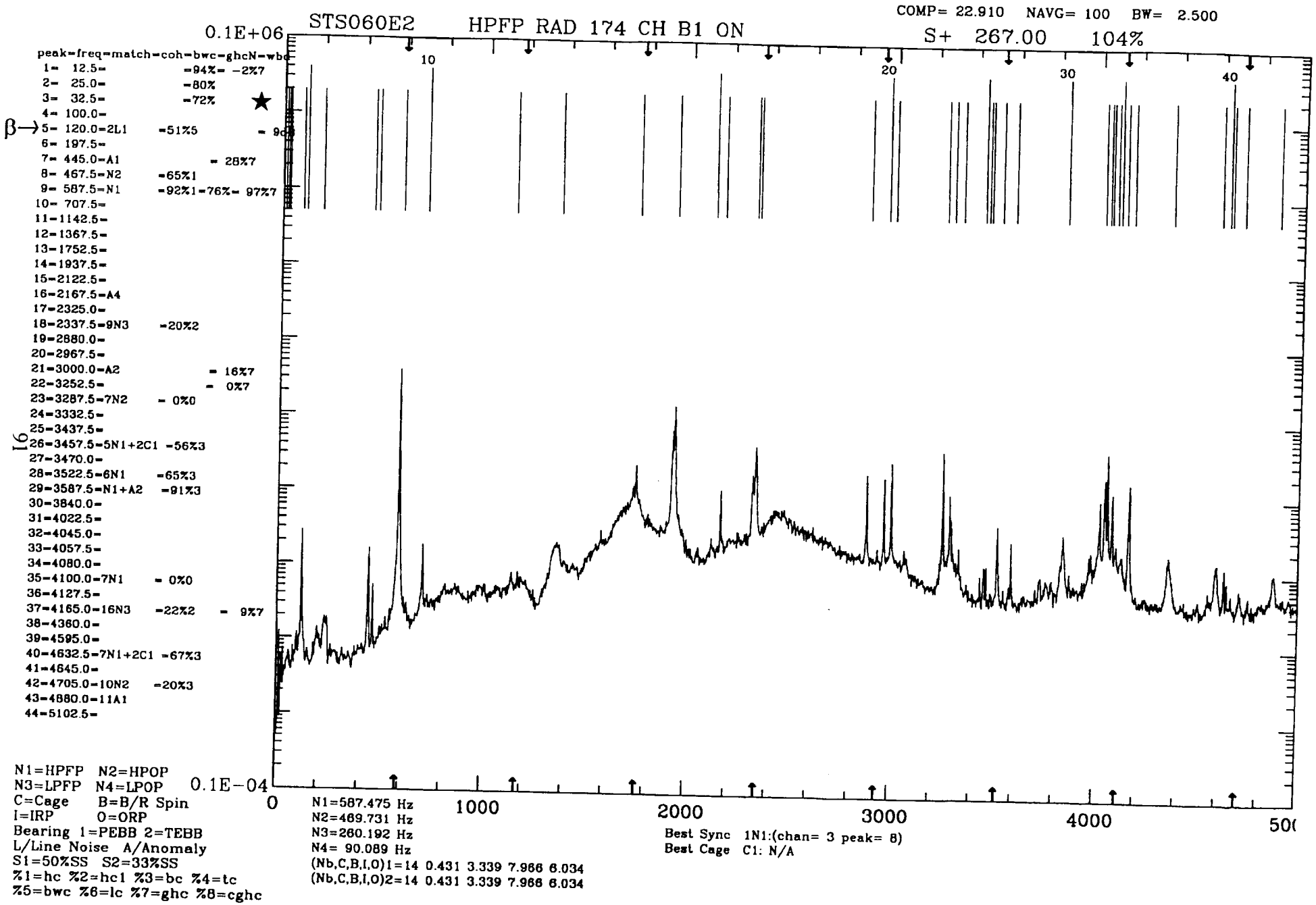

Figure 2.8.10.6 ADIS PSD: Strong WBD SNR at β indicating Wideband Modulation Phenomenon between β and the entire vibration signal.

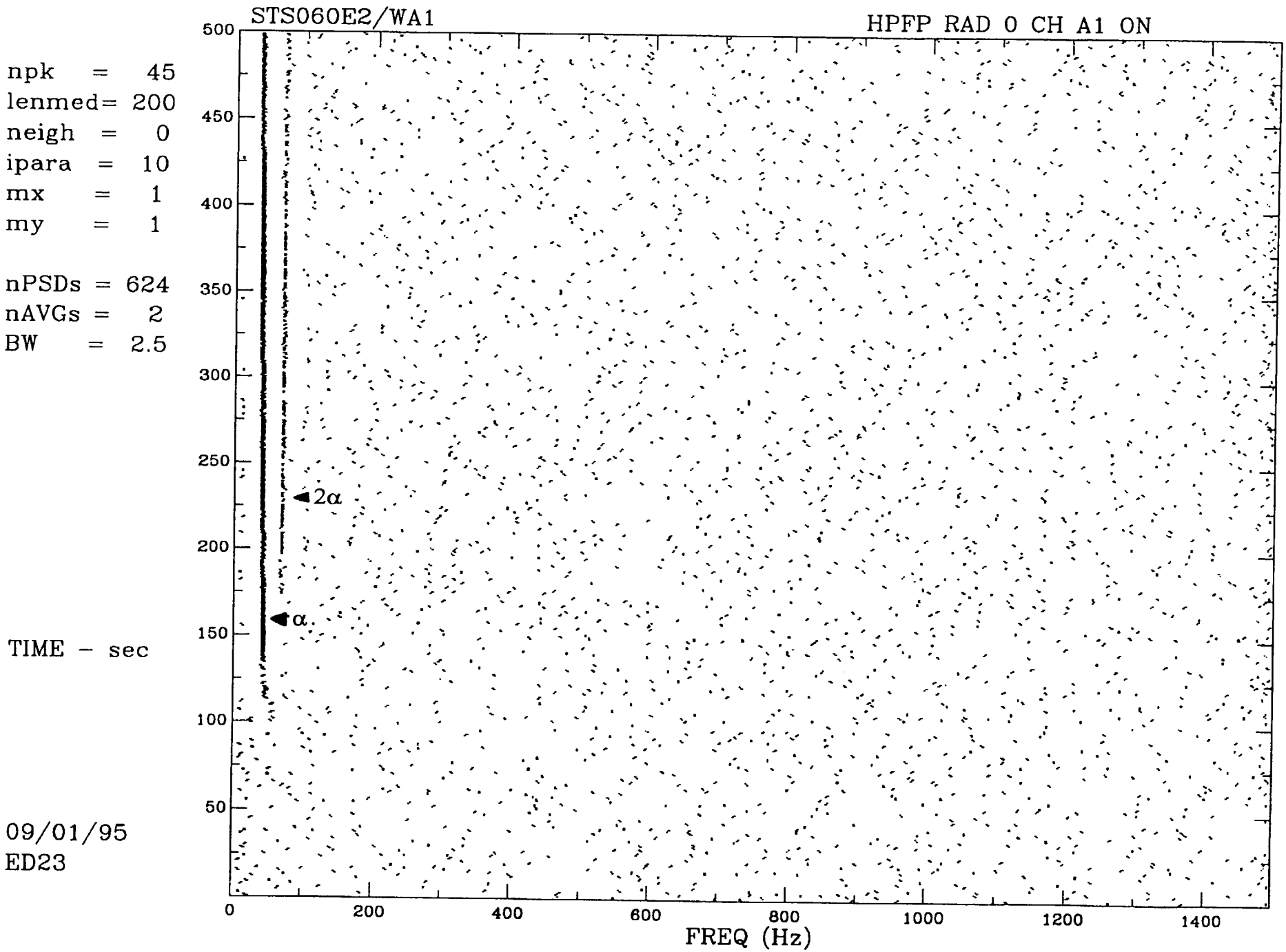

Figure 2.8.10.7 WBD PSD Topo: WBD Signature at α and 2α.

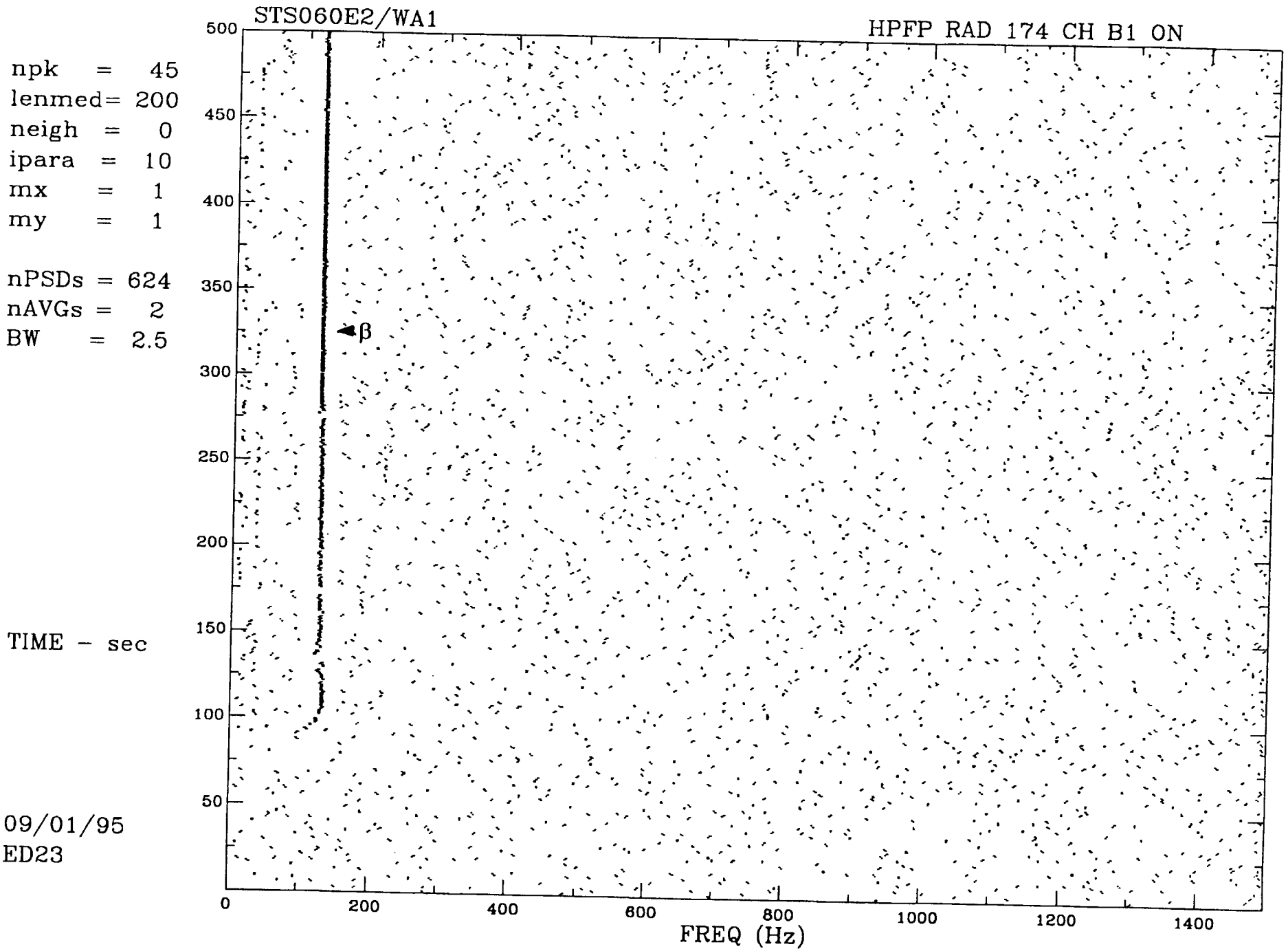

Figure 2.8.10.8 WBD PSD Topo: WBD Signature at β.

REFERENCE:

[1] Tandon, N. and Nakra, B. C., "Defect Detection in Rolling Element Bearings by Acoustic Emission Method", Journal of Acoustic Emission, Volume 9, NO. 1.

[2] Rose, H. J., "Diagnostic System Research Applicable to Helicopter Transmissions", 44th MFPG Meeting, Cavalier Hotel, Virginia Beach, Virginia, USA, April 1990

[3] Gadd, P., "The Integration of health Monitoring Techniques for Helicopter gearboxes", eleventh European Rotor Craft Forum, London, England.

[4] Stewart, R. M. et al, "Monitoring of Rotorcraft Dynamic Systems", Stewart Hughes Ltd. Document SHL/162, February 1985.

[5] Astridge, D. G., "Helicopter Manufacturer's Requirements and Experience with Advanced HUM Systems on Westland Helicopters", IMechEng Aerospace Industries Division Publication, Health and Usage Monitoring in Helicopter Mechanical Systems, April 1986.

[6] Astridge, D. G., "Vibration Health Monitoring of the Westland 30 Helicopter Transmission - Development and Service Experience", 41st MFPG Meeting, NATC Patuxent River, Maryland, USA, October 1986.

[7] Broyles, W. R. and M. A. Deatt. "Analysis of bandpass Signal on the HP Fourier Analyzer", GE Technical Information Series, NO. 80, POD3, 1980.

[8] Ktonas, W. R., Nicola Papp "Instantaneous Envelope & Phase Extraction from real Signal: Theory, Implementation, & Application to EEG Analysis", Signal Processing, Vol 2, NO. 4, Oct. 1980.

[9] Jong J., Jones J., Jones P., Nesman T., Zoladz T., Coffin T., "Nonlinear Correlation Analysis for Rocket Engine Turbomachinery Vibration Diagnostics", 48th Meeting of the Mechanical Failure Prevention Group (MFPG). April, 1994.

[10] Jong J. Y. and Coffin T., "Diagnostic Assessment of Turbomachinery by the Hyper-Coherence Method", NASA Conference Publication 2436, Advanced Earth-to-Orbit Propulsion Technology, May 1986.

[11] Jong J. Y. and Coffin T., "A Nonlinear Coherence Function and Its Application to Machine diagnostics", 110th Meeting of the Acoustical Society of America, November 1985.

[12] Jong J., Jones J., Mcbride J. "Some Recent Development in Turbomachinery Fault Detection", NASA Conference on Advanced Earth-to-Orbit Propulsion Technology, 1992.

[13] Dowling, Martin. AM and FM Digital Demodulation Technique for Electric Power. Final Report to Naval Ship Systems Engineering Station, FRC Project 5847-05, - 13, Feb., 1984.

[14] Jong J., Jones J., McBride J., Coffin T., "Correlation Identification Between Spectral Components in Turbomachinery Measurements by Generalized Hyper-Coherence", 3rd International Machinery Monitoring And Diagnostic Conference, December, 1991.

[15] Jong J., Jones J."Anomaly Identification for Space Shuttle main Engine Diagnostics"., 48th Meeting of the Mechanical Failure Prevention Group (MFPG). April, 1994.

[16] McFadden, P. D. "Interpolation Techniques for the Time Domain Averaging of Vibration Data with Application to Helicopter Gear Box Monitoring", Aero Propulsion Technical Memo 437, AR-004-448, DoD S&T. Aeronautical Research Lab., Australia, 1986.

[17] Jong J., Jones J. "Phase Synchronized Enhancement Method for Space Shuttle Main Engine Diagnostics", NASA Conference on Advanced Earth-to-Orbit Propulsion Technology, 1994

3.0 ATMS Menu System and Computer Codes

3.1 ATMS Menu System

The ATMS program can be directly executed within the OISPS system. To load the ATMS program, the user first types in "atms". After loading all the necessary files, the program will ask user to enter the number of menu file. This number is range from 0-9. User can choose from the range or the program will select the last active menu. A clips command "(batch atms.bat)" will then be executed in the background which will activate the clips environment and load the ATMS knowledge base including a set of rules and user-defined clips functions. An ATMS main menu will show up after this command. All the required information for automated SSME dynamic signal processing can be selected and changed within this main menu and its sub-menus. Figure 3.1.1 shows the overall ATMS Main Menu and its sub-menus items. Explanation of these menu/sub-menu items are sequentially discussed below:

The first menu displayed is the ATMS main menu, which shows the following:

ATMS main menu

*** ATMS MAIN MENU ***

(0) START EXECUTING(AFTER MENU SETUP COMPLETED)
(1) TESTID: 9040259 (online)
(2) INPUT DATA SOURCE(1/TAPE; 2/OPT. DISK; 3/HD): 3 ==> FFT DOMAIN
(3) PUMP SELECTION STATUS: (sub-menu)
(4) STORAGE DISK FILE: (sub-menu)
(5) PUMP CHANNEL SELECTION ATTRIBUTES: (sub-menu)
(6) START FROM(1/ROLL-IN; 2/(I)FFT; 3/ASPS; 4/ADIS): 3
(7) STOP AFTER(1/ROLL-IN; 2/(I)FFT; 3/ASPS; 4/ADIS): 4
(8) ASPS OPTIONS: (sub-menu)
(9) ADIS OPTIONS: (sub-menu)
(10) STORE RESULT TO DATABASE(0/NO; 1/YES): 1
(11) TIME TO SLEEP TO START RUNNING ATMS: (IN HOURS) 0.000
(12) POWER LEVEL PROFILE: 11
(13) VENT LOX PROFILE: 0
(14) VENT FUEL PROFILE: 0
(15) PLOTTING DEVICES: (sub-menu)
(16) Engine/Pump series number
(98) SAVE
(99) EXIT
Enter your choose?? (1-16/MODIFY)....1

There are 19 submenus that the user can choose from in the ATMS main menu. Following are detailed explanations of each submenu.

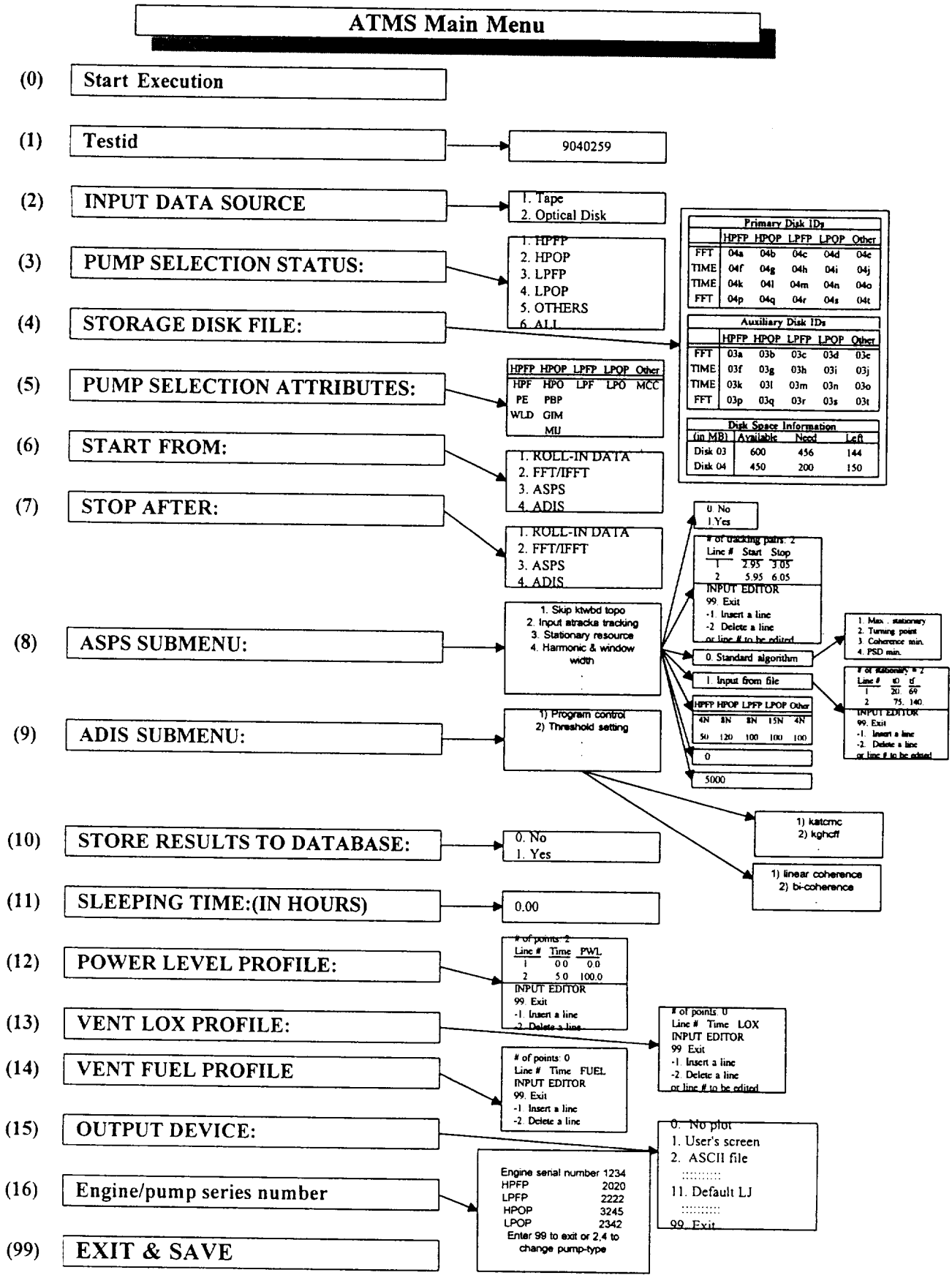

Figure 3.1.1 Overall ATMS Menu

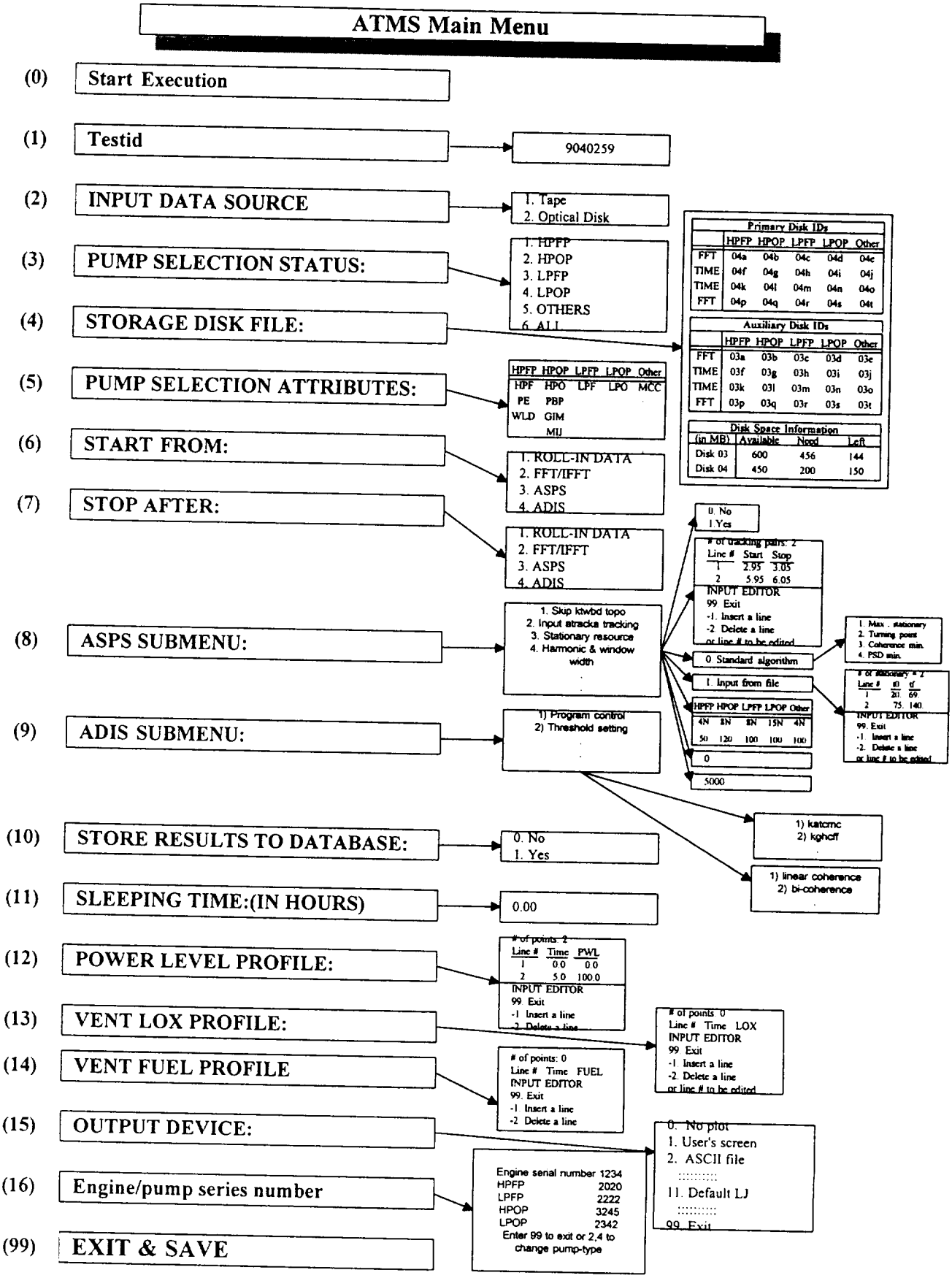

Figure 3.1.1 Overall ATMS Menu

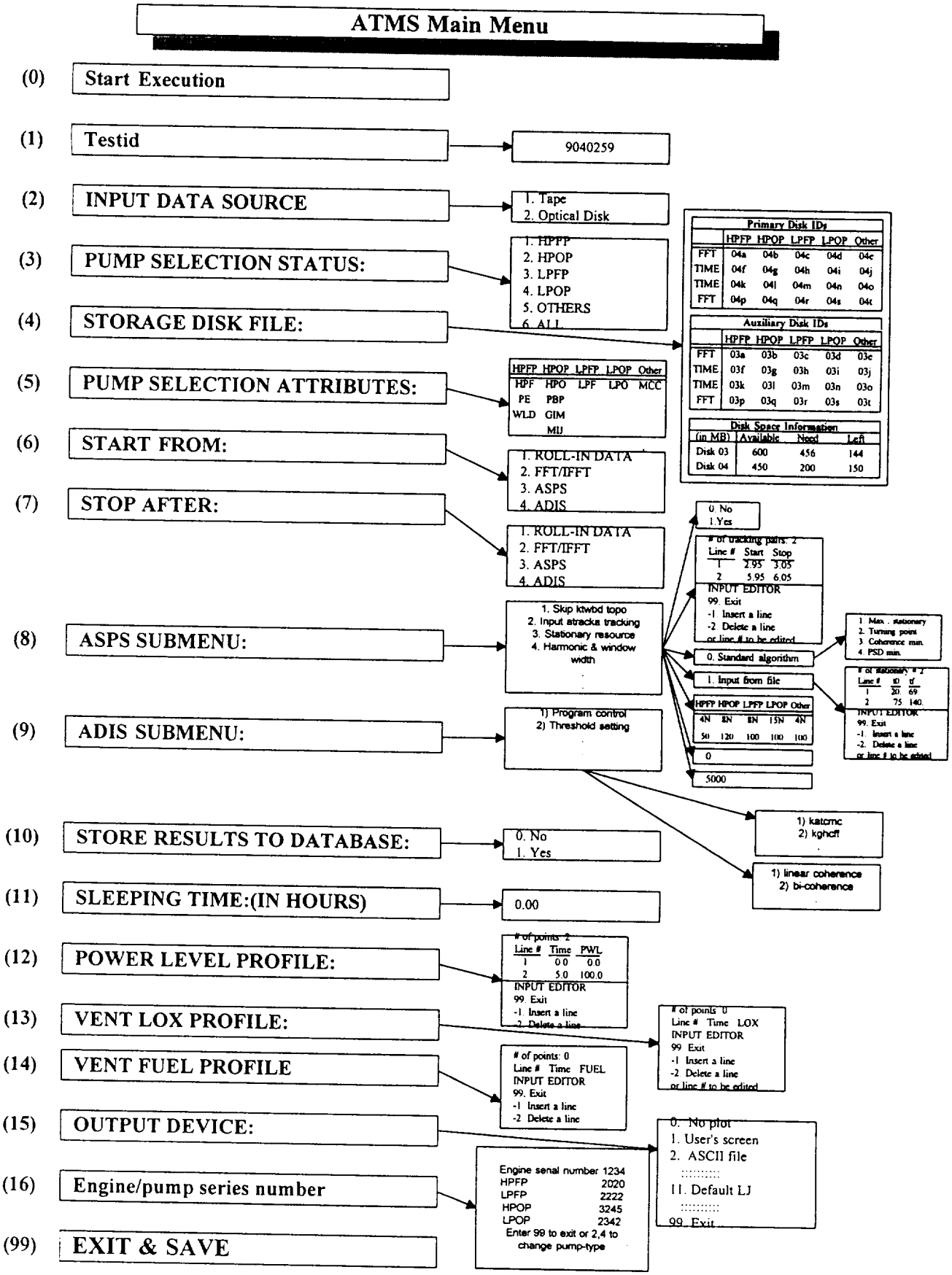

Figure 3.1.1 Overall ATMS Menu

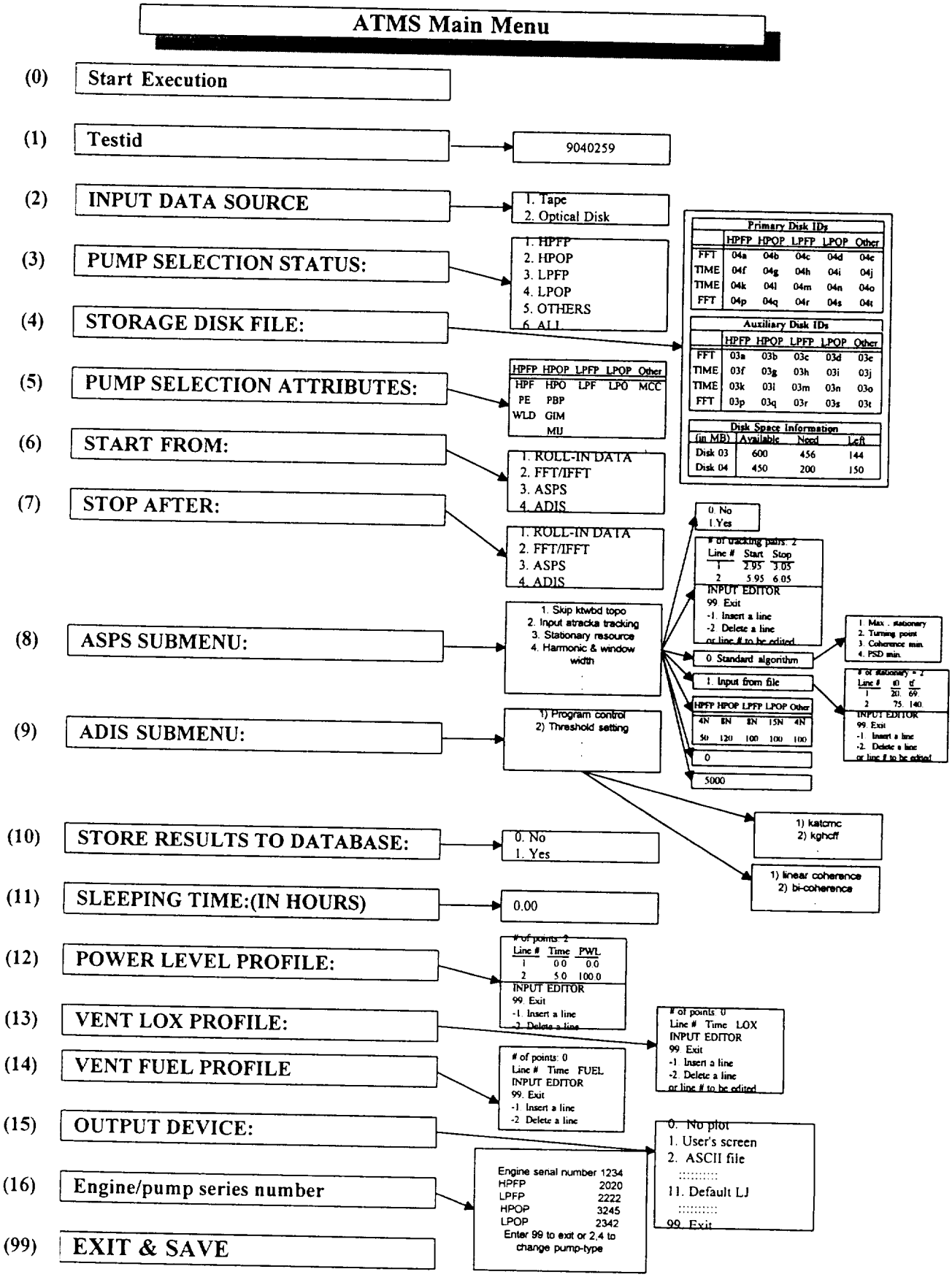

Figure 3.1.1 Overall ATMS Menu

ATMS main menu option 0:

User should choose this option only after all the necessary parameters are entered properly. Choosing this option will start the ATMS data analysis process. During processing time, user can stop the program by entering the following command:

ctrl Z

and then

kill atms

ATMS is control by the CLIPS Expert System. Using the parameters set by the user, the CLIPS Expert System will 'fire' the processes one by one until all are done. The process may take a few hours on the Gomez system, depending on the system traffic and the massive of the data being processed. User may suspend the ATMS process for a few hours until late evening or midnight. The method of suspending the ATMS process is explained in option 11.

ATMS main menu option 1:

User is asked to input the test-id for this run. The test-id is provided by the test-engineer. If improper test-id is entered, the process will stop. The test-id also is the subdirectory for that particular test case. User is responsible for creating that particular subdirectory before executing ATMS. Part of the process information will be saved in this particular subdirectory. This test-id subdirectory is different from the working-subdirectory, which is also created by the user. Both subdirectories should be available before executing ATMS. Different processing information will save on this two subdirectories. User can not modify the test-id once the ATMS process is underway.

```
Enter test ID = 9040259
```

ATMS main menu option 2:

User is asked to enter the data files source-disk. The data files can reside on tape, optical disk or hard disk. In addition, the data files can be in FFT or TIME format. It is the user's responsibility to provide the accurate information on the source-disk. ATMS may not work properly if wrong information is entered.

Enter 1 for tape, 2 for optical disk or 3 for hard disk. For the type of data on Hard Disk, enter 1 for FFT and 2 for TIME format.
Enter storage media(1/tape; 2/optical disk; 3/hard disk)=?? 3

What type of data on Hard Disk(1/FFT; 2/TIME)=?? 1

ATMS main menu option 3:

The program will show the available pump type and the corresponding number of channels associated with each pump. User can activate one particular pump by toggling it. A '*' in front of the pump id-name indicates that particular pump is selected for analysis. The Maximum channels available for each pump is shown next to the pump id-name. If number of channels for one particular pump is 0, this indicates that the information source file with the extension 'ssme' on the testid-subdirectory is not available or incomplete. This may also indicate that the particular testid is not validated. Check with the test-engineer for more information.

```
   *** Pump Selecting Submenu ***

            # of channels
            ------------
   1 *HPFP        10
   2 *HPOP        10
   3 *LPFP        6
   4 *LPOP        4
   5  OTHER       0

   Enter line #(1, 2, 3, 4, 5) to toggle or
99/EXIT??
```

ATMS main menu option 4:

User enters the data filenames and the program will automatically show the available disk space on that particular system and the number of Mb of disk space needed. If there is not enough disk space for processing, a warning will show up and the user should execute the proper procedure to ensure that enough working disk space is available. User may want to delete some old test case files. The name of the data files should correspond to the particular test case. It is the user's responsibility to ensure the information is correct.

*** Disk File Submenu ***

	1	2	3	4	5	
	HPFP	HPOP	LPFP	LPOP	OTHER	
1	04a	04b	04c	04d	04m	FFT
2	04f	04g	04h	04i	04j	TIME PRIMARY
3	04p	04q	04r	04s	04t	WORKING
4	04c	04f	04i	04l	04o	FFT/WBD
nchan	10	10	6	4	0	

Disk Space (MB):		
AVAILABLE	NEED	LEFT
300 Mb	126Mb	176Mb

Enter row # and column # to modify (0, 0) to EXIT: (row, column) = ??

ATMS main menu option 5:

Pump type Attributes are selected in this option. The available 'attributes' for the pump is fixed. User may choose the pump type attribute by entering the corresponding column and row number for the pump of interest, example:

2,2

will let user select the HPOP pump attribute 'PBP'. The available channels for each pump is then calculated and displayed.

*** Pump Type Attributes Submenu ***

	1	2	3	4	5
	HPFP	HPOP	LPFP	LPOP	OTHER
1	HPF	HPO	LPF	LPO	***
2		PBP			
3		GIM			
4					
5					
6					
nchan	10	10	6	4	0

Enter row # and column # to modify (0, 0) to exit
(row, column) = ?? 0,0
Total = 30

ATMS main menu option 6:

User choose from where ATMS start the processes.

1) For pre-process processing.
2) FFT data or Ifft data
3) ASPS-process
4) ADIS-process

```
Enter start step (1/Roll in data; 2/FFT or IFFT; 3/ASPS; 4/ADIS)=?? 3
```

ATMS main menu option 7:

User choose from where ATMS end processes.

1) For pre-process processing.
2) FFT data or Ifft data
3) ASPS-process
4) ADIS-process

It is important that the ending process number should be larger than the starting process number.

```
Enter stop step (1/Roll in data; 2/FFT or IFFT; 3/ASPS; 4/ADIS)=?? 4
```

ATMS main menu option 9:

Choosing this option brings the user to the Automated Signal Processing Subsystem submenu. There are 14 submenu's in this catalog and each submenu is explained in the next section.

```
   *** ASPS Option Selection Submenu ***
(1) Skip WBD topo (0/NO; 1/YES)          1
(2) Input 'atracka' tracking ranges      0
(3) Stationary Resource                  0
(4) Harmonic & Window Width for Tracking 0
(5) Minimum Frequency for Plotting       0
(6) Maximum Frequency for Plotting       5000
(7) Define afft parameters               0
(8) Define ktopo parameters              0
(9) Reference frequency in katcmc (fref) 1
(10) Define kisoplot parameters          0
(11) Define ksta parameters              0
(12) Skip ASPS process (0/NO; 1/YES)     1
(13) RESERVED                            0
(14) RESERVED                            0
(15) Program Control                     0
(99) EXIT
```

ASPS submenu option 1:

User can choose to execute the WBD topo process or skip it. Enter 0 will execute the WBD-topo process and 1 skips it.

```
Enter 0 for no skip WBD topo or 1 for skip WBD topo: ??
```

ASPS submenu option 2:

User chooses the type of pump to be analyzed. The program displays the available pump-type with the correspond number of channels that is associated with that particular pump. A '*' in front of the pump-id name indicates that particular pump is selected. User can choose from 1 to the maximum number of channels correspond to the particular pump. A '*" in front of the channel number indicates that particular channel is selected for that pump. This selection also sets up the available channels of each pump in the ADIS process. A zero in the # of ranges indicates that particular pump is not available.

```
*** Atracka Tracking Ranges Submenu ***

   PUMP TYPE      # OF RANGES
   ==========     ============
   1 * HPFP        10
   2 * HPOP        10
   3 * LPFP        6
   4 * LPOP        3
   5   OTHER
```

(asterisk [*] indicates pump is selected)
Enter your choose?? (99/MAIN MENU; 1-5/MODIFY)....99

ASPS submenu option 3:

User may choose the method of processing the stationary period in the data sets. The default is the Standard Algorithm. For more information of the different algorithm's methods, please read the technical section of this report.

```
   *** Stationary Resource Submenu ***

(0) * STANDARD ALGORITHM
(1) INPUT STATIONARY PERIODS TO FILE(statnry.dat)
    DIRECTLY WITHOUT ALGORITHM
(2)  AUXILIARY ALGORITHM 1
(3)  AUXILIARY ALGORITHM 2

Enter your choose?? (99/MAIN MENU; 0-3/SELECTION)....99
```

ASPS submenu option 4:

This option allows the user to set the tracking harmonic and Window Width using the ASPS process. User may use the default values set by the program or choose to enter new values. To change the default values, user will enter the column and row number corresponding to the particular item of interest, example:

1,2

will allow the user to change the 'tracking harmonic' for pump HPFP. After all modifications, user may enter

0,0

to exit from this option.

*** Tracking Harmonic & Window Width Submenu ***

	1	2	3	4	5	
	HPFP	HPOP	LPFP	LPOP	OTHER	
1	4N	8N	8N	15N	1N	current harmonic
	(4N)	(8N)	(8N)	(15N)	(1N)	default harmonic
2	100	150	200	100	50	current window width
	(100)	(150)	(200)	(100)	(50)	default window width

(row, column) = ??

Enter row # and column # to modify (0, 0) to exit

ASPS submenu option 5:

User enters the minimum frequency used in the plotting process. This will set the x-axis minimum value. This value is used for all plotting that involves frequency domain in the x-axis. The unit is in Hz. The default is 0 and user may enter any value less than the maximum set in the next option.

```
Enter min. frequency for plotting(default=0)...0
```

ASPS submenu option 6:

User enters the maximum frequency used in the plotting process. This will set the x-axis maximum value. This value is used for all plotting that involves frequency domain in the x-axis. The unit is in Hz. The default is 5000. User may enter any value more than the minimum set in the last option.

```
Enter max. frequency for plotting(default=5000)..    5000
```

ASPS submenu option 7:

This option allows the user to enter the parameters used in the FFT process. User may choose to use the default set up by the program or change the default to some suitable values. The default of overlap and number of window applications are set to 1. The CPWBD is set to 4. To modify the default value, user must enter the line # for that particular item of interest, example:

```
1
```

will allow user to modify the number of overlaps used in the ASPS process. After all modifications, user may enter 99 to exit from this option.

```
    **** AFFT Parameter Definition ****

(1) # of overlap, pmenu(5) ..... 1.000
(2) # of window applications, pmenu(7) ..... 1.000
(3) CPWBD(4/PO-CPWBD; 5/AM-CPWBD), pmenu(10).... 4.000
(4) RESERVED ..... 0.000
(5) RESERVED ..... 0.000
(99) EXIT

Enter line # to update; 99/Exit to option menu? 99
```

ASPS submenu option 8:

This option allows the user to set the parameters used in the Ktopo process. User may use the default values set by the program or enter new values for each parameter. To modify the default values, enter the line number for that particular item of interest, example:

1

this will allow the user to set the 'Medium filter length or rainfall db" used in the ASPS process. After all the modifications, enter 99 to exit this option.

```
   *** Ktopo Parameters Definition ***

(1) Medium filter length or rainfall dB ..... 100.000
(2) neigh = freq peak window ..... 4.000
(3) ipara = Peakyness parameter window ..... 9.000
(4) noise floor (0/No; -/both; +/# region)... -5.000
(5) RESERVED ..... 0.000
(99) EXIT

Enter line # to update; 99/Exit to option menu? 99
```

ASPS submenu option 9:

This option allows the user to set KATCMC reference frequency. The default is set by the program to have a value of 1. User may change the default values by entering a new value. To add more line # user enter 0 at the prompt and a '-' to delete the line. To modify any line, enter the correspond line number of interest and then enter the frequency. After all modifications, enter 99 to exit this option.

```
   **** KATCMC REFERENCE FREQUENCY ****

  line #    frequency
  ------    ---------
    1       1.000
    1       3.000
    1       6.000
  Enter choose(-/delete; 0/append; +/modify; 99/exit)?? 99
```

ASPS submenu option 10:

This option allows the user to set the parameters used in the Kisoplot process. User may use the default values set by the program of enter new values. To modify the default values, enter the line number of the item of interest, example:

1

this will allow user to set the 'Threshold" used in the ASPS process. After all modifications, enter 99 to exit this option.

```
   *** Kisoplot Parameters Definition ***

(1) Threshold %(-/abs) ..... 90.000
(2) Skewness (-1/L, 0/No, 1/R, 2/R more)..... 0.000
(3) 0/raw PSD; else/med. filter or rainfalldb .. 100.000
(4) RESERVED ..... 0.000
(5) RESERVED ..... 0.000
(99) EXIT

Enter line # to update; 99/Exit to option menu? 99
```

ASPS submenu option 11:

This option allows the user to set the parameter for the Ksta process. User may use the default values set by the program or enter new values. To modify the default values, enter the line number of the item of interest, example:

1

this will allow user to set the '# of points for STA waveform " used in the ASPS process. After all modifications, enter 99 to exit this option.

```
*** KATS Parameters Definition ***

(1) # of point for STA waveform(<= 4096) .... 128.000
(2) Harm. # of Speed Meas. (4/NA/8/15/1)..... 4.000
(3) RESERVED ..... 0.000
(4) RESERVED ..... 0.000
(5) RESERVED ..... 0.000
(99) EXIT

Enter line # to update; 99/Exit to option menu? 99
```

ASPS submenu option 12:

User may choose to execute the ASPS process or skip it. There may be cases where a user only needs to execute the ADIS portion of the ATMS process. By entering 0 user will execute the ASPS process. A 1 will skip it.

Enter new value for line # 12? 1

ASPS submenu option 15:

This is the ASPS program control section. There are 19 subprocesses under the ASPS submenu. User can choose which subprocess to execute. An '*' in front of the subprocess's name indicates that particular subprocess is selected and will be executed. To set or unset the process, enter the line number and the program will toggle between the 'set' or 'unset'. After all modifications, enter 99 to exit this option.

```
*** Program Control Submenu ***

* (1) aforeign          (11) asyncphas
* (2) ainvfft           * (12) akorbit
* (3) afft              * (13) kpsd
* (4) asyncfreq         * (14) kwbd
* (5) stationary        * (15) klincohxf
* (6) aplotsync         * (16) katcmc
* (7) ktopo             * (17) krice
* (8) kplot             * (18) kisoplot
* (9) atrackn           * (19) ksta
* (10) atracka          * (20) RESERVED
Enter line # to toggle; 99/Exit to option menu? 99
```

This ends the ASPS option.

ATMS main menu option 9

Choosing this option will bring the user into the ADIS submenu. There are only six submenus under the ADIS submenu. Each submenu is explained in the next section.

```
   *** ADIS Option Selection Submenu ***

(1) Program control ..... 0
(2) Threshold setting ..... 0
(3) Pump & Channel selection for ADIS ..... 2
(4) Stationary time period selection for ADIS. 1
(5) PSD peak selection (kjpsd) ..... 0
(6) PSD peak identification (kmatch) ..... 3
(7) RESERVED ..... 0
(8) RESERVED ..... 0
(99) EXIT
```

ADIS submenu option 2:

This is the program control for ADIS. User can choose which subprocess to execute. To choose or skip the subprocess, the user must first choose the number that corresponds to the subprocess and then enter 2 as asked. Entering 1 will execute the particular subprocess. To modify the default values, user may enter the line number of the item of interest, example:

3

this will allow the user to set the 'asyncfreq" process. 1 in this case indicates that this particular process will be executed. A 2 will skip this process. After all the modifications, user may enter 99 to exit this option.

*** ADIS Program Control Submenu ***

```
(1) katcmc ..... 1
(2) kghcff ..... 2
(3) asyncfreq (1/run 2/skip)..... 1
(4) kharmid  (1/run 2/skip)..... 1
(5) kfeedthru (1/run 2/skip)..... 1
(6) kbearing  (1/run 2/skip).....1
(7) kghcff   (1/run 2/skip)..... ..1
(8)kwbdadis  (1/run 2/skip).....1
(9)kadisplot (1/run 2/skip)..... .1
(10) program_10        1
(99) EXIT

Enter line # to update; 99/Exit to main menu?  99
```

ADIS submenu option 2:

This option allows the user to set the threshold values used in the ADIS process. User may use the default values set by the program or enter new values. To modify the default values, user enters the line number of the item of interest, example:

2

this will allow user to set the 'Threshold used in linear coherence " used in the ADIS process. After all modifications, enter 99 to exit this option.

```
**** ADIS Threshold Setting Submenu ****

(1) linear coherence    0.000
(2) bi-coherence        0.000
(3) tri-coherence       0.000
(4) GHC-coherence       0.000
(5) reserve_5           0.000
(6) reserve_6           0.000
(7) reserve_7           0.000
(8) reserve_8           0.000
(9) reserve_9           0.000
(10) reserve_10         0.000
(99) EXIT

Enter line # to update; 99/Exit??  99
```

ADIS submenu option 3:

This option allows user to select the available channels to be process for each pump. Example,

1

will allow user to select the channel of pump HPFP.

```
**** ADIS Pump & Channel Selection ****

                    ASPS          ADIS
                # of channels  # of channels
                -------------  -------------
  1 HPFP            10             2
  2 HPOP            10            13
  3 LPFP             6             0
  4 LPOP             4             0
  5 OTHER            0             0


   Enter line # to update; 99/EXIT?? 1
```

User may enter the line number to toggle. A '*' in front of the Channel id-name indicates that particular channel is selected . As standard, enter 99 to exit the option.

```
**** ADIS Channel List for Pump HPFP  ****

 1 * HPFP SPD NFD
 2   HPFP RAD 84 ACC
 3 * HPFP RAD 96 ACC
 4   HPFP RAD 180 ACC
 5   HPFP RAD 90 ACC
 6   HPFT RAD 90 ACC
 7   HPFT RAD 180 ACC
 8   FASCOS HPFP 20
 9   FASCOS HPFP 174
10   FASCOS HPFP 186

Enter channel # to toggle; 99/EXIT?? 99
```

ADIS submenu option 4:

This option allows user to select the 'STATIONARY" used in the ADIS process. User enters the line # to toggle. A '*' in front of the 't0' value indicates that particular 'STATIONARY' is selected. To exit this option, enter 99.

```
**** STATIONARY SELECTION SUBMENU ****

  #     t0       tf     power level
 --- --------- --------- -----------
  1     6.00     10.00     100.00
  2    *12.00    36.00     104.00
  3     42.00    59.00     65.00
  4     65.00    89.00     104.00
  5     95.00    99.00     65.00

Enter line # to toggle; 99/Exit??  99
```

ADIS submenu option 5:

This option allows user to set the 'ADIS PSD Peak'. User may use the default values provided by the program or choose to alter it. To modify the default values, user enters the line number of the item of interest, example:

1

this will allow user to set the 'Maximum # of peaks to be selected from PSD" used in the ADIS process. After all modifications, enter 99 to exit this option.

```
**** ADIS PSD Peak Selection for KJPSD ****

1)  Maximum # of peaks to be selected from PSD              1
2)  # of user-selected peaks at given fixed frequencies     2
3)  # of user-selected peaks at given fixed Sync-Ration freq.  0
4)  # of PSD peaks whose SNR exceeding a specified SNR       0
5)  Length of median filter for noise floor identification   0
6)  No peak to be selected within ? bandwidth                0
7)  reserve_7                                                0
8)  reserve_8                                                0
9)  reserve_9                                                0
10) reserve_10                                               0

Enter line # to update; 99/EXIT??  99
```

ADIS submenu option 6:

This option allows user to set the 'ADIS PSD Peak Identification Option for KMATCH'. User may use the default values provided by the program or choose to alter it. To modify the default values, enter the line number of the item of interest, example:

1

this will allow user to set the 'Bearing frequency selection options " used in the ADIS process. After all modifications, enter 99 to exit this option.

```
**** ADIS PSD Peak Identification Option for KMATCH ****

1) Bearing frequency selection options          0
2) Other sync-related frequency selection options  1
3) Other fixed-frequency selection options       1
4) Electronic noise (for all pumps)              1

Enter line # to update; 99/EXIT??  99
```

This end the ADIS option.

ATMS main menu option 10:

User is asked if the results should be stored in the database or not. A "0" indicates that the results will not be saved in the database. A "1" will save the data.

```
Store results to database(0/NO; 1/YES)=??  1
```

ATMS main menu option 11:

ATMS is designed such that the process can be delayed for execution. This is particular significant if during the daytime when the system is busy, there may not be enough memory for ATMS. User can choose to temporarily suspend ATMS process for a number of hours before executing. The time of delay is given in hours. Start time is when the user chooses option "0" in the ATMS main menu.

```
Time to sleep to start running (in hours) =??  0
```

ATMS main menu option 12:

This option allows user to set the 'Power profile'. User may use the default values provided by the program or choose to alter it. To modify the default values, user enters the line number of the item of interest, example:

1

this will allow user to set the set line 1 values. After all modifications, enter 99 to exit this option.

# of pairs: 11

LINE #	Time (second)	Power Level(%)
1	0.00	0.00
2	5.00	100.00
3	11.00	100.00
4	11.00	104.00
5	37.00	104.00
6	41.00	65.00
7	60.00	65.00
8	64.00	104.00
9	90.00	104.00
10	94.00	65.00
11	100.00	65.00

***** LINE EDITOR MENU *****

99 EXIT
-1 Insert a line
-2 Delete a line
OR Line # to be modified (1 - 11)
Enter your choose 99

ATMS main menu option 13:

This option allows user to set the VENT LOW PROFILE. Enter the time as asked. To exit from this option, enter -1.

Enter Time (second) for pair # 1 (-1 to quit) =? -1

ATMS main menu option 14:

This option allows user to set the VENT FUEL PROFILE. Enter the time as asked. To exit from this option, enter -1.
Enter Time (second) for pair # 1 (-1 to quit) =? -1

ATMS main menu option 15:

User chooses the plotting device for the plotting processes. "0" indicates that no plots are produced and "1" sends the plots to the user graphics screen. The printers that are available are located in the NASA/Gomez terminal room or the ASRI office.

```
   *** Plotting Devices Submenu ***

 0. No plot
 1. Users graphics screen.          Where-ever     ALL
 2. Tabulate data to ascii file.    local disk     ALL
 3. Tektronix 4014 graphics file.   ~/plots dir    ALL
 4. Tektronix 4325 graphics file.   ~/plots dir    ALL
 5. Postscript graphics file.       ~/plots dir    ALL
 6. Color postscript graphics file. ~/plots dir    ALL
 7. QMS #1  (4610 computer room).   Printlink II   ALL
 8. QMS #2  (4610 computer room).   Printlink II   ALL
 9. QMS2000 (5th floor 4610).       FTP-ethernet   ALL
10. Local serial 4014 printer.      /dev/tty2      Local only
11. Default LJ (Local computer room). Print Spooler  Local only
12. HP LJ4si #1 (4610 computer room). Print Spooler  SUNs
13. HP LJ4si #2 (4610 computer room). Print Spooler  SUNs
14. HP LJ4si #3 (ED33).             Print Spooler  SUNs
15. HP LJ4si #4 (Rockwell).         Print Spooler  SUNs
16. HP LJ4si  (4610 room 4012).     Print Spooler  SUNs
17. QMS 1725 #1 (4610 CSC room).    Print Spooler  SUNs
18. QMS 1725 #2 (4610 CSC room).    Print Spooler  SUNs
Enter your choose(99/Exit to main menu; 0-18/device)99
```

ATMS main menu option 16

This option show the corresponding engine and pump series name. All the information should be available from the data file testid.ssme. If that particular pump is typed 'P&W", a "yes" shows up under the 'P&W' column. If there are no series names available, user can choose to set that particular pump to either Rocketdyne or P&W type by toggling the line.

```
1) Engine Series #  0422     P&W
2) HPFP             4207R3   No
3) LPFP             2316     No
4) HPOP             8010R3   Yes
5) LPOP             0210     No
```

ATMS main menu option 99

This will exit the ATMS process .

Do you want to save main menu??(0/NO; 1/YES) 0

3.2 ATMS Software and Files Structure in OISPS/Gomez System

ATMS complete system is written in three different languages, C, Fortran and CLIPS. Figure 3.2.1 shows the overall file system structure of ATMS. The source files are located in different subdirectory under the root directory as follows:

3.2.1. 'user':

This subdirectory is under root and is the parent directory for all the subdirectory that contain most of the ATMS files. It contains two subdirectories, 'atms' and 'atmsmenu'. Each subdirectory contains important source and processed files for the ATMS system.

3.2.2 'atmsmenu':

This subdirectory is under 'user' and contains the menu file for 'atmsmain' program. There are 10 menu files under this subdirectory that range from '.dat0' to '.dat9'. 'Atmsmain' reads all the ATMS parameters from this menu file. The user can modified the parameters according to each case study. The modified information is then rewritten into this file. Without this file, 'atmsmain' will not run.

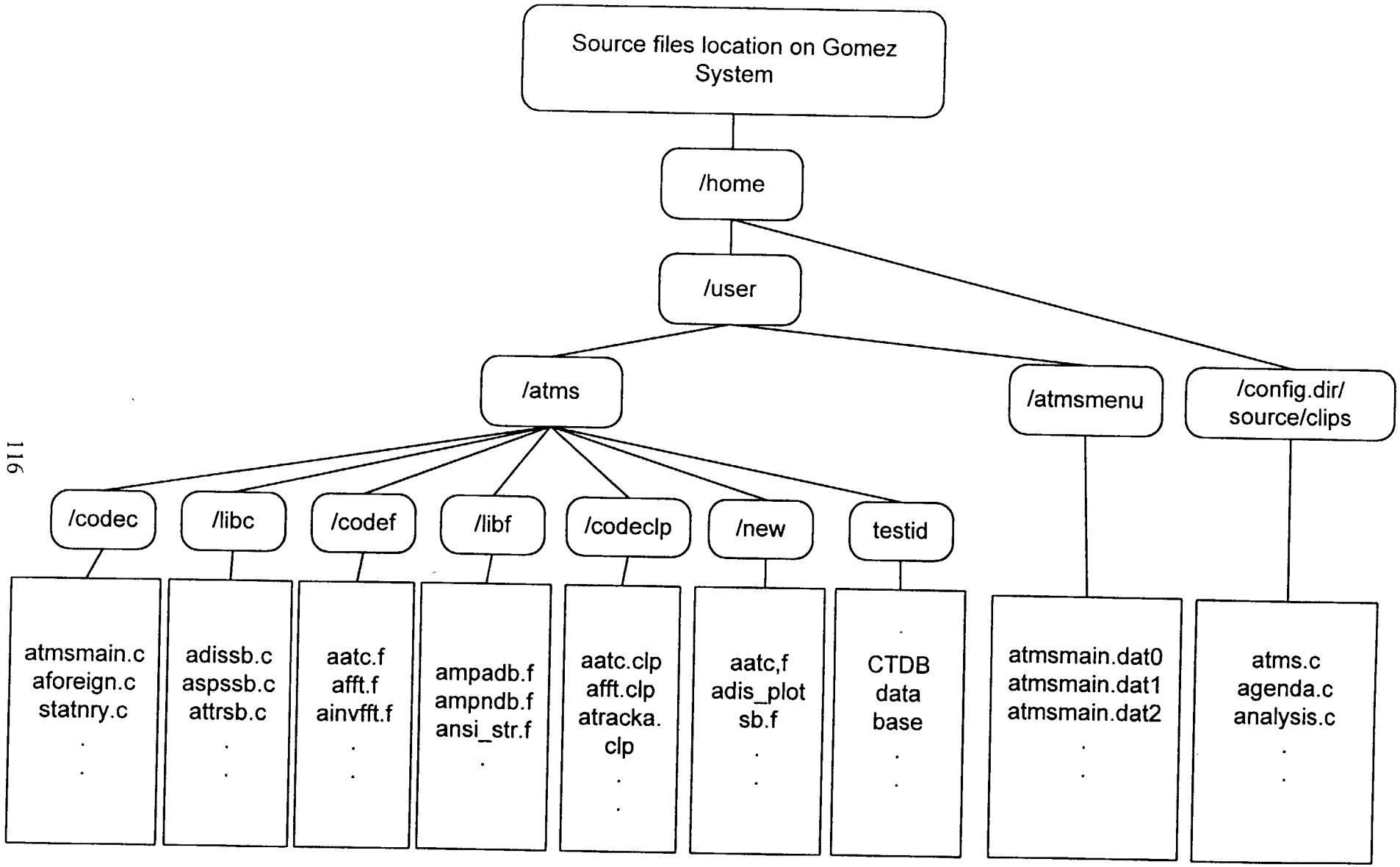

Figure 3.2.1 ATMS Overall File System Structure

3.2.3 'atms':

This subdirectory is under 'user'; It contains 7 subdirectories. These are '/codec', '/libc', '/codef', '/libf', '/codeclp', '/new' and '/testid'.

3.2.3.1 'config.dir/source/clips':

This subdirectory is under 'atms/clips' and contain all the C, Fortran and CLIPS basic building block files. The atms.c in this subdirectory is the most important file which setsup the ATMS processes.

3.2.3.2 'codec':

This subdirectory is under 'atms'. It contains the 'atmsmain.c' and other necessary ATMS files written in C.

Following are the tables of all the subdirectories and files.

/home/jen/atms/codec

adis_hd.h bsdcompat.h functions.h prod.h	ansi_str.h common_var.h header.h tape.h	atmschd.h defines.h messages.h
aforeign.c atmspwldb.c test.c ventmain.c	atmsmain.c statnry.c ventinit.c	

3.2.3.3 'libc':

This subdirectory is under 'atms'. It contains the function and subroutine ATMS file written in C.

//home/jen/atms/libc

adissb.c disksb.c isclips.c pwlsb.c unpack.c	aspssb.c editln.c menusb.c resetsb.c ventsb.c	attrsb.c findtest.c mktestdir.c ssmesb.c	bearsb.c getfsize.c pack.c statsb.c	del.c getint.c pumpsb.c strsb.c
adis_hd.h atmschd.h defines.h header.h prod.h	ansi_str.h common_var.h functions.h messages.h			

3.2.3.4 'codef':

This subdirectory is under 'atms'. It contains the 'afftf' and other necessary ATMS files written in Fortran.

//home/jen/atms/codef

aatc.f asyncfreq.f common_var.f graphics.f syncharmdb.f	afft.f asyncphas.f dbrecall.f header.f del.f	ainvfft.f atmsrdhd.f defines.f max_chan.f va2.f	akorbit.f atmssize.f mediansb.f va2test.f recall.h	alincohxf.f atracka.f ferror.f plotcom.f zrecall.f
ansi_str.f atrackn.f fva2stubs.f plplhead.f	aplotsync.f colors.f fvastubs.f progs.f	atmsfhd.h		

3.2.3.5 'libf':

This subdirectory is under 'atms'. It contains the function and subroutine ATMS files written in Fortran.

/home/jen/atms/libf

ampadb.f findipsd.f lcohdb.f postunpk.f strcmpr.f	ampndb.f findpump.f maindb.f prepk.f syncdb.f	ansi_str.f findtest.f mkbafn.f progs.f topodb.f	bcohdb.f getfm1clp.f mkdbfn.f psddb.f upper.f	checkrwclp.f getfm22clp.f mkmenudir.f pwldb.f va2.f
chkclp.f getfm2clp.f mktestdir.f rcmenu.f ventdb.f	chkdual.f getioclp.f plfreq.f reddb.f wbddb.f	cmptopo.f getmenuclp.f plotcom.f s1chclp.f	common_var.f graphics.f plplhead.f s2chclp.f	defines.f grpchan.f pltime.f ssmedb.f
defpump.f header.f pltopo.f statdb.f	atmsfhd.h recall.h			

3.2.3.6 'new':

This subdirectory is under 'atms'. It contains the Fortran files for ASPS and ADIS process.

{ong}//home/jen/atms/new

aatc.f ken.f ktopo.f	adis_plotsb. f kfalerls.f ktpsd.f	adis_plotsb_ 021097.f kfascos1.f ktpsd1c.f	ansi_str.f kfda.f ktpsdbrg.f	antbear.f kfeedthru.f ktpsdmp.f
kffterror.f ktrack.f working.f	bearing.f kfilter.f ktracka.f	bearingsb.f kgcomb.f ktrackabc.f	cfft.f kgetdata.f ktrackatc.f	cohsball.f kghc.f ktracklin.f
colors.f kghcff.f ktrackn.f	common_var.f kghcmc.f ktrackp.f	cpwbdsb.f kgroup.f ktransf.f	defines.f kharmid.f ktsem.f	del.f khilbert.f ktu2d.f
fda2t.f khypcoh.f ktum.f	fdatest.f khypfil.f ktum1p.f	fdpktopo.f kintegra.f ktum32.f	fdpktopon.f kintegra1.f ktumb:f	fdpktoponew. f kisoplot.f ktumrynd.f
fdpktopoold. f kisotu.f ktuxy.f	ferror.f kisotusb.f ktwbd.f	fft842.f kjpsd.f kwbd.f	fftcorrsb.f kjpsd_includ e.f kwbdadis.f	ffto.f kjpsdbrg.f kwheq.f
fftsub.f kkurtos.f kwidrow.f	fftsubap.f klincoh.f kwiener.f	filesize.f klincoh0.f masub.f	filter1.f klincoh1.f matchbrg.f	freq_match_o ld.f klincohxf.f max_chan.f
fvastubs.f klinoch.f mediansb.f	getmenuclp.f kmafilter.f ndig.f	ghcdel.f kmanipu.f noisefloor.f	graphics.f kmoment.f outputsb.f	hcohdsp.f* kmsin.f pl10head.f
hcoher.f korbit.f pl10sb.f	header.f kparameter.f pl10sb1.f	histgm.f* kpeak.f plotcom.f	isortmax.f kphase.f plotsbm.f	isotusb.f kplot.f plplhead.f
jfftsub.f kpoint.f plplotctr.f	kacor.f kpoint1.f plplotsb.f	kadisplot.f kpointmc.f progs.f	kadisplot_02 1097.f kpsd.f replot.f	kafag53.f kpsem.f simupoint.f
kahc.f kpsemold.f temp.f	kahcmc.f krice.f temp1.f	kaleag53.f kseal.f test.f	karmah.f kshock.f test1.f	katc.f ksinsweep.f test2.f
katcmc.f ksorbit.f testbear.f	kbearing.f ksrs.f testfft.f	kcepstrum.f ksta.f testfft1.f	kclipcheck.f kstasb.f testspeed.f	kcolor.f ktatc.f va2.f
kcomb.f ktatc0.f va2test.f	kcycoh.f ktatcmp.f wbd%.f	kcztsub.f ktda.f wbdcoh.f	kdecim.f ktdpsd.f wbdtest.f	kduqu.f ktdpsd1.f
ansi_str.h bsdcompat.h defines.h header.h prod.h	atmschd.h colors.h functions.h khypcoh.h progs.h	atmsfhd.h common_var.h graphics.h messages.h tape.h		

3.2.3.7 'testid':

This subdirectory is under 'atms'. It contains the CTDB database files generated from the ATMS process..

3.2.3.8 'codeclp':

This subdirectory is under 'atms'. It contains all the 'CLIPS' files used in the ATMS system.

//home/jen/atms/codeclp

aatc.clp atracka.clp kghcff.clp kwbd.clp stationary.clp	afft.clp atrackn.clp kharmid.clp kwbdadis.clp strat.clp	aforeign.clp bear-tab.clp kisoplot.clp mt_bear.clp syncharmdb.clp	ainvfft.clp header.clp kjpsd.clp peak-tab.clp true-n.clp	
alcoh.clp kahcmc.clp kplot.clp prn-pat.clp	aplotsync.clp katcmc.clp kpsd.clp prn-pk-1.clp	asyncfreq.clp kbearing.clp ksta.clp prn-pk-2.clp	asyncphas.clp kfeedthru.clp ktopo.clp start.clp	
adis.sub delplot.sub getlogin.sub readmain.sub stepflag.sub	bearing.sub findnum.sub harmwind.sub readmast.sub testid.sub	chksync.sub findtpend.sub matchapp.sub saveplot.sub whichprn.sub	atms.bat akorbit.clp kadisplot.clp klincohxf.clp prn-adis.clp	

3.2.3.9 CLIPS:

This subdirectory is under 'atms'. It contains all the original 'CLIPS' files

.

/config.dir/source/clips

agenda.c dffctcmp.c factmngr.c lgcldpnd.c reteutil.c	analysis.c dffctdef.c factprt.c main.c retract.c	argacces.c dffctpsr.c factrete.c memory.c router.c	bload.c dffnxbin.c factrhs.c miscfun.c rulebin.c	bmathfun.c dffnxcmp.c filecom.c modulbin.c rulebld.c
bsave.c dffnxexe.c filertr.c modulbsc.c rulebsc.c	classcom.c dffnxfun.c generate.c modulcmp.c rulecmp.c	classexm.c dffnxpsr.c genrcbin.c moduldef.c rulecom.c	classfun.c dfinsbin.c genrccmp.c modulpsr.c rulecstr.c	classinf.c dfinscmp.c genrccom.c modulutl.c ruledef.c

classini.c	classpsr.c	clsltpsr.c	commline.c	conscomp.c
drive.c	edbasic.c	edmain.c	edmisc.c	edstruct.c
genrcexe.c	genrcfun.c	genrcpsr.c	globlbin.c	globlbsc.c
msgcom.c	msgfun.c	msgpass.c	msgpsr.c	multifld.c
ruledlt.c	rulelhs.c	rulepsr.c	scanner.c	strngfun.c
constrct.c	constrnt.c	crstrtgy.c	cstrcbin.c	cstrccom.c
edterm.c	emathfun.c	engine.c	evaluatn.c	expressn.c
globlcmp.c	globlcom.c	globldef.c	globlpsr.c	immthpsr.c
multifun.c	objbin.c	objcmp.c	objrtbin.c	objrtbld.c
strngrtr.c	symblbin.c	symblcmp.c	symbol.c	sysdep.c
cstrcpsr.c	cstrnbin.c	cstrnchk.c	cstrncmp.c	cstrnops.c
exprnbin.c	exprnops.c	exprnpsr.c	extnfunc.c	factbin.c
incrrset.c	inherpsr.c	inscom.c	insfile.c	insfun.c
objrtcmp.c	objrtfnx.c	objrtgen.c	objrtmch.c	pattern.c
textpro.c	tmpltbin.c	tmpltbsc.c	tmpltcmp.c	tmpltcom.c
cstrnpsr.c	cstrnutl.c	default.c	defins.c	developr.c
factbld.c	factcmp.c	factcom.c	factgen.c	facthsh.c
insmngr.c	insmoddp.c	insmult.c	inspsr.c	insquery.c
pprint.c	prccode.c	prcdrfun.c	prcdrpsr.c	prdctfun.c
tmpltdef.c	tmpltfun.c	tmpltlhs.c	tmpltpsr.c	tmpltrhs.c
dffctbin.c	dffctbsc.c	agenda.h	analysis.h	argacces.h
factlhs.c	factmch.c	defins.h	developr.h	dffctbin.h
insqypsr.c	iofun.c	factmngr.h	factprt.h	factrete.h
prntutil.c	reorder.c	match.h	miscfun.h	modulbin.h
utility.c	watch.c	retract.h	router.h	rulebin.h
bload.h	bmathfun.h	bsave.h	classcom.h	classexm.h
dffctbsc.h	dffctcmp.h	dffctdef.h	dffctpsr.h	dffnxbin.h
factrhs.h	filecom.h	filertr.h	generate.h	genrcbin.h
modulbsc.h	modulcmp.h	moduldef.h	modulpsr.h	modulutl.h
rulebld.h	rulebsc.h	rulecmp.h	rulecom.h	rulecstr.h
classfun.h	classinf.h	classini.h	classpsr.h	clips.h
dffnxcmp.h	dffnxexe.h	dffnxfun.h	dffnxpsr.h	dfinsbin.h
genrccmp.h	genrccom.h	genrcexe.h	genrcfun.h	genrcpsr.h
msgcom.h	msgfun.h	msgpass.h	msgpsr.h	multifld.h
ruledef.h	ruledlt.h	rulelhs.h	rulepsr.h	scanner.h
clipsmem.h	clsltpsr.h	commline.h	conscomp.h	constant.h
dfinscmp.h	drive.h	ed.h	engine.h	evaluatn.h
globlbin.h	globlbsc.h	globlcmp.h	globlcom.h	globldef.h
multifun.h	network.h	objbin.h	objcmp.h	object.h
setup.h	shrtlnkn.h	strngfun.h	strngrtr.h	symblbin.h
constrct.h	constrnt.h	crstrtgy.h	cstrcbin.h	cstrccmp.h
expressn.h	exprnbin.h	exprnops.h	exprnpsr.h	extnfunc.h
globlpsr.h	immthpsr.h	incrrset.h	inherpsr.h	inscom.h
objrtbin.h	objrtbld.h	objrtcmp.h	objrtfnx.h	objrtgen.h
symblcmp.h	symbol.h	sysdep.h	tmpltbin.h	tmpltbsc.h
cstrccom.h	cstrcpsr.h	cstrnbin.h	cstrnchk.h	cstrncmp.h
extobj.h	factbin.h	factbld.h	factcmp.h	factcom.h
insfile.h	insfun.h	insmngr.h	insmoddp.h	insmult.h
objrtmch.h	pattern.h	pprint.h	prccode.h	prcdrfun.h
tmpltcmp.h	tmpltcom.h	tmpltdef.h	tmpltfun.h	tmpltlhs.h
cstrnops.h	cstrnpsr.h	cstrnutl.h	default.h	
factgen.h	facthsh.h	factlhs.h	factmch.h	
inspsr.h	insquery.h	insqypsr.h	lgcldpnd.h	

prcdrpsr.h tmpltpsr.h	prntutil.h tmpltrhs.h	reorder.h utility.h	reteutil.h watch.h	

4.0 Conclusion

Test evaluation of ATMS using actual SSME test data has demonstrated that the ATMS can perform detailed dynamic data analyses of large volumes of dynamic data without human interface thereby reducing the analysis man-hours. ATMS has also been used to support anomaly/incident investigations for the Advanced Turbopump (AT) HPFTP program, which has demonstrated ATMS will be a useful tool for detail dynamic signal analysis for failure investigation.

With the automation capability for signal processing, ATMS will significantly reduce manpower requirements for processing and analyzing large volumes of rocket engine flight/test dynamic data for diagnostic and performance evaluation. ATMS will allow NASA engineers to quickly evaluate rocket engine operational conditions of flight/test data, thereby reducing launch turn-around time and enhancing flight safety and reliability. ATMS will provide timely assessments of the engine performance, identify probable causes of malfunction/anomalies, and indicate feasible engineering solutions to enhance engine performance. In addition, failure history, fault symptoms, and anomalous signatures created in the CTDB will provide a foundation for future propulsion development programs. It is recommended that ATMS be utilized extensively in the future for analysis of NASA engine test data. To enhance the ATMS diagnostic capability, any newly observed critical engine vibration signature can be included in the list for anomaly detection and identification

An intelligent and fully automated rocket engine diagnostic system has considerable commercial application potential outside the NASA's propulsion area. Such a system would greatly increase the performance of monitoring and providing diagnostic data for critical mechanical/drive-train components of many industrial systems used by power plants, transportation, and manufacturing sectors.

APPENDIX-A

ATMS ASPS Output Package Example

using SSME test 9010853

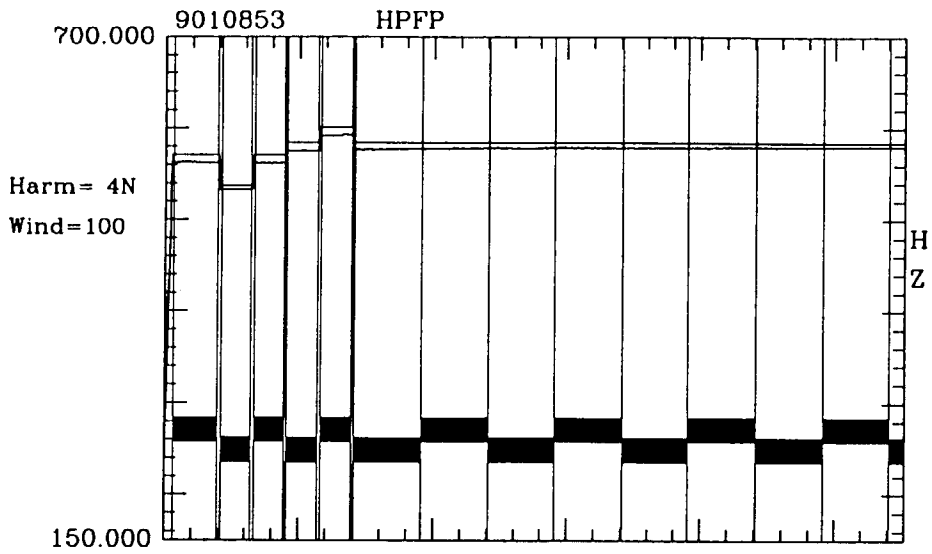
9010853
HPFP
700.000
150.000
Harm= 4N
Wind=100
H
Z

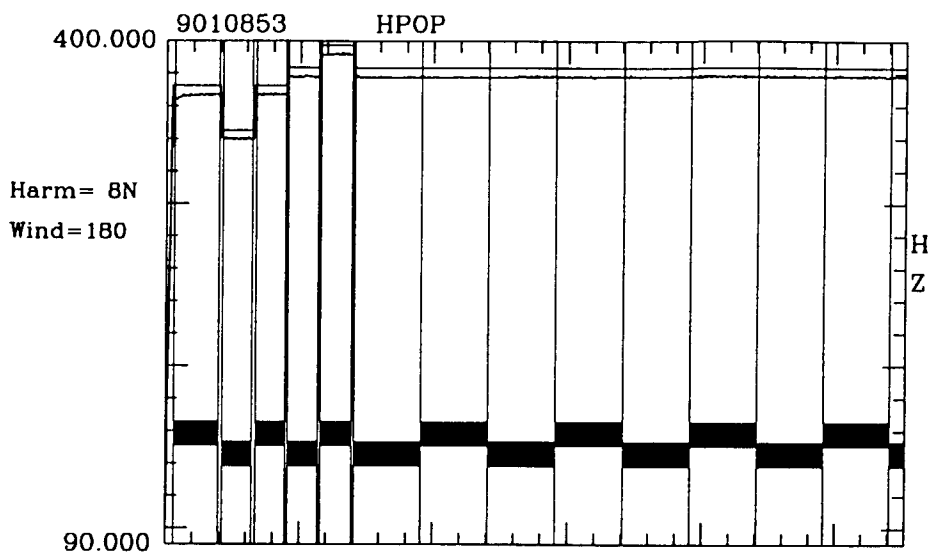
9010853
HPOP
400.000
90.000
Harm= 8N
Wind=180
H
Z

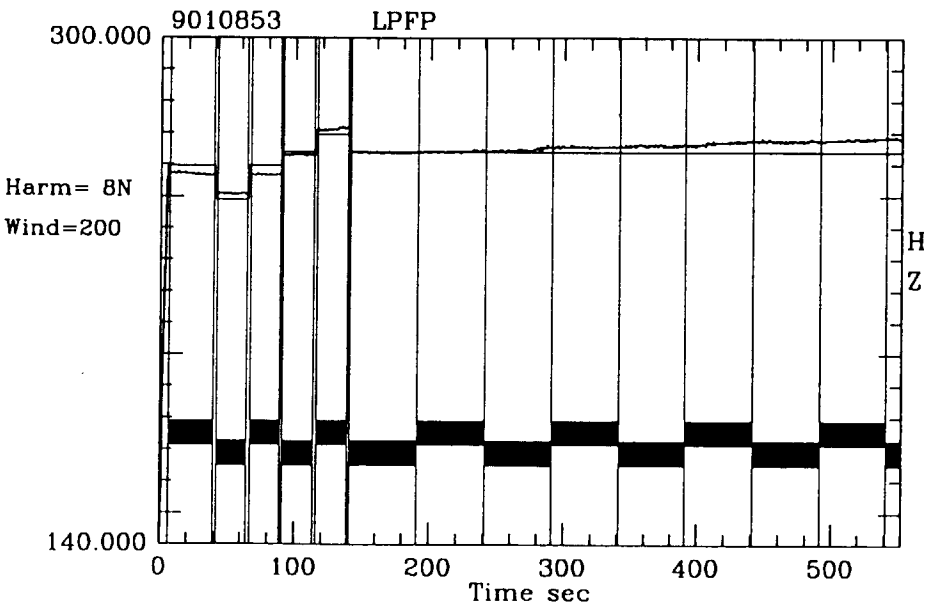
9010853
LPFP
300.000
140.000
Harm= 8N
Wind=200
H
Z
0
100
200
300
400
500
Time sec

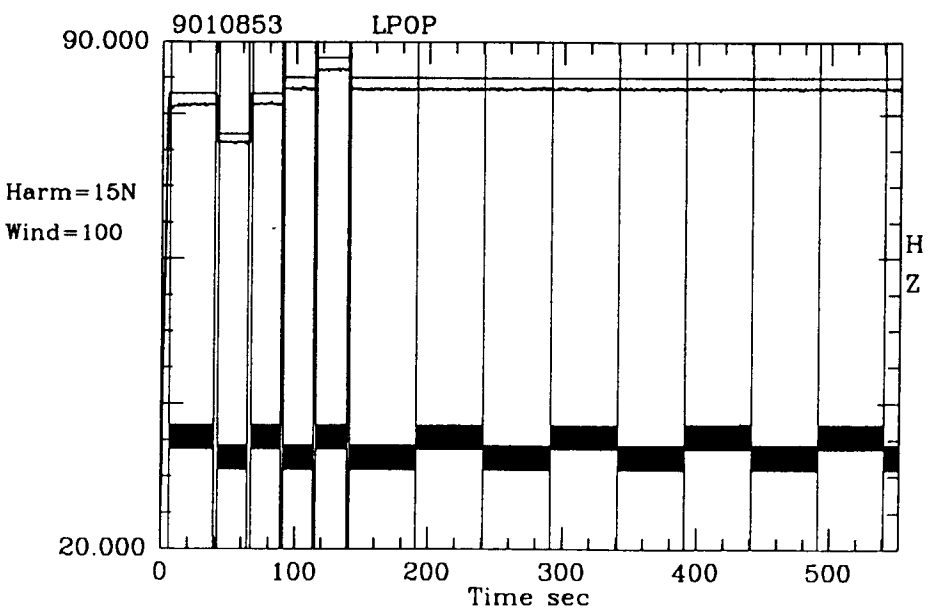
9010853
LPOP
90.000
20.000
Harm=15N
Wind=100
H
Z
0
100
200
300
400
500
Time sec

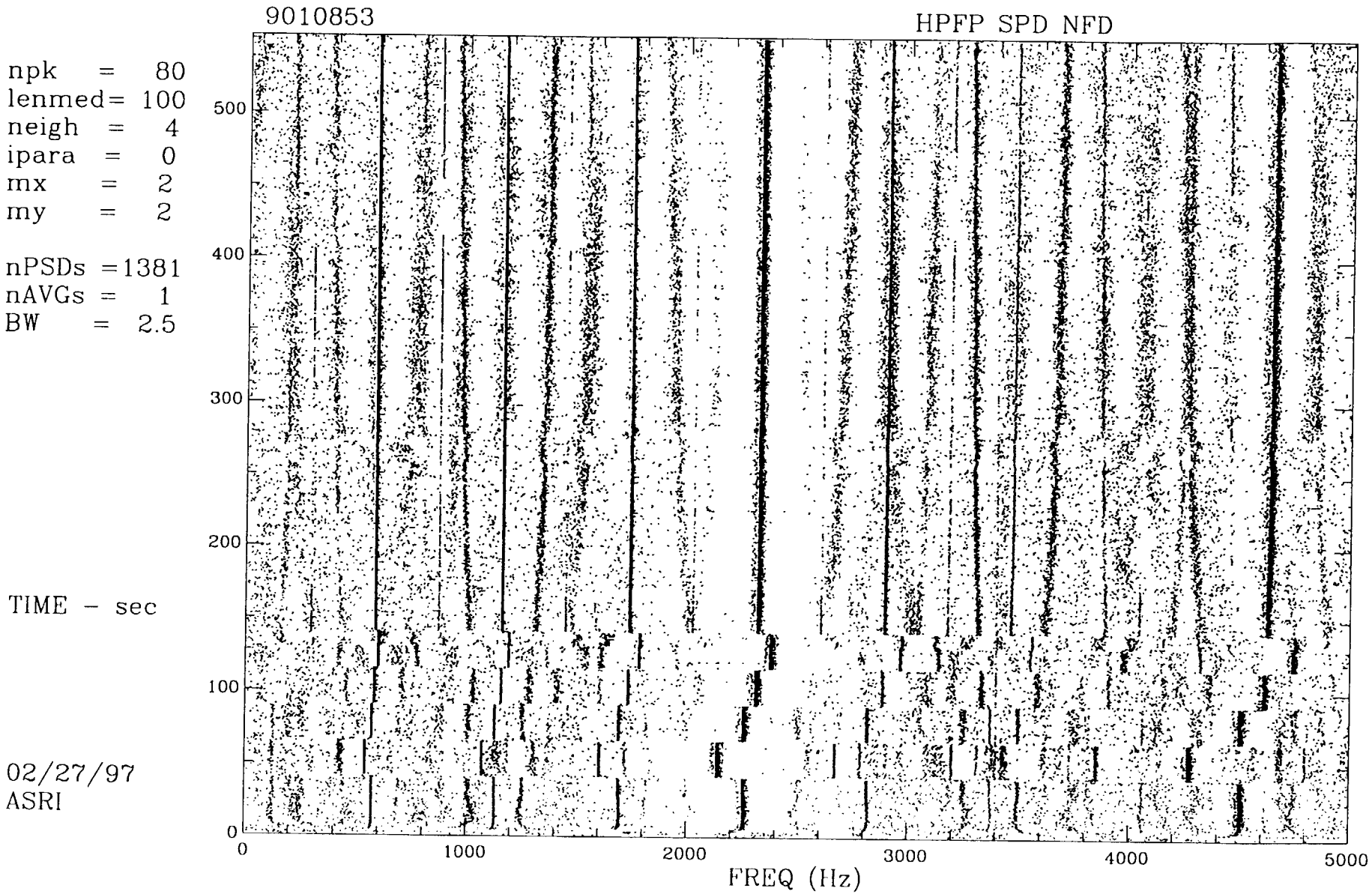
9010853
HPFP SPD NFD
npk = 80
lenmed= 100
neigh = 4
ipara = 0
mx = 2
my = 2
nPSDs =1381
nAVGs = 1
BW = 2.5
TIME - sec
02/27/97
ASRI
0
100
200
300
400
500
0
1000
2000
3000
4000
5000
FREQ (Hz)

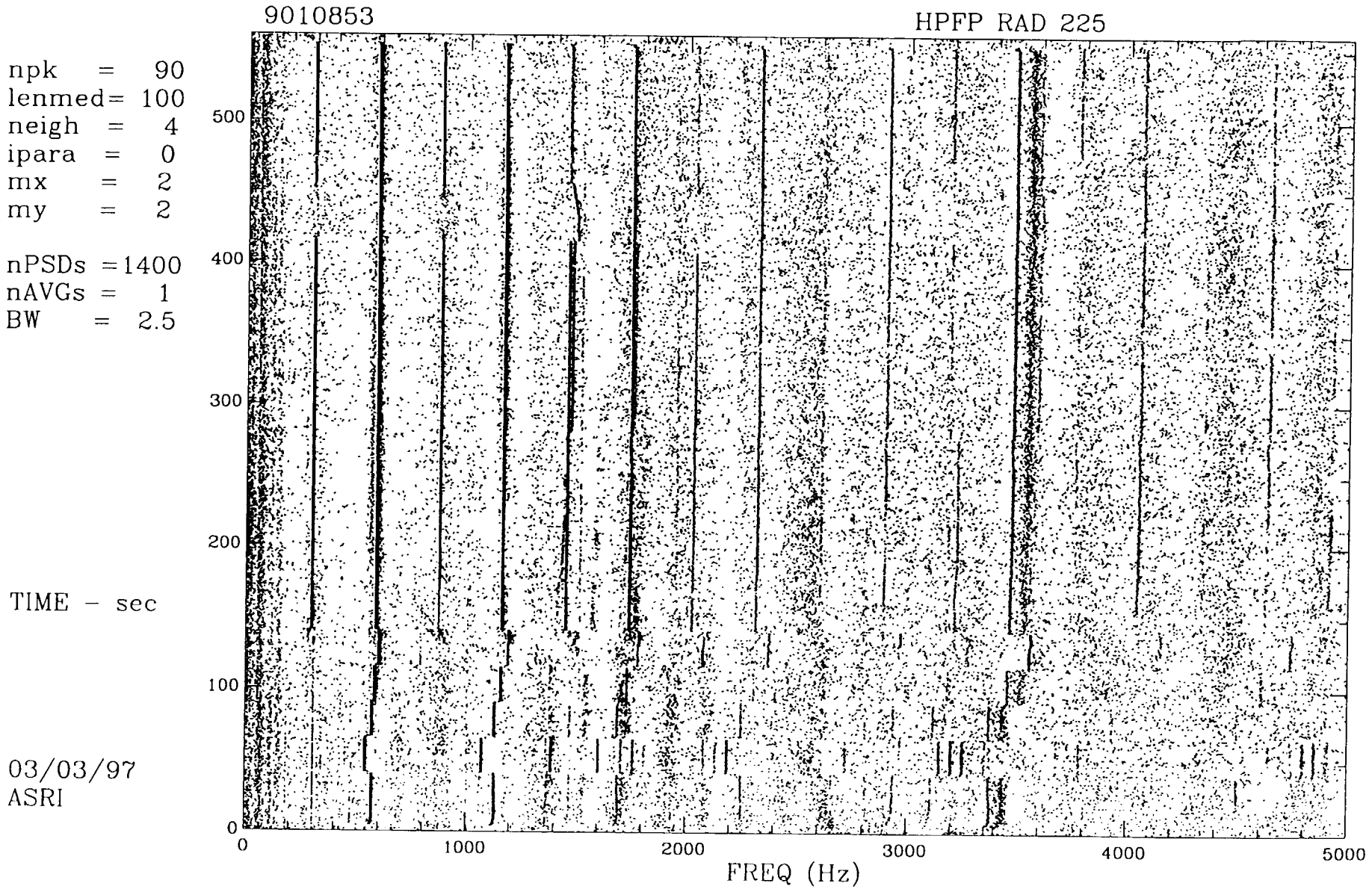
9010853
HPFP RAD 225
npk = 90
lenmed= 100
neigh = 4
ipara = 0
mx = 2
my = 2
nPSDs =1400
nAVGs = 1
BW = 2.5
TIME - sec
03/03/97
ASRI
500
400
300
200
100
0
0
1000
2000
3000
4000
5000
FREQ (Hz)

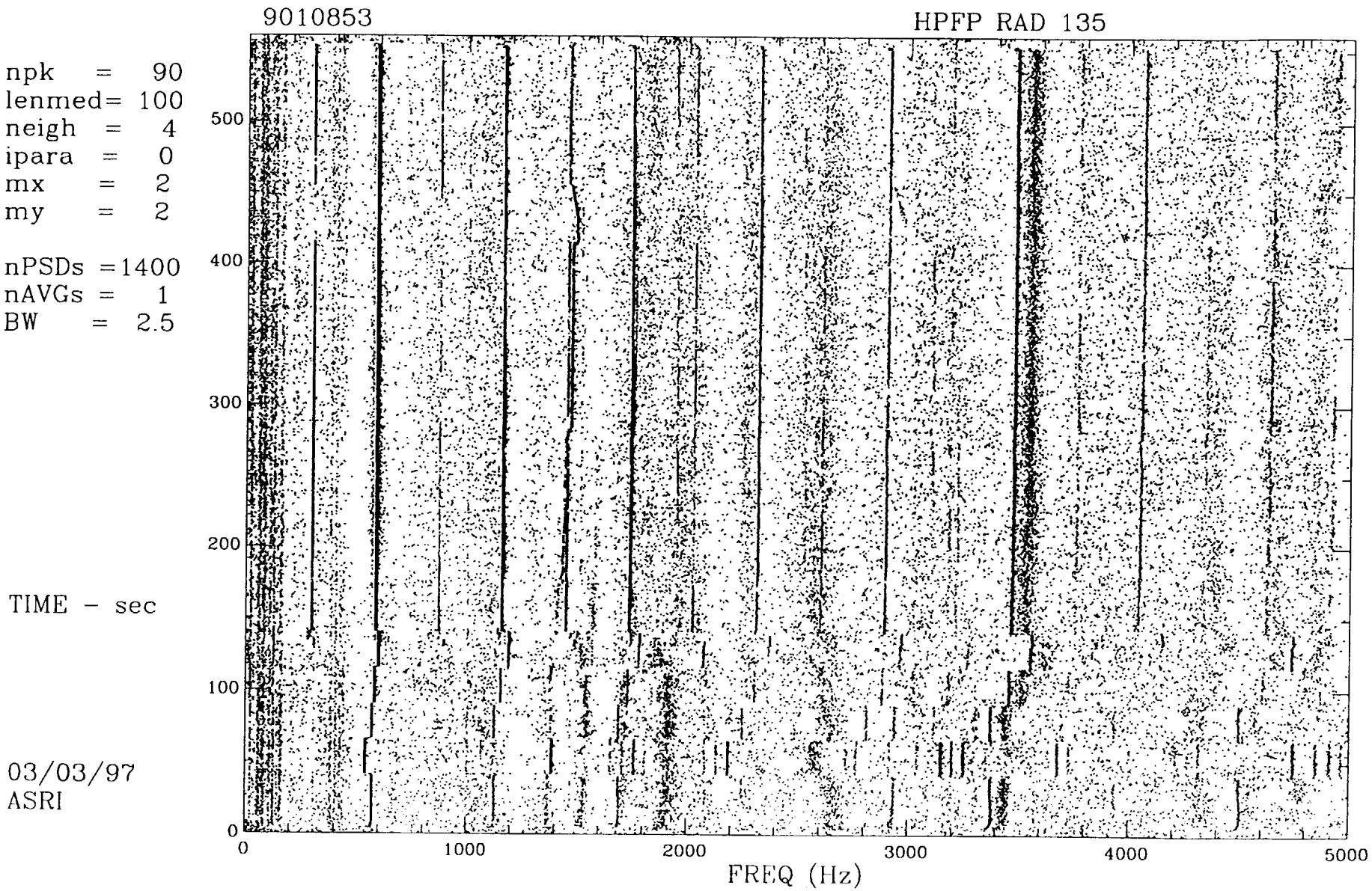
9010853
HPFP RAD 135
npk = 90
lenmed= 100
neigh = 4
ipara = 0
mx = 2
my = 2
nPSDs =1400
nAVGs = 1
BW = 2.5
TIME - sec
0
100
200
300
400
500
0
1000
2000
3000
4000
5000
FREQ (Hz)
03/03/97
ASRI

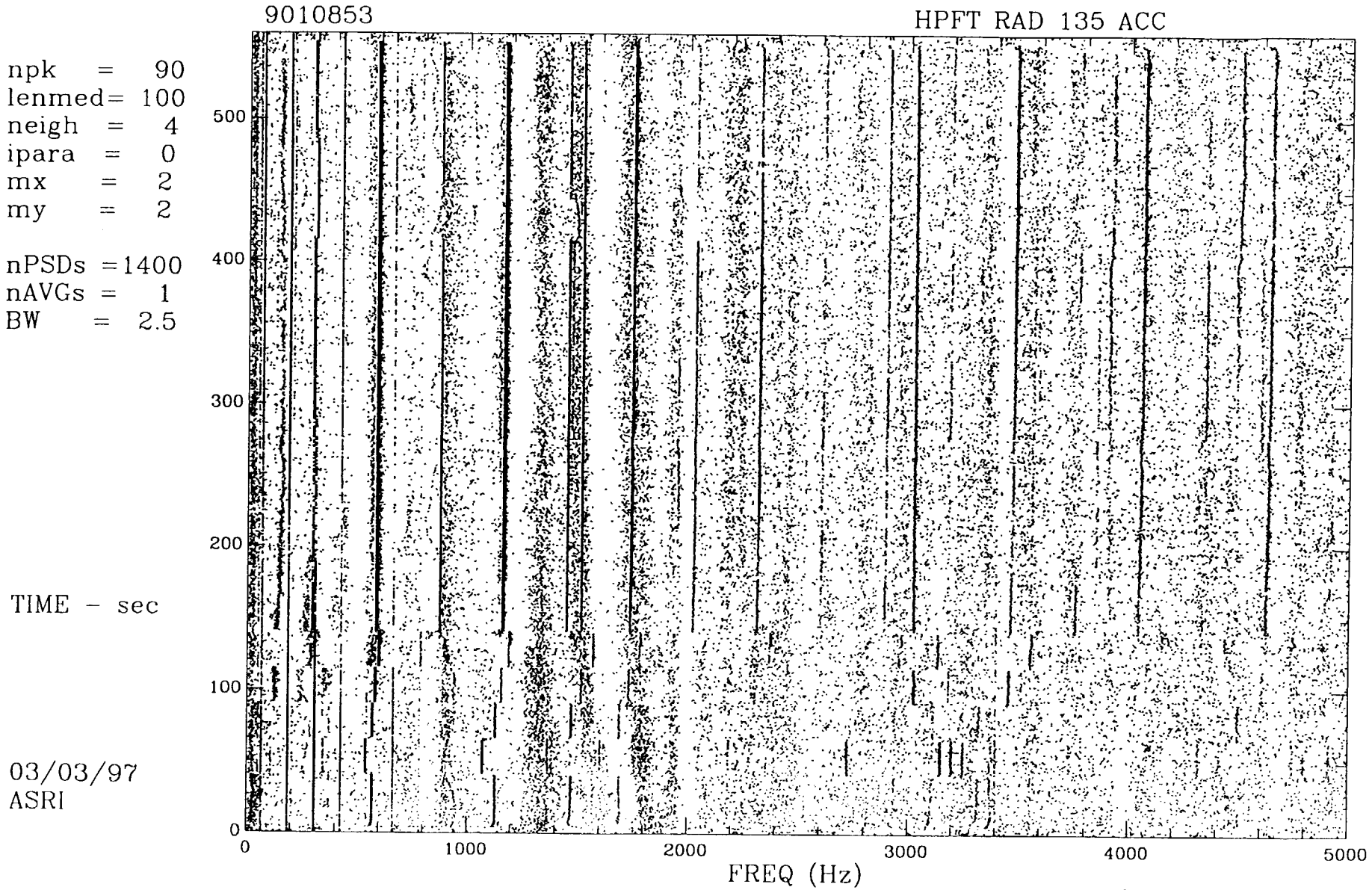
9010853
HPFT RAD 135 ACC
npk = 90
lenmed= 100
neigh = 4
ipara = 0
mx = 2
my = 2
nPSDs =1400
nAVGs = 1
BW = 2.5
TIME - sec
03/03/97
ASRI
0
100
200
300
400
500
0
1000
2000
3000
4000
5000
FREQ (Hz)

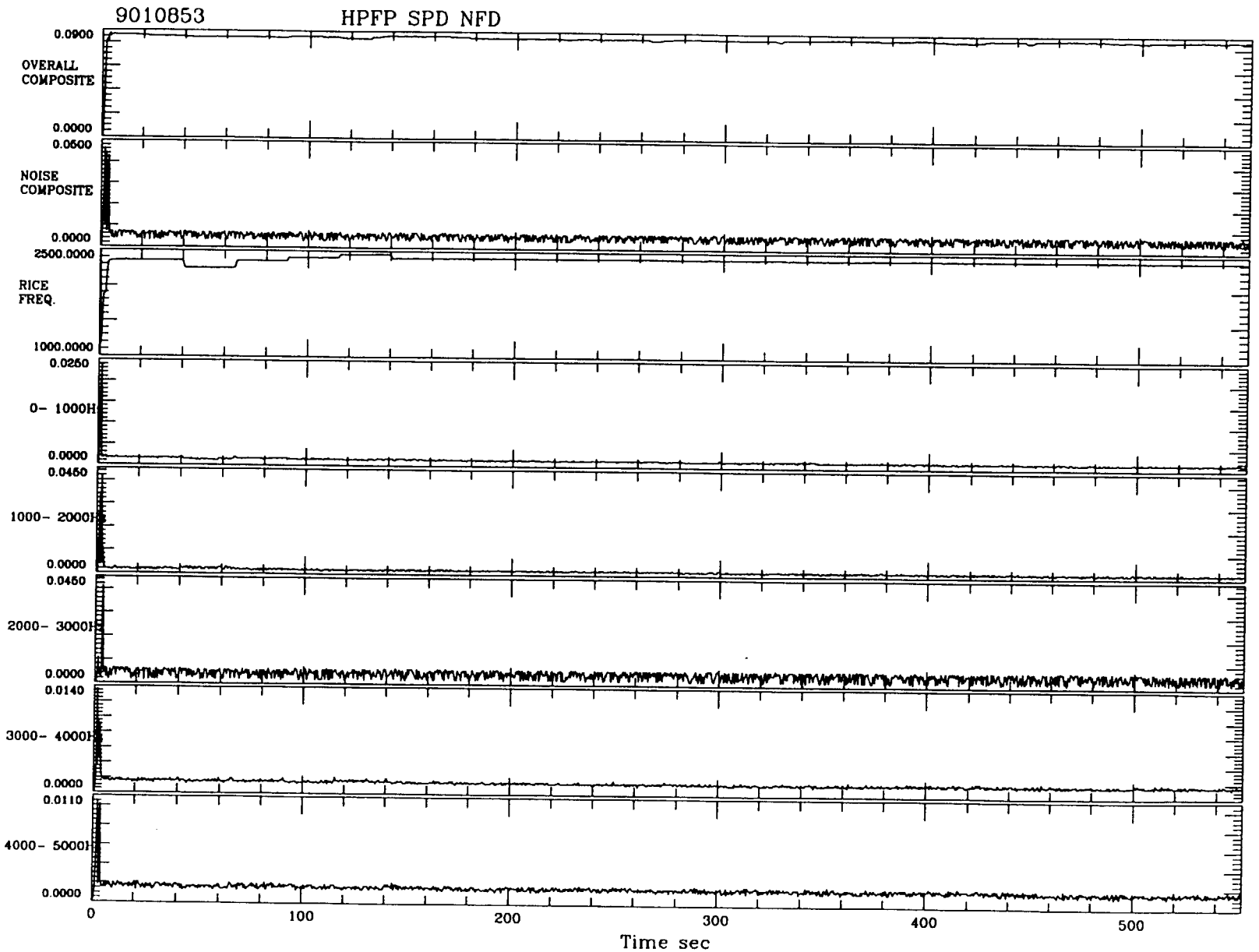

NOISE FLOOR (V RMS; nAVG = 1)

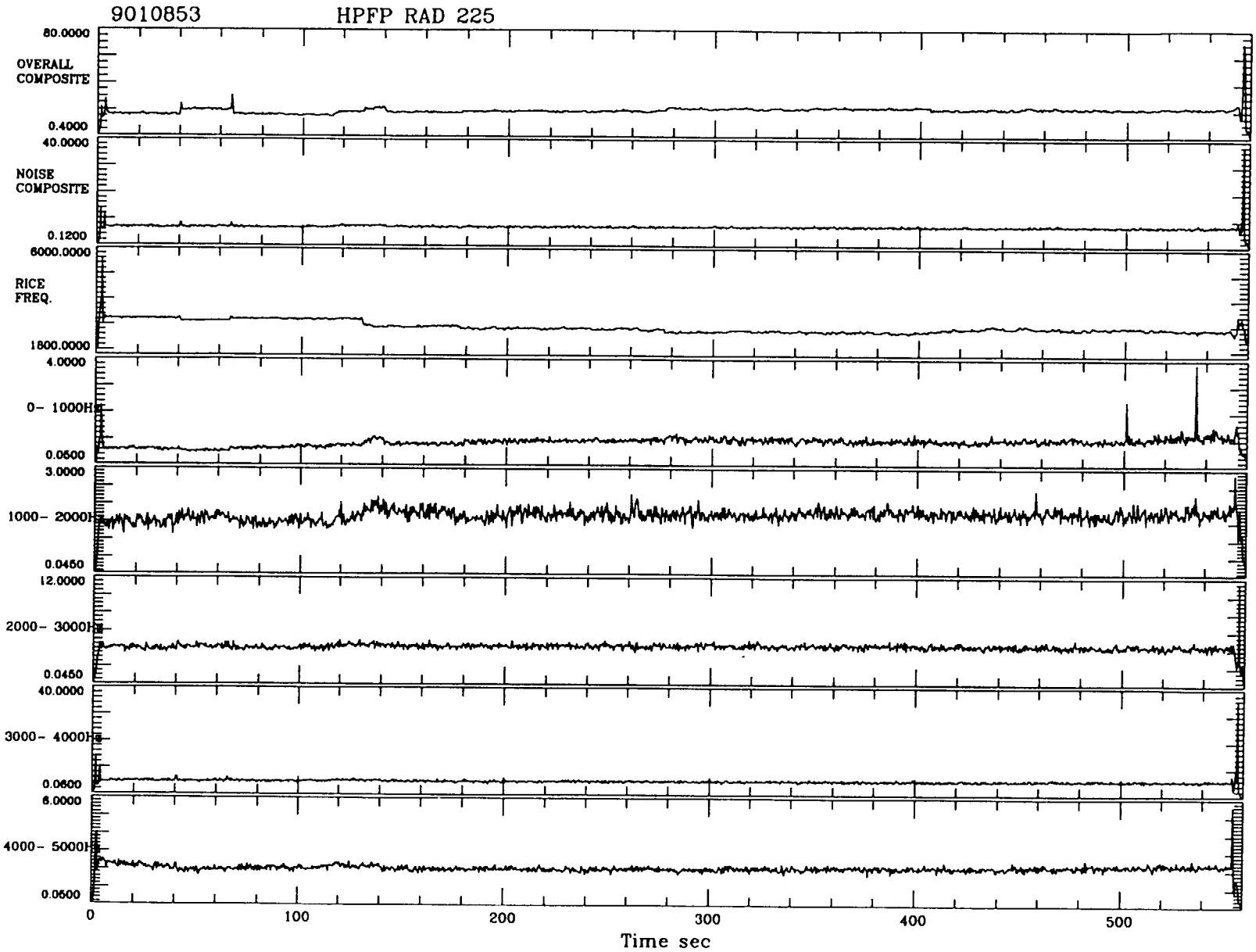

NOISE FLOOR (G RMS; nAVG = 1)

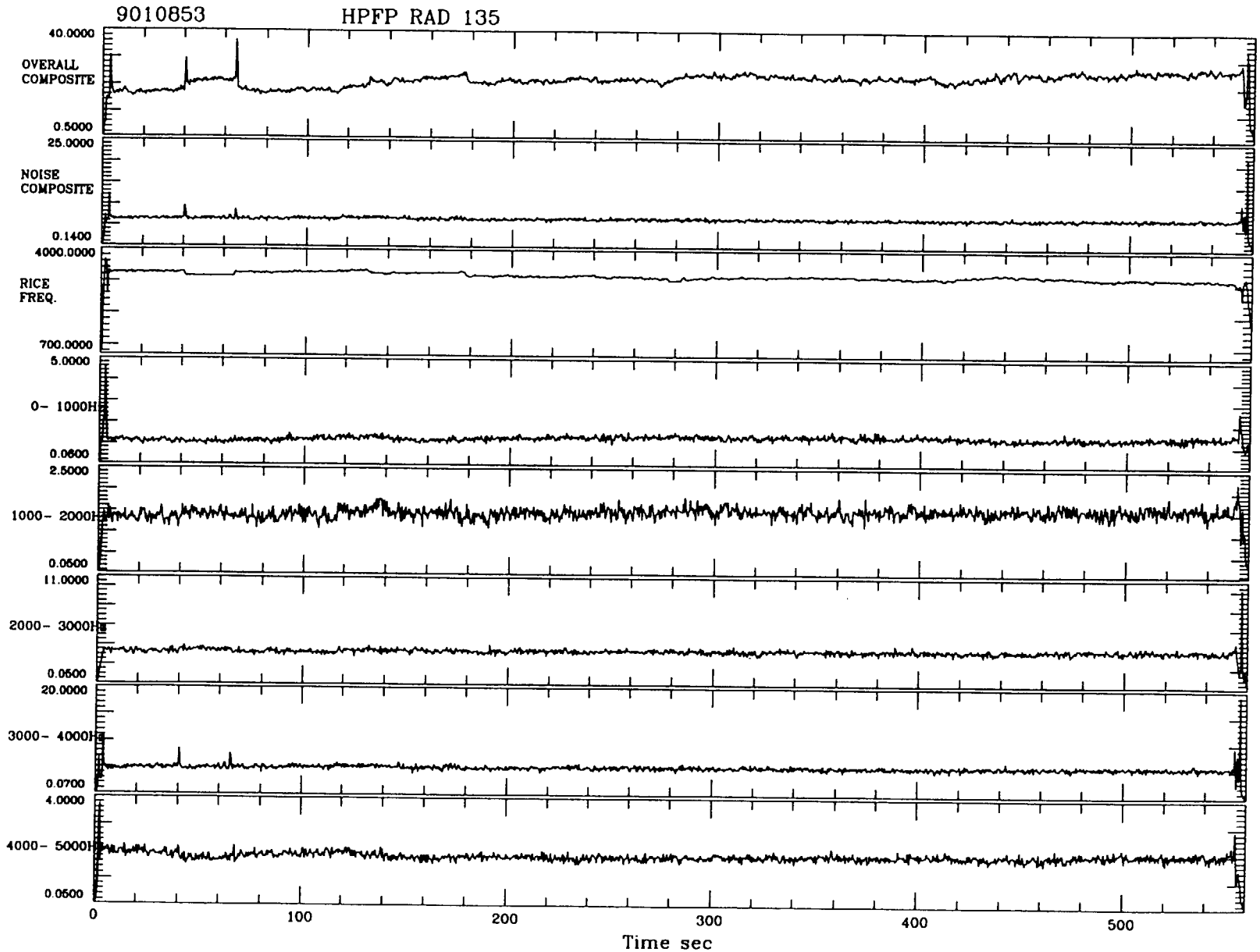

NOISE FLOOR (G RMS; nAVG = 1)

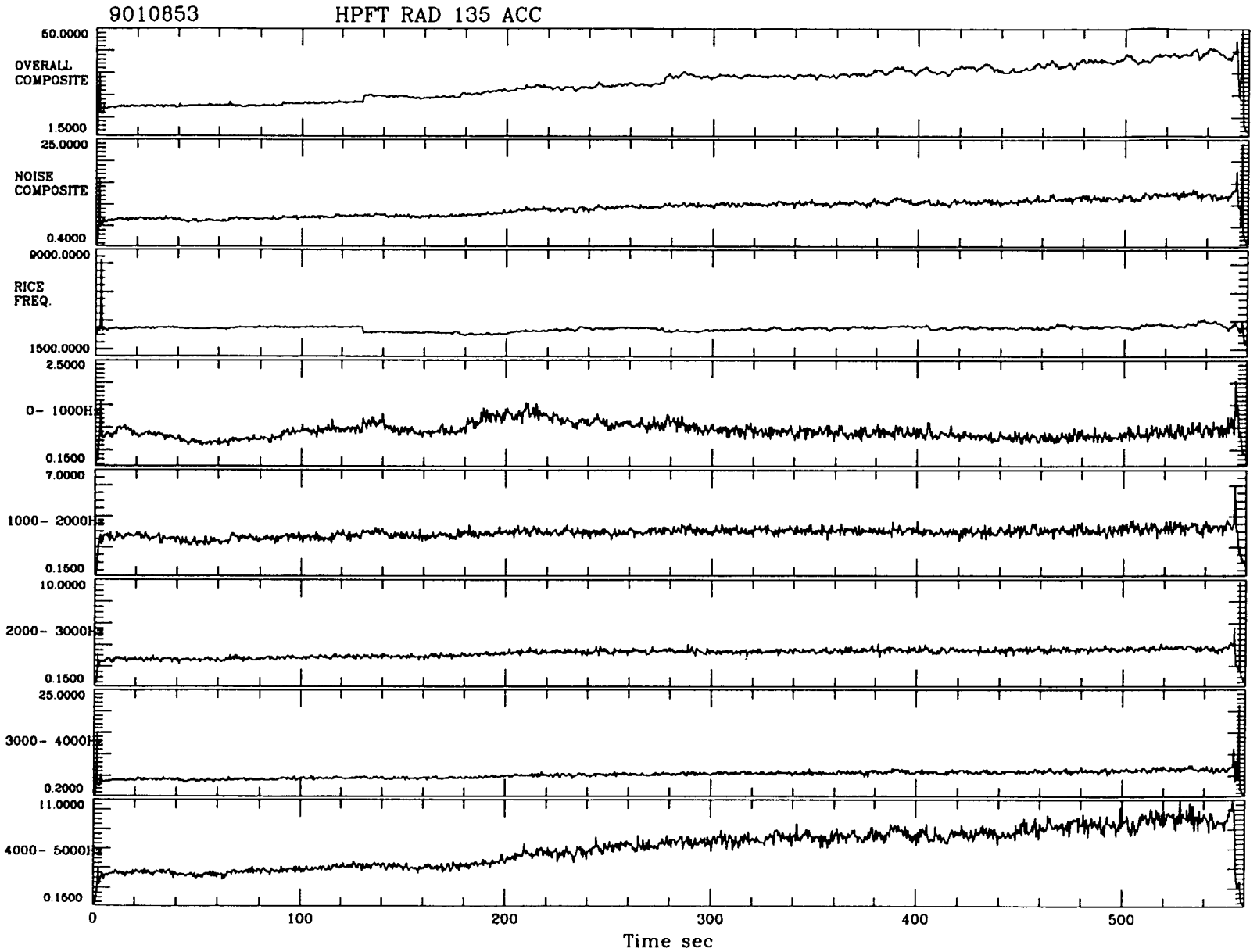

NOISE FLOOR (G RMS; nAVG = 1)

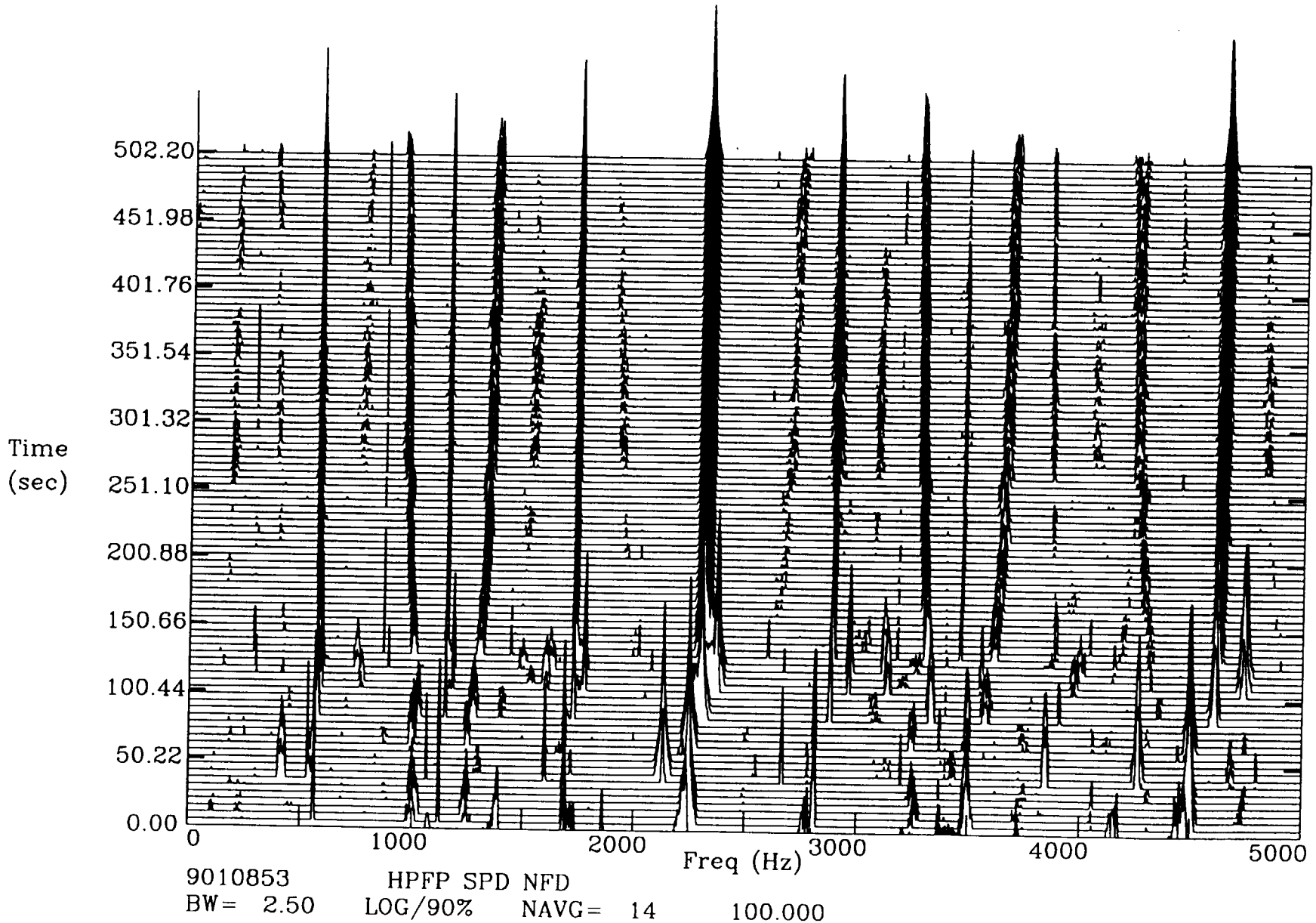
502.20
451.98
401.76
351.54
301.32
251.10
200.88
150.66
100.44
50.22
0.00
Time
(sec)
0
1000
2000
3000
4000
5000
Freq (Hz)
9010853 HPFP SPD NFD
BW= 2.50 LOG/90% NAVG= 14 100.000

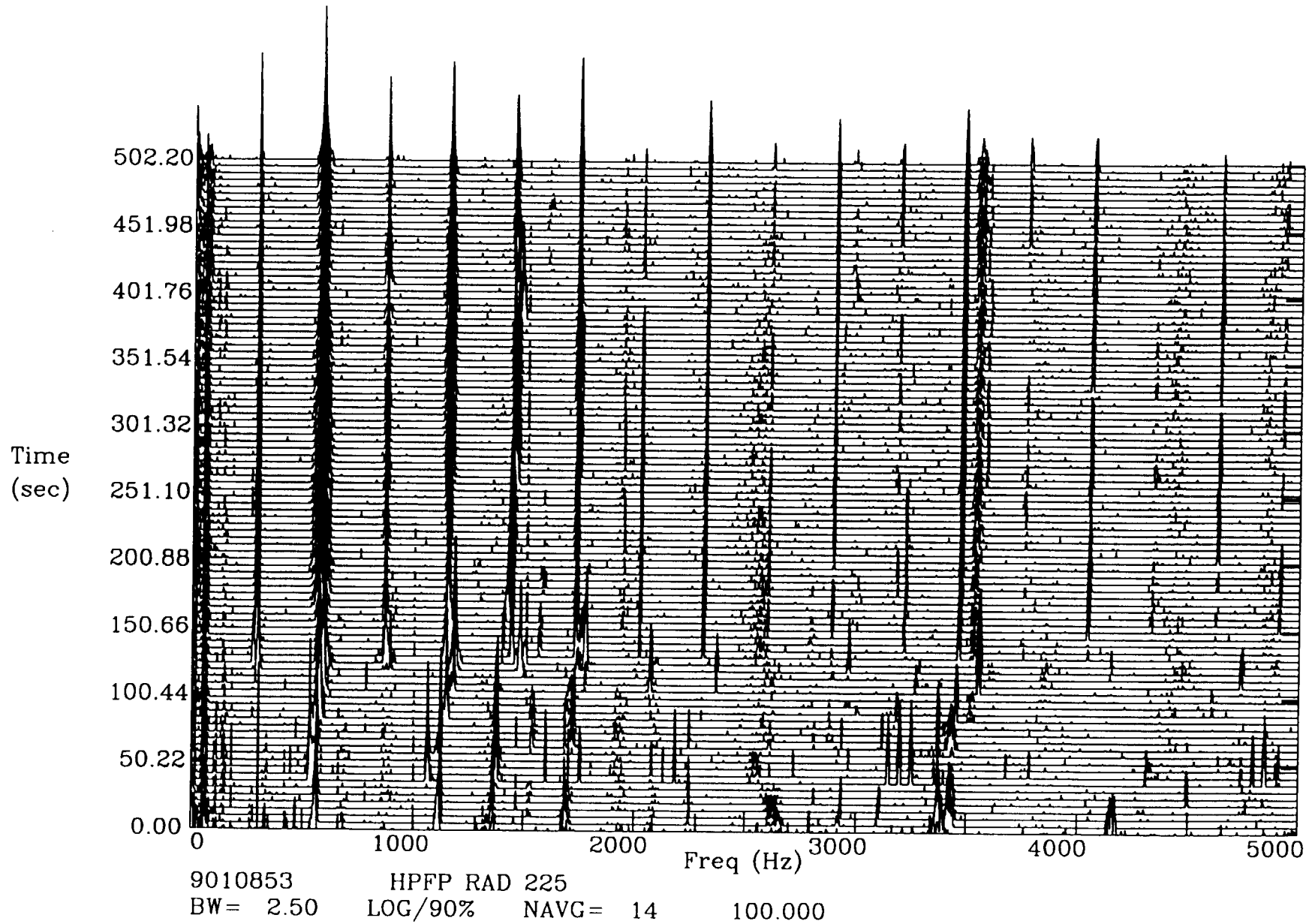
502.20
451.98
401.76
351.54
301.32
251.10
200.88
150.66
100.44
50.22
0.00
Time
(sec)
0
1000
2000
3000
4000
5000
Freq (Hz)
9010853 HPFP RAD 225
BW= 2.50 LOG/90% NAVG= 14 100.000

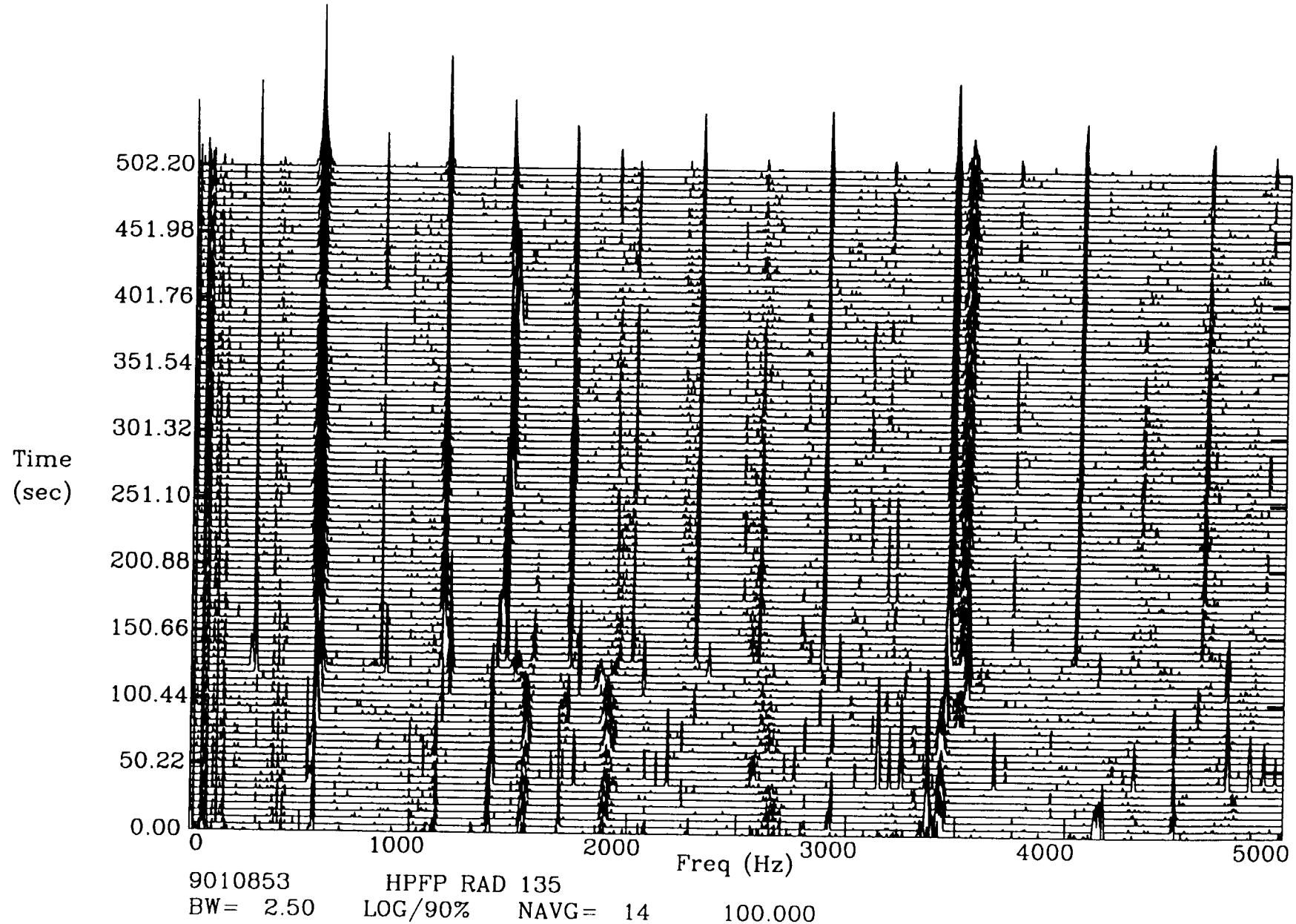
502.20
451.98
401.76
351.54
301.32
251.10
200.88
150.66
100.44
50.22
0.00
Time
(sec)
0
1000
2000
3000
4000
5000
Freq (Hz)
9010853 HPFP RAD 135
BW= 2.50 LOG/90% NAVG= 14 100.000

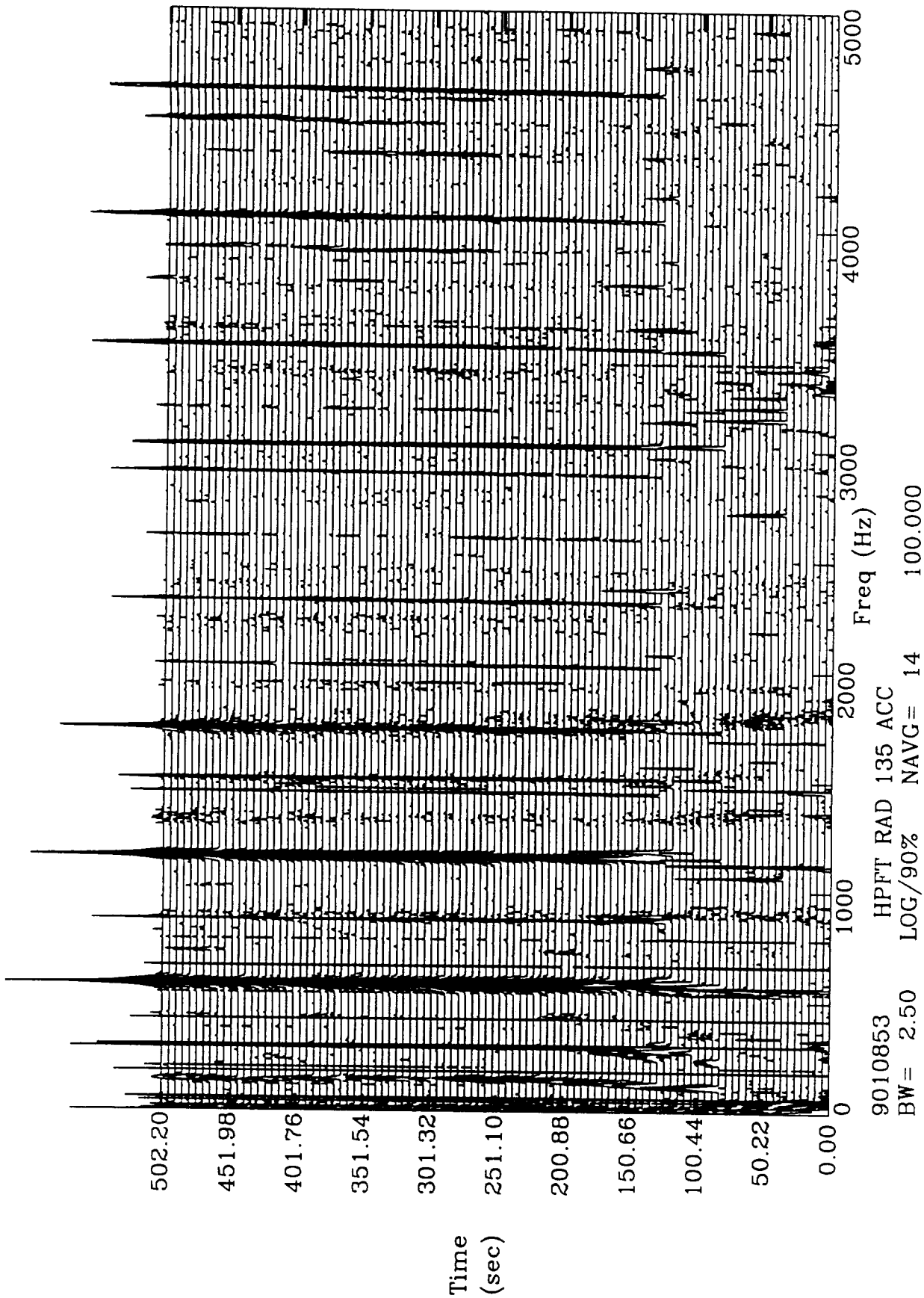
502.20
451.98
401.76
351.54
301.32
251.10
200.88
150.66
100.44
50.22
0.00
Time (sec)
0
1000
2000
3000
4000
5000
Freq (Hz)
9010853 HPFT RAD 135 ACC
BW= 2.50 LOG/90% NAVG= 14 100.000

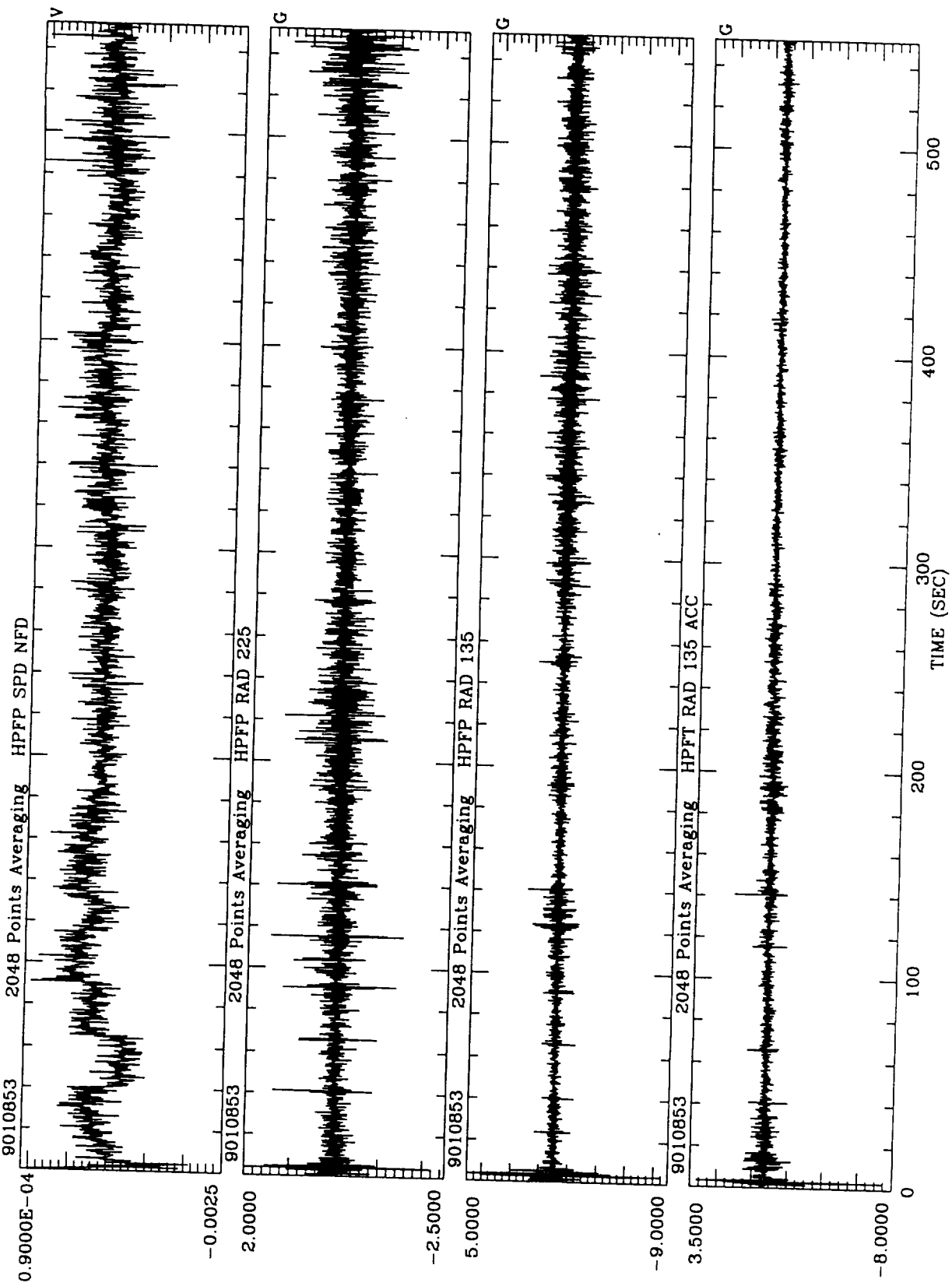
V
G
G
G
9010853
2048 Points Averaging
HPFP SPD NFD
HPFP RAD 225
HPFP RAD 135
HPFT RAD 135 ACC
0.9000E-04
-0.0025
2.0000
-2.5000
5.0000
-9.0000
3.5000
-8.0000
0
100
200
300
400
500
TIME (SEC)

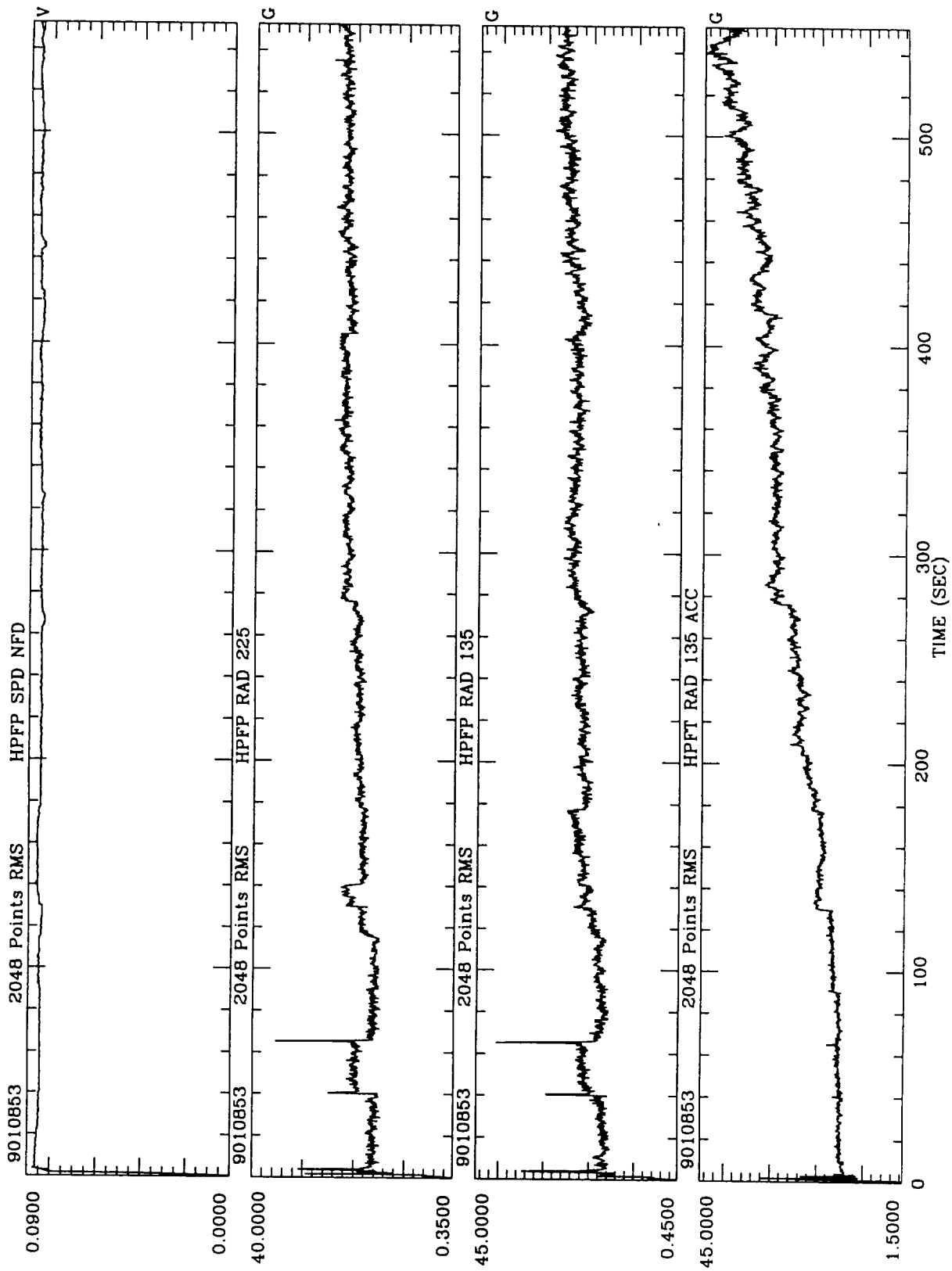
9010853 2048 Points RMS HPFP SPD NFD
V
0.0900
0.0000
9010853 2048 Points RMS HPFP RAD 225
G
40.0000
0.3500
9010853 2048 Points RMS HPFP RAD 135
G
45.0000
0.4500
9010853 2048 Points RMS HPFT RAD 135 ACC
G
45.0000
1.5000
0
100
200
300
400
500
TIME (SEC)

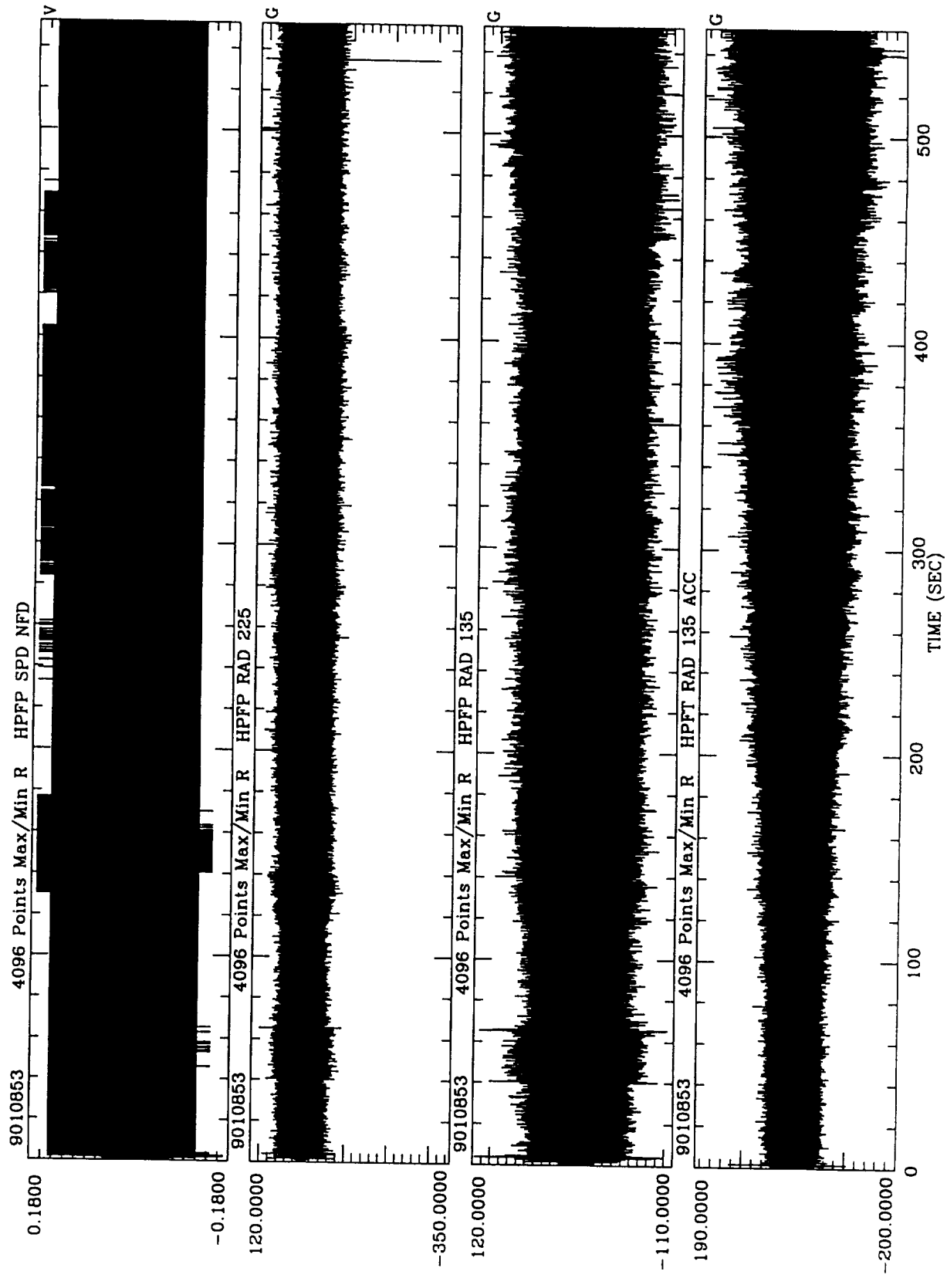
9010853 4096 Points Max/Min R HPFP SPD NFD
V
0.1800
-0.1800
9010853 4096 Points Max/Min R HPFP RAD 225
G
120.0000
-350.0000
9010853 4096 Points Max/Min R HPFP RAD 135
G
120.0000
-110.0000
9010853 4096 Points Max/Min R HPFT RAD 135 ACC
G
190.0000
-200.0000
0
100
200
300
400
500
TIME (SEC)

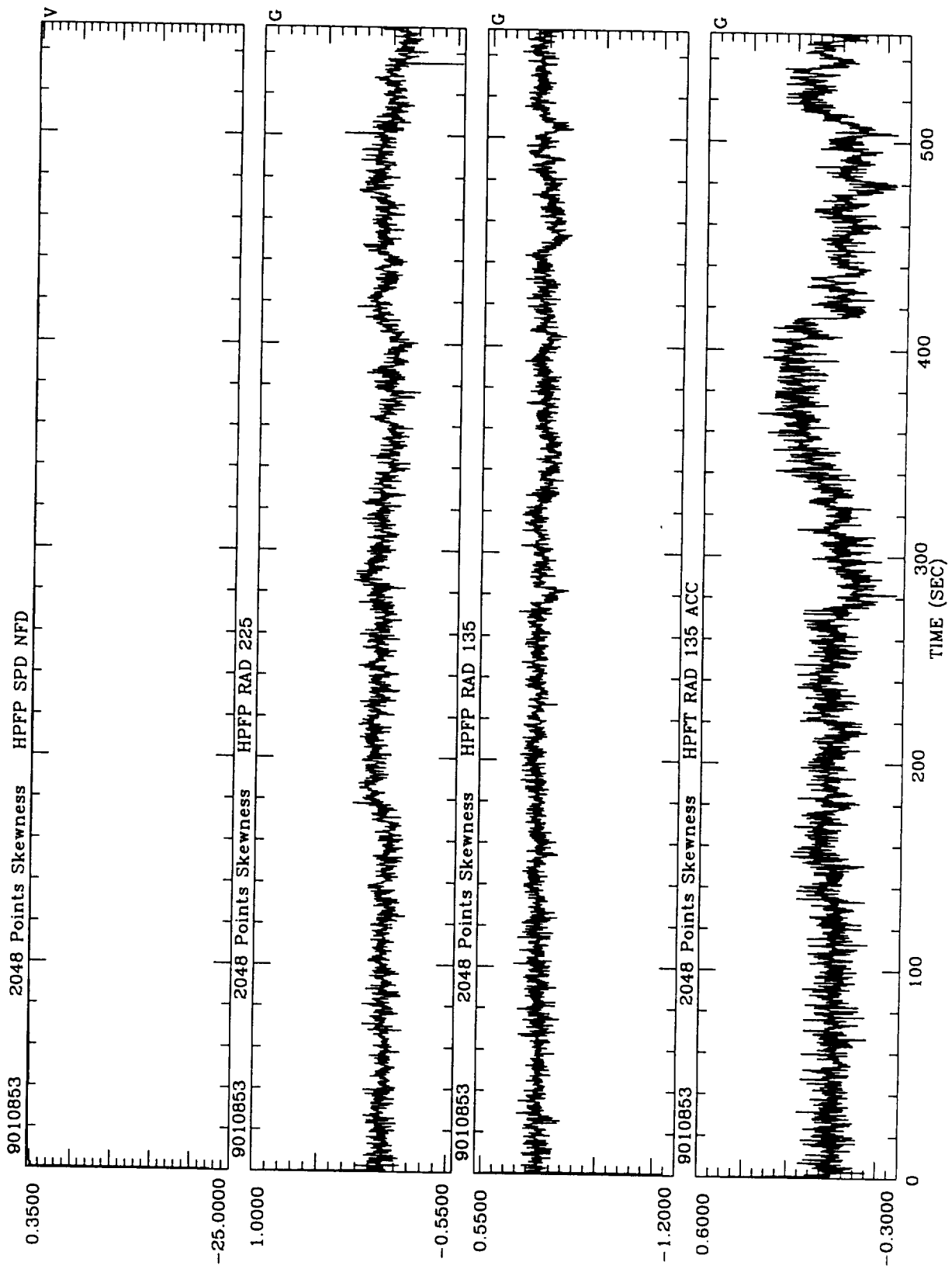
9010853 2048 Points Skewness HPFP SPD NFD
V
0.3500
-25.0000
9010853 2048 Points Skewness HPFP RAD 225
G
1.0000
-0.5500
9010853 2048 Points Skewness HPFP RAD 135
G
0.5500
-1.2000
9010853 2048 Points Skewness HPFT RAD 135 ACC
G
0.6000
-0.3000
0
100
200
300
400
500
TIME (SEC)

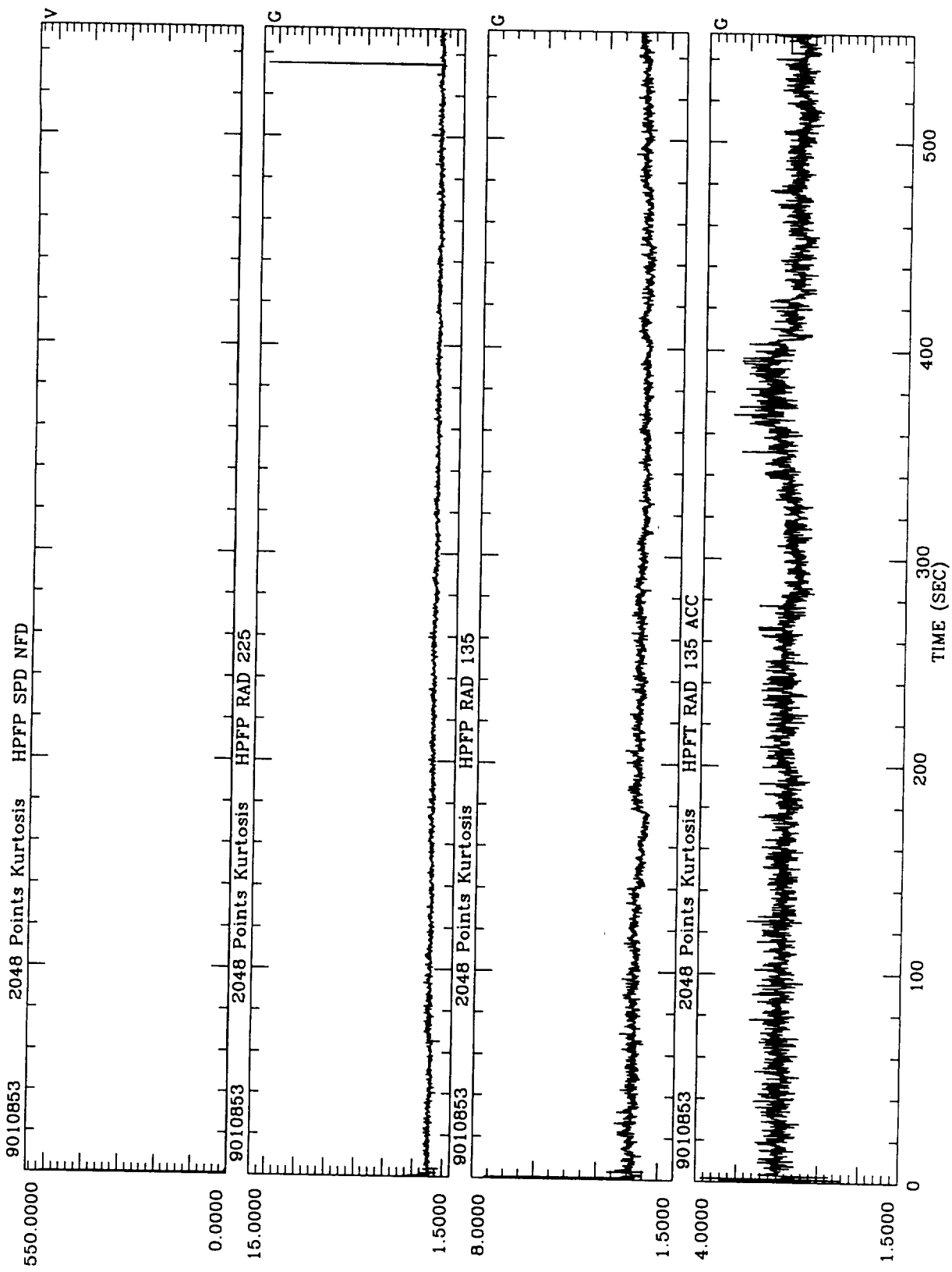
9010853
2048 Points Kurtosis
HPFP SPD NFD
V
550.0000
0.0000
9010853
2048 Points Kurtosis
HPFP RAD 225
G
15.0000
1.5000
9010853
2048 Points Kurtosis
HPFP RAD 135
G
8.0000
1.5000
9010853
2048 Points Kurtosis
HPFT RAD 135 ACC
G
4.0000
1.5000
0
100
200
300
400
500
TIME (SEC)

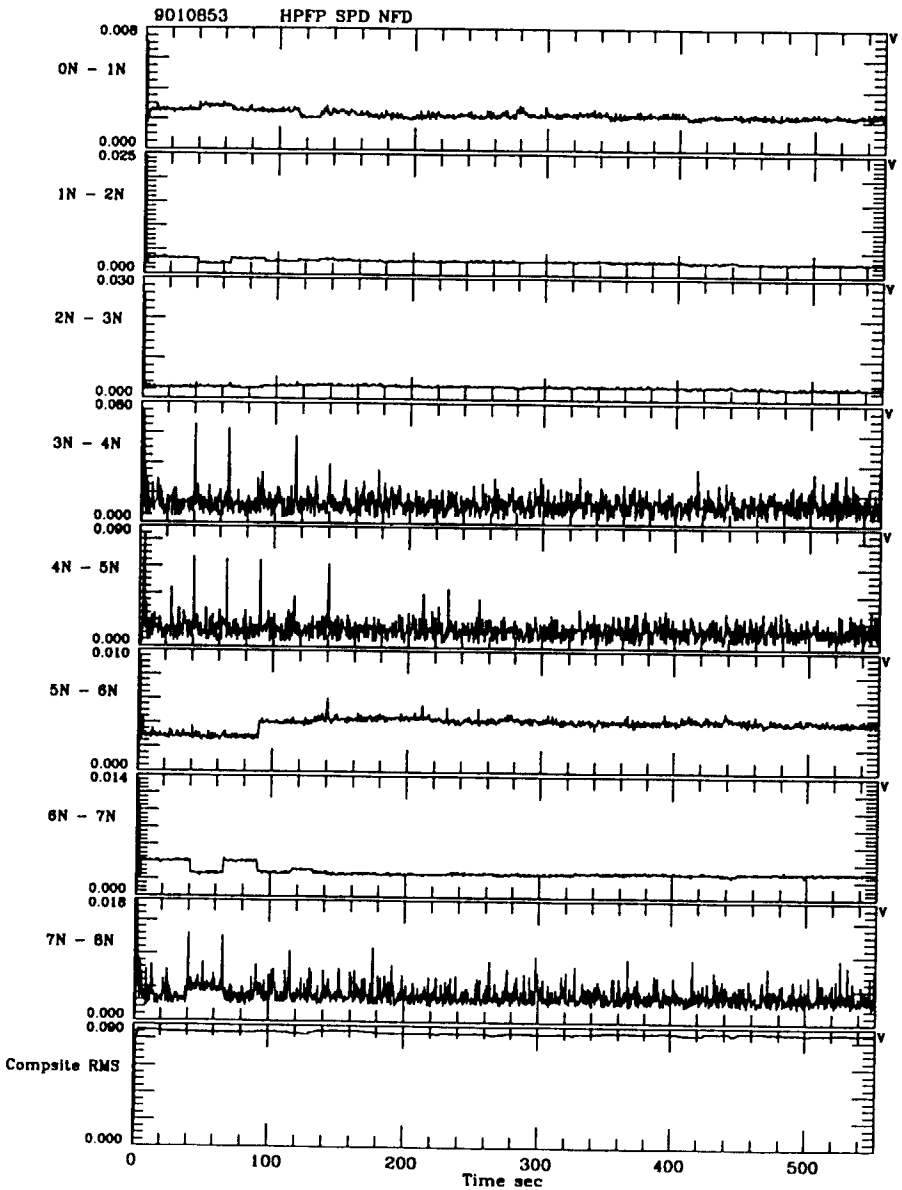

Between Harmonic RMS Tracking

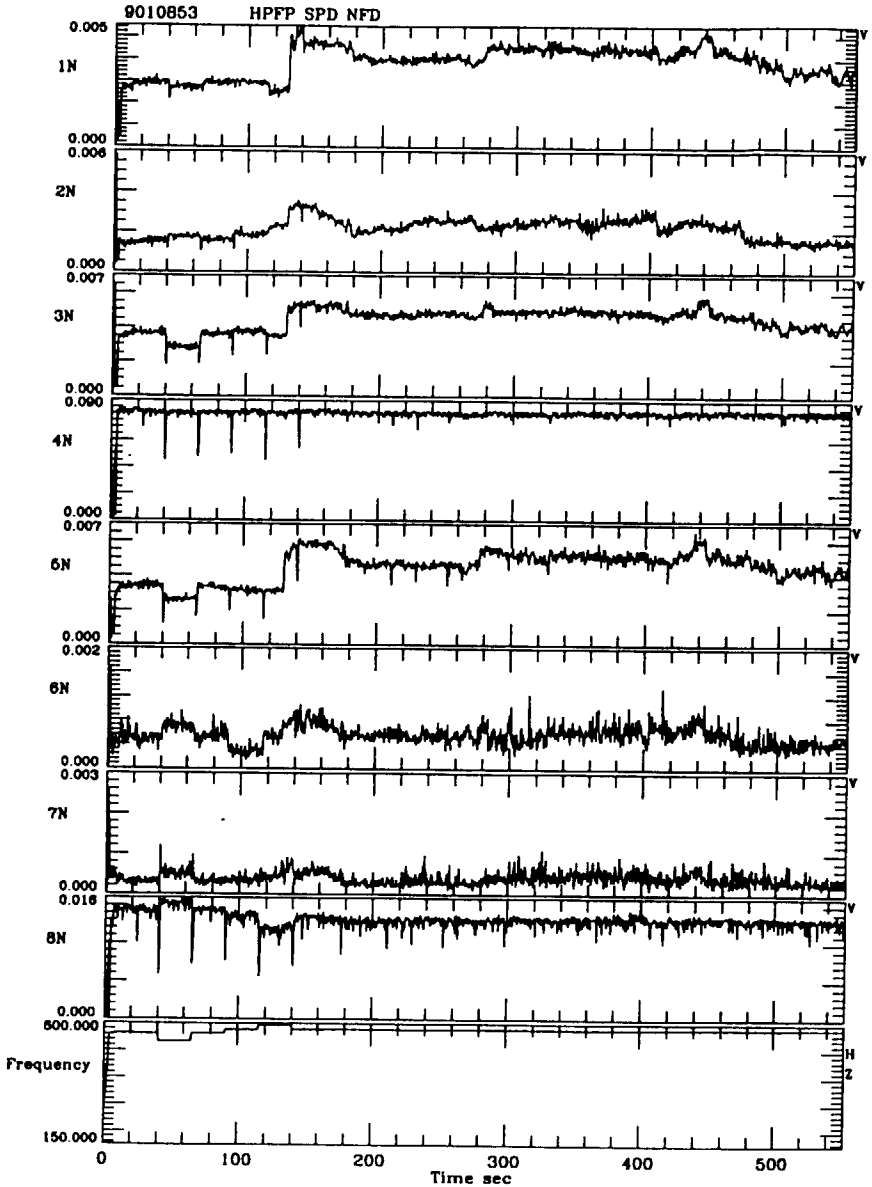

Sync/Harmonic RMS Tracking

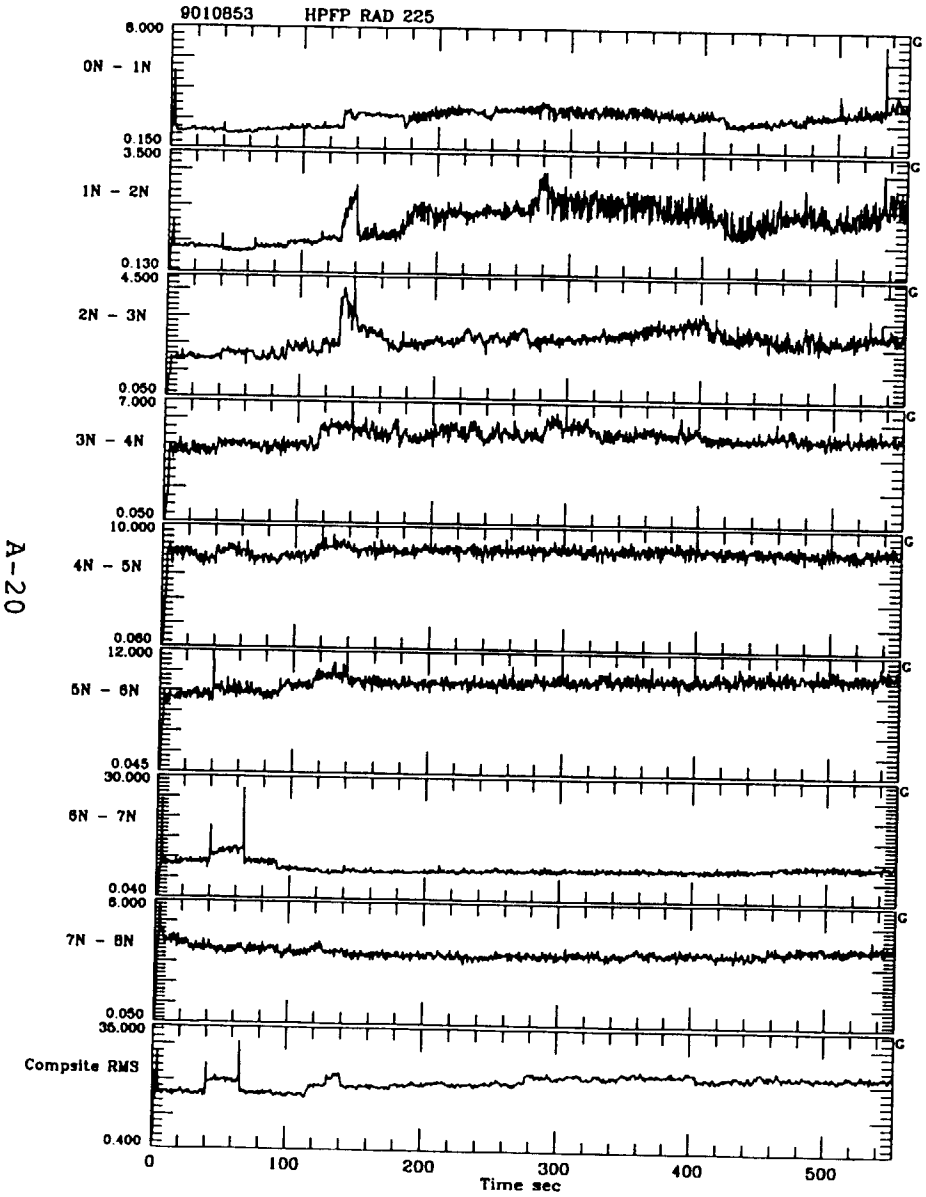

Between Harmonic RMS Tracking

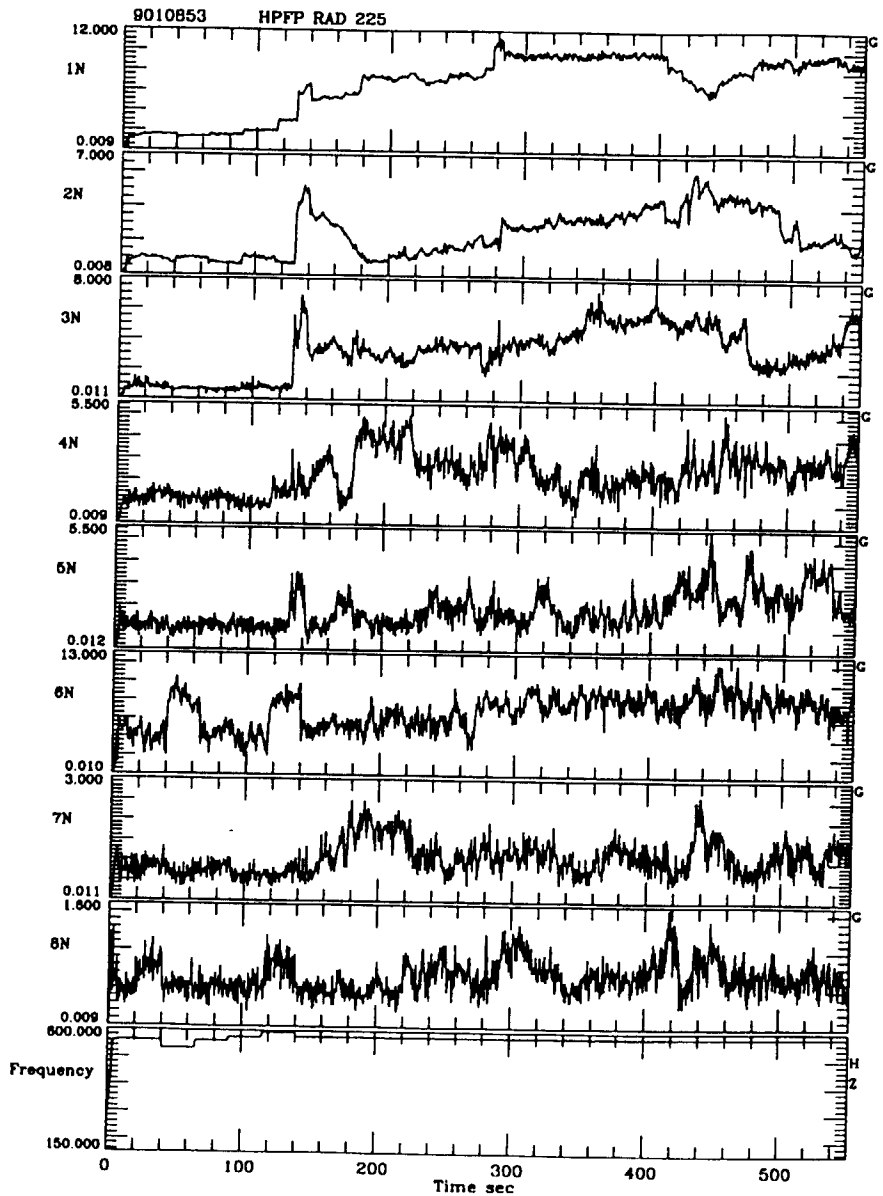

Sync/Harmonic RMS Tracking

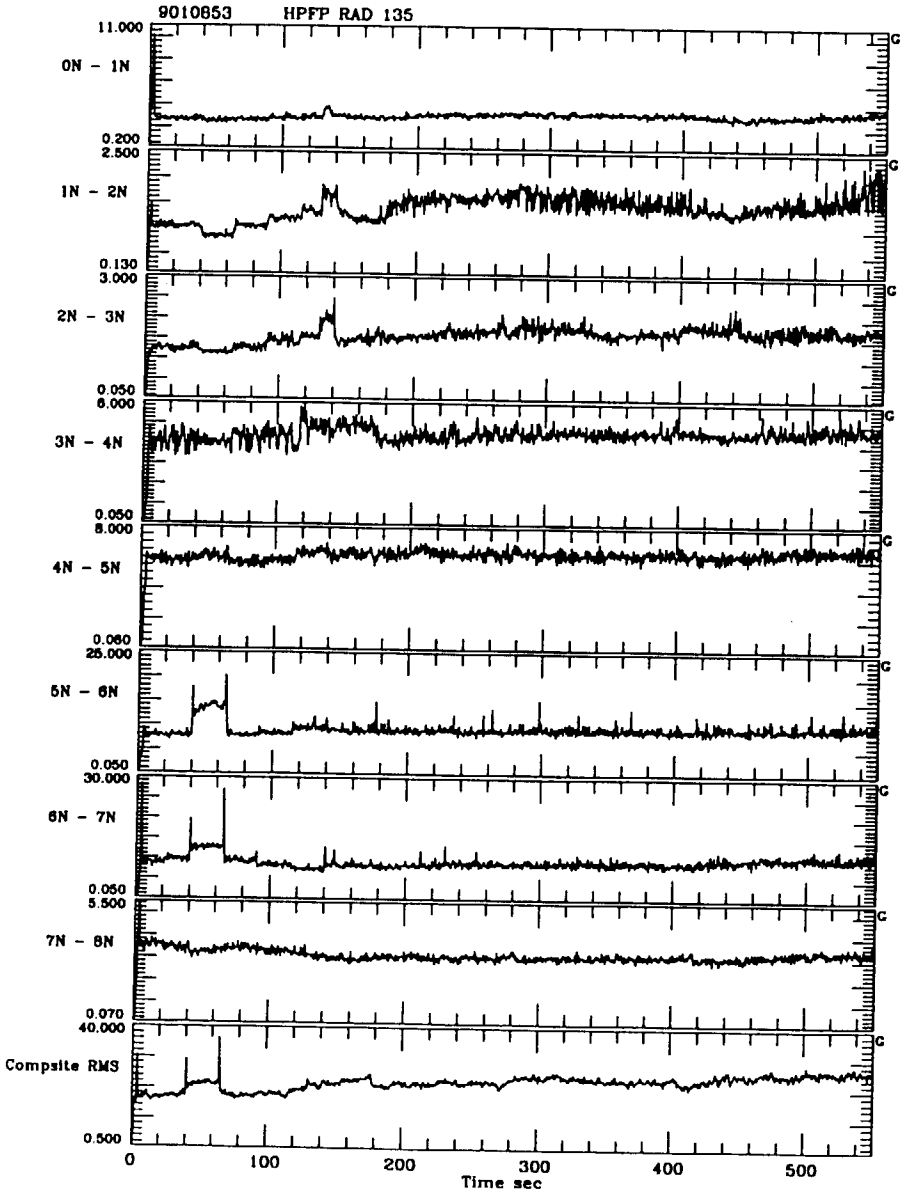

Between Harmonic RMS Tracking

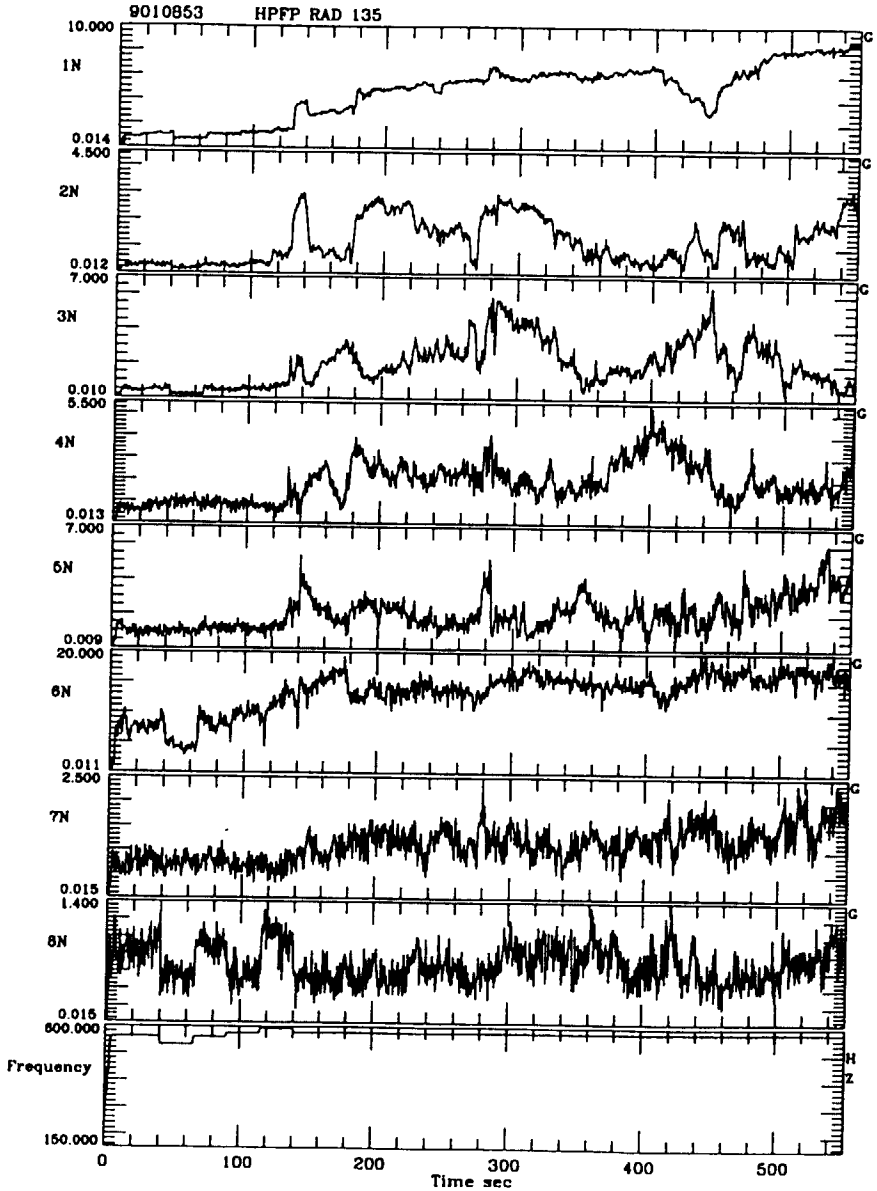

Sync/Harmonic RMS Tracking

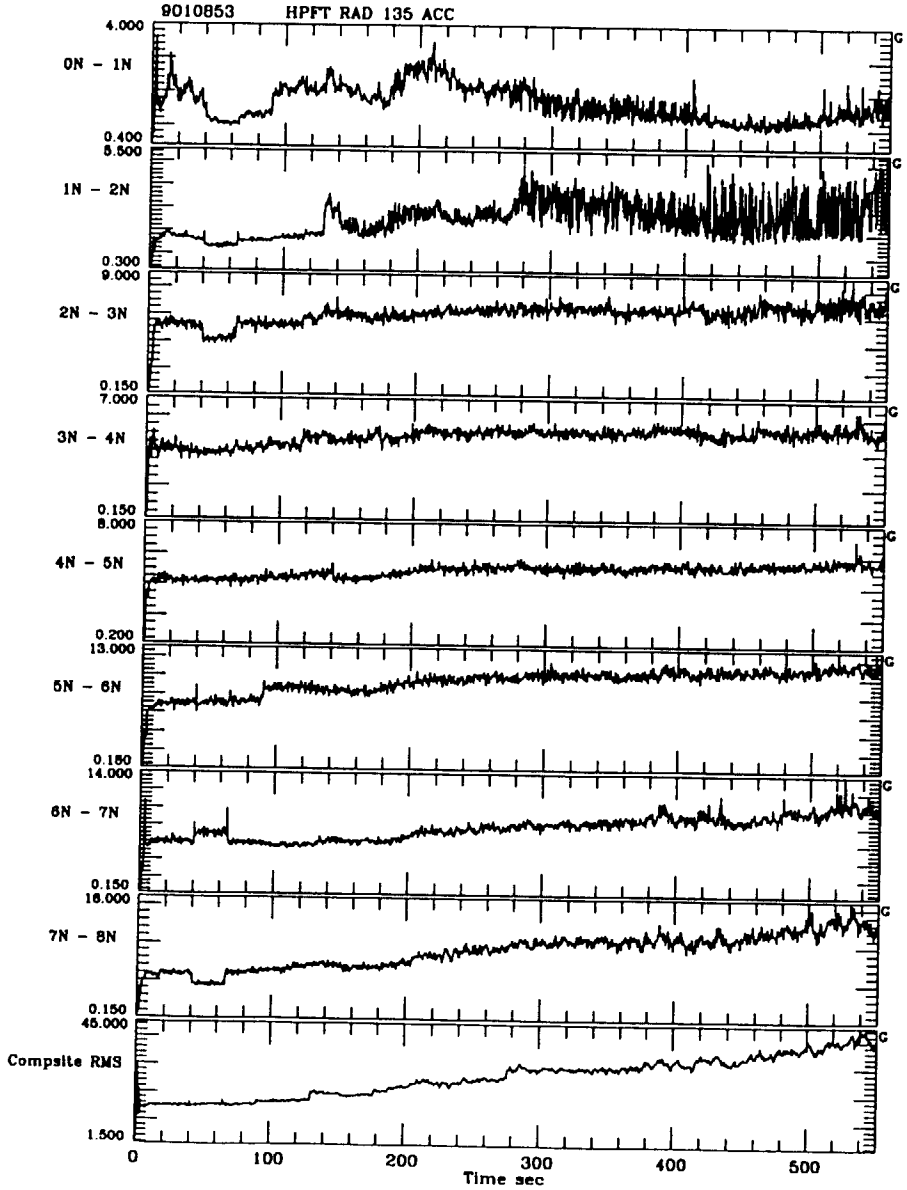

Between Harmonic RMS Tracking

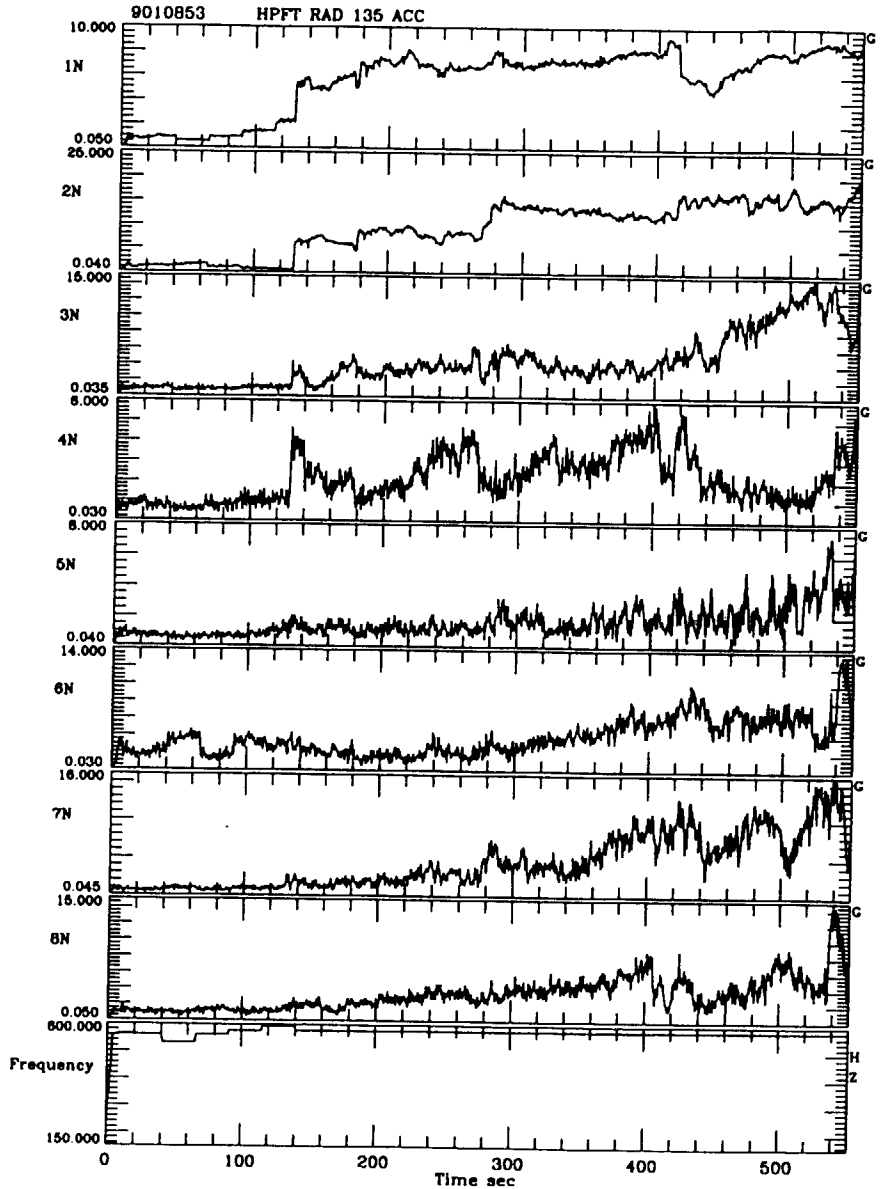

Sync/Harmonic RMS Tracking

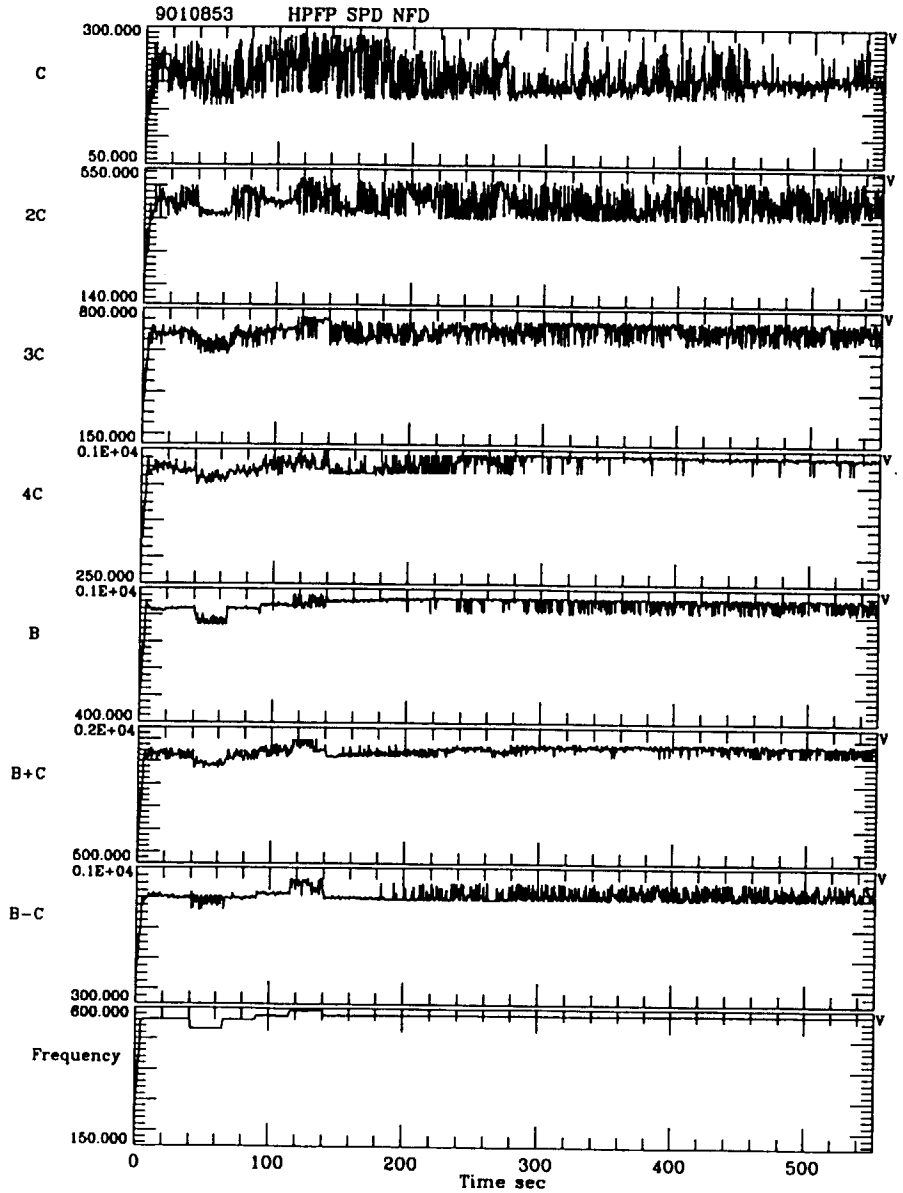

Bearing Frequency Tracking

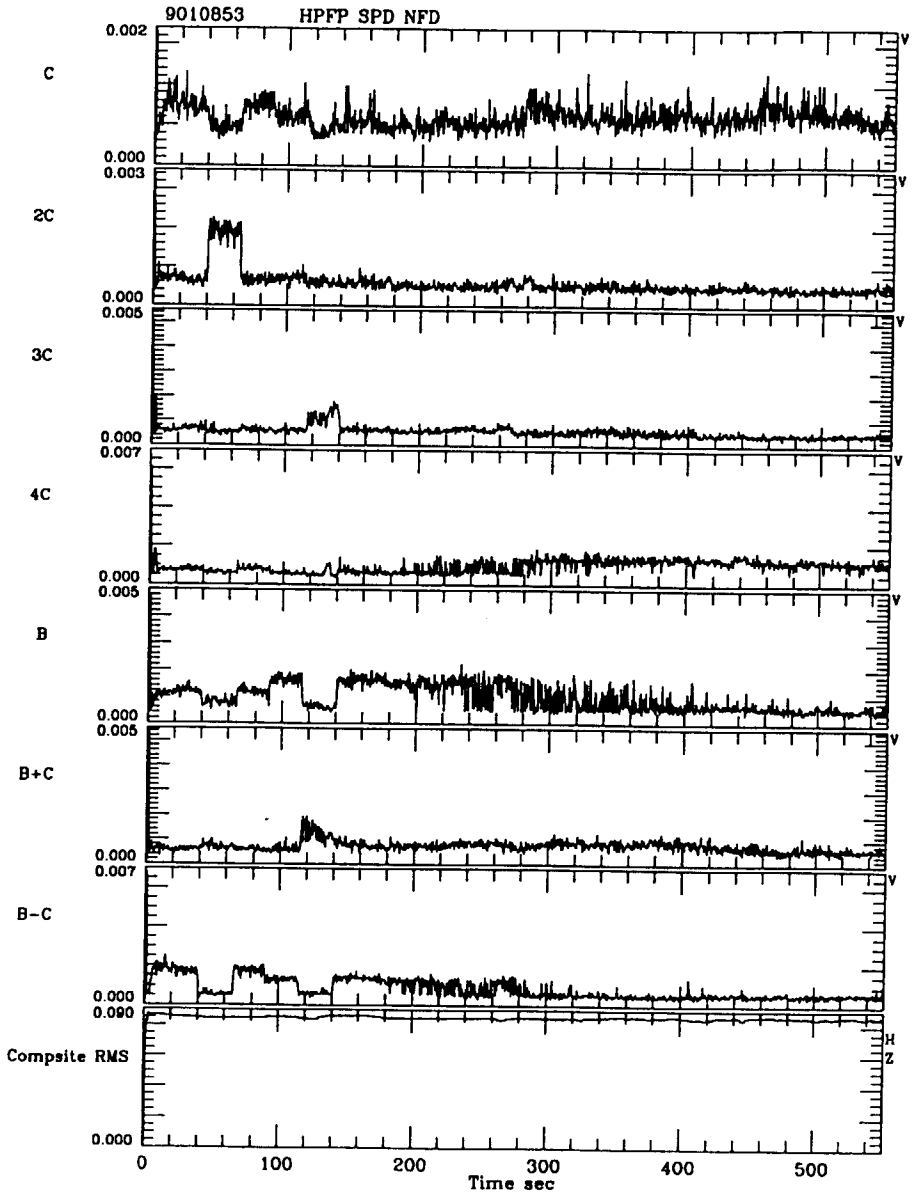

Bearing RMS Tracking

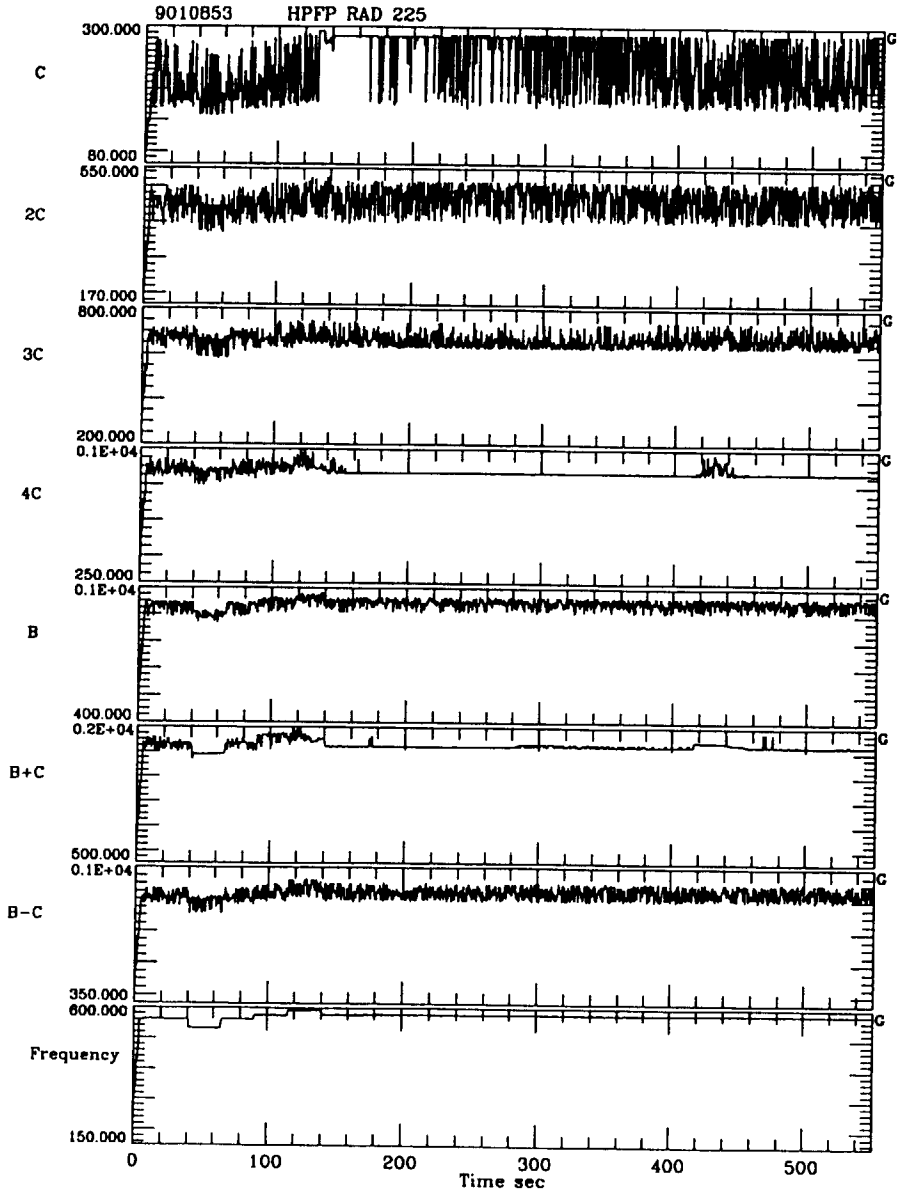

Bearing Frequency Tracking

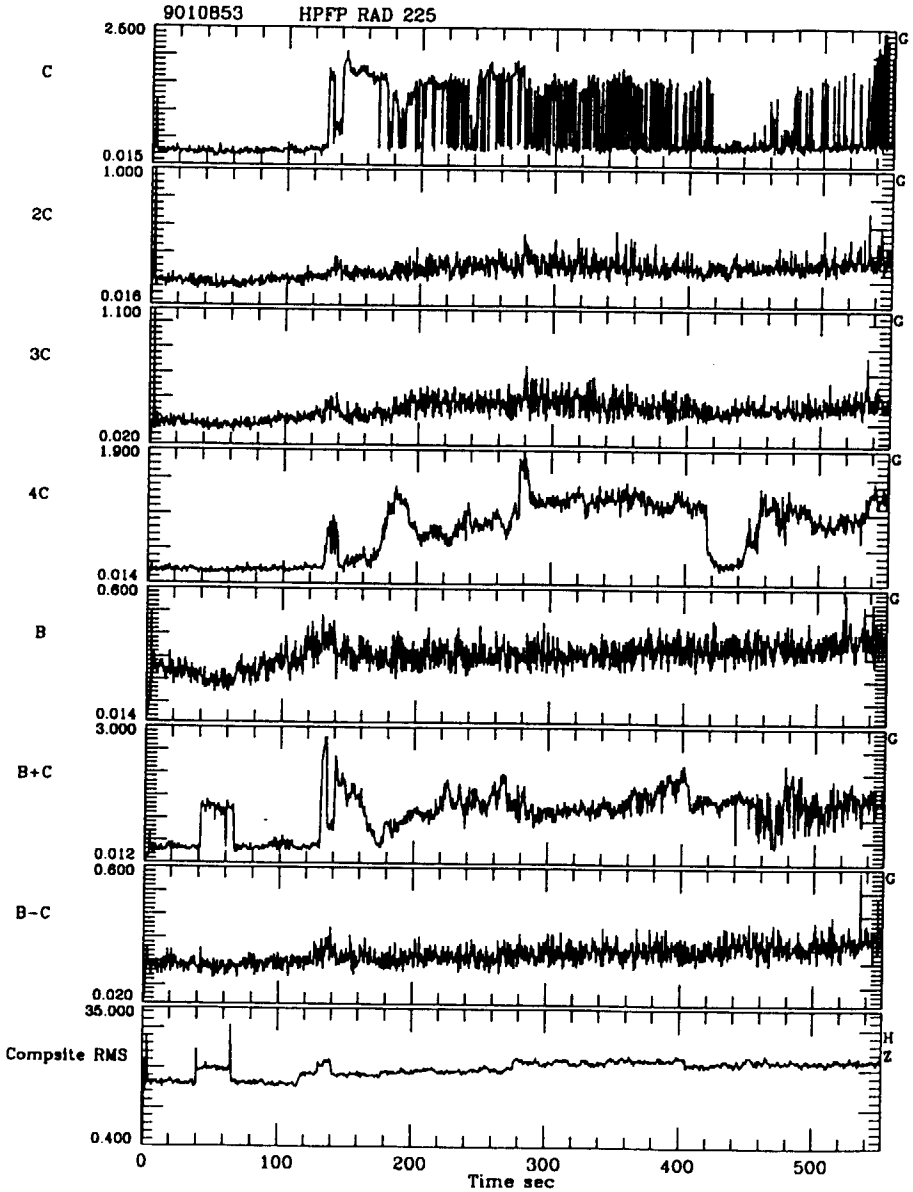

Bearing RMS Tracking

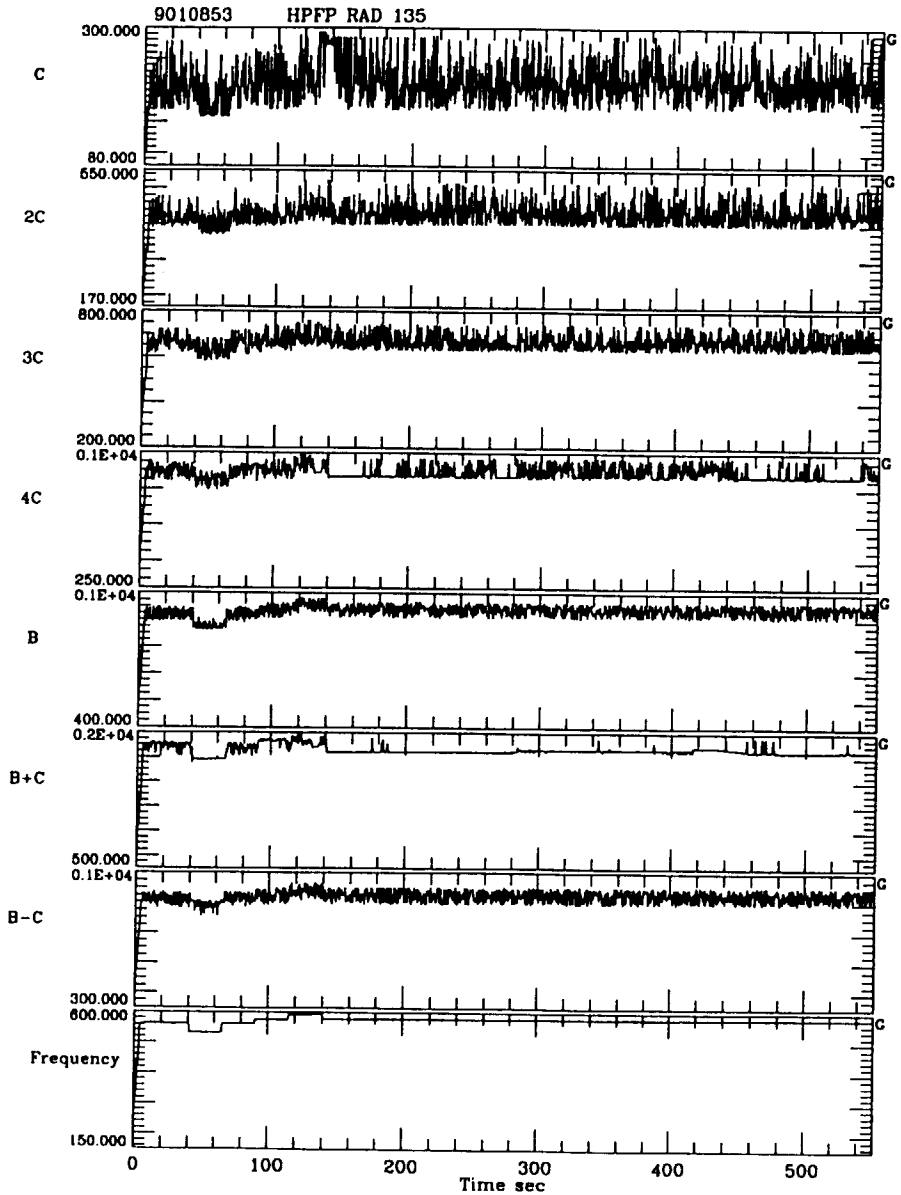

Bearing Frequency Tracking

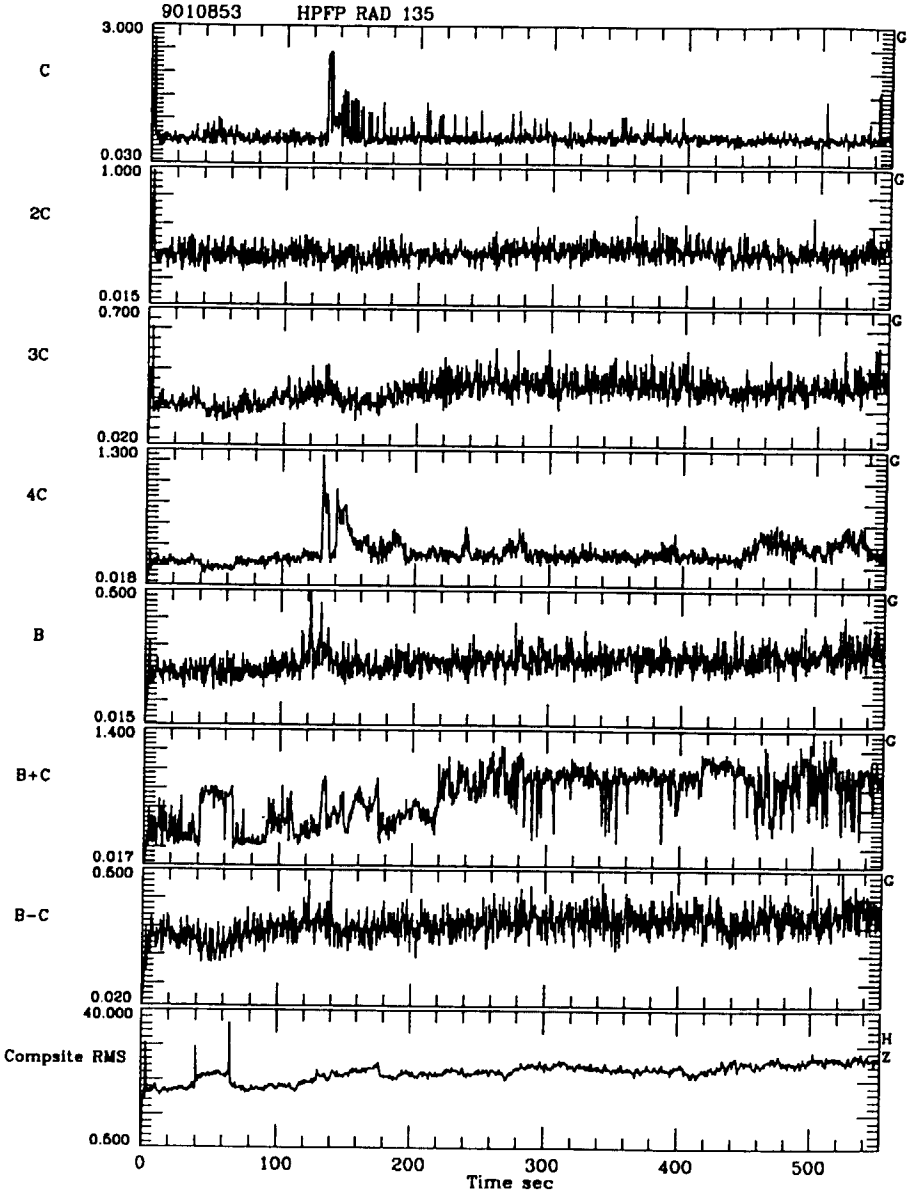

Bearing RMS Tracking

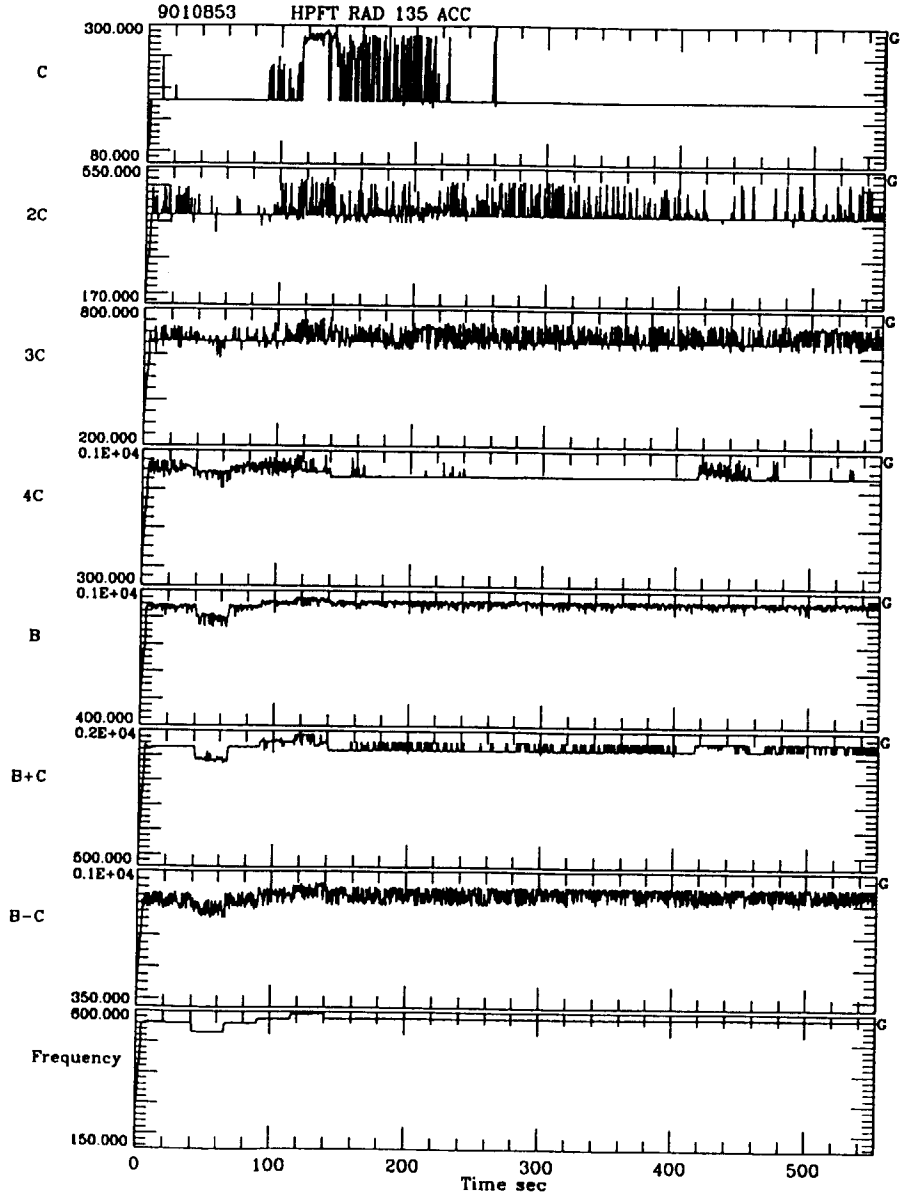

Bearing Frequency Tracking

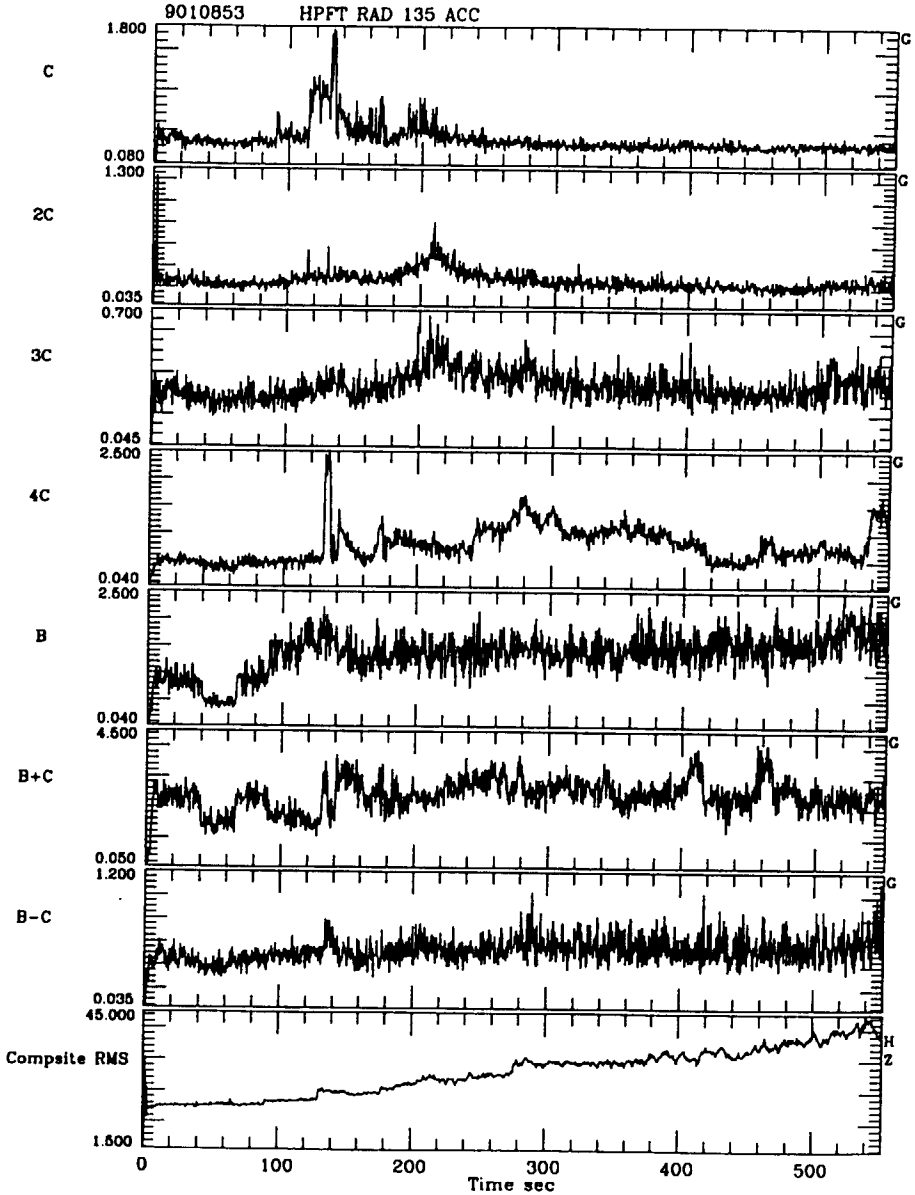

Bearing RMS Tracking

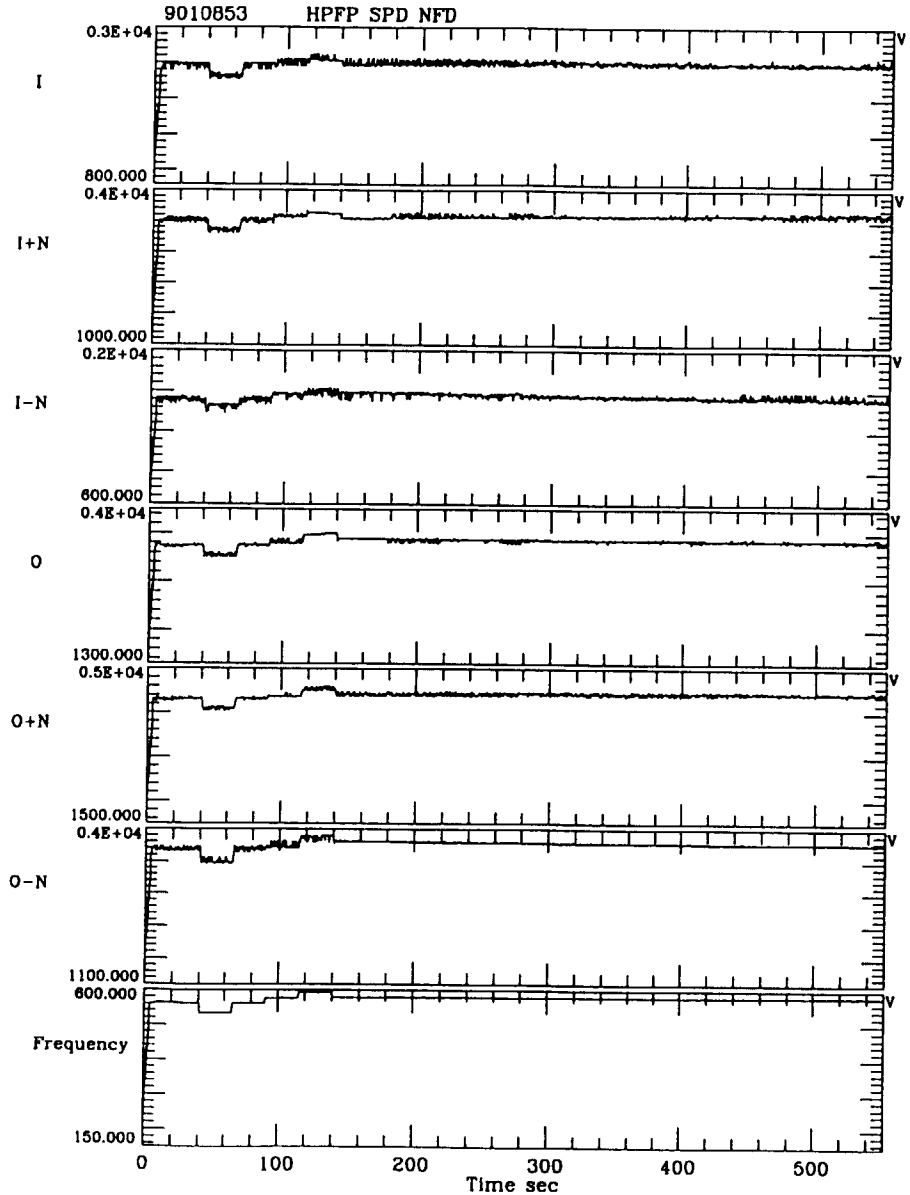

Bearing Frequency Tracking

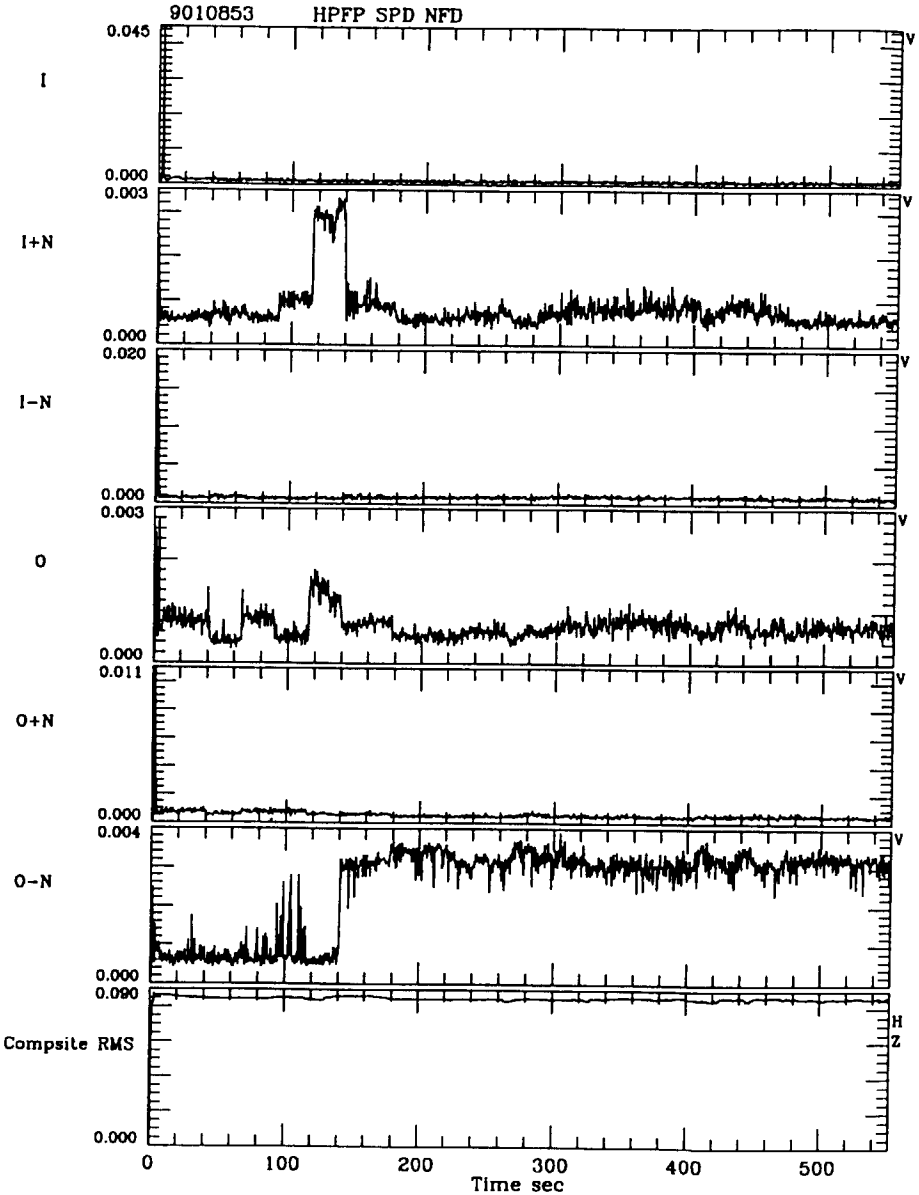

Bearing RMS Tracking

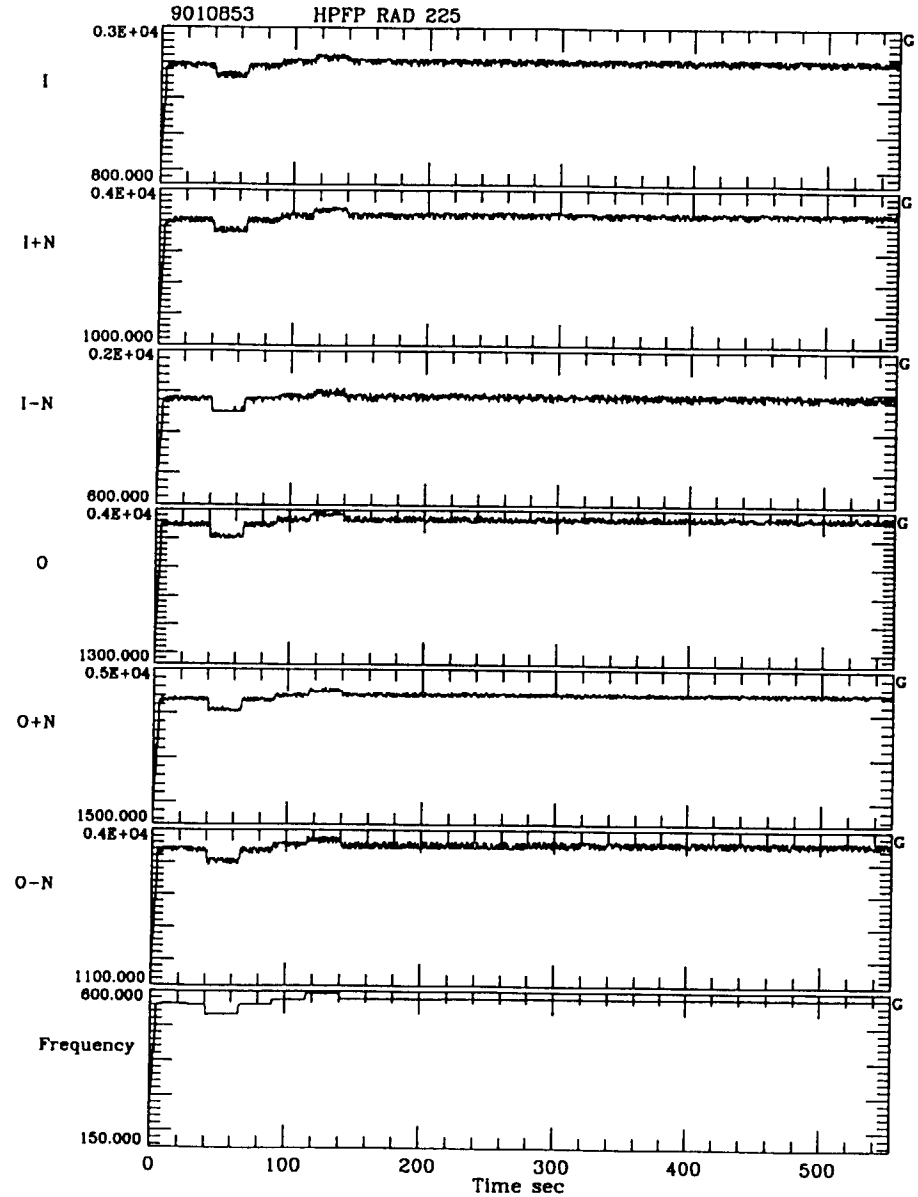

Bearing Frequency Tracking

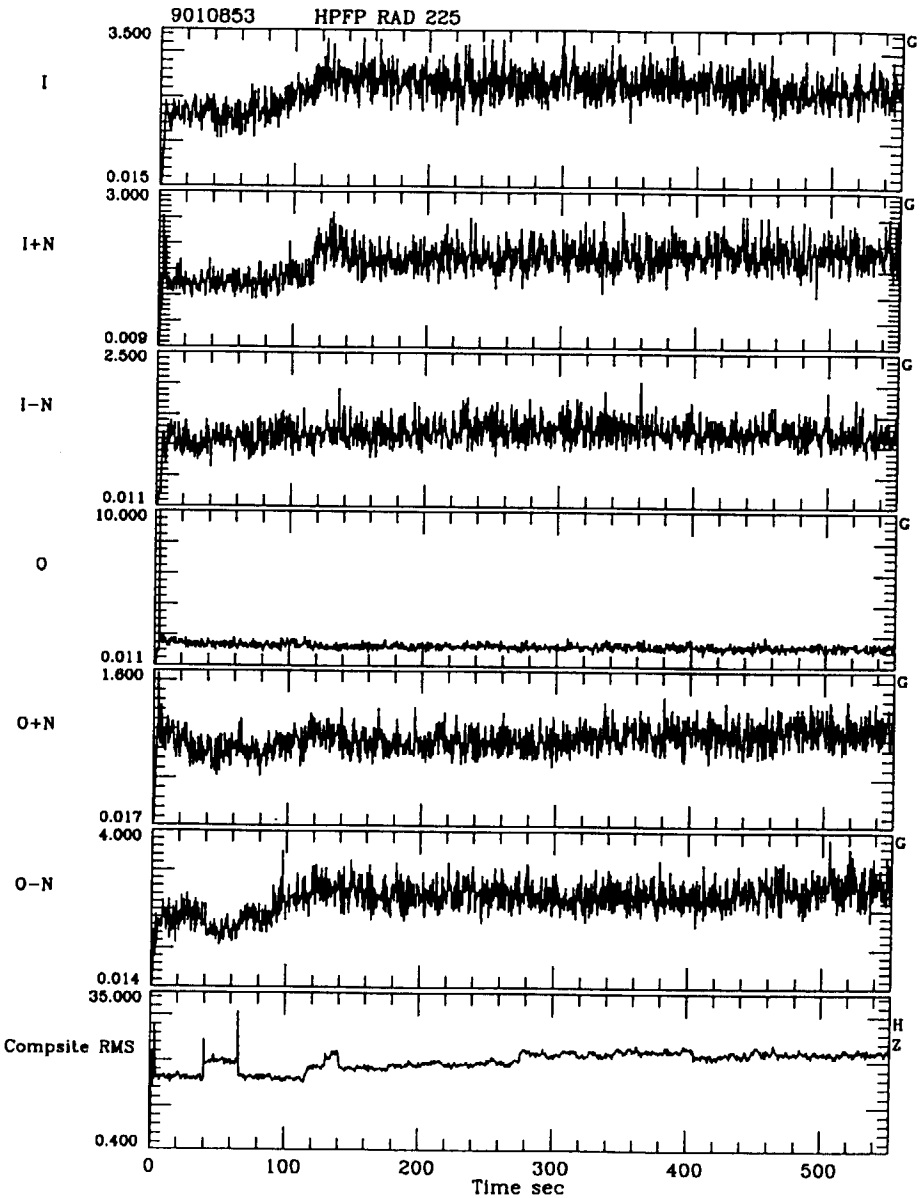

Bearing RMS Tracking

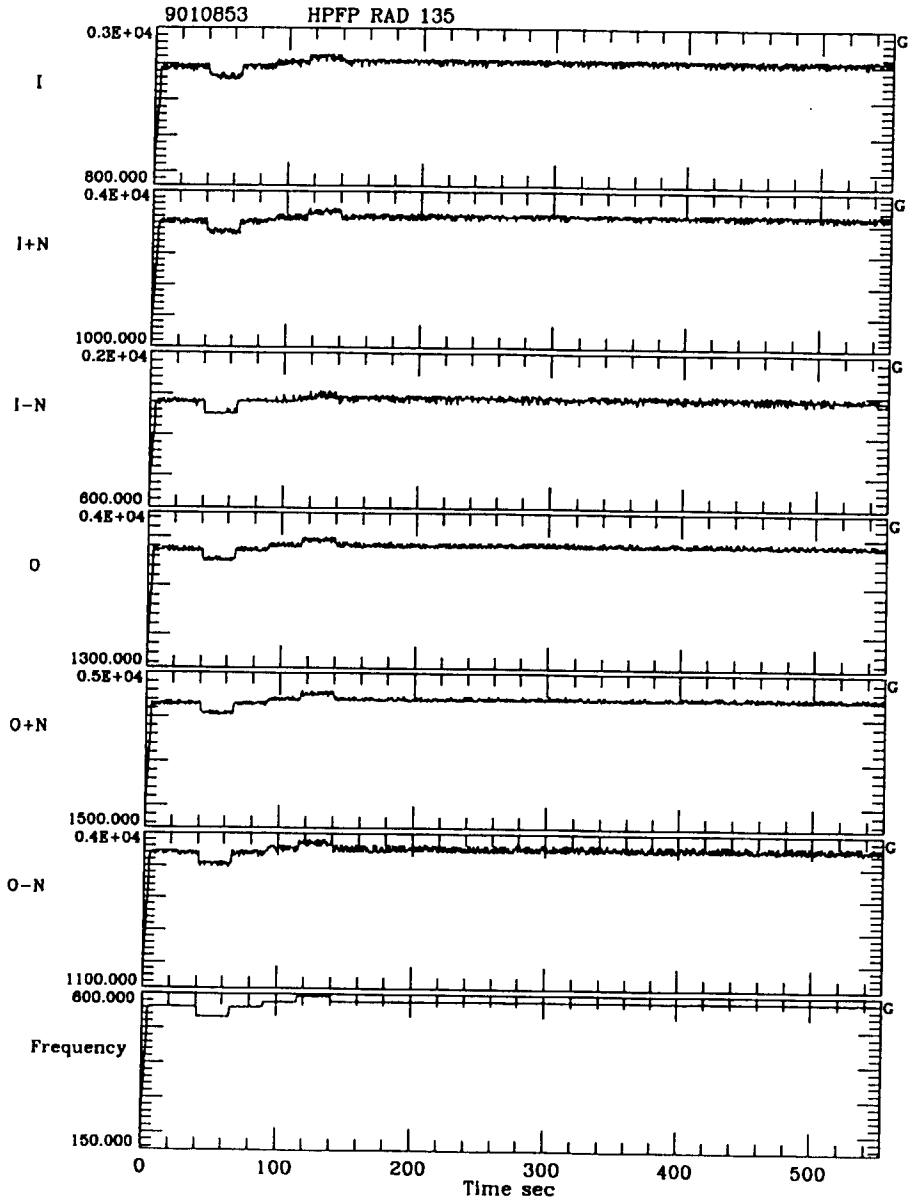

Bearing Frequency Tracking

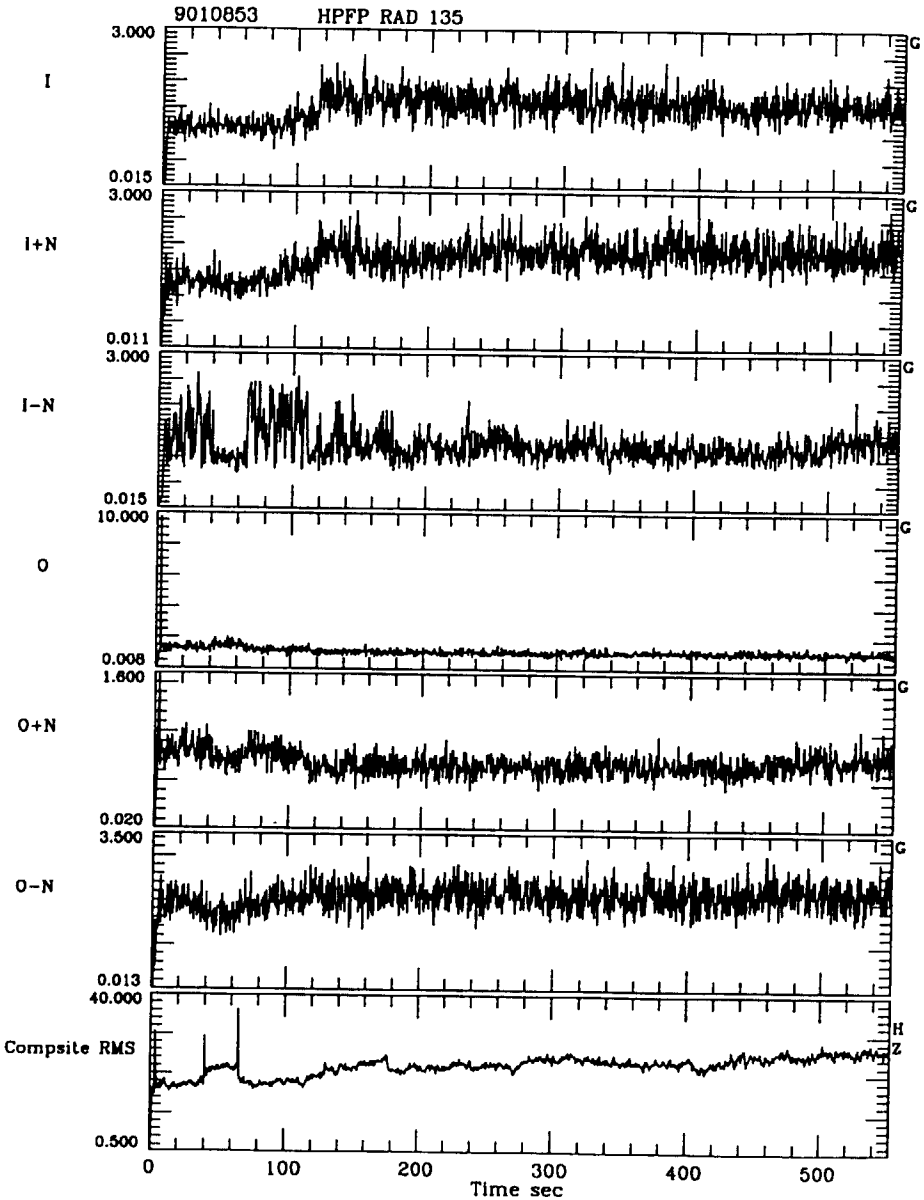

Bearing RMS Tracking

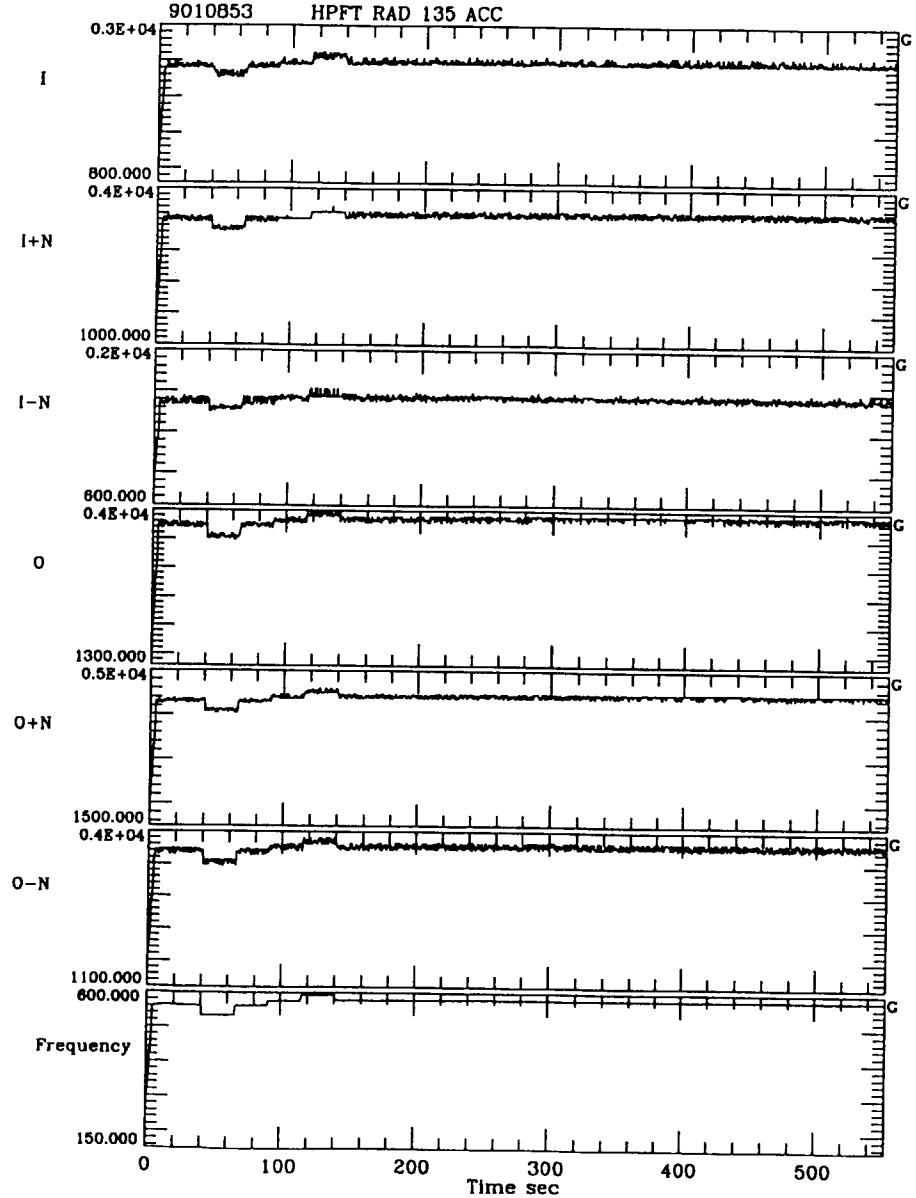

Bearing Frequency Tracking

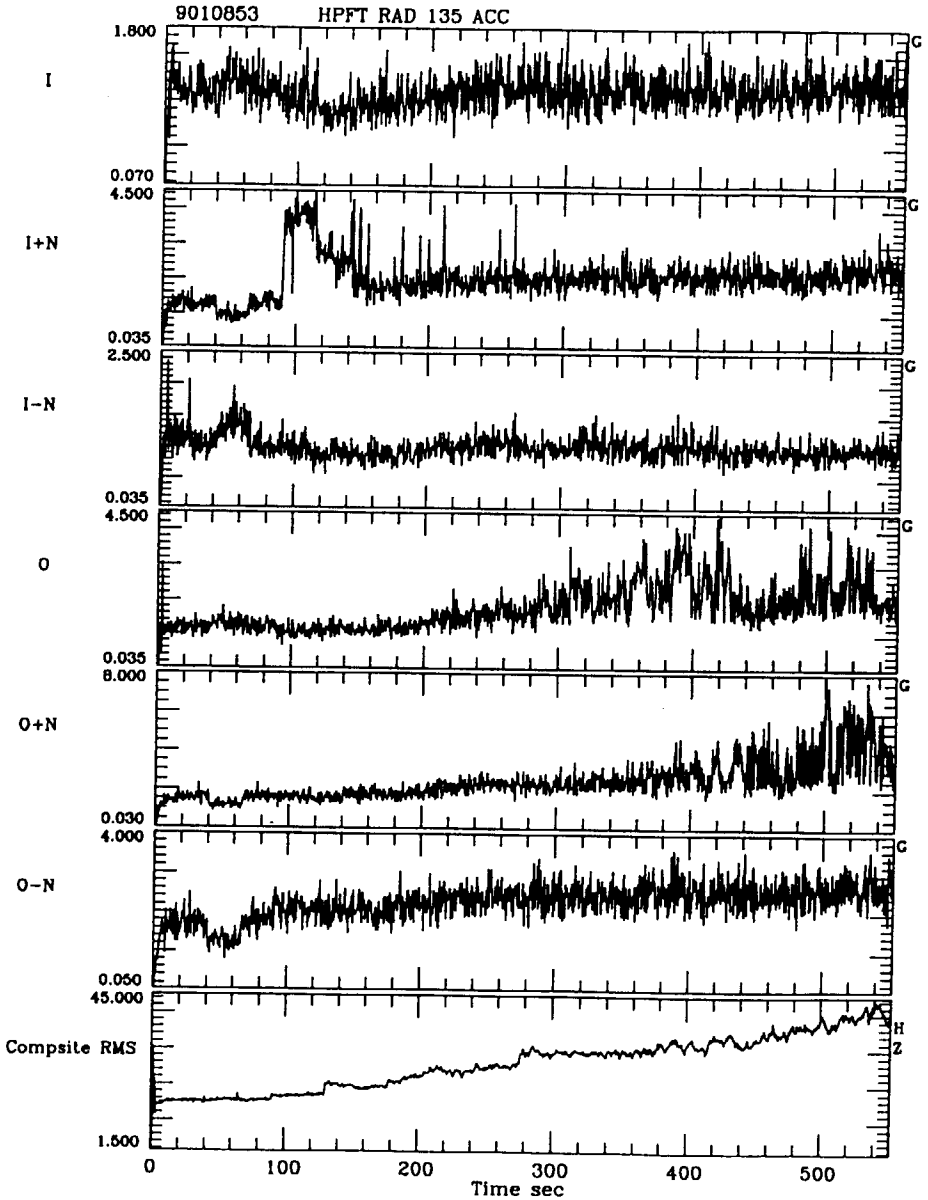

Bearing RMS Tracking

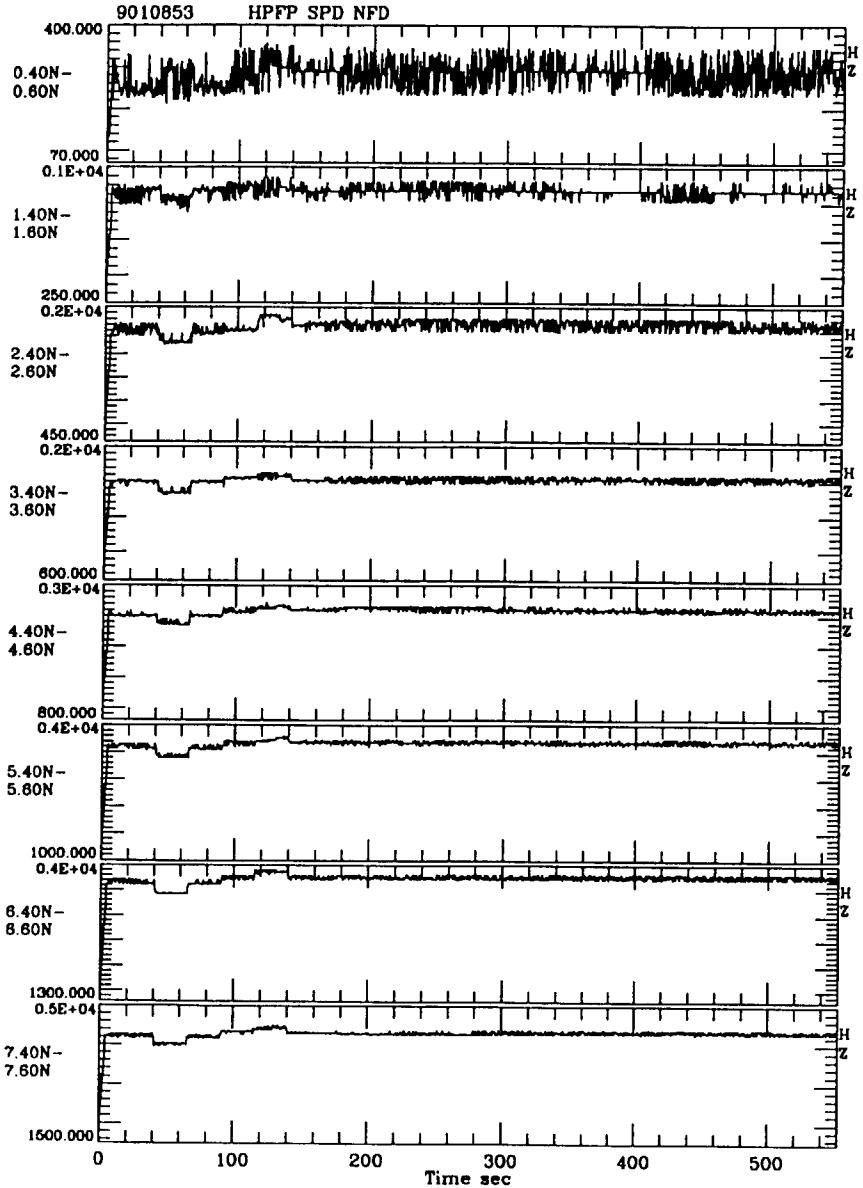

Anomaly Frequency Tracking

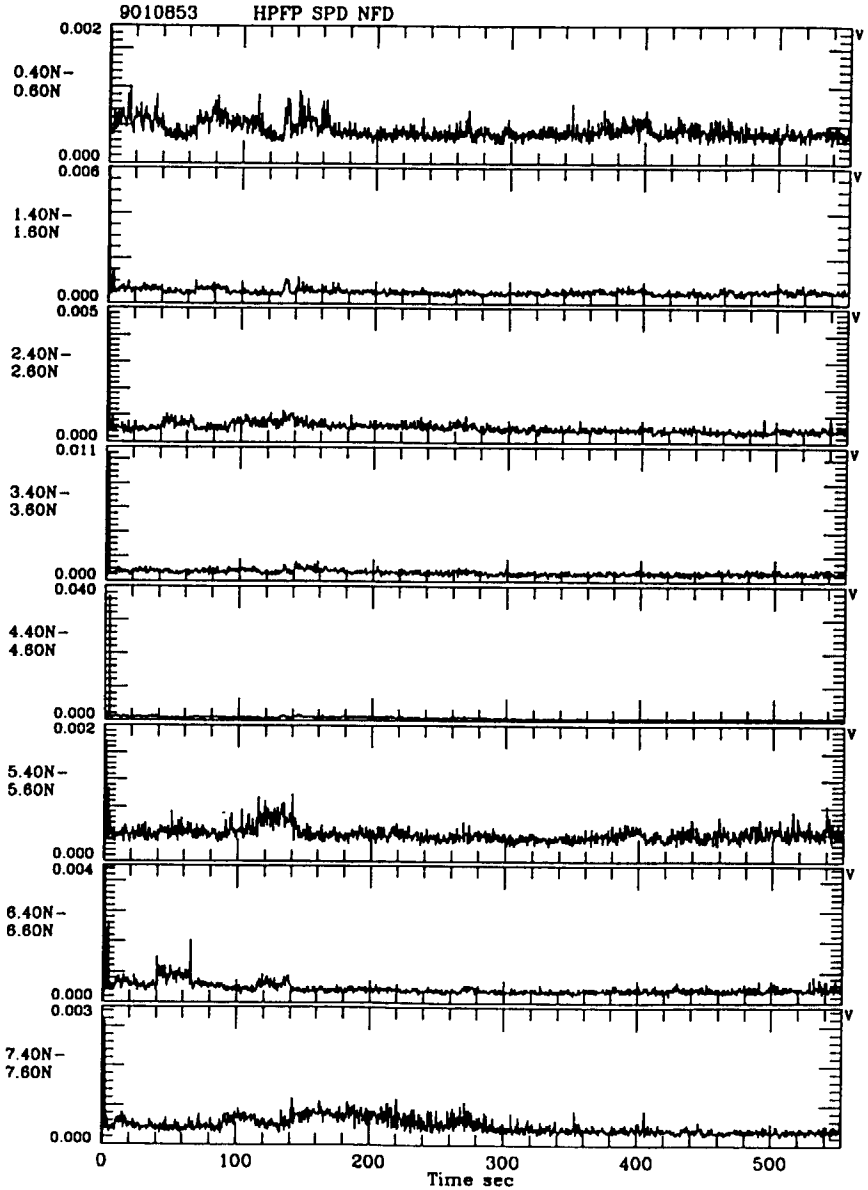

Anomaly Amplitude Tracking

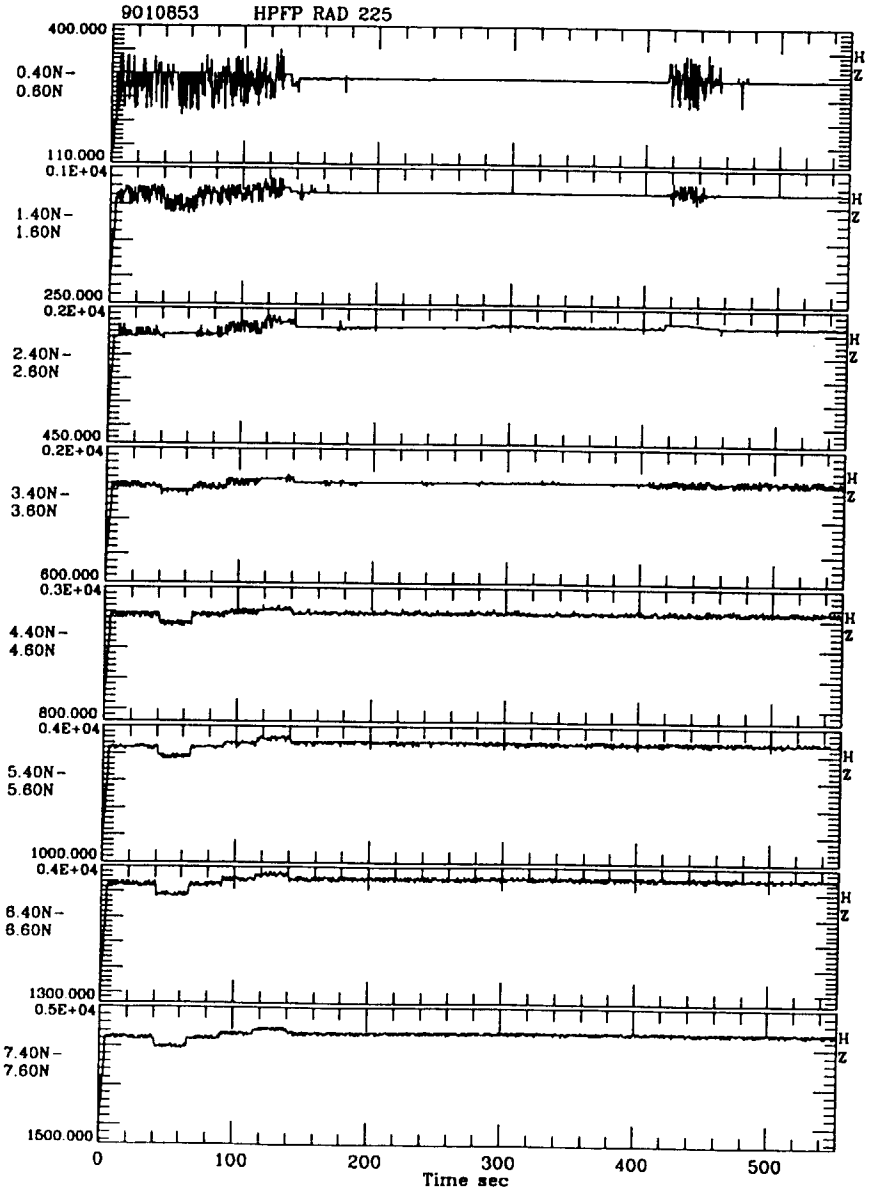

Anomaly Frequency Tracking

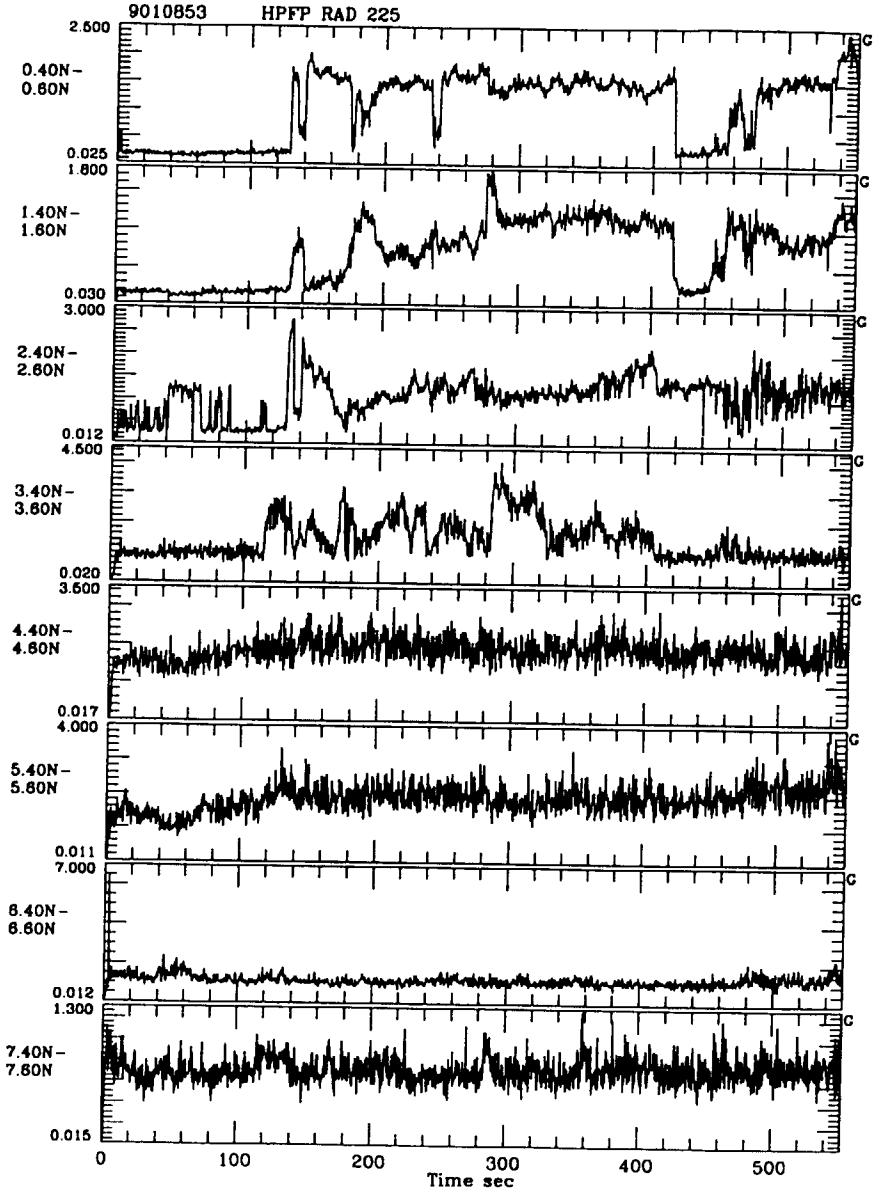

Anomaly Amplitude Tracking

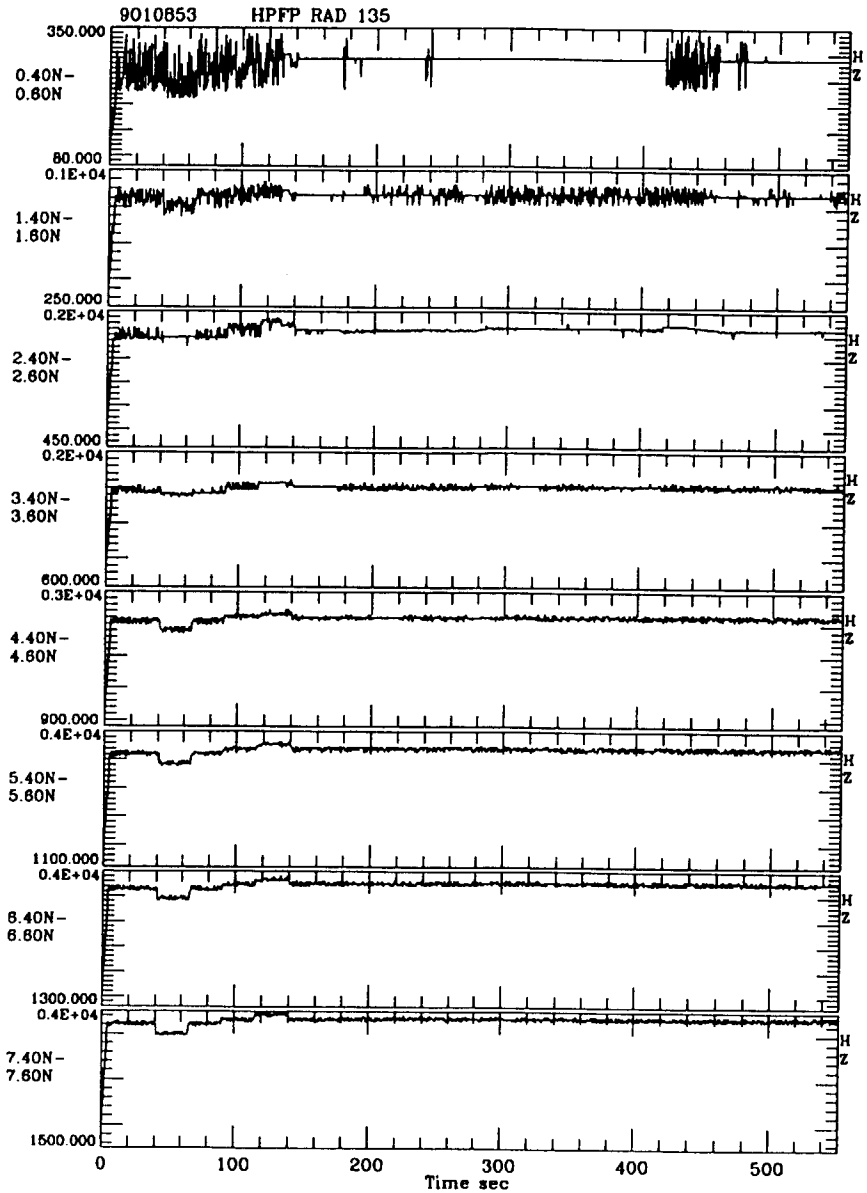

Anomaly Frequency Tracking

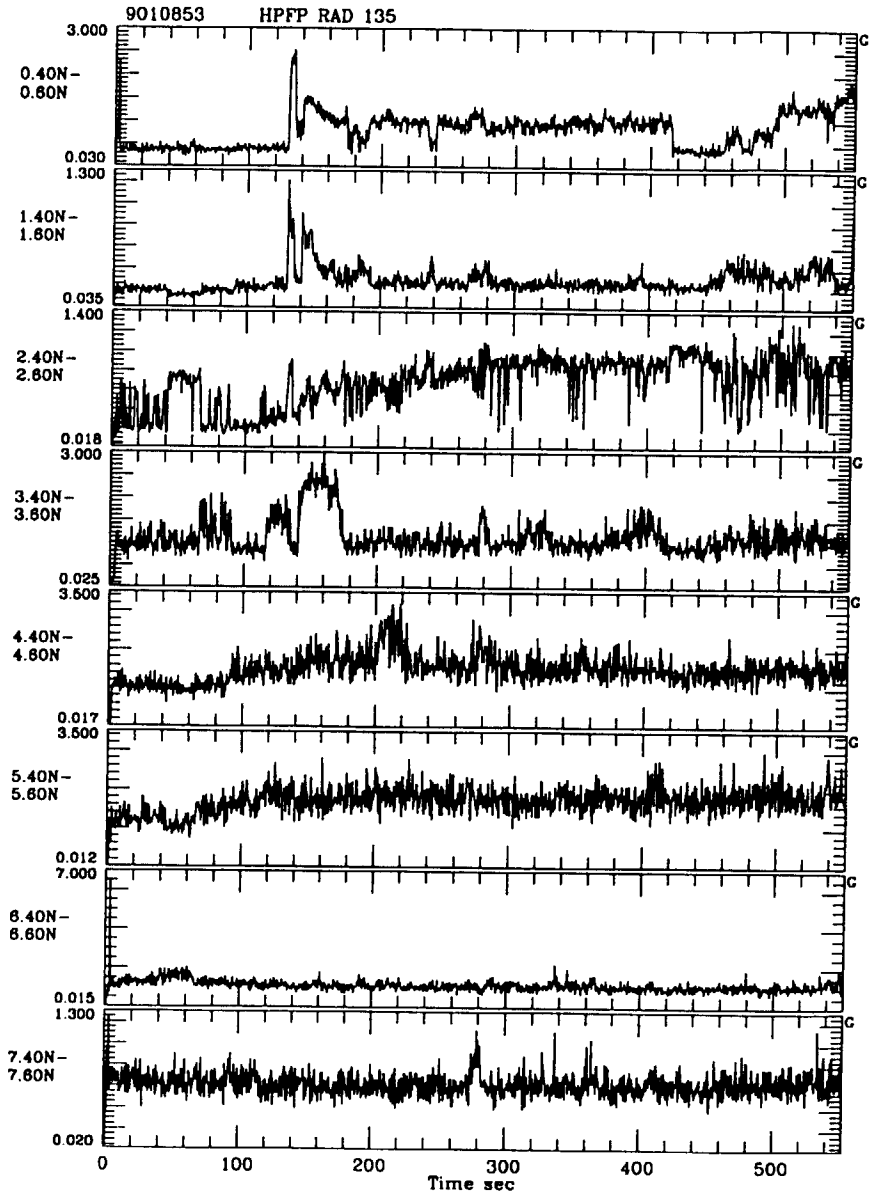

Anomaly Amplitude Tracking

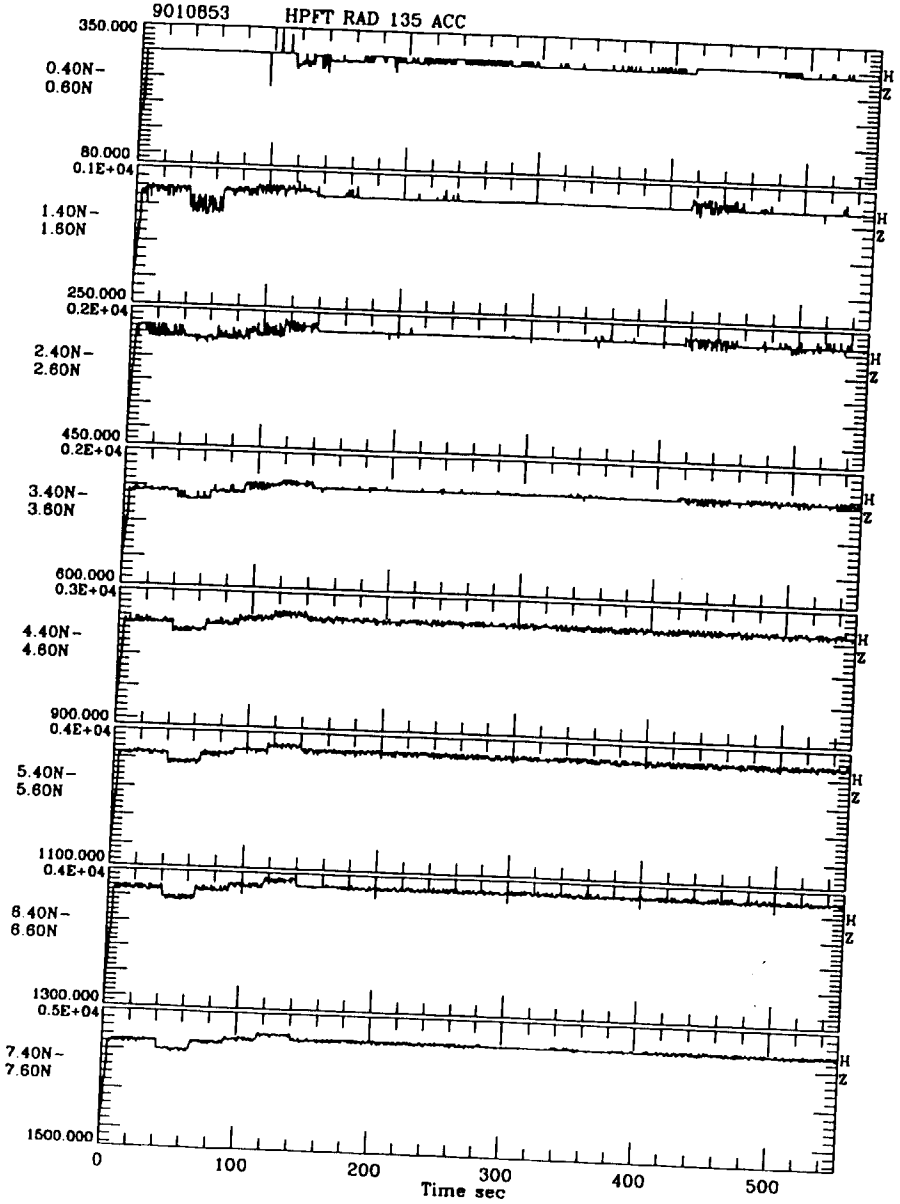

Anomaly Frequency Tracking

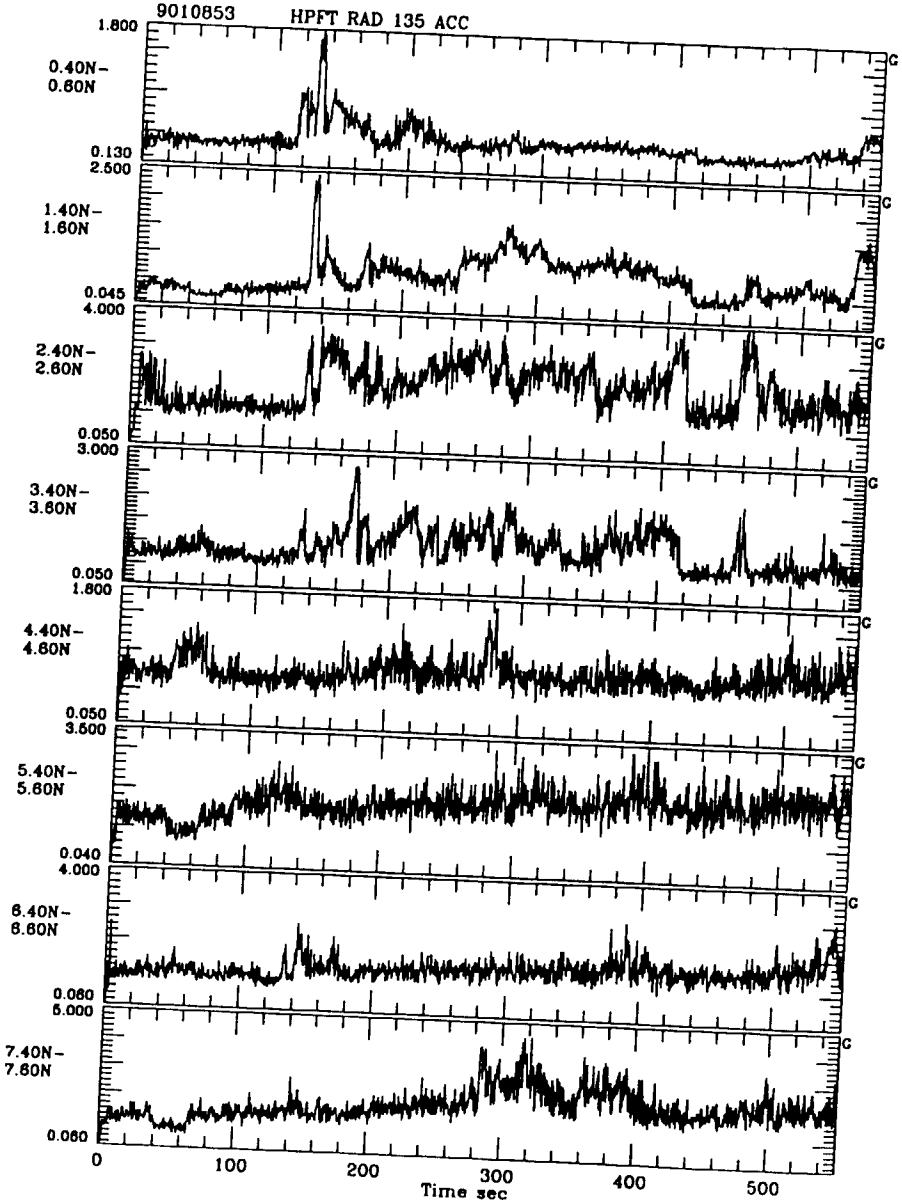

Anomaly Amplitude Tracking

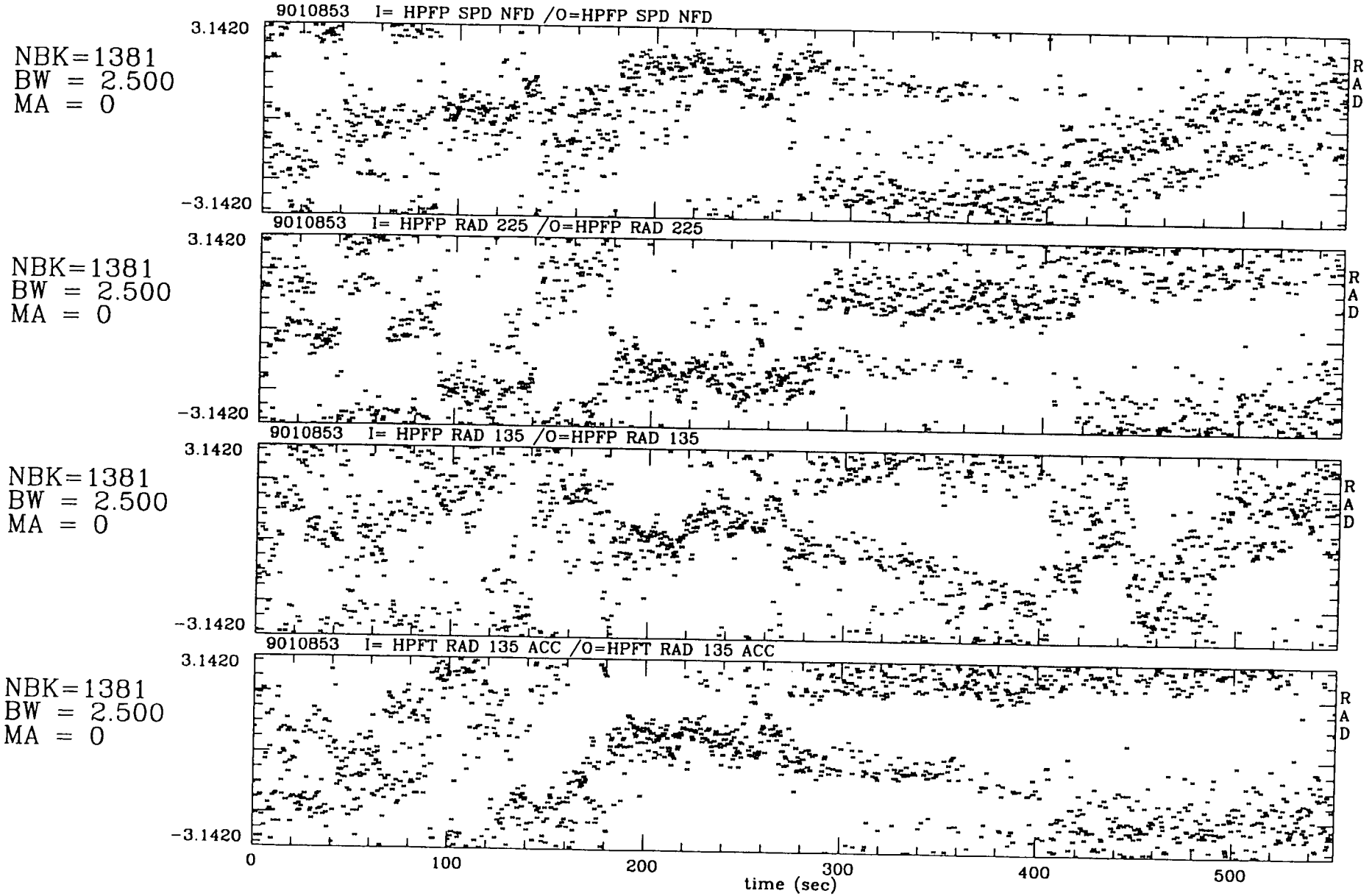

Hyper-coherence Phase Tracking at 2-nd Harmonic

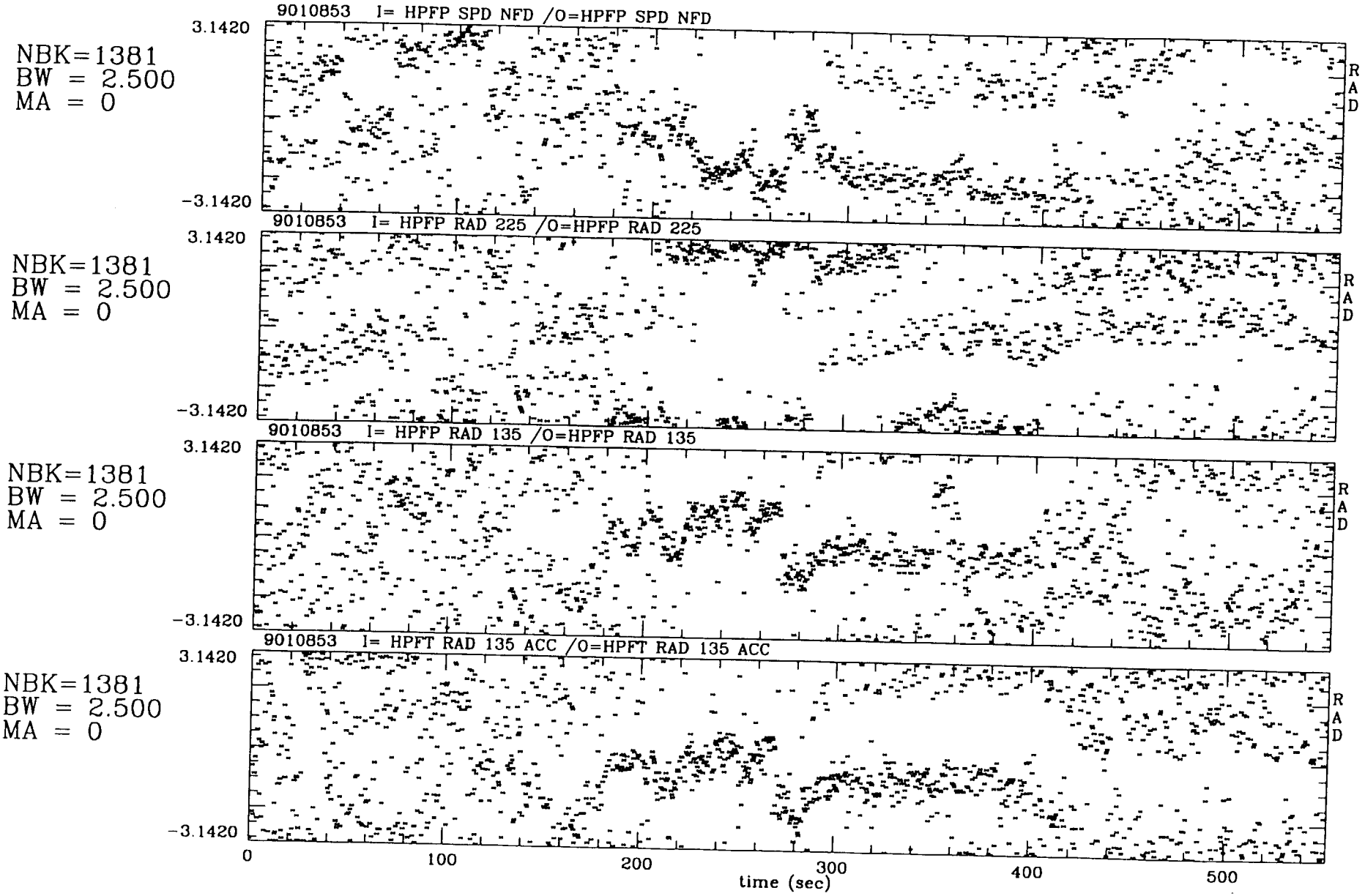

Hyper-coherence Phase Tracking at 3-rd Harmonic

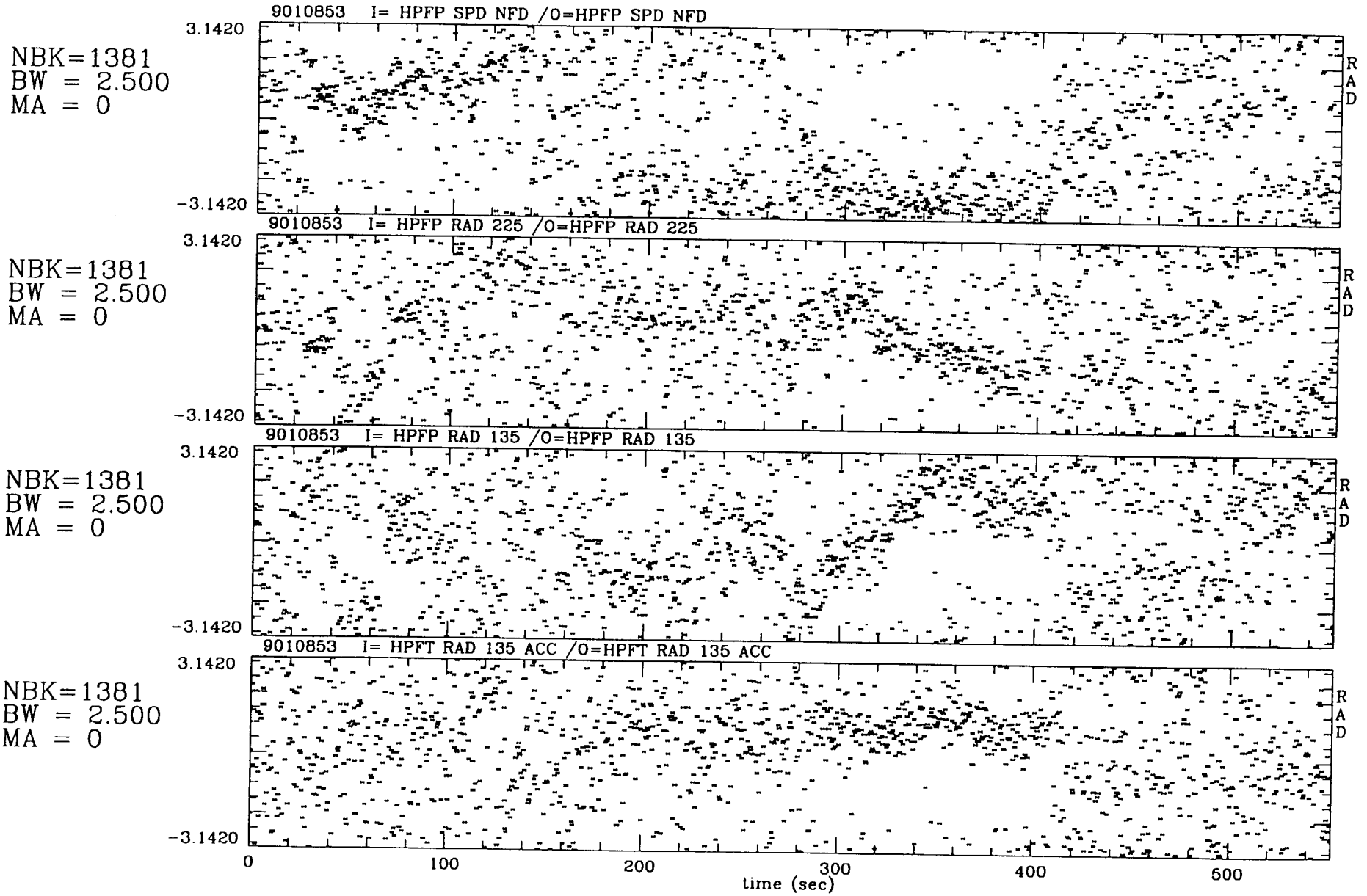

Hyper-coherence Phase Tracking at 4-th Harmonic

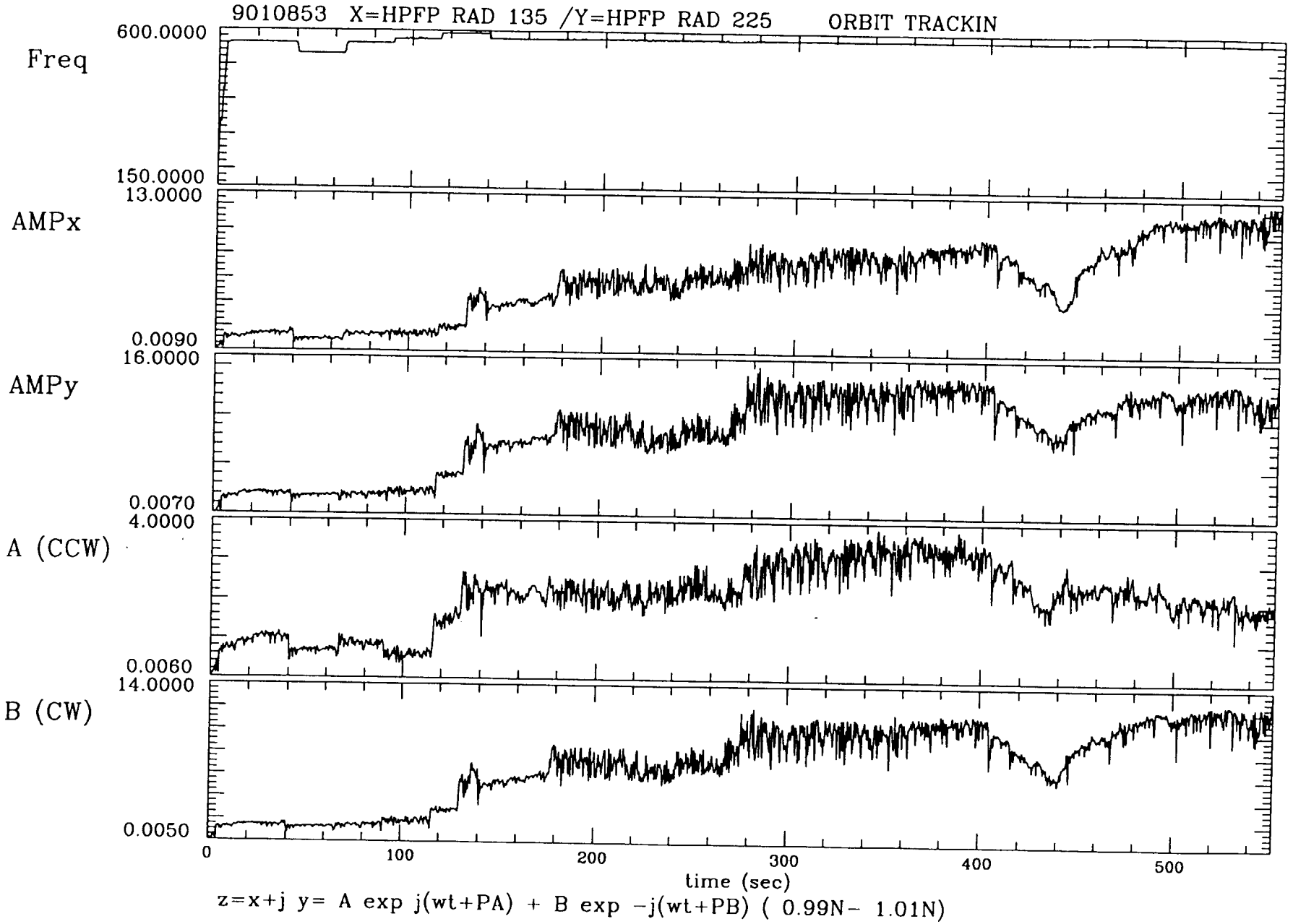
9010853 X=HPFP RAD 135 /Y=HPFP RAD 225 ORBIT TRACKIN
Freq
600.0000
150.0000
AMPx
13.0000
0.0090
AMPy
16.0000
0.0070
A (CCW)
4.0000
0.0060
B (CW)
14.0000
0.0050
0
100
200
300
400
500
time (sec)
z=x+j y= A exp j(wt+PA) + B exp -j(wt+PB) (0.99N- 1.01N)

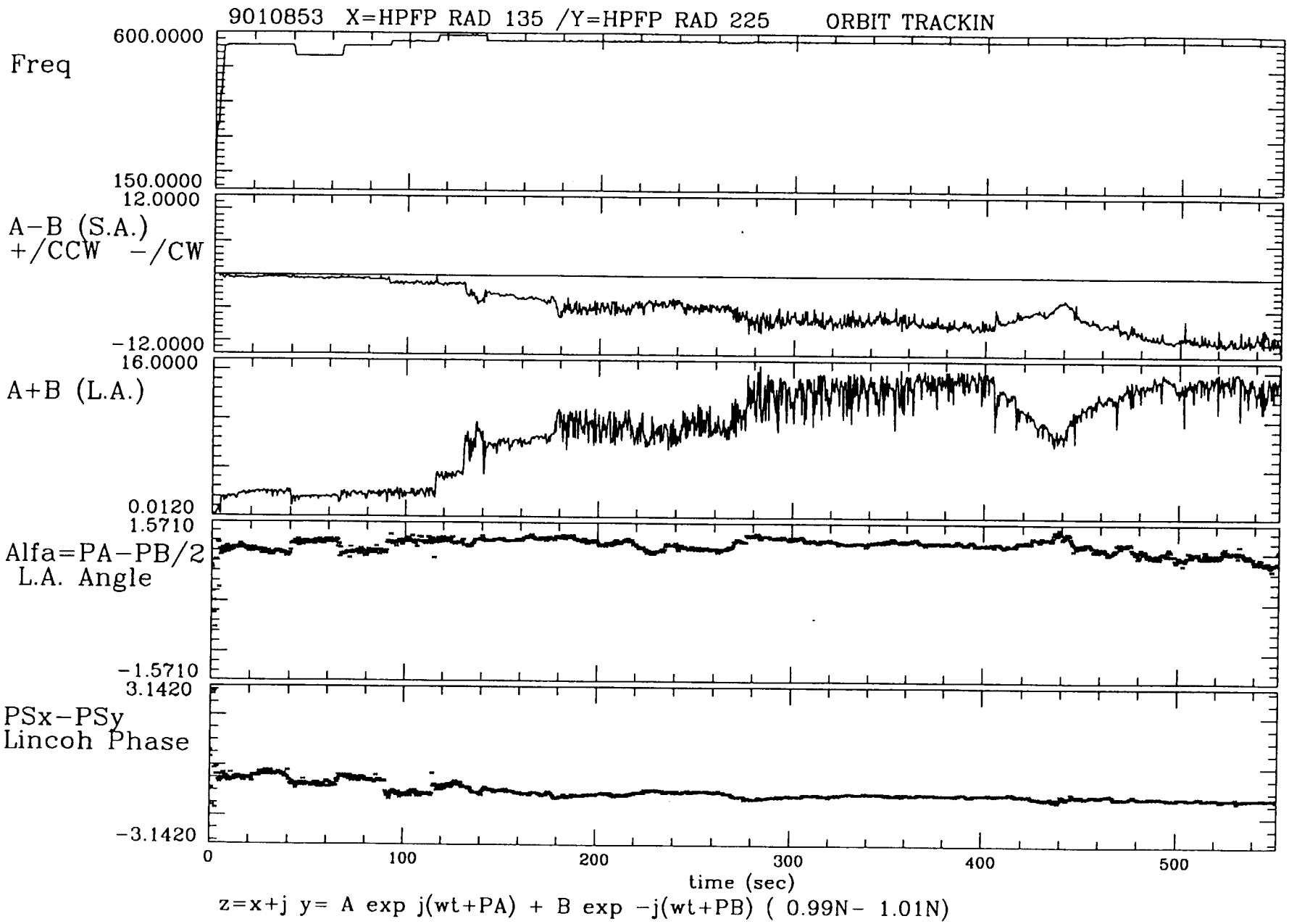
9010853 X=HPFP RAD 135 /Y=HPFP RAD 225 ORBIT TRACKIN
Freq
600.0000
150.0000
A-B (S.A.)
+/CCW -/CW
12.0000
-12.0000
A+B (L.A.)
16.0000
0.0120
Alfa=PA-PB/2
L.A. Angle
1.5710
-1.5710
PSx-PSy
Lincoh Phase
3.1420
-3.1420
0
100
200
300
400
500
time (sec)
z=x+j y= A exp j(wt+PA) + B exp -j(wt+PB) (0.99N- 1.01N)

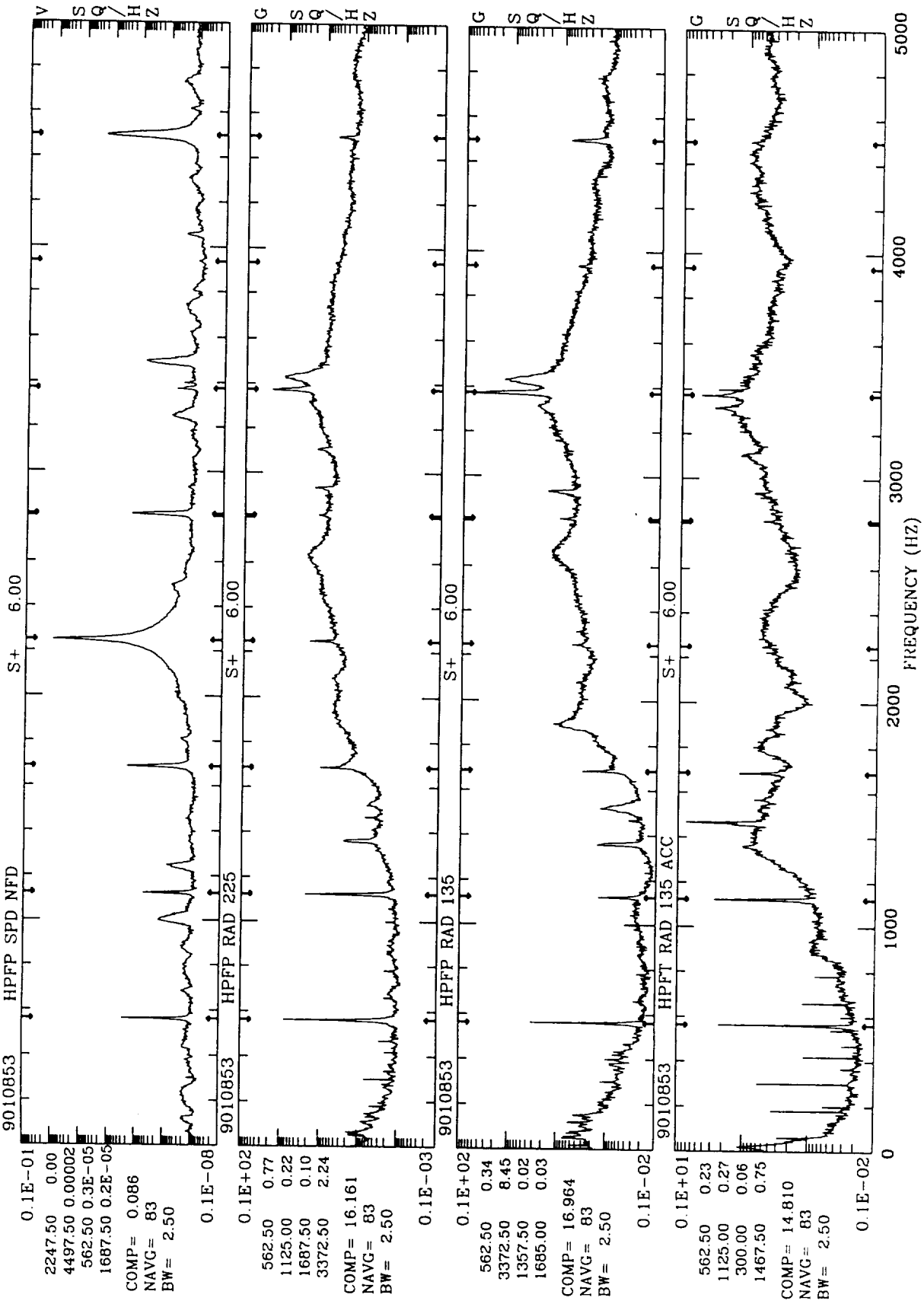
9010853 HPFP SPD NFD S+ 6.00
V S Q / H Z
0.1E-01
2247.50 0.00
4497.50 0.00002
562.50 0.3E-05
1687.50 0.2E-05
COMP= 0.086
NAVG= 83
BW= 2.50
0.1E-08
9010853 HPFP RAD 225 S+ 6.00
G S Q / H Z
0.1E+02
562.50 0.77
1125.00 0.22
1687.50 0.10
3372.50 2.24
COMP= 16.161
NAVG= 83
BW= 2.50
0.1E-03
9010853 HPFP RAD 135 S+ 6.00
G S Q / H Z
0.1E+02
562.50 0.34
3372.50 8.45
1357.50 0.02
1685.00 0.03
COMP= 16.964
NAVG= 83
BW= 2.50
0.1E-02
9010853 HPFT RAD 135 ACC S+ 6.00
G S Q / H Z
0.1E+01
562.50 0.23
1125.00 0.27
300.00 0.06
1467.50 0.75
COMP= 14.810
NAVG= 83
BW= 2.50
0.1E-02
0 1000 2000 3000 4000 5000
FREQUENCY (HZ)

PSD

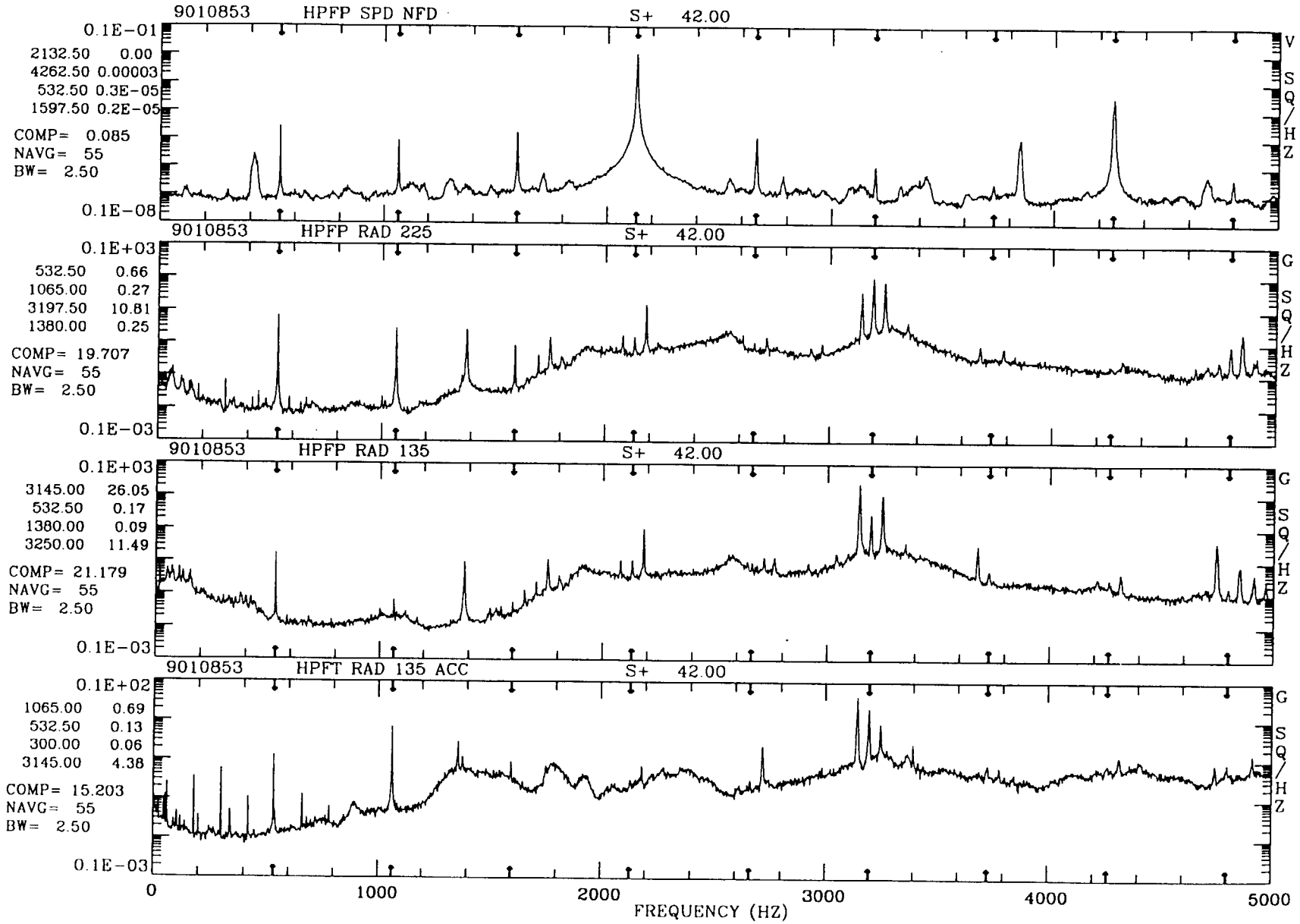
9010853 HPFP SPD NFD S+ 42.00
0.1E-01
2132.50 0.00
4262.50 0.00003
532.50 0.3E-05
1597.50 0.2E-05
COMP= 0.085
NAVG= 55
BW= 2.50
0.1E-08
V
S
Q
/
H
Z
9010853 HPFP RAD 225 S+ 42.00
0.1E+03
532.50 0.66
1065.00 0.27
3197.50 10.81
1380.00 0.25
COMP= 19.707
NAVG= 55
BW= 2.50
0.1E-03
G
S
Q
/
H
Z
9010853 HPFP RAD 135 S+ 42.00
0.1E+03
3145.00 26.05
532.50 0.17
1380.00 0.09
3250.00 11.49
COMP= 21.179
NAVG= 55
BW= 2.50
0.1E-03
G
S
Q
/
H
Z
9010853 HPFT RAD 135 ACC S+ 42.00
0.1E+02
1065.00 0.69
532.50 0.13
300.00 0.06
3145.00 4.38
COMP= 15.203
NAVG= 55
BW= 2.50
0.1E-03
G
S
Q
/
H
Z
0
1000
2000
3000
4000
5000
FREQUENCY (HZ)

PSD

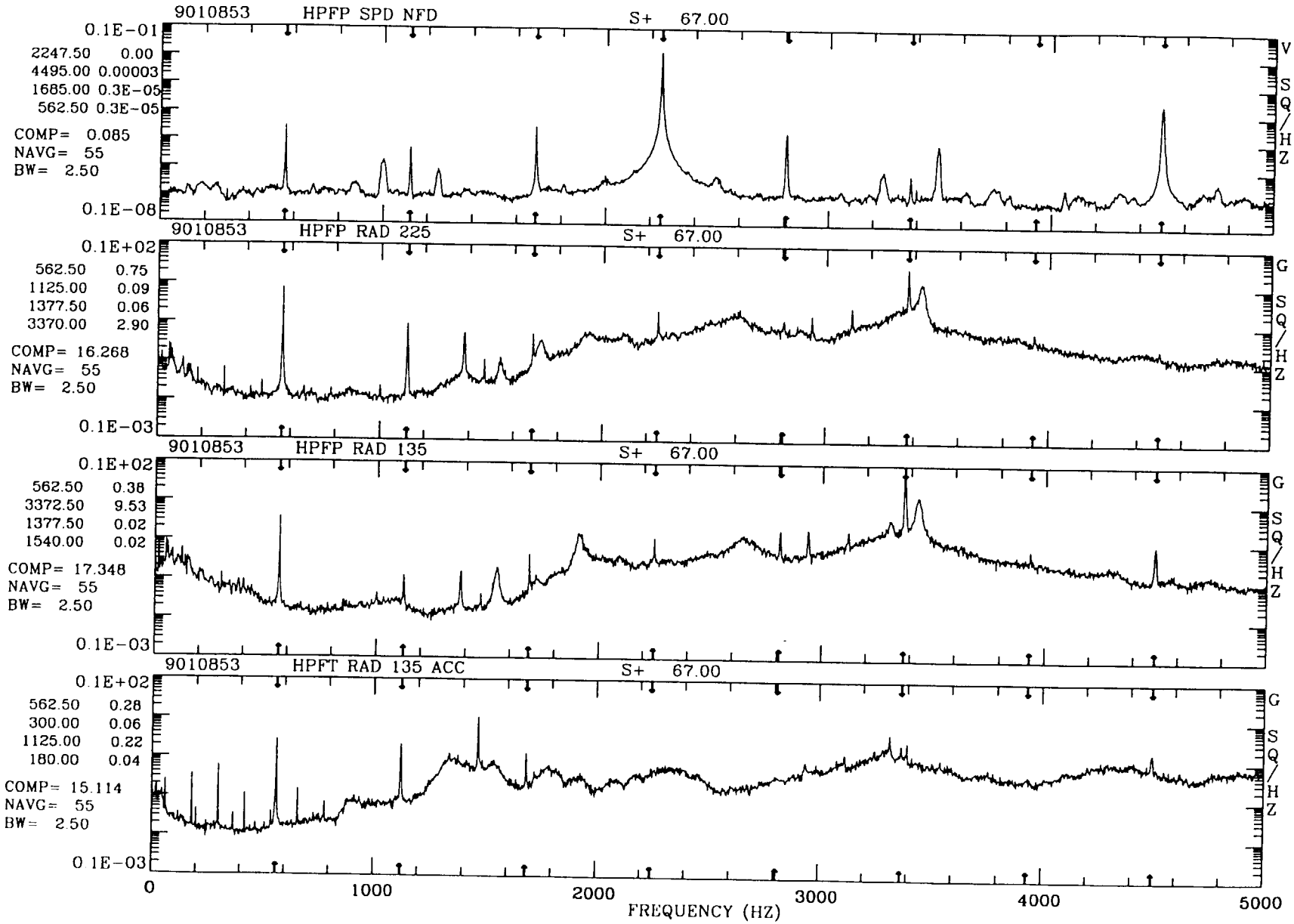
9010853 HPFP SPD NFD S+ 67.00
0.1E-01
2247.50 0.00
4495.00 0.00003
1685.00 0.3E-05
562.50 0.3E-05
COMP= 0.085
NAVG= 55
BW= 2.50
0.1E-08
V SQ/HZ
9010853 HPFP RAD 225 S+ 67.00
0.1E+02
562.50 0.75
1125.00 0.09
1377.50 0.06
3370.00 2.90
COMP= 16.268
NAVG= 55
BW= 2.50
0.1E-03
G SQ/HZ
9010853 HPFP RAD 135 S+ 67.00
0.1E+02
562.50 0.38
3372.50 9.53
1377.50 0.02
1540.00 0.02
COMP= 17.348
NAVG= 55
BW= 2.50
0.1E-03
G SQ/HZ
9010853 HPFT RAD 135 ACC S+ 67.00
0.1E+02
562.50 0.28
300.00 0.06
1125.00 0.22
180.00 0.04
COMP= 15.114
NAVG= 55
BW= 2.50
0.1E-03
G SQ/HZ
0
1000
2000
3000
4000
5000
FREQUENCY (HZ)

PSD

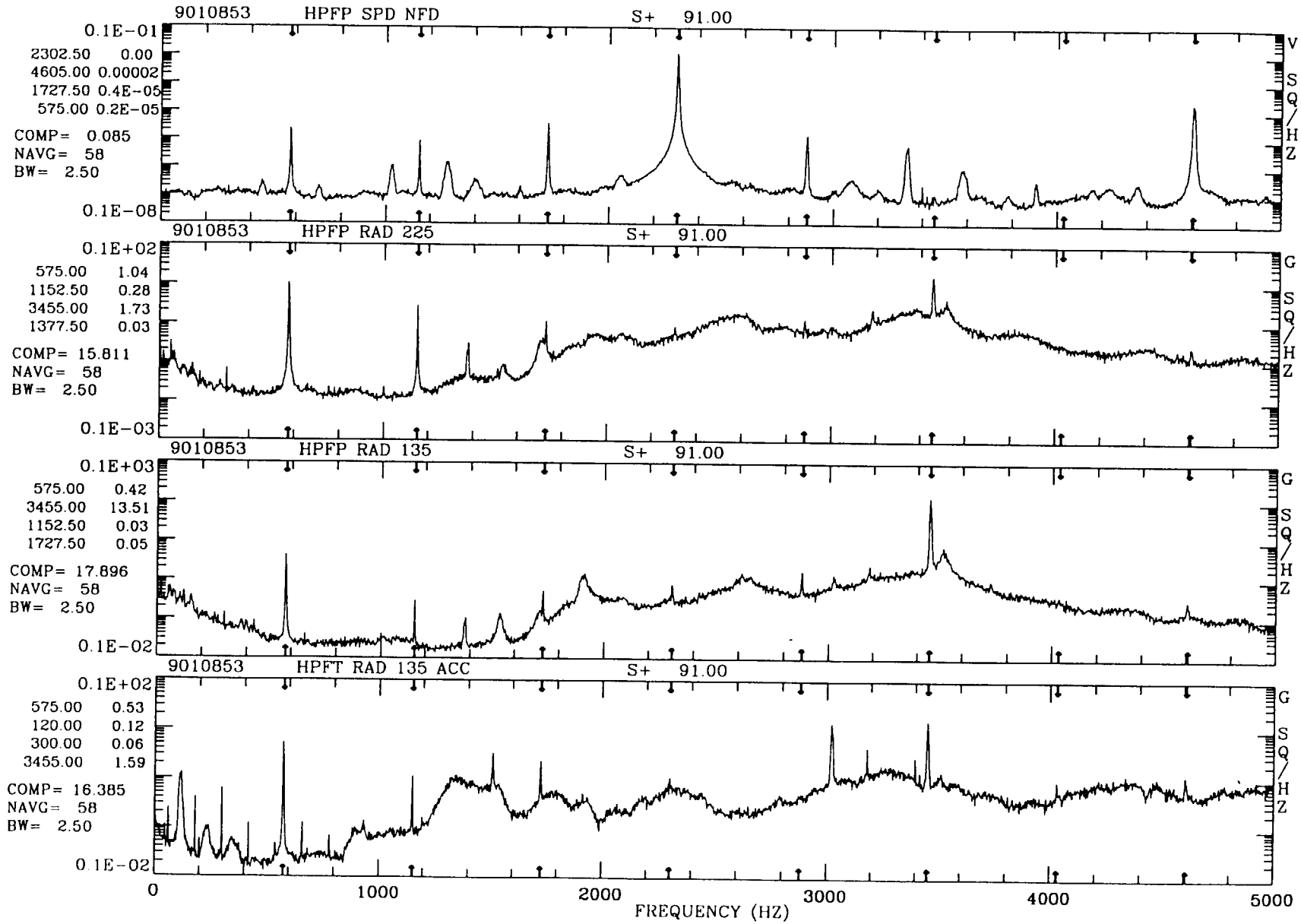
9010853 HPFP SPD NFD S+ 91.00
0.1E-01
2302.50 0.00
4605.00 0.00002
1727.50 0.4E-05
575.00 0.2E-05
COMP= 0.085
NAVG= 58
BW= 2.50
0.1E-08
V SQ/HZ
9010853 HPFP RAD 225 S+ 91.00
0.1E+02
575.00 1.04
1152.50 0.28
3455.00 1.73
1377.50 0.03
COMP= 15.811
NAVG= 58
BW= 2.50
0.1E-03
G SQ/HZ
9010853 HPFP RAD 135 S+ 91.00
0.1E+03
575.00 0.42
3455.00 13.51
1152.50 0.03
1727.50 0.05
COMP= 17.896
NAVG= 58
BW= 2.50
0.1E-02
G SQ/HZ
9010853 HPFT RAD 135 ACC S+ 91.00
0.1E+02
575.00 0.53
120.00 0.12
300.00 0.06
3455.00 1.59
COMP= 16.385
NAVG= 58
BW= 2.50
0.1E-02
G SQ/HZ
0
1000
2000
3000
4000
5000
FREQUENCY (HZ)

PSD

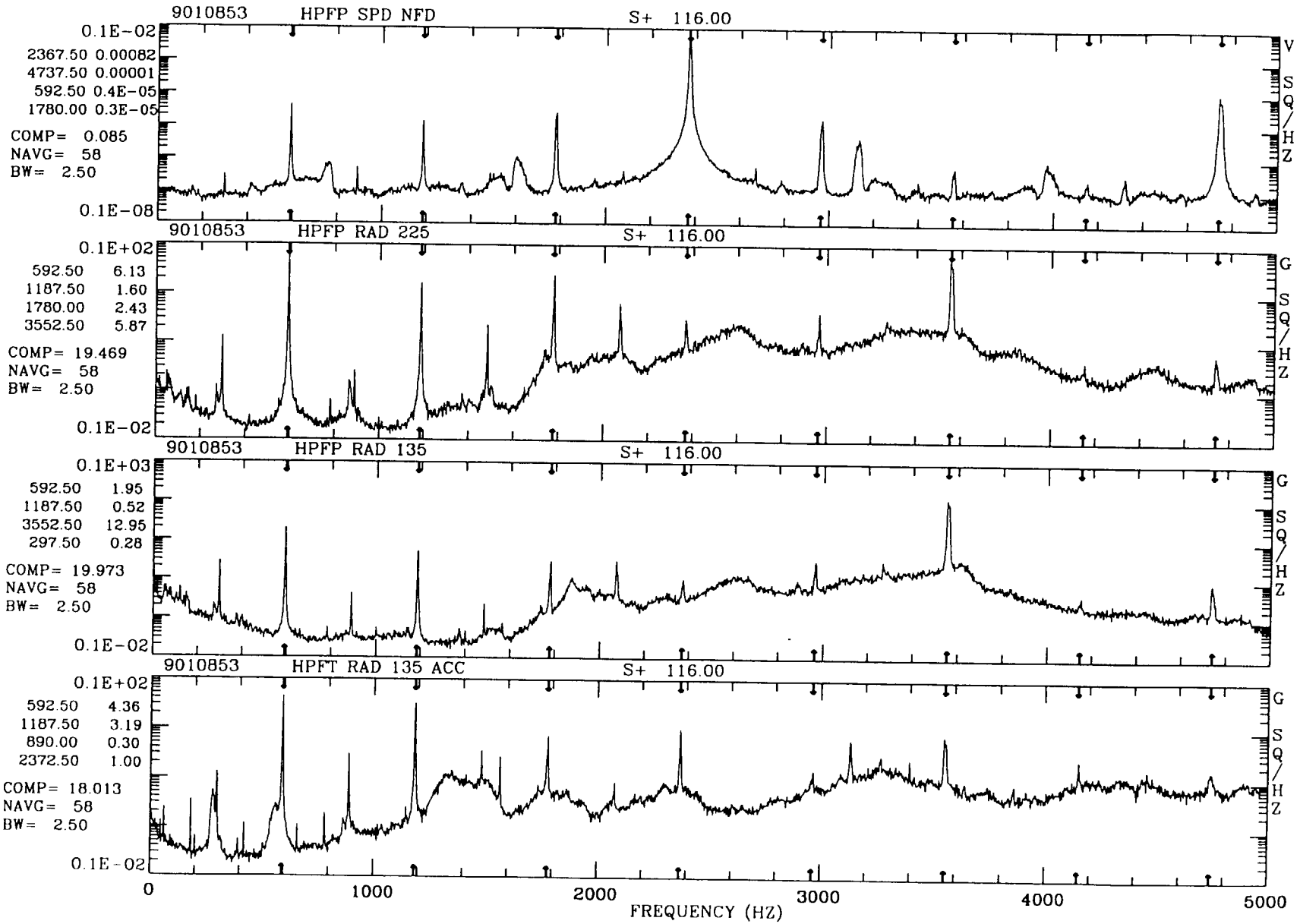
9010853 HPFP SPD NFD S+ 116.00
0.1E-02
2367.50 0.00082
4737.50 0.00001
592.50 0.4E-05
1780.00 0.3E-05
COMP= 0.085
NAVG= 58
BW= 2.50
0.1E-08
V
S
Q
/
H
Z
9010853 HPFP RAD 225 S+ 116.00
0.1E+02
592.50 6.13
1187.50 1.60
1780.00 2.43
3552.50 5.87
COMP= 19.469
NAVG= 58
BW= 2.50
0.1E-02
G
S
Q
/
H
Z
9010853 HPFP RAD 135 S+ 116.00
0.1E+03
592.50 1.95
1187.50 0.52
3552.50 12.95
297.50 0.28
COMP= 19.973
NAVG= 58
BW= 2.50
0.1E-02
G
S
Q
/
H
Z
9010853 HPFT RAD 135 ACC S+ 116.00
0.1E+02
592.50 4.36
1187.50 3.19
890.00 0.30
2372.50 1.00
COMP= 18.013
NAVG= 58
BW= 2.50
0.1E-02
G
S
Q
/
H
Z
0
1000
2000
3000
4000
5000
FREQUENCY (HZ)

PSD

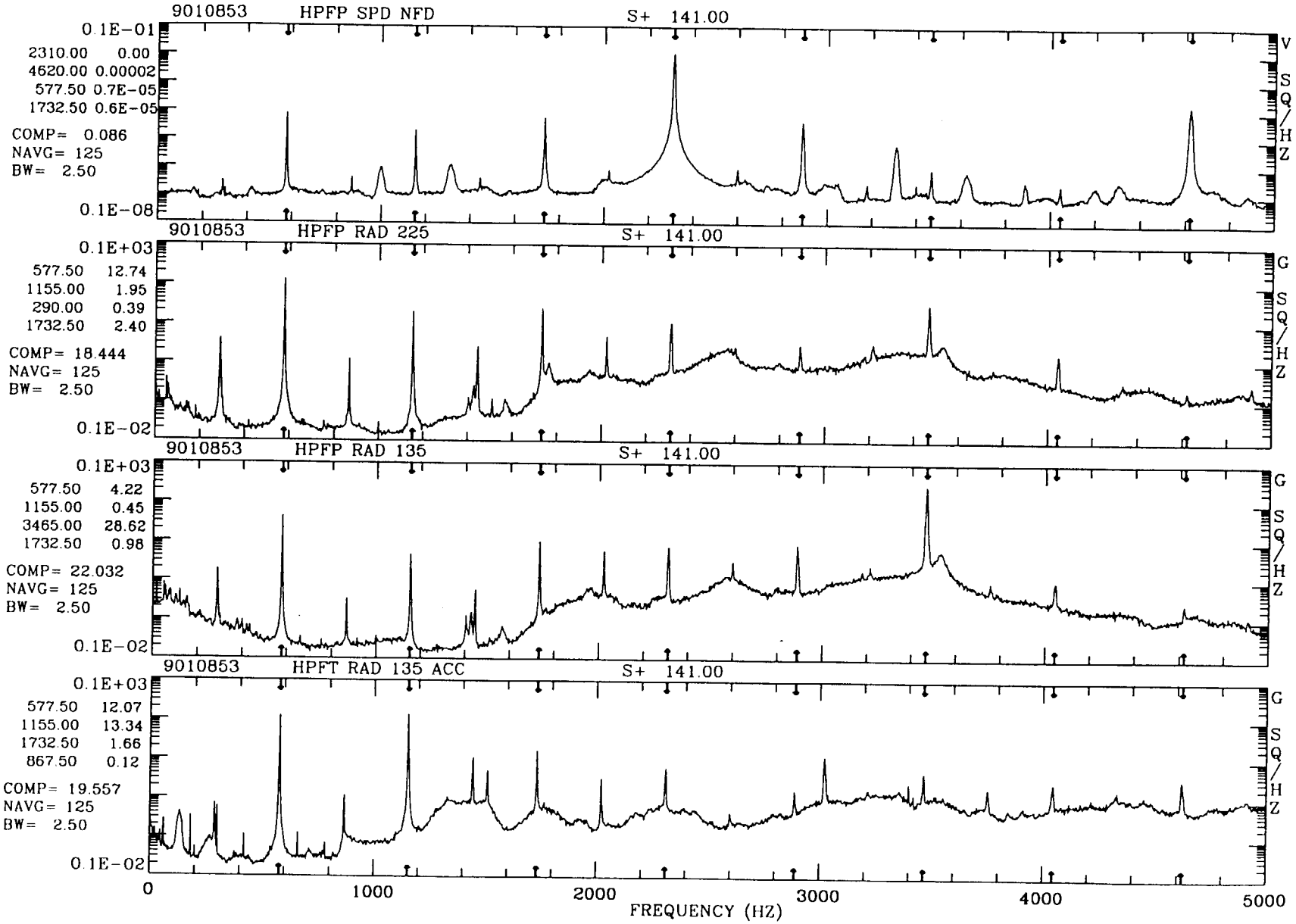
9010853 HPFP SPD NFD S+ 141.00
0.1E-01
2310.00 0.00
4620.00 0.00002
577.50 0.7E-05
1732.50 0.6E-05
COMP= 0.086
NAVG= 125
BW= 2.50
0.1E-08
V SQ/HZ
9010853 HPFP RAD 225 S+ 141.00
0.1E+03
577.50 12.74
1155.00 1.95
290.00 0.39
1732.50 2.40
COMP= 18.444
NAVG= 125
BW= 2.50
0.1E-02
G SQ/HZ
9010853 HPFP RAD 135 S+ 141.00
0.1E+03
577.50 4.22
1155.00 0.45
3465.00 28.62
1732.50 0.98
COMP= 22.032
NAVG= 125
BW= 2.50
0.1E-02
G SQ/HZ
9010853 HPFT RAD 135 ACC S+ 141.00
0.1E+03
577.50 12.07
1155.00 13.34
1732.50 1.66
867.50 0.12
COMP= 19.557
NAVG= 125
BW= 2.50
0.1E-02
G SQ/HZ
0
1000
2000
3000
4000
5000
FREQUENCY (HZ)

PSD

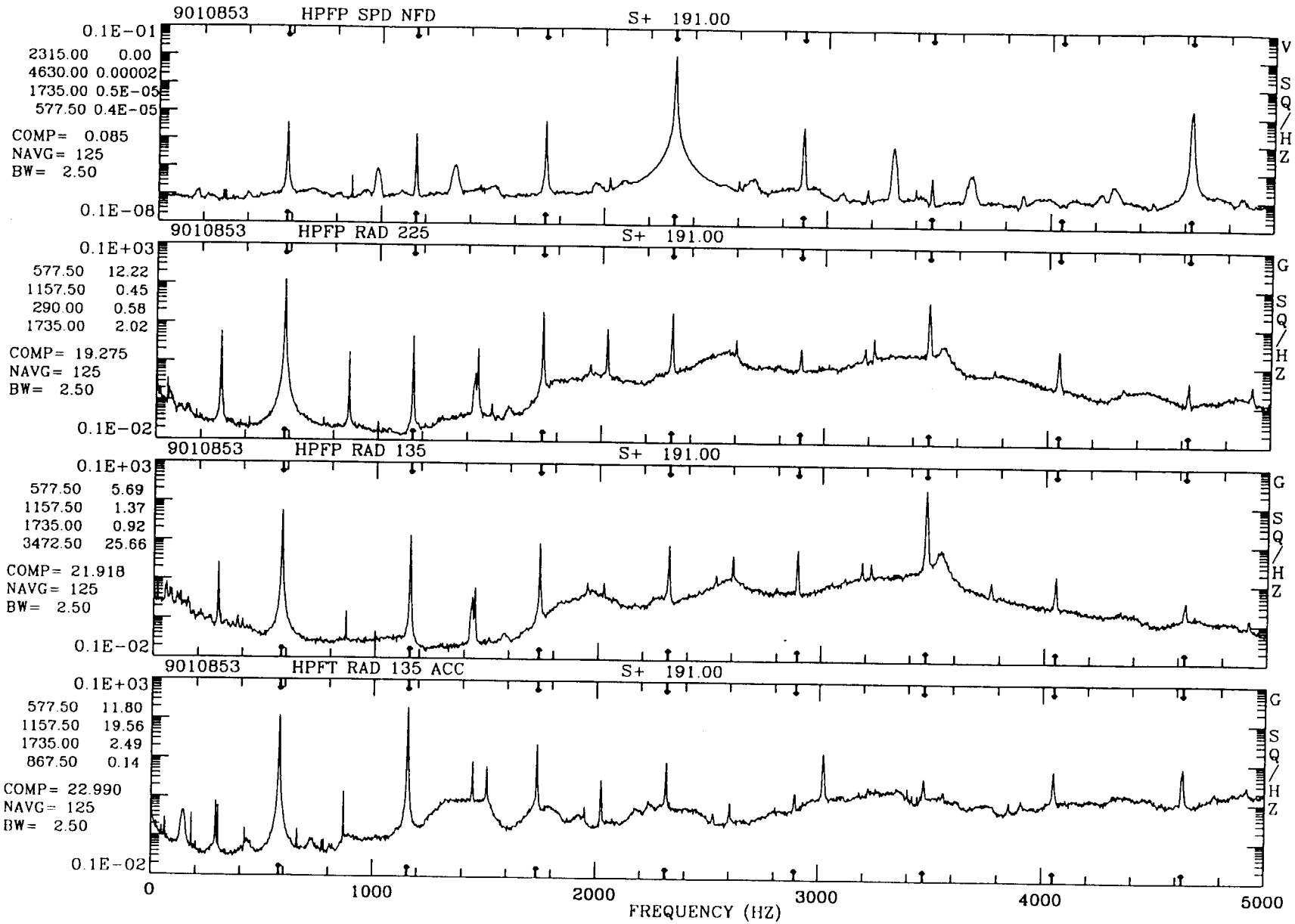
9010853 HPFP SPD NFD S+ 191.00
0.1E-01
2315.00 0.00
4630.00 0.00002
1735.00 0.5E-05
577.50 0.4E-05
COMP= 0.085
NAVG= 125
BW= 2.50
0.1E-08
V SQ/HZ
9010853 HPFP RAD 225 S+ 191.00
0.1E+03
577.50 12.22
1157.50 0.45
290.00 0.58
1735.00 2.02
COMP= 19.275
NAVG= 125
BW= 2.50
0.1E-02
G SQ/HZ
9010853 HPFP RAD 135 S+ 191.00
0.1E+03
577.50 5.69
1157.50 1.37
1735.00 0.92
3472.50 25.66
COMP= 21.918
NAVG= 125
BW= 2.50
0.1E-02
G SQ/HZ
9010853 HPFT RAD 135 ACC S+ 191.00
0.1E+03
577.50 11.80
1157.50 19.56
1735.00 2.49
867.50 0.14
COMP= 22.990
NAVG= 125
BW= 2.50
0.1E-02
G SQ/HZ
0
1000
2000
3000
4000
5000
FREQUENCY (HZ)

PSD

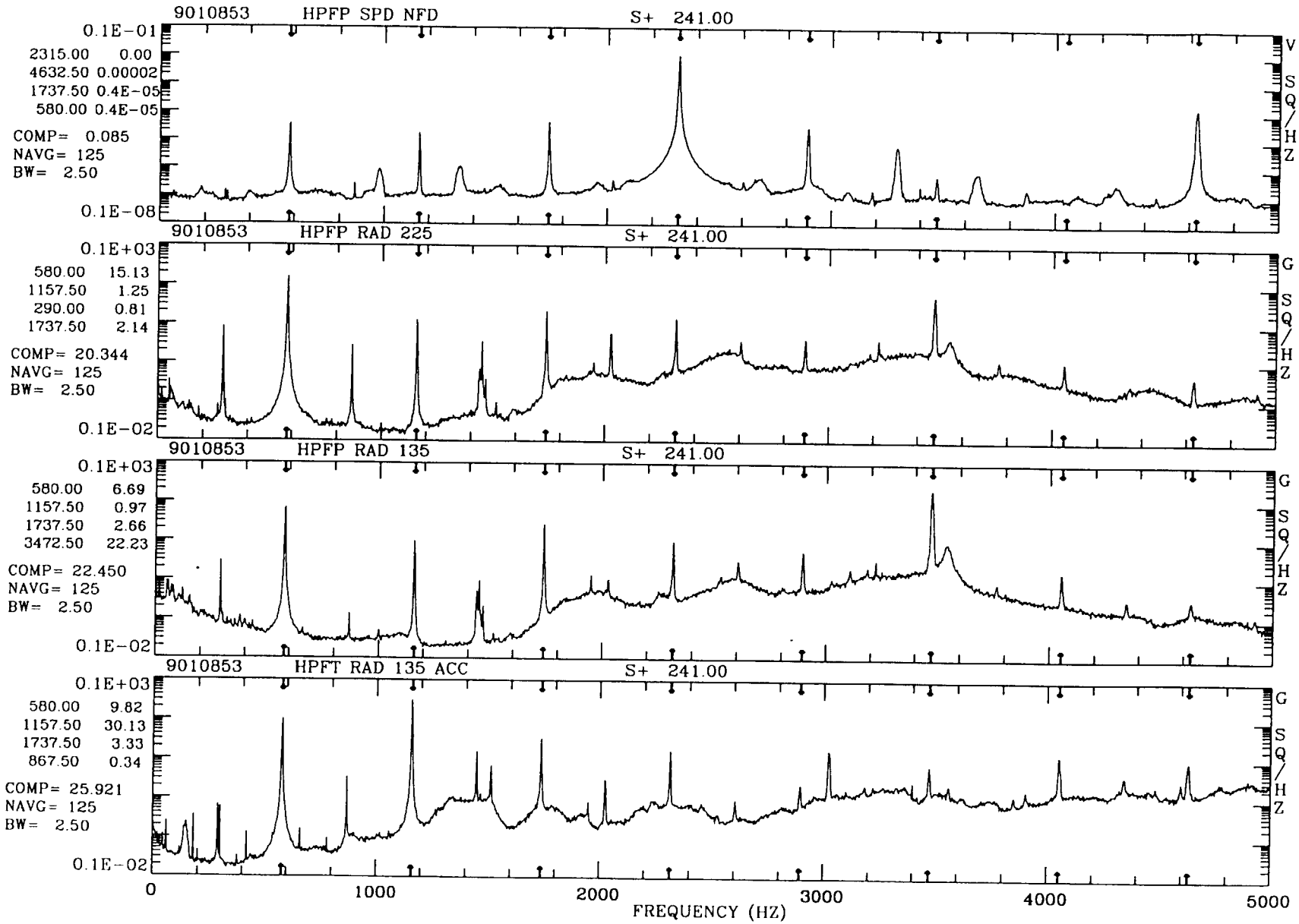
9010853 HPFP SPD NFD S+ 241.00
0.1E-01
2315.00 0.00
4632.50 0.00002
1737.50 0.4E-05
580.00 0.4E-05
COMP= 0.085
NAVG= 125
BW= 2.50
0.1E-08
V S Q / H Z
9010853 HPFP RAD 225 S+ 241.00
0.1E+03
580.00 15.13
1157.50 1.25
290.00 0.81
1737.50 2.14
COMP= 20.344
NAVG= 125
BW= 2.50
0.1E-02
G S Q / H Z
9010853 HPFP RAD 135 S+ 241.00
0.1E+03
580.00 6.69
1157.50 0.97
1737.50 2.66
3472.50 22.23
COMP= 22.450
NAVG= 125
BW= 2.50
0.1E-02
G S Q / H Z
9010853 HPFT RAD 135 ACC S+ 241.00
0.1E+03
580.00 9.82
1157.50 30.13
1737.50 3.33
867.50 0.34
COMP= 25.921
NAVG= 125
BW= 2.50
0.1E-02
G S Q / H Z
0
1000
2000
3000
4000
5000
FREQUENCY (HZ)

PSD

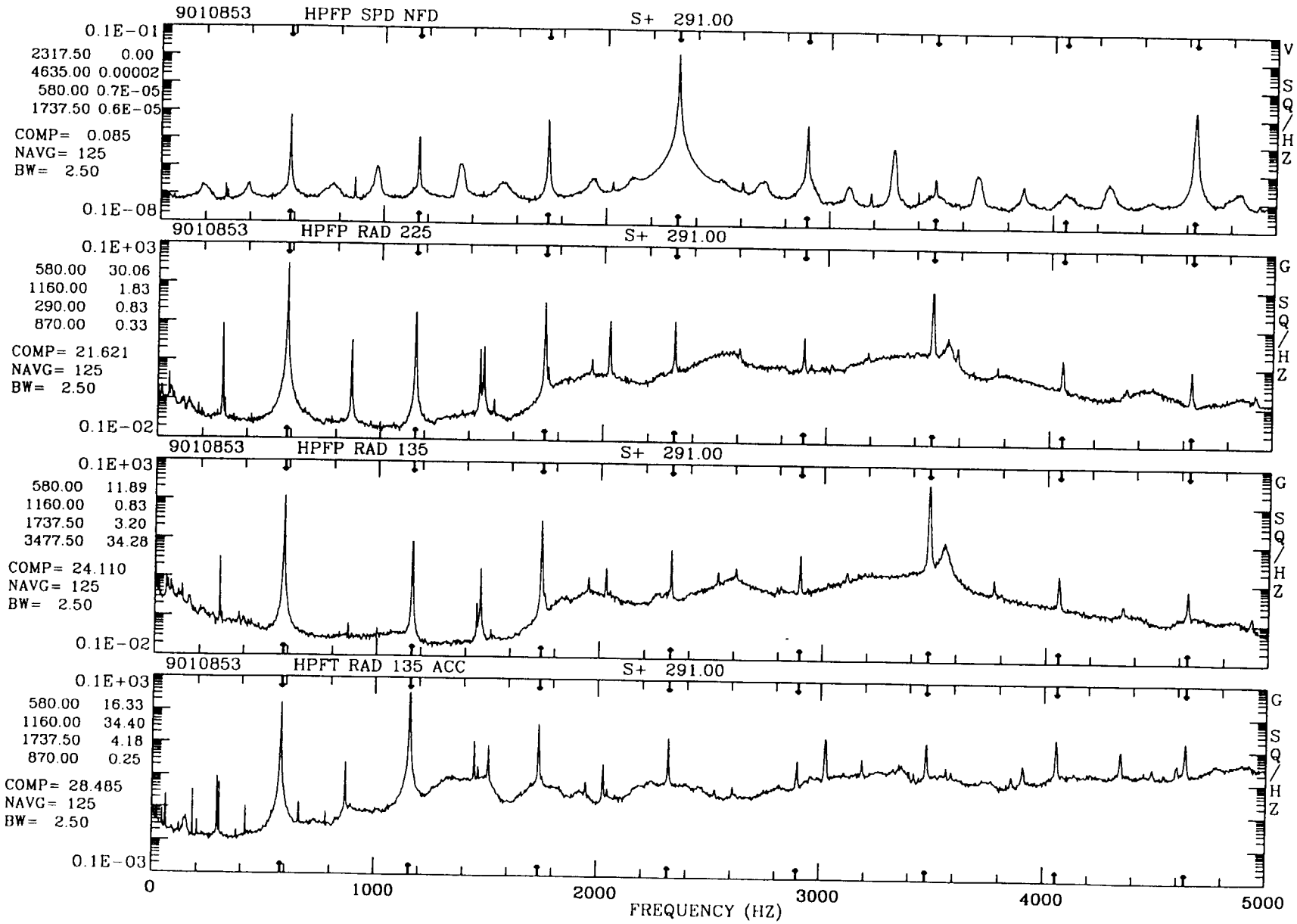
9010853 HPFP SPD NFD S+ 291.00
0.1E-01
2317.50 0.00
4635.00 0.00002
580.00 0.7E-05
1737.50 0.6E-05
COMP= 0.085
NAVG= 125
BW= 2.50
0.1E-08
V SQ/HZ
9010853 HPFP RAD 225 S+ 291.00
0.1E+03
580.00 30.06
1160.00 1.83
290.00 0.83
870.00 0.33
COMP= 21.621
NAVG= 125
BW= 2.50
0.1E-02
G SQ/HZ
9010853 HPFP RAD 135 S+ 291.00
0.1E+03
580.00 11.89
1160.00 0.83
1737.50 3.20
3477.50 34.28
COMP= 24.110
NAVG= 125
BW= 2.50
0.1E-02
G SQ/HZ
9010853 HPFT RAD 135 ACC S+ 291.00
0.1E+03
580.00 16.33
1160.00 34.40
1737.50 4.18
870.00 0.25
COMP= 28.485
NAVG= 125
BW= 2.50
0.1E-03
G SQ/HZ
0
1000
2000
3000
4000
5000
FREQUENCY (HZ)

PSD

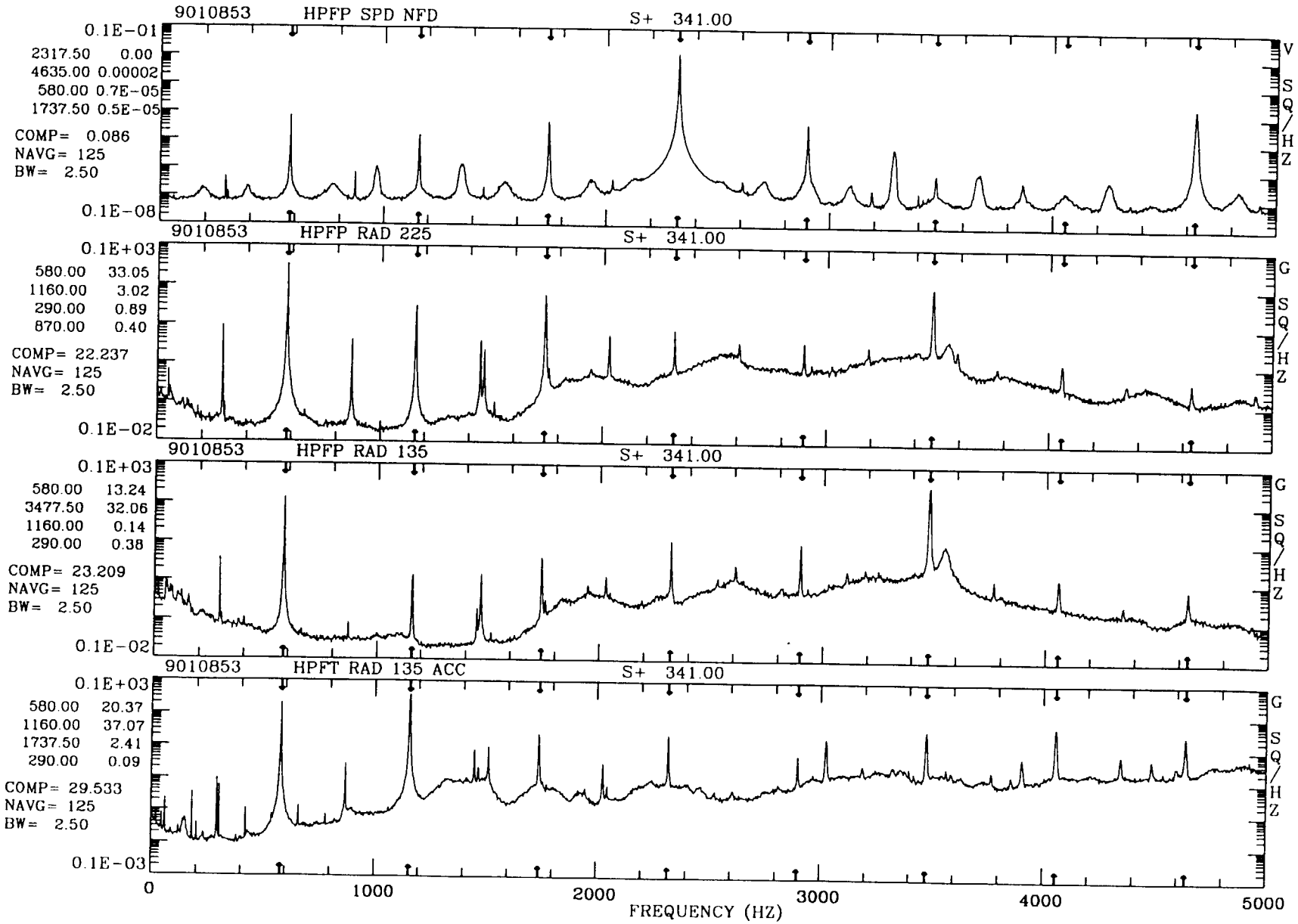
9010853 HPFP SPD NFD S+ 341.00
0.1E-01
2317.50 0.00
4635.00 0.00002
580.00 0.7E-05
1737.50 0.5E-05
COMP= 0.086
NAVG= 125
BW= 2.50
0.1E-08
V
S
Q
/
H
Z
9010853 HPFP RAD 225 S+ 341.00
0.1E+03
580.00 33.05
1160.00 3.02
290.00 0.89
870.00 0.40
COMP= 22.237
NAVG= 125
BW= 2.50
0.1E-02
G
S
Q
/
H
Z
9010853 HPFP RAD 135 S+ 341.00
0.1E+03
580.00 13.24
3477.50 32.06
1160.00 0.14
290.00 0.38
COMP= 23.209
NAVG= 125
BW= 2.50
0.1E-02
G
S
Q
/
H
Z
9010853 HPFT RAD 135 ACC S+ 341.00
0.1E+03
580.00 20.37
1160.00 37.07
1737.50 2.41
290.00 0.09
COMP= 29.533
NAVG= 125
BW= 2.50
0.1E-03
G
S
Q
/
H
Z
0
1000
2000
3000
4000
5000
FREQUENCY (HZ)

PSD

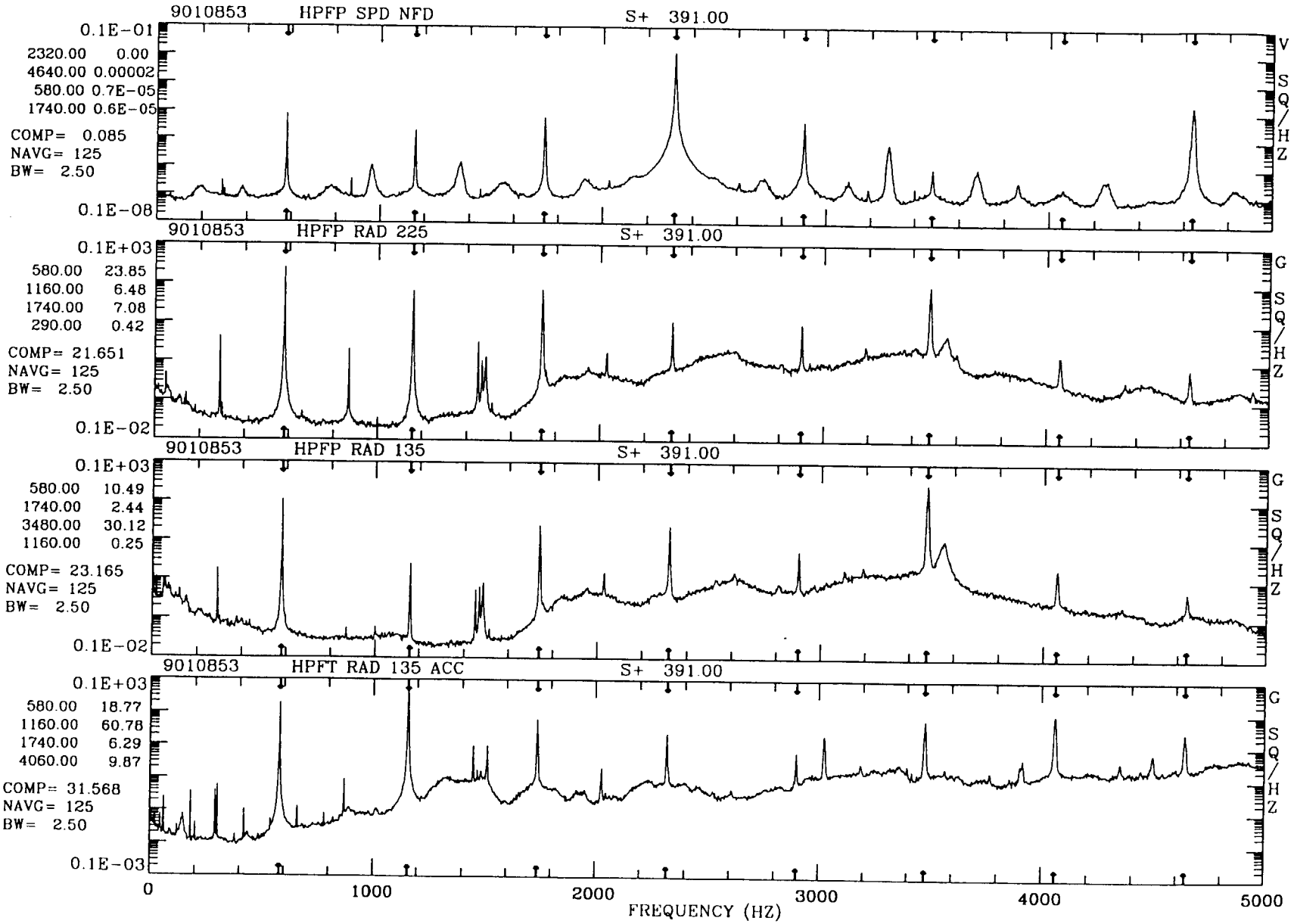
9010853 HPFP SPD NFD S+ 391.00
0.1E-01
2320.00 0.00
4640.00 0.00002
580.00 0.7E-05
1740.00 0.6E-05
COMP= 0.085
NAVG= 125
BW= 2.50
0.1E-08
V
S
Q
/
H
Z
9010853 HPFP RAD 225 S+ 391.00
0.1E+03
580.00 23.85
1160.00 6.48
1740.00 7.08
290.00 0.42
COMP= 21.651
NAVG= 125
BW= 2.50
0.1E-02
G
S
Q
/
H
Z
9010853 HPFP RAD 135 S+ 391.00
0.1E+03
580.00 10.49
1740.00 2.44
3480.00 30.12
1160.00 0.25
COMP= 23.165
NAVG= 125
BW= 2.50
0.1E-02
G
S
Q
/
H
Z
9010853 HPFT RAD 135 ACC S+ 391.00
0.1E+03
580.00 18.77
1160.00 60.78
1740.00 6.29
4060.00 9.87
COMP= 31.568
NAVG= 125
BW= 2.50
0.1E-03
G
S
Q
/
H
Z
0
1000
2000
3000
4000
5000
FREQUENCY (HZ)

PSD

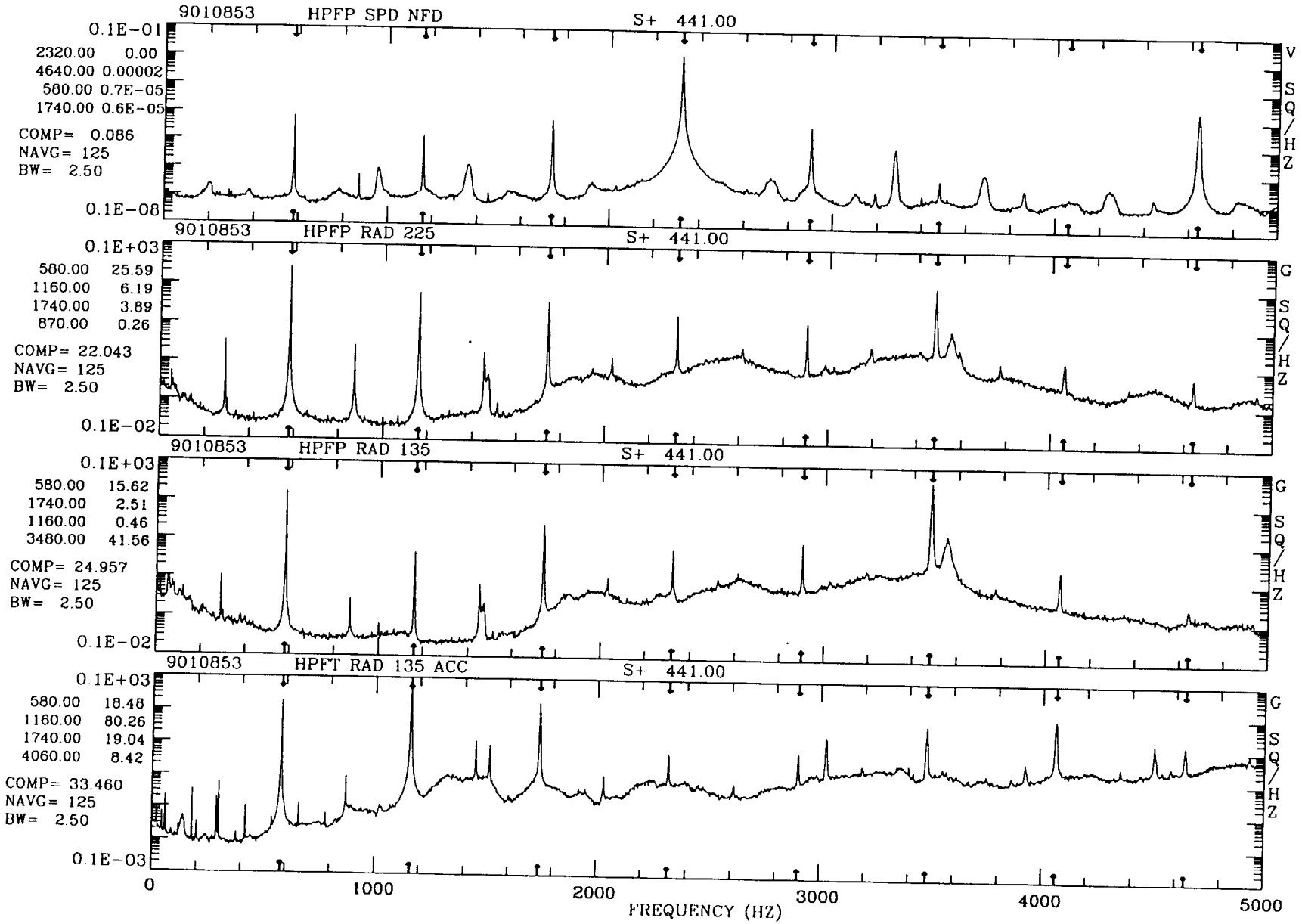
9010853 HPFP SPD NFD S+ 441.00
0.1E-01
2320.00 0.00
4640.00 0.00002
580.00 0.7E-05
1740.00 0.6E-05
COMP= 0.086
NAVG= 125
BW= 2.50
0.1E-08
V S Q / H Z
9010853 HPFP RAD 225 S+ 441.00
0.1E+03
580.00 25.59
1160.00 6.19
1740.00 3.89
870.00 0.26
COMP= 22.043
NAVG= 125
BW= 2.50
0.1E-02
G S Q / H Z
9010853 HPFP RAD 135 S+ 441.00
0.1E+03
580.00 15.62
1740.00 2.51
1160.00 0.46
3480.00 41.56
COMP= 24.957
NAVG= 125
BW= 2.50
0.1E-02
G S Q / H Z
9010853 HPFT RAD 135 ACC S+ 441.00
0.1E+03
580.00 18.48
1160.00 80.26
1740.00 19.04
4060.00 8.42
COMP= 33.460
NAVG= 125
BW= 2.50
0.1E-03
G S Q / H Z
0 1000 2000 3000 4000 5000
FREQUENCY (HZ)

PSD

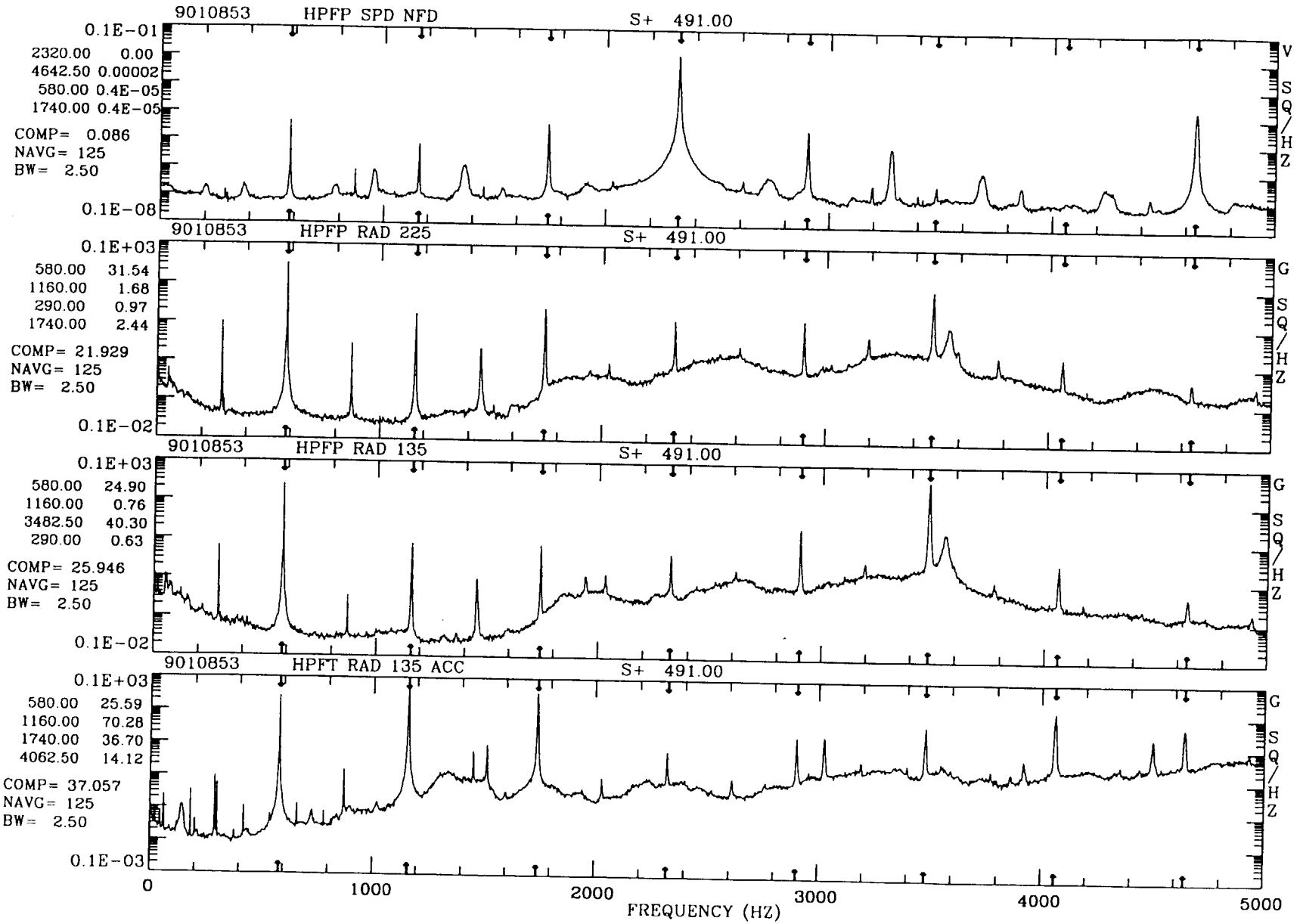
9010853 HPFP SPD NFD S+ 491.00
0.1E-01
2320.00 0.00
4642.50 0.00002
580.00 0.4E-05
1740.00 0.4E-05
COMP= 0.086
NAVG= 125
BW= 2.50
0.1E-08
V SQ/HZ
9010853 HPFP RAD 225 S+ 491.00
0.1E+03
580.00 31.54
1160.00 1.68
290.00 0.97
1740.00 2.44
COMP= 21.929
NAVG= 125
BW= 2.50
0.1E-02
G SQ/HZ
9010853 HPFP RAD 135 S+ 491.00
0.1E+03
580.00 24.90
1160.00 0.76
3482.50 40.30
290.00 0.63
COMP= 25.946
NAVG= 125
BW= 2.50
0.1E-02
G SQ/HZ
9010853 HPFT RAD 135 ACC S+ 491.00
0.1E+03
580.00 25.59
1160.00 70.28
1740.00 36.70
4062.50 14.12
COMP= 37.057
NAVG= 125
BW= 2.50
0.1E-03
G SQ/HZ
0
1000
2000
3000
4000
5000
FREQUENCY (HZ)

PSD

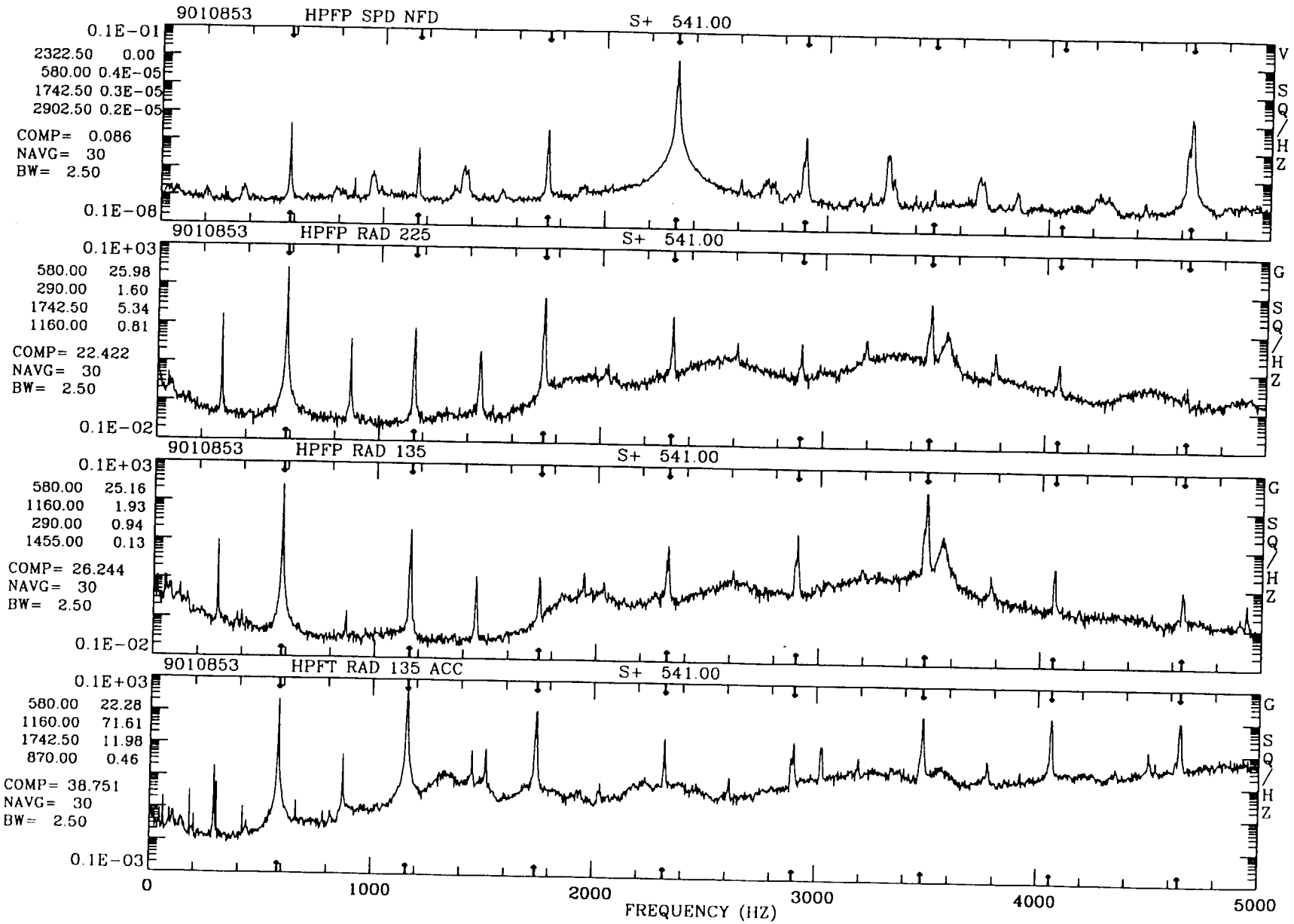
9010853 HPFP SPD NFD S+ 541.00
0.1E-01
2322.50 0.00
580.00 0.4E-05
1742.50 0.3E-05
2902.50 0.2E-05
COMP= 0.086
NAVG= 30
BW= 2.50
0.1E-08
V
S
Q
/
H
Z
9010853 HPFP RAD 225 S+ 541.00
0.1E+03
580.00 25.98
290.00 1.60
1742.50 5.34
1160.00 0.81
COMP= 22.422
NAVG= 30
BW= 2.50
0.1E-02
G
S
Q
/
H
Z
9010853 HPFP RAD 135 S+ 541.00
0.1E+03
580.00 25.16
1160.00 1.93
290.00 0.94
1455.00 0.13
COMP= 26.244
NAVG= 30
BW= 2.50
0.1E-02
G
S
Q
/
H
Z
9010853 HPFT RAD 135 ACC S+ 541.00
0.1E+03
580.00 22.28
1160.00 71.61
1742.50 11.98
870.00 0.46
COMP= 38.751
NAVG= 30
BW= 2.50
0.1E-03
G
S
Q
/
H
Z
0
1000
2000
3000
4000
5000
FREQUENCY (HZ)

PSD

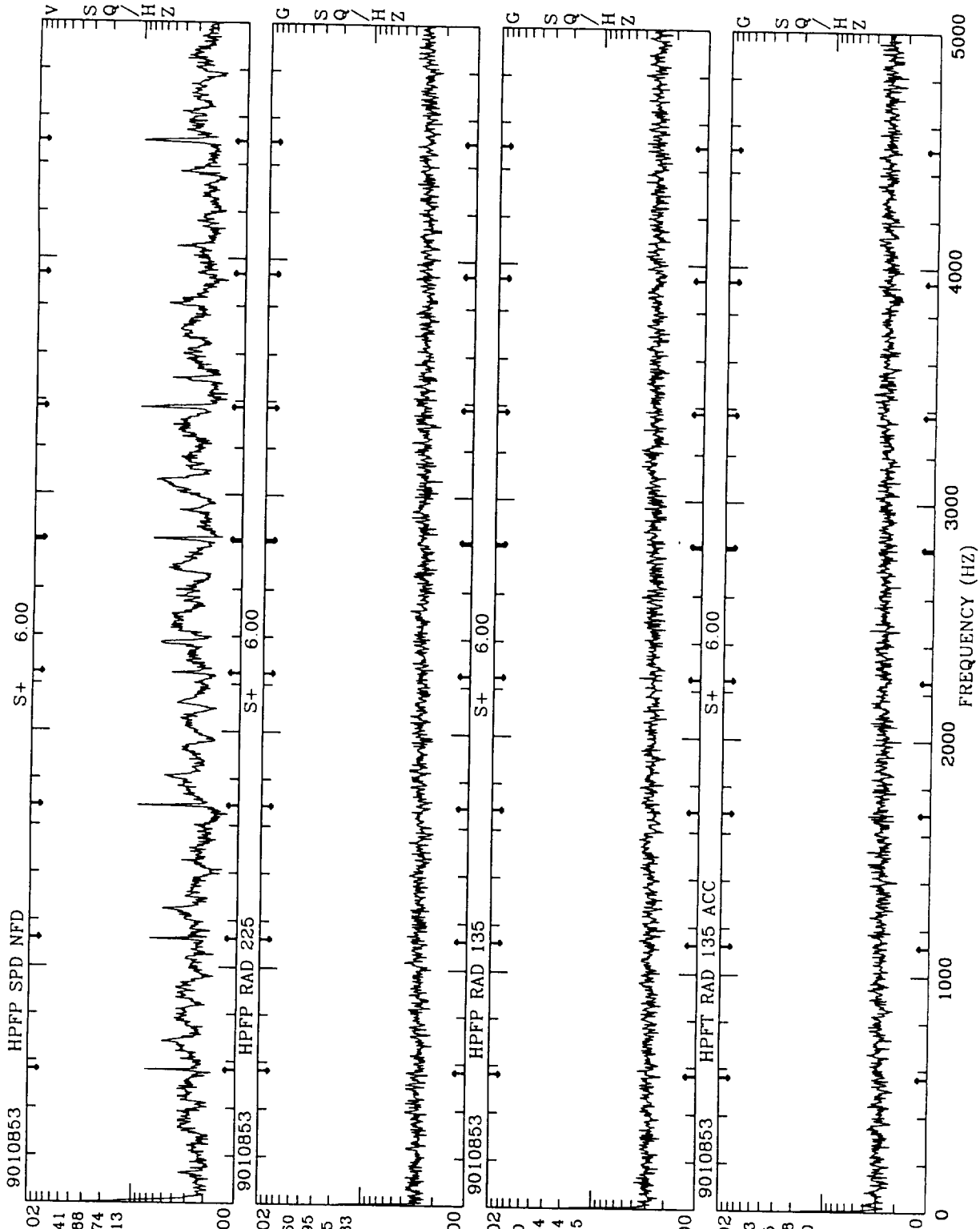
9010853 HPFP SPD NFD S+ 6.00
0.1E+02
0.1E+00
V S Q / H Z
1687.5 0.941
3372.5 0.988
4495.0 0.974
2812.5 0.713
COMP= 37.390
NAVG= 83
BW= 2.50
9010853 HPFP RAD 225 S+ 6.00
0.1E+02
0.1E+00
G S Q / H Z
1965.0 0.360
1030.0 0.395
5.0 1.575
2520.0 0.383
COMP= 38.287
NAVG= 83
BW= 2.50
9010853 HPFP RAD 135 S+ 6.00
0.1E+02
0.1E+00
G S Q / H Z
5.0 1.600
1945.0 0.364
1142.5 0.364
3220.0 0.395
COMP= 38.277
NAVG= 83
BW= 2.50
9010853 HPFT RAD 135 ACC S+ 6.00
0.1E+02
0.1E+00
G S Q / H Z
1530.0 0.403
30.0 0.415
1477.5 0.398
447.5 0.370
COMP= 38.352
NAVG= 83
BW= 2.50
0 1000 2000 3000 4000 5000
FREQUENCY (HZ)

CP -- WBD

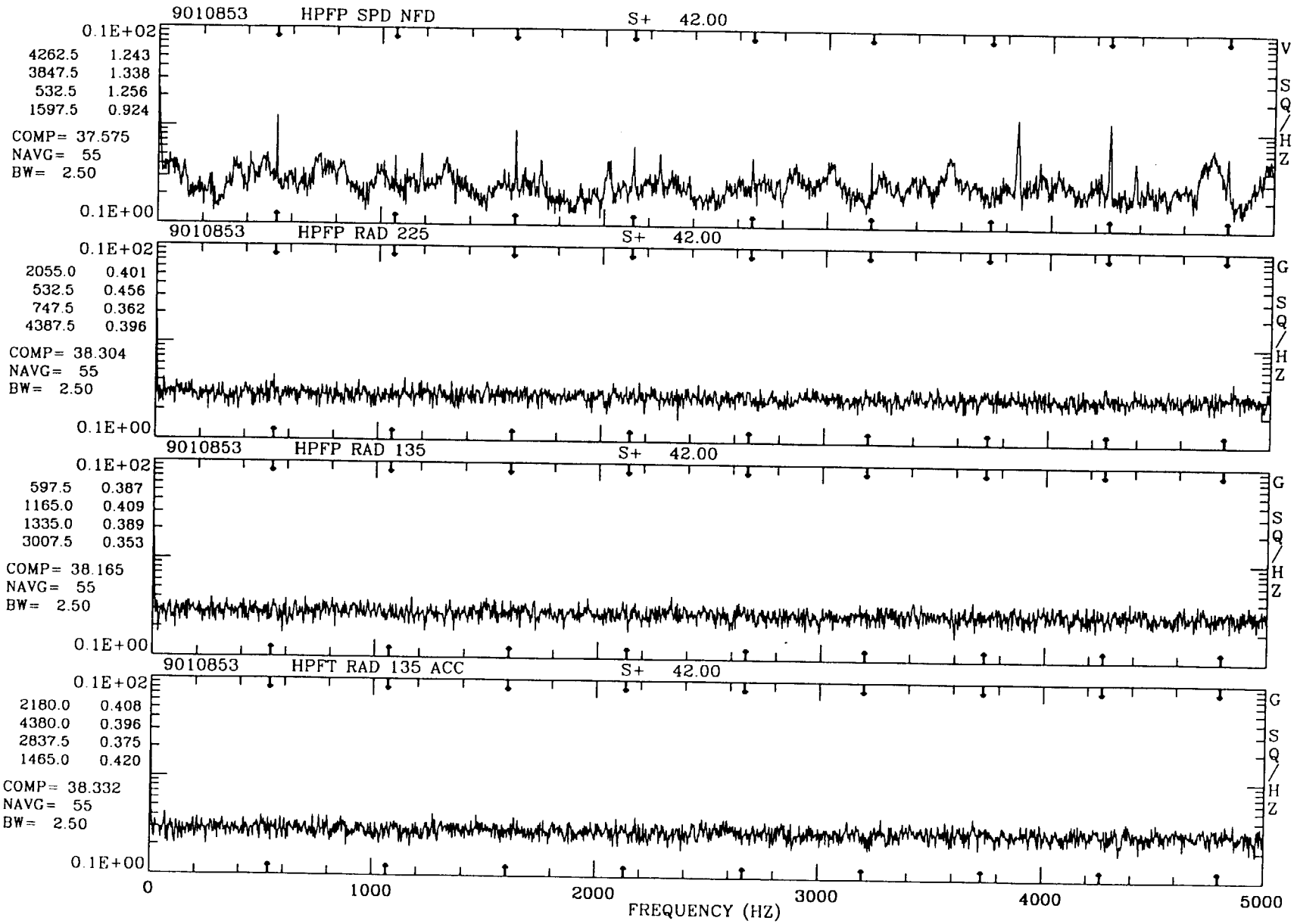
9010853 HPFP SPD NFD S+ 42.00
0.1E+02
4262.5 1.243
3847.5 1.338
532.5 1.256
1597.5 0.924
COMP= 37.575
NAVG= 55
BW= 2.50
0.1E+00
V
S
Q
/
H
Z
9010853 HPFP RAD 225 S+ 42.00
0.1E+02
2055.0 0.401
532.5 0.456
747.5 0.362
4387.5 0.396
COMP= 38.304
NAVG= 55
BW= 2.50
0.1E+00
G
S
Q
/
H
Z
9010853 HPFP RAD 135 S+ 42.00
0.1E+02
597.5 0.387
1165.0 0.409
1335.0 0.389
3007.5 0.353
COMP= 38.165
NAVG= 55
BW= 2.50
0.1E+00
G
S
Q
/
H
Z
9010853 HPFT RAD 135 ACC S+ 42.00
0.1E+02
2180.0 0.408
4380.0 0.396
2837.5 0.375
1465.0 0.420
COMP= 38.332
NAVG= 55
BW= 2.50
0.1E+00
G
S
Q
/
H
Z
0
1000
2000
3000
4000
5000
FREQUENCY (HZ)

CP-WBD

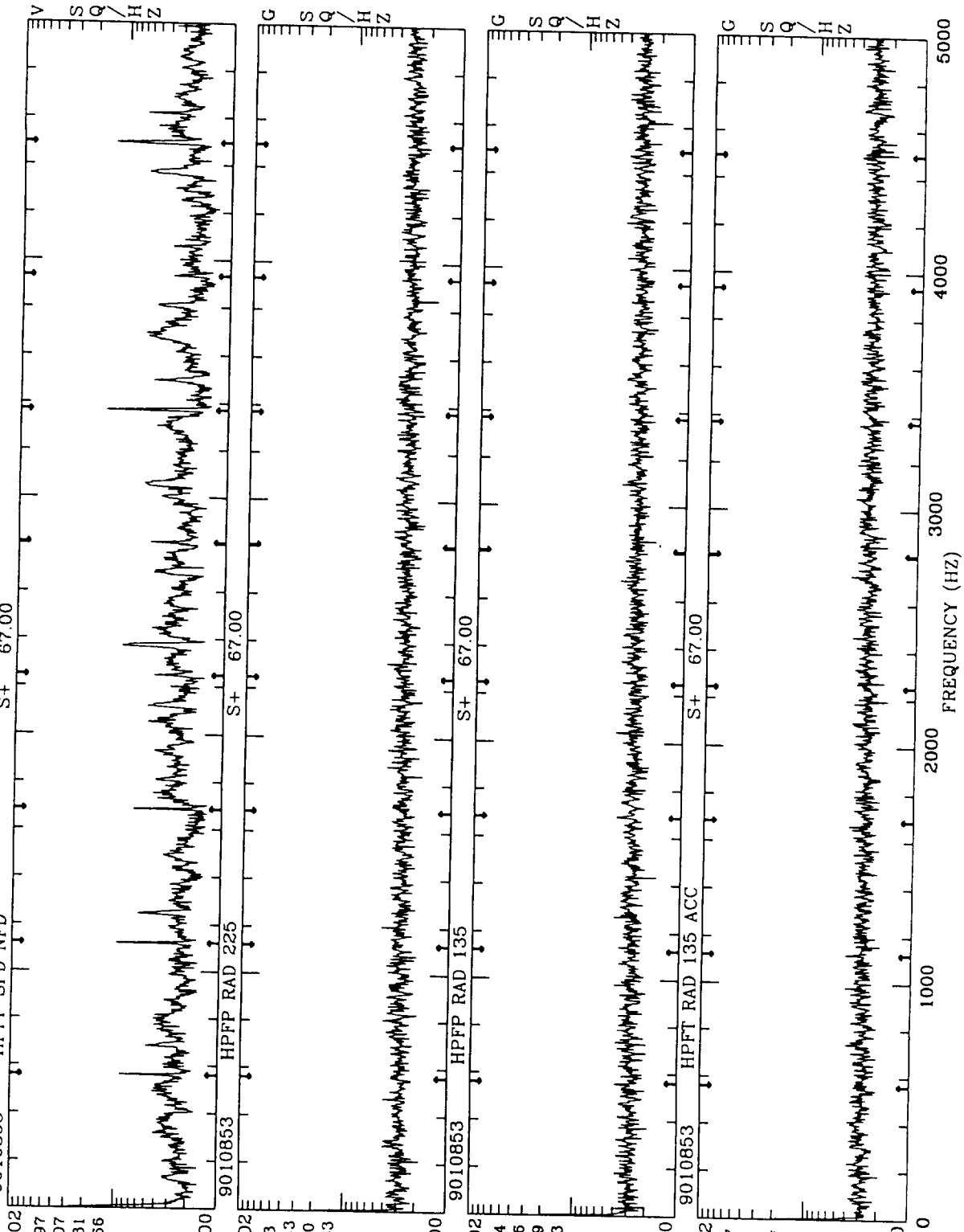
9010853 HPFP SPD NFD S+ 67.00
0.1E+02
0.1E+00
V S Q / H Z
3372.5 1.497
4495.0 1.307
1125.0 0.981
2372.5 0.966
COMP= 37.247
NAVG= 55
BW= 2.50
9010853 HPFP RAD 225 S+ 67.00
0.1E+02
0.1E+00
G S Q / H Z
5.0 1.853
1205.0 0.443
475.0 0.410
3102.5 0.383
COMP= 38.291
NAVG= 55
BW= 2.50
9010853 HPFP RAD 135 S+ 67.00
0.1E+02
0.1E+00
G S Q / H Z
4047.5 0.404
2042.5 0.436
4810.0 0.369
2455.0 0.383
COMP= 38.284
NAVG= 55
BW= 2.50
9010853 HPFT RAD 135 ACC S+ 67.00
0.1E+02
0.1E+00
G S Q / H Z
2720.0 0.427
740.0 0.411
1665.0 0.414
835.0 0.371
COMP= 38.328
NAVG= 55
BW= 2.50
0 1000 2000 3000 4000 5000
FREQUENCY (HZ)

CP – WBD

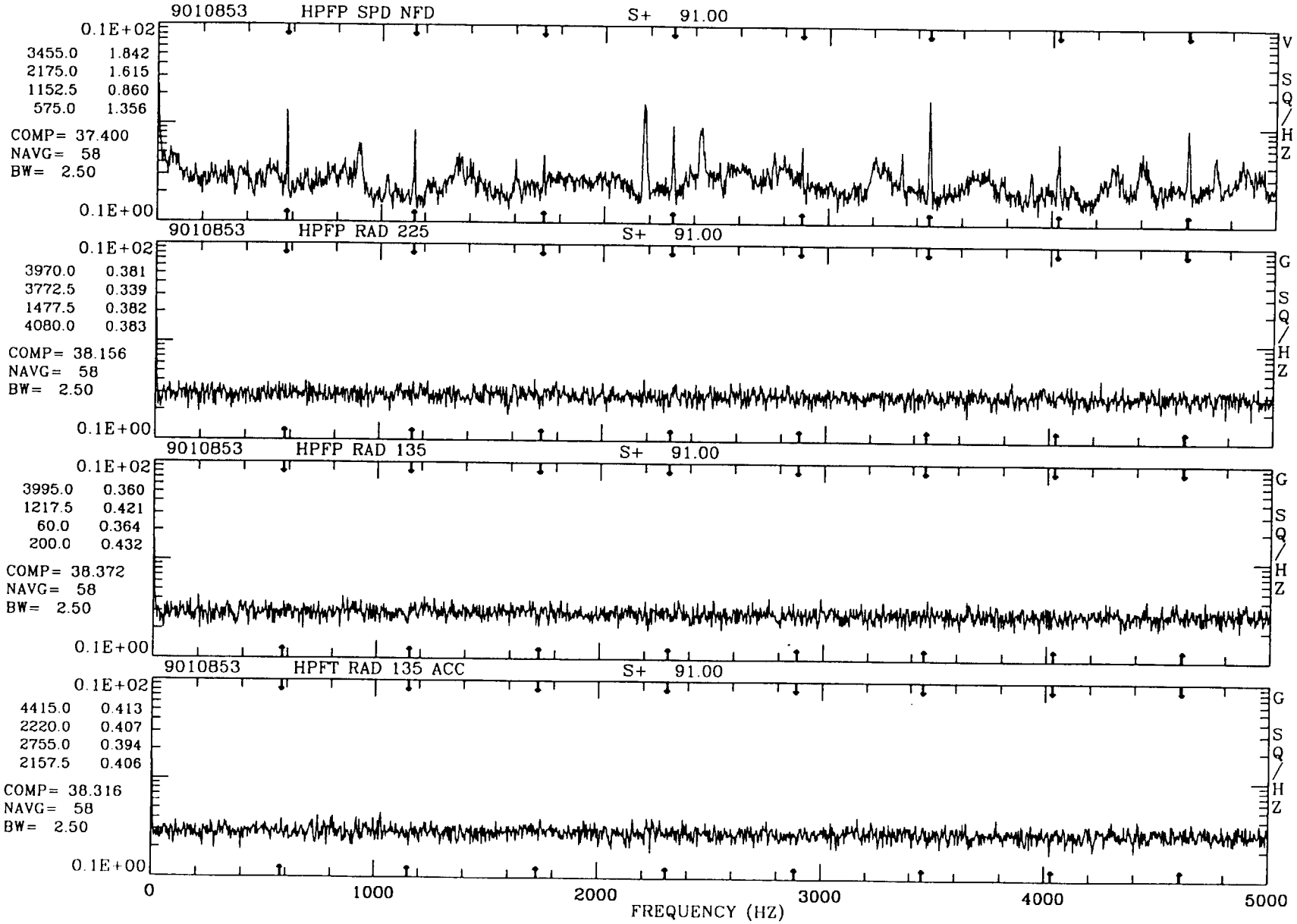
9010853 HPFP SPD NFD S+ 91.00
0.1E+02
3455.0 1.842
2175.0 1.615
1152.5 0.860
575.0 1.356
COMP= 37.400
NAVG= 58
BW= 2.50
0.1E+00
V SQ/HZ
9010853 HPFP RAD 225 S+ 91.00
0.1E+02
3970.0 0.381
3772.5 0.339
1477.5 0.382
4080.0 0.383
COMP= 38.156
NAVG= 58
BW= 2.50
0.1E+00
G SQ/HZ
9010853 HPFP RAD 135 S+ 91.00
0.1E+02
3995.0 0.360
1217.5 0.421
60.0 0.364
200.0 0.432
COMP= 38.372
NAVG= 58
BW= 2.50
0.1E+00
G SQ/HZ
9010853 HPFT RAD 135 ACC S+ 91.00
0.1E+02
4415.0 0.413
2220.0 0.407
2755.0 0.394
2157.5 0.406
COMP= 38.316
NAVG= 58
BW= 2.50
0.1E+00
G SQ/HZ
0
1000
2000
3000
4000
5000
FREQUENCY (HZ)

CP-WBD

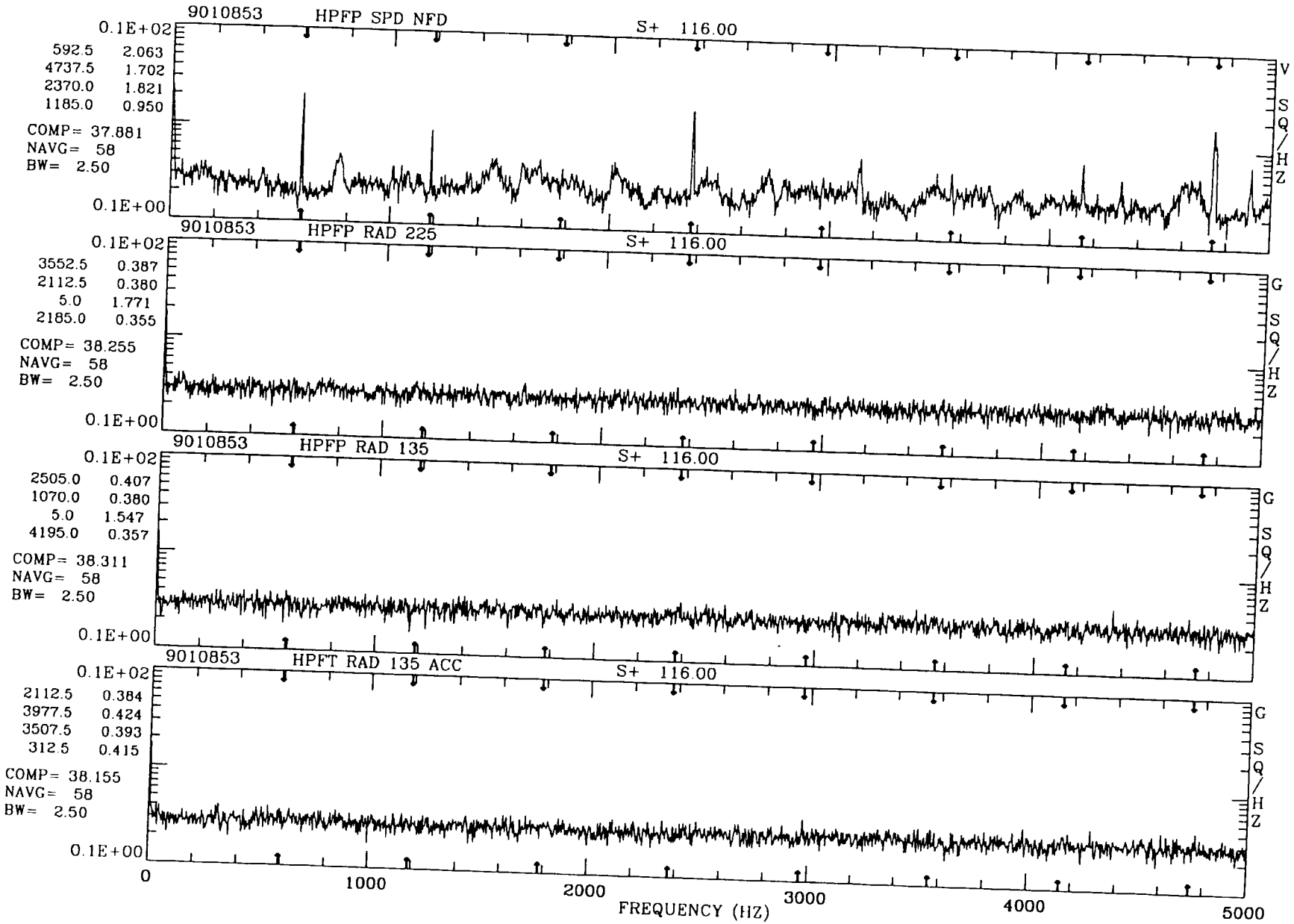
9010853 HPFP SPD NFD S+ 116.00
0.1E+02
592.5 2.063
4737.5 1.702
2370.0 1.821
1185.0 0.950
COMP= 37.881
NAVG= 58
BW= 2.50
0.1E+00
V SQ/HZ
9010853 HPFP RAD 225 S+ 116.00
0.1E+02
3552.5 0.387
2112.5 0.380
5.0 1.771
2185.0 0.355
COMP= 38.255
NAVG= 58
BW= 2.50
0.1E+00
G SQ/HZ
9010853 HPFP RAD 135 S+ 116.00
0.1E+02
2505.0 0.407
1070.0 0.380
5.0 1.547
4195.0 0.357
COMP= 38.311
NAVG= 58
BW= 2.50
0.1E+00
G SQ/HZ
9010853 HPFT RAD 135 ACC S+ 116.00
0.1E+02
2112.5 0.384
3977.5 0.424
3507.5 0.393
312.5 0.415
COMP= 38.155
NAVG= 58
BW= 2.50
0.1E+00
G SQ/HZ
0
1000
2000
3000
4000
5000
FREQUENCY (HZ)

CP-WBD

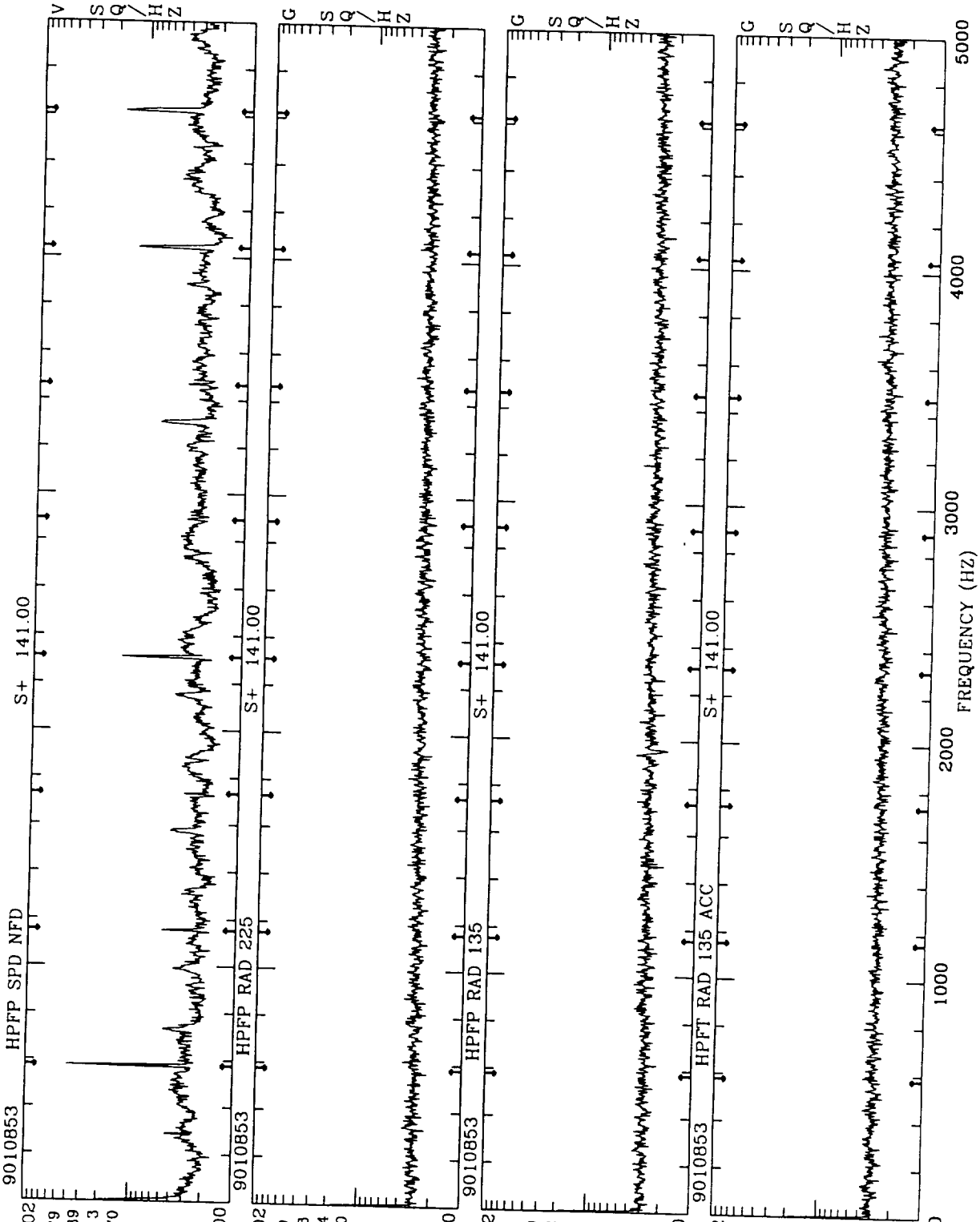
9010853
HPFP SPD NFD
S+ 141.00
0.1E+02
577.5 3.979
2310.0 1.439
4042.5 1.213
4620.0 1.670
COMP= 37.540
NAVG= 125
BW= 2.50
0.1E+00
9010853
HPFP RAD 225
S+ 141.00
0.1E+02
5.0 1.739
335.0 0.368
3360.0 0.354
4057.5 0.370
COMP= 38.312
NAVG= 125
BW= 2.50
0.1E+00
9010853
HPFP RAD 135
S+ 141.00
0.1E+02
967.5 0.371
2082.5 0.370
2750.0 0.372
1022.5 0.354
COMP= 38.257
NAVG= 125
BW= 2.50
0.1E+00
9010853
HPFT RAD 135 ACC
S+ 141.00
0.1E+02
1367.5 0.373
457.5 0.376
3632.5 0.381
5.0 1.810
COMP= 38.401
NAVG= 125
BW= 2.50
0.1E+00
0
1000
2000
3000
4000
5000
FREQUENCY (HZ)
V
G
S
Q
H
Z

CP-WBD

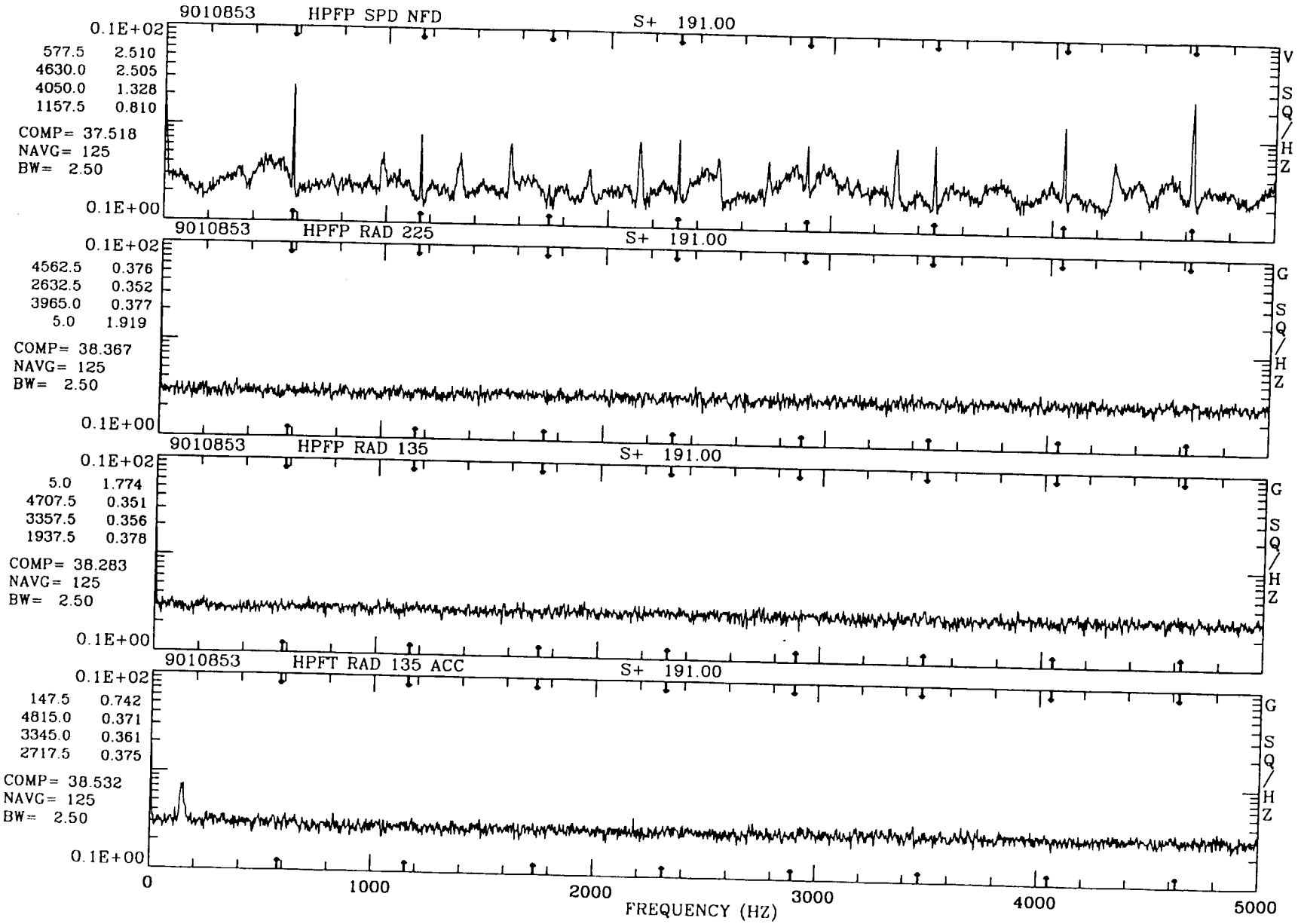
9010853 HPFP SPD NFD S+ 191.00
0.1E+02
577.5 2.510
4630.0 2.505
4050.0 1.328
1157.5 0.810
COMP= 37.518
NAVG= 125
BW= 2.50
0.1E+00
V SQ/HZ
9010853 HPFP RAD 225 S+ 191.00
0.1E+02
4562.5 0.376
2632.5 0.352
3965.0 0.377
5.0 1.919
COMP= 38.367
NAVG= 125
BW= 2.50
0.1E+00
G SQ/HZ
9010853 HPFP RAD 135 S+ 191.00
0.1E+02
5.0 1.774
4707.5 0.351
3357.5 0.356
1937.5 0.378
COMP= 38.283
NAVG= 125
BW= 2.50
0.1E+00
G SQ/HZ
9010853 HPFT RAD 135 ACC S+ 191.00
0.1E+02
147.5 0.742
4815.0 0.371
3345.0 0.361
2717.5 0.375
COMP= 38.532
NAVG= 125
BW= 2.50
0.1E+00
G SQ/HZ
0
1000
2000
3000
4000
5000
FREQUENCY (HZ)

CP-WBD

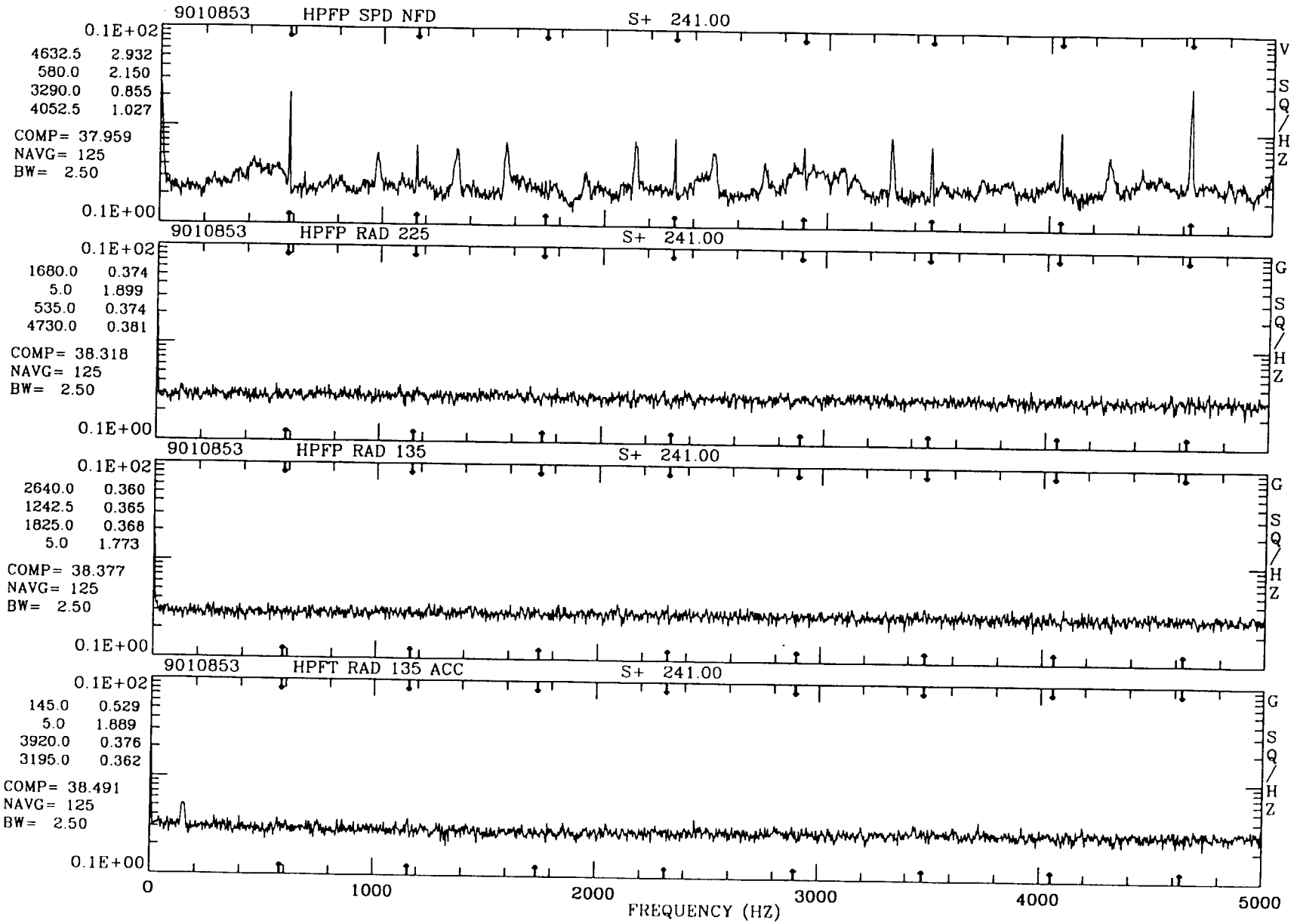
9010853 HPFP SPD NFD S+ 241.00
0.1E+02
4632.5 2.932
580.0 2.150
3290.0 0.855
4052.5 1.027
COMP= 37.959
NAVG= 125
BW= 2.50
0.1E+00
V SQ/HZ
9010853 HPFP RAD 225 S+ 241.00
0.1E+02
1680.0 0.374
5.0 1.899
535.0 0.374
4730.0 0.381
COMP= 38.318
NAVG= 125
BW= 2.50
0.1E+00
G SQ/HZ
9010853 HPFP RAD 135 S+ 241.00
0.1E+02
2640.0 0.360
1242.5 0.365
1825.0 0.368
5.0 1.773
COMP= 38.377
NAVG= 125
BW= 2.50
0.1E+00
G SQ/HZ
9010853 HPFT RAD 135 ACC S+ 241.00
0.1E+02
145.0 0.529
5.0 1.889
3920.0 0.376
3195.0 0.362
COMP= 38.491
NAVG= 125
BW= 2.50
0.1E+00
G SQ/HZ
0
1000
2000
3000
4000
5000
FREQUENCY (HZ)

CP-WBD

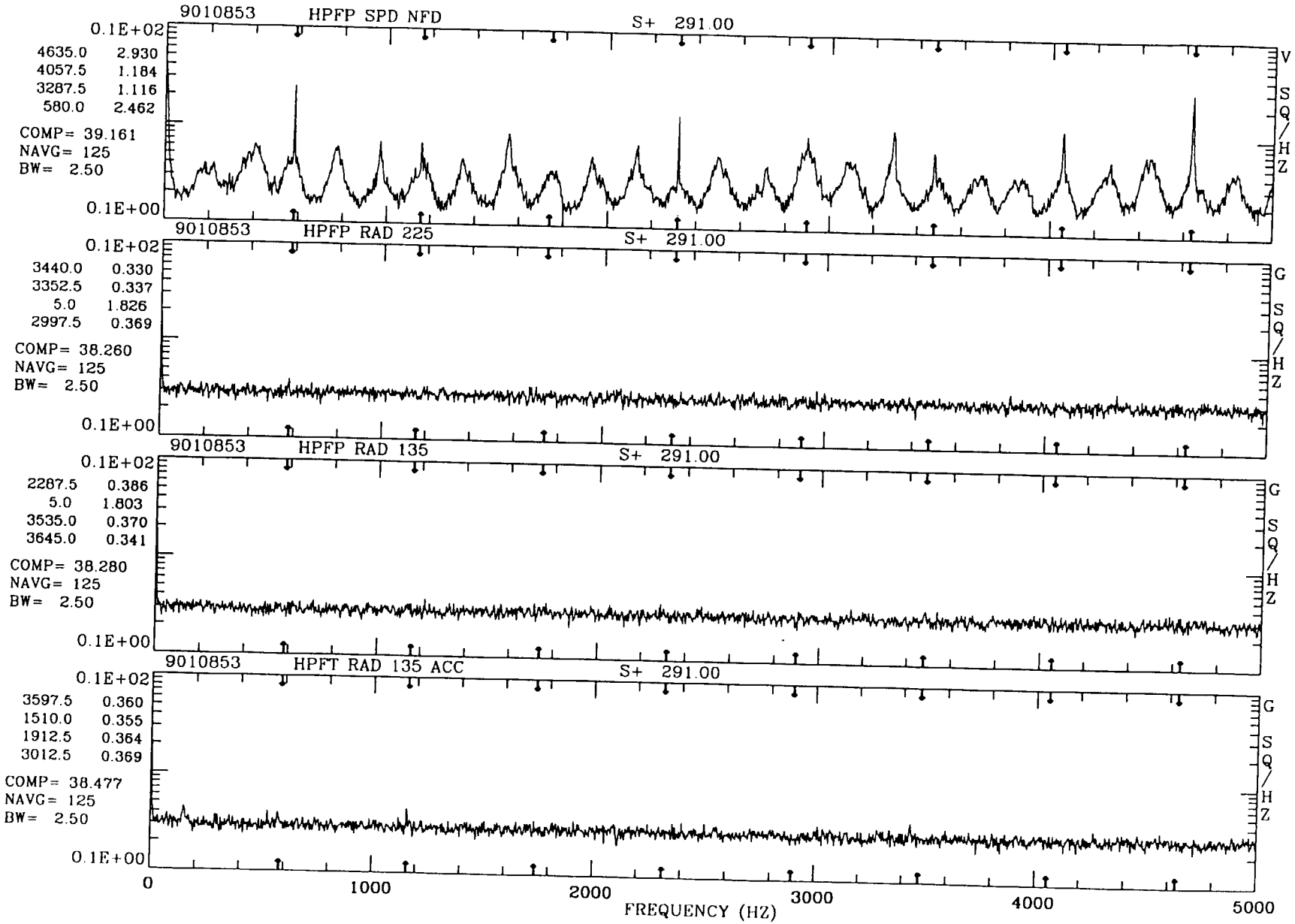
9010853 HPFP SPD NFD S+ 291.00
0.1E+02
4635.0 2.930
4057.5 1.184
3287.5 1.116
580.0 2.462
COMP= 39.161
NAVG= 125
BW= 2.50
0.1E+00
V SQ/HZ
9010853 HPFP RAD 225 S+ 291.00
0.1E+02
3440.0 0.330
3352.5 0.337
5.0 1.826
2997.5 0.369
COMP= 38.260
NAVG= 125
BW= 2.50
0.1E+00
G SQ/HZ
9010853 HPFP RAD 135 S+ 291.00
0.1E+02
2287.5 0.386
5.0 1.803
3535.0 0.370
3645.0 0.341
COMP= 38.280
NAVG= 125
BW= 2.50
0.1E+00
G SQ/HZ
9010853 HPFT RAD 135 ACC S+ 291.00
0.1E+02
3597.5 0.360
1510.0 0.355
1912.5 0.364
3012.5 0.369
COMP= 38.477
NAVG= 125
BW= 2.50
0.1E+00
G SQ/HZ
0
1000
2000
3000
4000
5000
FREQUENCY (HZ)

CP-WBD

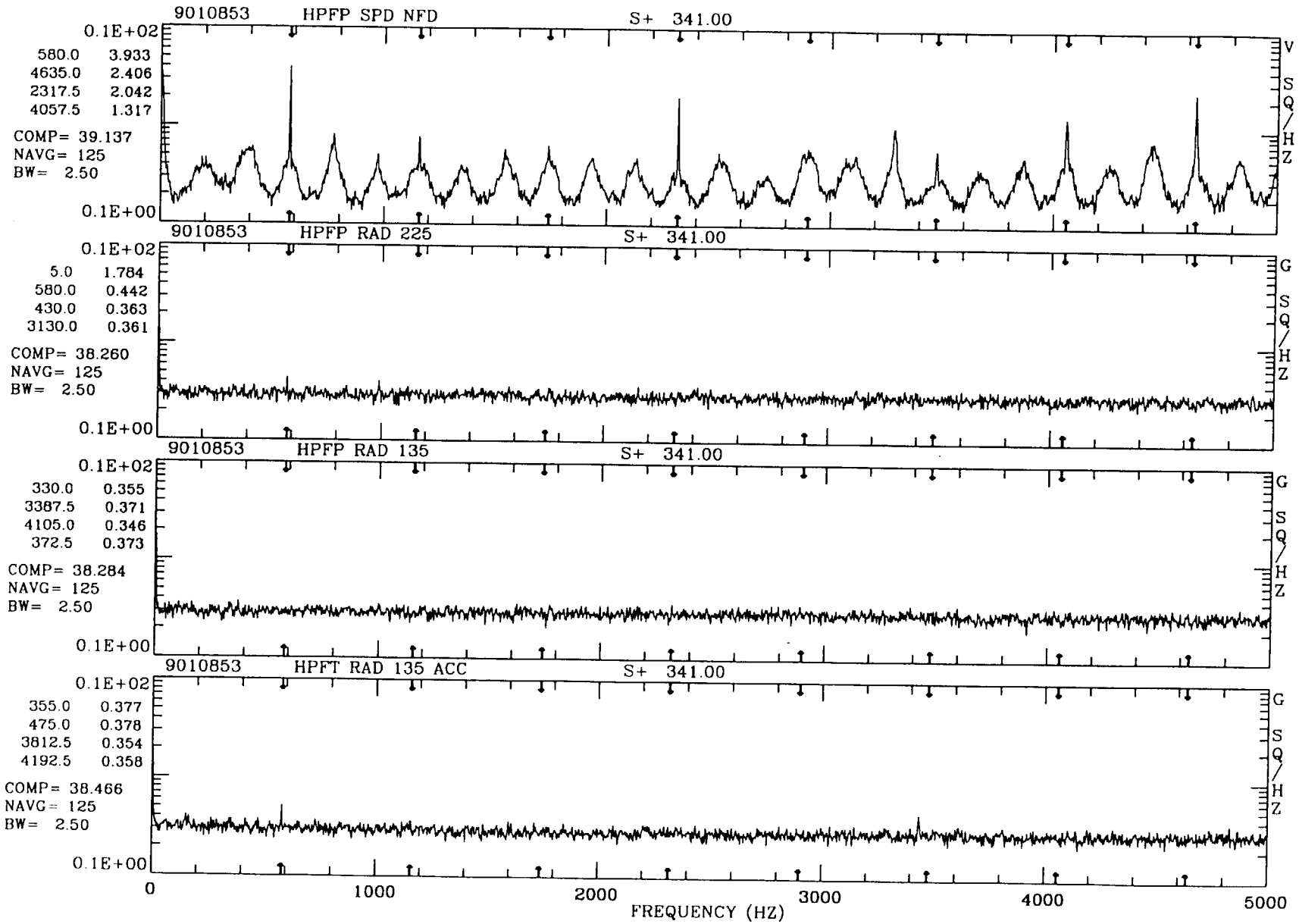
9010853 HPFP SPD NFD S+ 341.00
0.1E+02
580.0 3.933
4635.0 2.406
2317.5 2.042
4057.5 1.317
COMP= 39.137
NAVG= 125
BW= 2.50
0.1E+00
V SQ/HZ
9010853 HPFP RAD 225 S+ 341.00
0.1E+02
5.0 1.784
580.0 0.442
430.0 0.363
3130.0 0.361
COMP= 38.260
NAVG= 125
BW= 2.50
0.1E+00
G SQ/HZ
9010853 HPFP RAD 135 S+ 341.00
0.1E+02
330.0 0.355
3387.5 0.371
4105.0 0.346
372.5 0.373
COMP= 38.284
NAVG= 125
BW= 2.50
0.1E+00
G SQ/HZ
9010853 HPFT RAD 135 ACC S+ 341.00
0.1E+02
355.0 0.377
475.0 0.378
3812.5 0.354
4192.5 0.358
COMP= 38.466
NAVG= 125
BW= 2.50
0.1E+00
G SQ/HZ
0
1000
2000
3000
4000
5000
FREQUENCY (HZ)

CP-WBD

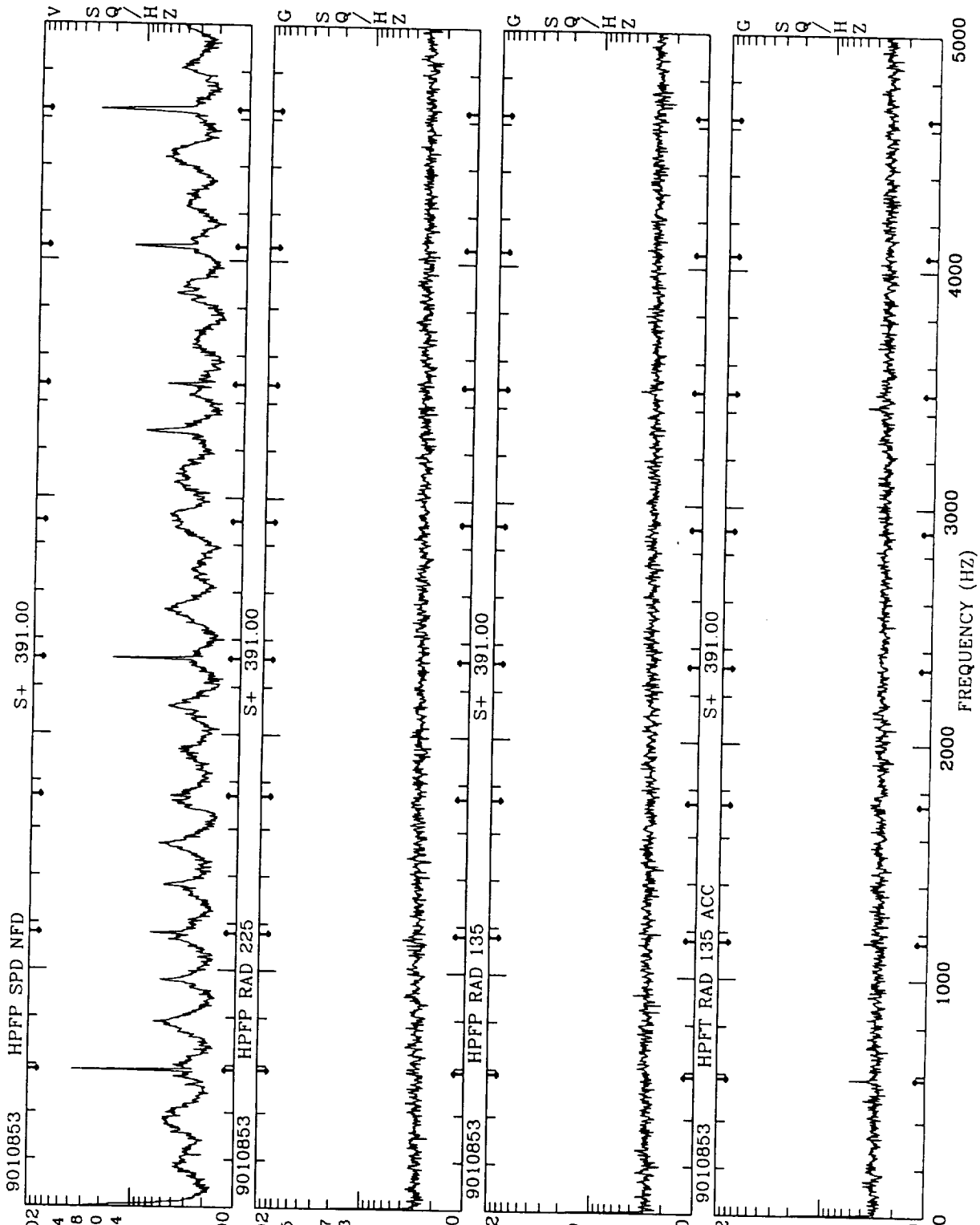
9010853
HPFP SPD NFD
S+ 391.00
0.1E+02
0.1E+00
580.0 3.714
4640.0 2.668
2320.0 1.710
4060.0 1.214
COMP= 38.473
NAVG= 125
BW= 2.50
V
S
Q
H
Z
9010853
HPFP RAD 225
S+ 391.00
900.0 0.385
5.0 1.842
1487.5 0.377
3185.0 0.363
COMP= 38.261
NAVG= 125
BW= 2.50
G
9010853
HPFP RAD 135
S+ 391.00
5.0 1.648
27.5 0.326
2240.0 0.361
4077.5 0.369
COMP= 38.270
NAVG= 125
BW= 2.50
9010853
HPFT RAD 135 ACC
S+ 391.00
580.0 0.529
3427.5 0.441
1160.0 0.409
1637.5 0.361
COMP= 38.483
NAVG= 125
BW= 2.50
0
1000
2000
3000
4000
5000
FREQUENCY (HZ)

CP–WBD

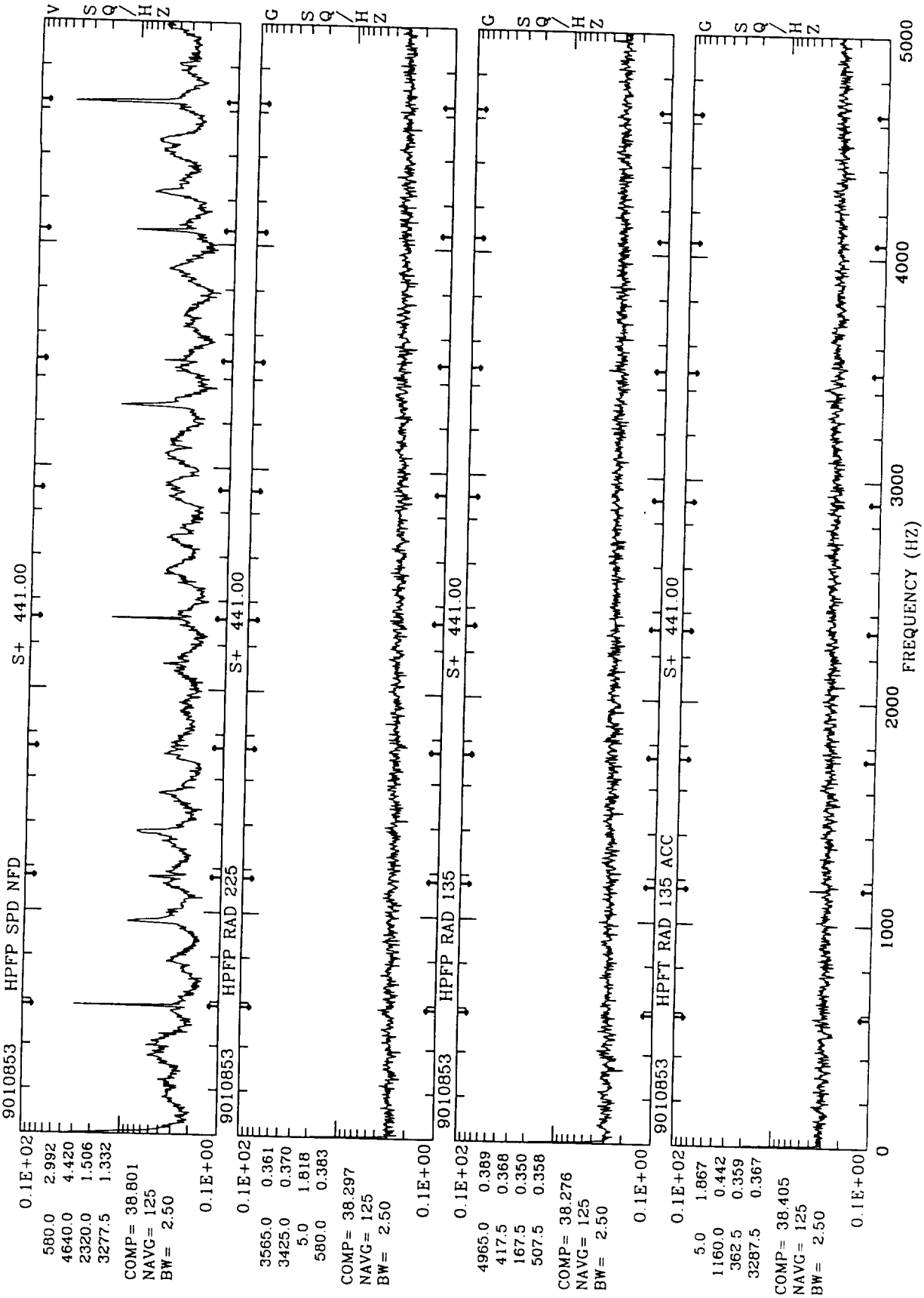
9010853 HPFP SPD NFD S+ 441.00
0.1E+02
580.0 2.992
4640.0 4.420
2320.0 1.506
3277.5 1.332
COMP= 38.801
NAVG= 125
BW= 2.50
0.1E+00
9010853 HPFP RAD 225 S+ 441.00
0.1E+02
3565.0 0.361
3425.0 0.370
5.0 1.818
580.0 0.383
COMP= 38.297
NAVG= 125
BW= 2.50
0.1E+00
9010853 HPFP RAD 135 S+ 441.00
0.1E+02
4965.0 0.389
417.5 0.368
167.5 0.350
507.5 0.358
COMP= 38.276
NAVG= 125
BW= 2.50
0.1E+00
9010853 HPFT RAD 135 ACC S+ 441.00
0.1E+02
5.0 1.867
1160.0 0.442
362.5 0.359
3287.5 0.367
COMP= 38.405
NAVG= 125
BW= 2.50
0.1E+00
0 1000 2000 3000 4000 5000
FREQUENCY (HZ)
V S Q / H Z
G S Q / H Z

CP-WBD

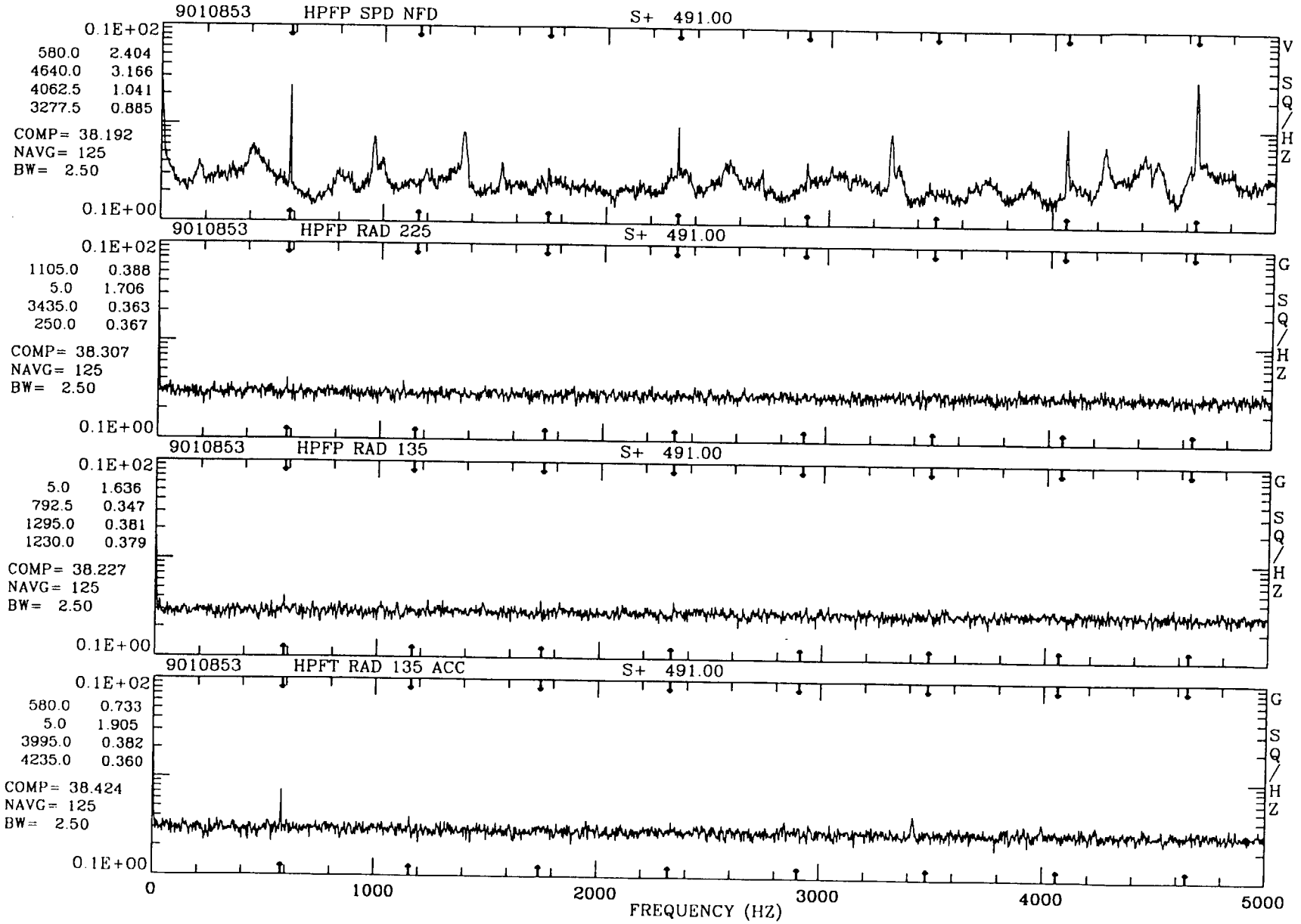
9010853 HPFP SPD NFD S+ 491.00
0.1E+02
580.0 2.404
4640.0 3.166
4062.5 1.041
3277.5 0.885
COMP= 38.192
NAVG= 125
BW= 2.50
0.1E+00
V SQ/HZ
9010853 HPFP RAD 225 S+ 491.00
0.1E+02
1105.0 0.388
5.0 1.706
3435.0 0.363
250.0 0.367
COMP= 38.307
NAVG= 125
BW= 2.50
0.1E+00
G SQ/HZ
9010853 HPFP RAD 135 S+ 491.00
0.1E+02
5.0 1.636
792.5 0.347
1295.0 0.381
1230.0 0.379
COMP= 38.227
NAVG= 125
BW= 2.50
0.1E+00
G SQ/HZ
9010853 HPFT RAD 135 ACC S+ 491.00
0.1E+02
580.0 0.733
5.0 1.905
3995.0 0.382
4235.0 0.360
COMP= 38.424
NAVG= 125
BW= 2.50
0.1E+00
G SQ/HZ
0
1000
2000
3000
4000
5000
FREQUENCY (HZ)

CP-WBD

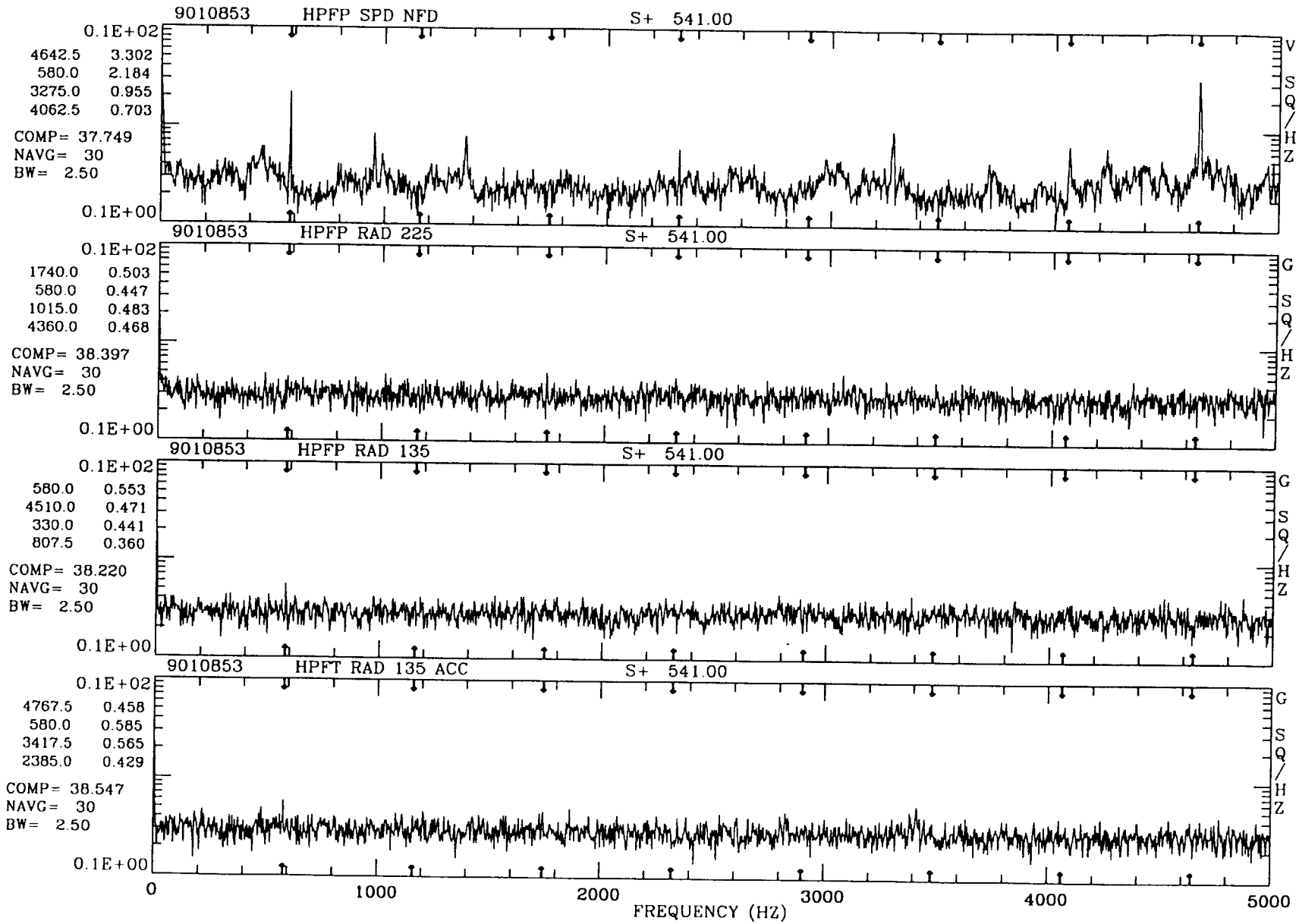
9010853 HPFP SPD NFD S+ 541.00
0.1E+02
4642.5 3.302
580.0 2.184
3275.0 0.955
4062.5 0.703
COMP= 37.749
NAVG= 30
BW= 2.50
0.1E+00
V SQ/HZ
9010853 HPFP RAD 225 S+ 541.00
0.1E+02
1740.0 0.503
580.0 0.447
1015.0 0.483
4360.0 0.468
COMP= 38.397
NAVG= 30
BW= 2.50
0.1E+00
G SQ/HZ
9010853 HPFP RAD 135 S+ 541.00
0.1E+02
580.0 0.553
4510.0 0.471
330.0 0.441
807.5 0.360
COMP= 38.220
NAVG= 30
BW= 2.50
0.1E+00
G SQ/HZ
9010853 HPFT RAD 135 ACC S+ 541.00
0.1E+02
4767.5 0.458
580.0 0.585
3417.5 0.565
2385.0 0.429
COMP= 38.547
NAVG= 30
BW= 2.50
0.1E+00
G SQ/HZ
0
1000
2000
3000
4000
5000
FREQUENCY (HZ)

CP-WBD

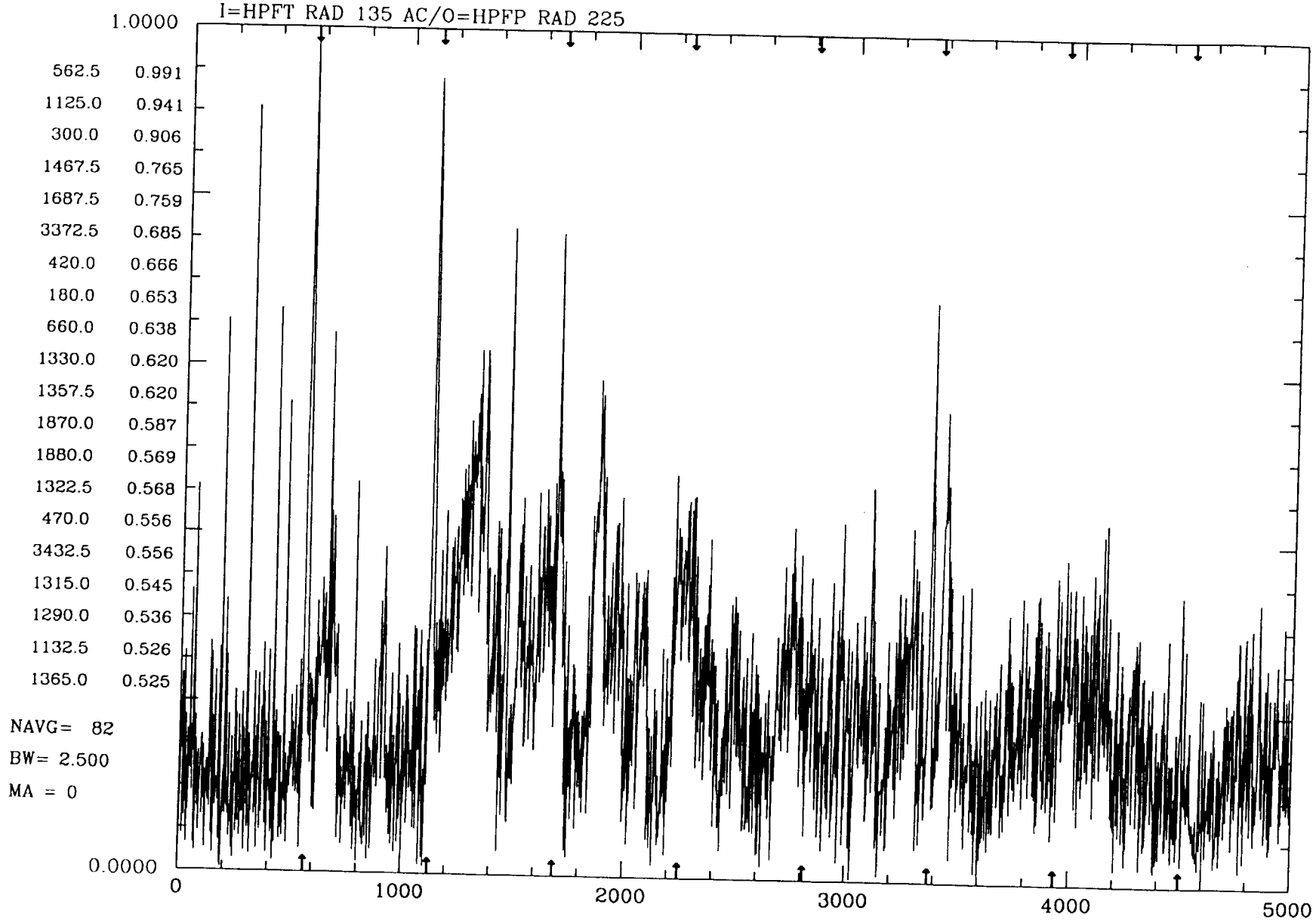
I=HPFT RAD 135 AC/O=HPFP RAD 225
1.0000
562.5 0.991
1125.0 0.941
300.0 0.906
1467.5 0.765
1687.5 0.759
3372.5 0.685
420.0 0.666
180.0 0.653
660.0 0.638
1330.0 0.620
1357.5 0.620
1870.0 0.587
1880.0 0.569
1322.5 0.568
470.0 0.556
3432.5 0.556
1315.0 0.545
1290.0 0.536
1132.5 0.526
1365.0 0.525
NAVG= 82
BW= 2.500
MA = 0
0.0000
0
1000
2000
3000
4000
5000
9010853 LINEAR-COH: NFFT= 4096 TIME = 6.0 - 38

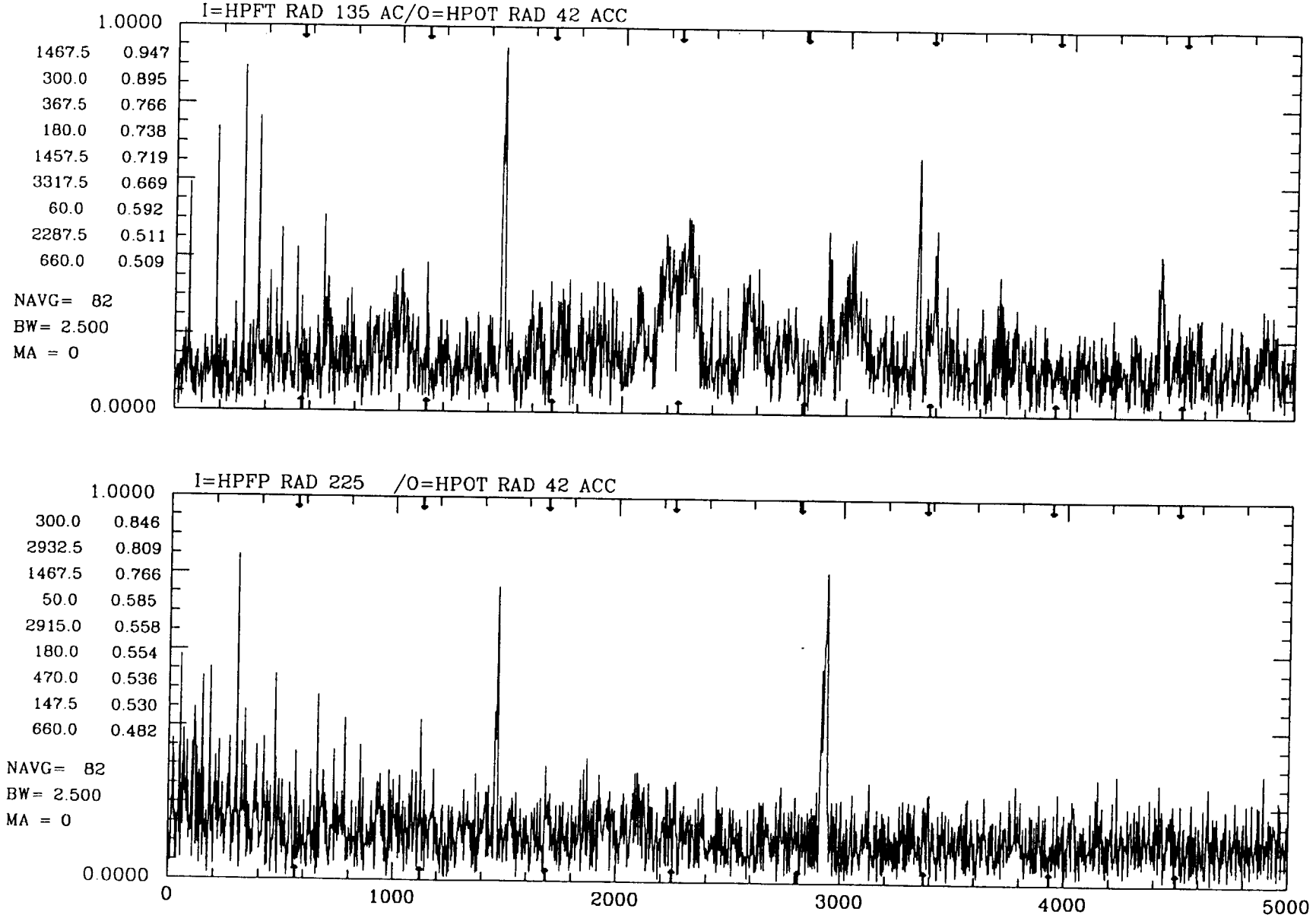

9010853 LINEAR-COH: NFFT= 4096 TIME = 6.0 - 38

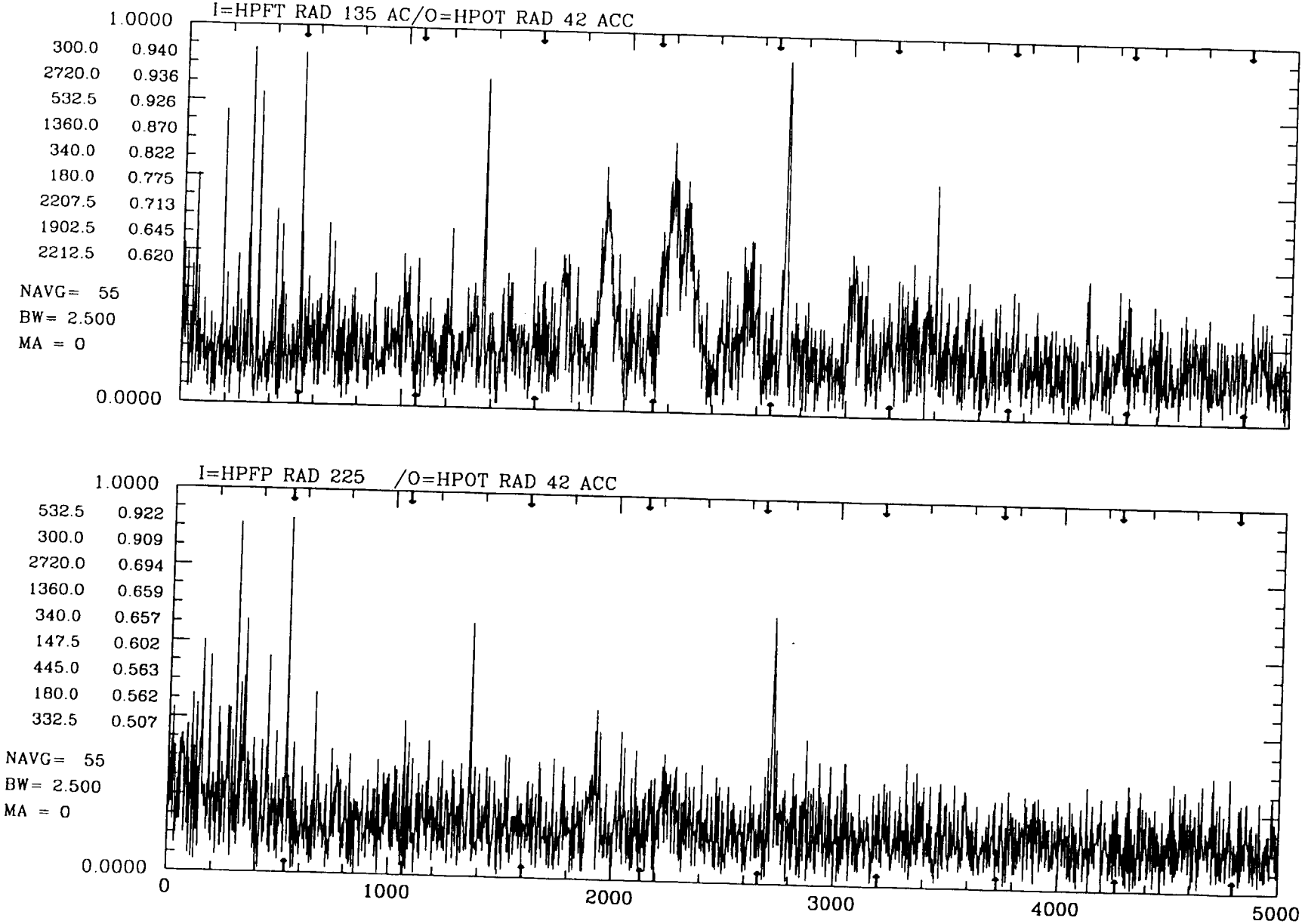

9010853 LINEAR-COH: NFFT= 4096 TIME = 42.0 - 64

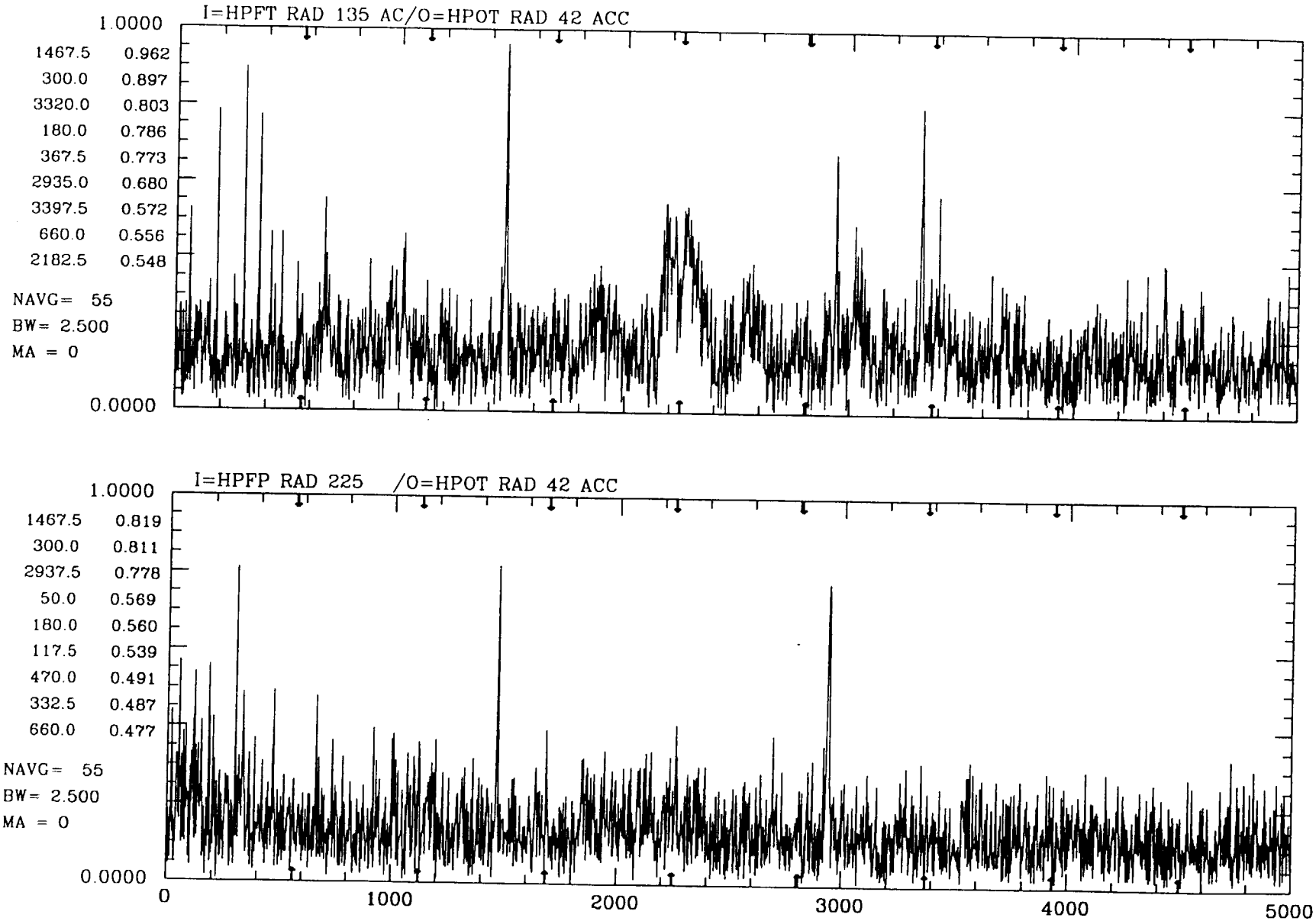

9010853 LINEAR-COH: NFFT= 4096 TIME = 67.0 - 89

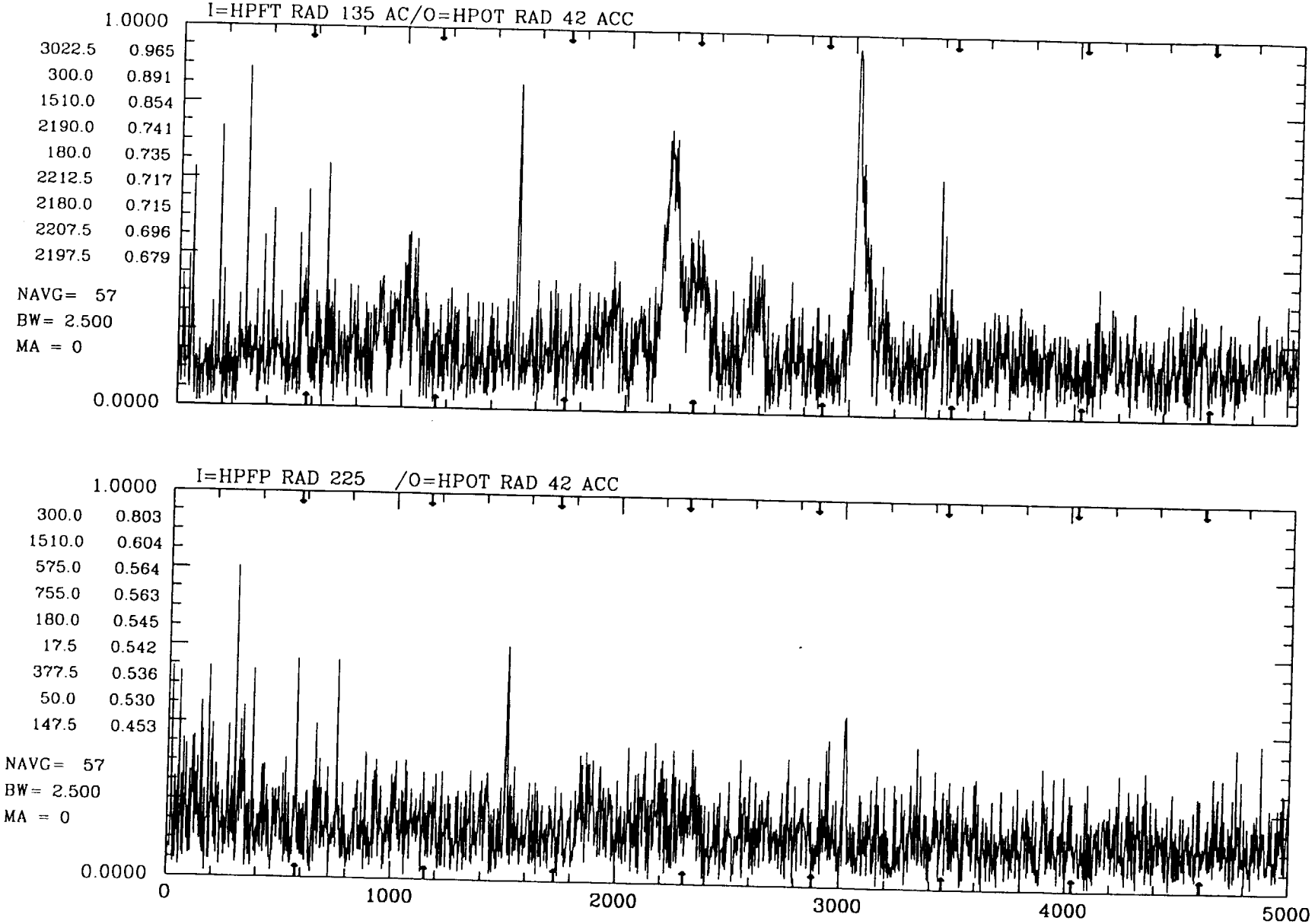

9010853 LINEAR-COH: NFFT= 4096 TIME = 91.0 - 113

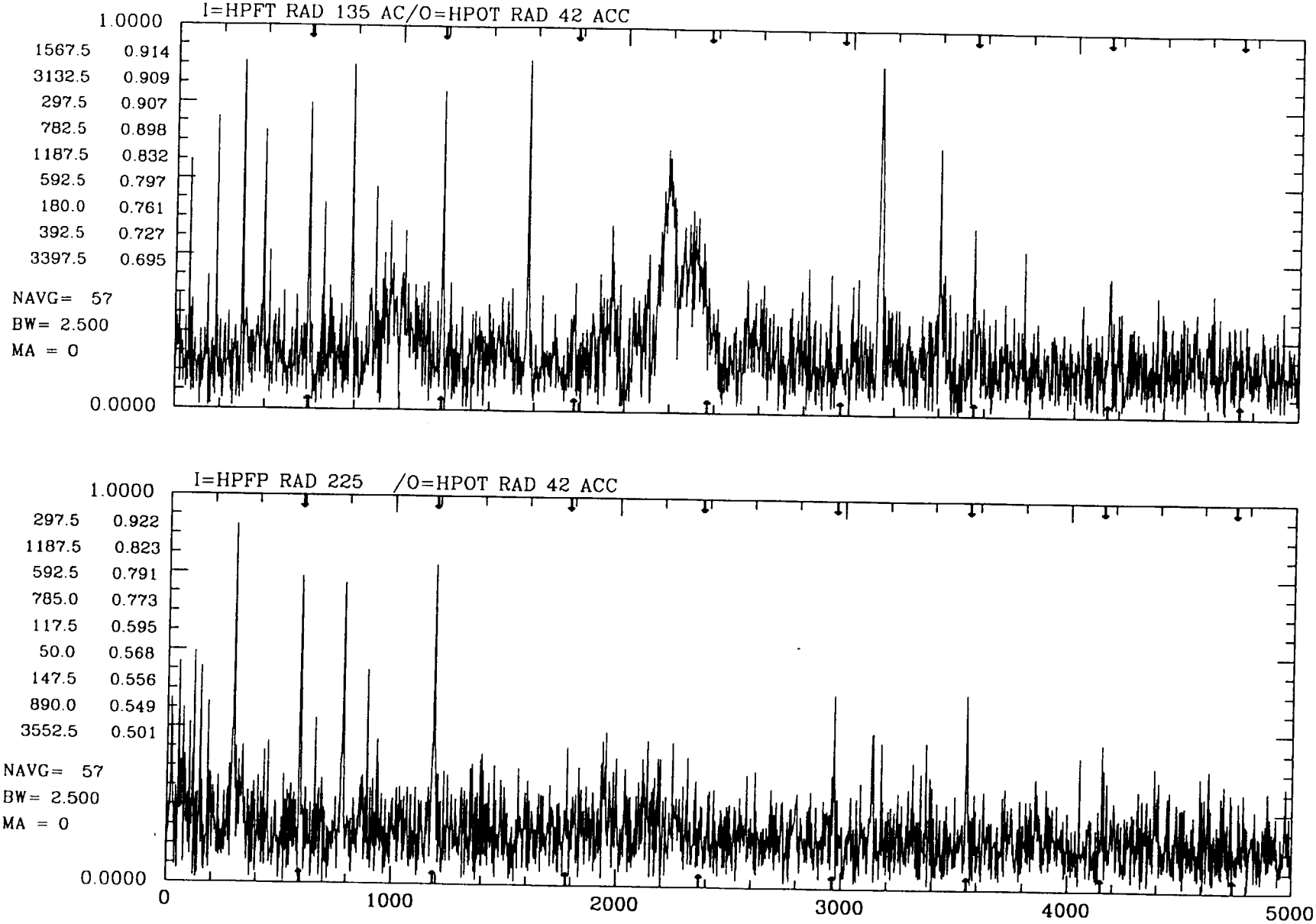

9010853 LINEAR-COH: NFFT= 4096 TIME = 116.0 - 138

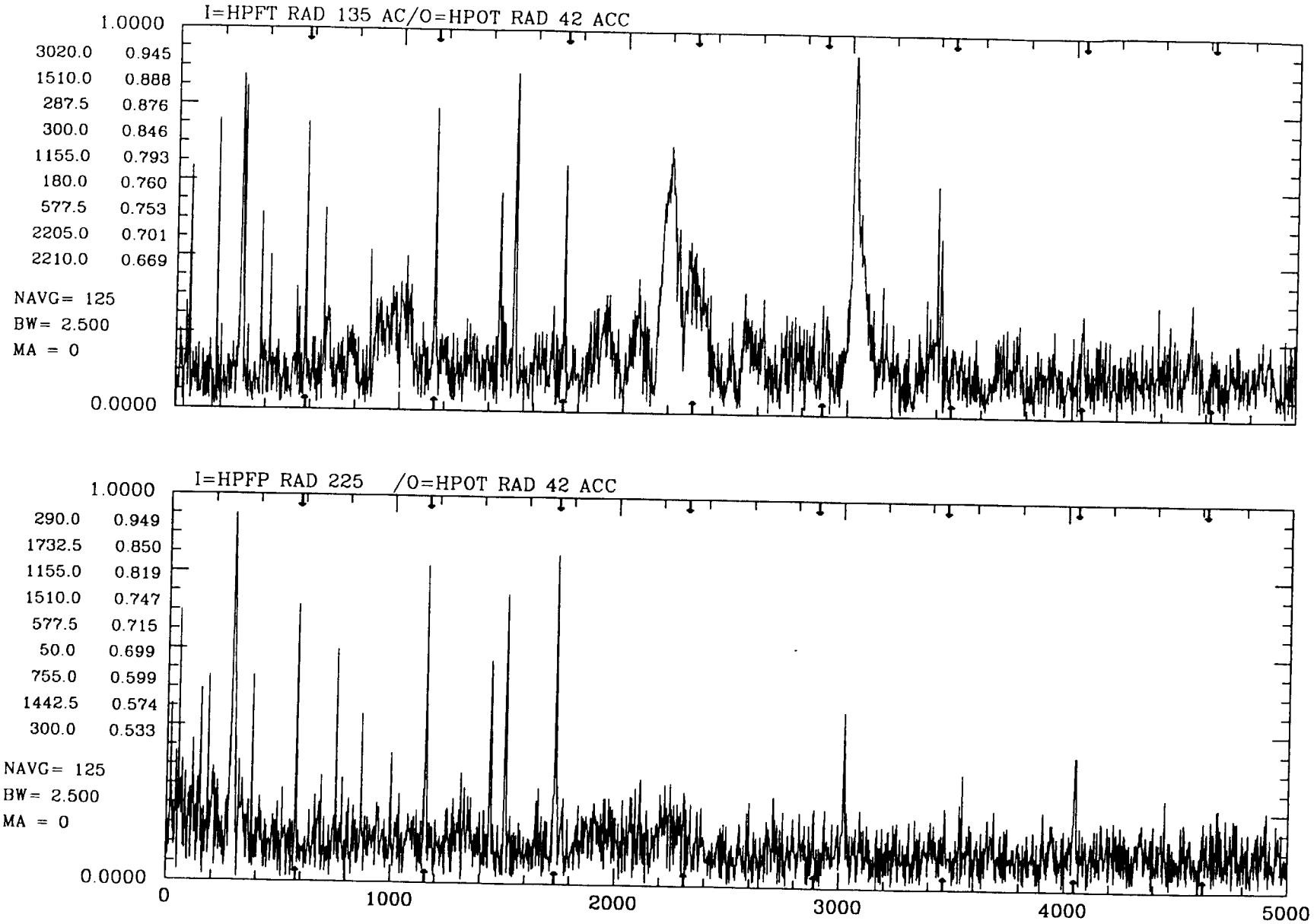

9010853 LINEAR-COH: NFFT= 4096 TIME = 141.0 - 191

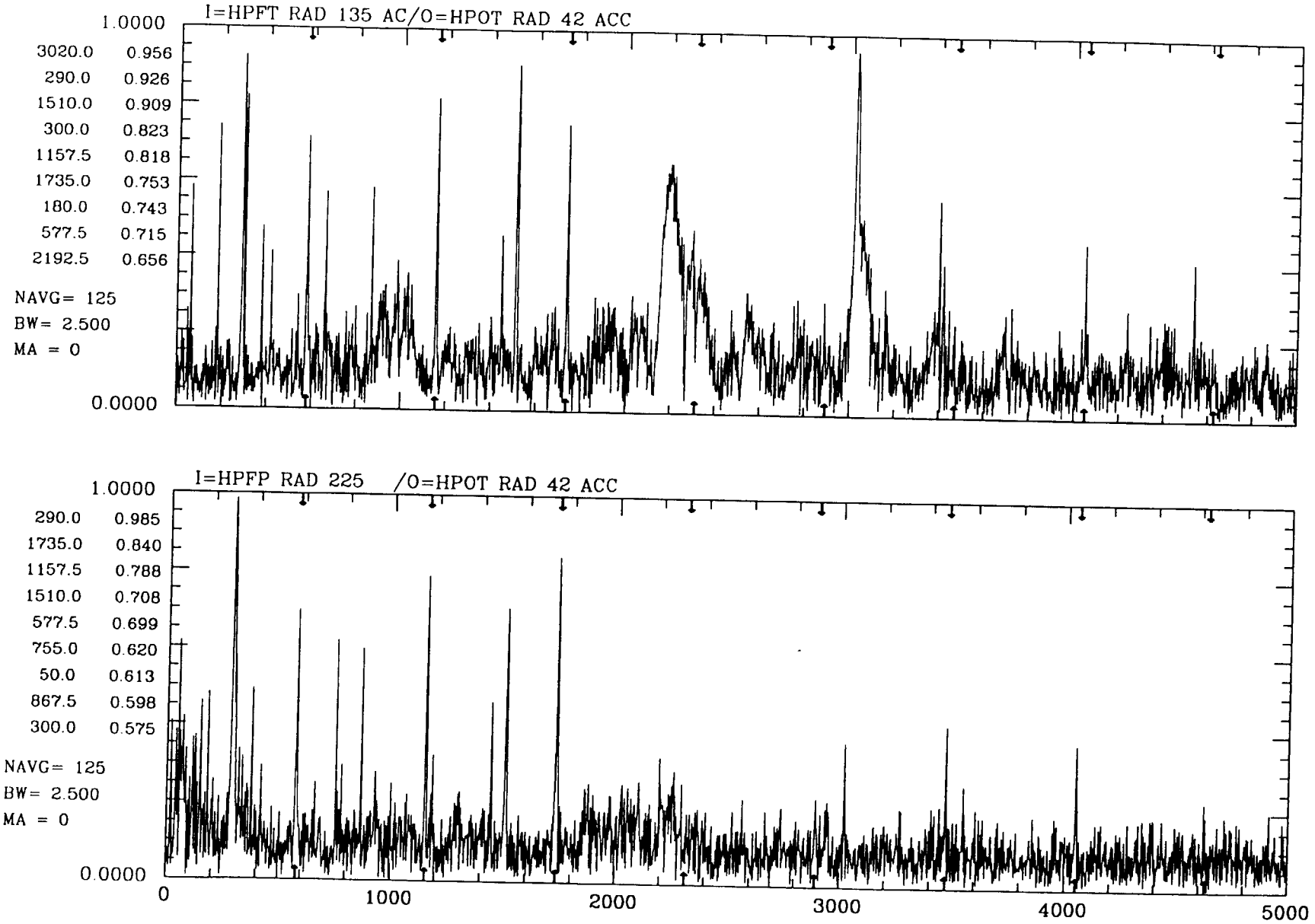

9010853 LINEAR-COH: NFFT= 4096 TIME = 191.0 - 241

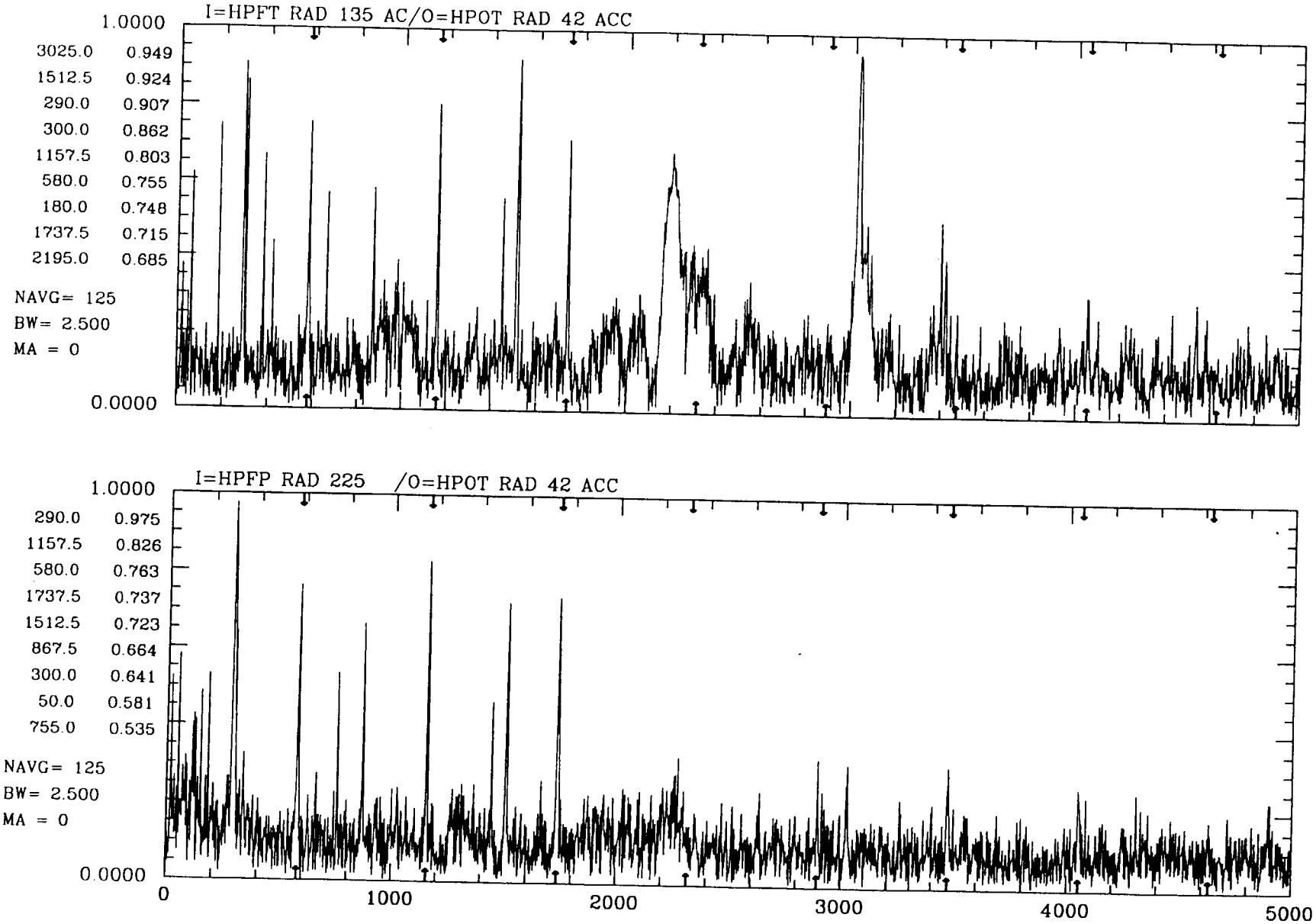

9010853 LINEAR-COH: NFFT= 4096 TIME = 241.0 - 291

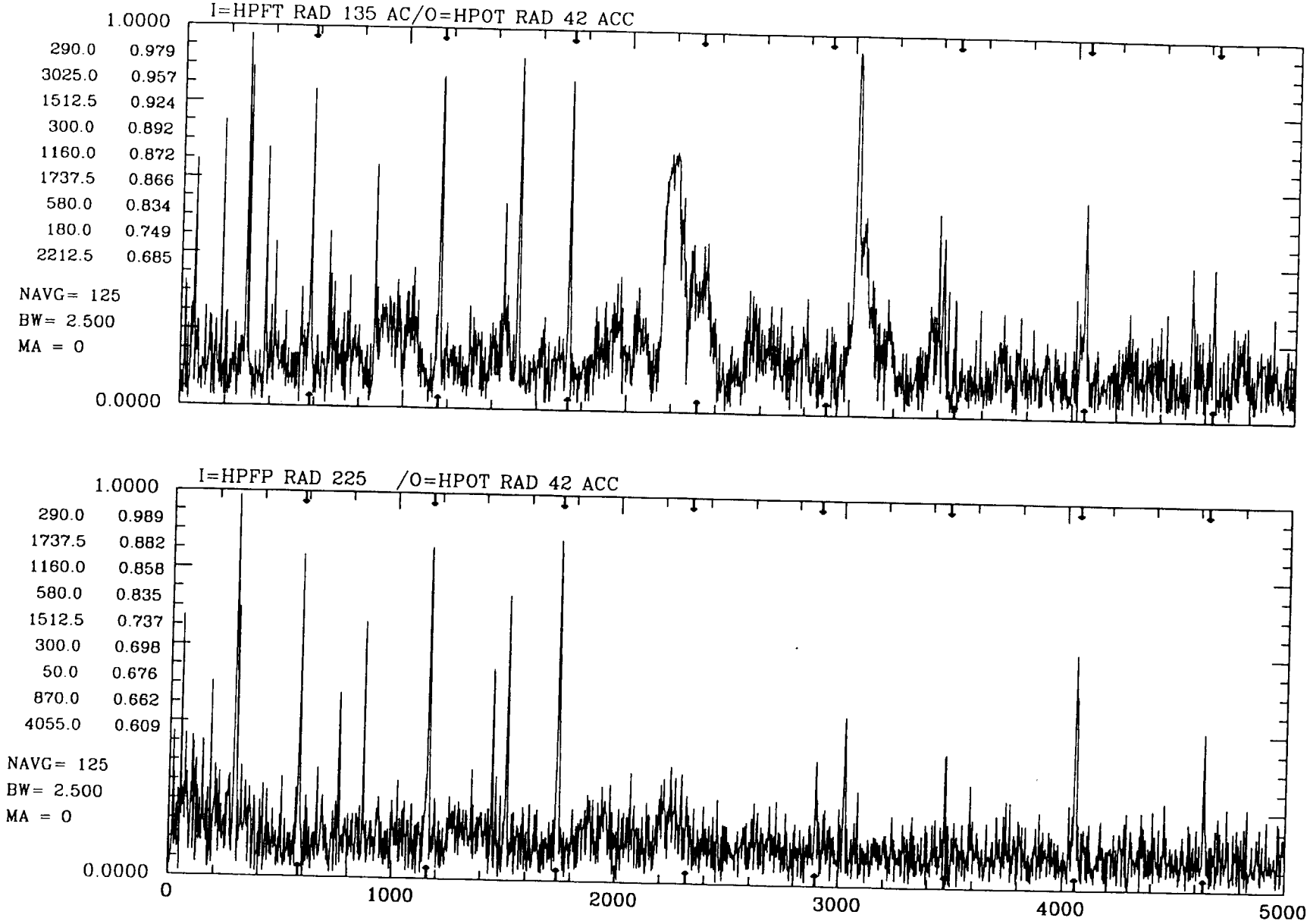

9010853 LINEAR-COH: NFFT= 4096 TIME = 291.0 - 341

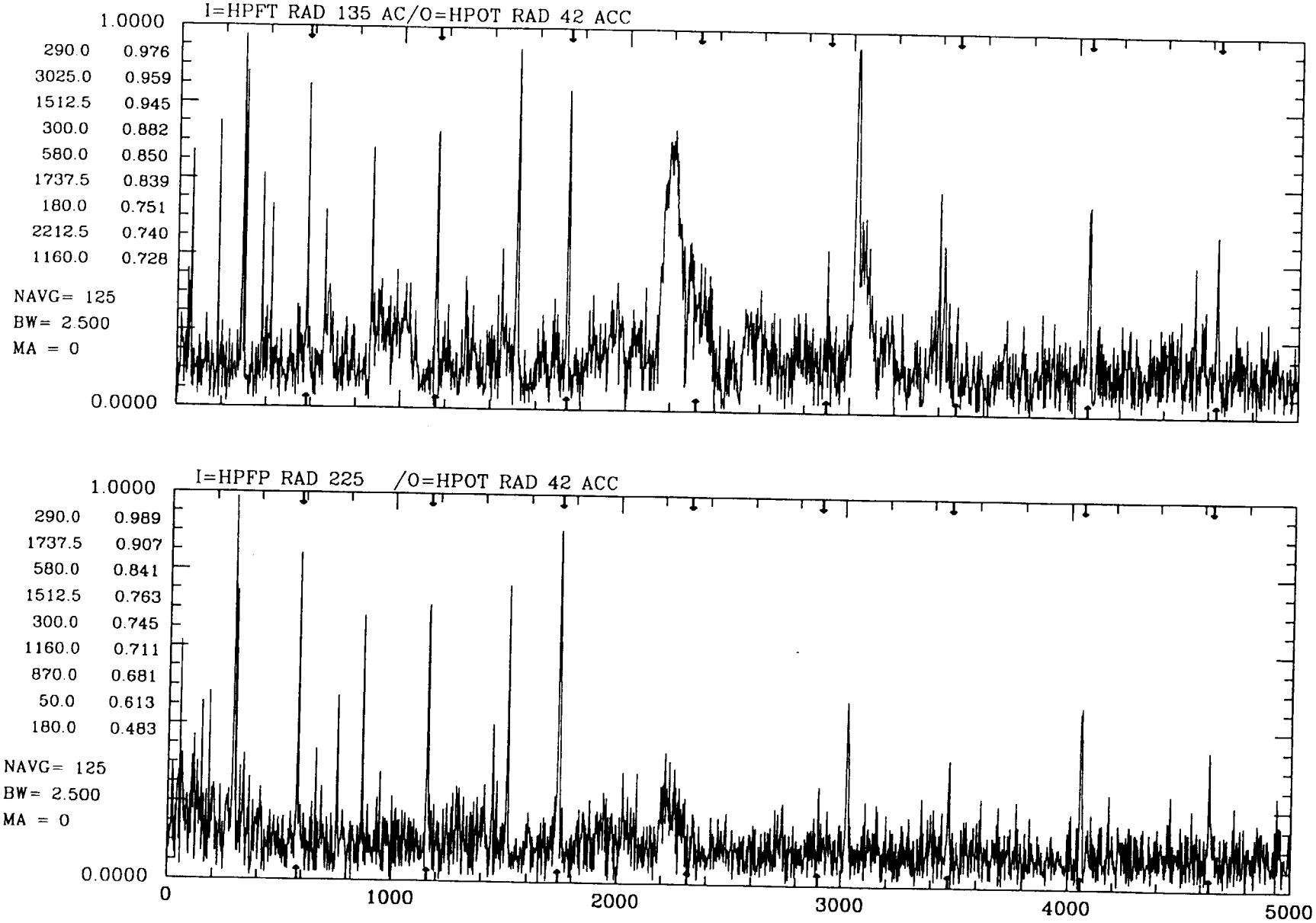

9010853 LINEAR-COH: NFFT= 4096 TIME = 341.0 - 391

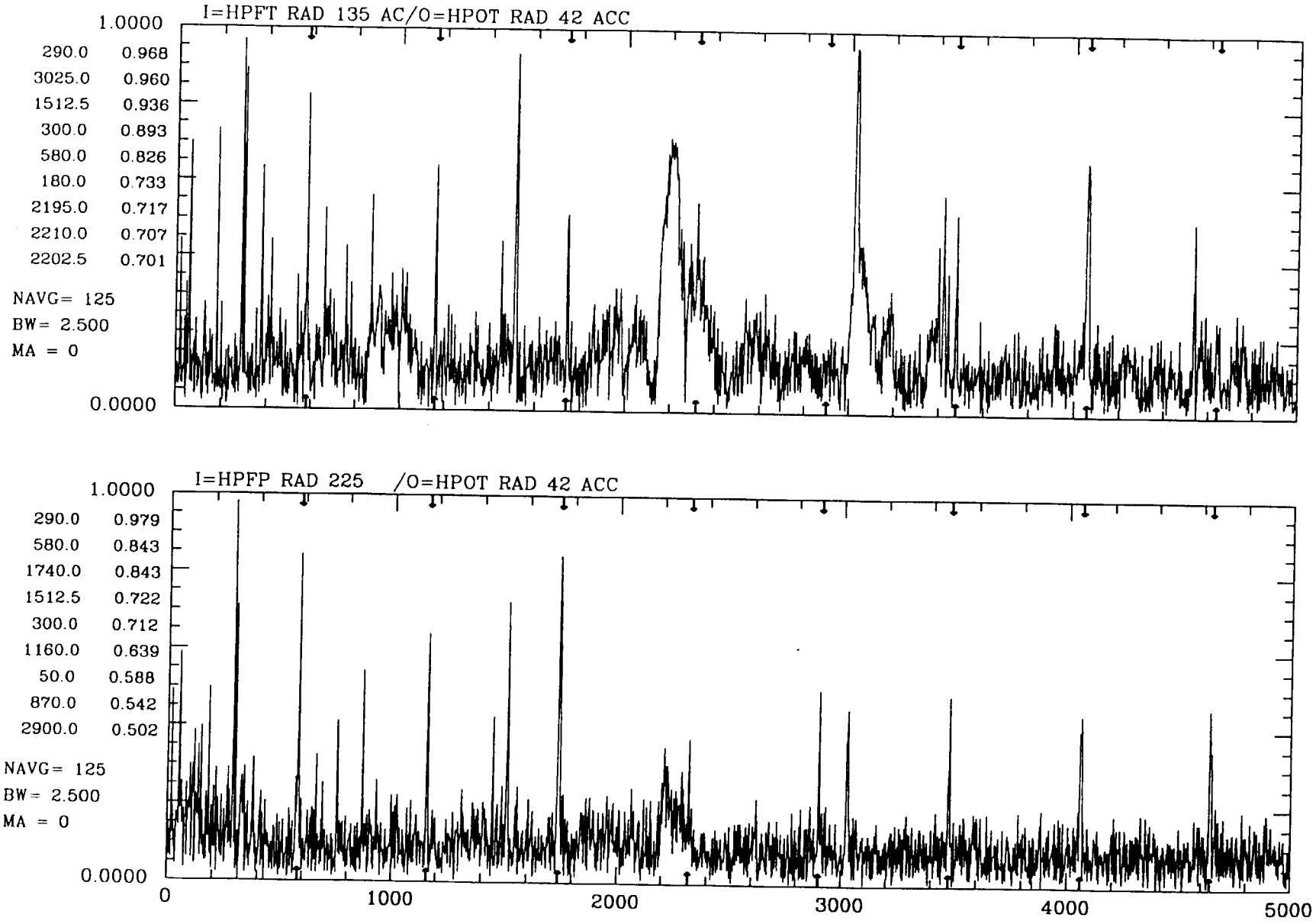

9010853 LINEAR-COH: NFFT= 4096 TIME = 391.0 - 441

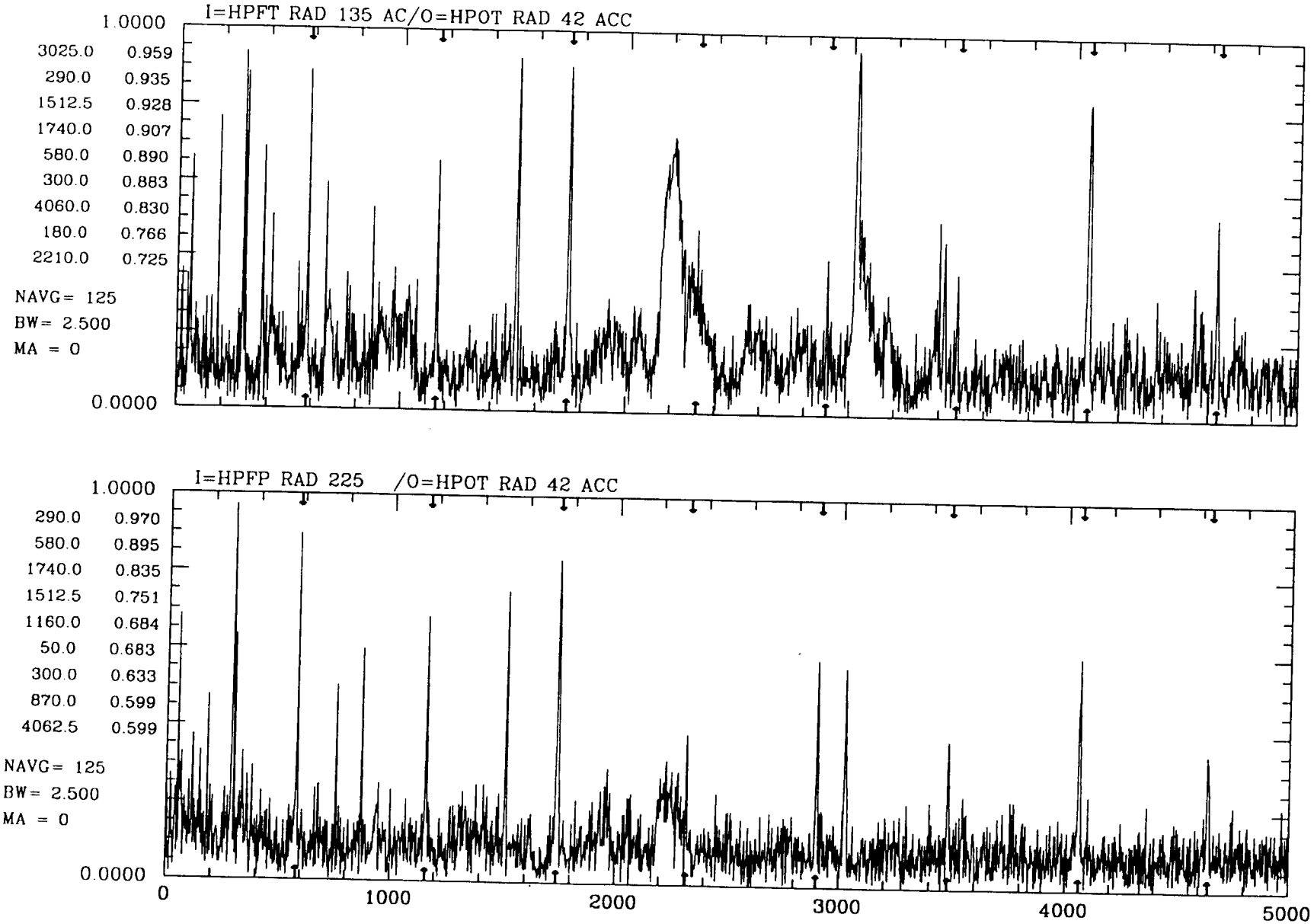

9010853 LINEAR-COH: NFFT= 4096 TIME = 441.0 - 491

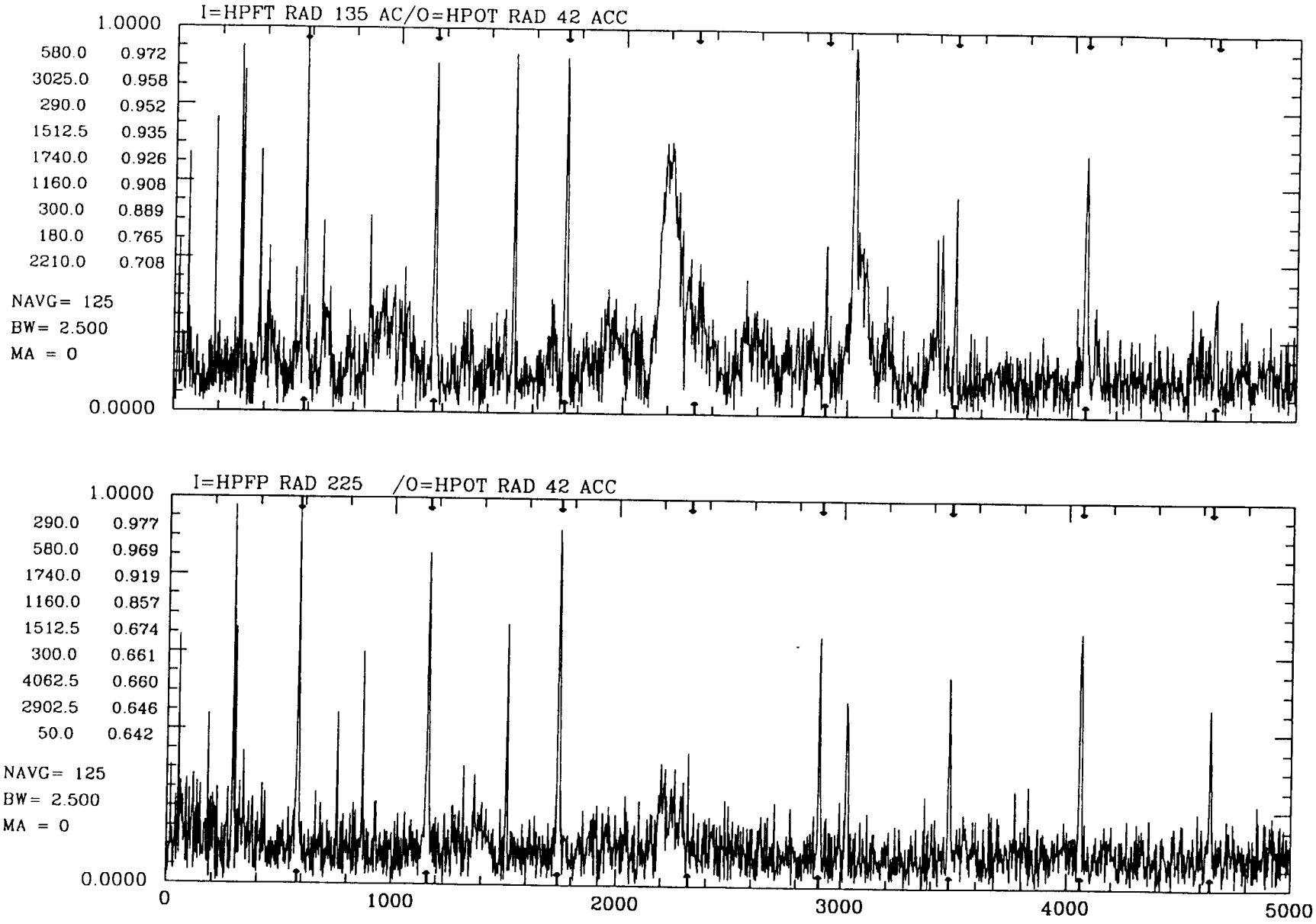

9010853 LINEAR-COH: NFFT= 4096 TIME = 491.0 - 541

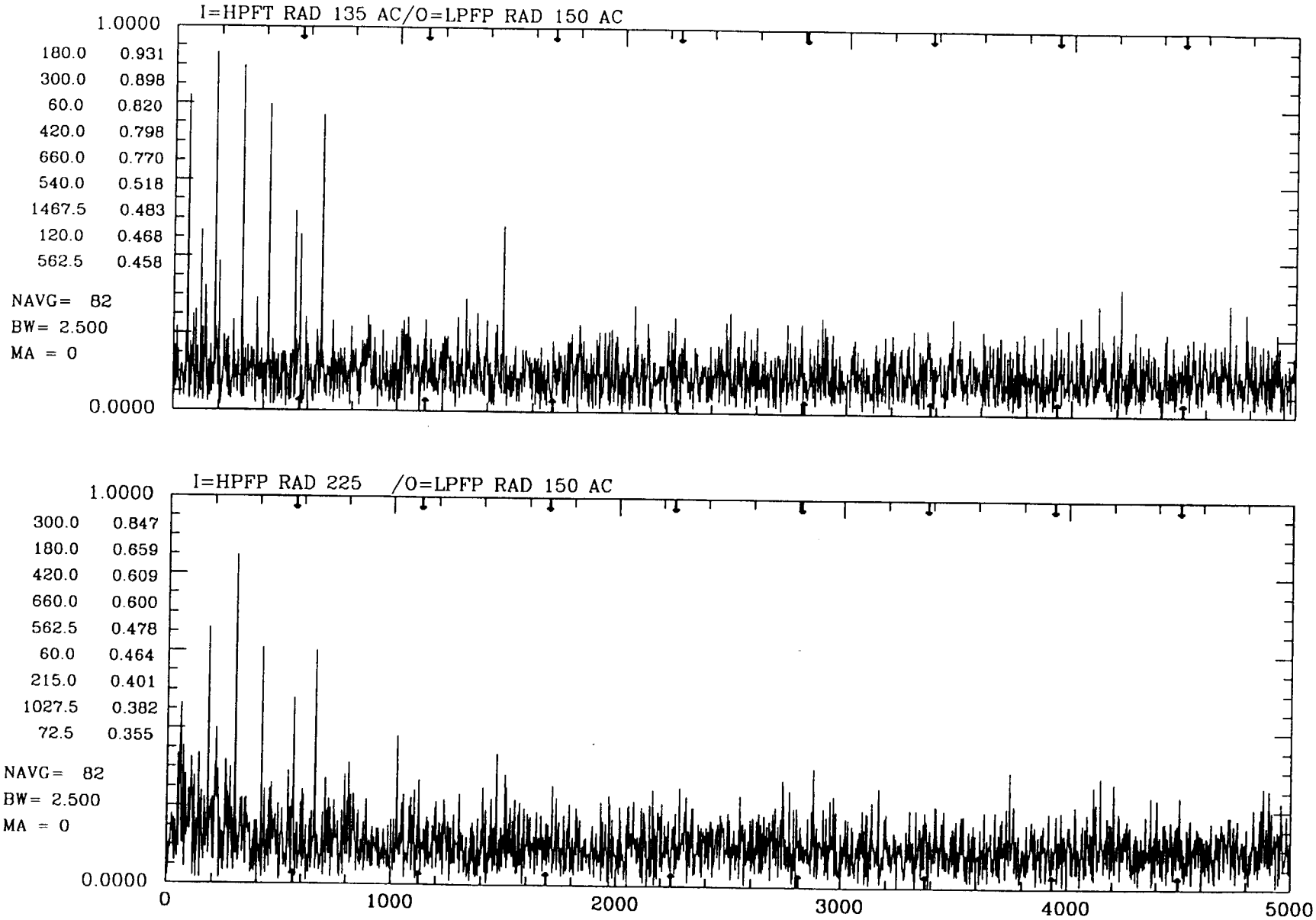

9010853 LINEAR-COH: NFFT= 4096 TIME = 6.0 - 38

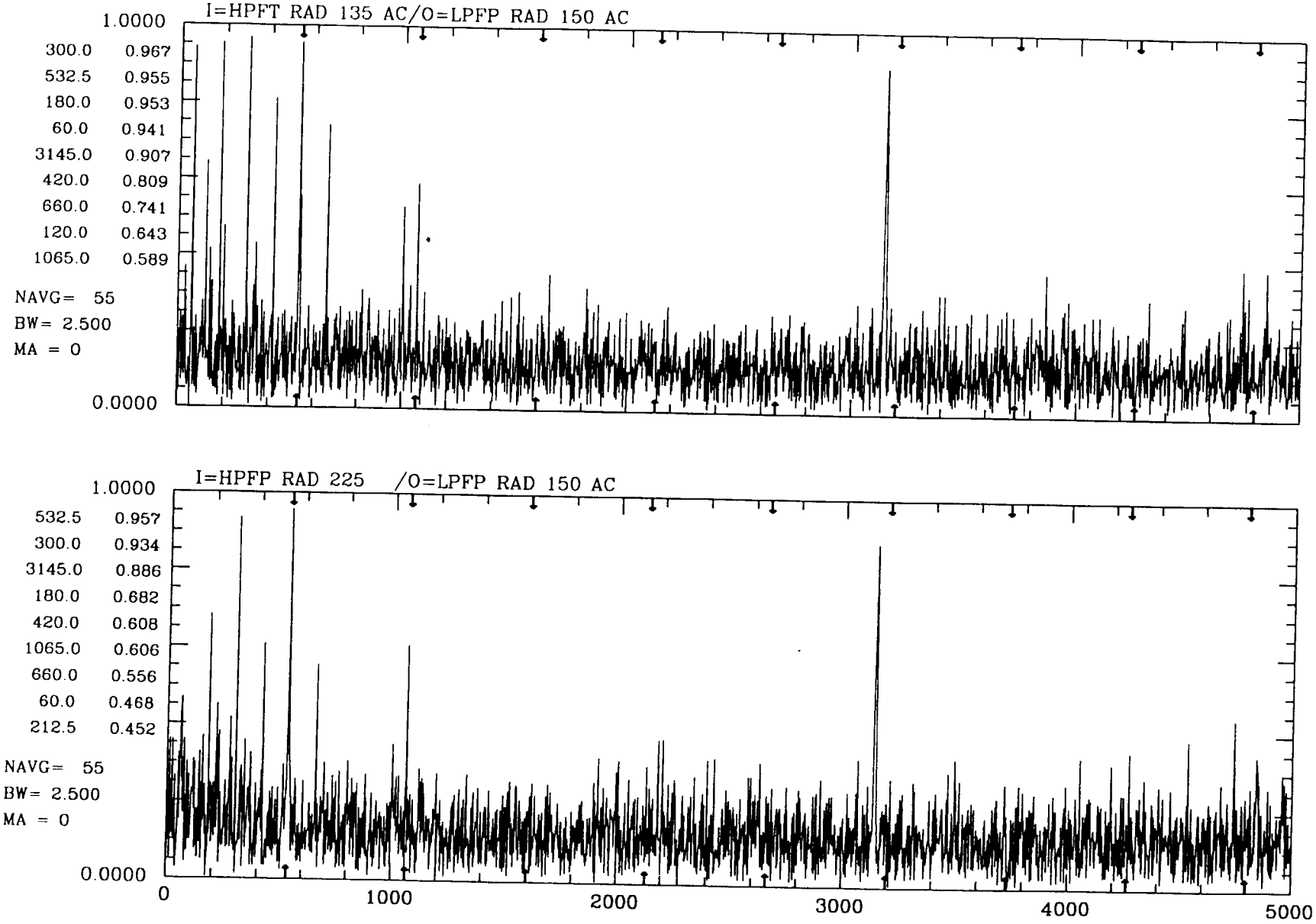

9010853 LINEAR-COH: NFFT= 4096 TIME = 42.0 - 64

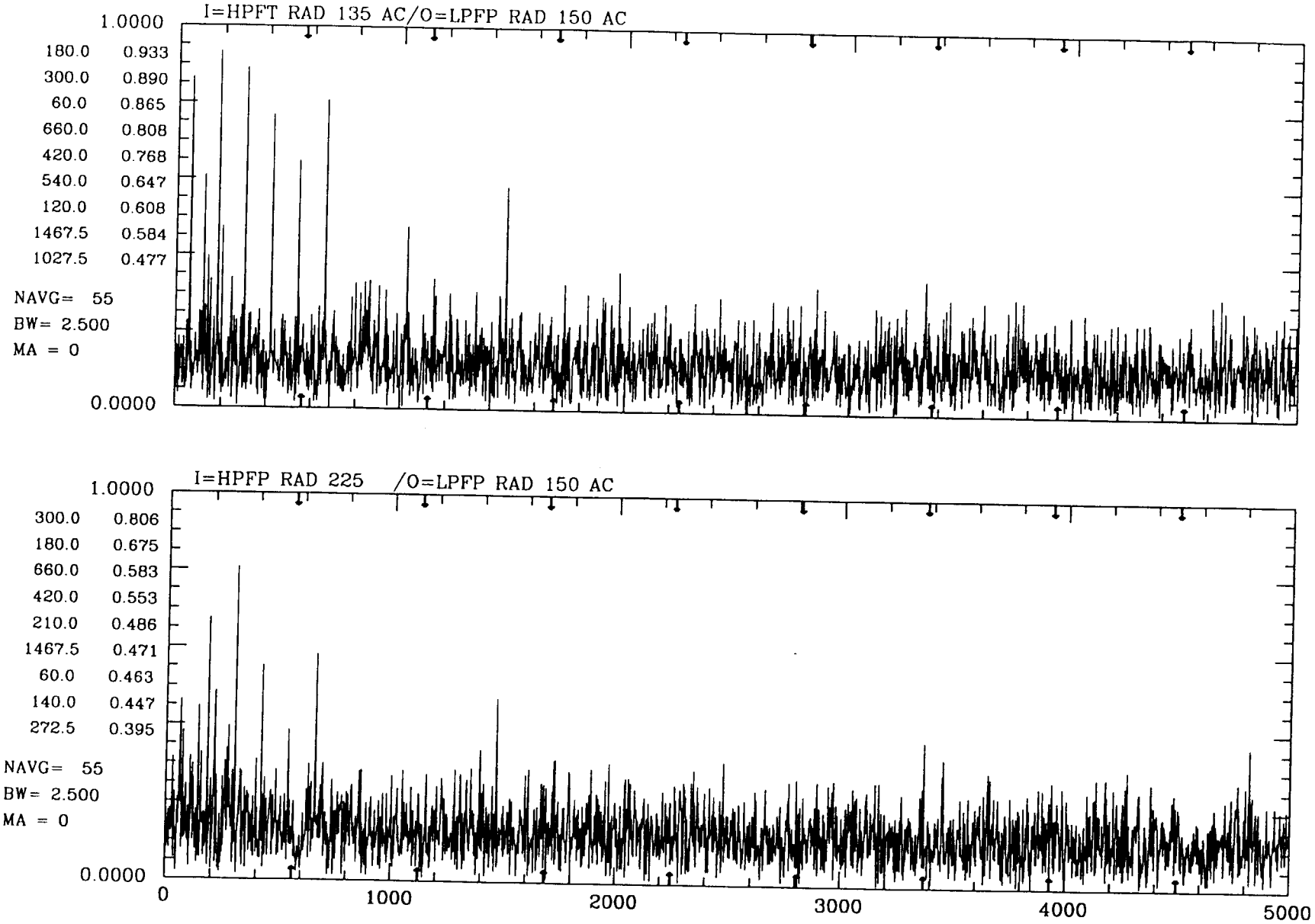

9010853 LINEAR-COH: NFFT= 4096 TIME = 67.0 - 89

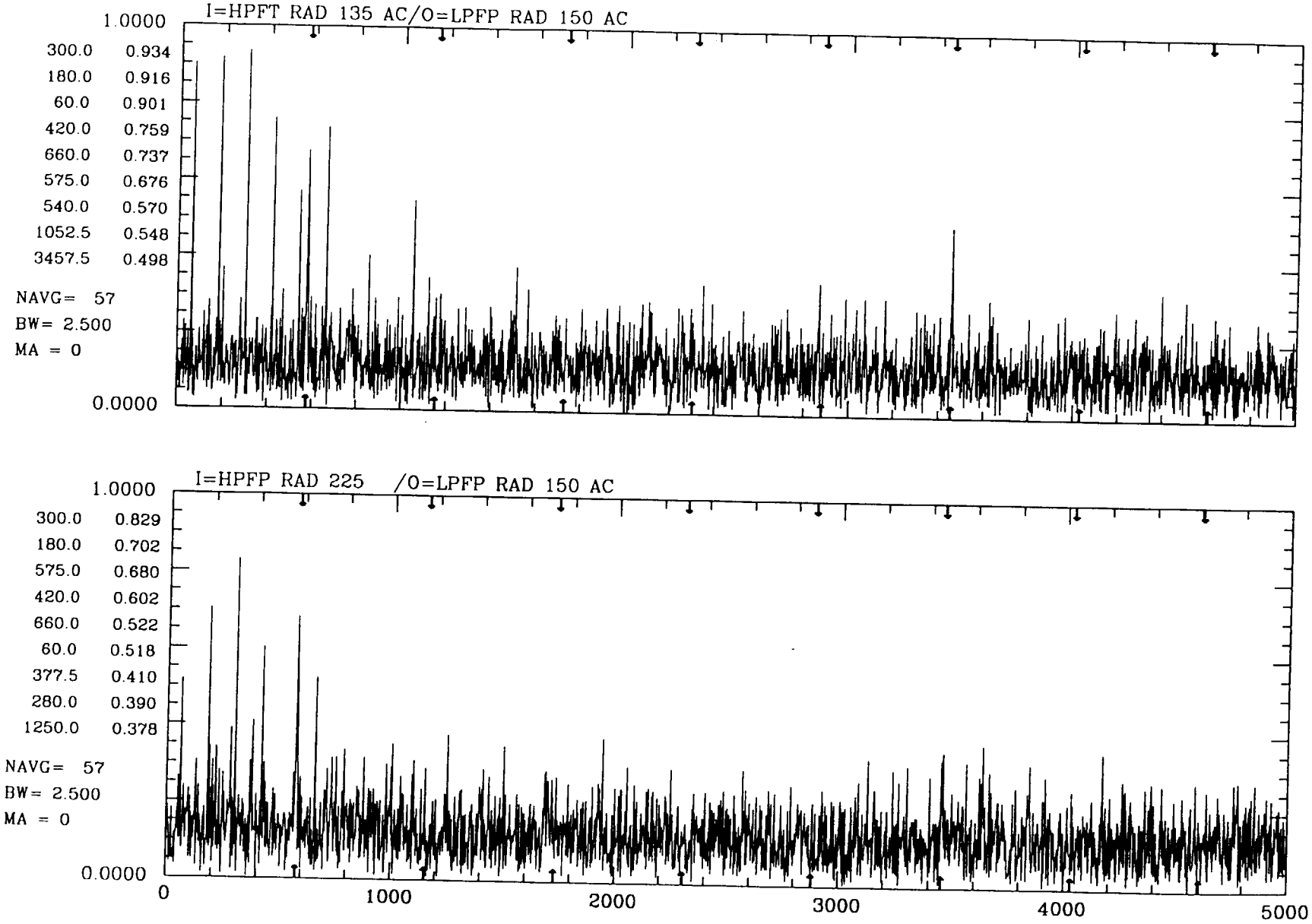

9010853 LINEAR-COH: NFFT= 4096 TIME = 91.0 - 113

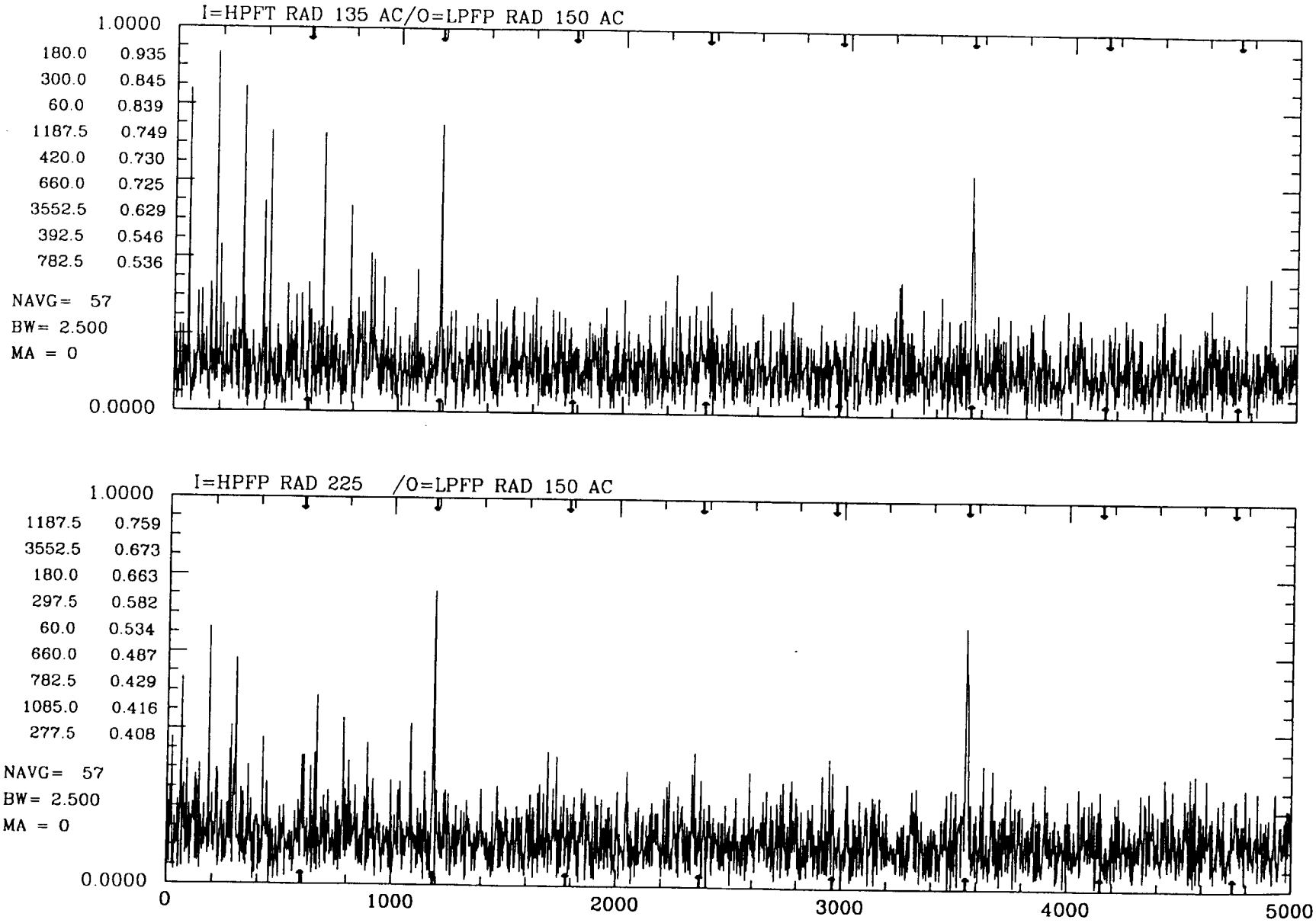

9010853 LINEAR-COH: NFFT= 4096 TIME = 116.0 - 138

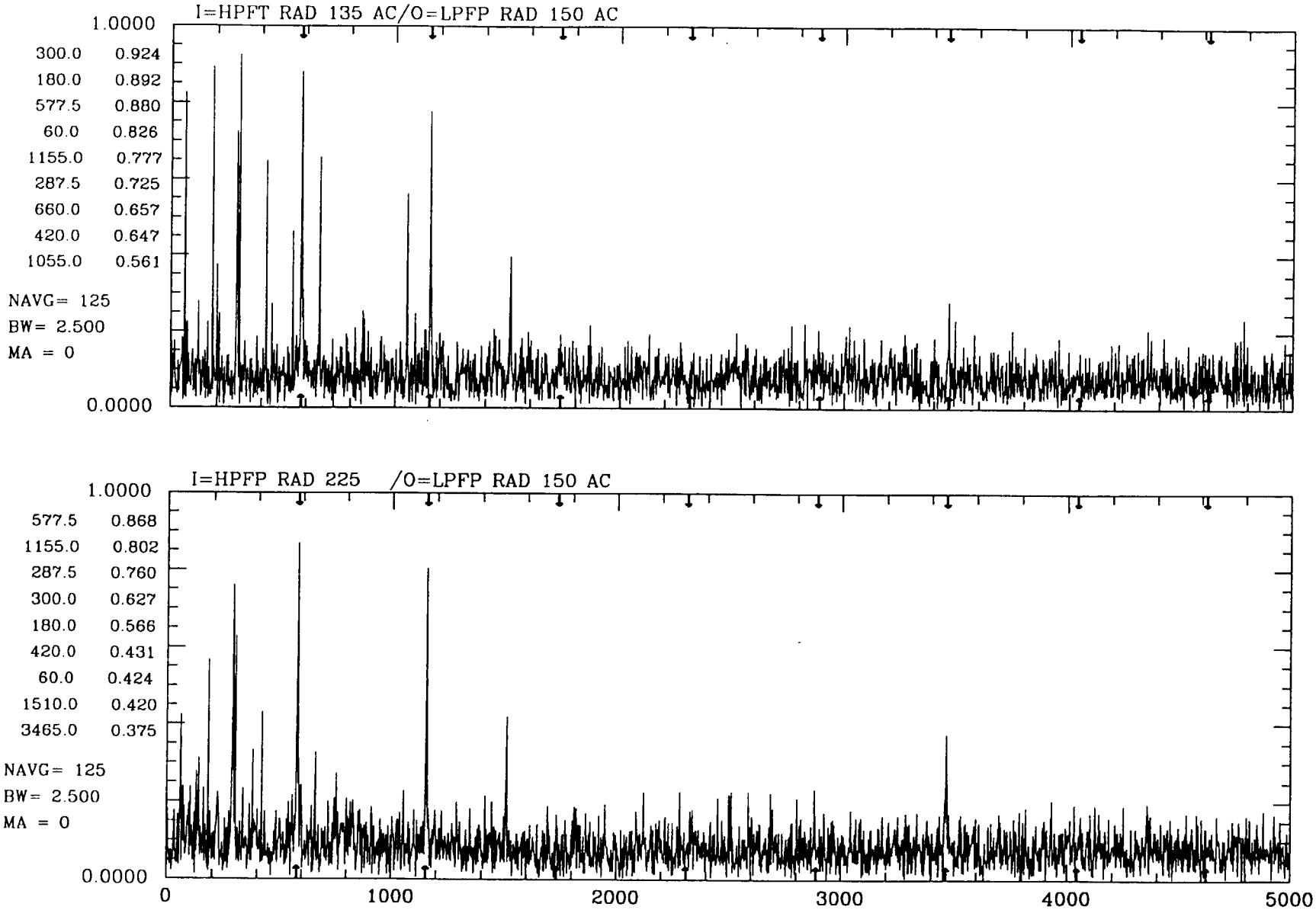

9010853 LINEAR-COH: NFFT= 4096 TIME = 141.0 - 191

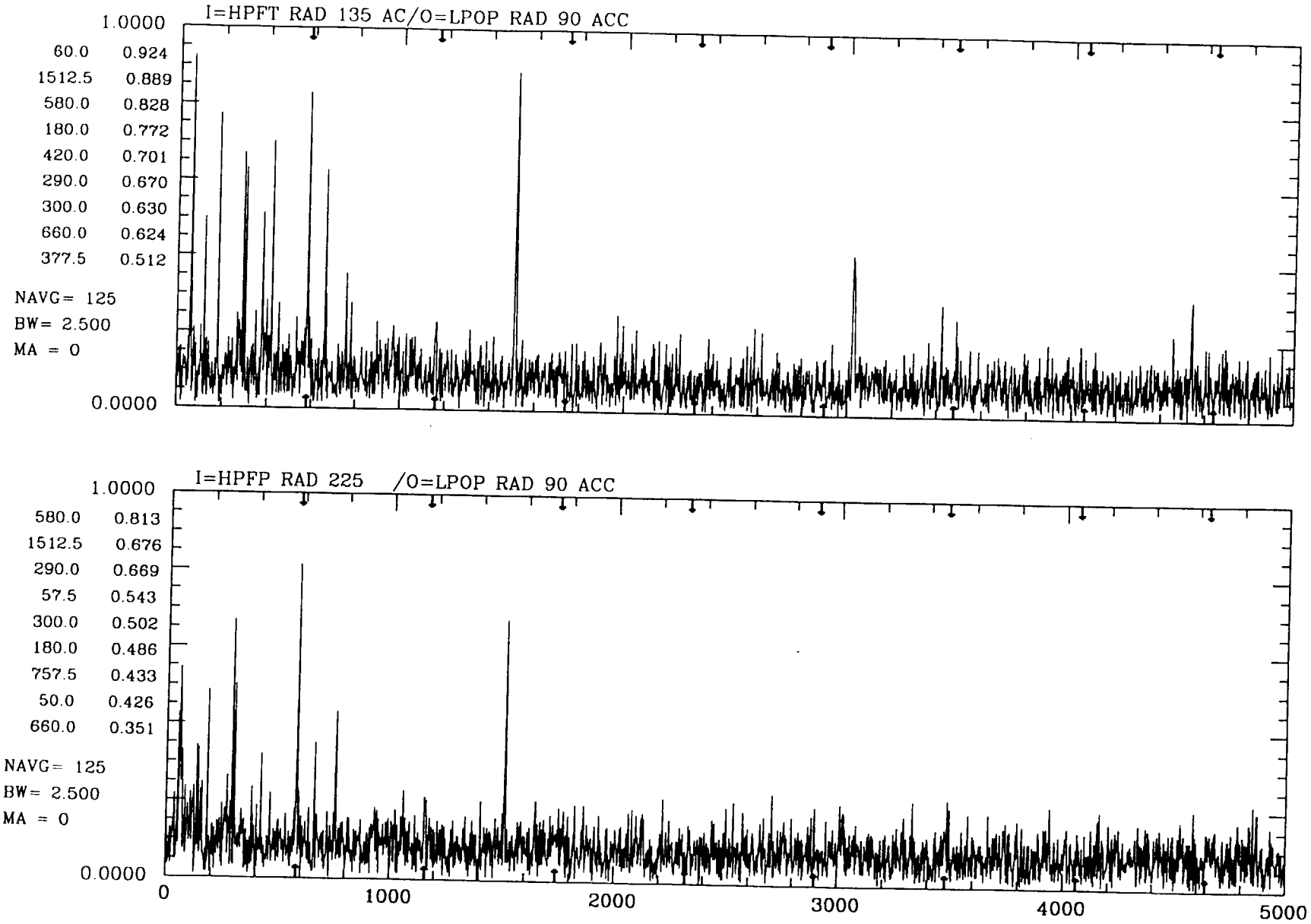

9010853 LINEAR-COH: NFFT= 4096 TIME = 391.0 - 441

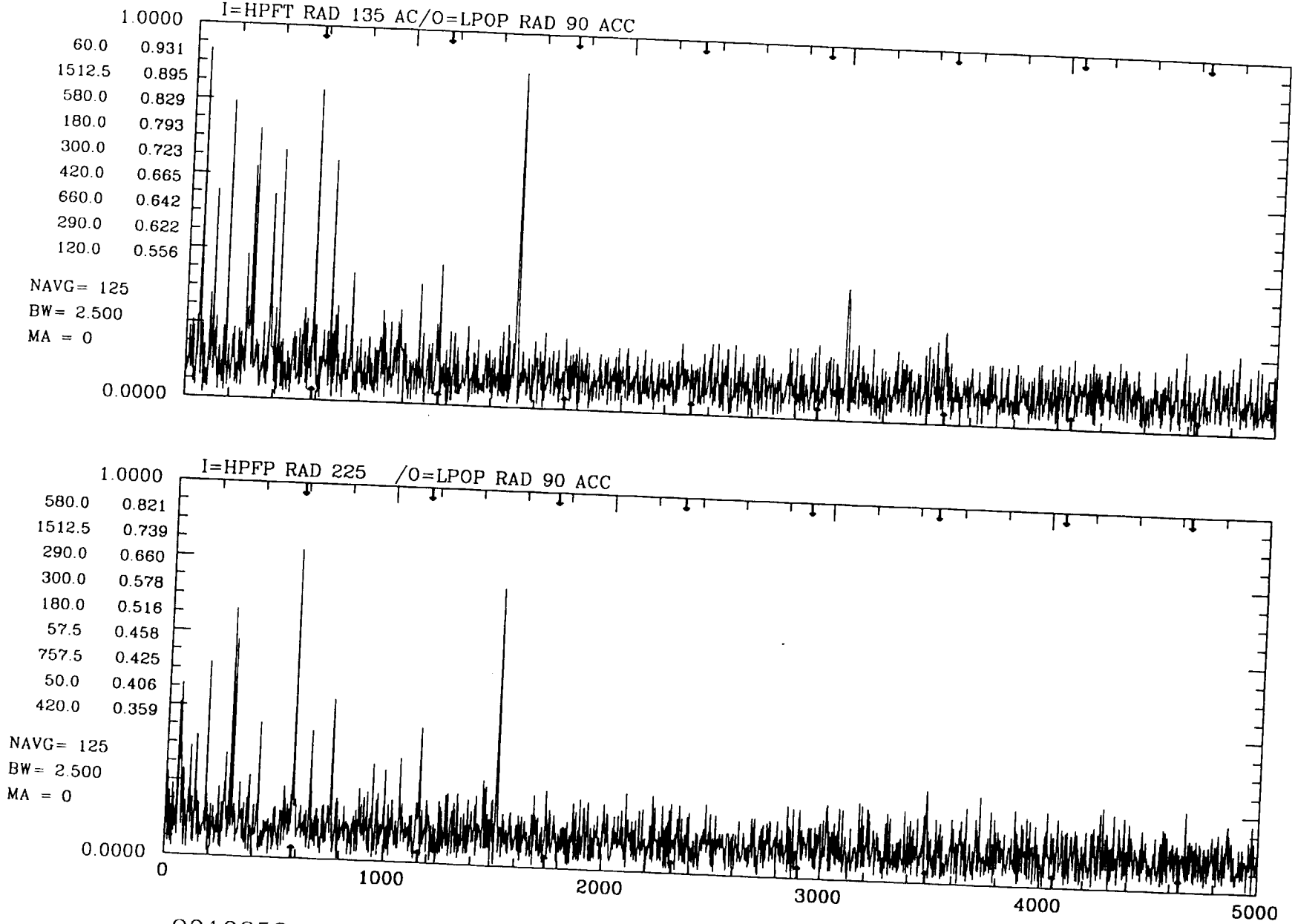

9010853 LINEAR-COH: NFFT= 4096 TIME = 441.0 - 491

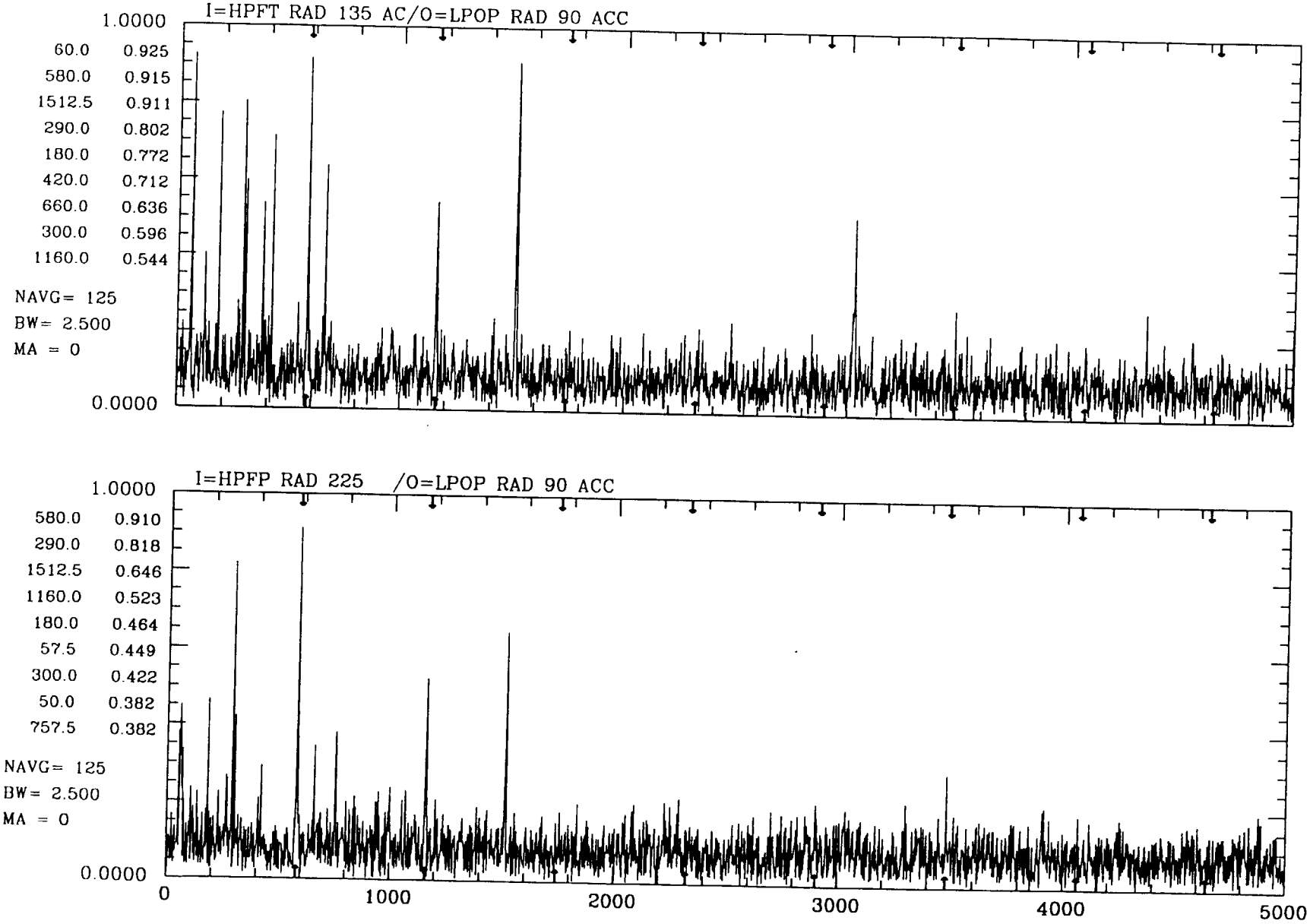

9010853 LINEAR-COH: NFFT= 4096 TIME = 491.0 - 541

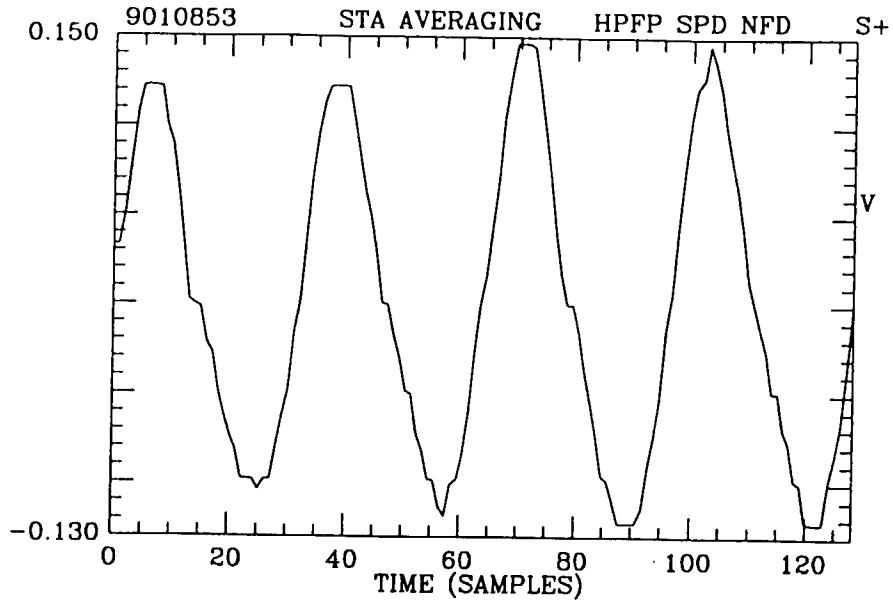

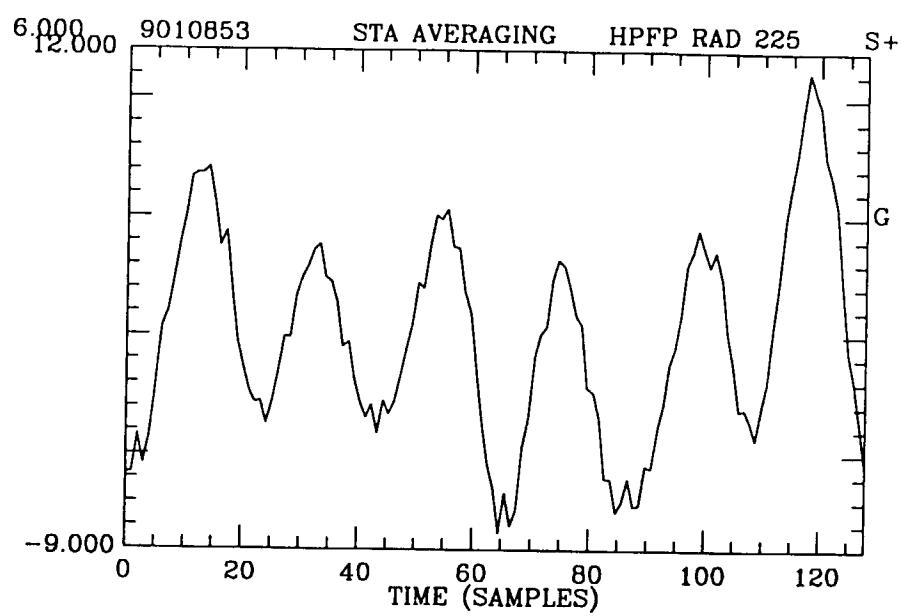

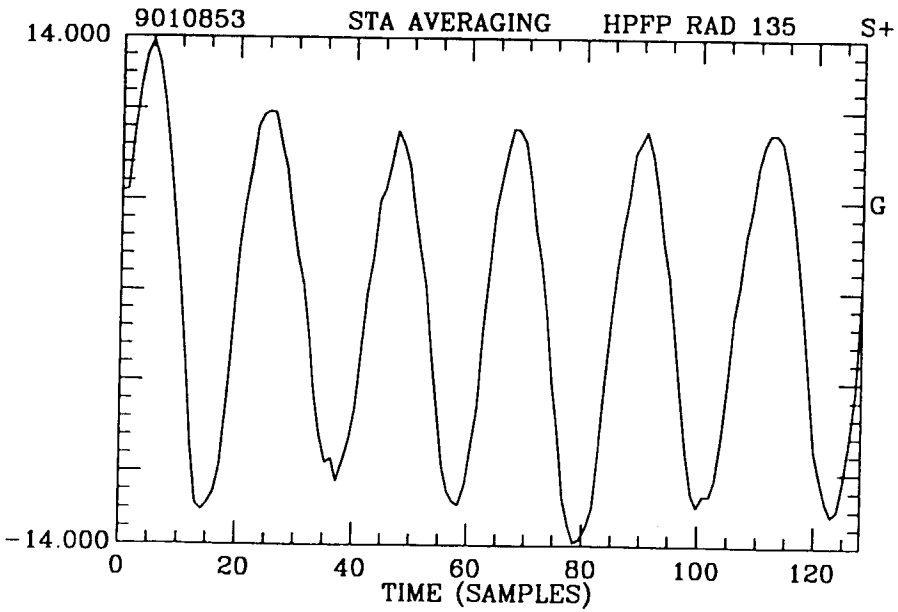

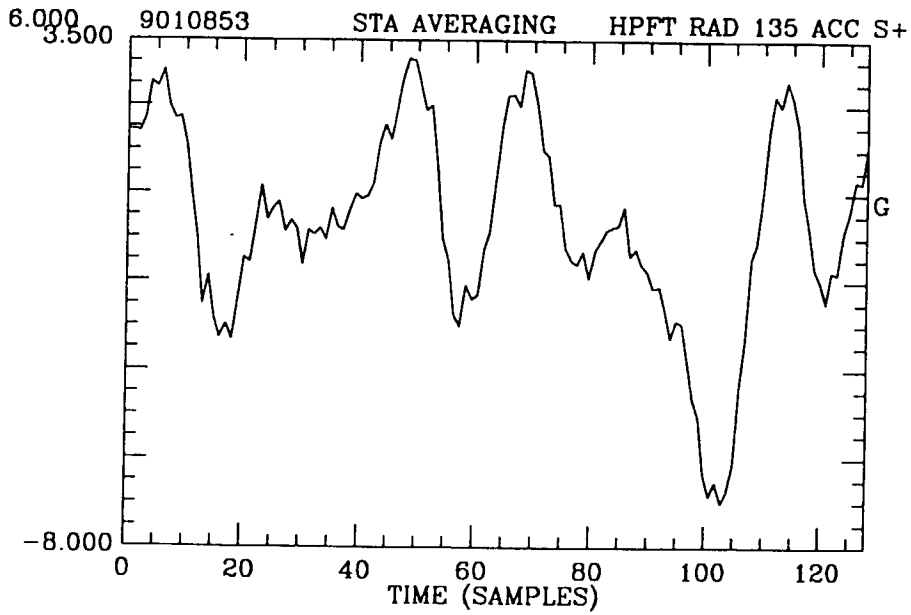

Upcrossing Frequency of 0.00= 558.849 Hz, NAVG= 18442

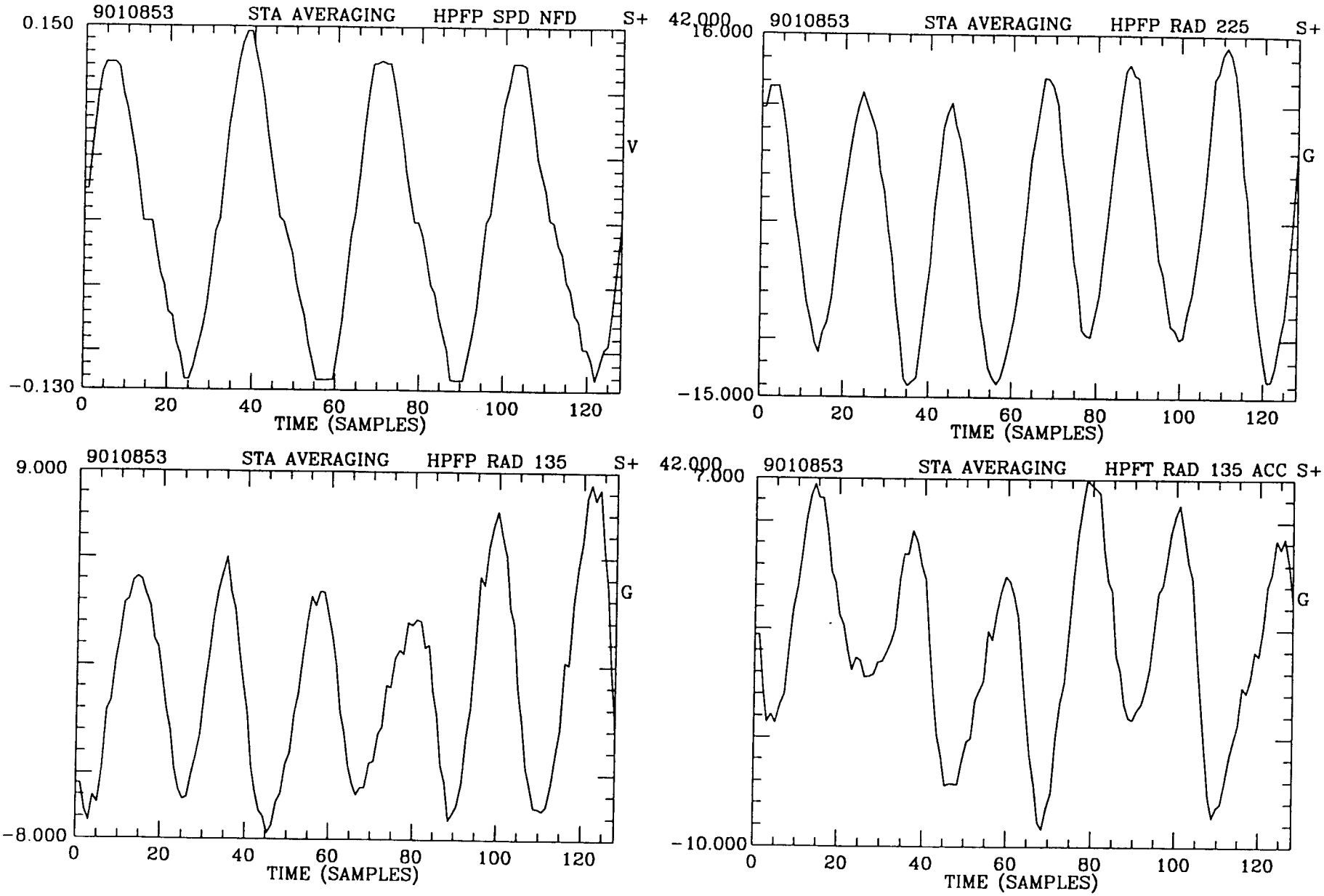

Upcrossing Frequency of 0.00= 532.864 Hz, NAVG= 11723

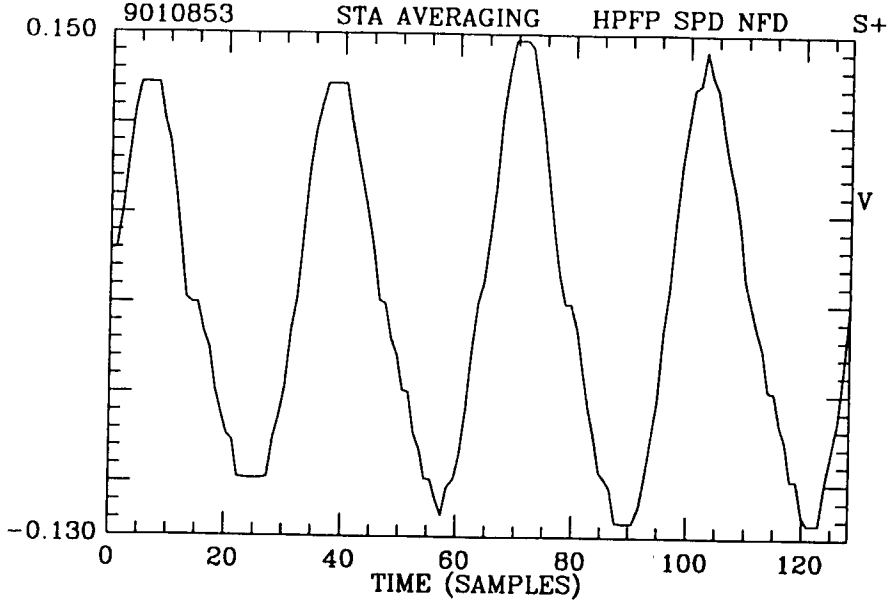

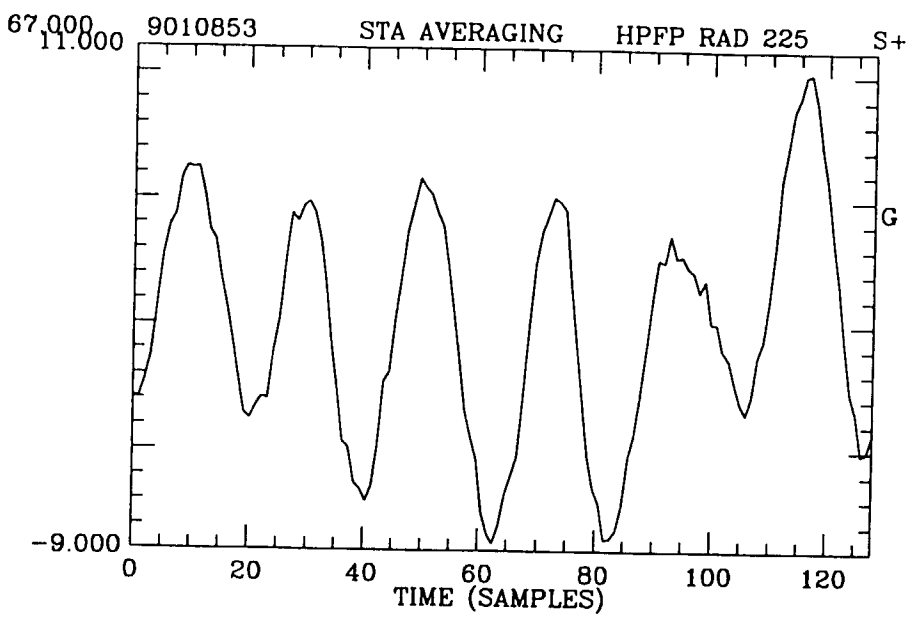

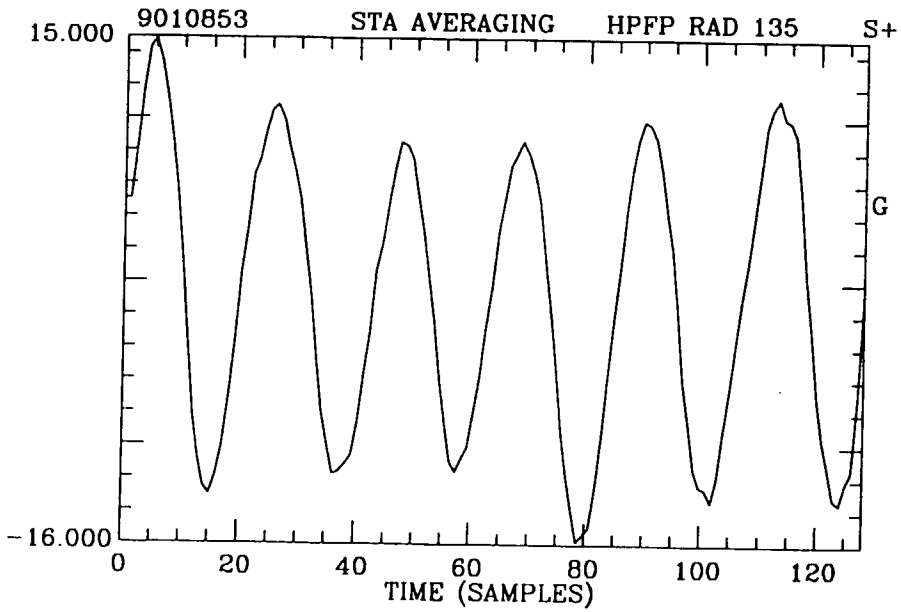

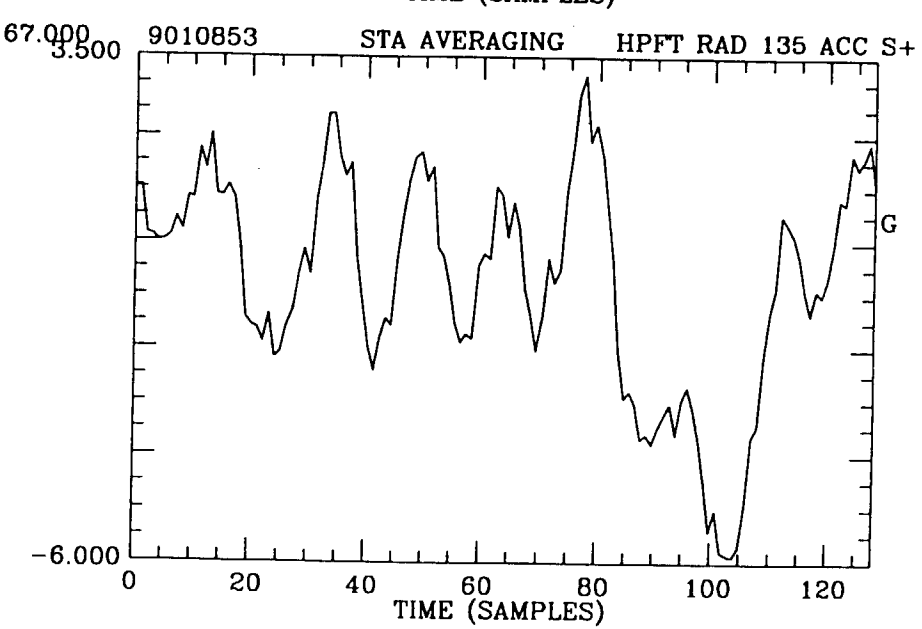

Upcrossing Frequency of 0.00= 562.000 Hz, NAVG= 12364

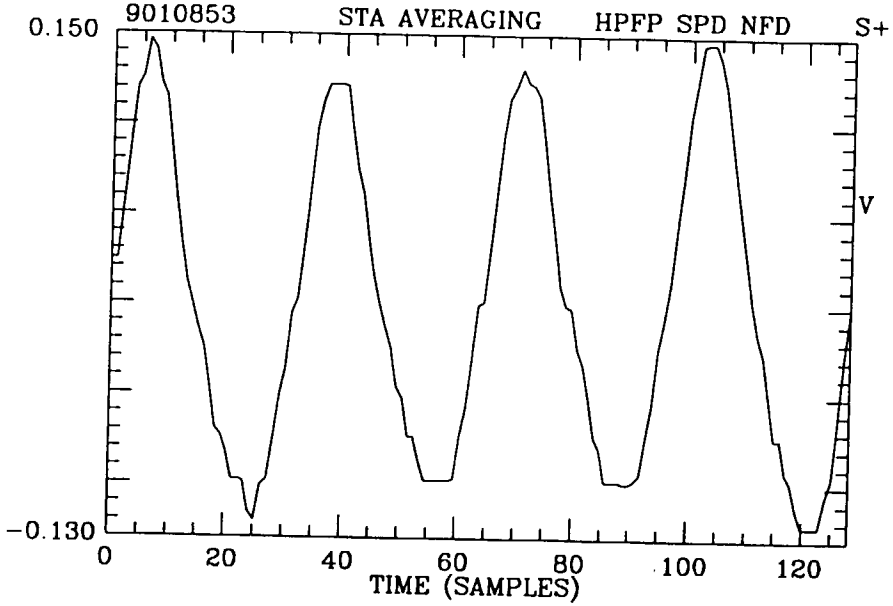

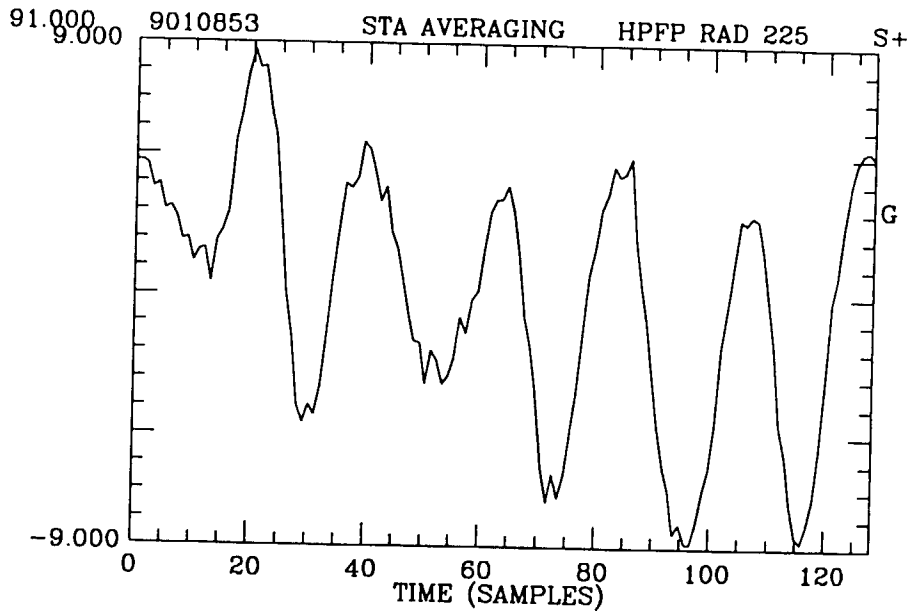

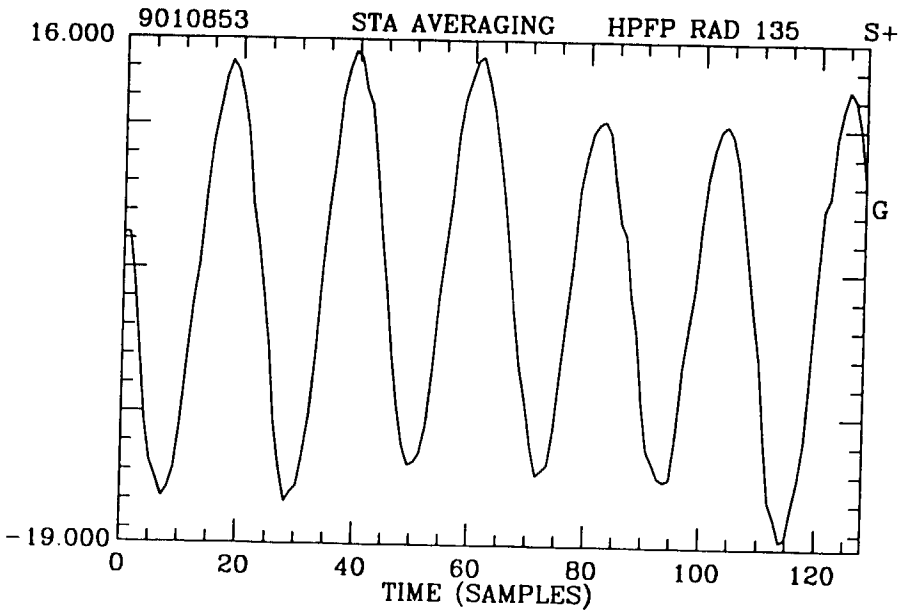

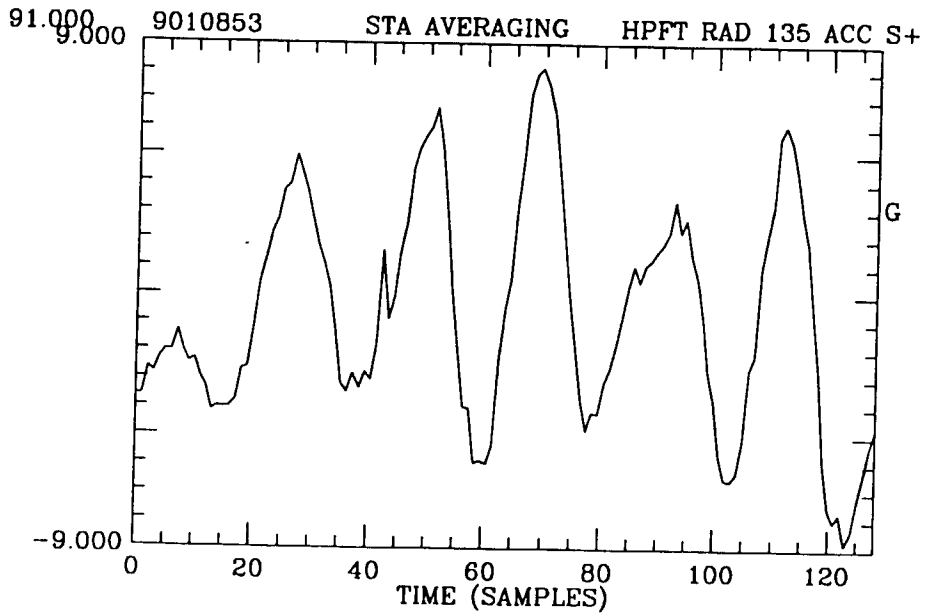

Upcrossing Frequency of 0.00= 570.913 Hz, NAVG= 13131

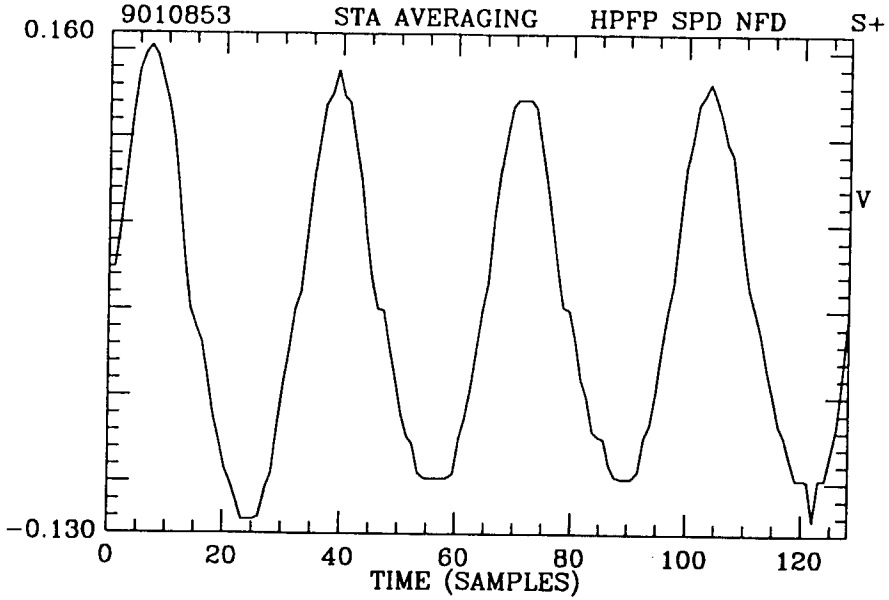

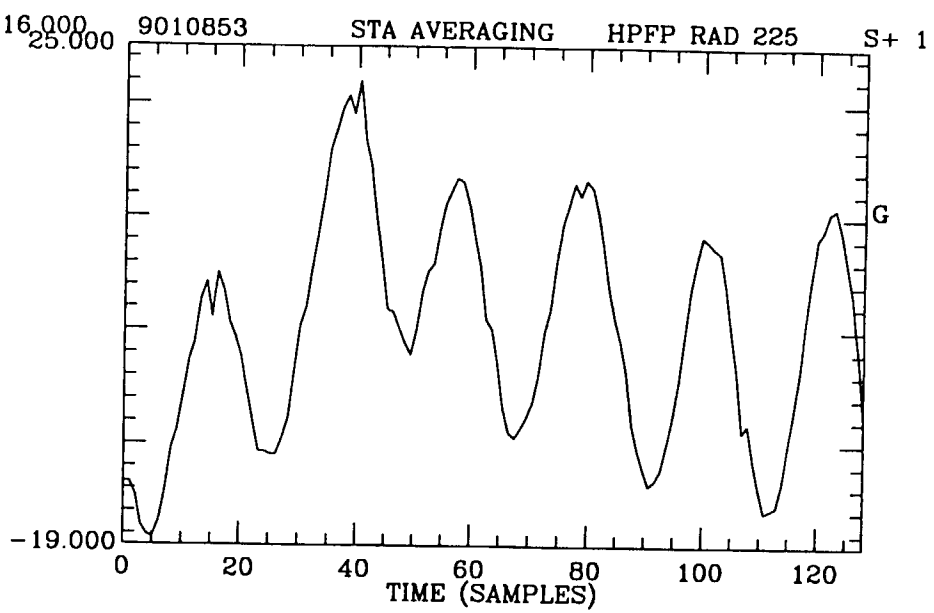

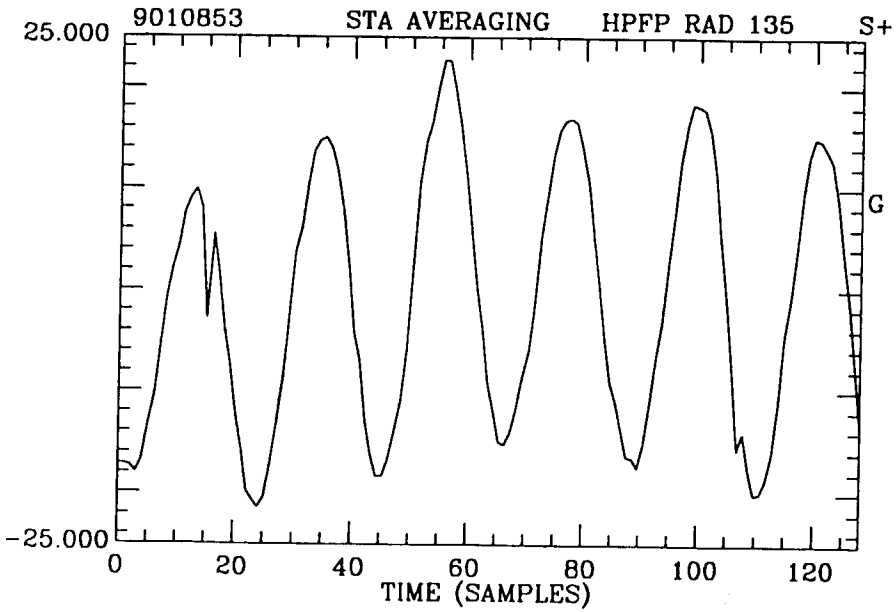

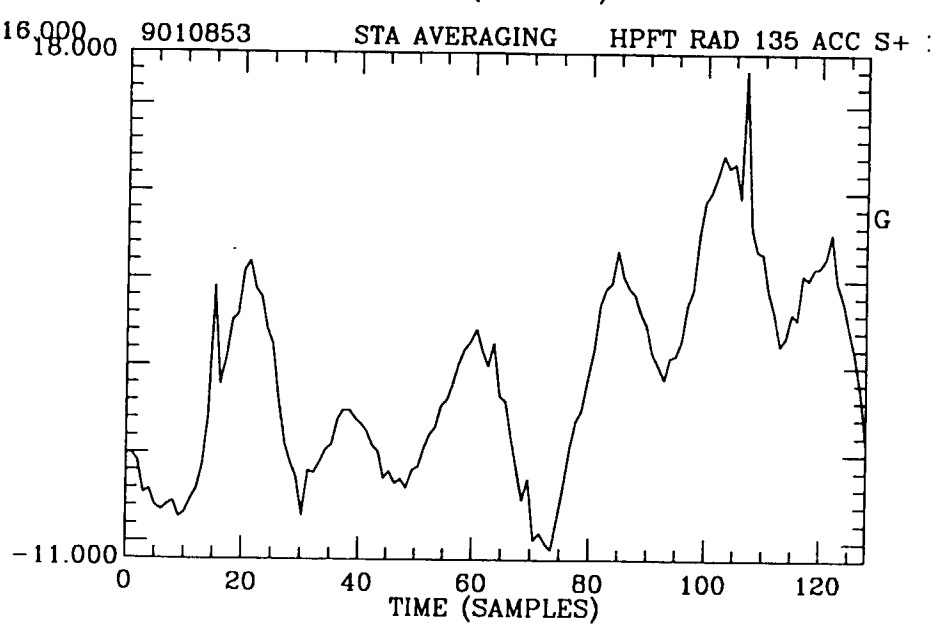

Upcrossing Frequency of 0.00= 587.391 Hz, NAVG= 13510

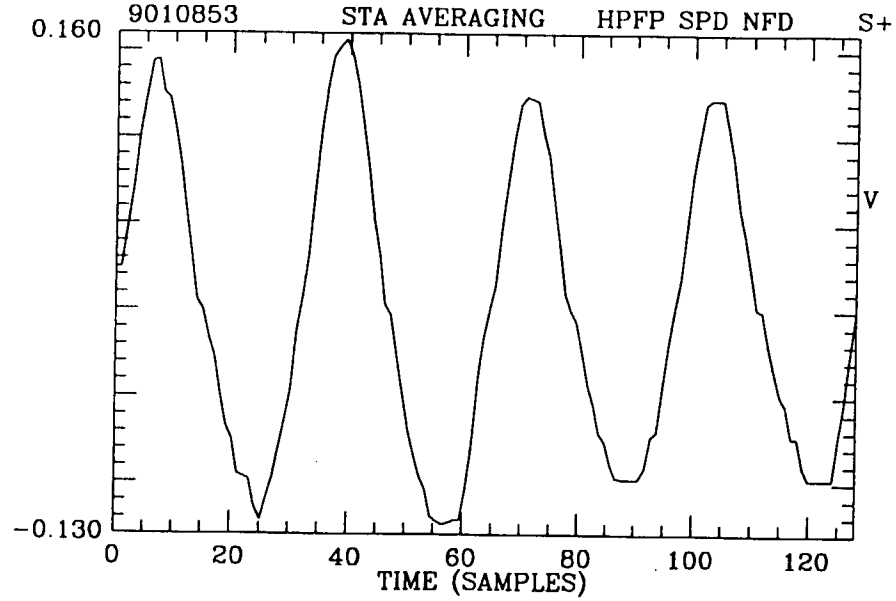

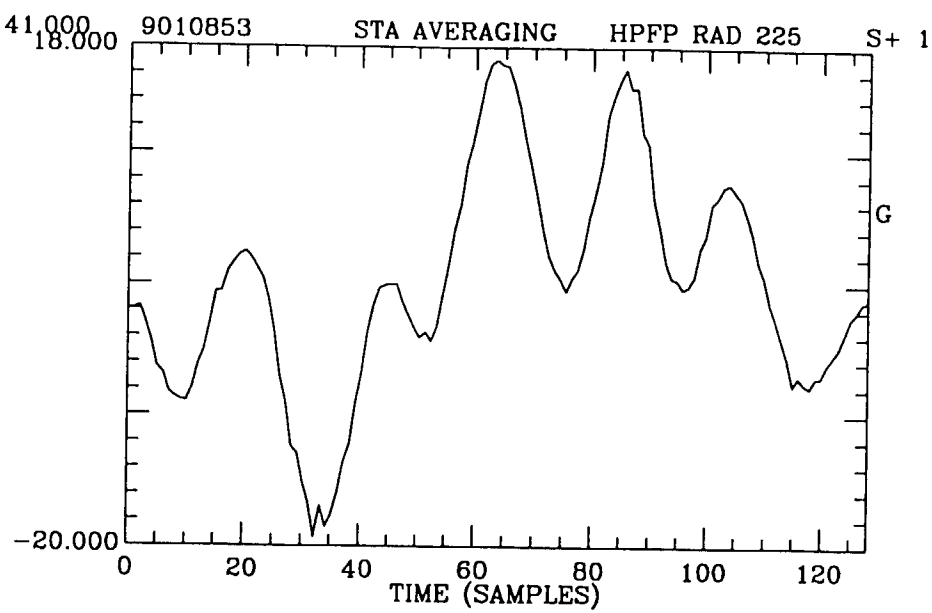

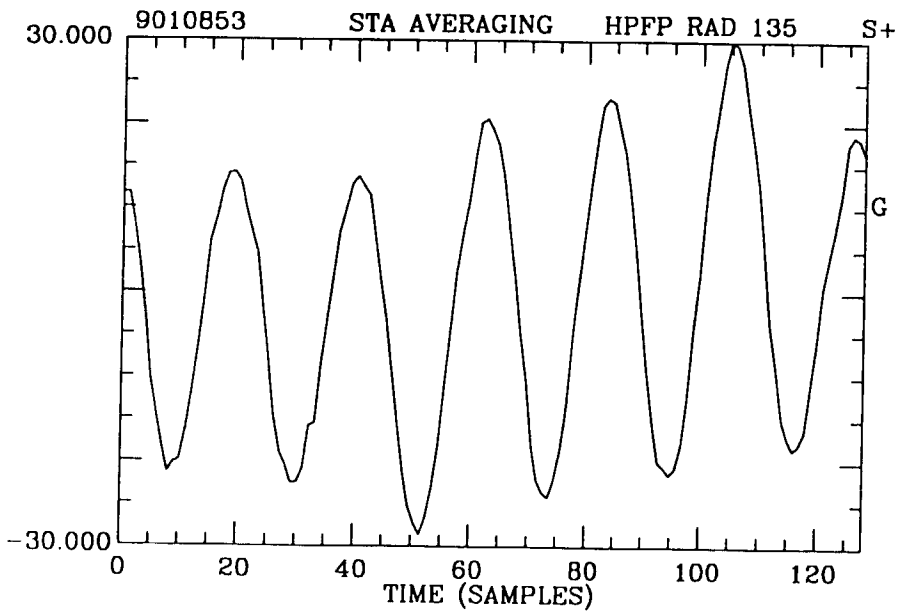

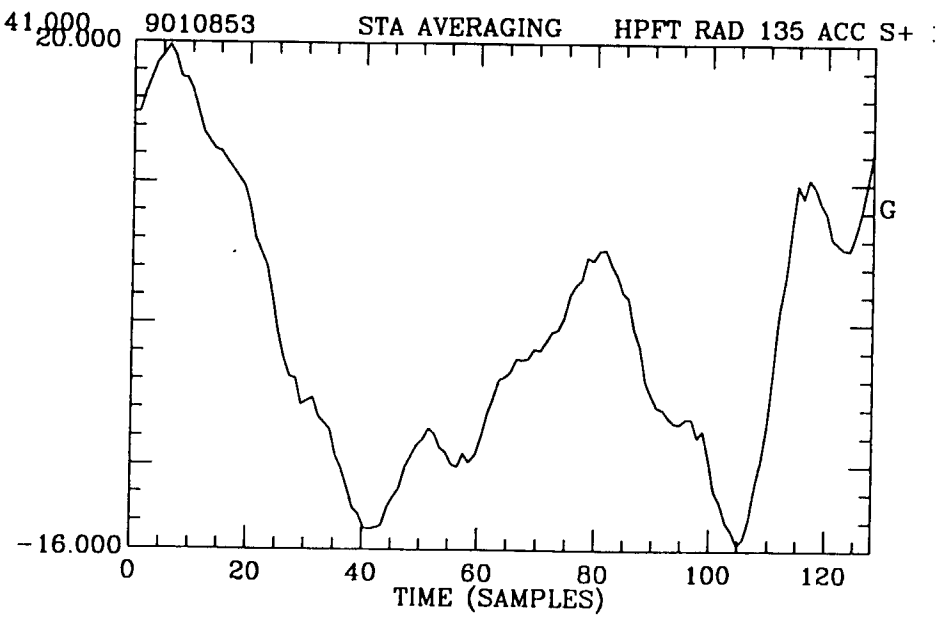

Upcrossing Frequency of 0.00= 577.660 Hz, NAVG= 28883

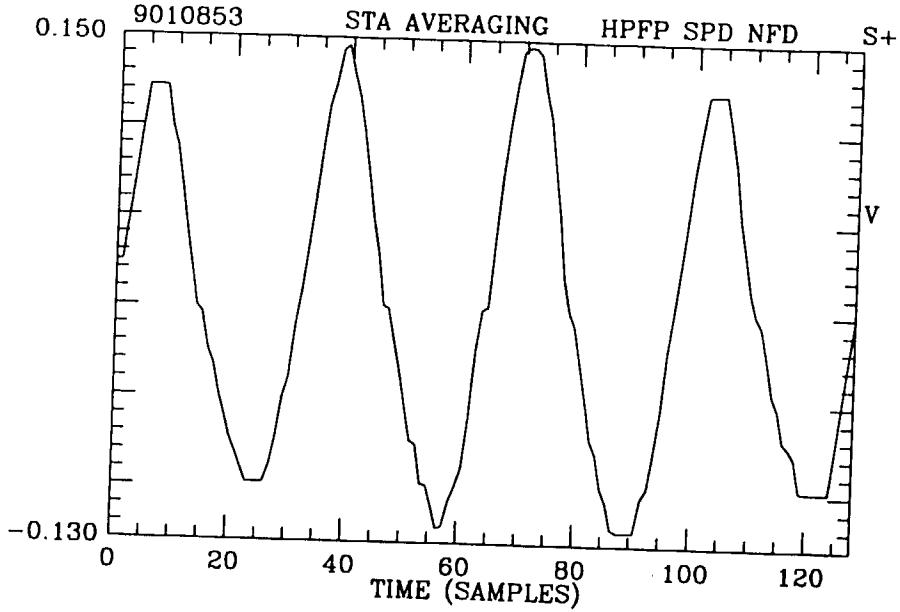

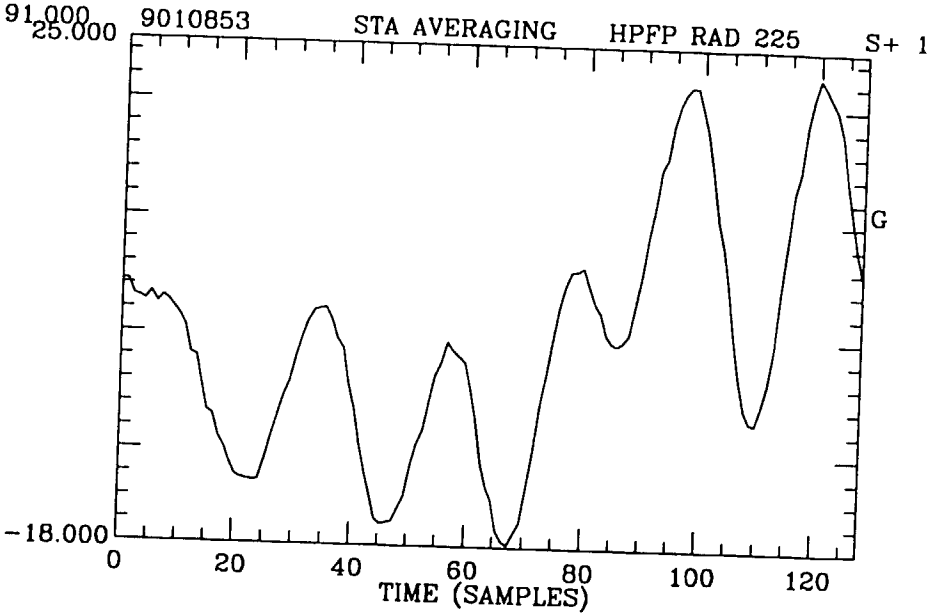

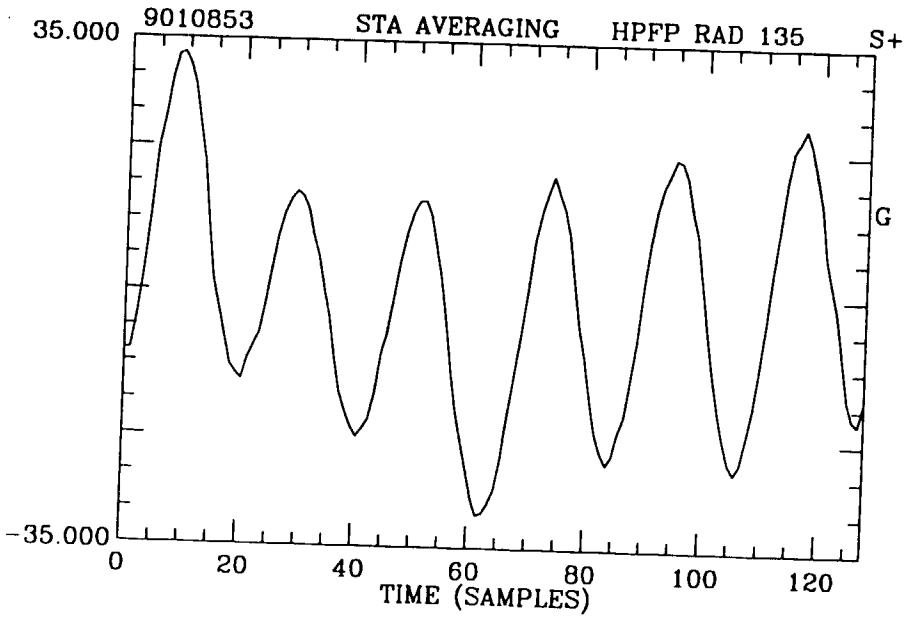

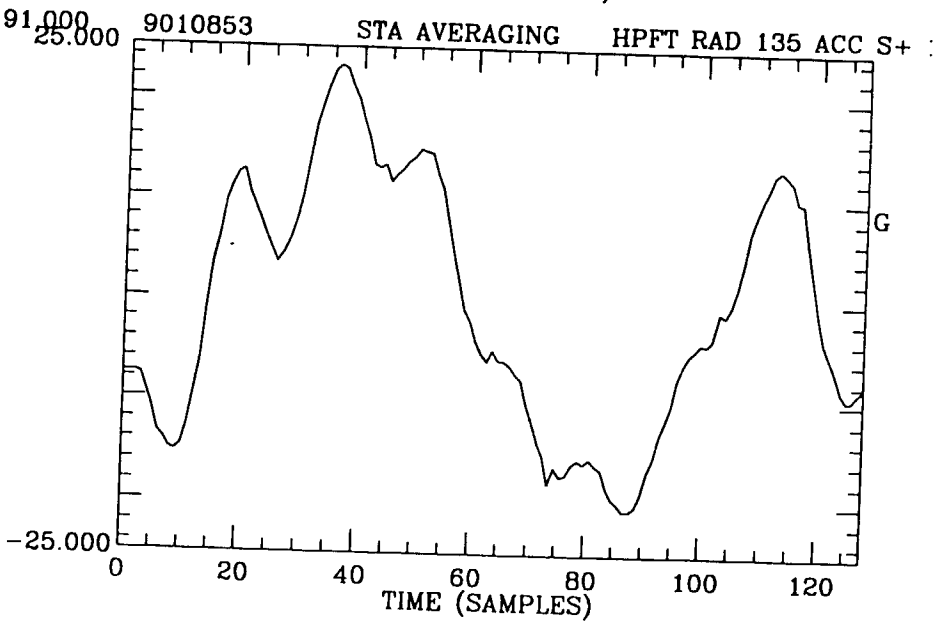

Upcrossing Frequency of 0.00= 578.540 Hz, NAVG= 28927

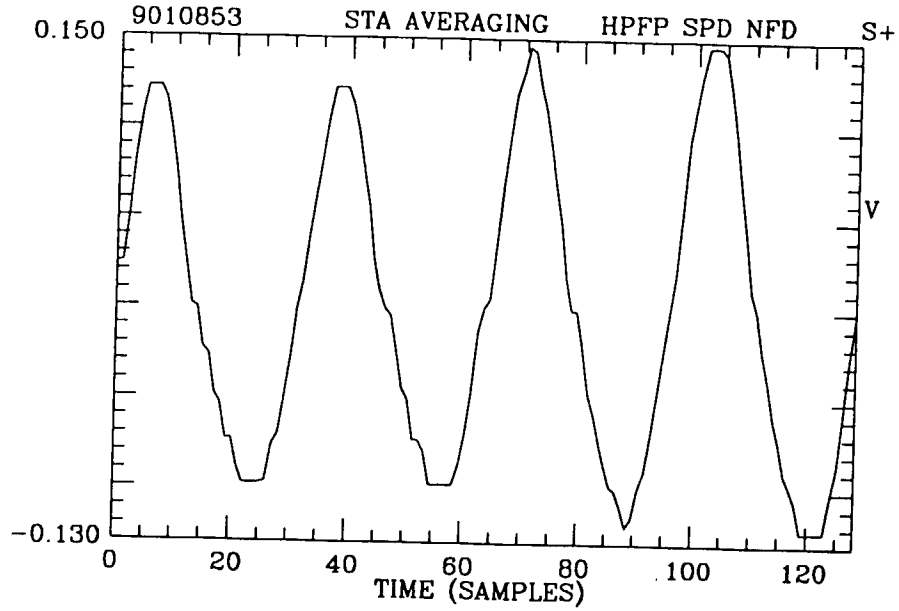

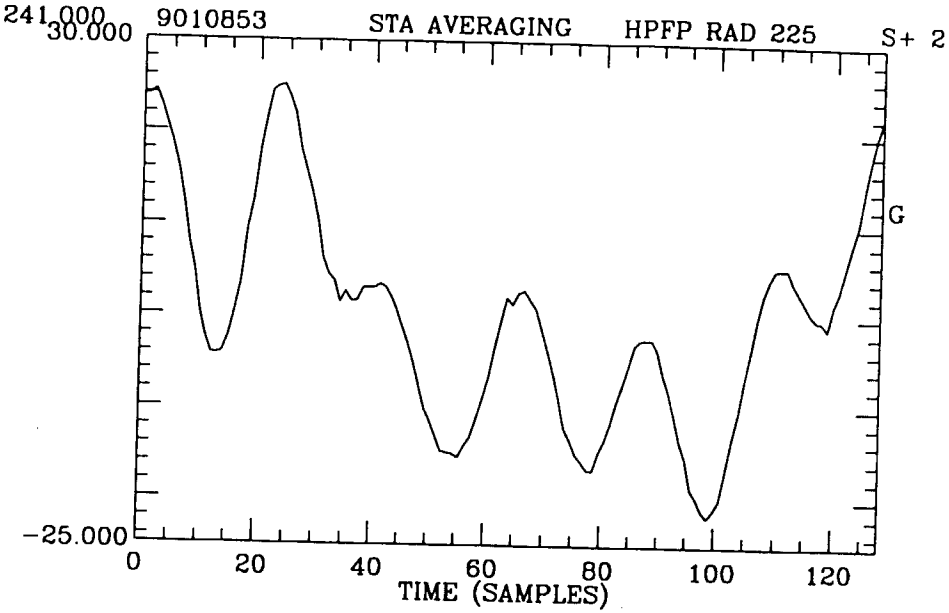

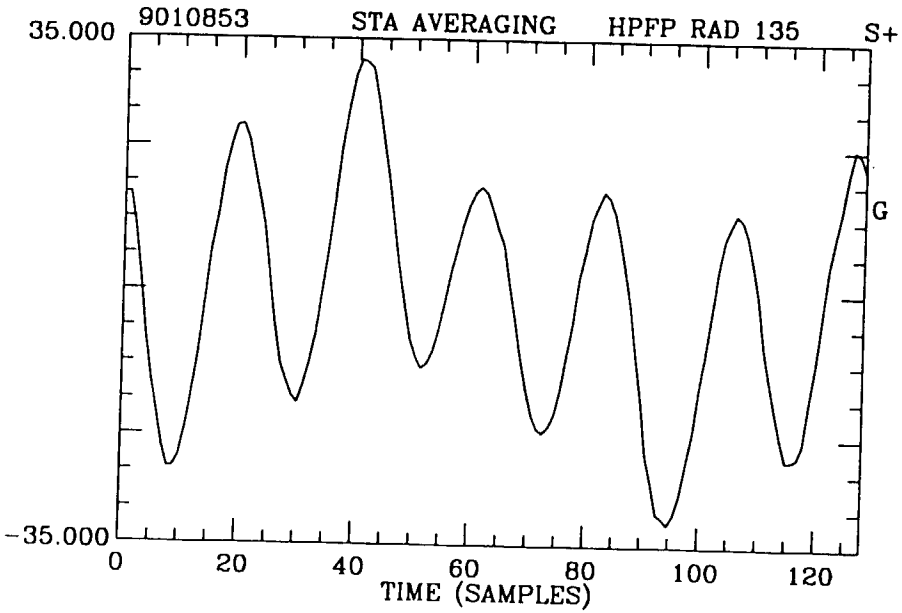

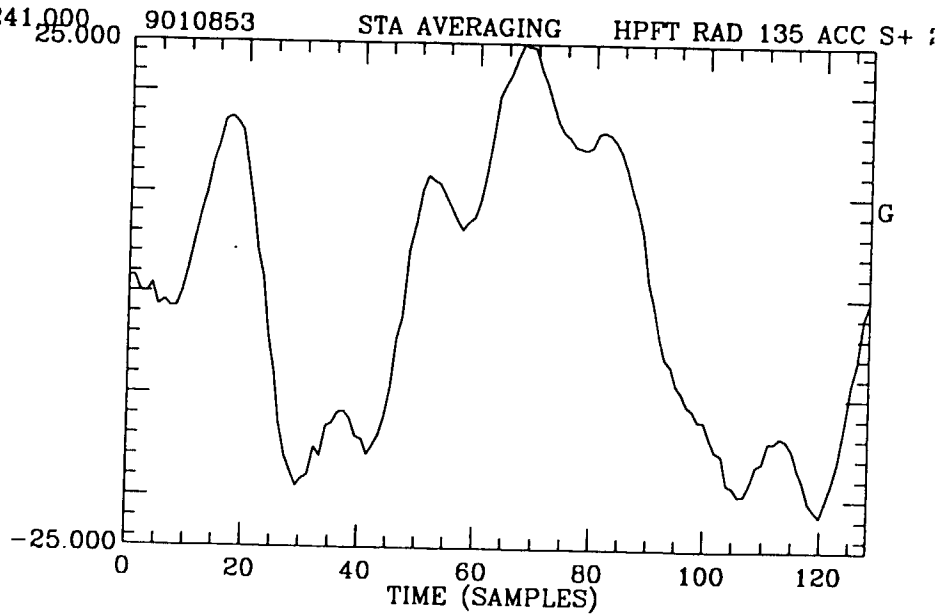

Upcrossing Frequency of 0.00= 578.840 Hz, NAVG= 28942

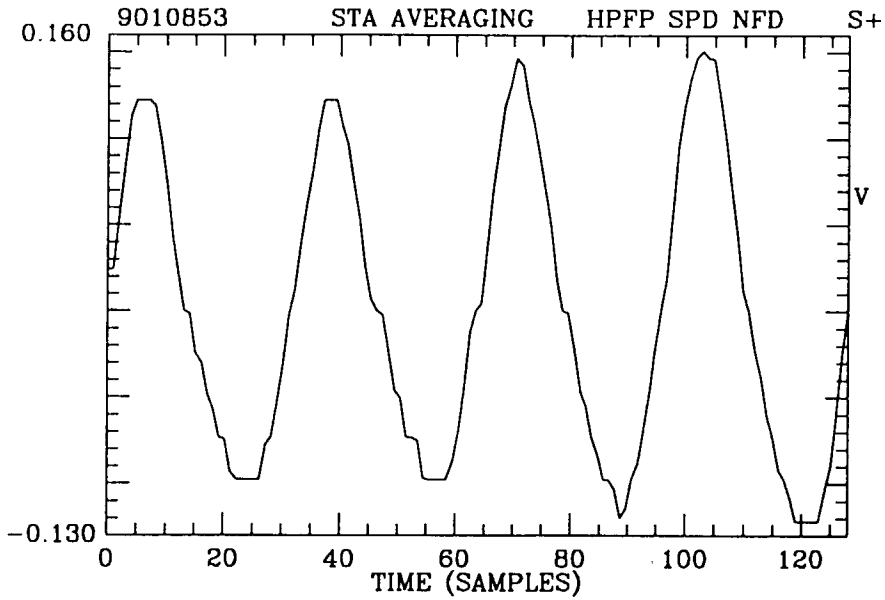

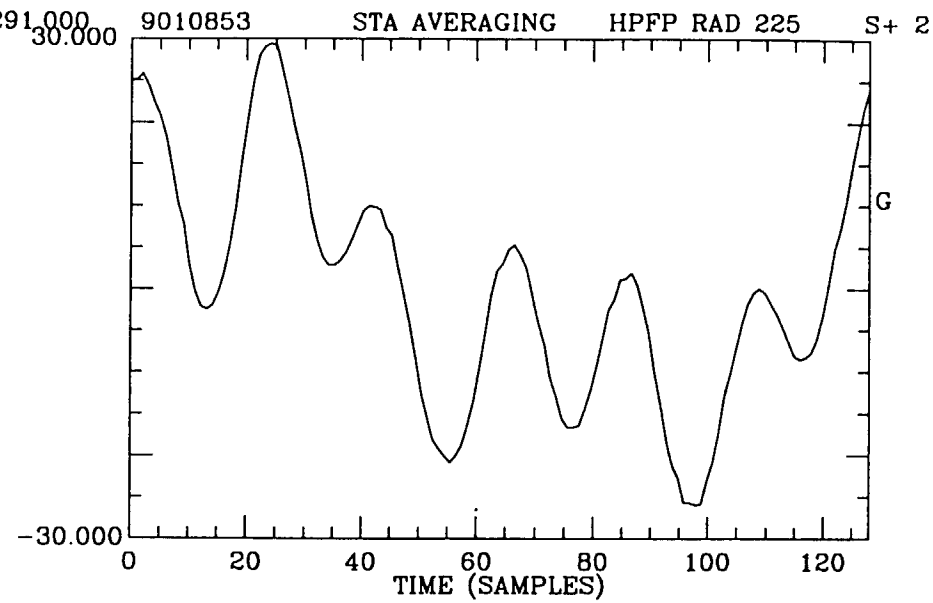

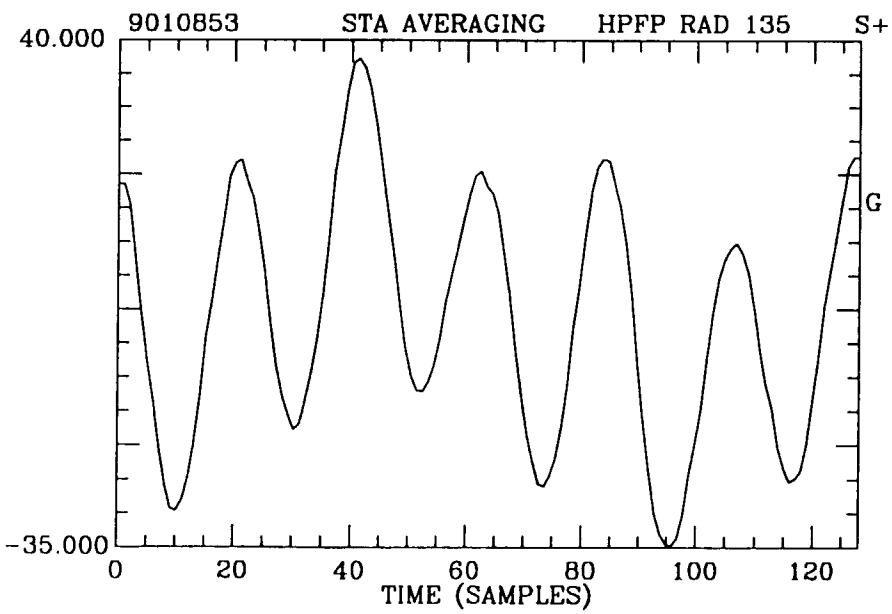

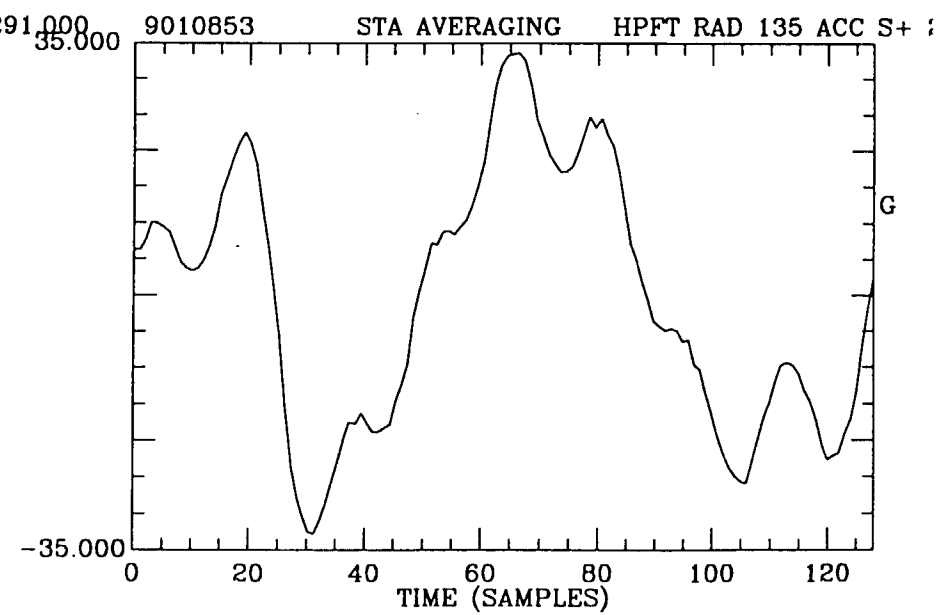

Upcrossing Frequency of 0.00= 579.400 Hz, NAVG= 28970

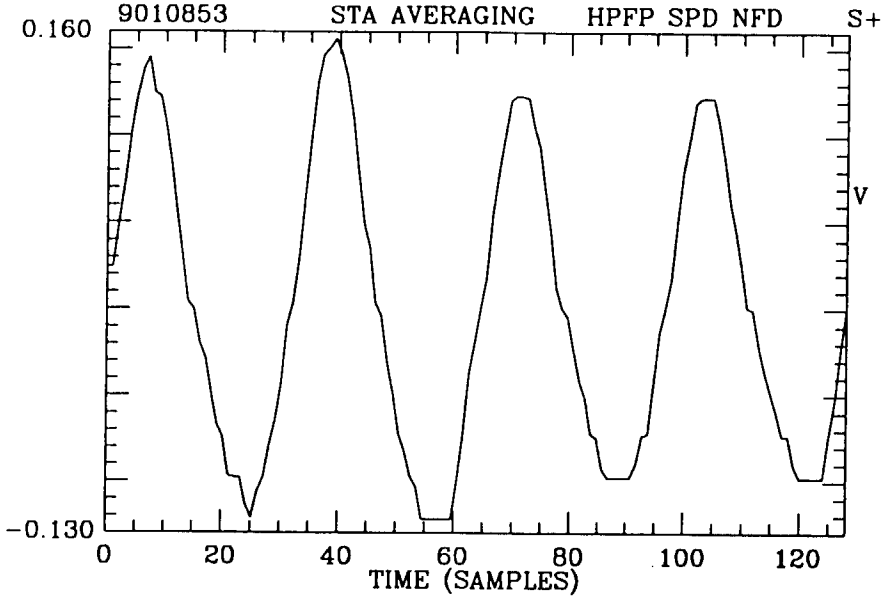

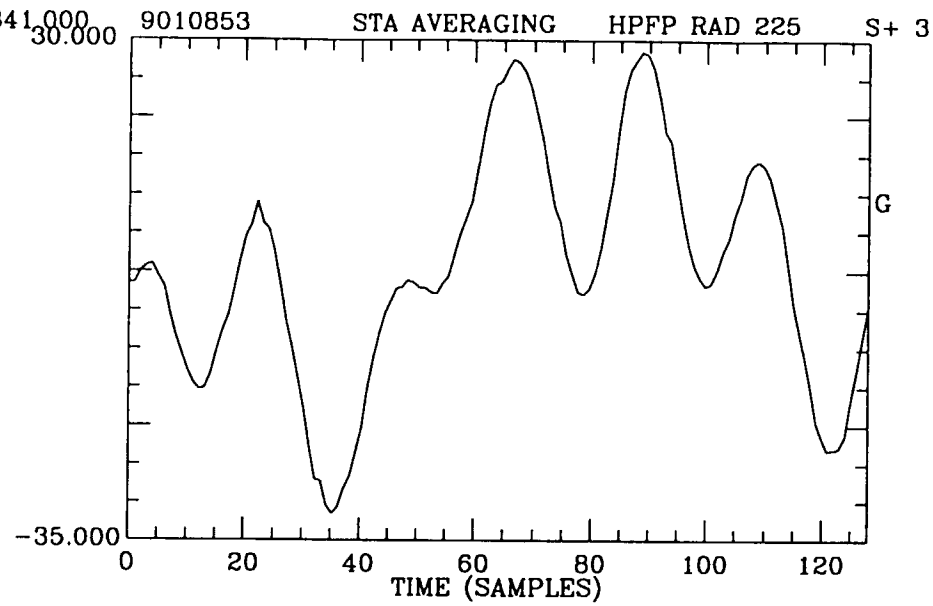

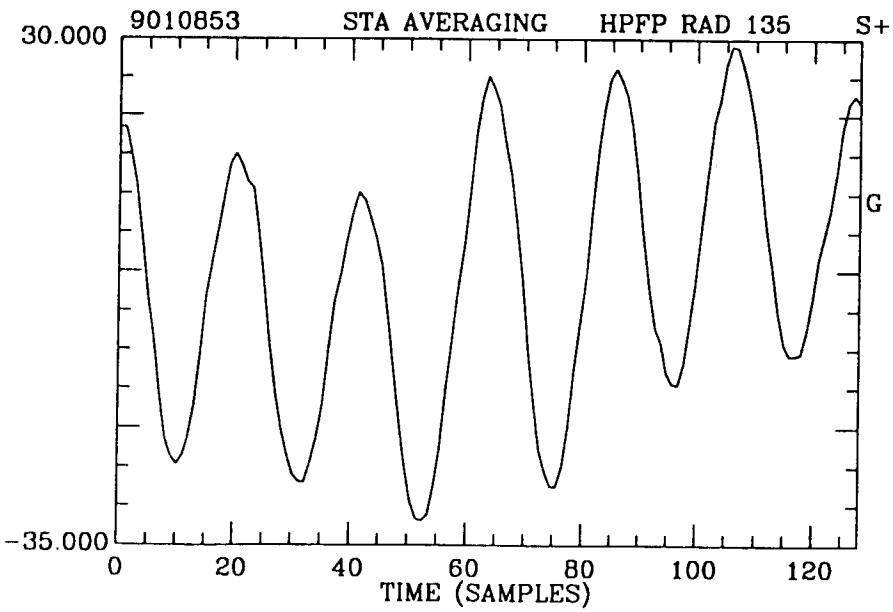

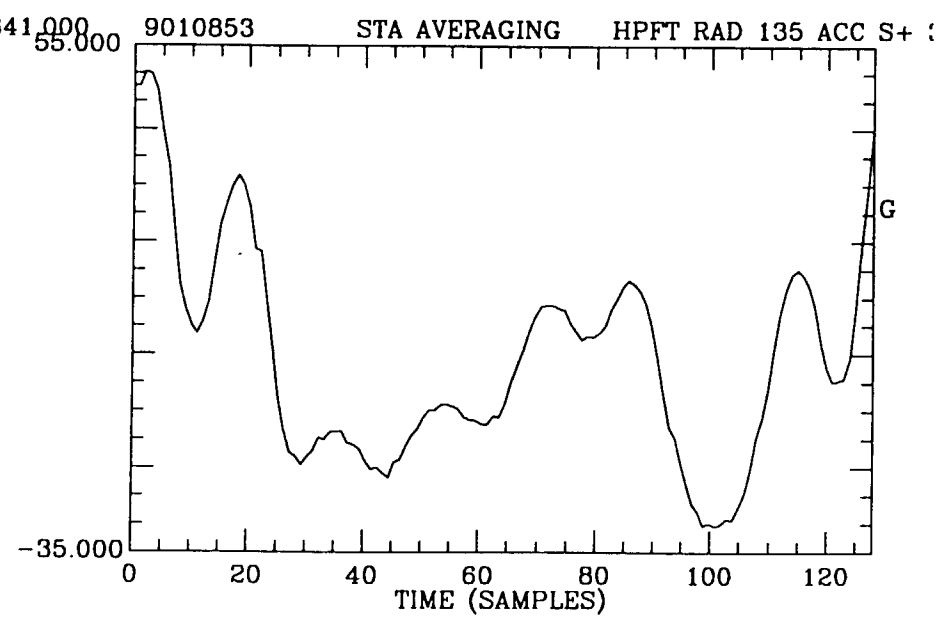

Upcrossing Frequency of 0.00= 579.540 Hz, NAVG= 28977

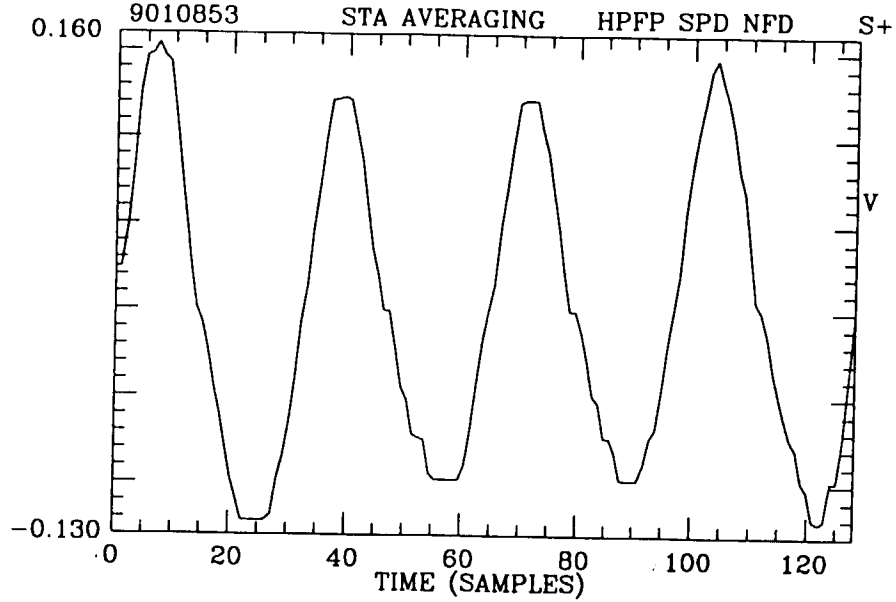

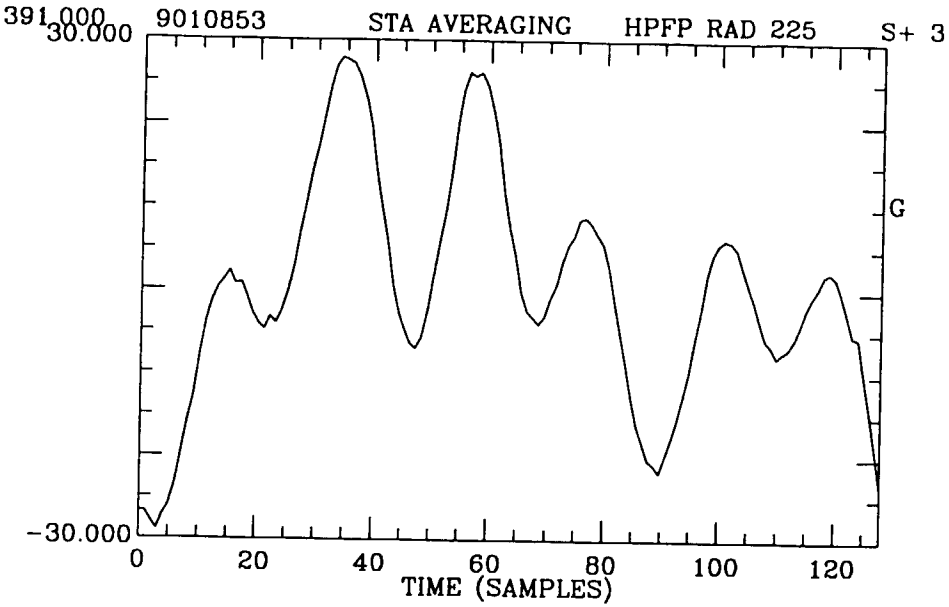

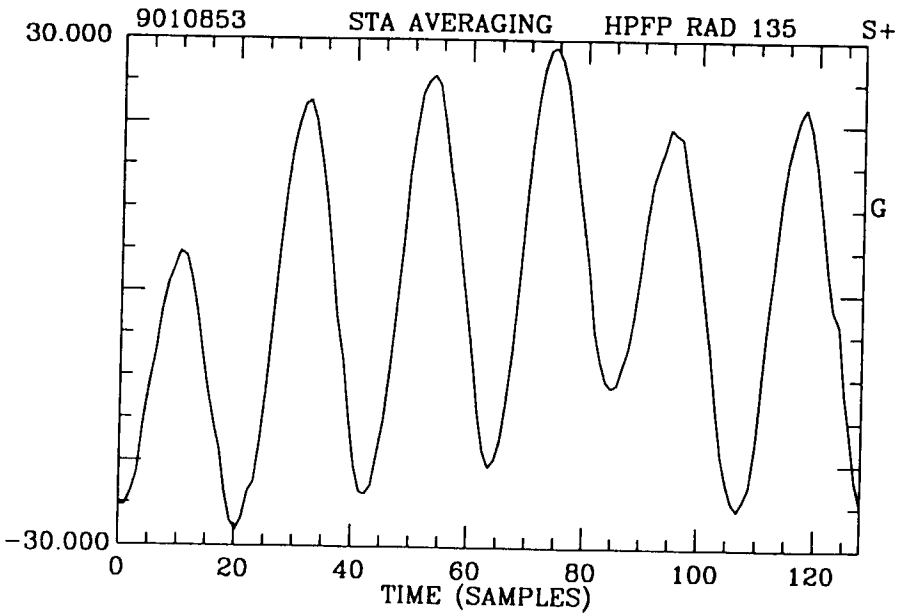

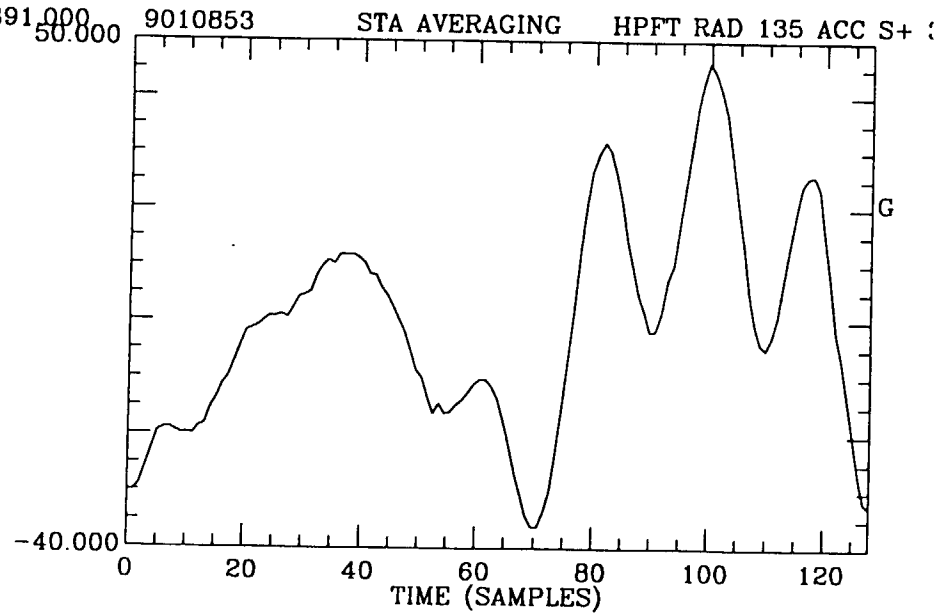

Upcrossing Frequency of 0.00= 579.920 Hz, NAVG= 28996

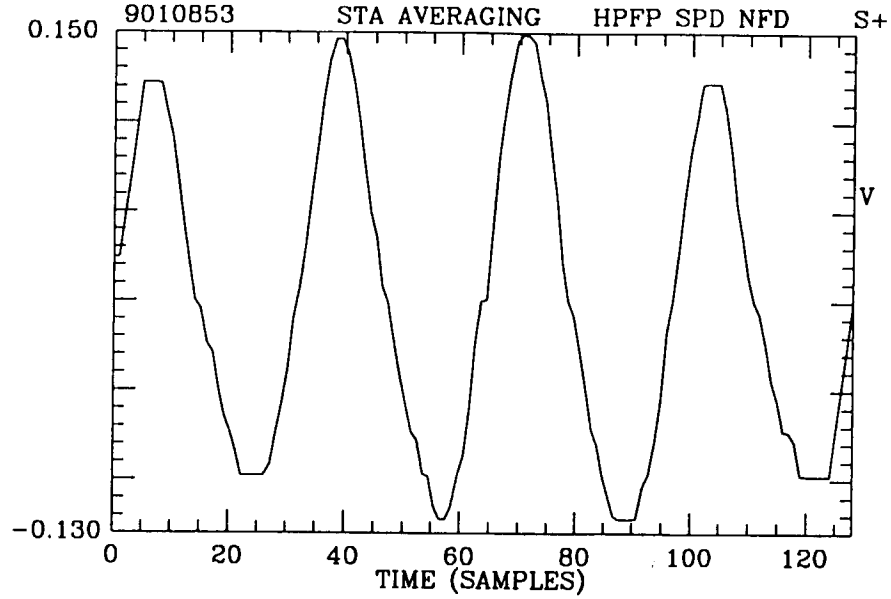

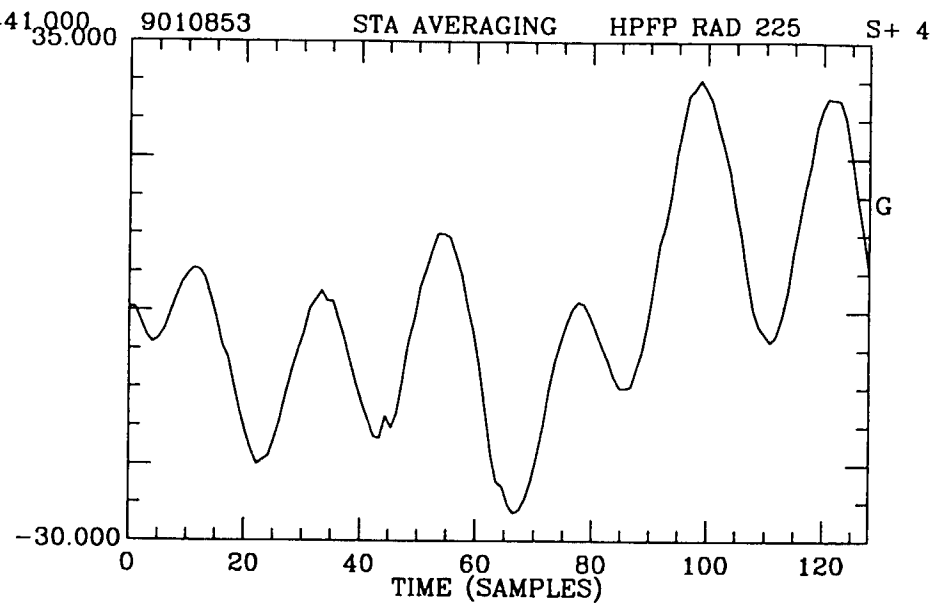

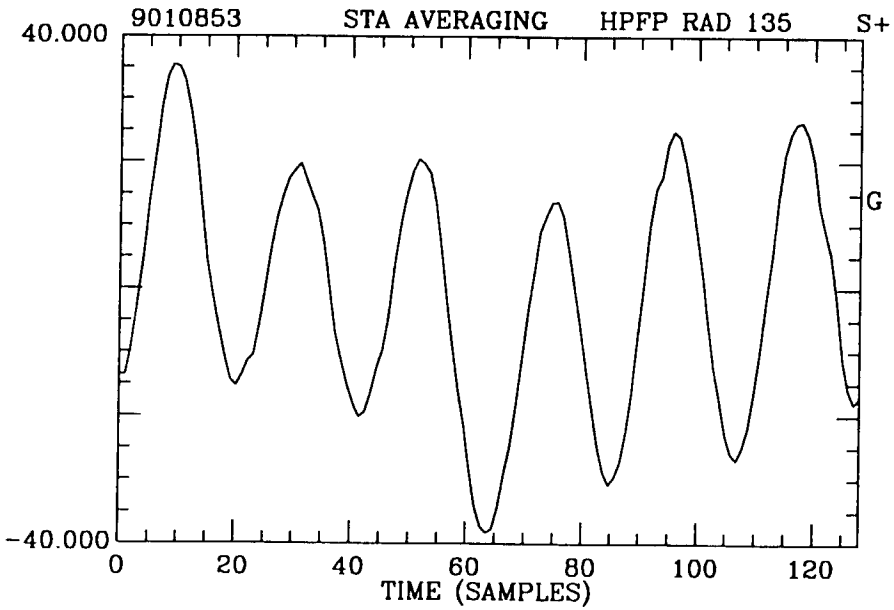

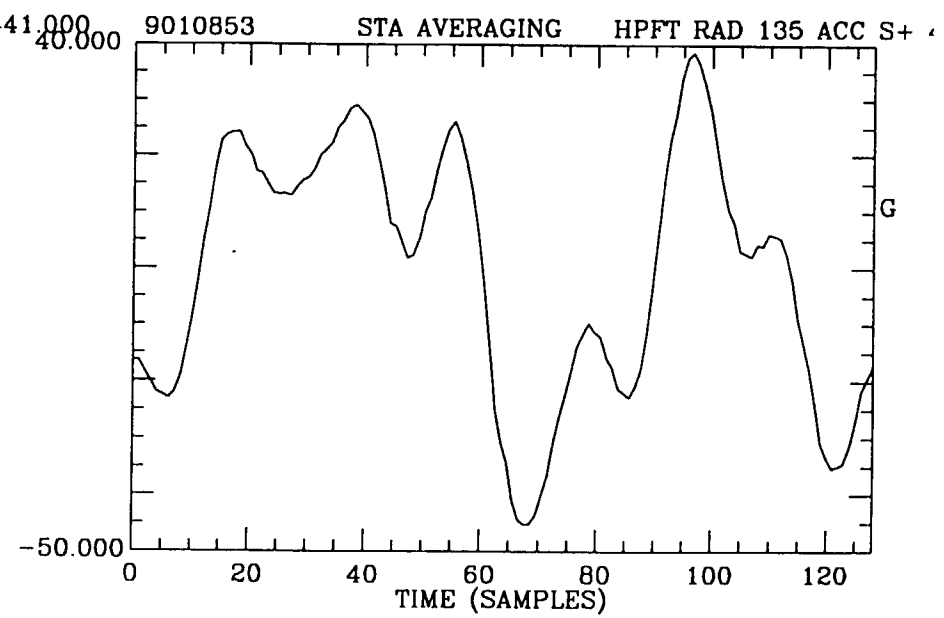

Upcrossing Frequency of 0.00= 580.060 Hz, NAVG= 29003

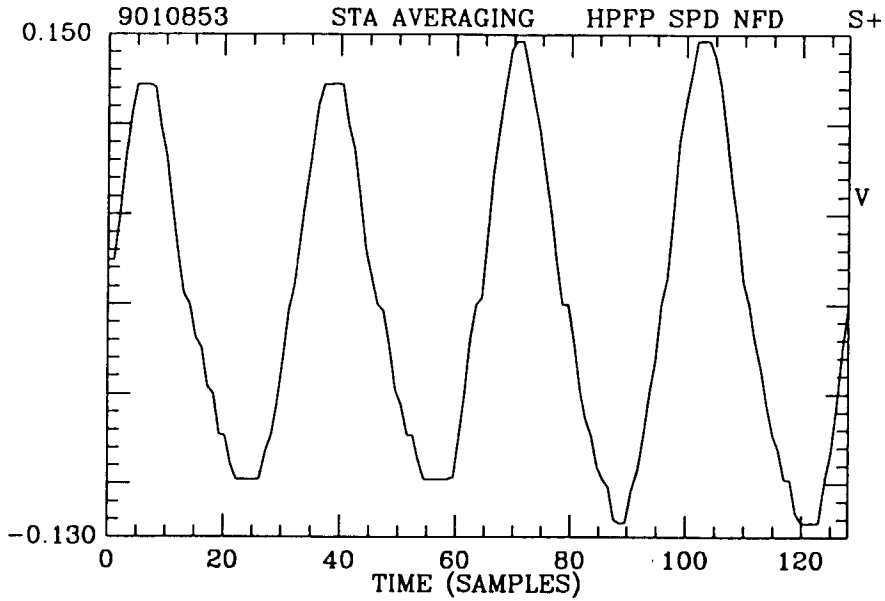

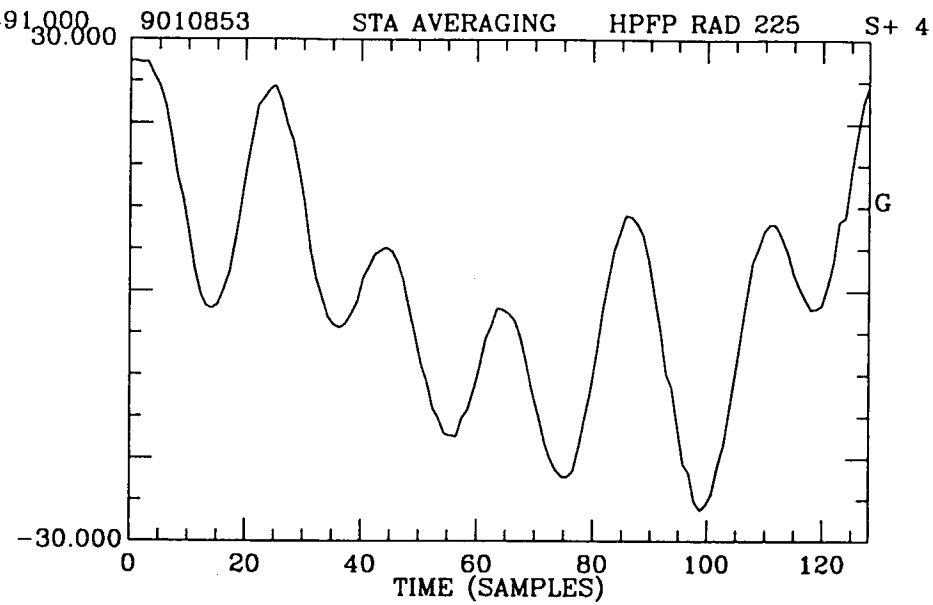

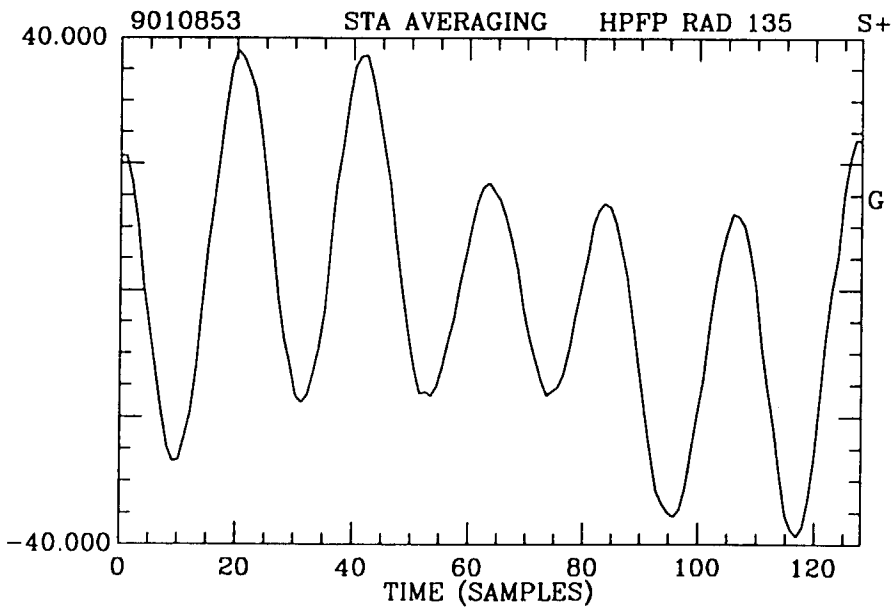

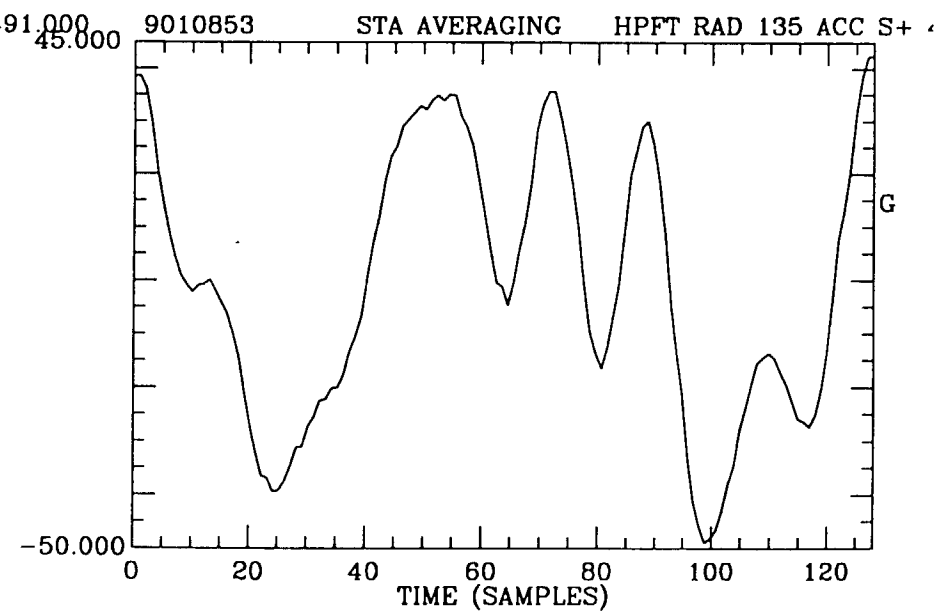

Upcrossing Frequency of 0.00= 580.240 Hz, NAVG= 29012

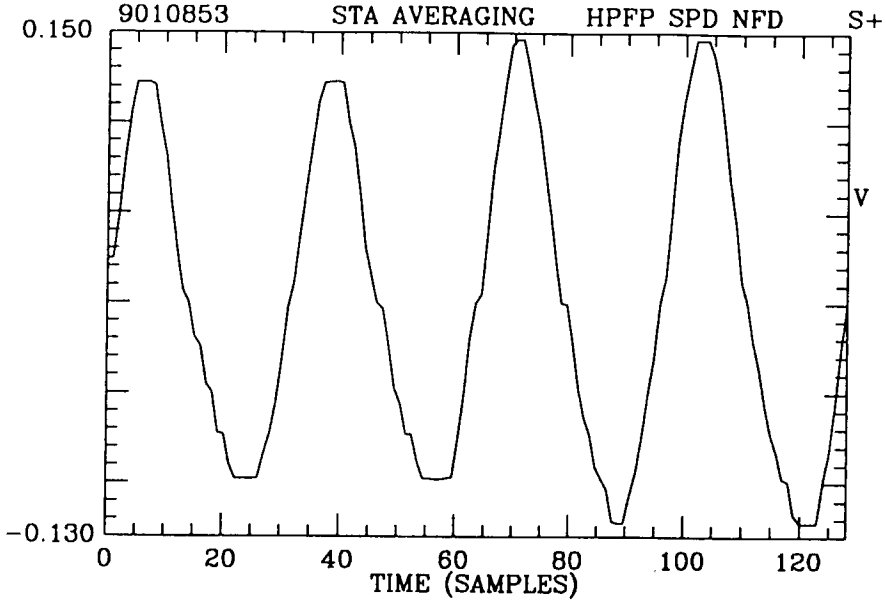

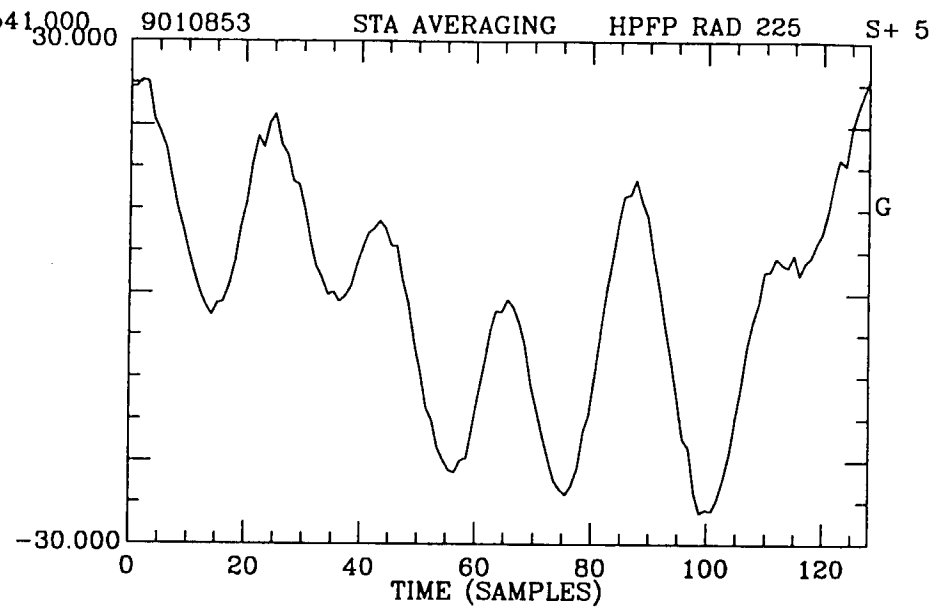

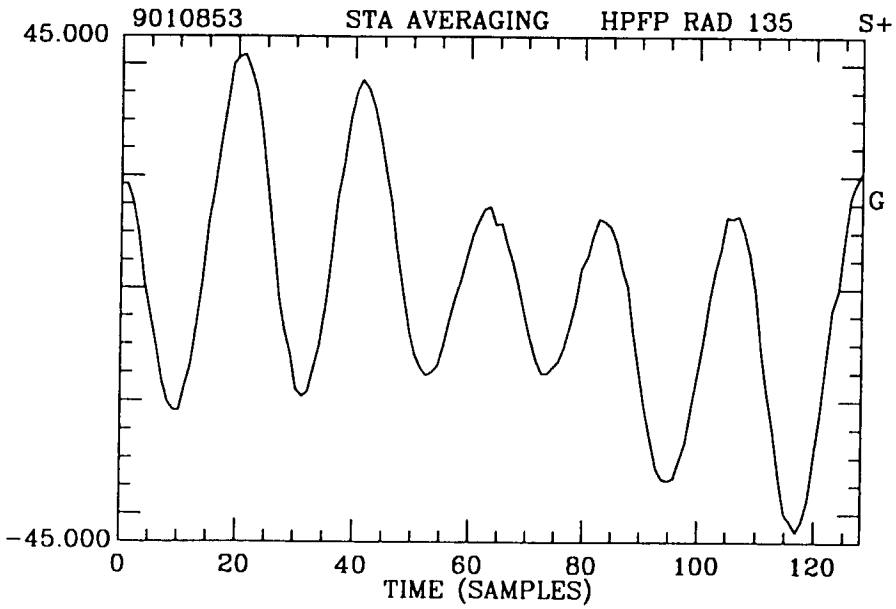

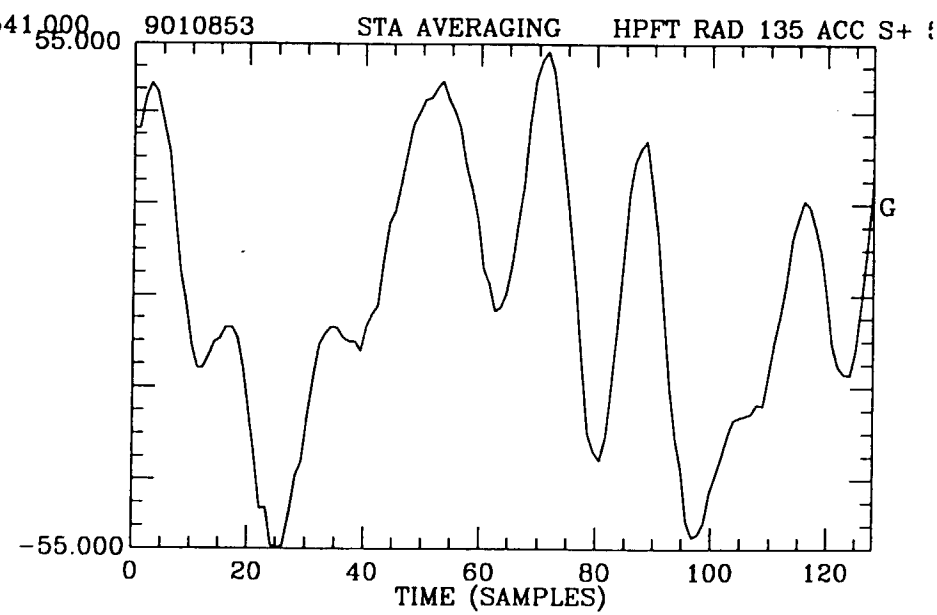

Upcrossing Frequency of 0.00= 564.766 Hz, NAVG= 6732

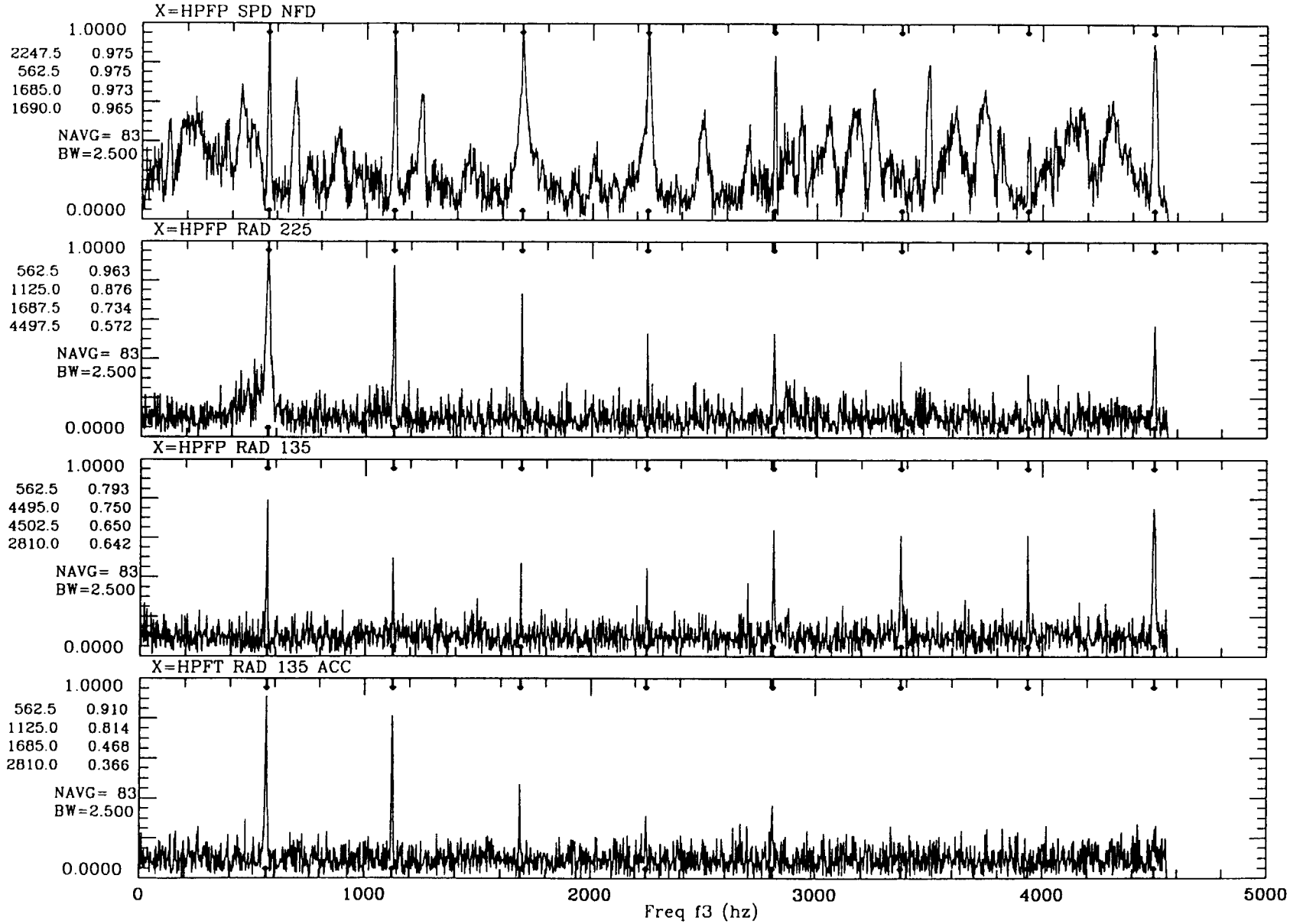

9010853 Txxxx(f1= 0.00,f2= 562.176,f3),S+ 6.00

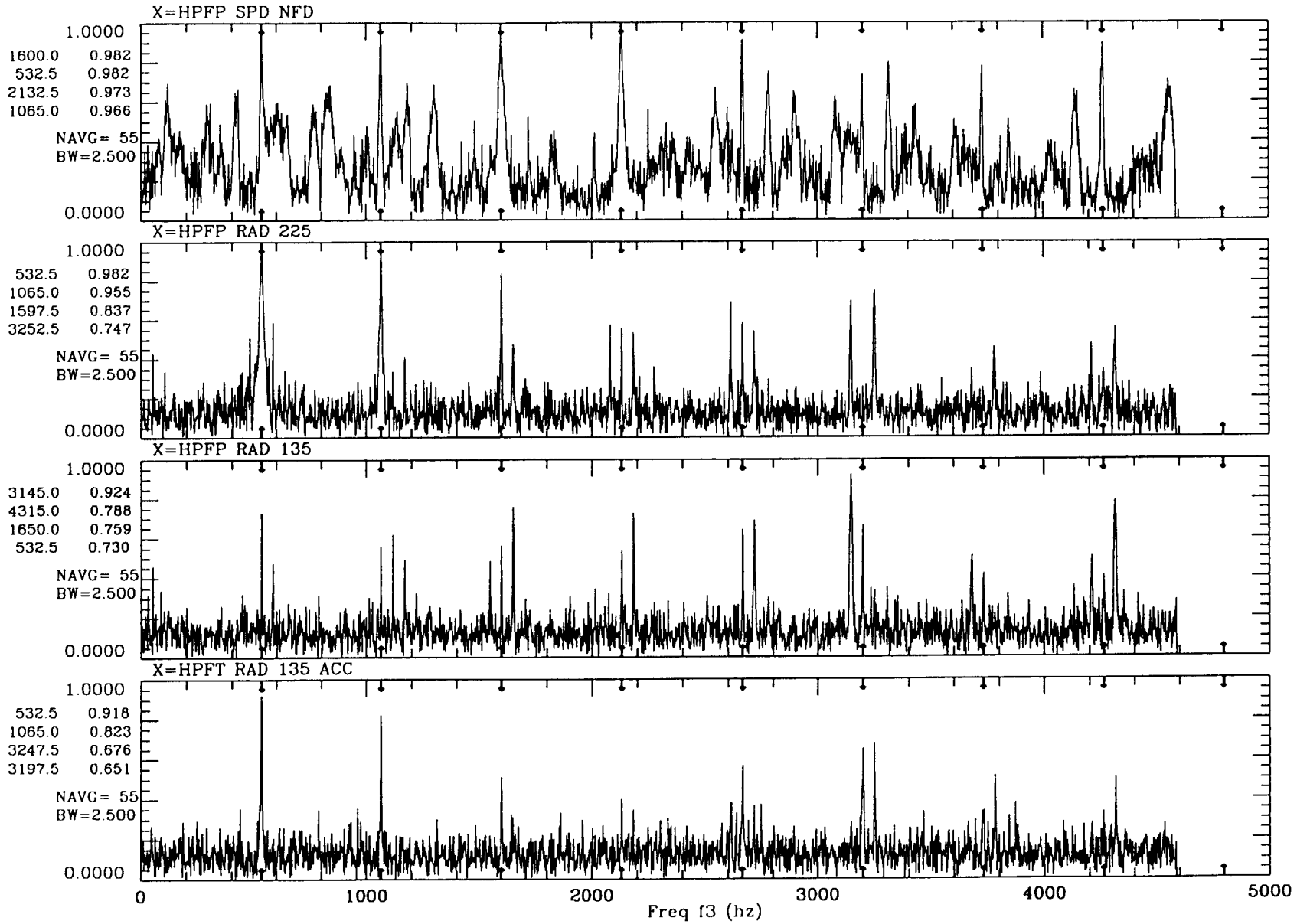

9010853 Txxxx(f1= 0.00,f2= 532.812,f3),S+ 42.00

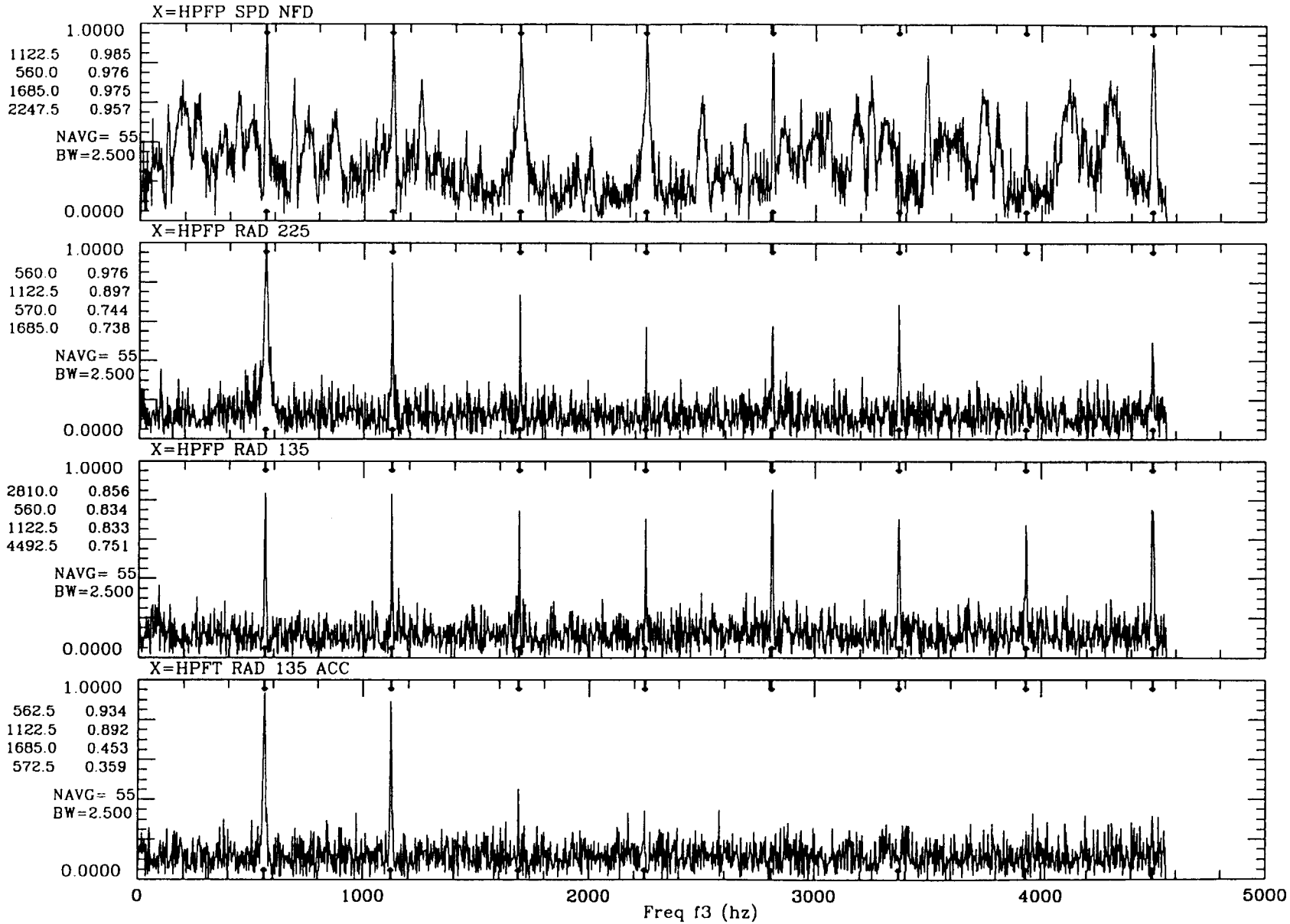

9010853 Txxxx(f1= 0.00,f2= 561.942,f3),S+ 67.00

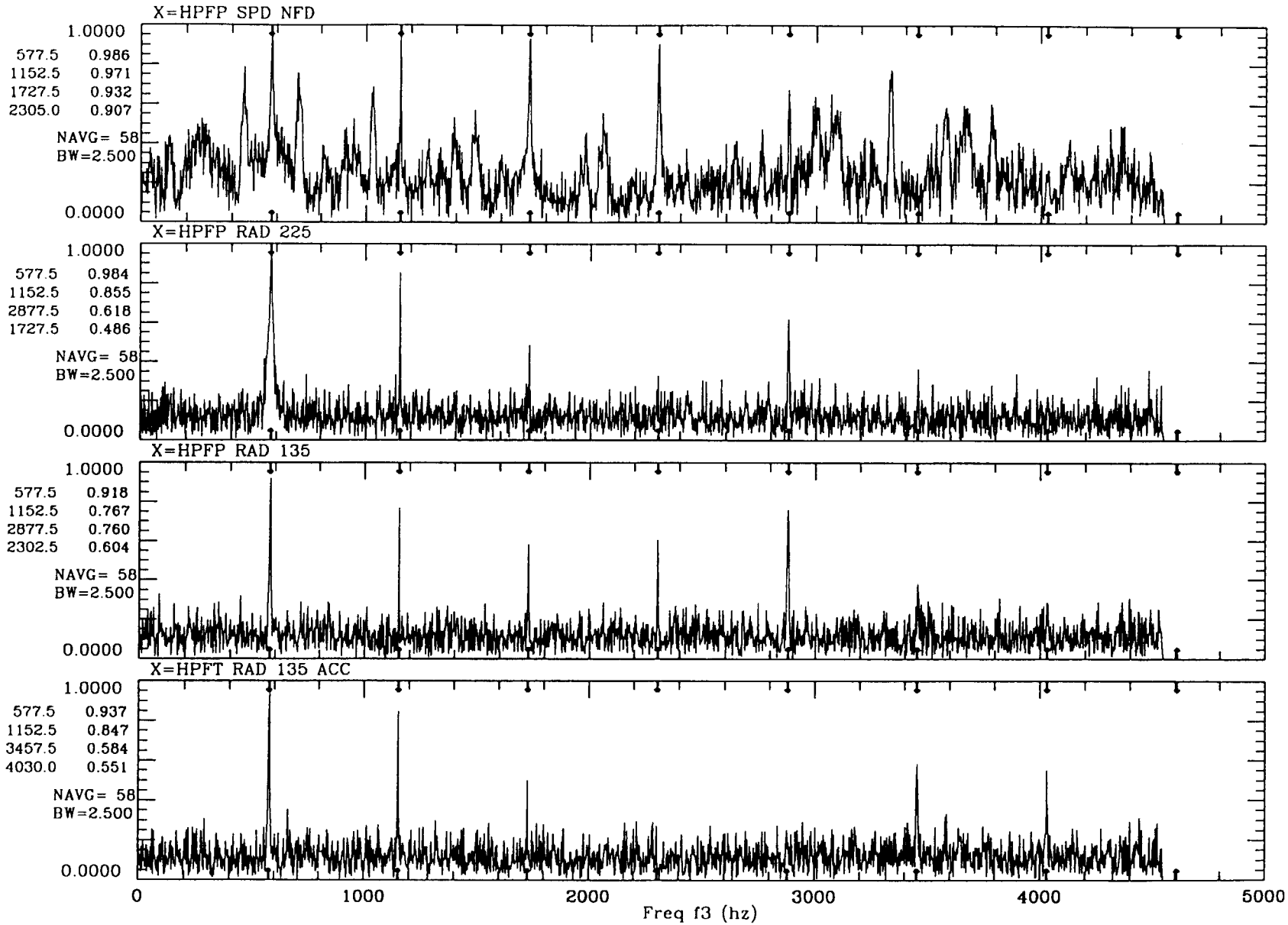

9010853 Txxxx(f1= 0.00,f2= 575.890,f3),S+ 91.00

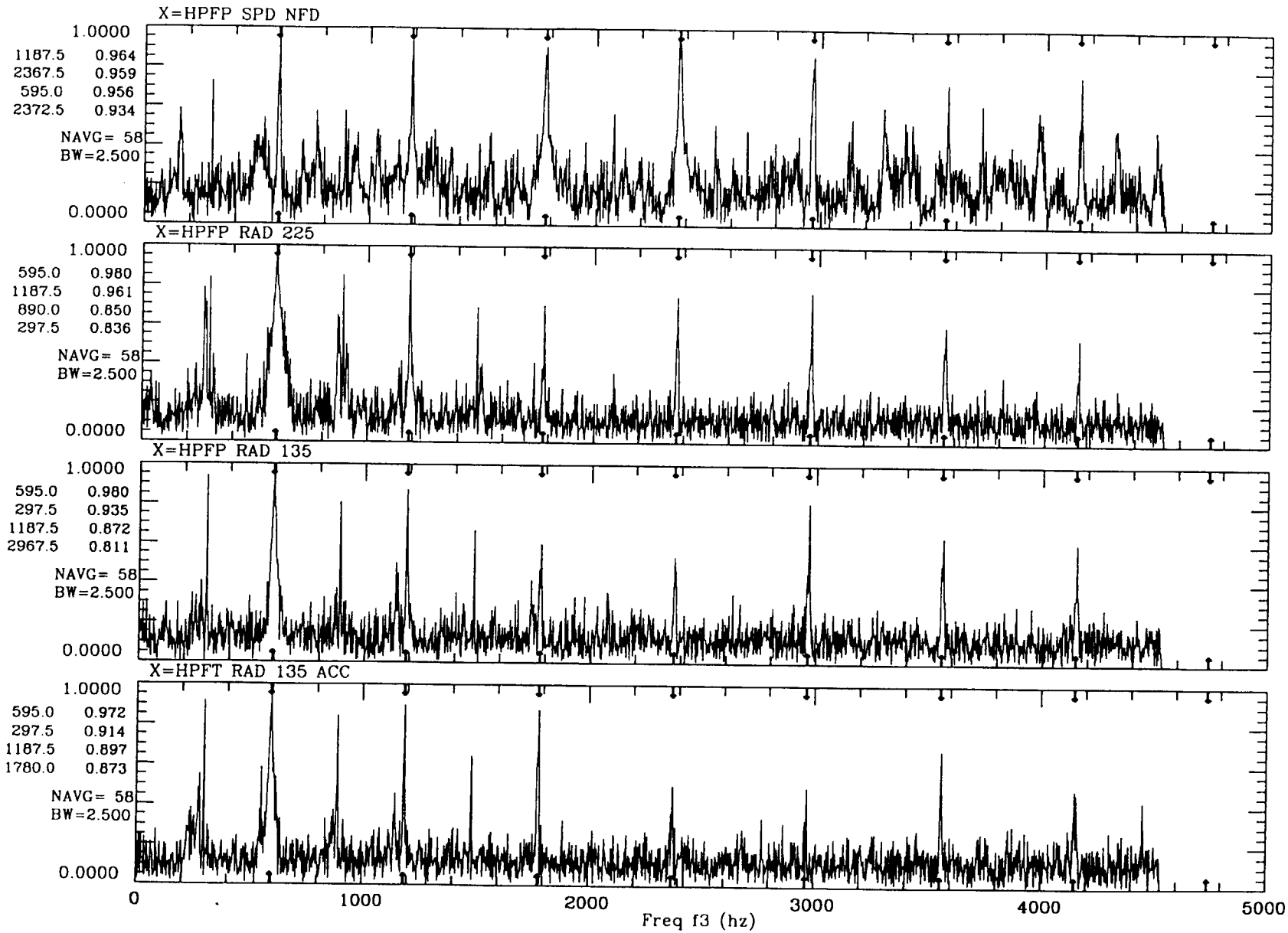

9010853 Txxxx(f1= 0.00,f2= 592.522,f3),S+ 116.00

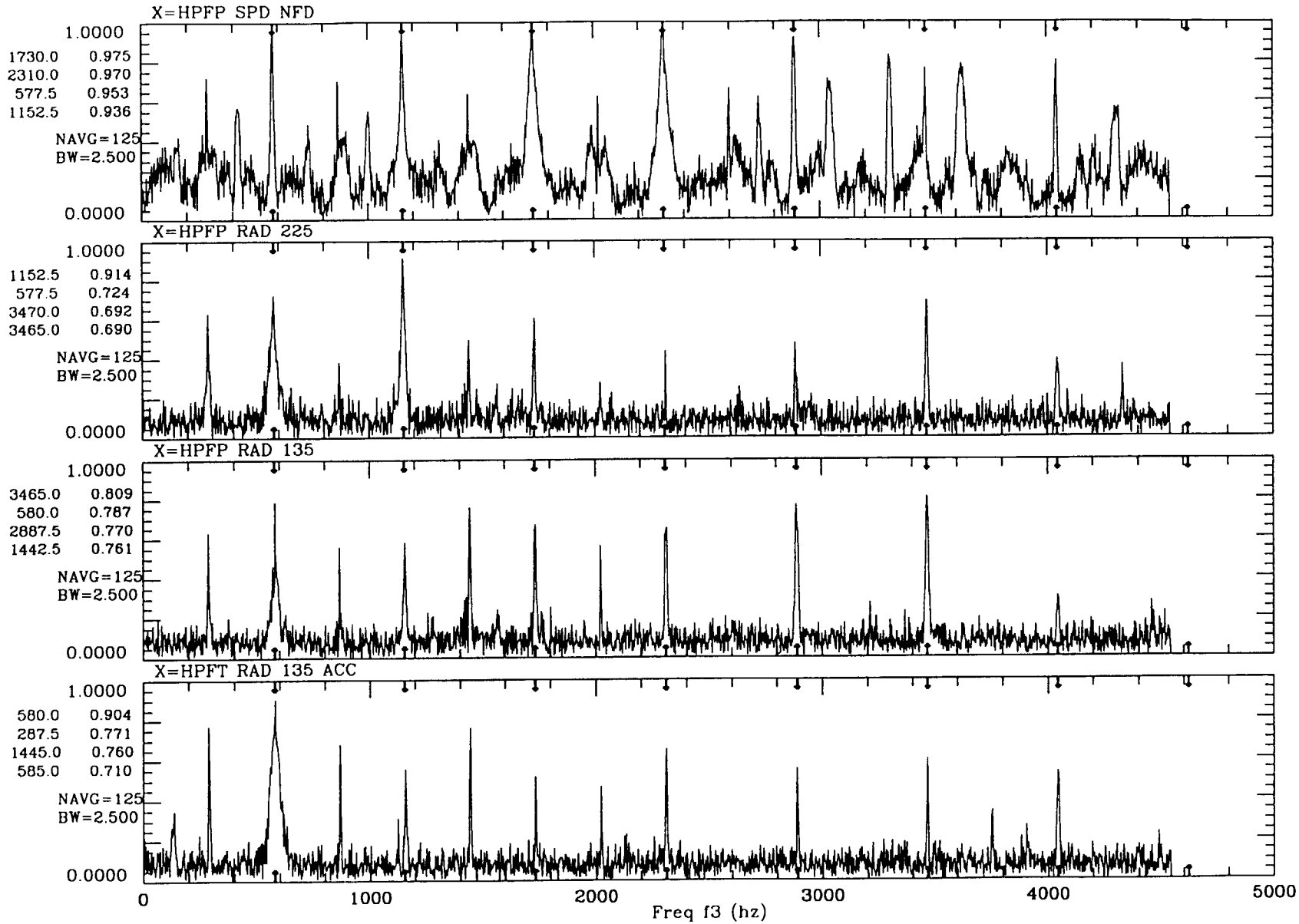

9010853 Txxxx(f1= 0.00,f2= 577.674,f3),S+ 141.00

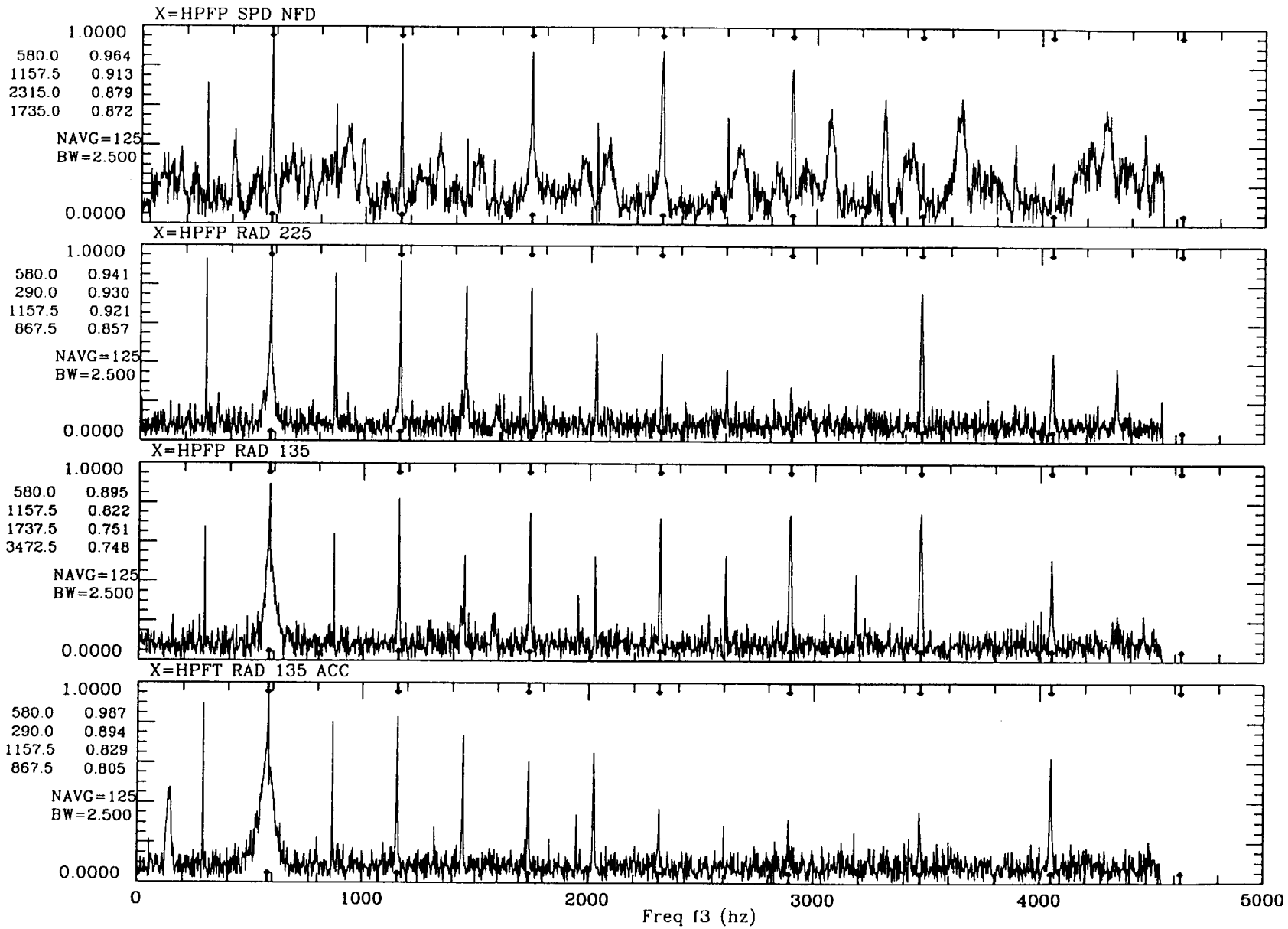

9010853 Txxxx(f1= 0.00,f2= 578.512,f3),S+ 191.00

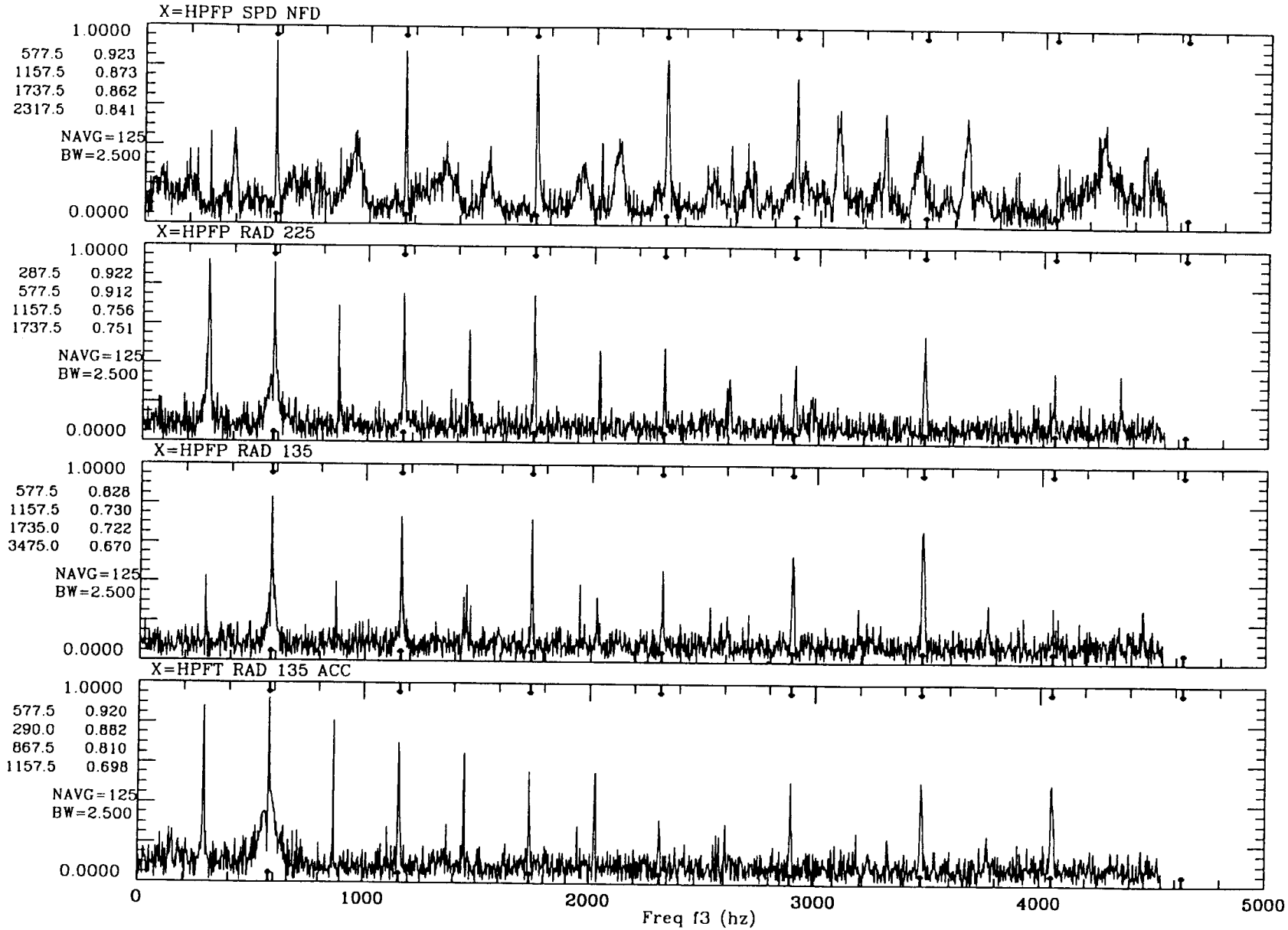

9010853 Txxxx(f1= 0.00,f2= 578.834,f3),S+ 241.00

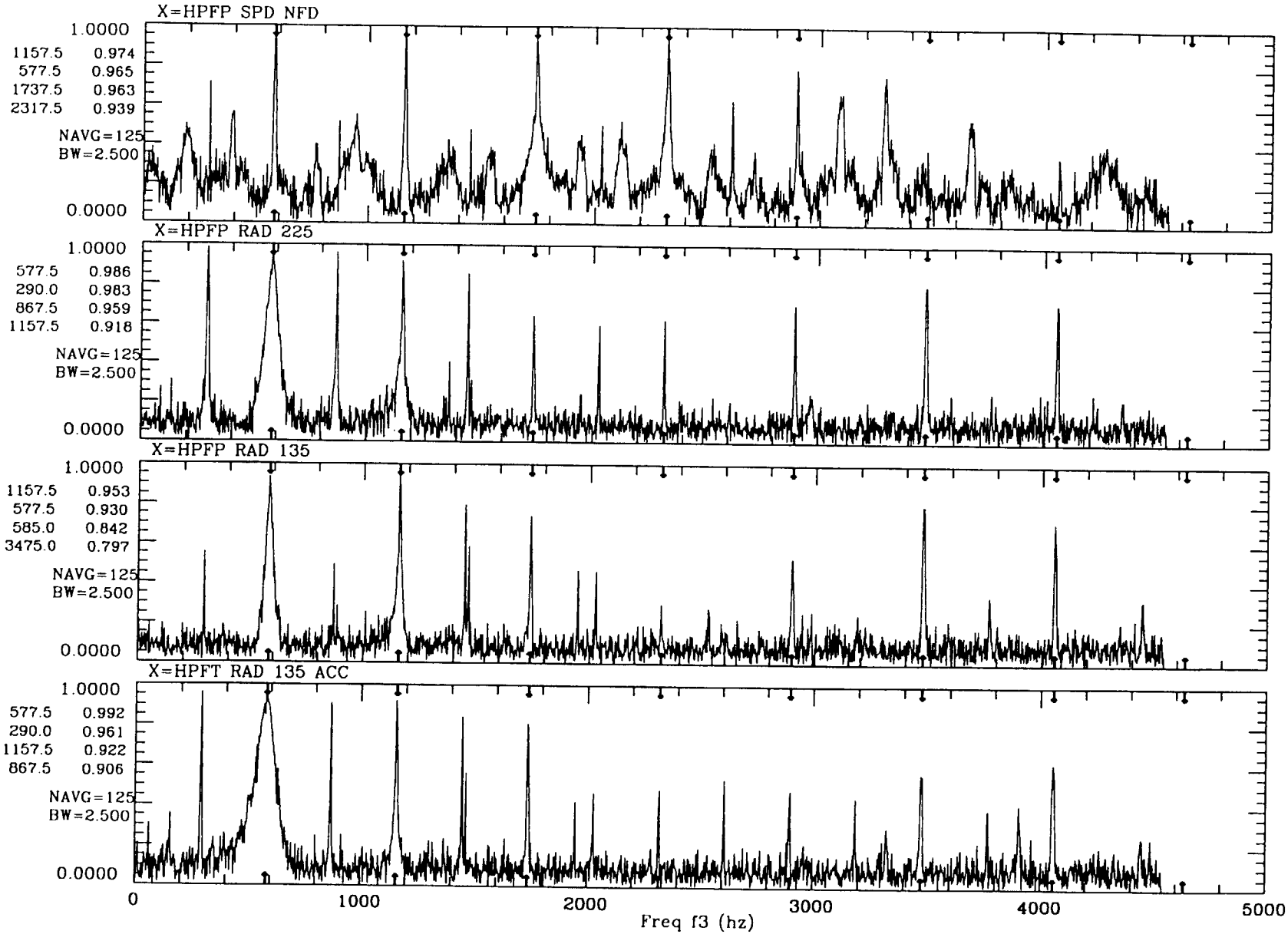

9010853 Txxxx(f1= 0.00,f2= 579.405,f3),S+ 291.00

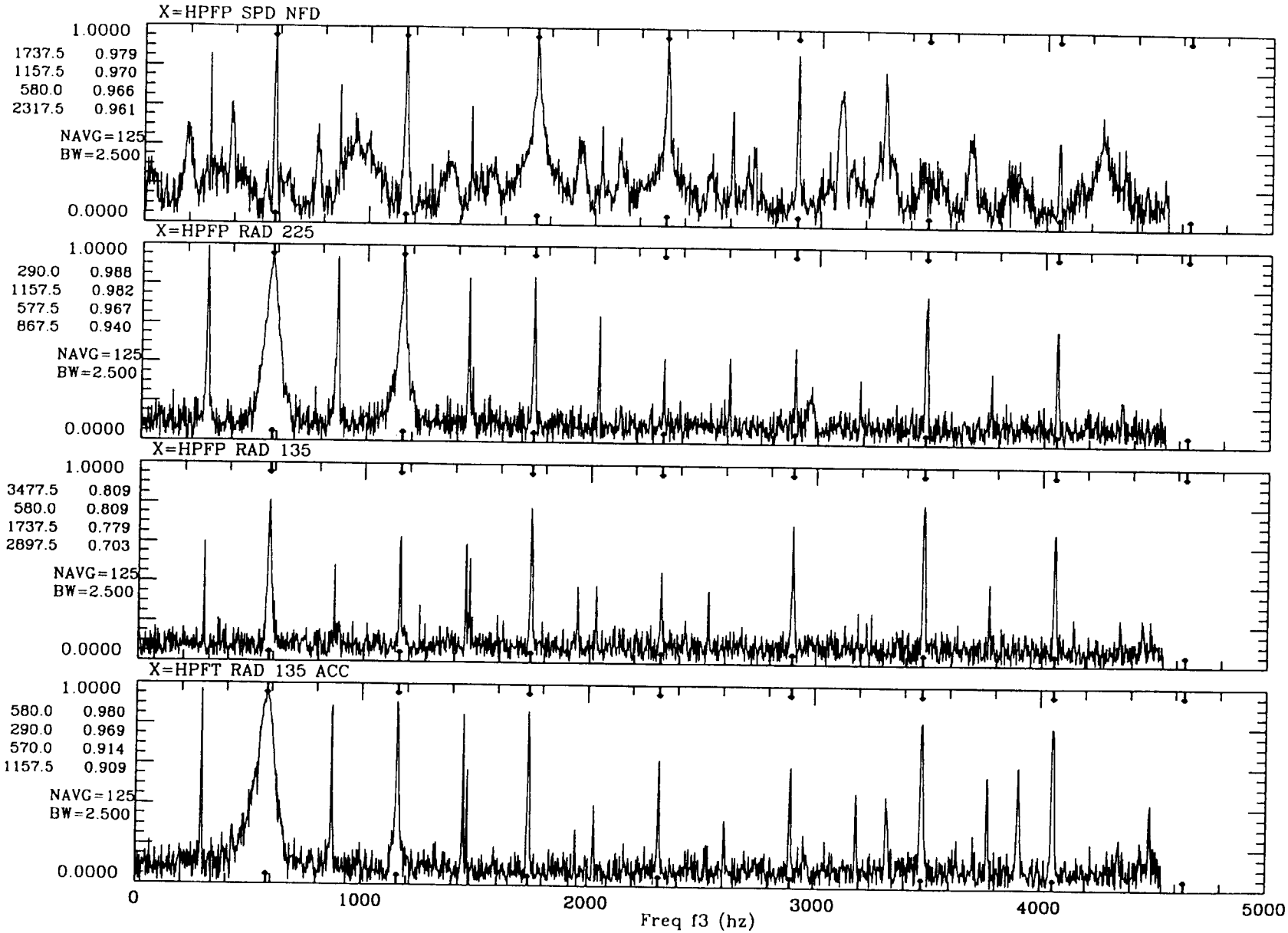

9010853 Txxxx(f1= 0.00,f2= 579.534,f3),S+ 341.00

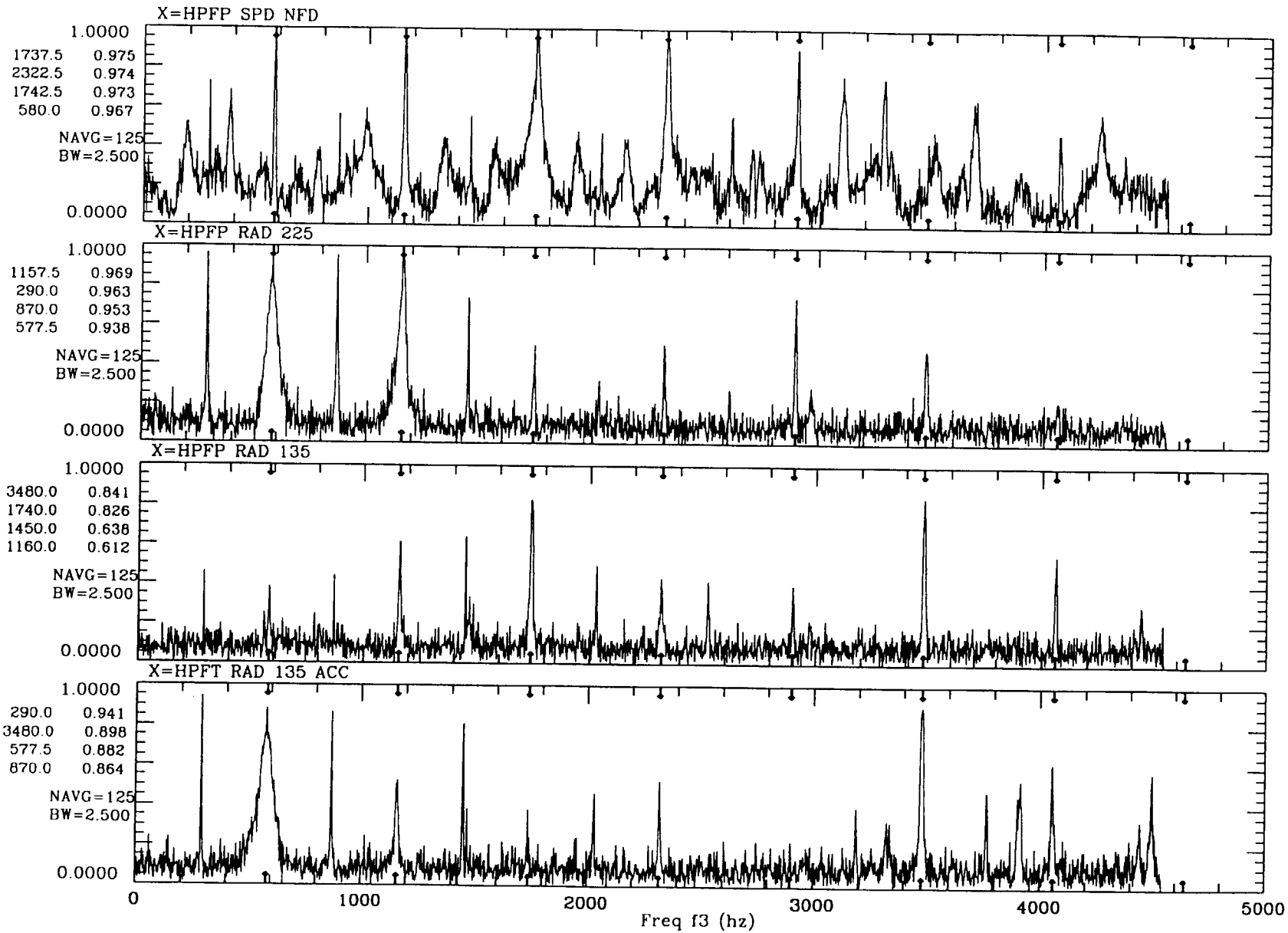

9010853 Txxxx(f1= 0.00,f2= 579.891,f3),S+ 391.00

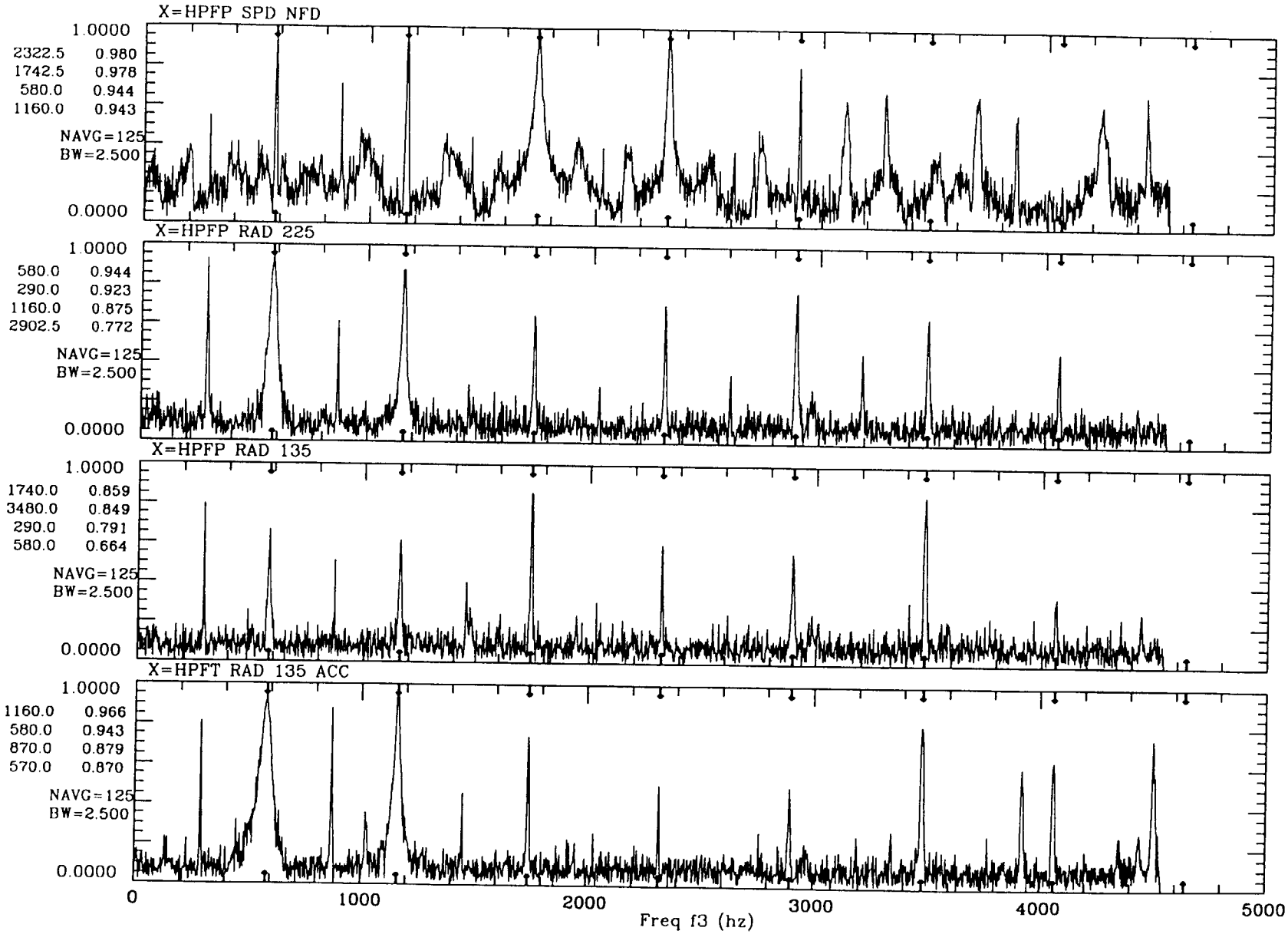

9010853 Txxxx(f1= 0.00,f2= 580.055,f3),S+ 441.00

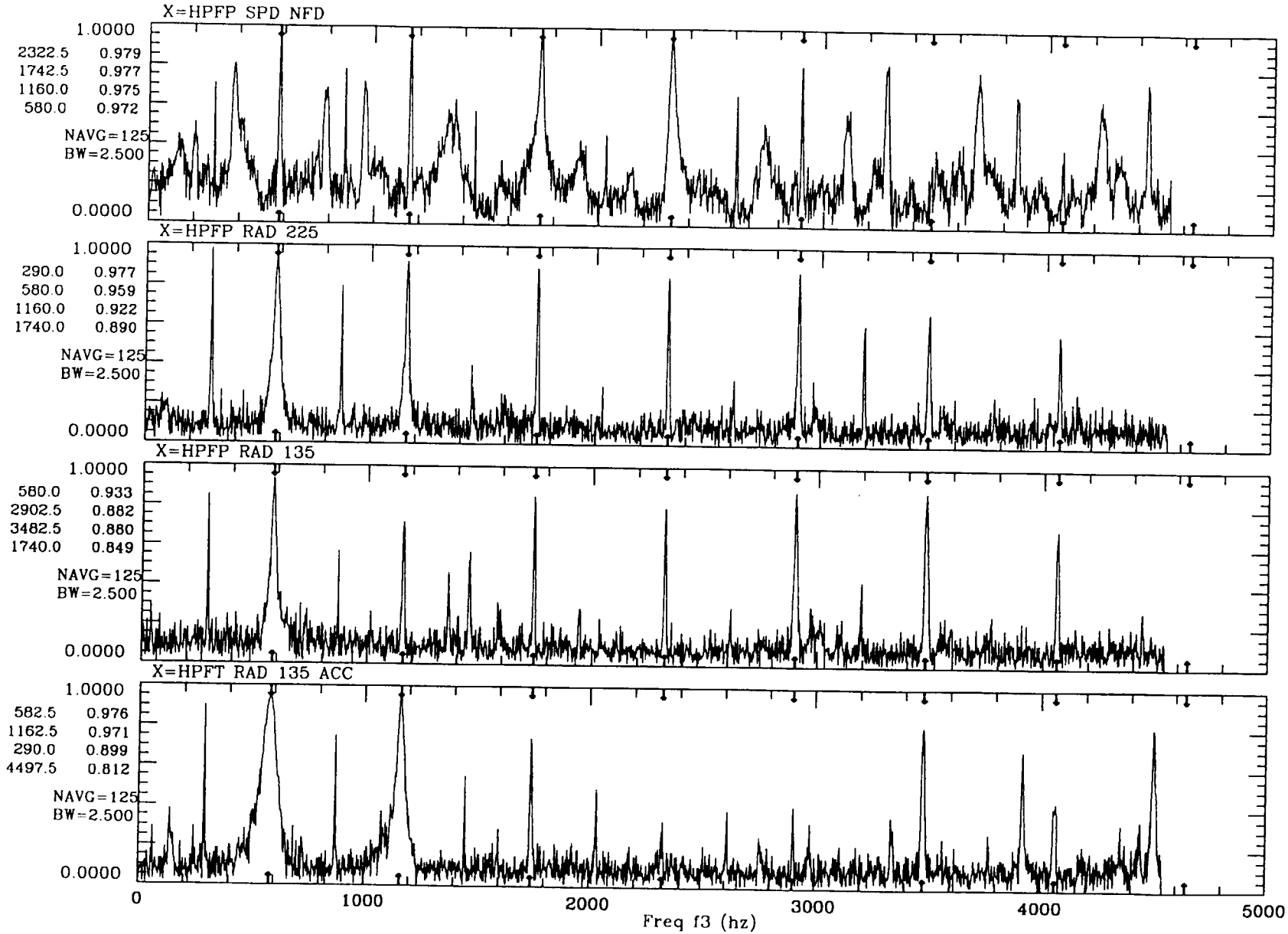

9010853 Txxxx(f1= 0.00,f2= 580.253,f3),S+ 491.00

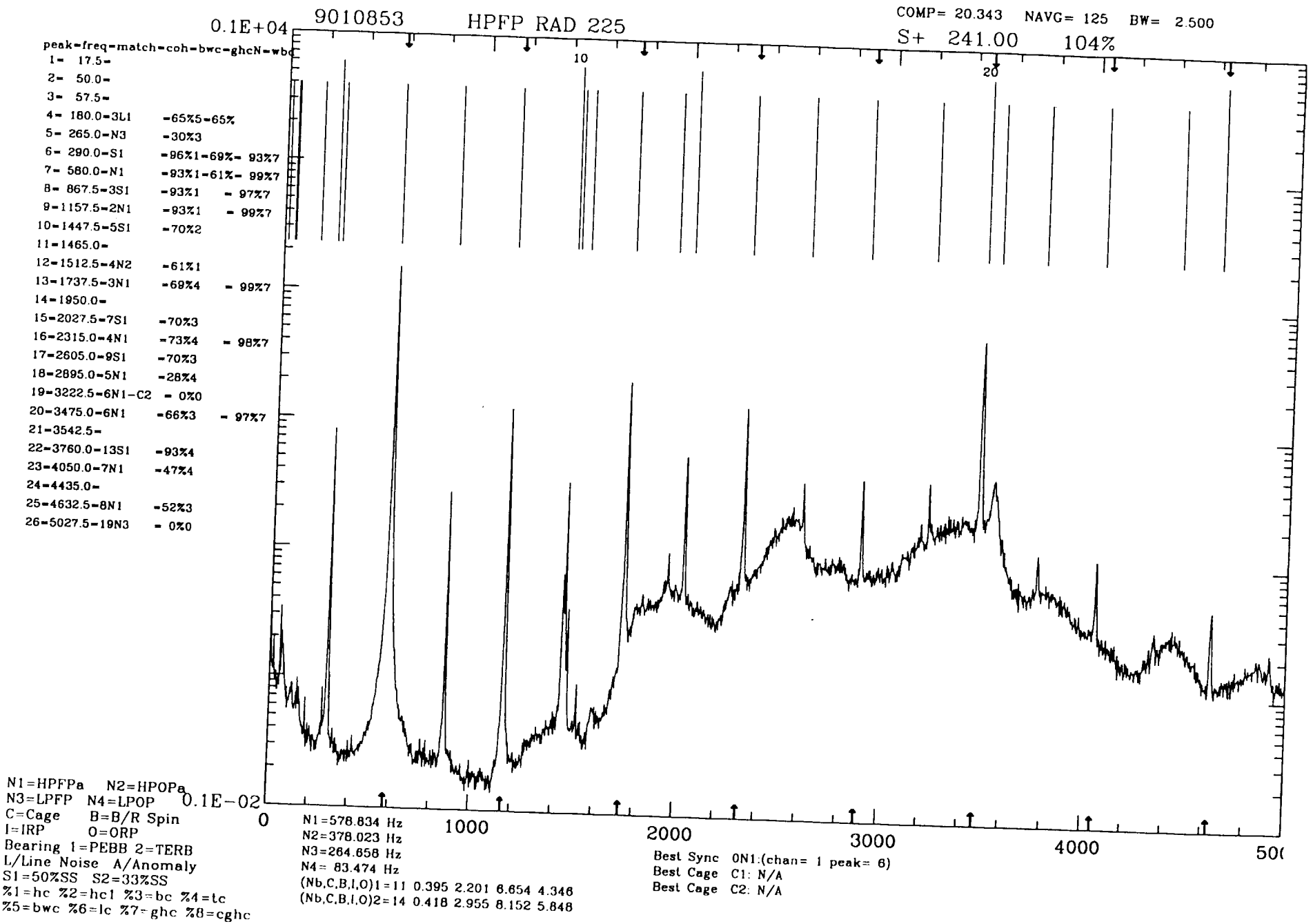
0.1E+04
9010853 HPFP RAD 225
COMP= 20.343 NAVG= 125 BW= 2.500
S+ 241.00 104%
peak-freq-match-coh-bwc-ghcN-wbc
1- 17.5-
2- 50.0-
3- 57.5-
4- 180.0-3L1 -65%5-65%
5- 265.0-N3 -30%3
6- 290.0-S1 -96%1-69%- 93%7
7- 580.0-N1 -93%1-61%- 99%7
8- 867.5-3S1 -93%1 - 97%7
9-1157.5-2N1 -93%1 - 99%7
10-1447.5-5S1 -70%2
11-1465.0-
12-1512.5-4N2 -61%1
13-1737.5-3N1 -69%4 - 99%7
14-1950.0-
15-2027.5-7S1 -70%3
16-2315.0-4N1 -73%4 - 98%7
17-2605.0-9S1 -70%3
18-2895.0-5N1 -28%4
19-3222.5-6N1-C2 - 0%0
20-3475.0-6N1 -66%3 - 97%7
21-3542.5-
22-3760.0-13S1 -93%4
23-4050.0-7N1 -47%4
24-4435.0-
25-4632.5-8N1 -52%3
26-5027.5-19N3 - 0%0
10
20
0.1E-02
0
1000
2000
3000
4000
N1=578.834 Hz
N2=378.023 Hz
N3=264.658 Hz
N4= 83.474 Hz
(Nb,C,B,I,O)1=11 0.395 2.201 6.654 4.346
(Nb,C,B,I,O)2=14 0.418 2.955 8.152 5.848
Best Sync 0N1:(chan= 1 peak= 6)
Best Cage C1: N/A
Best Cage C2: N/A
N1=HPFPa N2=HPOPa
N3=LPFP N4=LPOP
C=Cage B=B/R Spin
I=IRP O=ORP
Bearing 1=PEBB 2=TERB
L/Line Noise A/Anomaly
S1=50%SS S2=33%SS
%1=hc %2=hc1 %3=bc %4=tc
%5=bwc %6=lc %7=ghc %8=cghc

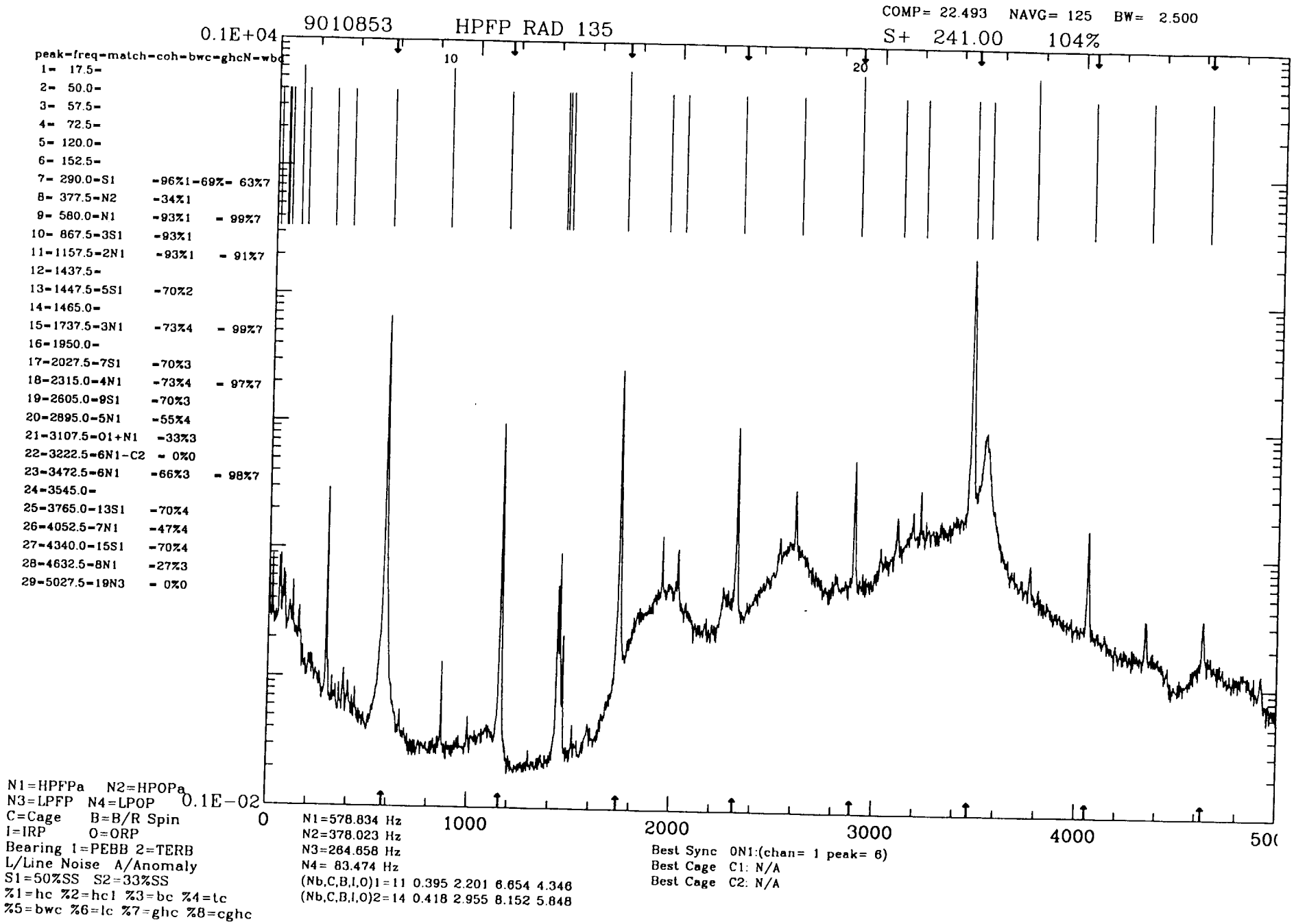
9010853 HPFP RAD 135
COMP= 22.493 NAVG= 125 BW= 2.500
S+ 241.00 104%
0.1E+04
0.1E-02
peak-freq-match-coh-bwc-ghcN-wbc
1= 17.5-
2= 50.0-
3= 57.5-
4= 72.5-
5= 120.0-
6= 152.5-
7= 290.0-S1 -96%1-69%- 63%7
8= 377.5-N2 -34%1
9= 580.0-N1 -93%1 - 99%7
10= 867.5-3S1 -93%1
11=1157.5-2N1 -93%1 - 91%7
12=1437.5-
13=1447.5-5S1 -70%2
14=1465.0-
15=1737.5-3N1 -73%4 - 99%7
16=1950.0-
17=2027.5-7S1 -70%3
18=2315.0-4N1 -73%4 - 97%7
19=2605.0-9S1 -70%3
20=2895.0-5N1 -55%4
21=3107.5-O1+N1 -33%3
22=3222.5-6N1-C2 - 0%0
23=3472.5-6N1 -66%3 - 98%7
24=3545.0-
25=3765.0-13S1 -70%4
26=4052.5-7N1 -47%4
27=4340.0-15S1 -70%4
28=4632.5-8N1 -27%3
29=5027.5-19N3 - 0%0
10
20
0
1000
2000
3000
4000
N1=HPFPa N2=HPOPa
N3=LPFP N4=LPOP
C=Cage B=B/R Spin
I=IRP O=ORP
Bearing 1=PEBB 2=TERB
L/Line Noise A/Anomaly
S1=50%SS S2=33%SS
%1=hc %2=hc1 %3=bc %4=tc
%5=bwc %6=lc %7=ghc %8=cghc
N1=578.834 Hz
N2=378.023 Hz
N3=264.658 Hz
N4= 83.474 Hz
(Nb,C,B,I,O)1=11 0.395 2.201 6.654 4.346
(Nb,C,B,I,O)2=14 0.418 2.955 8.152 5.848
Best Sync 0N1:(chan= 1 peak= 6)
Best Cage C1: N/A
Best Cage C2: N/A

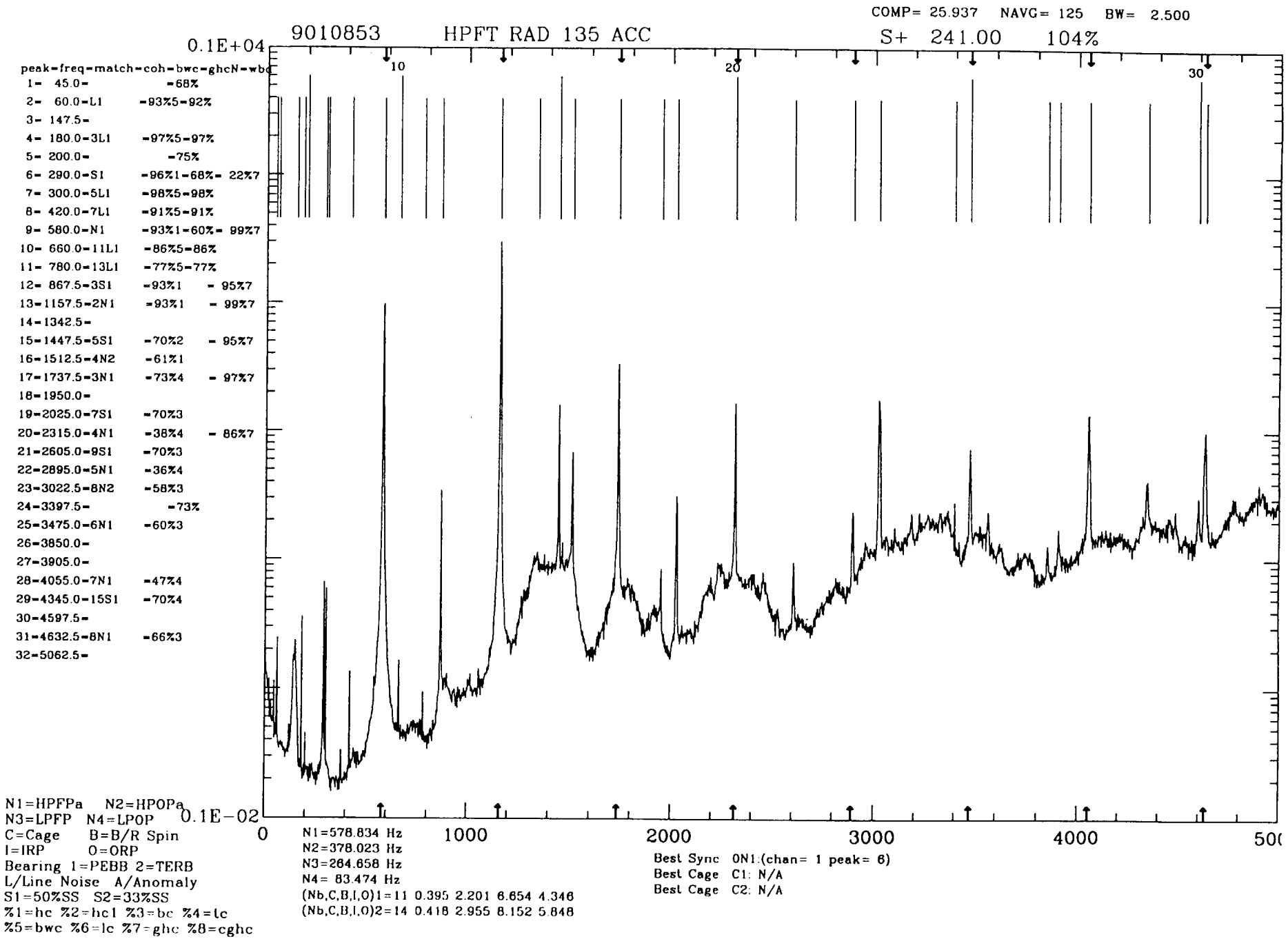
COMP= 25.937 NAVG= 125 BW= 2.500
9010853 HPFT RAD 135 ACC
S+ 241.00 104%
0.1E+04
0.1E-02
peak-freq-match-coh-bwc-ghcN-wbc
1= 45.0- =68%
2= 60.0-L1 =93%5-92%
3= 147.5-
4= 180.0-3L1 =97%5-97%
5= 200.0- =75%
6= 290.0-S1 =96%1-68%- 22%7
7= 300.0-5L1 =98%5-98%
8= 420.0-7L1 =91%5-91%
9= 580.0-N1 =93%1-60%- 99%7
10= 660.0-11L1 =86%5-86%
11= 780.0-13L1 =77%5-77%
12= 867.5-3S1 =93%1 - 95%7
13=1157.5-2N1 =93%1 - 99%7
14=1342.5-
15=1447.5-5S1 =70%2 - 95%7
16=1512.5-4N2 =61%1
17=1737.5-3N1 =73%4 - 97%7
18=1950.0-
19=2025.0-7S1 =70%3
20=2315.0-4N1 =38%4 - 86%7
21=2605.0-9S1 =70%3
22=2895.0-5N1 =36%4
23=3022.5-8N2 =58%3
24=3397.5- =73%
25=3475.0-6N1 =60%3
26=3850.0-
27=3905.0-
28=4055.0-7N1 =47%4
29=4345.0-15S1 =70%4
30=4597.5-
31=4632.5-8N1 =66%3
32=5062.5-
10
20
30
0
1000
2000
3000
4000
N1=HPFPa N2=HPOPa
N3=LPFP N4=LPOP
C=Cage B=B/R Spin
I=IRP O=ORP
Bearing 1=PEBB 2=TERB
L/Line Noise A/Anomaly
S1=50%SS S2=33%SS
%1=hc %2=hc1 %3=bc %4=lc
%5=bwc %6=lc %7=ghc %8=cghc
N1=578.834 Hz
N2=378.023 Hz
N3=264.658 Hz
N4= 83.474 Hz
(Nb,C,B,I,O)1=11 0.395 2.201 6.654 4.346
(Nb,C,B,I,O)2=14 0.418 2.955 8.152 5.848
Best Sync 0N1:(chan= 1 peak= 6)
Best Cage C1: N/A
Best Cage C2: N/A

REPORT DOCUMENTATION PAGE

Form Approved
OMB No. 0704-0188

1. AGENCY USE ONLY *(Leave blank)*	2. REPORT DATE	3. REPORT TYPE AND DATES COVERED
	March 31, 1997	Final Report

4. TITLE AND SUBTITLE

Develop Advanced Nonlinear Signal Analysis Topographical Mapping System

5. FUNDING NUMBERS

NAS8-39393

6. AUTHOR(S)

Jen-Yi, Jong

7. PERFORMING ORGANIZATION NAME(S) AND ADDRESS(ES)

AI SIGNAL RESEARCH, INC.
3322 South Memorial Parkway, Suite 67
Huntsville, AL 35801

8. PERFORMING ORGANIZATION REPORT NUMBER

TR-4002-Final

9. SPONSORING/MONITORING AGENCY NAME(S) AND ADDRESS(ES)

Procurement Office, AP29-I
George C. Marshall Space Flight Center
NASA
Marshall Space Flight Center, AL 35812

10. SPONSORING/MONITORING AGENCY REPORT NUMBER

11. SUPPLEMENTARY NOTES

12a. DISTRIBUTION/AVAILABILITY STATEMENT

12b. DISTRIBUTION CODE

13. ABSTRACT *(Maximum 200 words)*

During the development of the SSME, a hierarchy of advanced signal analysis techniques for mechanical signature analysis has been developed by NASA and AI Signal Research Inc. (ASRI) to improve the safety and reliability for Space Shuttle operations. These techniques can process and identify intelligent information hidden in a measured signal which is often unidentifiable using conventional signal analysis methods. Currently, due to the highly interactive processing requirements and the volume of dynamic data involved, detailed diagnostic analysis is being performed manually which requires immense man-hours with extensive human interface. To overcome this manual process, NASA implemented this program to develop an Advanced nonlinear signal Analysis Topographical Mapping System (ATMS) to provide automatic/unsupervised engine diagnostic capabilities. The ATMS will utilize a rule-based Clips expert system to supervise a hierarchy of diagnostic signature analysis techniques in the Advanced Signal Analysis Library (ASAL). ASAL will perform automatic signal processing, archiving, and anomaly detection/identification tasks in order to provide an intelligent and fully automated engine diagnostic capability. The ATMS has been successfully developed under this contract. In summary, the program objectives to design, develop, test and conduct performance evaluation for an automated engine diagnostic system have been successfully achieved. Software implementation of the entire ATMS system on MSFC's OISPS computer has been completed. The significance of the ATMS developed under this program is attributed to the fully automated coherence analysis capability for anomaly detection and identification which can greatly enhance the power and reliability of engine diagnostic evaluation. The results have demonstrated that ATMS can significantly save time and man-hours in performing engine test/flight data analysis and performance evaluation of large volumes of dynamic test data.

14. SUBJECT TERMS			15. NUMBER OF PAGES 245
			16. PRICE CODE
17. SECURITY CLASSIFICATION OF REPORT	18. SECURITY CLASSIFICATION OF THIS PAGE	19. SECURITY CLASSIFICATION OF ABSTRACT	20. LIMITATION OF ABSTRACT